

A Thesis Submitted for the Degree of PhD at the University of Warwick

Permanent WRAP URL:

<http://wrap.warwick.ac.uk/100748>

Copyright and reuse:

This thesis is made available online and is protected by original copyright.

Please scroll down to view the document itself.

Please refer to the repository record for this item for information to help you to cite it.

Our policy information is available from the repository home page.

For more information, please contact the WRAP Team at: wrap@warwick.ac.uk

AIR CORED LINEAR MACHINES
FOR GROUND TRANSPORTATION

E Abel, B.Sc, CEng, MIEE

submitted for the degree of PhD

Department of Engineering Science

University of Warwick

September 1981

Volume One of two volumes

To, Diana, who with her consideration, help and
thoughtfulness over the past four years has been
most responsible for the completion of this thesis.

SUMMARY

The most important areas of interest concerning air cored linear machines (ACLM), their design, development and application to guided ground transportation are presented. A description of the origins of high speed guided ground transportation (HSGGT) is given which covers tracked air cushion vehicle and linear induction motor development, as well as the electromagnetic and electrodynamic systems of levitation.

ACLM began as the favoured propulsion option for the electrodynamic system, and the machine characteristics of the linear synchronous motor (LSM) are discussed with optimization techniques given for choice of wavelength. Stress factors for rectangular coils with tight corner radii can be calculated using a circular coil equivalent.

The linear commutator motor (LCM) provides a means of achieving high local track power density without degrading overall machine performance. Several forms are examined and the trade off and comparison with LSM made. The system comparison of the electrodynamic and electromagnetic systems (EDS and EMS) of magnetic levitation indicates that specifying just lift to drag ratio and specific energy intensity is an insufficient base. Comparison is made of the German EMS and EDS designs, together with a comparison of other groups' EDS vehicles. The German EDS design is found to be heavily penalised by excessive low speed suspension weight.

Several variations of a new type of ACLM using on board flux pumping are proposed. The advantages are that a passive track structure is possible, and a cryogenically cooled winding can be used as a cost effective alternative to a superconducting coil.

Application of ACLM to propulsion of advanced duorail vehicles is set out together with the possibility of speed extension with reduced track wear and initial capital cost, as well as reduced manning and maintenance cost. An Advanced Passenger Train with LSM would appear to be a feasible option for future transport needs, and extension to a low speed urban vehicle using for example liquid nitrogen cooled pool boiling coils would similarly present a low cost system.

An indexed bibliography containing over 400 HSGGT references is included, with a bias to EDS and ACLM.

TABLE OF CONTENTS

Page No

VOLUME ONE

SUMMARY	iii
ACKNOWLEDGEMENT	vii
DECLARATION	vii
LIST OF TABLES	viii
LIST OF FIGURES	ix
LIST OF SYMBOLS	xii
ABBREVIATIONS	xv
1. INTRODUCTION	1
2. LINEAR MACHINE DEVELOPMENT - AN OVERVIEW	5
2.1 Early Linear Machines	5
2.2 Tracked Air Cushion Vehicles	8
2.2.1 General Considerations	8
2.2.2 American Systems	9
2.2.2.1 UMTA Projects	9
2.2.2.2 FRA Projects	10
2.2.3 Tracked Hovercraft Ltd	12
2.2.4 The Aerotrain	13
2.2.5 Other TACV	15
2.3 The Electromagnetic System of Levitation	16
2.3.1 General Development	16
2.3.2 German Systems	18
2.3.2.1 German Development	18
2.3.2.2 German Test Vehicles	22
2.3.3 Japanese Systems	25
2.3.3.1 Japanese Development	25
2.3.3.2 Japanese Vehicles	27
2.3.4 Other Systems	29
2.3.4.1 UK Development	29
2.3.4.2 American Development	30
2.3.4.3 Russian Development	31
2.4 The Electrodynamic System of Levitation	31
2.4.1 General Development	31
2.4.2 American Systems	33
2.4.2.1 Levitation Research	33
2.4.2.2 The Magneplane Project	36
2.4.3 Japanese Development	39
2.4.3.1 Initial Research	39
2.4.3.2 CSPG	40
2.4.3.3 The Miyazaki Test Line	42
2.4.4 Canadian Research	47
2.4.4.1 Overall Development	47
2.4.4.2 Test Facilities	52

	Page No
2.4.5 German Development	58
2.4.6 UK Development	63
2.4.7 French Research	73
2.5 Other Machine Variants	73
2.5.1 Linear Induction Machines	74
2.5.1.1 LIMRV	74
2.5.1.2 Transverse Flux LIM	76
2.5.1.3 ROMAG	77
2.5.1.4 ISPS	77
2.5.1.5 ICTS	79
2.5.1.6 Brush-BR Mickleover Tests	80
2.5.2 Linear Synchronous Motors	80
2.5.2.1 Heteropolar LSM	81
2.5.2.2 Homopolar LSM	83
2.5.2.3 Linear Reluctance Motors	85
2.5.3 Linear DC Motors	86
2.6 Future Near Term Developments	89
3. PERFORMANCE CHARACTERISTICS OF LSM	93
3.1 Equivalent Circuit Representation	93
3.1.1 Basic Requirements	93
3.1.2 Load Angle Derived Equations	95
3.1.3 Current Angle Derived Equations	98
3.1.4 Operation at Minimum S_T	102
3.2 Inductance and Induced Emf Modelling	103
3.2.1 Mutual Inductance	103
3.2.2 Track Inductance	104
3.2.3 Back Emf	106
3.3 Wavelength Optimization	110
3.4 Shape Effects on Coil Stress	113
4. LINEAR COMMUTATOR MOTOR	118
4.1 Original Design Philosophy	118
4.2 Model LCM	121
4.3 Comparison with LSM	123
5. MACHINE ECONOMICS AND SYSTEMS COMPARISONS	127
5.1 The Need for Systems Comparisons	127
5.2 German Maglev Revenue Passenger Vehicles	128
5.3 Maglev Vehicle Weight Breakdown	134
5.4 Specific Energy Intensity	134
6. FLUX PUMPING AND CRYOGENICALLY COOLED MACHINES	136
6.1 Pulsed and AC Operation of Coils	136
6.2 Application to HSGGT	137
6.3 Flux Pumping Motors	138
6.3.1 Components	138
6.3.2 Methods of Coil Energisation	140
6.4 Superconducting Homopolar LSM	142
7. HYBRID APPLICATIONS OF ACLSM	143
7.1 Introduction	143
7.2 Advanced Passenger Train with ACLSM	144
7.2.1 APT Origin	144
7.2.2 Problem Areas in High Speed Running	146
7.2.3 ACLSM Extension of APT Capability	148
7.3 Urban Vehicles with ACLSM	154

8. CONCLUSIONS	Page No	157
9. REFERENCES		160

VOLUME TWO

APPENDIX I	BIBLIOGRAPHY	177
	1. Scope of the Bibliography	177
	2. Books	178
	3. Special Issues	178
	4. Conference Proceedings	179
	5. Indexed Papers List	180
	5.1 Papers	180
	5.2 Author Index	228
	5.3 Corporate Index	236
APPENDIX II	SOLENOID MAGNET DESIGN	241
	1. Introduction	241
	2. Circular Coils	242
	2.1 Basic Field and Power Relationships	242
	2.2 Off Axis Field of a Finite Solenoid	246
	3. Rectangular Coils	247
	3.1 Line Filament Solutions	247
	3.2 Finite Sections	249
	4. Racetrack Coils	251
APPENDIX III	DERIVATION OF TRACK INDUCTANCE	
	1. Introduction	253
	2. Track Inductance	254
	2.1 Phase Leakage Inductance	254
	2.2 Elemental Inductance	254
	3. Self Inductance Structure	255
	4. Mutual Inductance Structure	258
APPENDIX IV	FLUX LINKAGE AND INDUCED EMF IN AIR CORED MACHINES (Reference 222)	
	1. Introduction	262
	2. Derivation of Back Emf Relationships	262
	3. Rectangular Coils	268
	4. Circular and Racetrack Coils	272
	5. Conclusions	273
	Appendix. Rate of Change of Flux Linkage for a Rectangular Coil	274
APPENDIX V	COMPARISONS OF ALTERNATIVE MAGLEV REVENUE VEHICLE SYSTEMS	
	1. Reference 134, Electronics and Power	291
	2. Reference 135, IEEE Transactions on Magnetics	294

ACKNOWLEDGEMENT

The study of Air Cored Linear Synchronous Machines began as part of the Warwick University Maglev Research Programme, which was largely funded by the Wolfson Foundation. I therefore acknowledge and express appreciation for my association with the project and the other research fellows involved, especially Jeff Howell, Joe Mahtani, and Jan Rakels, and of course the Project Director, Professor Rene Rhodes.

Audrey Poffley deserves special thanks for her diligence and good nature in converting an untidy manuscript into a presentable and ordered document.

DECLARATION

Some of the material contained in this thesis has already been published, both before and since its beginning. The relevant sections are referenced whether they are freely available or Warwick University reports. Mr Mahtani produced some of the calculation embodied in the AMMA paper (Reference 130), but the remainder of the material originates from the author.

LIST OF TABLES

	Following Page No
I TACV with Linear Motor Propulsion	10
II German EMS Vehicles	22
III Japanese EMS Vehicles	28
IV EDS Test Tracks	38
V EDS Rotating Test Facilities	40
VI Linear Machine Test Tracks	75
VII Linear Machine Test Rigs	78
VIII Characteristics of LCM Superconducting Coil	122
IX Magneplane Parameters	124
X Optimisation Parameters	126
XI Conceptual Maglev Revenue Vehicles	128
XII Apparent Efficiency of the German Vehicles	131

LIST OF FIGURES

		Following Page No
1	Linear Synchronous Motor	33
2	Superconducting Paddlewheel	35
3	Superconducting Helix	35
4	Combined System of Propulsion and Guidance	41
5	Power Supply and Control System for LSM	44
6	Split Track	66
7	Claw-Pole Motor	81
8	Heteropolar Inductor Motor	82
9	Aberdeen Transverse Flux Heteropolar Machine	82
10	Kemper's Homopolar Machine with Levitation	83
11	Double Sided HLSM	83
12	Aberdeen Transverse Flux Homopolar Machine	84
13	Homopolar Inductor Motor	84
14	Voltage Fed Equivalent Circuit	93
15	Phasor Diagram for Representative Phase	93
16	Efficiency, Power Factor and Product with Load Angle	97
17	Efficiency, Power Factor and Product with Load Angle	- 97
18	Current Angle for Minimum S_T	101
19	Efficiency for Minimum S_T	102
20	Power Factor and Product for Minimum S_T	102
21	Terminal Voltage	102
22	Phase Current	102
23	Power Input	102
24	Performance Characteristics of LSM at Cruise	102
25	Mutual Inductance between Parallel Current Elements	103
26	Coordinates for Mutual Inductance	103
27	Armature Winding Representation	104
28	Asymptotic Self and Mutual Inductance	106

29	Generalised Vehicle and Track Coils	106
30	Field Conventions Adopted for Rectangular Coils	108
31	Neighbouring Coil Contribution to $\frac{d\phi}{dx}$	108
32	Effect of Neighbouring Coils on Rate of Change of Flux	109
33	Thrust per Unit Stator Length x Current	112
34	Optimum Wavelength for Machine Width and Airgap	113
35	Lorentz Forces on Simple Elements	114
36	Balance of Body Forces and Restraining Forces	115
37	Element for Cylindrical Coil Stressing	115
38	Central Field Change for Non Circular Coils	116
39	Tube Equivalents to Radiused Coils	116
40	Fractional Power Loss in Block Sectioned Armature	119
41	LCM, Distributed Progressive Winding	119
42	LCM, Discrete Winding	119
43	Superconducting Model LCM	122
44	Magneplane Characteristics at 504 km/h	124
45	Annual Unit Track Armature Cost	125
46	Optimisation for G and A	125
47	Loci of Optimum G, A, for Different Wavelengths	125
48	Costs as a Function of Wavelength	125
49	Specific Primary Energy Cost of Transport Modes	127
50	Distribution Diagram for the EDS LSM	129
51	Distribution Diagram for the EMS LIM	129
52	Distribution Diagram for the EMS LSM	129
53	Total Active Power of Systems	130
54	Relative System Active Power Requirements	131
55	Total Complex and Active Power of Systems	132
56	Relative System Total Complex Power Requirements	132
57	Subsystem Weight Breakdown (% Gross)	134

58	Subsystem Weight Breakdown	134
59	Flux Pumping Motor Coil Array	138
60	Methods of Coil Energisation	140
61	Superconducting Homopolar Linear Synchronous Motor	142
62	Power Requirements for APT	148
63	Cryostat End View	149
64	Propulsion Magnet	150
65	APT with Track Winding and Removeable Cryostats	154
66	Mixed μ Suspension and Transverse Flux LSM Propulsion	156
67	The Elemental Loop	242
68	Current Sheet	242
69	Saturation of Current Sheet Central Field	242
70	Finite Thickness Uniform Current Density Solenoid	244
71	Constant Fabry Factor Contours	244
72	Coil Geometry for Thick Coil	246
73	Superposition of Semi Infinite Solenoids	246
74	GMD/AMD for Equal Parallel Rectangles	247
75	Current Element, dl	248
76	Volume Superposition	248
77	Axial Field Variation for Coils	249
78	Normalized Field for Square Coil	249
79	Field for Finite Section Coils	249
80	Field Functions for Infinitely Long Bar	249
81	Field Function for Finite Length Bar	251
82	Field Function for Finite Length Bar	251
83	Race Track Coil Field Components	251
84	Off Axis Field for a Quadrant	251

LIST OF SYMBOLS

a	No of parallel paths per phase; coil radius, m
a _{1,2}	Coil inner, outer radius, m
A	Conductor cross section, A/m ²
b	Track half width; coil half height, m
B ₀	Central flux density, T
B _{x,y,z}	Longitudinal, Lateral, normal flux density, T
C	Bending moment coefficient; annual cost, \$/yr-m
C _{I,C,P}	Inverter, cable and power cost, \$/kVA,kg,kWh
D	End turn coefficient
e	Coil half width, m
E _{B,T}	Back emf; terminal voltage, V
F	Fractional phase displacement; Field factor
F _{B,N}	Thrust; normal force, N
G	Section Length, m; Fabry factor
h	Coil height, m
H	Optimum coefficient; solenoid field, AT/m
I	Phase current; coil current
I _{C,F,V}	Conductor Current, field equivalent current; coil AT, A
I _T	Track peak phase current, A
j	(-1) ^{1/2} ; current density, A/m ²
k	Repayment factor, %
l	Element length, m
L	Track phase inductance, H
L _{a,e,i}	Asymptotic, elemental, initial, inductance, H
L _{G,T}	Section length, strip self, inductance, H
m	No phases; no elements
M _{a,i,G}	Asymptotic, initial, section length, inductance, H
M _A	Per unit length track mass, kg/m
M _{FA}	Field-armature mutual inductance, H

n	No elements
\bar{n}	Average vehicle frequency, vehicles/h
N	No poles, no turns
P_A	Per unit length track power loss, W/m
$P_{B,T}$	Mechanical(propulsive), average terminal (active), power, W
P_M	Magnetic pressure, N/m ²
$Q_{B,T}$	Internal, terminal, reactive power, VA
r	Corner radius, m
R	Normalized radial offset; phase resistance, ohms
s	Solenoid inner radius, m; term defined by equation 22
t	Coil thickness, m
$T_C(H)$	Transition temperature, K
v	Velocity, m/s
\bar{v}	Average speed, km/h
$V_{1,2}$	Active, reactive, terminal voltage, V
w	Track width, m; loading density, N/m
W	Coil power, W
x	Longitudinal coordinate, m
X	Phase reactance, ohms
y	Transverse coordinate, m
z	Vertical coordinate; levitation height, m
Z	Normalized coil elevation
α	Force, current, angle, radians; coil diameter shape ratio
β	Coil shape ratio
γ	Coil breadth ratio
δ	Coil height ratio
ϵ	Longitudinal offset ratio
η	Efficiency
θ	Power factor angle, radians

λ	Wavelength, m; space factor
μ_0	Free Space Permeability, H/m
ρ	Resistivity, ohm-m
σ	Conductor density, kg/m ³
$\sigma_{r,s,\theta}$	Radial, sheer, hoop, stress, N/m ²
τ	Load angle, radians
ϕ	Flux linkage, Wb-T
$\Phi_{A,F}$	Armature, field, flux, Wb
ψ	Specific energy intensity, J/passenger-km
ω	Angular frequency, radians/s

ABBREVIATIONS

ACLM	Air Cored Linear Machine
ACLSM	Air Cored Linear Synchronous Motor
ACV	Air Cushion Vehicle
AEG	Allgemeine Elektrizitas-Gesellschaft
AFLIM	Axial Flux Linear Induction Motor
APT	Advanced Passenger Train
ASEA	Allmanna Svenska Elektriska Aktiebolaget
AVF	Anwendungsnahe Versuchsfahrzeug
AVR	Automatic Voltage Regulator
BBC	Brown Boveri Co.
BMFT	Bundesministerium für Forschungs und Technologie
BR	British Rail
CIGGT	Canadian Institute of Guided Ground Transportation
CIT	Cranfield Institute of Technology
CSL	Canadair Services Ltd.
CSPG	Combined System of Propulsion and Guidance
DCLM	DC Linear Motor
DoE	Department of the Environment
DoT	Department of Transportation
DSLIM	Double Sided Linear Induction Motor
DSLMS	Double Sided Linear Synchronous Motor
EDS	Electrodynamic System
EET	Erlangen Test Carrier
EMS	Electromagnetic System
FET	Field Effect Transistor
FPM	Flux Pumping Motor
FRA	Federal Railroad Administration
FS	Italian State Railways
GE	General Electric Co.
GEC	General Electric Co. Ltd.
GFR	German Federal Railways
GMD	Geometric Mean Distance
HELMS	Heteropolar Linear Synchronous Motor
HFLRM	Hybrid Flux Linear Reluctance Motor
HLSM	Homopolar Linear Synchronous Motor
HSB	Hochleistungsschnellbahn
HSGGT	High Speed Guided Ground Transportation
HSGT	High Speed Ground Transportation

HSGTC	High Speed Ground Transportation Centre
HSST	High Speed Surface Transportation
HST	High Speed Train
ICLSM	Iron Cored Linear Synchronous Motor
ICTS	Intermediate Capacity Transit System
INTERMAG	International Conference on Magnetism
ISPS	Integrated Suspension/Propulsion System
JAL	Japan Air Lines
JIS	Japan Iron and Steel
JNR	Japanese National Railways
LCM	Linear Commutator Motor
LCP	Large Coil Program
LEM	Linear Electrical Machine
LFPM	Linear Flux Pumping Motor
LHP	Lineare Hochgeschwindigkeitsprufstand
LIM	Linear Induction Motor
LIMRV	Linear Induction Motor Research Vehicle
LML	Le Moteur Lineal
LRM	Linear Reluctance Motor
LSM	Linear Synchronous Motor
MAGLEV	Magnetic Levitation
MBB	Messerschmitt-Bolkow-Blohm GmbH
MHD	Magnetohydrodynamics
MIT	Massachusetts Institute of Technology
NRC	National Research Council
NRDC	National Research and Development Corporation
PCU	Power Conditioning Unit
PM	Projektgruppe Magnetschwebbahn
PTACV	Prototype Tracked Air Cushion Vehicle
PWM	Pulse Width Modulated
RANN	Research Applied to the National Need
ROSY	Rotating Synchronous Test Wheel
RTV	Research Test Vehicle
SCR	Silicon Controlled Rectifier
SLIM	Single Sided Linear Induction Motor
SMES	Superconducting Magnetic Energy Storage
SNCF	Societe Nationale des Chemins de Fer
SRC	Science Research Council
SSFP	Semiconductor Switched Flux Pump
TACV	Tracked Air Cushion Vehicle

TARP	Transportation Advanced Research Projects Program
TDA	Transportation Development Agency
TFLIM	Transverse Flux Linear Induction Motor
TGV	Tres Grandes Vitesse
THL	Tracked Hovercraft Ltd.
TLRV	Tracked Levitated Research Vehicle
TMLV	Tracked Magnetically Levitated Vehicle
TSFP	Thermally Switched Flux Pump
TTI	Transportation Technology Inc.
TV	Test Vehicle
UHV	Ultra High Voltage
UMTA	Urban Mass Transit Authority
UTDC	Urban Transportation Development Corporation
VV	Variable Voltage

CHAPTER ONE
INTRODUCTION

1. Introduction

The main concepts of high speed guided ground transportation were established at the beginning of this century. It was not until the decade before 1970, however, that several countries began programmes of work to specifically produce tracked systems that could displace conventional wheel-on-rail trains and rival aircraft in centre to centre trip times. The impetus to these programmes was naturally a combination of factors. It was generally acknowledged that intercity trains would soon reach a practical speed limitation accompanied by deterioration in ride quality and increases in maintenance costs from excessive track and vehicle wear. Indeed, to provide very high speed ground transport without a completely new infrastructure would have been impractical. Air travel had reached the state that major new airports would have to be built remote from population centres because of their environmental impact, and this meant an access penalty would have to be paid in the total trip time. Existing air traffic routes, especially in Europe, were approaching saturation, resulting in scheduling and turn around problems for the air lines.

The solution to these problems appeared to be some new form of exclusive surface-guideway vehicle with non-contacting suspension, guidance and propulsion. Preliminary economic studies indicated that for densely populated areas the land acquisition and civil engineering costs dominated the system capital cost, and that the choice of vehicle support became of secondary importance.

Any new system would have to meet the following criteria:

Cruise speed in range 300-500 km/h

Access to city centres

Low specific energy intensity

Reasonable cost

High degree of safety and reliability

Minimal environmental disturbance

Good ride quality

Initially tracked hovercraft appeared to be the ideal candidate for a new system. While large scale prototype vehicles were being built, two alternative schemes were investigated, namely the electromagnetic system (EMS) and electrodynamic system (EDS) of magnetic levitation (Maglev). Both Maglev schemes indicated much better suspension and guidance power densities, and effectively curtailed the air cushion programmes. Linear machine propulsion was considered essential for Maglev vehicles, with the EMS relying on the more mature linear induction motor (LIM) technology, using essentially conventional machine constructional techniques and advances in power electronics.

The EDS required a machine that could operate with an airgap of 200-300mm, so it was not feasible to use a LIM because of the large levels of inductive power that would need to be supplied. Once practical superconductors were being used in rotating machines, it became apparent that linear as well as rotating superconducting machines could be built, and that the use of iron in the magnetic circuit was no longer essential to provide adequate flux linkage between machine windings. The air cored linear machine (ACLM) configuration chosen by the majority of research groups provided air gap magnetization with a superconducting magnet array, and with an air cored polyphase track winding constituted a linear synchronous machine (LSM). Such a machine could transfer power efficiently across the large airgaps with reasonably small levels of power dissipation in the track winding because the equivalent current sheet average values may vary by as much as three orders of magnitude. The machine could also be designed with high power factors, partly because the track is iron free, but also because there is no significant requirement for air gap magnetization to be derived from the power supply unit.

Although a single superconducting field array is the most common arrangement, the ACLM can have topological variation, as can any motor group. The machine can be double sided, laterally transverse, produce force components other than just thrust, or have a track winding that is locally commutated rather than converter fed. The field coils can be cryogenically cooled and need not be superconducting, in some applications. Time varying currents can be fed to the coils to match a variable reluctance track, or the coils can be sequentially switched to produce an induction effect.

With all the variants, common techniques have had to be evolved to cope with design parameter choice and optimization. The superconducting (or cryogenic) winding in particular must be designed so that the electromagnetically produced stresses can be accommodated, and the field profile at the winding cross section and track level can be accurately computed. The track winding must be physically realizable, and must have its primary parameters calculated. If possible the machine should be represented by an equivalent circuit so that performance can be predicted and its sensitivity to parameter change modelled. Finally the machine's interaction with the system's other subcomponents must be analysed, so that the overall vehicle and guideway operation meets required criteria. This thesis presents the most important aspects of air cored linear machines, as applied to ground transportation. Initially an overview of linear machines and high speed ground transportation is performed, and this is supported by an indexed bibliography as an appendix. The three main types of ACLM are described, and the LSM performance characteristics are detailed.

The philosophy of the linear commutator machine (LCM), which was originally conceived as a short energised section LSM is given, followed by an economic study of full sized systems, including their relationship with long and short stator iron cored propulsion EMS.

The concept behind the linear flux pumping machine (LFPM), which represents a novel class, is described. This machine can be operated in an induction, reluctance or synchronous mode, and could produce significant thrust with unenergised track structure and no power pickup. Because of the operational constraints on the field winding, a cryogenically cooled winding would be the most suitable, although a pulsed superconductor would be the eventual aim. Conventional wheeled transport can also use ACLM to produce enhanced performance in terms of increased speed, reduced capital and maintenance costs. The conceptual design behind such systems is introduced as having realistic potential in providing compact propulsion units for future generation trains.

CHAPTER TWO

LINEAR MACHINE DEVELOPMENT - AN OVERVIEW

2. Linear Machine Development - An Overview

The development of air cored linear machines has been a fairly recent occurrence. Largely it has been closely tied to the development of electrodynamic Maglev systems, which in turn rival or complement electromagnetic Maglev and Tracked Air Cushion Vehicles, depending on one's point of view. A balanced overview of linear machine development must sensibly include descriptions of EMS and TACV progress as they represent contributory factors in ACLM development. This chapter provides an account of the main methods of levitation and the linear machines employed, starting with the earliest known linear machines, followed by TACV, EMS and EDS Maglev, and then subsidiary motor development.

Although this development is referenced, a bibliography is included as Appendix I, which lists the majority of these and additional references. The bibliography is arranged to give the most relevant conference and German Statusseminar proceedings, and then over 400 references are arranged in chronological order. Author and author affiliation indices are included to allow cross reference of common publications.

2.1 Early linear machines

The first recorded linear machine was built by Wheatstone between 1841 and 1845, but it was not until 1889 that the first practical linear machine was proposed. This consisted of a 3000 feet long array of solenoids which sequentially attracted a moving car, and was operated for a few months in 1890 by Dolbear and Williams in America. About the same time Wheeler and Bradley⁽¹⁾ were granted patents for a double sided induction machine which used passive iron "inductors" on the vehicle and an ac dynamo feeding the three phase track winding. Around 1901 Rosenfield and Zelenay^(2,3) suggested a tangential traction system where rail vehicles could be propelled using a linear induction motor with fixed stator blocks in the guideway.

A little later Zehden^(4,5) was granted patents in Europe and America for a double sided linear motor configuration which could be used as a propulsion unit for a steel wheel on rail railway.

A few years on, the Electric Carrier Company^(6,7) and Emile Bachelet⁽⁸⁾ produced two different schemes for transporting mail. The former scheme, which was developed as an alternative to pneumatic despatch tubes, used three phase current collection to supply moving primary windings with variable frequency. A track secondary was fitted into a one foot gauge duorail, within a three feet diameter tube. Both the driving and the trailing cars were six feet long and had capacities of eighteen cubic feet, their weights being 1250 lb and 1000 lb respectively. A demonstration of the system on a 1000 feet loop test track which incorporated a 100 feet inclined section was performed in Paterson, New Jersey on 25 September 1913, when the cars were each loaded with 200 lb of sand and driven at speeds of 25 mph. The driven car could climb the incline at the same speed, when loaded with 1000 lb of sand.

Bachelet's scheme involved the use of iron cored electromagnets to produce eddy currents for levitation in outboard "Wings" attached to a tubular vehicle. Propulsion could be provided by several means, depending on the application; if the vehicle was in a closed tube, suction could be used, but the preferred method had solenoids placed at intervals along the track which were switched in and out by the vehicle motion. Similarly, only the eight electromagnets directly under the vehicle were energised at any one time, the switch being accomplished by another set of brushgear on the vehicle. Several other configurations were tried, including a single aluminium sheet under the vehicle, and also vehicle mounted coils. Bachelet expected the system to be capable of carrying 500 lb loads at speeds of 300 mph, and initially had no intention of producing a passenger carrying version. When showed in Great Britain the system received a great deal of interest, but

also bad technical reaction. The main objections were that air resistance was thought to provide an insuperable problem, and that the track capital costs would be excessive.

In 1936 Kemper began work in Germany on electromagnetic levitation for European passenger transportation, and built several demonstration models⁽¹⁰⁾. In 1953 his system was more clearly defined⁽¹¹⁾ and a three phase propulsion winding was let into slots on the levitation magnet pole face, producing in effect a homopolar linear machine which combined the lift and propulsion functions. The lift magnet produced a transverse bulk flux in the levitation rail, and separate magnets were proposed for guidance. Kemper contemplated a 40 tonne, 20 metre long vehicle running at 250 km/h or 500-1000 km/h in an evacuated tube, requiring about 22MW of power at the top speed. This system formed the basis of further work by Messerschmitt - Bolkow-Blohm GmbH and Krauss-Maffei AG in the late 1960's.

During World War II, Westinghouse built two linear induction motors called Electropulsts for launching heavily loaded planes from short runways in the Pacific atolls⁽¹²⁻¹⁴⁾. The largest track secondary was made up of 76 sections 18.2 feet long (a total length of 1382 feet), by one foot wide. The first 55 accelerating sections had four changes in bar resistance to give a near constant acceleration to the plane. Up to 12MW of power were transferred to the moving shuttle to which the plane was attached, through brushgear carrying 7kA. The last 382 feet of track were used to provide dynamic braking with dc injection. A typical launch of a 10,000 lb plane to a take off speed of 117 mph would be accomplished in 340 feet and 4.2 seconds, the shuttle itself being capable of 225 mph. The US Navy continued to use the Electropulsts for the experimental assisted launch of pilotless and jet propelled planes, after the war.

At the Royal Aircraft Establishment, Farnborough, a 15 metre long linear dc motor was built in 1954⁽¹⁵⁾. The machine was fed by accumulators with a field power of 25 MVA and an armature power of 4MVA. The armature weight was less than 1 kg, and typical speeds were in the order of 500 m/s. Similar

work was performed by NASA to simulate the effect of meteorite impacts on space vehicles, in 1961.

Also in the 1950's Laithwaite at Manchester University began his work on linear induction machines that provided the stimulus for so much of the subsequent world wide research and development effort on linear machines. Two demonstration test tracks were built, one at Manchester, and a later version funded by the British Transport Commission, at British Railways' Gorton Locomotive Works. The Gorton machine used steel wheels on a duorail track about a hundred yards long, and a double sided primary. The primary was guided along the vertical reaction rail by an auxiliary set of wheels, so that expansion joint misalignment of the reaction rail could be accommodated. With a synchronous speed of 34 m/h the top speed was 30 m/h.

The ensuing development of linear machines became dominated by the high speed ground transportation (HSGT) schemes that were proposed mainly by government sponsorship in France, Great Britain, U.S.A., Germany and Japan. The systems of levitation made different configurations of machines necessary, and the economic pressures indicated that long stator machines would not be favoured, and that high speed current collection would be obligatory. The linear machine had now begun to be an important component in completely different types of transport systems.

2.2 Tracked Air Cushion Vehicles

2.2.1 General Considerations

Tracked Air Cushion Vehicle (TACV) research and development lasted for just over a decade, between 1963 and 1976. As the first of the new levitation technologies it attracted high technology companies such as Rohr, Grumman and LTV in the USA, and with liberal administration, large scale testing of prototype vehicles became the apparent immediate aim. More modest programmes in Europe and Japan were established, and after some years of experimentation it was concluded that alternative levitation schemes showed more promise. The track cross section required horizontal and vertical surfaces to provide the necessary support and guidance, and the three main guideway choices were

the inverted 'T' (or top-hat), the rectangular box, and the U (or trough). The smallest feasible air gaps were in the 3-5mm range, and naturally there was a continual need to replace the suspension air.

The systems achieved near revenue operation and various vehicles carried passengers. Speeds of up to 400 km/h were reached with jet propulsion, and although some vehicles were fitted with large linear machines these were not proved at their full output powers within the projects' duration.

Virtually all work had been concluded by 1976. The technical reasons for project cancellation were that the systems were generally noisy and had high energy demands compared to magnetic suspensions (mainly because the air for support and guidance has to be captured and pressurised). Political decisions to abandon projects in mid term were less tractable; in the UK, THL were closed because there was thought to be insufficient market potential for such systems, and in the USA, all high speed projects were the subject of an executive cut in 1975.

2.2.2 American Systems

2.2.2.1 UMTA Projects

In America the Kennedy administration passed two acts which in effect started off high speed ground transport. The first act, the Urban Mass Transportation Act of 1964, resulted in the establishment of the Urban Mass Transportation Administration and allowed government to provide 67% of the cost of urban transportation equipment. The UMTA financed many schemes which aimed to improve local urban services at essentially low transit speeds, being compatible with existing highway trip times. One particular scheme, that of Transportation Technology Inc (TTI), a subsidiary of OTIS Elevator Co received \$1.5m from UMTA to build a demonstration unit for the Transpo 72 exhibition in Washington⁽¹⁶⁾. The vehicle was supported on air cushion pads and was propelled by a single sided linear induction motor, which allowed a much simplified guideway design through switches. Apart from this demonstration, no permanent installation transpired.

Another UMTA project was the Prototype Tracked Air Cushion Vehicle (PTACV), which allowed Rohr Industries and LTV Aerospace Corporation to produce full sized mockup vehicles for exhibition at Transpo '72. The PTACV was meant to be an urban vehicle for airport access and high density corridor applications, carrying 60 passengers at speeds up to 250 km/hr. Rohr had already expanded from its rapid transit origins by acquiring manufacturing rights of the French Aerotrain, in 1970, and subsequently won a further \$1.5m contract to produce an engineering study on a TACV for demonstration at the Pueblo Test Center, Colorado.

In 1972 a further \$5m development contract was secured to allow construction of the vehicle. A project involving an Aerotrain link to Los Angeles Airport failed to materialize.

The Rohr TACV structure was mainly aluminium, with roof and sidewalls patterned after the BART cars, using common tooling⁽¹⁷⁾. The double sided linear induction motor and the power collection equipment were designed and built by Le Moteur Linear (LML), a subsidiary of Merlin Gerin of Grenoble. GEC Traction provided the thyristor control equipment. The motor peak thrust was 45kN and at a top speed of 250 km/h the output power would be about 1.9MW. Vehicle details are given in Table 1. Low speed trials were completed at Rohr's Chula Vista facility in 1974, when it was delivered to Pueblo, the project then coming under the Federal Railroad Administration. Further development and testing were curtailed in 1975.

2.2.2.2 FRA Projects

The High Speed Ground Transportation Act of 1965 directed the Secretary of Commerce "to undertake research and development in high-speed ground transportation". It was felt that in heavily congested travel corridors it was necessary to have a ground alternative to air transport, at surface speeds greater than 300 km/h. Although the North East corridor (Washington-New York-Boston) was the prime route, other links such as San Francisco - Los Angeles were also considered to be the possible congested zones of the near future.

TABLE 1 - TRACKED AIR CUSHION VEHICLES WITH LINEAR MOTOR PROPULSION

Vehicle	Grumman TACV (THLV)	Rohr TACV (PTACV)	THL RTV 31	Krauss-Haefel Transrapid 03	Aerotrain S44	Inst. Aeronautics Palermo, IAP03
Length	15.6	28.6	22.1	11.7	14.3	13.2
Width x height	3.7 x 4.1	3.4 x 3.4	3.7 x 3.8	2.9 x 2.5	2.2 x 3.2	
Weight	26	29.6	23	9.6	12	10
Design/Achieved						
Speed	480	270/232	480/172	140/140	180/180	250/2
Seating Capacity	4	60	0	2	40	
Guideway						
Location	Pueblo HSGTC Trough	Pueblo HSGTC Inverted T	Earlith Box	Munichen-Allach Inverted T	Gomutz Inverted T	Trapain-Milo Trough
Type						
Length Built/Planned	4.8+/35	4.8/8.9	2/5	0.93/0.93	3/3	
Motor						
Type	2DSLIMIntandem*	DSLIM	SLIM	DSLIM	DSLIM	SLIM
Manufacturer	AiResearch	LML	GFC	Merlin&Gerin	Merlin&Gerin	
Weight	2.03		1.95			
Thrust-cont/max	44.4/66.6	22.3/45	2.06/45.6	/29	(140 kW)	
Voltage	C-4.12	0-4.16	0-6.6			
Frequency	0-165	60	50	50		
Current-cont/max	530/700		750			
Cooling	Water	forced air	air			
AirGap	38		30-60			
Reaction Rail						
Material		Al	Al+Fe	Al	Al	
Height x width	0.6 x 6.35	0.84 x 44-17				
Pickup						
Voltage	8.25	4.16	0-6.6			
Frequency	60	60	50			

*Only one DSLIM+PCU built; figures for pair of units +Only 3.5km electrified

The Department of Transportation was formed in 1967 and the Secretary of Commerce HSGGT work was handed over to the Federal Railroad Administration (FRA). In parallel (and relative isolation from) the UMTA TACV work, the FRA funded extensive development and demonstration projects, with the emphasis on TACV and linear induction machines. In 1968 LTV Aerospace teamed up with General Electric to tender for a high speed TACV for the Department of Transportation, but in the event in 1970 the contract went to the Grumman Aerospace Corporation who unveiled their vehicle at Transpo'72 after static levitation tests. The Grumman TACV was originally supplied with three United Aircraft JT 15D-1 turbo fans to give a maximum speed of 200 km/h. Between May and December 1973 the top speed of 147 km/h was reached, limited by 4.8km of track. In the latter half of 1974, the TACV was converted to LIM propulsion, the design and construction being subcontracted to the AiResearch Manufacturing Co division of the Garrett Corporation⁽¹⁸⁾. AiResearch had already built and tested the Linear Induction Motor Research Vehicle (LIMRV) at Pueblo on 10 km of duorail track, so the TACV LIM and power conditioning unit represented a second generation of design, and incorporated extensive water cooling. Relative power to weight ratios were 1.68 (TACV) and 1.0 (LIMRV) MW/tonne. The other advance was that Garrett had developed a three phase power collection system that had been tested to 500 km/h. This was fed with 60Hz 8.25 kV, and on board conditioning produced variable frequency and voltage for the double sided LIM. A synchronous condenser was used to correct the power factor and keep an ac voltage that could line commutate the inverter. The motor consisted of two tandem units each supplying 33kN peak thrust, 22 kN continuous running to 165 Hz at 480 km/h and 4.12 kV l-n. Table I gives details of the vehicle, guideway and motor.

Static testing of the LIM and PCU was carried out at Torrance between May and October in 1973. By late 1974 the LIM and PCU were installed in the vehicle and initial tests to 100 km/h began on 500m of electrified section. By this time DOT had two large TACV at Pueblo, and renamed the Grumman TACV Tracked

Levitated Research Vehicle (TLRV) on the assumption that it would be used later as a maglev test vehicle. Track testing continued from December 1975 to July 1976 on the 3.5 km electrified section⁽²⁰⁾.

In 1974 the Transportation Advanced Research Projects (TARP) program was organized within DOT, and in 1975 FRA were forced to turn their attention to more pressing near term railroad problems. The TARP program⁽²¹⁾ assumed responsibility for all continued non contact suspension and propulsion technology R and D and began a worldwide reassessment of the work. It was decided to concentrate on technologies that were not receiving attention elsewhere, and to keep abreast of other schemes through interaction with foreign projects.

2.2.3 Tracked Hovercraft Ltd

UK experience of linear motor propelled aircushion vehicles centred on Tracked Hovercraft Ltd (THL)⁽²²⁾. THL was formed as a subsidiary of NRDC in September 1967 to explore the possibilities of air cushion suspension and LIM propulsion for HSGGT. From the start the program attempted to foresee the problems that would arise with a Revenue Vehicle, and incorporate possible solutions in the test vehicles and rigs. Fairly early on a commitment was made to an all electric vehicle since this was thought to be less intrusive on the environment, and a rectangular box section track was chosen as being the simplest guideway element that could provide adequate lateral and vertical stiffness, and be self clearing of debris.

The motor choice in 1969 was for a single sided axial flux linear induction motor, rather than a double or sesquisided version. Work at Imperial College suggested that a transverse flux machine might be possible eventually, after some initial tests, and this showed advantage in that a larger pole pitch lighter core weight configuration would be possible. Two test vehicles were planned that could run on a elevated box track which would accommodate different designs of reaction rail. RTV22 would run at 240 km/h on pneumatic tyres and test the motor and current collection equipment; RTV31 would have air cushion support and guidance and reach 480 km/h. As work proceeded,

RTV31 was built first and made its first run in December 1971, and finally reached a top speed of 171 km/h on only 1.9 km of track, in January 1973. RTV22 was held back as a possible test vehicle for a large scale transverse flux LIM. A 1/5 scale model was constructed by Linear Motors Ltd and tested on a 90m track and model test vehicle RTV41, but the full sized motor was never built.

Towards 1973 THL attempted to evaluate alternative suspension systems, such as EMS, EDS, and Laithwaite and Eastham's Magnetic River Transverse Flux LIM. NRDC spun out one year's funding over two years, and in February 1973 the project was closed completely, before the remaining track sections were erected and RTV31 could reach its design speed.

2.2.4 The Aérotrain

Jean Bertin was responsible for the most organised and technically successful TACV program. Air cushion vehicle studies began at Société Bertin in 1957, and a systematic development of the Aérotrain was undertaken from 1961. After patents were taken out in Britain and France in 1962, Bertin formed Société de l'Aérotrain in 1965 to specifically develop and promote air cushion vehicles. The first two vehicles were half scale models to allow comparisons to be made to calculations before proceeding to full size vehicles.

Aérotrain experimental 01 started tests in December 1965 and reached its design speed of 200 km/hr on its fifth run. In the next two years it reached up to 345 km/h with an improved suspension and additional boosters.

Aérotrain expérimental 02 was designed in 1967 and 1968 to establish air cushion behaviour at high speed, especially at the supercritical speeds when the ram air pressure exceeds cushion pressure. In 1968, it reached 390 km/h with a 12 kN thrust PWA JT12 turbojet, and in January 1969 reached 422 km/h with an additional 5 kN thrust from a solid propellant rocket. Both of the test vehicles ran on an inverted T track 6.7km long at Gometz la Ville near Paris.

The Paris Air Show in July 1969 saw the first public display of the Aerotrain I-80 "Orléans", an 80 passenger full size prototype vehicle initially driven by ducted propeller. The test track was laid along the line of a prospective route from Paris to Orleans, and was an 18 km long elevated inverted T structure. Between 1969 and 1971 the vehicle regularly reached 260 km/h, and by 1972 had logged 710 hours of operation and carried 10,000 passengers. After fitting with a Pratt and Whitney PWA JT8D turbofan, the Orléans reached 430 km/h in 1973. An extensive program of trials was concluded in 1975.

A fourth vehicle, S-44, was built and tested from 1969 at Gometz on a new 3km track built alongside that used for 01 and 02. This was also a full sized vehicle, designed for suburban rather than intercity use. It held 40 passengers and in 1973 exceeded 170 km/h. The double sided 400 kW LIM was built by Merlin and Gerin.

Results from the full sized test vehicles prompted the French Government to authorise a 24 km demonstration LIM propelled system that would link the new town of Cergy-Pontoise and the office complex at La Défense in suburban Paris. The proposed vehicle would have been a bidirectional twin unit train travelling at 180 km/h and could also have had intermediate sections for increased traffic density. The scheme lost Government support in 1974⁽²⁴⁾.

A final vehicle, the Tridim Aérotrain was designed to suit urban traffic where station spacing was between a few kilometres and several hundred metres. Propulsion could be either LIM, friction drive or rack and pinion. Anticipated cruise speeds ranged from 40-80 km/h, and the system used a relatively simple track structure. The ability to tolerate sharp bends and steep slopes was the source of the name Tridim, for three dimensions^(24,25). Vehicle capacity could vary between 4 to 100 depending on the traffic requirements. A four/six seat prototype was run on a 300 metre test track in mid 1973, which incorporated a 20m radius bend, 10m curve switch and 20% slope, and demonstrated the cheap steel pipe structure used for track support.

Société Bertin continued work on dynamic noise measurement of jet engines at Gometz, where a GEJ85 turbojet replaced the PWA JT12 on the Aérotrain 02, and in conjunction with SNECMA* this noise research program continued between 1974 and 1976⁽²⁶⁾. Further part funding of Guimbal's LIM work at Merlin and Gerin in Grenoble continued, but no significant developments matured within the Aérotrain program.

2.2.5 Other TACV

Germany, Italy, Japan and USSR all had experimental TACV running. Krauss Maffei A.G. built a 930m inverted T dual purpose test track to permit comparison trials between magnetic levitation and air cushion vehicles. The EMS vehicle, Transrapid 02 had its first public demonstration in October 1971, and in the autumn of 1972 Transrapid 03, the ACV began comparison tests. The double sided LIM was built by Merlin & Gerin and had a maximum thrust of 29 kN. The ACV tests were successful, but the comparisons indicated that EMS had clear advantages. Further work was halted in the beginning of 1974 in mutual agreement with the Federal Ministry of Research and Technology (BMFT), who provided the funding. Table I shows outline details of the vehicle and track.

Italian work was based at the Institute of Aeronautics at the University of Palermo. They built two experimental TACV in the course of their research program, which began in 1967. Both vehicles only ran at low speeds, the first, IAP 2 was fitted with a propeller, and the second, IAP3, a single sided LIM, to allow better switching. Trial runs of IAP3 were held on a trough track at Trapain-Milo Airport in Sicily in 1972. The Institute then concentrated on magnetic levitation and linear motor propulsion.

Japanese National Railways began looking at new types of HSGGT systems as early as 1962. Initially they were concerned with LIM propulsion systems, but also considered TACV⁽²⁷⁾. The effort was superceded by their commitment to EDS.

*Société Nationale d'Etude et de Construction de Moteurs d'Aviation, Paris

Russia apparently had two separate projects on ACV; one run at the Institute of Internal Combustion Locomotive Engineering near Moscow developed a diesel engined TACV, and at Kiev, a LIM propelled vehicle was built and tested.

2.3 The Electromagnetic System of Levitation

2.3.1 General Development

The concept of providing contactless levitation by controlling the current in a dc magnet attracted to a steel guideway to maintain a constant gap, was first proposed by Kemper in Germany. EMS Maglev was subsequently researched and developed in Germany and Japan, and to a lesser extent in the UK and USA. The major division in effort was whether EMS was to be applied to high speed intercity or low speed urban transport. Germany and Japan largely chose high speed applications, whereas the UK and the USA chose urban vehicles as most suited to their particular requirements.

In America, early analysis of transport modes that might be applied to the Northeast Corridor suggested that High Speed Ground Transport (HSGT) alternatives only showed advantages (in operating costs) over air travel when the range was up to about 650 kilometres, and no allowance was made for the cost of passenger time⁽²⁸⁾. If a premium was put on passenger time, this dropped to around the 300 km level⁽²⁹⁾. No attempt had been made to account for the large capital costs required to implement a HSGT scheme, and so development had no particular aim following Federal withdrawal in 1975.

European population densities and existing use of transport modes differ significantly from the USA patterns. In Western Europe roughly 50% of the distances between major cities are below 300km^(30,31). Also any increase in traffic densities in air or road transport incur environmental penalties. The modal split has been such that over the last two decades railways have had their market share progressively decreased. In an attempt to redress the balance and evolve an acceptable transportation system preliminary studies indicated that HSGT could in fact be a viable alternative in a European context⁽³²⁾. The German Government through BMFT began a

broad spectrum development program which investigated the three main methods (TACV, EMS and EDS) of HSGT, with the objective of identifying the most suitable system.

Krauss Maffei and Messerschmitt-Bolkow-Blohm both began work on EMS test vehicles and together with the EDS researchers produced designs for an "Anwendungsnahe Versuchsfahrzeug" (AVF), or prototype experimental vehicle that could carry 200-400 passengers at speeds of 400-500 km/h⁽³³⁻³⁵⁾.

It was planned that these vehicles would be built and tested at a major test facility in Donaueschingen, but as the development continued, it was decided to opt for one system. After an exhaustive comparison of the rival designs,^(36,37) it was decided on 8 December 1977 to develop only the EMS Maglev, and to construct a test facility at Emsland in North Germany for testing to 400 km/h. The EDS study was successfully completed, and work on the superconducting LSM continued with track tests at Erlangen.

The Japanese EMS research began as an in-house development at Japan Air Lines, who were investigating ways of reducing city centre to airport access times. Starting from essentially a Krauss-Maffei configuration, two test vehicles were built, and design of a pre-production prototype has begun. This project, together with a low speed EMS program and Japanese National Railways EDS research have been combined under the charge of the Ministry of Transport who will directly fund future developments⁽³⁸⁾.

American effort in the low speed EMS was limited to work performed at Ford, MIT and Mitre on dynamic test rigs, and a vehicle built by General Motors at Detroit. Under the Transportation Advanced Research Projects (TARP) program an American and German Cooperative Project investigated the vehicle and guideway dynamics to establish limits for roughness and flexibility⁽²¹⁾.

The KOMET test vehicle was used to provide data over its guideway which could have its flexibility changed by removal of supporting piers.

The UK development began with research undertaken by Jayawant at Sussex University, and this was followed by an independent study performed by

broad spectrum development program which investigated the three main methods (TACV, EMS and EDS) of HSGT, with the objective of identifying the most suitable system.

Krauss Maffei and Messerschmitt-Bolkow-Blohm both began work on EMS test vehicles and together with the EDS researchers produced designs for an "Anwendungsnahe Versuchsfahrzeug" (AVF), or prototype experimental vehicle that could carry 200-400 passengers at speeds of 400-500 km/h⁽³³⁻³⁵⁾.

It was planned that these vehicles would be built and tested at a major test facility in Donauried, but as the development continued, it was decided to opt for one system. After an exhaustive comparison of the rival designs,^(36,37) it was decided on 8 December 1977 to develop only the EMS Maglev, and to construct a test facility at Emsland in North Germany for testing to 400 km/h. The EDS study was successfully completed, and work on the superconducting LSM continued with track tests at Erlangen.

The Japanese EMS research began as an in-house development at Japan Air Lines, who were investigating ways of reducing city centre to airport access times. Starting from essentially a Krauss-Maffei configuration, two test vehicles were built, and design of a pre-production prototype has begun. This project, together with a low speed EMS program and Japanese National Railways EDS research have been combined under the charge of the Ministry of Transport who will directly fund future developments⁽³⁸⁾.

American effort in the low speed EMS was limited to work performed at Ford, MIT and Mitre on dynamic test rigs, and a vehicle built by General Motors at Detroit. Under the Transportation Advanced Research Projects (TARP) program an American and German Cooperative Project investigated the vehicle and guideway dynamics to establish limits for roughness and flexibility⁽²¹⁾.

The KOMET test vehicle was used to provide data over its guideway which could have its flexibility changed by removal of supporting piers.

The UK development began with research undertaken by Jayawant at Sussex University, and this was followed by an independent study performed by

British Rail who were indirectly Government funded. Both groups built operational development vehicles that could carry passengers for demonstration.

EMS Maglev has been the prime application of linear induction motor research. Although JAL still plan to use LIM propulsion for 300 km/h, the German effort has switched to an iron cored linear synchronous motor with a track stator. The ICLSM can also provide substantial lift and guidance forces, and was chosen for both the Hamburg and Emsland vehicle designs. A final choice on whether all of the three main functions of levitation, guidance and propulsion are to be economically achieved with the ICLSM has yet to be made.

2.3.2 German Systems

2.3.2.1 German Development

As previously mentioned, Kemper began work on EMS Maglev in the mid 1930's in Germany. It was not until the second half of the 1960's that Krauss-Maffei and Messerschmitt-Bolkow-Blohm (MBB) began detailed systems appraisal and decided to develop a Maglev based high speed ground transportation system. Both companies built test rigs for levitation and linear machine experiments, and began building linear test tracks with medium sized vehicles. In 1969 the German Federal Minister of Transport commissioned a wide ranging study of the economic and operational management aspects of high speed transport from the Hochleistungsschnellbahn-Studiengesellschaft mbH (made up of German Federal Railways, STRABAG and MBB)⁽³⁹⁾. The "HSB Study" conclusions were that such new systems as Maglev could operate economically, and this prompted the Federal Government and Industry to increase the development effort. The Federal Ministry of Research and Technology (BMFT) provided the majority of funding for the test vehicles' program, and in the same year Krauss Maffei presented the first electromagnetically levitated functional model with linear propulsion, Transrapid 01 which weighed about 3 tonnes and ran on a 40m track at 36 km/h. MBB followed by producing the

first passenger carrying vehicle, the Magnetmobil in 1971. Various other vehicles followed from both companies (see next section) and in 1974 Krauss-Maffei and MBB combined their Maglev research and development activities into the one company of Transrapid-EMS. Other firms such as Rheinstahl (Thyssen Henschel), Krupp, as well as TU Braunschweig were actively connected to the company.

As research and design studies continued for large vehicles with maximum speeds of 500 km/h, it became apparent that the use of the single sided axial flux LIM posed special problems. The motors needed to be about 6 metres long to counteract end effects, and would run at air gaps of about 20mm. Because of the low power factor-efficiency product the on board power converter was large even though a heat pipe cooler was developed. The volume constraint was such that at 400 km/h there was virtually no space for a pay load. The thrust power also had to be transmitted to the vehicle, and this proved to be problematic; copper plated aluminium rails with current pickup had unsatisfactory brush wear, and current arc transmission suffered from excessive arc voltage drop and electromagnetic radiation interference. Weh at TU Braunschweig investigated the iron cored linear synchronous motor with a long stator in about 1973, and in the next year the Rheinstahl Company built a 100m track and vehicle which combined long stator LSM propulsion and lift functions. Weh also built a difference flux version of the integrated lift and propulsion LSM on 30m of track at Braunschweig.

Following on the development of Transrapid 02 and 03, and a Magnet Test Vehicle at Ottobrunn propelled by a hot water rocket, Krauss Maffei as part of Transrapid-EMS constructed Transrapid 04 at Munchen Allach. The vehicle was propelled by a double sided horizontally mounted LIM along a 2.4km elevated guideway. MBB built another hot water rocket propelled component test vehicle KOMET on a 1.3km track at Manching^(40,41). The Lineare Hochgeschwindigkeitsprufstand (LHP) was meant to test components of EMS and LIM up to 400 km/h. As well as having a rigid body frame to which the

magnets for support and guidance were fixed, the centralized on board computer system allowed control system configuration and control parameter change by modification of software. Vehicle test data could be PCM coded and telemetered to a ground station, and an instrumented test rail was included in the track.

The second version of KOMET included a decentralized hierarchical control system for the magnets. KOMET-M embodied two magnet bogies connected through a secondary suspension to the cabin, and to the six independently controlled support magnets through the primary suspension^(42,43). This system was known as the Magnetic Wheel since the modular mechanical and electrical structure closely mimicked wheeled independent suspension. Its advantages were that a more consistent force profile for in line magnet systems was possible, track tolerance could be relaxed, and the levitation height could be reduced (resulting in lower power requirement in the magnets).

In 1977, the HSB Studiengesellschaft cooperated with the Federal Railway to compare track investment costs of a Maglev system and a conventional new railway track⁽⁴⁴⁾. Since the Maglev system did not rely on wheel friction for traction and braking, steeper gradients were possible, and since guidance forces could be controlled, tighter radii also became possible. Route tracing virtually at-grade construction, or on elevated track as opposed to the traditional tunnel-cutting-viaduct working meant that the Maglev system compared most favourably with steel wheel or steel rail infrastructure cost.

At the end of 1977, the BMFT decided to concentrate entirely on EMS Maglev, and the EDS group members (BBC, Siemens and AEG) combined with Transrapid-EMS to form Konsortium Magnetbahn Transrapid. Siemens continued work on the air cored LSM and converted their Erlangen test track from LIM to LSM propulsion, and the track tests began in 1979. The Konsortium built the demonstration vehicle Transrapid 05, the "IVA-Bahn Hamburg" for the International Traffic and Transportation Fair in Hamburg in June 1979^(45,46). The vehicle

used Magnetic Wheels and Weh's iron cored long stator LSM as a propulsion and lift unit, and was in public operation for 12-14 hours daily from March to July 1979 with only one minor breakdown.

Large scale testing of pre-production vehicles has always been an aim of the BMFT. Initially a full size system comparison was to be made between steel wheel on steel rail, EMS and EDS vehicles at a Test Center in the Donaured Area of Bavaria. A large complex with 75km of track and 500 km/h test vehicles met local environmental opposition, and the BMFT finally chose a site in northern Germany at Emsland^(47,48). By this time work on EDS was concluded, and although initial plans were to provide an adaptable track and vehicle to accept LIM, Air Cored LSM as well iron cored LSM, the eventual choice was for the integrated EMS and iron cored LSM long stator propulsion. The definition phase began on 1 July 1978, and later in that year construction began. It is expected that the active test program should begin in 1982.

Work on urban vehicles has been overshadowed by the high speed program. Krauss Maffei produced a system known as Transurban-TAKT in the early 1970's^(16,49). This system which used EMS levitation and single sided LIM propulsion was chosen by Toronto to be their new urban transportation mode. Difficulties were encountered with excessive vehicle weight, unexpected interaction of the LIM and EMS forces and switch transitions on the guideway. The German Government also withdrew support from Krauss Maffei as it was thought at the time that there was insufficient need for new urban systems, and Krauss Maffei withdrew from the contract and paid a penalty fee.

Siemens have produced a wheeled system propelled by synchronous linear motor called H-Bahn. A demonstration elevated track vehicle exists at Erlangen. Weh also has a demonstration vehicle and track at TU Braunschweig called Magnetbahngesellschaft (M-Bahn) which uses ICLSM long stator drive with excitation assisted with permanent magnets⁽⁵⁰⁾.

Residual forces in levitation are taken up by small diameter plastic wheels. AEG are involved in the commercial application of Magnetbahn. Weh continued to refine the combined levitation and propulsion system and produced design variations using permanent magnets to provide the bulk of the static forces^(51,54). The immediate advantage of this technique is that the control power is reduced. Transverse flux guidance controlled permanent magnets with very small power loss in a mild steel strip rail have also been considered.

2.3.2.2 German Test Vehicles

MBB were the first to present a passenger carrying vehicle, on 7 May 1971, when their Magnetmobil carried eight people on a 660m test track at Manching⁽⁵⁵⁾. The vehicle was supported by eight levitation magnets and four guidance magnets, driven by three phase SCR controllers. The propulsion was by a vertical aluminium reaction rail and double sided LIM, which produced about 200 kW of power and a top speed of 90km/h. The Magnetmobil tested rigid body control strategies and general feasibility of EMS levitated vehicles. Details of this and subsequent vehicles are given in Table II.

Krauss-Maffei's first passenger carrying vehicle was displayed on 11 October 1971 at a 930m test track built near München Allach. It used 16 U shaped magnets which provided both levitation and guidance against a U shaped rail, the magnets being laterally offset to give guidance. The vehicle weighed nearly 12 tonnes and the track incorporated an 800 metre radius curve. Propulsion was with a double sided vertical rail LIM built by AEG which ran at fixed supply voltage and frequency. The Transrapid 02 track also accommodated the air cushion vehicle Transrapid 03, and as discussed in 2.2.5 comparison trials were completed. TRO2 could be controlled remotely, and its top speed of 164 km/h was first reached in early 1972.

TABLE II GERMAN EMS VEHICLES WITH LINEAR MOTOR PROPULSION

Vehicle	MAGNETHOBIL	TRANSRAPID 02	TRANSRAPID 04	TRANSURBAN TAKT	KOMET	HMB2	LSV 301/2	TRO5	TRO6
		TRO2	TRO4	TU02	LHP				
Length	7.6	11.7	15	6	8.5	5		26	54
Width & Height	2.1 x 1.8	2.9 x 2.9	3.4 x 2.8	2 x 2	2.5 x 1.7				3.8 x 3.7
Weight	5.8	11.3 + 2	18.5		8.8+	2.5		36	102 + 20
Maximum speed	90	164	253.2	70	360*	36	2.2	75	400
Seating capacity	8	9	20	12	-	-	-	68	200
Guideway									
Location	Ottobrunn	München Allach	München Allach		Manching	Kassel	TU Braunschweig	Hamburg	Emsland
Length	0.66	0.930	2.4		1.3	0.1	0.03	0.908	31.5
Motor									
Type	DSLIM	DSLIM	Horizontal DSLIM	SLIM	LIM*	Iron cored LSM+lift	Difference flux ICLSM+Lift	ICLSM+ Lift	ICLSM+ Lift
Manufacturer	MBB	AEG	(1) (2) AEG						
Type No		LAM d 14950	LAD,12, 220/5						
Weight	0.8	1.26	3.36	0.65	0.42			28	85
Thrust	10	31	40	13	2.25			1.17	4.15
Voltage	0.38	2.6	3.5	v.v	0-1.1		380	0-200	0-215
Frequency	50	50	50	v.f	0-160		0-100	580kW	7,000
Power	200kW	5,000	6,200				100		
No of Poles		5	6	9	5				
Pole Pitch		0.52	0.61		0.384		0.3		
Length	2	2.84	3.66	2.65	1.8				
AirGap	32	47					15		
Synchronous Speed		186	440						

*Linear Motor Test Unit top speed 360km/h;

Main propulsion unit Rocket Sled DANIEL

Max speed with sled 401.3 km/h

MBB built several hot water rocket propelled test vehicles. The first vehicle at Ottobrunn was operational by 1972 and ran up to 225 km/h over instrumented test rails in the 660m Magnetmobil track. Different magnets and sensors could be incorporated into the basic test frame. MBB then built a new facility and used a hot water rocket sled "DANIEL" which was automatically disengaged from the component test vehicle "KOMET" after travelling 300 metres. KOMET then passed through 300 metres of highly accurate track and then was automatically braked in the final 700 metres. With accelerations of up to 4 gee's available, the top speed of 401.3 km/h was recorded on 19 February 1976, two years after the system was built⁽⁴⁰⁾. The main frame carried 10 levitation and 8 guidance magnets and had available 2.5 tonnes payload for a test object support frame. A 5 pole linear motor test unit was run at speeds up to 360 km/h. In 1977 KOMET was rebuilt to accommodate a modular system of magnets with decentralized control and independent primary suspension.

Krauss Maffei began building Transrapid 04 in 1973. The guideway was elevated and various constructional techniques tried out. The full length of 2.4km included 800 metre and 3.1 km curves with a straight central section over which top speeds of 250 km/h were reached. The vehicle was 15 metres long and weighed 18.5 tonnes. It had 20 seats and guidance and levitation was accomplished with 23 magnets. The propulsion was with a horizontally mounted double sided LIM, and two motors were tried out. The AEG machine was Gramme ring wound and incorporated substantial damping cages around the back iron to screen out the leakage fields. Maximum thrust was 70 kN from the 6 metre long motor, which had a design synchronous speed of 440 km/h.

HMB2 was built largely by Thyssen-Henschel at Kassel, in 1974, and became operational in early 1975. The final vehicle weighed 2.5 tonnes and accelerated up to 36 km/h in the first 60 metres of a 100 metre track. Thyssen examined the economics and production techniques required to

fabricate the long stator packets, and how to automate the winding process⁽⁵⁶⁾. The combined lift and propulsion iron cored LSM stator was made in two parallel runs at the track gauge.

HMB2 had resulted directly from Weh's work at Braunschweig⁽⁵⁷⁻⁵⁹⁾. His first experimental model was a 42kg vehicle running on a 10 metre track. A much larger experimental model LSV 301 was built with a full sized guideway and a double air gap stator system with one air gap inclined (the difference-flux system). This gave combined lift, propulsion and guidance in one system. The 2.2 tonne vehicle reached a top speed of 25 km/h on the 30 metre indoor track. The vehicle was operational in November 1975 and was later given an individual spring and damper suspension for each of the four corner magnet sets. The renamed LSV02 used linear bearings in the suspension to avoid tilting the pole faces, and also spring and dashpot suspension were included for lateral motions.

The combined lift and propulsion iron cored long stator LSM became the eventual choice for the TR05 vehicle at Hamburg. The track was 908 metres long and a top speed limit of 75 km/h was legally required. The machine gave a thrust of 28kN (570 kW at 73 km/h) and was fed by a 0-200 Hz inverter. This system will also be used for the Emsland vehicle TR06 where 85kN thrust will propel the 122 tonne vehicle to over 400 km/hr. On board power requirement for the magnets will be provided by a linear generator, which picks up the stator slot harmonics in two phase pole face windings and is rectified to top up a battery conditioning unit above about 30 km/h. Batteries provide all the on board power below this speed.

Krauss Maffei's Transurban-TAKT system was propelled by a 650 kg single sided 9 pole LIM which had an iron backed aluminium reaction rail⁽⁶⁰⁾. A variable voltage, variable frequency inverter was used for the motor supply and the vehicle had a top speed of 70 km/h. Testing began in 1973, and a 8km track was planned for Toronto. Ironically, TAKT was meant to signify the rhythmical operation of the system running at 30-40 second headways.

2.3.3 Japanese Systems

2.3.3.1 Japanese Development

As with German development both high speed intercity and low speed urban transport systems have been examined. Japan Air Lines (JAL) have been the principal organization concerned with a High Speed Surface Transport (HSST) scheme, and have been largely funded both directly and indirectly by the Japanese Government. A low speed system was funded directly by the Ministry of Transport and coordinated University and Industry research⁽⁶¹⁾.

JAL formed a special unit to plan and research the development of HSST as early as 1971⁽⁶²⁻⁶⁴⁾. The main reason behind the project was growing awareness of the increasing times required to reach out of town airports from the centres of population, in an environmentally unobtrusive fashion. There were two major town-to-airport links that JAL had in mind. The first was the New Tokyo International Airport at Narita, some 66 kilometres away from central Tokyo, and 80km away from the domestic Airport at Haneda. The second was between Chitose Airport and the city of Sapporo, on Hokkaido. Because of the high traffic density on the Narita-Tokyo Expressway, the travel time may be two hours to and three hours from the airport. Chitose does not have a high traffic density problem but the roads are inadequate and the 40 kilometres may take over an hour. The intercity trip might take therefore, allowing up to an hour from Tokyo to Haneda, perhaps five hours, with only one hour 40 minutes in the air. The rail trip by the new Japanese National Railways (JNR) Shinkansen extension is only six and a half hours, so air flight has only minimal competitive advantage.

During 1973 JAL evaluated the various schemes being developed worldwide, and initially expected to only have to license a particular system. It was decided, however, to pursue an in house development using the aerospace technology and expertise available within JAL. In the next year an experimental vehicle was designed by the JAL Engineering Centre at Haneda Airport, and on 22 December 1975 the two seat test vehicle HSST-01 was first tested on a 200 metre track at Sugita, near Yokohama. The levitation configuration chosen was the offset pair

of inverted U shaped magnets reacting on a U rail developed by Krauss-Maffei.

The propulsion unit was a single sided LIM with a thrust of 3.4kN. Maximum speed was limited by the track length to about 35 km/h, and it was decided to build a longer 1.3km track.

In 1976 the new track was constructed on reclaimed land at Higashi Ogijama, a man made island in the Kawasaki area of Tokyo Bay. The site was subject to subsidence and allowance was made for adjustment to the longitudinal beams; maximum sinkage was about half a metre in the first year. In 1977 HSST 01 began running on the new track and reached a top speed of 219.3km/h with the LIM propulsion. Addition of rockets to boost the acceleration when the vehicle reached 150 km/h under the LIM meant that over 300 km/h could be reached in the 1300 metres. The top speed of 307.8 km/h was reached on 14 February 1978.

A second vehicle HSST-02 was built and tested in January 1978 for the first time. It used the same track as HSST-01, and could carry up to eight passengers and one driver, at speeds to 100 km/h. Several thousand members of the public have been given demonstration rides.

Towards the end of 1978 and into 1979 the test track was reconstructed past the 900 metre mark to include two curved and banked sections. The curve radii were 2 kilometres and 280 metres, and the total track length became 1.6 kilometres. In March 1979 both vehicles were successfully tried out on the extended track.

HSST-01 and -02 had run 850 and 1500 km by May, respectively. LIM only propulsion on HSST-01 produced a top speed of 236.8 km/h in April 1979.

Substantial Government funding allowed JAL to proceed with the design of an 80 seat prototype of an operational vehicle, HSST-03, which has the same cross section as the production vehicle, but is double headed and shorter. This will be tested at 300 km/h on a 15km test track. So far a full size mockup has been built⁽⁶⁵⁾, and a further 20 billion yen is required to complete the development into engineered hardware.

Although the application of HSST by JAL was originally for airport to city centre links, the intercity link is beginning to feature in their philosophy as a replacement for conventional railway systems.

In 1974 the Ministry of Transport began a special project to develop a low environmental pollution railway and concluded after some study, that the EMS of supporting a vehicle showed most promise. The main purposes were to produce a system with minimal noise and vibration, and negligible air pollution. Having set up some baseline design characteristics such as 120 km/h speed for a 10 car train with minimal headways of 2 to 3 minutes, a running test facility was constructed. The EML-50 vehicle and track tests were carried out in 1975 and 1976, using a strip of land already acquired as an extension route for an existing railway. The system was dismantled in 1977 to allow the extension railway to be built and a new track was planned at a different location.

2.3.3.2 Japanese Vehicles

The first JAL vehicle HSST-01 was constructed in a light alloy semi-monocoque shell with a streamlined outer skin. Wind tunnel testing was carried out to determine the pitch instability since the centroid and centre of gravity were close together. Pitch and yaw damping were achieved by fitting a pair of tail fin stabilizers to the rear part of the body shell.

Initially the vehicle was controlled on board by one of the two passengers. When moved to Kawasaki a remote control system was installed, which operated the LIM at a predetermined slip to give near zero normal force⁽⁶⁶⁾. The variable voltage variable frequency supply is fed to the vehicle through brushgear, and is derived from a 200 kVA alternator, driven by two 150 hp automotive engines.

HSST-02 has a similar semi-monocoque light alloy shell, but mainly differs in that all the vehicle magnets are mounted on a primary suspended flexible chassis. The passenger compartment is linked to the chassis through a

secondary suspension. The main advantages are that either the track tolerances can be relaxed, or the magnet power can be reduced. Follow up of track irregularities is also masked from the passenger ride. Gap sensing is accomplished mainly by inductive transducers, although HSST-02 uses accelerometers for lateral control. The track steel work is standard JIS channel section, and the magnets have extended pole faces to minimize the excessive leakage flux. The levitation rails are fixed to regularly spaced sleepers bolted to longitudinal beams. For the first 1000 metres these beams are reinforced concrete, and the remainder of the track uses steel section. Screw jacks can realign the longitudinal beams as the track settles.

The single-sided LIMs for both vehicles were similar in construction and performance, and reacted against a composite secondary consisting of a 9mm iron plate faced with either 5, 3 or 2mm aluminium. The 5mm ran for the first 200 metres of track, the 3mm for the next 320 metres, and the 2mm for the remainder.

Both magnets have similar ampere turns, but differ in length and area⁽⁶⁷⁾. The HSST-01 magnets are 0.6 metre long and weight 30kg, those of HSST-02 are 1 metre long and weight 47kg. HSST-01 relies totally for levitation power from an on board battery, whereas HSST-02 rectifies the picked up power to supply the magnets, in addition to back up batteries. Other vehicle details are given in Table III.

The Ministry of Transport sponsored research vehicle EML-50 weighed 1.8 tonne and was supported and guided by 8 separate U magnets with pole face windings reacting against L shaped rails⁽⁶⁸⁾. The power supply for the single sided LIM was fed to the vehicle through brushgear, and LIM speed control was by pole changing. The track length was 165.5 metres, with a 160m 5 rail power collection system, two rails for the magnet power and three rails supplying the 420 volt 50Hz power to the motor. A top speed of 40 km/h was possible on the existing track. The aluminium

TABLE III - JAPANESE EMS VEHICLES WITH LINEAR MOTOR PROPULSION

		<u>HSSTOI</u>	<u>HSSTOI</u>	<u>HSSTOI</u>	<u>HSSTO2</u>	<u>EML50</u>
<u>Vehicle</u>						
Length	m		4.2		6.84	2.8
Width x Height	m		2.6 x 1.1		2 x 1.75	1.7 x 2.1
Weight	tonne		1		1.8 + .6	1.8
Maximum Speed	km/h	35		307.8*	100	40
Seating Capacity			2		1+(6-8)	
<u>Guideway</u>						
Location		Sugita		Ogishima Kawasaki		Tukimino Kanagawaken
Length	m	200		1600		165.5
<u>Motor</u>						
Type			SLIM		SLIM	SLIM
Thrust	kN		3.4		3	
Voltage	V		0-600		0-600	420
Frequency	Hz		0.350		0-120	50
Power	kVA		200		200	
No of Poles			14			
Pole Pitch	m		0.144			
Length	m		2.141			
Airgap	mm		13		12	15
<u>Reaction Rail</u>						
Material			Al+Fe		Al+Fe	Al+Fe
Thickness	mm		5,3,2 Al 9 Fe			

*Rocket assisted acceleration on 1300m track
219.3 km/h LIM only

reaction rail was backed by unlaminated iron plate. Further studies into sensitivity of ride to track irregularities at 120 km/h and 15mm gap were planned, but were absorbed into JAL work in 1978.

2.3.4 Other Systems

2.3.4.1 UK Development

In the UK two groups produced working experimental EMS vehicles propelled by LIM. Jayawant at the University of Sussex constructed a 1 tonne vehicle with funding from the Wolfson Foundation⁽⁶⁹⁾, and continued research with Science Research Council grants. The vehicle was designed to operate on 30 metres of track and carry up to four passengers.

British Railways Board Research and Development Division were invited by the Department of the Environment to undertake a program of exploratory research into magnetic suspension and guidance of vehicles, following the withdrawal of support for Tracked Hovercraft Ltd. In doing so they constructed a 110 metre track at Derby on which a 3.5 tonne vehicle carrying up to 12 passengers ran⁽⁷⁰⁾. Continuing this research, The Transport and Road Research Laboratory supported BR to produce a project definition study of magnetically suspended Minitram type vehicles⁽⁷¹⁾, as part of a larger program on Automated Urban Transport. BR's conclusion was that a second generation design of magnetically suspended vehicle could be significantly cheaper than a wheeled system in both capital and operating costs, despite the low power factor-efficiency product of the LIM. TRRL's published view resulting from the total program was that there was at that time no case for preferring a magnetically suspended vehicle instead of an equivalent wheeled system.

More recently, the West Midlands County Council have been successful in persuading the Government to part fund an EMS Maglev link from Birmingham Airport to Birmingham International Station and the National Exhibition Centre, for full operation in 1984⁽⁷²⁾. The scheme is for a twin 600 metre elevated track with 6 metre long 2.25m wide vehicles carrying 49

passengers each, at speeds up to 47 km/h. A consortium called the People Mover Group made up of seven companies including GEC, Brush, Balfour Beatty and Metro Cammell will put up £557k, with £480k from British Rail and £750k from the Departments of Transport and Industry. West Midlands County Council is to put up £980k. The system should be ready in early 1983 to give 12 months preoperational experience. Brush are to be responsible for the LIM propulsion and its overall control, and GEC Rectifiers will produce the transistorized inverter. Initially three vehicles will be provided, and eventually a fourth vehicle will allow two coupled vehicles per track.

2.3.4.2 American Development

American activity in EMS Maglev using dc magnets has been relatively limited. Borcherts and Wilkie at Ford Motor Company investigated the dynamic characteristics of attractive Maglev in 1972, with experiments on a 305mm diameter wheel. These were followed by a larger wheel test rig in 1974, but a vehicle was not constructed. Similarly the METREK Division of the MITRE Corporation completed analytical work in 1973 with confirmation on a 2.2kg magnet secondary suspended test stand.

General Motors actually built a 1.8 tonne vehicle which used the Krauss-Maffei arrangement of 8 offset levitation magnets to provide lateral guidance⁽⁷³⁾. The fibre glass shell was supported on fore and aft aluminium box frames which housed the magnets, electronics and two LIM's. The LIM's allowed 0.1gee acceleration or deceleration (equivalent to 1.76kN thrust) at an airgap of 7.5mm. The 480V three phase power was supplied through brushgear and converted to 650V dc for the magnet drivers and for the LIM's the voltage was varied in magnitude and phase sequence. The reaction rail was 4.8mm aluminium backed by 6.3mm unlaminated iron. The power electronics used high voltage transistor bridge PWM choppers and optical isolation between high and low power circuits. Although the track length was only 15 metres and top speed only 9km/h a reasonably sophisticated trajectory control system based on a Texas Instruments STI

Programmable Controller was used. This system checked out vehicle status before a run, and also controlled the position and velocity profiles. The vehicle is reported to have made over 2500 round trips and achieved good reliability, but as yet there have been no published plans to further the development within General Motors.

2.3.4.3 Russian Development

The Soviet Union is reported to have built and tested a magnetically levitated prototype passenger vehicle weighing 10 tonnes, in 1978⁽⁷⁴⁾. The vehicle could carry 36 passengers and was 9 metres long, 2.7 metres wide and 2 metres high. The first installation was to be in Alma Ata, the capital of Kazakhstan in 1979. The track length was to be 14 kilometres crossing the city, with two stations. Eventually there was to be a 65km extension to the Kapchagai Reservoir, a suburban recreational area and resort. Various reports differ as to whether the vehicles would be levitated by EMS or permanent magnets, but linear motor propulsion was to be used. It is known that both EMS and EDS systems are being studied in Russia analytically⁽⁷⁵⁾, and that Research Institutes in Moscow, Leningrad and Kiev have had substantial teams of engineers organised to investigate Maglev schemes.

2.4 The Electrodynamic System of Levitation

2.4.1 General Development

The electrodynamic system of levitation was suggested by Americans working in the field of superconductivity applied to particle accelerators. Several variations of the basic scheme involving vehicle mounted superconducting magnets were proposed, the main difference being choice of track conductor. In the first years after 1970 research groups began basic investigative programmes in Japan, USA, Canada, Germany and the UK. Japanese development centred on their need to find a non polluting low noise and vibration alternative to the Shinkansen. The maintenance cost of keeping track alignment under the severe duty cycle was correctly

anticipated as being of major importance. From the beginning the Japanese had decided to run 16 car trains in the ultimate revenue system, and chose a loop levitation conductor over the sheet conductor adopted universally by other groups. Their reasons were that loop guideways can give better lift to drag ratios, and are simpler to realign and position than sheet guideways. The remaining groups designed revenue vehicles usually to run singly or in not more than three car trains, the overriding reason being that traffic passenger density on the routes to be used did not warrant multiple unit training.

Propulsion choice on the mature designs has been for the linear synchronous motor, with exception of the Ford baseline revenue vehicle. Ford opted for a ducted turbo fan, based on the Hamilton Standard Q-fan. With acoustic shielding the Q fan noise levels would be acceptable in low population density intercontinental travel, but would be totally unacceptable in the higher densities of the USA North East Corridor, Europe and Japan.

Guidance schemes generally relied on null flux operation of LSM magnets either on an additional array of null flux track loops, or null flux connected armature windings. The UK system differed, in that guidance forces were generated by shaded pole action of the vehicle magnets with the edge discontinuities of the levitation conductor.

The decade of the seventies has generally suffered in economic downturn, and this has naturally affected high speed guided ground transportation research. The American research was closed by an executive decision to halt all HSGGT work in 1975. German development of EDS was discontinued as a choice was made in favour of EMS Maglev. UK development has continually suffered from shortage of funds, and Canadian work has been at a low ebb in recent years. JNR in Japan seem to be the major group fully committed to establishing full size EDS at 500 km/h and are in the process of reconstructing their inverted T 7 kilometre track at Miyazaki in the form of a trough guideway, and will run a 3 car train. Russian research has

recently been apparent, although it has merely extended and repeated already published information. It is not known whether there has been any significant hardware development.

2.4.2 American Systems

2.4.2.1 Levitation Research

Powell first suggested the use of superconducting coils to provide levitation of a passenger carrying train, in 1963⁽⁷⁶⁾. The rail system could be a laminated conductor, but initial preference was given to a superconducting rail pair, over which a superconducting coil straddled. Later, in 1966, in collaboration with Danby, he proposed a more practical system where the track component was an array of normally conducting aluminium coils⁽⁷⁷⁾. Further work produced modification of the basic concept and two superconducting coil arrays were placed either side of the track coils within a re-entrant cryostat, the so called null flux system⁽⁷⁸⁾. With this configuration, only a small percentage of the vehicle flux linked the track coils providing a stiff suspension with high lift-to-drag ratio. The track coils could also be suitably powered with variable voltage and frequency to form a linear synchronous motor (LSM), as shown in Figure 1⁽⁷⁹⁾.

In 1967 Williams and Gerstle at Sandia Laboratories became interested in propelling high speed rocket sleds which were magnetically suspended. Guderjahn and Wipf of Atomics International, assisted by Coffee and Chilton of Stanford produced a viable scheme based on conducting sheet suspensions. During this study the method of impedance modelling to be used by later researchers was tried as part of the design process⁽⁸⁰⁾. Guderjahn and Wipf proposed the conducting sheet suspension as an alternative to Powell and Danby's loop track for high speed trains, and incorporated a composite upper section of the channel with a ferromagnetic member to carry the lift force of the vehicle and increase the lift to drag ratio⁽⁸¹⁾.

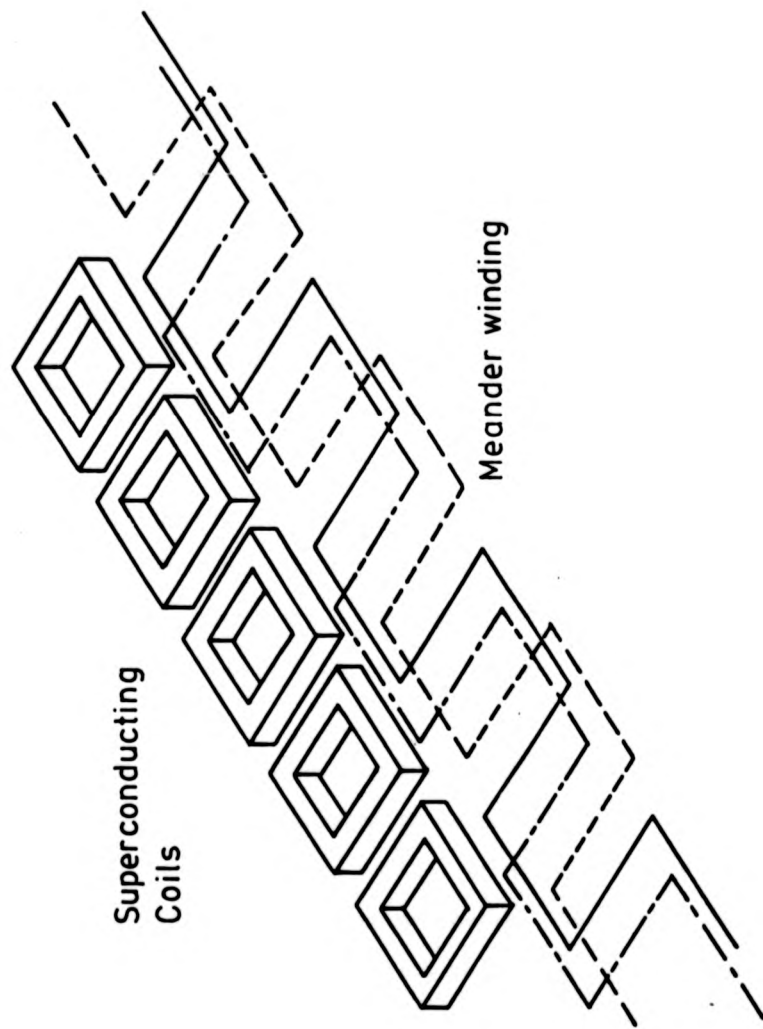


FIGURE 1. LINEAR SYNCHRONOUS MOTOR

Richards and Tinkham produced a systematic analysis of conducting sheet suspensions to incorporate normal and null flux systems, using Fourier analysis of the magnets' fields. An attempt was made to estimate the characteristics of linear synchronous machines, and the linear dc machine with track switching was briefly considered⁽⁸²⁾.

Both Stanford and Ford received support from US DOT for research into magnetic levitation, and Appendix I lists the reports to the DOT. Stanford concentrated on building a 152 metre guideway and a 300 kg wheeled vehicle which bore four superconducting magnets and a telemetry system at speeds up to 42 km/h^(83,84). Propulsion was by a glider towing winch and testing began in 1972. The dewar used to house the magnets used compressed fibreglass to transmit the loads to the outer walls but provide low heat leak paths. In the second half of the experiments, vertical side walls were tack welded to the horizontal track, and lateral instabilities were observed because of the discontinuity at the edge. Full seam welding produced stabilizing guidance forces. To analyse ride comfort criteria, damping coils were placed on the vehicle and it was taken through lateral and vertical step and ramp displacements and joints. A six degree of freedom programme was written to verify the dynamic behaviour of the vehicle.

Studies at Ford Motor Company began in 1970 on small scale wheel tests with ceramic magnets, and progressed to larger wheels with suspended and instrumented superconducting coils. By April 1974 the scale of tests had increased to 0.6 and 1.5m diameter wheels. Reitz and Davis of Ford produced many analyses of different magnet configurations, especially the method of calculating lift, drag and guidance forces of rectangular coils moving over flat or corner-channel guideways. Parametric studies of the magnetic forces for a revenue vehicle suggested that for an acceptable level of drag force the aluminium guideway should be about 25mm thick and the vehicle magnets should be at least 2 metres long. A proposed revenue

vehicle design initially chose coils 0.5 x 3 metres.

In evaluating propulsion units for their proposed revenue vehicle, Ford analysed the double sided LIM, a superconducting paddle wheel and helix, and a Q fan turbojet engine⁽⁸⁵⁾. The LIM study was one of the first to use a three dimensional analysis of series connected constant current and parallel connected constant voltage fed primaries. Fourier transform methods were used in the same way as levitation analysis was carried out, and the results when compared to a two dimensional analysis, showed poor correlation. The combination of the LIM with the high clearance electrodynamic suspension had to provide active normal suspension of the motor from the vehicle without degrading the lateral ride quality. The two superconducting motors used on board prime movers providing the motive power to rotate either "paddle wheels" or "helices" of superconducting windings. The paddle wheel configuration, Figure 2 consisted of meander wound wheels whose alternating magnetic field directly reacted on the sides of the aluminium guideway to produce an induction motor effect. Since only a small portion of the wheel would prominently link the guideway, an attempt to increase the linkage produced the helical arrangement, Figure 3, where the helix effectively moves as a screw. Both schemes would require major development and might only provide overall power to weight ratios comparable to LIM.

As part of the Tracked Magnetically Levitated Vehicle (TMLV) Technology Program of the US DOT Ford embarked on two major tasks in the second half of 1974⁽⁸⁶⁾. The first task was to produce a conceptual design of a passenger carrying system which could meet specified ride quality objectives, with the major emphasis on levitation and guidance design aspects⁽⁸⁷⁾. The second task was to design and test a high speed rocket propelled test vehicle which could provide the engineering data relevant to the conceptual design. Both projects were curtailed by the executive decision to abandon the majority of high speed ground transport

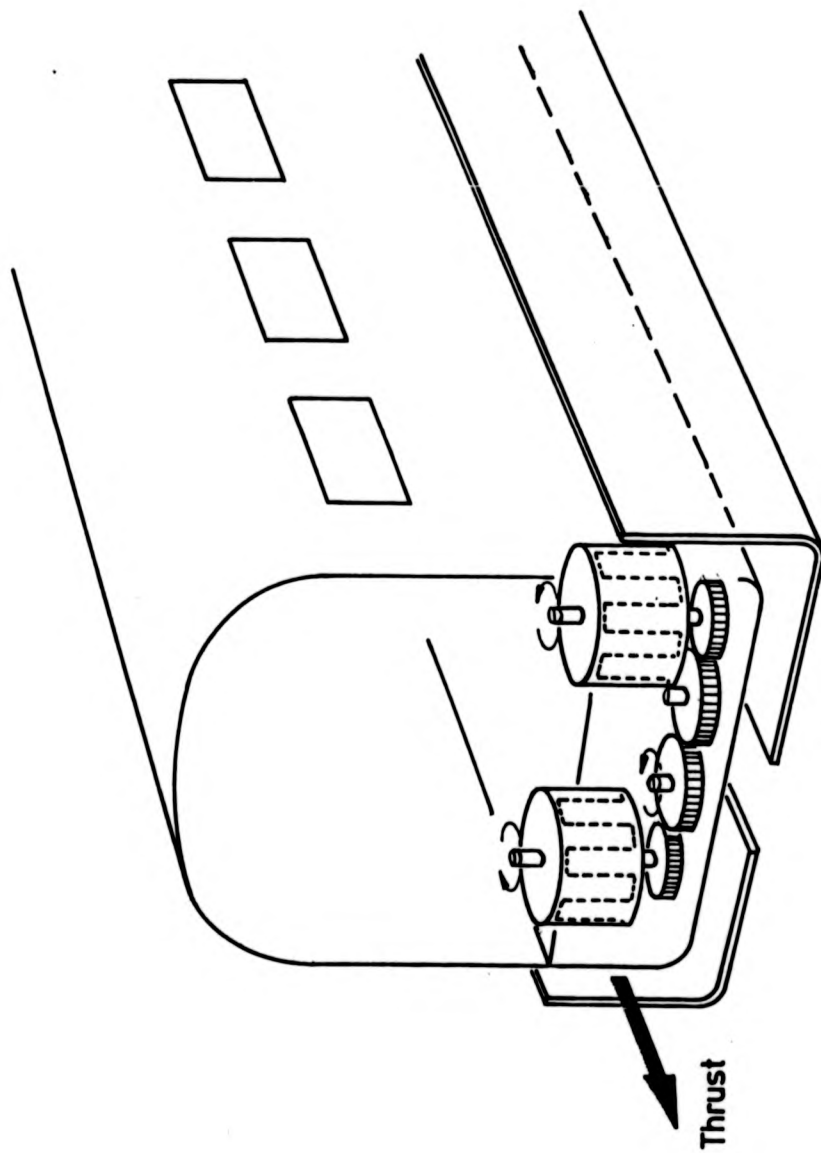


FIGURE 2. SUPERCONDUCTING PADDLEWHEEL

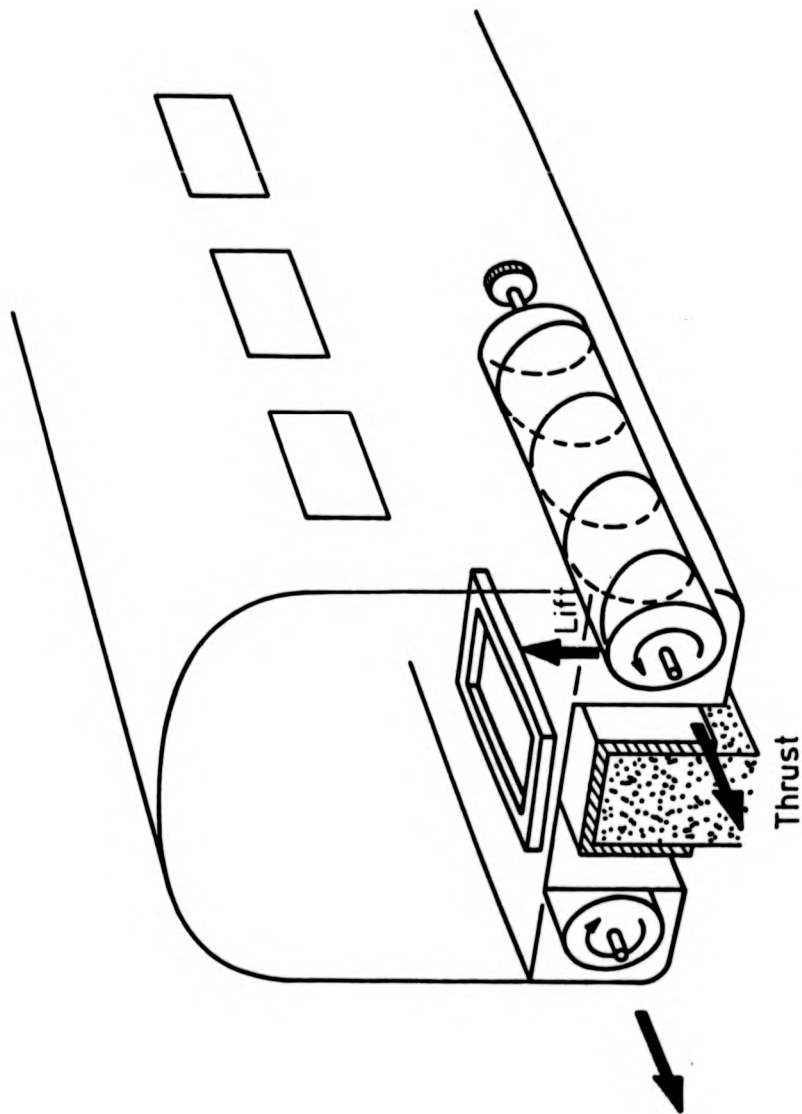


FIGURE.3 SUPERCONDUCTING HELIX

research on 3 January 1975. Ford continued and completed the conceptual design under internal funding.

The test vehicle was to weigh approximately 3 tonnes and would have been supported by four superconducting magnets at up to 480 km/h. The guideway would have been an inverted tee 1km long, located at the Naval Weapons Center, China Lake, California. Propulsion would have been solid fuel propellant rockets.

The conceptual study was largely performed by the Transportation Systems Department of the Aeronutronics Ford Corporation (Philco-Ford). The 80 seat vehicle was powered by two noise suppressed ducted fans, driven by regenerative gas turbines, and ran on an inverted tee guideway. The vehicle propulsion was also studied by the Raytheon Company who suggested a detailed design for a double sided LSM. Philco-Ford disagreed with the Raytheon recommendations and suggested the Q fan as being the most easily engineered solution, having much lower weight and complexity.

2.4.2.2 The Magneplane Project

The Magneplane Project evolved between June 1970 and July 1971 as a result of co-operation between Thornton and Kolm at MIT. Their patent⁽⁸⁸⁾ describes a vehicle that is magnetically guided, suspended and propelled, using a tandem array of superconducting coils along the curved lower arc of the cylindrical body. The coils interact with outer conducting strips to provide levitation forces, and the inward component of this radial levitation force provides the guidance. Propulsion was supplied by the interaction of the coils' alternating magnetic field with a track polyphase meander winding in the centre of the part-cylindrical trough, acting as a linear synchronous motor.

The project gained momentum when support from MIT was assisted by AVCO Systems, and the Raytheon Company, which enabled a systems approach to be taken embracing all aspects of vehicle design and evaluation⁽⁸⁹⁾. AVCO performed initial vehicle dynamic design and defined the overall

characteristics of the magneplane vehicle. Raytheon were concerned with magnetic performance of the lift and guidance magnets and cycloconverter control of the LSM. MIT established design guidelines for the cryogenics and magnetic shielding required in the passenger compartment.

Further funding under the RANN program of the National Science Foundation allowed Thornton to begin detailed design study of both electrodynamic levitation systems⁽⁹⁰⁾ and linear synchronous motor performance⁽⁹¹⁾.

Together with United Engineers (a Raytheon subsidiary) and Raytheon, a full size Magneplane Vehicle was designed⁽⁹²⁾ and a 1/25 scale model constructed and tested with both permanent and superconducting magnet fuselages⁽⁹³⁾. The full scale design was for a 50 metre, 140

passenger vehicle approximately 3.8 metre wide by 4.35 metre high. The vehicle weighed 44.8 tonne and was levitated and propelled by sixteen elliptical pancake coils which curved along the bottom arc of the vehicle.

Bucking coils above the main coils reduced the passenger compartment field to less than 0.01 Tesla. The coils were cooled by forced flow of supercritical helium through the rectangular cross section of the winding. Vehicle fuselage construction was based on aerospace technique of frames and stringers supporting a lightly stressed skin, as employed in the Boeing 707. In the description the Magneplane is likened to a low flying aircraft, which cruises at a height of about one foot and is free to bank in the guideway around curves taken at high speed. The guideway was a cylindrical trough of 4 metre diameter and 120° arc, the central 40° being taken up by the propulsion winding.

Propulsion by LSM is through large self supporting meander busbars cranked to provide active length with integral end windings.

The 1/25 scale model was built at the Raytheon Equipment Division Laboratory site at Wayland, Massachusetts, and consisted of a 116 metre guideway supported on pipe legs. The purpose of the project was to

establish and study propulsion levitation and guidance as an integral system rather than as separate decoupled components, and to try out control strategies on the cycloconverter, such as active heave compensation. Two permanent magnet fuselages were built, one based on Alnico 8 and the second on samarium cobalt magnets. Chu and Tang at Raytheon backed up Harrold's magnet optimisation and design by computing the lift and guidance forces that would be obtained from in line and laterally displaced magnet arrays, and these calculations were extended to include the revenue vehicle design⁽⁹⁴⁾. The guideway was constructed from two parallel rolled aluminium levitation conductors whose diameter of roll was about 0.23 metre. A 40° arc at the centreline exposed the flat meander LSM armature winding which was formed into three phases at a pole pitch of 75mm out of 10 gauge aluminium wire. Details of the track and vehicle are given in Table IV. After an acceleration section of 55 metres the vehicle had reached 98 km/h. If a controlled speed profile run had been achieved from the cycloconverter, the vehicle dropped down on the last 18 metres of track where the levitation strips acted as eddy current brakes.

During the last stages of the project, before it was terminated in June 1975 when funding was discontinued, a study was made of the guideway edge effects. Tang's analysis suggested that significant edge generated guidance was possible, and that this could be enhanced by addition of a keel magnet within the main pancake magnet plan^(94,5). This effect was not successfully incorporated into a redesigned Magneplane revenue vehicle, and would have modified the roll stiffness achieved, constraining the free roll philosophy adopted by Kolm and Thornton.

TABLE IV EDS TEST TRACKS WITH LINEAR MOTOR PROPULSION

Vehicle	Magneplane	LSM 200	ML 100	ML100A	LEM Model	ML 500	LSM Model	EET01	EET02
Length x width x height, m	1 x 0.20	4x1.5x.6	7x2.5x1.93	5x2.2x1.4	2 x 7 x 7	13.5x3.7x2.63	0.455x.305x.130	12x3.8x3.6	12.45x3.8x3.6
Weight, tonnes	14kg	2	3.5	3.6	0.75	10	8.1kg	17	14
Maximum speed, km/h	86.4	50	60	60	26	500	13	150	180
<u>Guideway</u>									
Location	Hayland	Tokyo	Tokyo	Tokyo	Tokyo	Miyazaki	Kingston	Erlangen	
Length, m	116	220	480		104 Loop	7000	25.2 circular	860 circular	
<u>Magnet</u>									
No coils	3	2	4	8*		16*	4	4	2
Coil size, l x w, m		1.2x.4		1.55x.3			56 x 75mm	1 x .3	1.20
Strength, kAT	60	320	250	450		450	-	515	1000
Levitation Height, mm	20	50-90	100	250		270	>1	100	100
<u>Armature</u>									
Type	LSM	LSM	LIH*	DSLMS	DSLMS	DSLMS	LSM	DSLIM	LSM
No Phases	3	1		3	3	3	3	3	3
Pole Pitch, m	75mm	1.4		1.8	0.24		60mm	0.33	1.4
Coil Size, l x w, m		1.3x.4				1.1x.7	60x80mm	w = .74	1.4x1.2
Section (or Feedable) length, m	(98)	(150)	(350)	(151)	4.32	29.4	3.6	2.874	430
No sections	8		64 primaries		25	240	7	9 poles	2
Thrust, kN			10			44		22/35	20
Air Gap, mm	20	-		190			>1	50	250
<u>Power Converter</u>									
Type	Cycloconverter	Cycloconverter	2 x VV	Cyclo-converter	Cyclo-converter	Cyclo-converter	Cycloconverter	Inverter	
Power Output kVA									
Current A	30kW					9600	12	5000	500
Voltage V					10	1100	60	1000	
Frequency Hz	0-200		50	0-46	200	2900	30-120	0-3000	0-2700
					0-15	0-33.1	0.5-40	0-105	0-20

*track primary
 †half for propulsion/guidance
 half for suspension

2.4.3 Japanese Development

2.4.3.1 Initial Research (96-98)

EDS development in Japan has centered on Japanese National Railways, and has been actively supported by the major engineering firms Toshiba, Hitachi, Mitsubishi, Fuji and Sumitomo. Preliminary investigation into railway systems to succeed Shinkansen had begun in 1962, and had covered aircushion and permanent magnet suspensions as well as LIM propelled wheeled rolling stock. In January 1970, Kyotani, the then Deputy Director of the Technical Development Department of JNR, suggested a superconducting levitated linear motor propelled train for intercity passenger transport, which could surpass speed limitations of conventional wheel vehicle adhesion and would be free from noise, vibration and air pollution. A research and development program was set up to look at the constituent systems and to produce an overall specification for a practical arrangement. Several test installations and many cryostats and superconducting magnets were built in the ensuing period to establish basic levitation and damping characteristics over the Powell and Danby loop tracks.

After the first round of rotational tests had verified the basic principles of EDS and agreement with theoretical predictions had been reached, it was decided to construct two linear test tracks, to test levitation and propulsion under dynamic conditions. The first track, LSM-200 was designed as a LSM running test facility, and consisted of a 220 metre straight track with horizontal track coils interacting with two superconducting coils each 1.2 metre by 0.4 metre pitched at 1.4 metre on a magnet carriage housing the cryostat. Vertical track coils on each side of the channel guideway were connected to a cycloconverter to produce a LSM. The 2 tonne vehicle was wheel guided and could be run either as a levitated test, or with the track coils connected, as combined LSM and levitation. A LIM auxiliary drive device ran alongside the LSM 200 track, and the cryostat could be

driven separately through a draw bar to provide data on just levitation without the constraints of the magnet car and LSM interaction. Initial tests in March 1972 were followed by public demonstration on 27 July 1972. Levitation height over 110 metres of levitation loops was approximately 90mm at 50km/h. Facility details are given in Table IV.

The second linear track was built partly to publicise the centenary of the railway in Japan, and was named ML-100 (Magnetic levitation - centenary). The 480 metre track had normally conducting track coils over 240 metres, and 350 metres had track primary LIM propulsion. The LIM was split into 64 ground primaries pitched at 5.5 metre intervals, with three bands of synchronous speed, 25, 50 and 75 km/h. The secondary on the vehicle was a 12mm thick 6 metre sheet of aluminium alloy. Power was supplied to the LIM alternately from two 50Hz variable voltage sources. Trials of the system began in September 1972 and in October public demonstration was staged. The two cryostats each housed two superconducting coils, and helium was vented to atmosphere at the end of a run. About 10kN thrust was obtained and levitation height was 100mm over the track coil section. Reasonable behaviour of the vehicle gave impetus to the plan for a field test of a Maglev vehicle at 500km/h on a 7 kilometre track.

2.4.3.2 Combined System for Propulsion and Guidance

Continuing the development of the Powell and Danby's loop track configurations, in November 1973 JNR and Hitachi built a rotating test device to confirm calculations on the null flux system of guidance⁽⁹⁹⁾. The wheel facility (Table V) could be used to test both null flux guidance and LSM performance, and consisted of a fixed cryostat with two coils energised to 250 kAT flanked by two discs which each had 18 LSM coils pitched at 0.468 metres, and 30 guidance coils. Running speed was 150 km/h and the cryostat could be given lateral and vertical offsets of +100mm and 50mm respectively. The tests showed that the null flux system could achieve high lift to drag ratios and that adequate guidance forces could be generated.

TABLE V EDS ROTATING TEST FACILITIES

<u>Wheel</u>	JNR CSPG	CIGGT	ROSY
Diameter m	3.124	7.6	5.8
Tip Speed km/h	150	105	144
Location	Tokyo	Kingston	Erlangen
<u>Magnet</u>			
Manufacturer	Hitachi	CIGGT	Siemens
No coils	2	1	1
Coil Pitch m	0.7		
Size, lxwxh, m	0.6 x 0.3	0.4 x 1.35	0.3 x 1.0
Strength,kAT	250	202	460
<u>Cryostat</u>			
Manufacturer	Hitachi	Oxford Inst.	Siemens
Size, lxwxh, m	1.6 x .25 x 1.04	? x 2.68 x .32	1.4x .6x .24
Weight, tonne	0.6	1.0	0.54
<u>Armature</u>			
Type	DSLMS	LSM	LSM
No Phases	3	3	3
No Wavelengths	6	24	48
Pitch, m	0.468	0.505	0.38
Mean Width, m	0.3	1.27	0.9
Slot Pitch, mm		84	
No.Cond/Phase		2	4
No Cond/Slot		1	
Cross section mm ²		125, Al	70,Cu
Distance between coil faces, m	0.25		
<u>Power Converter</u>			
Type	Cycloconverter	Inverter	Inverter
Power Output, kVA	40kW	60	240
Current,A		350	400
Voltage,V			390
Frequency,Hz	0-30	0-30	0-52.5

Following on from these wheel tests, work at Toshiba had shown that a L shaped cryostat design housing one vertical and one horizontal superconducting coil was feasible⁽¹⁰⁰⁾, so it was possible to apply this technique to design with tandem coils supplying lift and guidance/propulsion forces within the same cryostat.

A 19.6 metre diameter test track was also constructed to test out cycloconverter control of a LSM when an eight carriage model train passed through switched blocks. The fields on the model cars were produced by permanent magnets. Position and speed sensing was monitored from a telemetered signal derived from the modulation of a light beam on the model. Because of the success with the model control system and the wheel results, it was felt that the concepts could be extended by a linear track facility. Figure 4 shows the combined system of propulsion and guidance (CSPG) that was tried out on a conversion of the ML100 track. When a lateral offset occurs, the armature coils have an additional circulating current i_c flowing which supplies the null flux force to restore centre line motion of the vehicle. Each coil set has a terminal voltage e_t made up of voltages e_l or e_r for left and right hand coils, generated by mutual linkage with the moving vehicle coils, and the $\frac{L di}{dt} + R i$ drop, where i is the phase current i_p with any circulating current i_c adding or subtracting, depending on the offset direction. Only one phase is shown in the figure; to match conventional power equipment a three phase track winding would be used, with the null flux connection made between laterally opposite coils.

The ML100 track was therefore converted to provide in 1975 a LSM propelled vehicle (ML100A) using superconducting magnets⁽¹⁰¹⁾. The tests established that stable guidance was possible with the null flux connected armature coils, and experiments into passive heave damping control by aluminium sheets of various thickness were carried out. The guideway

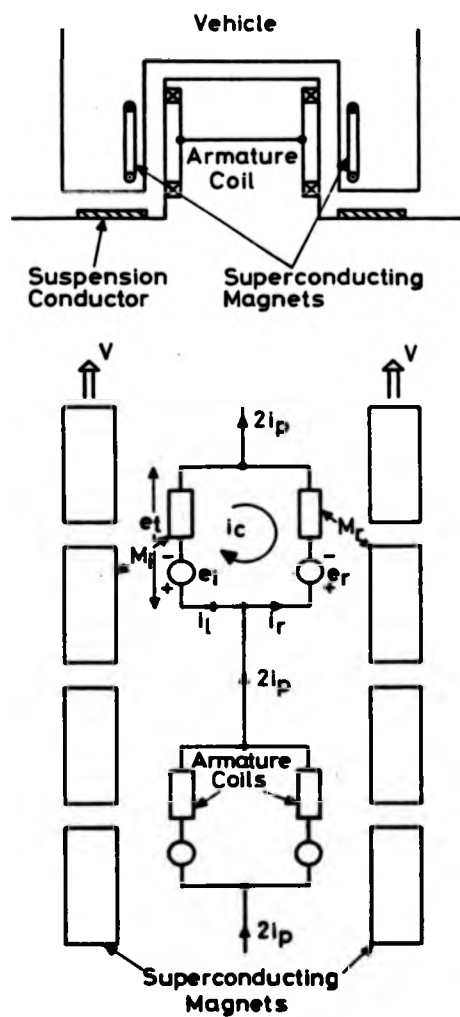


FIGURE 4. COMBINED SYSTEM OF PROPULSION AND GUIDANCE.

remained roughly the same length as for ML100, at 480 metres. Propulsion and guidance coils were installed over the 151 metres from the start of the track, levitation coils (remaining from ML100) ran from 64 to 200 metres, and the braking section ran for 65 metres from the 350 metre point. Only one way running was possible. The power supply consisted of two 860 kVA transformers feeding four 206kVA cycloconverters which ran at 375A from 0 to 4.6Hz. (Table IV). The cryostats used were L shaped and contained four superconducting coils, two for levitation and two for propulsion and guidance. The 3.6 tonne vehicle reached 60 km/h in about 100 metres and the distance between the coils and the guideway propulsion coils was about 190mm. Levitation characteristics were similar to ML100 with a levitation height of about 250mm. About 10kN thrust was generated by the propulsion, giving about 0.2gee acceleration. Guidance stiffness at 40 mm offset was more than 0.5 kN/mm.

2.4.3.3 The Miyazaki Test Line (102-4)

In 1974, JNR announced that a 7 kilometre test line facility was to be built in the Miyazaki Prefecture, Kyushu, between Hyuga and Tsuno, whose purpose was to test a near-actual sized vehicle running at the very high speed of 500 km/h. The Vehicle Testing Center was opened on 16 April 1976 to supervise the experiments and construction work, which had begun on 1 November 1975. By 26 July 1977 self propelled running tests commenced on the completed 1.3 kilometre section, and low speed tests to 100 km/h were performed from September 1977 to establish running characteristics and basic wheeled vehicle dynamics. The track structure was an all elevated guideway, about 6 metres wide, and constructed with the reinforced concrete and slab track techniques developed for the Sanyo Shinkansen. Track and vehicle details are given in Table IV. First stage tests were to be based on the inverted T configuration, and when performance was established, the centre section would be removed, and the U-track configuration would be explored. The inverted T structure was chosen as the most stable for the generation of lateral guidance forces, which when the facility was

designed, were still unqualified. Such a guideway would be unsuitable for a practical revenue system since it severely limits vehicle space. The tolerances on track construction were generally $\pm 10\text{mm}$ for first setting and $\pm 20\text{mm}$ for maintenance. Propulsion and levitation coil tolerances were to be kept to within $\pm 6\text{mm}$, measured relative to local guide datum rails. A Guideway Inspection Car could fully measure critical track dimensions at a running speed of 36 km/h.

Track grade was designed to minimise inertial forces on the test vehicle within the geographical constraints. At one end of the track near the Test Centre the down grade is 5/1000 and the guideway passes over the Nippo main line. Towards the other end a curvature of 10 kilometres is included. The acceleration rates of 0.3 to 0.4 gee are about 3 to 4 times that to be expected in a revenue vehicle, but permit 5 second running at 500 km/h, with the LSM thrust of 44 kN. This time is deemed sufficient to fully examine the vehicle dynamics, including damping characteristics.

The propulsion coils are wound using aluminium wire and are fixed either side of the inverted T and interconnected to make the null flux guidance operate. Their length is 1.1 metre by 0.7 metre wide, pitched at 1.4 metre. The coils have a moulded exterior with the location adjustment set in. A 50mm deviation from the straight ahead motion results in a guidance force of 50kN.

The vehicle carries no passengers and has an all up weight of 10 tonnes. Two L shaped cryostats on either side of the vehicle carry two levitation and two propulsion/guidance superconducting magnets each. The propulsion magnets run at 450 kAT, and the levitation coils are energised at 250 kAT to produce 270mm lift, with 120mm mechanical clearance. The vehicle width of 3.7 metres is roughly a revenue vehicle dimension, whereas the length of 13.5 is approximate half. Body construction was mainly out of aluminium alloys as used in aerospace manufacture. Coils are energised at the Test Center and switched into the persistent current mode by removing heating power from the thermal switches. The L cryostats employ return helium gas

and liquid nitrogen cooled shields, and can be operated as isochoric containers working up to 200 kN/m^2 pressure. Their capacity is about 400 litres of liquid helium, and heat leak is about 10W, with a roughly 10% lower heat leak when running. The lower heat leak observed as the vehicle moves is thought to be caused by more effective heat transfer in the vapour and liquid cooling of the intermediate temperature shields.

The general system of power supply and LSM control is shown in Figure 5. The ground coils are laid continuously along the track and are arranged in sections of length D, slightly longer than the train length d. The main power supply is a strong UHV buffered by a motor generator set at the main substation. The motor generator increases the utility frequency to provide a better harmonic content for the pair of subsequent cycloconverters. The utility sees a synchronous machine load. If the cycloconverters (or inverters) were not buffered, a low power factor load with high harmonic content would be presented to the utility with a resulting economic penalty. The sections are connected alternately to similar cycloconverters A or B, and the adjacent sections containing and expecting the vehicle are the only ones energised. The vehicle position is fed to the control centre from a 180 kHz signal transmitted on board into a transposed inductive track wire system.

The switching control is set up to allow the leap frog of cycloconverter connection through track side vacuum switches, which will only switch at zero current. This feeder switching must be accomplished in such a way that there is no fluctuation in propulsive force on the vehicle.

For the Miyazaki test track the ratio of train length to section length is about 0.45. Before the control system was finalised for ML500, a model linear motor and cycloconverter were tested by JNR on a 104 metre loop track. The vehicle length and section length of 2 and 4.32 metres were about 1/7 of the ML500 track, but had similar ratio. The 10 kVA cycloconverter was tested out using the actual control desk for the Miyazaki facility. Table IV includes brief details of this system. A choice was made for a section

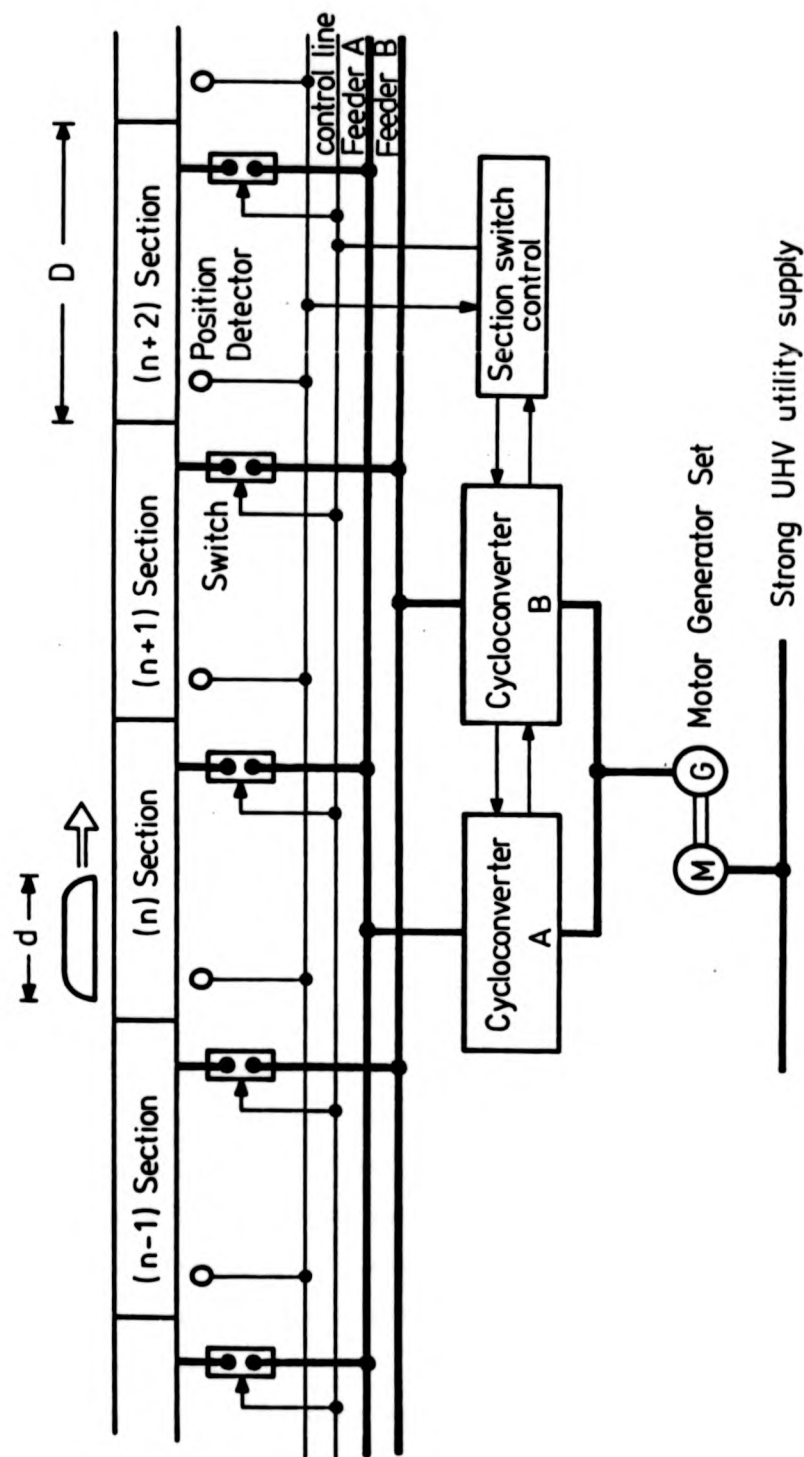


FIGURE 5. POWER SUPPLY AND CONTROL SYSTEM FOR LINEAR SYNCHRONOUS MOTOR.

length of 29.4 metres on the basis of sufficient switching time being available to the cycloconverter.

Phase angle and current control of the power converters was controlled by signals from optical reflection plates placed every 4.2 metres along the guideway. The position of the vehicle relative to a track propulsion coil is transmitted into a leaky feeder coaxial cable laid along the track.

After the preliminary low speed tests on the 1.3 kilometres length of the track had finished, and the extension to 3.1 kilometres was completed in November 1977, medium speed testing began, reaching 204 km/h in December. The levitated or guidance forces were checked independently, as support or guidance wheels were separately withdrawn. Eventually all auxiliary support was withdrawn and ML500 was allowed levitated flight. The next guideway extension to 4.7km in June 1978 meant that 300 km/h runs were possible, and in November 347 km/h was attained. By this time about 5,000 kilometres had been covered and 2,200 running tests conducted. August 1979 saw completion of the track to the full 7 kilometres and on 21 December 1979 the top speed of 517 km/h was reached. While the last extension to the track was being finished, aerodynamic tests on ML500 as it passed through a simulated tunnel 350 metres long, at 330 km/h were performed. Also on the 4.7km track, tests were made on the performance of a helium refrigerator. The refrigerator was manufactured in 1978 to operate under dynamic conditions and was fitted to ML500R, the ML500 body with part of the framework converted. Although the Miyazaki magnets operated in closed conditions, JNR expect to consider using a refrigerator per cryostat, with the provision of sealed off operations in the case of a power failure or refrigerator problems. The prototype could deliver 30W at 4.5K, and weighed 163kg. Because the test vehicle had no on board power, an i.c. engine was mounted on ML100R for the tests to 200 Km/h. The prototype worked satisfactorily, and gave information on possible improvements.

The first stage tests were completed in December 1979 with the satisfactory

repeated performance of the vehicle at speeds of up to 500 km/h. The track is now being reconstructed to form a U profile, and three test vehicles will be built to study multiple car running. The CSPG will be used, with levitation coils on board. It has been suggested that with increased mmf propulsion coils, CSPG requires no levitation coils on board. Typically for a revenue vehicle, 16 800 kAT superconducting magnets are sufficient for levitation as well as propulsion and guidance. On board power pick up is accomplished by placing normally conducting coils in the levitation coils position, and picking up the track levitation loops' reaction field harmonics. Up to 100 kW of power could be generated over 300 km/h to back up on board battery power for services and refrigeration loads.

Further studies are taking place to establish the power stability of revenue vehicle operations. Typically in acceleration, up to 1.9 times active power and 2.5 times reactive power are required compared to the steady state 500 km/h cruise values. For a 16 car Shinkansen type train, the commercial line power requirement is in the region of more than 160MVA. In a design study for the Tokyo-Osaka line 300 MVA transformers feeding 250MW motor generator sets were distributed every 36 kilometres and fed four cycloconverters, two for the up line, two for the down line. At accelerating sections the M-G sets would be placed every 9 kilometres. The power swing as a vehicle passes through a section is caused by having to reset the leap frogging cycloconverter to zero and resynchronizing it in the advanced section. At the M-G base of 250MW the power input swing might be as much as 120MW. The Miyazaki track presented a more severe problem because of the short switching times. However by designing sufficiently high inertia constant for the MG set the input active power swing was kept to less than twice that of the output swing, and was confined to the lower speed range of 70-90 km/h, and was adequately damped out at the running speed.

Provided the U track conversion and running of the three vehicle train set is satisfactory, JNR will redesign for a preproduction test train and track (about 40 kilometres long) to be built in either the Nagano or Yamanashi prefecture. It is likely that since the Japanese Ministry of Transport has begun to take charge of both the JNR and JAL effort, the track will be part of a dual facility to test both EMS and EDS systems. Initial spend on construction work will begin at around Y 10,000m in the form of a government grant.

2.4.4 Canadian Research

2.4.4.1 Overall Development

In 1970 the Canadian Institute of Guided Ground Transportation (CIGGT) was established at Queen's University Kingston to carry out investigations and research, both short and long term, towards improving Canadian guided ground transportation systems, and to involve graduate and undergraduate students in transportation studies. In February 1971 the Canadian Ministry of Transport's Transportation Development Agency (TDA) let a contract, to be administered by CIGGT, to investigate the use of superconducting magnets for suspension, guidance and linear synchronous propulsion of high speed transport, and to establish in Canada, a group of applied scientists competent in this field of research. Initially the Canadian Maglev Group was formed by physicists and engineers from Queen's and Toronto Universities, and later McGill University supplied computational and analytical expertise. The Group have produced a large number of papers describing various aspects of their work; the major results are included in the CIGGT annual progress reports to TDA⁽¹⁰⁵⁻⁹⁾, and a report by Hayes of the National Research Council⁽¹¹⁰⁾. From the beginning of the development programme emphasis has been placed on producing a viable design for a revenue vehicle, that would be suitable for Canadian conditions. The funding from TDA (later to be reorganised as the Transport Canada Research and Development Centre) was for three phases of

development. The first phase was for two years from February 1971 to March 1973 and cost \$59k. The work involved introductory studies into the design of levitation magnets, establishing LSM propulsion concepts, and producing a conceptual design for a Maglev test facility. The second phase development cost \$320k with additional funding of \$133k for Queen's University from the National Research Council to construct the test facility. Phase II lasted until March 1975 and allowed substantial progress to be made on several fronts. A 7.6 metre diameter test wheel which could attain 101 km/h was constructed and proved, and a 6 component force harness was designed and built to accommodate test cryostats and magnets. A preliminary revenue vehicle for a Toronto-Montreal via Ottawa route was subject to a reference design, on which technical and economic analysis could be based. The purpose was to further optimise the design of sub-components such as levitation magnets and their operating characteristics, LSM propulsion strategies, guidance requirements, guideway and vehicle construction.

The LSM received a high priority of effort. At Toronto the theoretical analysis was completed and optimization studies attempted to quantify trade offs in design. Current source inverters which had been under development for other applications were found to be applicable to LSM propulsion with little modification. An 8 metre model LSM was constructed at Queen's University and powered by a Toronto designed cycloconverter. The model vehicle had rare earth permanent magnets to simulate the field distribution of a superconducting magnet array on a revenue vehicle, and a six channel FM telemetry link provided control and data transmission.

In 1973 a LSM magnet coil was designed and wound. This magnet was near full size and was meant to prove the concepts of LSM propulsion using the large test wheel facility. The 1 tonne cryostat was delivered in May 1974, but suffered cold leak problems at a lower demountable seal which was eventually soldered up. The cryostat was fabricated by Oxford Instruments. Once this problem was overcome, the dewar and magnet operated satisfactorily and the

initial wheel tests with a rim mounted air cored armature winding proved successful, with no sign of magnet instabilities, despite severe mechanical vibration and voltage transients on loss of synchronism.

Finally levitation system analyses were performed to include parametric and economic investigations of sheet guideways, using integral equation, Fourier transform and dynamic circuit theory. Ladder guideway models were included in the study. A levitation magnet and cryostat were designed for testing on the wheel, and materials were procured, although the magnet was in fact never constructed.

Phase III began in April 1975 and was for a further two year period. The objectives were to continue with the practical tests on the wheel facility to verify design parameters, to develop suitable mathematical models that could describe levitation, guidance and stability as well as propulsion and dynamic performance of a vehicle over its entire speed range, and to identify a feasible Maglev system. A full description of the magnets and guideway components including the LSM control concepts was required.

The experimental work on the test wheel which began in Phase II was continued and the six component force harness was commissioned and allowed accurate measurement of LSM forces and moments to be made. A 42 kVA three phase variable frequency current source inverter from the University of Toronto supplied power to the LSM windings. The model LSM test track was provided with an improved FM telemetry system and a method of measuring force angle in the machine was tried out. Cycloconverter modifications allowed external analogue signal drive to select output waveforms as well as voltage and frequency. Two types of control strategy were developed, using either back emf sensing or vehicle position feedback, and were computer modelled under dynamic conditions. Both systems were tested on the small tracked vehicle. Further work on the levitation and guidance forces was pursued by the McGill group, who found the dynamic circuit theory proposed by Ooi to be the most satisfactory. Lift, drag and guidance forces were examined for finite width

strips and rectangular magnets and the results correlated well with experimental findings. Passive coil damping with normally conducting coils closely linked to the main windings electromagnetically, and attached physically to the secondary mass in parallel to the secondary suspension were examined. Configurations to damp all six degrees of freedom were proposed with coil masses in the order of 100 kilogrammes. To achieve low frequency damping (less than 0.5Hz) and to allow steady state deflection offset controlled hydraulic actuators would be included in the secondary suspension.

Toronto also investigate ladder and loop guideway configurations as comparisons to the sheet guideway reference design. Although the Japanese experience of low drag forces with low force pulsation were confirmed, with similar amounts of conductor material to a sheet track, the rapid build up in destabilising force for offset magnets was considered to be a problem with the Canadian flat track arrangement. For high speed turnout the levitation conductor would be loops with semiconductor switches to allow open or closed operation as the guidance direction is determined by null flux loops also containing semiconductor switches.

The test wheel facility was altered to allow levitation experiments to be performed. The LSM windings were removed, and the plywood rim was machined to take a 800mm wide x 10mm thick aluminium strip. The LSM magnet was used to determine the levitation drag and guidance forces, as well as the effects of joints in the conductor.

In the final year of Phase III the conceptual study and details of the proposed revenue Maglev vehicle and operating system were completed. Hayes at NRC integrated the work of groups within CIGGT and NRC in the engineering design study. The vehicle was based on the CIGGT reference designs which had matured through the previous six years of research. The flat track configuration, initially chosen because of the problem that might arise with snow accumulation in Canada was to be elevated to a mean height of 7 metres

in the urban and intercity route. Levitation, guidance and propulsion track conductors would be embedded in asphalt on the top surface of a prestressed box section carrying a reinforced concrete slab deck. The 30 tonne vehicle design is for 100 passengers at a cruise speed of 480 km/h between Toronto and Montreal, a 600 kilometre trip with an intermediate stop at Ottawa. Isochoric cryostats separately house ten levitation magnets, and the 56 LSM magnets are grouped in seven independent pods. Each eight pole pitches, space is required for end of pod cryostat insulation. Merely omitting a magnet would result in large interpod forces, so a mini magnet of half width is included at the end of each pod with reduced ampere turns (150 kAT, main magnets 500 kAT). The pod has a helium reservoir with 85 litre storage mounted above, within the pod support linkages. Pods are connected to the passenger compartment and are allowed to move laterally through a torsion bar secondary suspension and dampers, whereas levitation cryostats are constrained by their secondary suspension and dampers to move purely in the vertical direction. Main vehicle guidance would be derived from the interaction of the LSM magnets with track null flux loops laid in between the levitation strips. High overall apparent efficiency of 70% is determined by economic trade offs in guideway conductor and vehicle magnet design. For a 60% capacity vehicle the LSM produces nominal 40 kN thrust with track, conductor current of only 240A in the split phase three phase winding. Terminal rating at a section length of 5 kilometres is 7.56 MVA at 117 Hz. Following on from the completion of the conceptual vehicle design study, the economics of the system operating in the Toronto-Ottawa-Montreal corridor were investigated at CIGGT⁽¹¹¹⁻²⁾. The purpose was to establish whether the capital outlay for the system could be ultimately offset by the revenue generated by passengers and freight over the short haul route. As with studies by other Maglev groups the emphasis had changed from high speed intercity commuter orientated transport to high capacity transport with competitive specific energy density and dependence on renewable or at least

centrally generated energy supplies. Economic parity with conventional high speed rail systems running at elevated speeds of 300 km/h seemed to be especially attractive.

NRC has continued to refine the conceptual design for the revenue vehicle and magnet systems, and has also devoted effort to investigating alternative vehicle configurations, with emphasis on ride quality. The test wheel at Queen's has been converted to allow low speed tests on a SLIM under an US DOT contract with Mitre and Rohr. This programme is described in section 2.5.1.4.

2.4.4.2 Test Facilities

The two test facilities are both run by the CIGGT at Queen's University. The small scale model LSM facility consists of an eight metre diameter circular track, a rare earth magnet assembly mounted on a wheeled vehicle, which also carries sensors and a FM telemetry transmitter, and a 12 kVA cycloconverter. The second facility is based on a 7.6 metre diameter rotating wheel onto which guideway components can be fixed. A force measuring harness can accommodate a cryostat housing a superconducting magnet for propulsion and levitation tests at speeds up to 105 km/h, limited by centripetal accelerations of 21 gee. The test inverter comprised two basic forms of inverter, a three phase current source, and a three single phase current source, with each of the phases 120° electrically displaced. Both systems could deliver 350A rms with a frequency of up to 30 Hz.

The small scale model LSM facility was constructed to evaluate the operating requirements and control system strategies for full sized vehicles.

Preliminary work had examined iron cored LSM as being suitable for model work, but when the facility was designed it became apparent that an air cored armature showed more promise in available current density with minimal temperature rise, than a iron cored track. The full size system could also be more readily modelled using rare earth magnets for the field array. The vehicle was a light weight structure with machined model railway type wheels

running on the circular track aluminium rails placed either side of the armature windings. The four pole magnet array was made up of alternating polarity blocks of rare earth magnets 75mm wide pitched at 60mm. Each block was made of 4 wide by 3 long magnets which could be aligned to produce essentially a sinusoidal flux density profile longitudinally under the vehicle, and a square profile transversely, as would occur in a full sized LSM. Also on board the vehicle was a permanent magnet machine, which could be either driven by the LSM through gearing to the axle and allowed to dissipate power into a fixed resistor giving a load on the vehicle or left open circuit to act as a tachogenerator.

Two telemetry systems were tried on the model. The second system allowed force measurement, force angle and velocity signals to be transmitted to the control of the cycloconverter to allow more versatile operation of the LSM to be realized. The force angle was measured by a Hall effect probe which sensed the displacement of the vehicle magnetic field from the armature mmf wave. The probe measures the track field at ten equidistant positions over a wave length, and converts to a sinusoid equivalent which is zero crossing detected. A bistable circuit is latched at the beginning of a scan of the probes and unlatched when the zero crossing point is reached, thereby giving a position dependent output. Vehicle velocity and velocity error signals are derived from track posts being detected by vehicle phototransistors. The generated normal and longitudinal forces will be measured by strain gauges on a magnet harness to which the magnet assembly is fixed.

The cycloconverter is nominally rated at 12 kVA and gives an output of 60A three phase, 0.5-40 Hz. A special purpose three phase oscillator was built to produce a wide range output waveforms with the intention of improving the vehicle performance by applying a wider range of feedback control schemes than would be possible with just a sinusoidal oscillator.

Computer modelling of LSM control had indicated that velocity feedback to control the cycloconverter voltage magnitude was necessary to damp out the

force angle pulsations. With the telemetry system and improved cycloconverter oscillator, the control strategy was successfully demonstrated, as were automatic acceleration and deceleration and transient behaviour control following a system disturbance. The combination of both velocity and force angle feedback produced most acceptable vehicle performance; controlling vehicle velocity during steady state and transient operation essentially controls ride quality (at least in surge) and controlling the force angle near 90° maximizes the thrust force and minimizes normal force generation. Both parameters can be measured on or off the vehicle.

The large test wheel is mounted with its axis vertical and is made up of eight aluminium I beam spokes to which rim segments are bolted. The rim is built up of eight laminated plywood box sections with a tension wound outer wrap of epoxy impregnated glass fibre cloth, to take the hoop stress under the maximum speed of 105 km/h (70 rpm). A 120 kW dc motor is mounted through a gearbox to the drive shaft and can either motor the wheel at full speed or act as a drag force generator when connected to load resistance. The wheel rim was extended in width to take essentially full sized LSM windings made up from 10mm stranded aluminium on a 0.52m pitch. The three phase winding was splitphased, providing one conductor every 30 electrical degrees and two sections were provided to allow section entry testing. Eight slip rings take inverter power to the windings and are rated at 400A. The track rim can take a distributed load of 1 tonne at a width up to 1.45 metre. The support frame was strain gauged to allow for wheel balancing and to generally monitor structural vibrations. During the initial commissioning the structural resonance was traced to unbalance of the high speed drive shaft, and additional problems were apparent in the wheel hunting at speeds above 30 rpm. A control loop was designed for the drive motor to sense the rate of change of armature current, and by limiting the acceleration of the wheel to 20 revs/min^2 the wheel could be operated successfully to full speed.

The LSM Magnet was designed to be virtually full sized at 0.4 x 1.35 metres. The shape is a racetrack with an internal corner radius of 179mm. A high current density superconductor previously used for MHD coils was used because a lightweight design was required to enable the force measurement to be made sufficiently sensitive. The short sample critical current was 1900A at 5.5 Tesla which corresponded to $5.2 \cdot 10^5$ AT on the 252 turn LSM magnet. Initially designed for 60% short sample current of 1200 A, the coil was finally run at 800A (40% s.s. and 202 kAT total) which experimentally appeared to be near its limit of stability. The magnet was quench tolerant and ran with as little as 10% of its winding in LHe and has performed well despite rapidly applied forces and large voltage transients applied through the power supply.

Inverter design was based on the premise that the full sized LSM for a revenue vehicle was rated at 8.5MVA, 123Hz with a line voltage of 5.8kV and 490A. Reducing these values down to one magnet and a fifth of the speed, the inverter phase voltage is 40 volts and the maximum frequency 28 Hz with an inverter rating of 42kVA. As mentioned, the test inverter was made up of two configurations, and was supplied with a 100 kVA input service. The three phase inverter produced a square current waveform at 120 degrees and the three single phase systems can produce either 180 degree square current, 120 degree square current or a 15 step sine current approximation waveform. The band of frequencies possible are 2-30 Hz at 350A. Both inverters use water cooled thyristor stacks and were designed and built by the University of Toronto.

The test wheel was completed and low speed runs performed in late 1974. In March 1975 the first set of LSM propulsion tests began. The machine parameters such as phase resistance and inductance, mutual inductance between phases, and field to track mutual were measured through the slip rings. The wheel windage was calculated by decoupling the drive motor and measuring power input before and after driving the wheel. Using a simple force

measurement system the magnet was run as a LSM with the drive motor disconnected, and the inverter supplying approximately 200A. By ramping up the inverter frequency slowly as a function of time, the basic operation of the LSM could be confirmed. The current angle followed a predicted pattern until its value reached 90 degrees, when synchronism was lost. Control of the power factor angle was also established in the preliminary tests, and propulsion force roughly followed the predicted relationship.

With the completion of the more sensitive six degree of freedom force harness, more detailed examination of LSM behaviour could be made. The dewar total installed magnet helium capacity is about 80 litres which allowed run times in excess of 12 hours. Typically about 70 litres were required at 16-20 litres/hour to cool down the cryostat. A further 150 litres were needed to $\frac{1}{2}$ fill although these quantities could be less. The 450 litre delivery would last three days of tests with 10-12 hour operational runs per day.

Two motor control strategies were examined on the test wheel, the α and β . α control is where the internal voltage of the machine is measured and its angle with the current phasor is deduced. This is achieved by using a model of the stator resistance and subtracting the resistive drop from the terminal voltage in an analogue circuit. The resultant waveform models the internal voltage of the machine and the controller is required to force the stator current to a specific value in a set phase relationship to the internal voltage. For known ratios of stator and field currents this angle is an explicit function of the force angle. For much higher speeds the armature resistive drop is small compared to the internal voltage, and can be effectively ignored. The generated angle is now the power factor angle, θ , and the control strategy is known as θ control.

β control is LSM control based on position detection. On the test wheel optical sensors are fixed to the outer support structure and a series of stud markers are fitted to the wheel rim at a pitch of one wavelength. The

optical sensors are 60° pitched, coinciding with the stator winding pitch, and their triggered signals correspond directly to the armature displacement with respect to the fixed reference frame of the magnet. The signals can be used to control gating of the inverter throughout four quadrants of operation. Although this type of control is essentially advocated by JNR, CIGGT consider it only suitable for near station operation, to enable acceleration and deceleration rates to be closely controlled. α control is impractical at low speeds because the model has only a very small induced emf to make up the internal voltage.

Straightforward open loop control where the force angle adjusts itself (within stability limits) to match the motor thrust to the load drag was examined, but because the machine is so lightly damped, surge oscillation becomes marked and synchronism is soon lost. Programmed frequency ramping without position (β) or internal voltage (α) control might be possible with a sample voltage from the inverter providing a damping mechanism, but wheel tests were abandoned in favour of a laboratory test rig examination.

Two main sequences of test runs in August and December 1975 confirmed basic calculated predictions of LSM performance. Open circuit and short circuit tests at nominal air gaps of 220mm and 202 kAT were compared to predictions using mutual inductance programmes. Steady state load tests under β control over four quadrants generated test data on propulsion and levitation forces. Pitch roll and yaw moments were small and were equivalent to a 40mm offset of the magnet's geometric centre from that of the centre of force measured from the balance.

Harmonic content of the normal and thrust forces was observed to give a dominant sixth harmonic, when energised from the 120° square waveform currents, but agreed well with predictions. Higher harmonics were also observed in the measured force waveforms. Inverter control of sequential sections was established by leaving one half of the wheel winding unenergised. Resynchronisation and stable operation was achieved although the normal and thrust forces continued to ring for several cycles after

resynchronisation. Both α and β control were tested and validated, although α control required further stabilisation at high stator current magnitudes since the relationship of the internal power factor angle and the force angle are no longer unique.

Generally the CIGGT test wheel experiments confirmed the theoretical predictions of steady state performance of LSM at low speeds and modest frequencies and power levels. The next stage of wheel tests began with use of the LSM magnet to confirm predictions on levitation behaviour. The outer rim LSM windings were removed and an aluminium strip 0.8 metres wide by 10mm thick was fixed on. Lift and drag forces and their movements were measured, together with their variations over several different track joints.

2.4.5 German Development

German development has been financed by the Federal Government and EDS has been the responsibility of three companies, AEG-Telefunken, Brown Boveri and Siemens. The companies formed Projektgruppe Magnetschwebbahn in 1970 to investigate variations of tracks, test vehicles and revenue vehicle designs, together with development of hardware to demonstrate EDS with LSM propulsion. Other companies such as Linde provided expertise in developing forced LHe cooling systems for magnets and closed cycle on board refrigerator designs. As with the EMS development, results and analyses were presented at the annual BMFT Statusseminars (See Appendix I), and involved extensive designs of possible revenue vehicles.

In 1972 it was decided to build a track and test vehicle to acquire basic knowledge into the operation of an EDS system using state of the art cryogenics. The Erlangen Test Carrier (EET-01) represented a full sized test system for levitation magnets working on the normal flux principle. The 17 tonne vehicle ran on an inclined circular test track of 280 metre diameter, at the Siemens Research Laboratories, Erlangen⁽¹¹³⁾. Maximum speed of 150 km/h was reached several times with the vehicle levitated at 100mm clearance by four of the superconducting magnets built. An overall distance

of 1000 kilometres was travelled with energised magnets. The vehicle was first put into operation in 1973, with the chosen propulsion of a double sided LIM with electrohydraulic gap control. The LIM could produce 35kN thrust at low speed and 22kN at the rated speed under an inverter limitation of 5MVA and power limit of 1.2MW for the motor. The drive package was supplied by AEG (LIM) and BBC (inverter) and represented the largest variable voltage and frequency LIM installation in Europe. The motor (AEG No LAZD 3340/9) had a synchronous speed of 248 km/h and the triple layer winding was force air cooled.

Tests performed on the magnets included pre-installation attitude checks. Because the vehicle ran at a 45° inclination and because of the inertial forces on the coolant, forced LHe flow was chosen so that the four constructed levitation magnets and the proposed guidance magnets could adopt similar standard construction that was orientation independent. The levitation magnets were mounted into two subframes within the EET structure, and guidance was performed by the LIM servo controller and auxiliary guide wheels. Levitation characteristics had been calculated by Urankar⁽¹¹⁴⁾ and were confirmed by running tests. Vehicle and track details are given in Table IV.

From design studies for revenue vehicles it became apparent that a LIM propulsion was unsuitable, and that a LSM with active track would provide a better solution. The tests on the EET-01 were not extended to include guidance, so that a LSM programme could be followed. Continued levitation tests included a study of active damping on a EET magnet platform reacting against a watercooled copper mirror coil and on the EET itself at speeds up to 140 km/h, with real disturbances such as ramps and gaps. It appeared that an active control coil with about 3% of the main coil ampere turns could adequately damp motion with about 0.4 kVA/tonne required control power reducing maximum acceleration peaks to 0.1 m/s² from 2 m/s² at a resonance of 2 Hz. Passive damping could reduce this level to 0.7 m/s², but was

only effective to speed ranges below 90 km/h. This contrasts with the CIGGT calculated results that suggest passive damping is adequate for all speeds, even though their vehicle is lighter.

To test out the concepts of ACLSM, Siemens constructed a rotating test rig for air cored linear synchronous motors, ROSY, that had a 5.8 metre diameter and surface speed of 144 km/h⁽¹¹⁵⁾. The main wheel constructional material was propeller plywood, with the stator winding banded on with an epoxy impregnated fibreglass cloth, to take the high centripetal loads. Two separate Brown Boveri inverters each supplied 120 kVA to the split section tack winding, which enable section transition and inverter handover to be examined. Both inverters had a dc link voltage of 510 volts and pwm output with sub harmonic control from 0-52.5 Hz. An EET magnet fixed to a six degree of freedom frame allowed force and moment measurements to be made as the machine ran. Forced LHe cooling became particularly important in the configuration chosen of a vertical axis wheel, since the magnet plane was also vertical. The control concept chosen was based on a Siemens propriety unit known as TRANSVEKTOR, which identified the phase current into its d and q axis components⁽¹¹⁶⁾. No communication equipment is required between the vehicle and the inverter control as vehicle position is calculated from the terminal phase voltages and currents. AS with the CIGGT α and θ control, vehicle speed is given by the induced emf frequency, relative vehicle position is given by the phase of the emf, and the levitation height is determined by dividing the magnitude of the emf by the power supply frequency. In deriving a model of the LSM, an oscillator is phase locked to the emf frequency and the required reference signals can be obtained to feed the control system. Leonhard and Boning devised an alternative control scheme which used a microcomputer to derive force angle, thrust and velocity from the instantaneous values of voltages and currents at the inverter terminals⁽¹¹⁷⁾. The system was tried out on ROSY and gave results in thrust measurement accurate to 5% over the frequency range 53 to 2.5Hz.

Various other methods of vehicle position detection were tried on ROSY, including inductive sensing and an open loop ramp generator using a dynamic model of the vehicle (wheel). These were generally successful as was the correlation of experimental and theoretical predictions of force measurements and operation under pwm inverter control. Transition between sections occurred within about 100ms (compared to about 0.5s for a full sized vehicle) and there was no measurable disturbance in lift or thrust force.

At the end of 1977, the levitation work was completed and the LIM drive was removed from the circular track. During 1978 a LSM winding was installed in the centre section of the guideway⁽¹¹⁸⁾. The track winding was three phase consisting of single cables embedded in concrete winding supports with a plastic based mortar. There were 6 conductors per phase on a pole pitch of 1.4 metres, which lead to a 200 km/h synchronous speed at 20Hz. The track winding was split into two 440 metre sections, one with a copper and one with an aluminium conductor of 84 strands making 240mm² section. The 5MVA LIM inverter was used to power the sections, since it could be split into two similar parts, each with an output of 2.7kV and 500A. The effective track linear current density of 10.6 kA/m led to a thrust of 20kN for an airgap of 250mm and with the two pole magnet assembly, this was sufficient to get EET-02 to 180km/h. The EET-01 test vehicle was converted to take a 3.4 tonne open bath cryostat assembly, MELOT, which contained two 1.2 metre diameter oppositely polarised circular magnets. The superconducting magnets were energised to 1 MAT each, and pitched at 1.43 metres. The helium bath allowed operation at up to about 6 hours without refilling. MELOT was tested on a stationary mock up of the track winding before being installed in the converted EET chassis to form EET-02.

The initial open and short circuit tests were performed using a 150kW dc drive auxiliary on the vehicle in February 1979, at 150 km/h. This motor

could be used for later loading experiments. The control scheme used for EET-02 was essentially the same as that tested on ROSY, but with modifications to allow for the different parameters of various circuit configurations. There is no need for example to include additional phase inductance in the inverter feed line to more accurately simulate a full sized track winding. Control circuitry is included to eliminate dc offset and unbalance in the phase currents, which occurs even though the winding is fully transposed to match impedances.

Projektgruppe Magnetschwebbahn produced a more sophisticated LSM design for the Emsland vehicle, after the decision had been made to use EMS levitation, but a choice had not been made between iron or air cored LSM⁽¹¹⁹⁾. The two section vehicle, each section weighing 68 tonnes, was designed to run at 400 km/h. The required LSM thrust of 160kN was produced by 36 rectangular magnets energised to 1.15 MAT, interacting at an air gap of 300mm with a track winding linear current distribution of 7.5 kA/m. Six magnets were installed in one of three cryostat units per section, fabricated from cast aluminium, with an all up weight of 4 tonnes per unit.

The results of the Erlangen EET-02 tests have not been published, but they are believed to have been highly successful. Despite difficulties in laying the track winding the test programme was completed on schedule at the end of 1979 and both the Erlangen test track and the ROSY test rig have been dismantled. The majority of engineers involved have been redeployed on the Emsland test track, which is being supported by a consortium of companies including the members of Projektgruppe Magnetschwebbahn⁽¹²⁰⁾. There are no further plans to continue either EDS or ACLSM work in the foreseeable future.

2.4.6 UK Development

EDS development in the UK was initially funded by the Science Research Council (SRC). In September 1971 the SRC sponsored research at the University of Warwick and Cranfield Institute of Technology (CIT) to investigate the technical and economic merits of superconducting magnetic suspensions for high speed vehicles, over a twelve month period. Cranfield performed the economic analysis of full sized revenue vehicles and their operational requirements, the configurations being mainly conventional duorail low speed suspensions, normal conducting loop or null flux levitation, and turbo-prop or LIM propulsion. The main conclusion was that such a system of maglev vehicles was economically attractive compared to aircraft at short haul, or conventional duorail trains requiring special tracks⁽¹²¹⁾. Warwick analysed null flux and normal flux arrangements for vehicles that could run in trough guideways and evaluated their basic engineering design parameters and suspension characteristics⁽¹²²⁾.

In 1973, both groups received further funding, Cranfield from the Department of Environment, through the Transport and Road Research Laboratory, and Warwick from the Wolfson Foundation. Cranfield produced further economic study of duorail compatible vehicles and showed that operational and installed costs were consistently less than Tracked Hovercraft designs over many routes. First estimates were made of a far from optimum LSM design which used a dual configuration (two parallel) motor arrays. It was not thought to show significant advantages over a fixed 50 Hz LIM since the track structure became more complex, and little was known of the variable frequency operation and track section switching requirements⁽¹²³⁾.

The Warwick research project was centred on fundamental studies of levitation and propulsion concepts and was tied to design for a linear test facility. The test track was originally planned to be capable of carrying a 600 kilogramme magnetically levitated, guided, and propelled vehicle at up to 120 km/h with two passengers, or 250 km/h, unmanned. The main guideway would

have been a pier structure with a glass fibre reinforced concrete top deck to which the track conductors could be fixed. The effect of rapid inflation and a fixed value grant meant that the final design was for a 150kg unmanned vehicle on a 550 metre track with timber decking and a cable winched propulsion system.

Fairly early on in the project, tests with a three phase meander winding in a 1.5 metre diameter circle and a multipole ferrite field showed that LSM control could be achieved with low frequency starting. The armature current was 30 amperes, supplied from the slip frequency of a wound rotor teaching machine. The machine power factor was monitored to prevent pull out as the frequency supplied to the armature was raised. Reed relays around the outside of the track provided field position information which was compared to the induction motor slip frequency as an additional check on the force angle. As the experiment was successful, it was decided to build a more substantial apparatus using concentrated turns on the periphery of a 0.5 metre diameter drum, with a stationary field array of barium ferrite magnets. The armature winding eventually consisted of 24 concentrated turns on a double layer three phase connection. Power to the winding was supplied through slip rings close to the drum axle. A commutator was included to provide position information. The double layer winding was chosen as it gave reasonable packing density at the track and easy location of the potted winding was possible. A meander winding would have required a circumferential band to prevent conductors from lifting, and this would have reduced the cooling effect of wheel windage. The drum was also fed from the wound rotor slip frequency, and with the more accurate identification of armature pole position relative to the field, satisfactory control of the machine was possible on ramp frequency starting.

In parallel with the LSM tests, experiments were carried out using nitrogen cooled copper ac coils in various topological configurations. Conventional EDS of Maglev had provided vertical surfaces for guidance but SRI had experienced lateral instabilities on their towed test vehicle. Abel explained this as being a shaded pole action as the levitation magnets passed close to the edge discontinuity formed by the vertical and horizontal aluminium track members⁽¹²⁴⁾. Since CIT had shown the advantages of a flat track arrangement as being compatible with existing duorail systems, and allowing relatively easy switching, the ac coil experiments centred on flat track arrangements. It was found that by designing in a dual edge discontinuity lateral guidance could be achieved and the stiffness available was adequate from ride quality considerations, being a similar frequency to levitation. The simplest structure was a duorail of aluminium sheets with a central longitudinal gap and a transverse spanning coil, overlapping in plan the guideway conductor. Although the amount of superconductor required for levitation is increased, the amount of track conductor needed is substantially reduced. The central gap also allowed a track armature winding to be positioned under the maximum vertical field of the coil array producing combined lift, guidance and propulsion.

This "flat track" design was therefore a conscious effort to produce a self cleansing guideway that was easy to fabricate and switch, could be made compatible to existing duorail systems, and provided combined levitation, guidance and propulsion with at the minimum, one tandem magnet array. Controlled lateral stiffness could be designed in depending on the coil/guideway conductor overlap. As such it was a hybrid of the CIGGT and MIT designs, CIGGT having a flat track with separate lift and guidance systems, and MIT having a free rolling vehicle in a cylindrical trough. MIT attempted to control lateral (roll) stiffness by an additional keel magnet only much later on in their research.

A study of LIM research showed that Laithwaite and Eastham's transverse flux designs were appropriate for LSM too, and would benefit a revenue design. EDS magnets tend to require length in the direction of motion with minimal transverse end conductor; LSM magnets require the opposite. For a combined system a transverse flux arrangement means that long longitudinal pole pitches, and the resulting increases in ampere turns in the magnets can be replaced by relatively short flux paths across the vehicle width. This will keep magnet ampere turns low, and reduce the magnitude of the stray field in the passenger compartment, easing the amount of shielding required to meet design limits on passenger exposure. One revenue track that was examined is shown in Figure 6a⁽¹²⁴⁾. The windings have cranked end sections to minimise lost width, and can lay under the levitation conductors. The superconducting magnets are transverse flux energised providing tight lateral magnetic coupling. The LSM windings form a dual, and can be excited either separately to give yaw and roll control, or in conjunction. Width limitations on the Wolfson track meant that a single tandem magnet array had to be studied (Figure 6b). A dual LSM was later analysed by Burke for the CIGGT reference revenue vehicle⁽¹²⁵⁾. The linear machines studied as possible propulsion units included homopolar synchronous, induction and synchronous. The LIM, including transverse flux variants was discarded quickly, as its dependence on small gaps for reasonable performance was incompatible with large gap EDS Maglev even when mounted on a separate gap controlled tug. Homopolar machines were considered difficult to implement because with passive track secondaries, substantial amounts of power would have to be transferred to the vehicle. It was recognised that their power factor efficiency product should be superior to a LIM⁽¹²⁶⁾, because air gap magnetization derives from a dc winding. Preliminary designs of LSM track windings for the Wolfson facility showed that to achieve high accelerations with a modest number of vehicle coils, the track current loading had to be high. If the

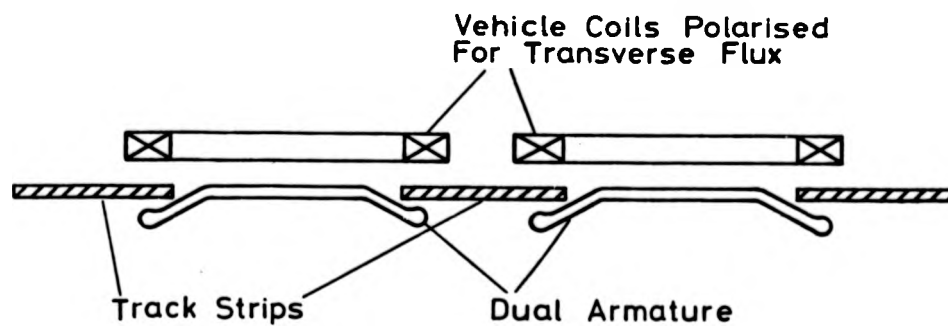


FIGURE 6a. REVENUE VEHICLE TRANSVERSE FLUX DUAL MOTOR.

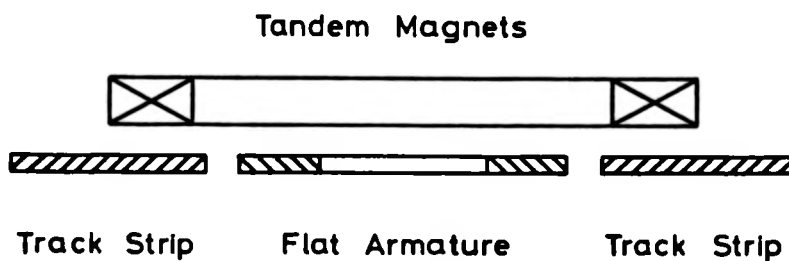


FIGURE 6b. WOLFSON TRACK ARRANGEMENT.

acceleration section (200-300 metres) was wound as one LSM unit, feeder voltage and track drop became significant for the impulse duty. The natural solution was to reduce the section length until it was slightly longer than the vehicle length, and to use trackside switches to energise the winding in response to vehicle position. In the limit the track switching could be performed on pole pitches less than the vehicle length, and the inverter or cycloconverter operation effectively transferred to the trackside. Such a machine can be described as a Linear Commutator Machine (LCM), and a parallel study of LSM and LCM was begun⁽¹²⁴⁾.

The three phase winding on the 0.5 metre diameter drum was reconnected as a LCM. Each coil had an individual thyristor whose gating signal was provided through moveable brushes running on the commutator. The 50Hz mains frequency was used to turn off the thyristors as the coils passed under the three pole pieces, so that the correct armature current paths were assured. By changing when the coils were energised relative to the pole positions, the machine could motor and brake. A superconducting coil 130mm square running at $3.7 \cdot 10^4$ AT was designed to model winding construction techniques and coil stresses for the Wolfson coils, and was used to drive the LCM with the ferrite poles removed. The superconducting machine was successfully operated several times, and the ac induced on the superconducting magnet did not affect its stability. A public demonstration of the superconducting LCM was made at the INTERMAG Conference in London September 1975, where it aroused a great deal of comment.

After a more detailed investigation of the LSM and LCM designs, using mutual inductance and equivalent circuit models it became apparent in 1975 that construction of a linear motor on the test facility would not be possible, because of limited finance. The vehicle dimensions were shrunk to two tandem 0.4 metre square coils housed in a cryostat and body shell 2.5 metres long by 0.5 metres wide and high. The vehicle propulsion winch

was capable of driving this load up to 160 km/h. Analytical studies of the flat track were based on impedance models, and Howell and Wong investigated the stability of vehicles travelling over split guideways, as applied to revenue duties⁽¹²⁷⁾.

The Science Research Council awarded two further grants to Warwick to support research into ac losses in composite conductors for magnetic levitation, and power generators, and also to extend the LSM and levitation analysis by measurements taken on a newly constructed test wheel facility. The test wheel was built from non magnetic materials on a horizontal axis. The surface speed was 160 km/h to match the Wolfson facility top speed. The wheel diameter at 3 metres was made from a plywood box section built between eight aluminium I beams. Speed control was through a Ward Leonard set derived from previous Departmental MHD experiments, and the drive motor was mounted on one of the concrete bearing pedestals. The outer rim consisted of plywood laminations secured by a final multilayer addition of epoxy impregnated fibreglass⁽¹²⁸⁻⁹⁾. Initial tests on levitation characteristics of split track guideways were performed on two aluminium rings that were thermally shrunk onto the wheel.

In 1976 Abel and Mahtani produced an assessment of LSM as used for maglev systems⁽¹³⁰⁾. The combined system of propulsion, guidance and levitation developed at Warwick used essentially tandem arrays of superconducting coils. From the levitation and guidance viewpoint long lengths of conductor were necessary in the direction of motion, and from the propulsion point of view, long lengths were required transversely. It was important therefore to attempt to establish optimization techniques that could indicate not just specific parameter optima, but also their sensitivity to change in the other base parameters. The assessment also clarified the wavelength optimisation for specific vehicle length. Thornton had previously tried to optimise wavelength on the basis of

thrust per pole maximization. However this assumes that vehicle length is unlimited, and the vehicle's thrust requirement can be matched by merely adding poles as necessary. A preferable approach provides maximization of thrust per unit of active conductor times current, which results in a wavelength choice about 1/3 of the MIT value. By performing a cost analysis, MIT, CIGGT and a full size LCM design with a 300 metre excited length were compared. It was discovered that wavelength choice is only loosely coupled to overall cost, so for a combined system a LCM with a relatively long pole pitch (to suit lift and guidance stiffness requirements) does not in fact pay a heavy penalty, and can be shown to be marginally cheaper than the other two systems.

Another study investigated the sensitivity of design to changes in coil shape⁽¹³¹⁾. Abel evaluated the coil stresses and field variations that occur as a rectangular or square coil changes its corner radius until a racetrack or circular coil is formed. Howell used the impedance modelling technique to establish the change in lift to drag ratio and lateral stiffness of an array of coils with a split track. It was found that from the coil stressing criteria, circular coils were preferable, but the motor performance suffered, requiring increased ampere turns or increased active length. The latter requirement is in conflict with lift to drag and lateral stiffness of circular coils, which require decreased split gap to maintain adequate values. The drag magnitude also increases with a circular array. The parameters can all be carefully manipulated to provide adequate standards of ride quality with reasonable stress increase factors on circular coil standards. Even for the worst case of a circular array the split track geometry shows economic advantage over other track designs.

In 1977, Leonhard published a comparison study of the EMS and EDS systems proposed by the Maglev groups in Germany⁽¹³²⁾. In the comparison

power consumption figures were given which suggested at first sight that EDS vehicles use over two and a half times as much active power as EMS vehicles. In order to establish the exact power balance in each of the cases, Abel examined the source material of the designs and presented it in such a way that active and reactive power requirements for different operating regimes were totally qualified⁽¹³³⁻⁴⁾. The main conclusions were that the EDS LSM was the most suitable form of propulsion for 400 and 500 km/h, the iron cored long stator LSM for EMS appeared to have reasonable characteristics at 400 km/h but these were degraded at 500 km/h, and that the LIM's studied by the Germans were unsuited to 500 km/h and did not perform particularly well at 400 km/h. It was obvious from the study that a strict comparison of system lift to drag ratio and specific power were insufficient to fully define the operating parameters, and a lot more detail was required.

In a continuation of the study it was shown that the German EDS design was further penalised by not adopting the aerospace type vehicle structure used by other EDS design groups⁽¹³⁵⁾.

Assembly difficulties had arisen with the Wolfson cryostat. Because the lid and body were made to be light weight structures, the side mating flange was of insufficient thickness to allow repetitive joining.

Distortion of the body had to be pulled out when the lid was fitted. Despite many attempts, an adequate vacuum was not achieved on the cryostat, and persistent cold leaks occurred on the coil and helium fill structure. A new lid was constructed with bracing ribs which were finally adequately secured by Alvis Ltd, who welded an additional flange onto the lid and base. The box could then be pulled to better than 10^{-6} torr and it was hoped that cryopumping would be possible from the coil assembly to further reduce the vacuum.

Both the LN_2 radiation shield and the coil assembly had insufficient attention paid to balancing the flow paths of liquid and gaseous nitrogen

and helium. The coil assembly had only a single 10mm tube for both fill and vent. Consequently there was no possibility of circulating cold gas through either structure. The coil assembly was repiped and the Rutherford Laboratory performed a nitrogen quench and leak checks on the structure. On its return to Warwick the coil assembly was rechecked for integrity. The radiation shield had had several unsuccessful attempts at cool down to nitrogen temperatures within the cryostat. Although there was no apparent cold leak into the interspace, support heat leak, radiation and high coolant path resistance resulted in a steady state being reached with the nitrogen shield at about 100K, and no liquid being retained. The radiation shield was discarded and the coil assembly was wrapped with superinsulation from Thor Cryogenics. The assembly was never completed because of lack of funding.

The Wolfson track was used for aerodynamic studies both under the initial funding, and then under separate SRC research by Howell. The 3 metre test wheel was successfully run by Mahtani, with published results of levitation tests on the split track, using first the small superconducting coil built and used on the 0.5 metre drum, and then using liquid nitrogen cooled pulsed coils. SRC further sponsored the continuation of work on the test wheel, and an interim report described progress⁽¹³⁶⁾. A LSM design for the wheel by Rakels was included, and details of a 375 kVA inverter that Brush had used on the Mickleover LIM tests and loaned to the Maglev Group were given. It was hoped that the next stage of development would be a full width winding on the wheel with a multipolar field assembly of superconducting or liquid nitrogen cooled pulsed coils. The wheel tests would confirm machine performance and establish control concepts incorporating active ride quality manipulation.

Towards the end of 1978 and in early 1979 a cooperative research programme was suggested which would revive interest in air cored LSM in the UK. The basic concept was for a hybrid system of transportation which

used the state of the art in both conventional wheeled vehicles and linear synchronous motors⁽¹³⁷⁻⁹⁾. By producing for example a LSM propelled Advanced Passenger Train, the advantages of APT tilting suspension and novel bogie design could be married with the simple track structure and ease of control and non contact transfer of thrust achieved by a LSM. Such a hybrid would be capable of operating on existing infrastructure, and would have initial lower first cost to conventional electrification schemes. The programme involved industry and the SRC in a cooperative funding of LSM research on the Warwick 3 metre wheel and 550 metre track facilities. Although the industrial sponsors were keen to pursue the development, they required at least British Rails' tacit approval of the scheme. Unfortunately BR failed to provide such approval and the application to SRC was not made. It is interesting to note with hindsight that of the parties involved in the first programme discussion meetings, namely British Rail, BICC, Balfour Beatty, Brush, Farebrother, Thor Cryogenics, the first four make up the new People Mover Group formed shortly afterwards to develop the British Rail EMS Maglev installation for Birmingham Airport⁽⁷²⁾. The purpose of promoting an exportable system is the same aim as discussed in the meetings at Warwick.

British Rail had performed their own research into LSM and EDS following discussion with Warwick University in 1976. Their funding came directly from the Department of Transport under an Advanced Ground Transport Consultancy Contract, to look at areas which were thought to have limited theoretical and experimental data. A linear desk top model was constructed, on which no meaningful measurements of force could be made, because of incorrect choice of field to armature ampere turns ratio⁽¹⁴⁰⁾.

2.4.7 French Research

French research into EDS and LSM propulsion has been mainly the concern of SNCF's Technical Division Research Department. Both EDS and EMS were the subject of a technical evaluation program which produced a design methodology for magnetically levitated and linear motor propelled trains. SNCF wrote a computer based model SYSMAG (Systèmes Magnétiques) which could calculate performance characteristics of the two Maglev systems⁽¹⁴¹⁾. The model was based on cooperative work from the Battelle Institute, Geneva, and the Institut National Polytechnique, Grenoble. LSM analysis was given a similar treatment, and a simplified theory and performance evaluation based on gradients of mutual inductance between conductors was encompassed in a programme called MOSYN⁽¹⁴²⁾. In common with British Rail, SNCF saw no conceivable future for Maglev in a European context.

2.5 Other Machine Variants

This section describes those remaining machines that have not been specifically mentioned with the previous suspension systems. The three main types are linear induction motors, including the combined ac propulsion and guidance/suspension systems of Rohr, Boeing, and Laithwaite and Eastham; iron cored linear synchronous and reluctance machines, especially those with a dc bias winding, and the JNR linear dc machine development.

Linear induction machines have inspired the large majority of linear machine research effort throughout the world over the last twenty years. There are two major specialist books on the subject^(143,144), a bibliography⁽¹⁴⁵⁾, and a multitude of descriptive and qualitative articles (eg 146-9). Although the German EMS Maglev Group have abandoned LIM as being suitable for speeds of 400 km/h, JAL propose to use single sided LIM (SLIM) for 300 km/h. The low power factor-efficiency product provoked investigation of iron cored LSM with a dc winding on the

stator providing the bulk of the airgap magnetization; the power supply sees a higher power factor as a result and the product is significantly improved. However the trade off of increased track structure cost and the energy cost is far from simple, and relatively complex analysis of the machines and their operating cycle are required before adequate judgement can be made between the two options.

JNR have developed an air cored track, iron cored field linear dc machine which uses thyristor commutation. The characteristics of the machine make it suitable for 300 or 500 km/h operation and it provides a backup development to the main cryogenic LSM and EDS research.

2.5.1 Linear Induction Machines

2.5.1.1. Linear Induction Motor Research Vehicle

The Linear Induction Motor Research Vehicle (LIMRV) was built by AiResearch Manufacturing Company^(18,150) to meet the Department of Transportation's requirement for full sized linear induction motor testing. The vehicle was meant to run on a 35km oval track at Pueblo, although only 10km were eventually built. It was felt that this vehicle would give insight into large LIM operation and characteristics that could be applied to other transport systems, such as high capacity brakes, classification yards, magnetic levitation and air cushion vehicles. The LIMRV suspension and guidance was derived from a set of steel wheels on steel rail, at standard gauge. Because of the relative unknowns of vehicle-track dynamic interaction at speeds up to 400 km/h, British Rail were consulted during the suspension design.

The double sided forced air cooled 1.86 MW LIM was supplied with variable voltage and frequency from a 3MW alternator which in turn was driven through a reducing gearbox from a gas turbine. There was therefore no need for current pick up. The aluminium alloy reaction rail was a hollow extrusion held to bed plates by spring clips, and welded every 30 metres to the next section. The stator was guided about the reaction rail by four

pairs of wheels, and was separately linked to the main vehicle frame. The LIM used a conventional five-sixths pitched double layer winding with diamond coils, and the lower end windings were cranked at right angles to the slots to allow a shorter reaction rail to be used. Table VI gives details of the LIM and Vehicle.

The contract from DOT was begun in March 1965 and design and construction of the LIM began in July 1967, followed a year later by the vehicle. Static tests of the LIM were carried out in 1969, and throughout 1970 till March 1971, the whole vehicle and installed LIM were given proving tests on a 500 metre track at the AIREsearch Works in Torrence, California. The inaugural LIMRV run was made at the official opening of the Pueblo Test Center with the DOT Secretary Volpe on board⁽²⁰⁾, in May 1971.

Subsequent tests on the LIMRV were carried out at various speeds on the 10km track, and it was decided that instead of completing the 35km oval, it would be cheaper to use two jet thrust boosters attached to the vehicle body. These allowed a maximum speed of 410 km/h to be reached on 14 August 1974, and running tests of the LIM at full speed and thrust within the short track length⁽¹⁵¹⁾. In late 1976 and 1977, tests were made with varying numbers of poles, to investigate the changes in LIM performance by extending the iron to the rear of the primary excitation. This was effected by exciting only the front five poles of the stator, and comparisons with only the rear five poles suggested that improvements with trailing iron were only minimal⁽¹⁵²⁾. Selective pole excitation allowed investigation of the mmf air gap waves induced by the finite length of the primary current sheet, or so called end effect waves⁽¹⁵³⁾. It was planned to convert the track to a single sided configuration in 1978. The LIMRV has had major implications in confirming theoretical calculations, and the DOT have used and collated five different theories, namely those of Elliott, Bolton, Oberretl, Yamamura and Mosebach. In the majority of cases the models predicted thrust and real input power fairly

TABLE VI LINEAR MACHINE TEST TRACKS

Vehicle	LIMRV	ICTS, TVI	BRAF-1	RTV	DCLM
Length x width x height, m	17.5 x 3 x 2.13		2 car DMU		6 x 1.6 x 0.7
Maximum speed, km/h	410	72	80		200
<u>Guideway</u>					
Location	Pueblo	Toronto	Mickleover	Loughborough	Tokyo
Length, km	10	2.5	0.240	0.080	0.500
<u>Motor</u>					
Type	DSLIM	SLIM	SLIM	HELIM	DCLM
Manufacturer	AiResearch	Thomson	Brush	Brush	JNR
Type No		TLM 134	BRAF1		
Weight, tonne	2.95	0.57	0.263		3.3
Thrust, kN	16.7	11	6		20
Voltage, V	0-1040	0-600			
Frequency Hz	0-173.3	0-40	0-50		
Armature Current, A					24kAT
Field Current, A				20	116.85 kAT
Power, kW	1865	130		55	~1500
No Poles	10	6	8	5	8
Pole Pitch, m	0.3556	0.287		0.18	0.60
Length, m	3.81	1.935	1.1	~0.99	4.8
Airgap, mm	38.1	11	~13	10	85
Synchronous Speed, km/h	450		86.4		
<u>Track</u>					
Thickness, mm	6.35				
Width, m	0.546		0.2		
Material	6061-T6Al	Al+Fe	Al+Fe	Fe	

close to measured values⁽¹⁵²⁾. They also all predicted similar airgap flux density distributions which showed a marked difference to the measured values, due mainly to additional leakage flux in the real machine producing a much higher value of slot leakage inductance. The consequence was optimistic estimates of power factor and reactive power levels.

2.5.1.2 Transverse Flux LIM

Laithwaite and Eastham were primarily responsible for developing the transverse flux LIM⁽¹⁵⁴⁾ (TFLIM). With conventional axial flux design, the pole pitch of a machine running at high speed would have to be large for 50 or 60 Hz operation, and the core depth and hence primary mass would also be large. Although variable frequency to higher frequencies would partly solve the length of pole pitch required, the payload of a vehicle would be reduced with an on board inverter. By examining the topology of the magnetic and electrical circuits, a transverse flux arrangement showed positive advantages. Primarily the core need only carry the slot flux rather than the pole flux, reducing the back iron depth, which is now independent of pole pitch.

A small machine was built by Linear Motors Limited and tested on the RTV41 test track at Tracked Hovercraft Limited, which was later passed to Brush Electrical Machines at Loughborough. The concept of the TFLIM was further extended to that of the "Magnetic River"⁽¹⁵⁵⁾ where the machine was proposed to give levitation, guidance and propulsion, by careful design of the magnetic and electrical circuits. This total suspension design was later suggested to be uneconomic in the primary reactive power requirement for the machine, when used as a high speed vehicle propulsion unit, but a TFLIM which provided one other force, either guidance or levitation was considered to still perform better than a conventional axial flux LIM⁽¹⁵⁶⁾ (AFLIM). The experimental work at Brush also confirmed that while TFLIM were more easily constructed and could generate additional forces compared to AFLIM, neither showed particular promise for high speed

propulsion simply because of the low power factor efficiency product⁽¹⁵⁷⁾.

2.5.1.3 ROMAG

J A Ross developed a system called ROMAG at Rohr Industries Inc. in 1970, which used a linear induction motor to provide both lift and thrust^(17,158,159). The track could be solid ferromagnetic rails for cruise, and laminated when higher thrust efficiency is required. The rails could also be notched to provide reluctance motor operation, and for even higher thrusts, short circuit bars could be placed in the track steel to give an effective damper cage winding. Two vehicles were built, a 20 passenger configuration which was demonstrated at Transpo '72 and a 6 passenger suspended vehicle at Rohr's Chula Vista test track. Both vehicles used a motor at each corner and PWM inverters. Preliminary reliability assessment gave meantime between failures of 53 thousand hours of operation.

In 1979 Boeing Aerospace Company received a research and development contract from UMTA to develop an integrated magnetic levitation and propulsion conceptual vehicle, which could carry 12 passengers at 65 km/h⁽¹⁶⁰⁾. Boeing acquired worldwide rights to ROMAG technology and renamed the system Mag-Transit. The project will involve building a full size prototype vehicle and test track. The power collection will be at 600v dc and power FET PWM inverters will allow high conversion efficiencies. The track will use an aluminium cage winding in a laminated rail.

2.5.1.4 Integrated Suspension/Propulsion System

ROMAG was initially aimed at low speed urban vehicles, but Rohr also proposed the use of LIM as an integrated suspension/propulsion system (ISPS), in 1974 for speeds up to 500 km/h. The US DOT sponsored an analytical modelling and laboratory experimentation program under TARP control⁽²¹⁾, with the Metrek Division of the Mitre Corporation

producing the analysis and design, the Rohr Corporation fabricating the LIM, and the CIGGT performing the experiments on the Queen's University Test Wheel. Mitre's preliminary calculations suggested that it was possible to offset the SLIM to the reaction rail to provide guidance forces (as with the Krauss-Maffei EMS). The analysis combined a two dimensional field approach to obtain self and mutual inductances and a circuit approach to evaluate thrust, lift and guidance forces, and allowed adequate description of transverse edge effects⁽¹⁶¹⁻²⁾.

The reaction rail was fitted to the CIGGT test wheel plywood rim, and the existing geared 110kW dc motor used to propel and brake the SLIM. Additional braking was required for full motoring operation, and locomotive type air brakes were used on a steel hub disc. The main parameters of the motor are given in Table VII. The stack length was 1.73 metres with 6 poles and half filled end slots. The Reliance Electric Company supplied the 200 kVA (350kVA peak) PWM inverter⁽¹⁶³⁻⁵⁾.

Two reaction rails, a cage rail and a solid steel rail have been tested; it is planned to study a sheet reaction rail by mounting an extruded cap onto the steel rail, to allow comparisons of three main rail configurations. Typically the tests performed ran the curved face SLIM at an air gap of 15mm and search coil data for airgap, tooth root and tip, pole and yoke flux densities were recorded. The primary was mounted in a force balance so that the six degrees of freedom could be measured, at speeds of up to 90km/h. Performance characteristics were measured throughout the plugging, motoring and dynamic braking speed regimes. The conclusions of the tests were that end effects did not dominate the design at the measured frequencies and speeds. For the steel rail secondary, it was found that transverse edge effects are apparently insensitive to rail widths greater than core width.

TABLE VII LINEAR MACHINE TEST RIGS

<u>Wheel</u>	ISPS	HELMS	HLSM	Toronto	Sussex	DCLM
Diameter m	7.8	1.1	1.4	1.98		1.73
Tip speed km/h	72	~ 68	402	108	18	500
Location	Kingston	Nottingham	Schneectady	Toronto	Falmer	Tokyo

Motor

Type	SLIM	HELMS	HLSM	HLSM	LRM	DCLM
Manufacturer	Rohr	Brush	GE			JNR
Weight kg				93		
Thrust N				240		
Voltage V	0-460		140		0-30	800
Frequency Hz	5-56	0-50	0-394.3	0-138	0-20	
Armature Current A	50-500	30.5	370	60		8.32kAT
Field Current A		80		15		
Power kW		~ 12	112			
No poles	6	6		3	4	1
Pole Pitch mm	250	180	141.7	109.2	150	
Chording	7/9		5/6	5/6	5/6	
Length m	1.73	1.15	0.85			
Stack Height mm	100		76			
Stack Width mm	101	400	410	55	152	
Airgap mm	10-30	20	15.2	5-10	12.5	

The maximum operational speed would be determined by the specific weight of the power conditioning unit (PCU), accepting that minimum airgap, required guidance to lift ratio, minimum acceptable lift to weight ratio for the SLIM have to be selected from mechanical considerations. With accepted state of the art values, maximum speed of an ISPS system can be approximately 300 km/h.

2.5.1.5 Intermediate Capacity Transit System (ICTS)

Following on from the Canadian Government's involvement with the Krauss Maffei scheme for a Toronto transportation system, the Urban Transportation Development Corporation (UTDC) were commissioned in 1975 to design, construct and test a rapid transit system which could provide a high level of service in the range of 5-15 thousand passenger per hour in both directions. UTDC's main contractor was Canadair Services Ltd (CSL) who designed a steerable axle truck to allow tight radii and low wear rates to be achieved⁽¹¹⁶⁾. Spar Aerospace Products Ltd designed and built various SLIM which were tested on their own 400 metre track⁽¹⁶⁷⁻¹⁶⁸⁾.

The UTDC constructed a test centre at Kingston and this included a 2.5km track with LIM reaction plate, steel rails and current pickup. A six percent gradient was built into the track and a 35 metre radius curve formed part of a loop around a mockup station platform and pair of sidings with maintenance shed^(169,170). The centre was opened on 29 September 1978, and the prototype test vehicle TV1 began the experimental system evaluation. The LIM for the ICTS, TLM134 was manufactured by Thomson Electrical Works Ltd and used a diamond 4 slots per pole winding in a 6 pole 1.935metre long stator. Motor details are given in Table VI. The motor was rigidly fixed to the steerable truck axles' bearings with a three point suspension system. The nominal airgap of 11mm is increased at the centre of the stator by a set bow to accommodate unequal thermal expansion within the stator. Air cooling in motion is assisted by ten fans over the stator end heads. The motor slip frequency was varied in conjunction with

the automatic train speed control, allowing headways down to 60 seconds at the top speed of 72 km/h⁽¹⁷¹⁾. High thrust and deceleration were possible since force transmission did not rely on the steel wheel on rail interface.

Following successful system evaluation it is planned to build two lines in Toronto, both about 6km long, one linking Union station with southern Toronto, and the other connecting industrial and residential zones in Hamilton.

2.5.1.6 Brush-British Rail Mickleover Tests

Brush Electrical Machines produced an experimental axial flux LIM under contract to the Department of Industry^(157,172-3). The machine, which could generate up to about 3kN of thrust was tested on the British Rail Research site at Mickleover near Derby, in 1976, with Brush and British Rail cooperation. 240 metres of aluminium reaction rail were laid on the top cheek of a steel I beam placed between a conventional duorail. The stator weighed 263kg and was supported on load cells to a bogie of a self powered two car rail set. On board conditioning consisted of a Brush 375kVA twelve pulse voltage fed inverter, with a resonant power controlled chopper to vary the dc link voltage. Tests could be performed with the train set running at a constant maximum speed of 80 km/h, and the motor taken through motoring, plugging and regenerative braking by setting the slip through the inverter frequency control. Machine details are given in Table VI.

A variety of track joints were tested to investigate their importance on the eddy current patterns in the secondary. Forced air cooling was employed to give up to three times the power output from an uncooled stator. Maximum apparent efficiency at 12mm air gap was 0.31.

2.5.2 Linear Synchronous Motors

The LSM in this section all have passive iron secondary track structures, with iron cored primaries carrying one or two superimposed windings. The

homopolar inductor and heteropolar linear synchronous machines (HLSM and HELSM) both have an ac and a dc winding which allows a theoretical unity power factor operation, as far as any on board converter is concerned. The linear reluctance motor (LRM) and its variants use the track saliency to provide reluctance interaction with a single ac primary winding. The LRM has a low power factor, since air gap magnetization is derived from the ac supply, but its overall performance is theoretically superior to a LIM. The existence of substantial normal forces have suggested that these LSM and the LRM may be used as combined suspension and propulsion systems.

2.5.2.1 Heteropolar Linear Synchronous Motors

The original HELSM was proposed by the North American Rockwell Corporation⁽¹⁷⁴⁾. The "Nadyne" track structure consisted of the claw-pole arrangement, where alternate north and south polarized blocks were connected to outboard longitudinal rails as shown in Figure 7. The dc magnetization was produced by a field winding establishing a transverse flux into the side rails. Within the field C core an axial flux armature winding produced the ac mmf wave linking the alternating north and south claws, and provided the closing path for the field flux. The machine consequently has a relatively long magnetic path, and a doubling of the air gap length.

Claw-pole machines were supplied by Rockwell to Disney World for a synchronous low speed operation. Due to difficulties with drift of the analogue control system the machines could not be made to operate synchronously so the dc winding was left unenergised and a reaction rail built in to allow induction motoring. It was hoped that at a later stage digital control would enable the inverters to track the vehicle motion successfully.

US DOT funding since 1973 prompted Levi to include the claw-pole machine as a more promising alternative to SLIM for high speed ground transport propulsion⁽¹⁷⁵⁻⁸⁾. In the preliminary study the claw-pole showed a

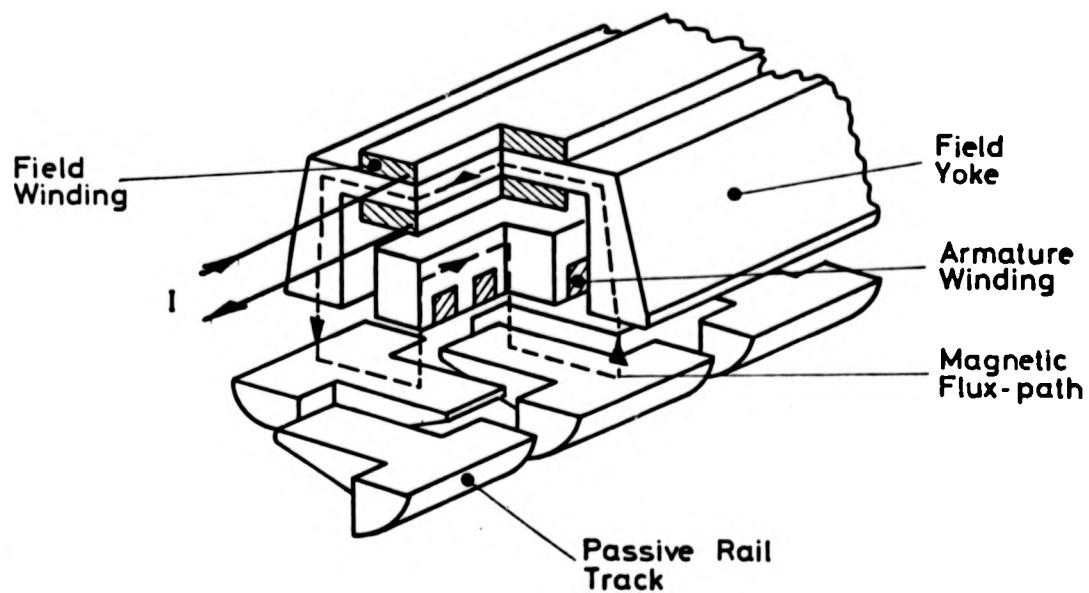


FIGURE 7. CLAW POLE MOTOR

power to weight ratio of 5.5 compared to 3.7 for HLSM and 2.5 for SLIM (kW/kg). A further 30 month exploratory study by General Electric for a 400 km/h, 5000hp comparison⁽¹⁷⁹⁾ suggested that this ratio should be modified to HELSM 0.48, HLSM 2.9, SLIM 0.9. For this reason the HELSM development ceased, and emphasis was placed on the HLSM in USA.

Levi also considered another form of heteropolar machine, in which the field windings and the armature windings produced fully longitudinal fluxes (Figure 8)⁽¹⁷⁸⁾. The track members are more simply made, but now require a fine lamination because they see high frequency alternating flux as the vehicle passes. This configuration only received a cursory examination before it was discarded as unsuited to ground rail transportation, because of increased track complexity.

Eastham designed a modified heteropolar machine based on a transverse flux core⁽¹⁸⁰⁾, where both the ac and dc winding fluxes were strictly transverse (Figure 9). The track structure then became simpler, being only staggered slabs of iron without side rails. A laboratory static model was built, followed by an arch motor mounted on a drum. Initial tests⁽¹⁸¹⁾ suggested that a fixed torque angle of 90° provided maximum output at near optimum efficiency, and that pole shaping and coarse lamination could improve power factor by reducing the longitudinal edge effect.

Brush built two motors based on Eastham's transverse flux principle but, to ensure mechanical rigidity used an axial flux longitudinally laminated core and side limbs with keyed in transverse laminated back iron carrying the dc winding⁽¹⁷²⁾. The linear motor had 5 poles and ran at a 10mm gap on the 80m test track at Brush⁽¹⁸²⁾ (Table VI). Several different pole shapes were tested as well as the original rectangular design, including T's and trapezoides. The trapezoidal poles attempt to maximise the useful plan area of the air gap, decreasing the effective reluctance at both the edges and centre. Search coils indicated that the flux paths were not wholly transverse as expected, and that a partly axial path was followed.

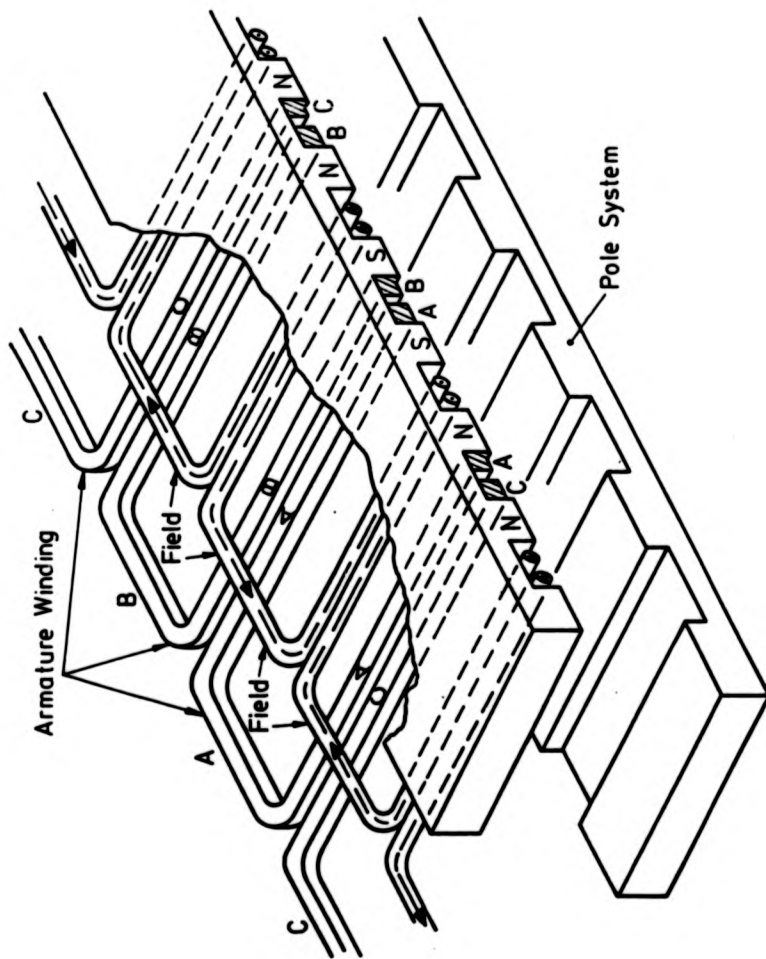


FIGURE 8 HETEROPOLAR INDUCTOR MOTOR

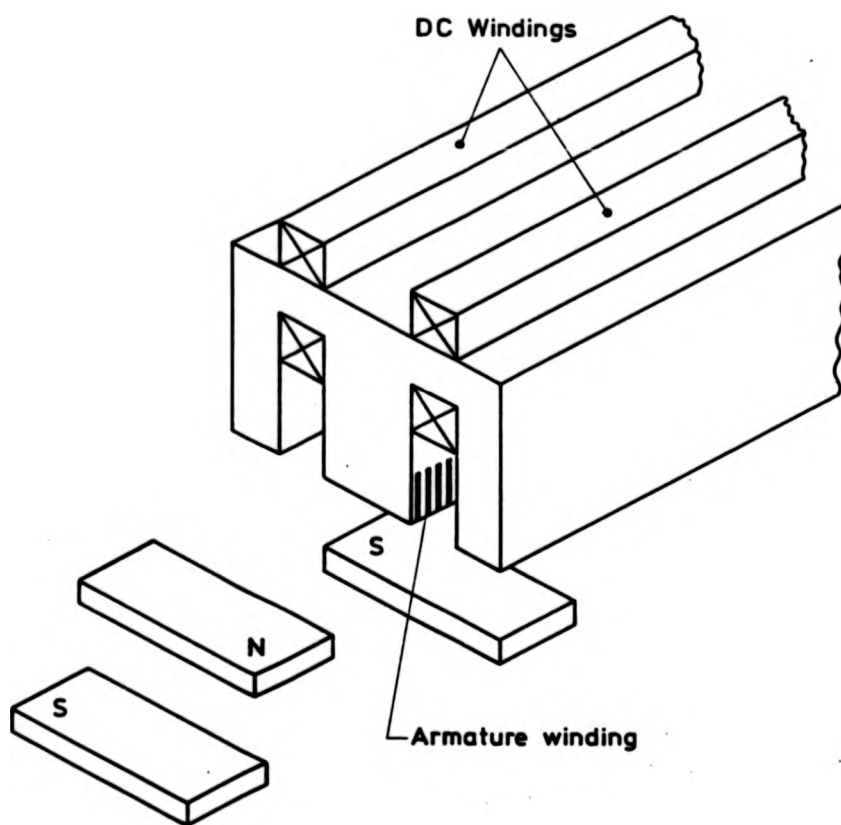


FIGURE 9 ABERDEEN TRANSVERSE FLUX HETEROPOLAR MACHINE

An improved core design with pole face windings on the outer limbs for the dc magnetization, solid back iron and axial flux centre limb was suggested for future designs.

The rotary version was tested at Nottingham University, and was built as a six pole arch motor reacting on a 1.1 metre drum (Table VII). It showed up the weakness of the design in that only about 11 percent of the dc coil flux reached the slotted armature core⁽¹⁸³⁾. Computation and test allowed pole shape optimization to be performed, with final close agreement between experiment and calculation. Work continues at Nottingham to design and test a HELSM which combines levitation with propulsion, to meet the Science Research Council Advanced Ground Transport Panel's specification for a 72 km/h, 3 tonne vehicle.

2.5.2.2. Homopolar Linear Synchronous Motors

Kemper's scheme for combined levitation and propulsion was based on a HLSM⁽¹¹⁾. The track consisted of an iron rail with side staggered poles which were cross magnetised by a dc winding on the back of an axial flux parallel pair of armature laminations (Figure 10). The armature slots were filled by straight through windings. Separate guidance magnets reacted against a vertical iron plate placed above the main rail. Nearly two decades later, Leitgeb at Siemens followed on the development with double sided designs for combined propulsion and guidance, which had the advantage of a very simple rectangular block track structure^(184,185). The LSM was to be used on an urban vehicle H-Cabins. The field winding could be either on a yoke straddling the vertical track, or split and placed behind each armature block (Figure 11 a,b). In the later case one half of the machine resembled Kemper's design. Leitgeb also suggested a single sided version in which one armature block reacted with an array of rectangular blocks mechanically supported by thin backing iron⁽¹⁸⁶⁾.

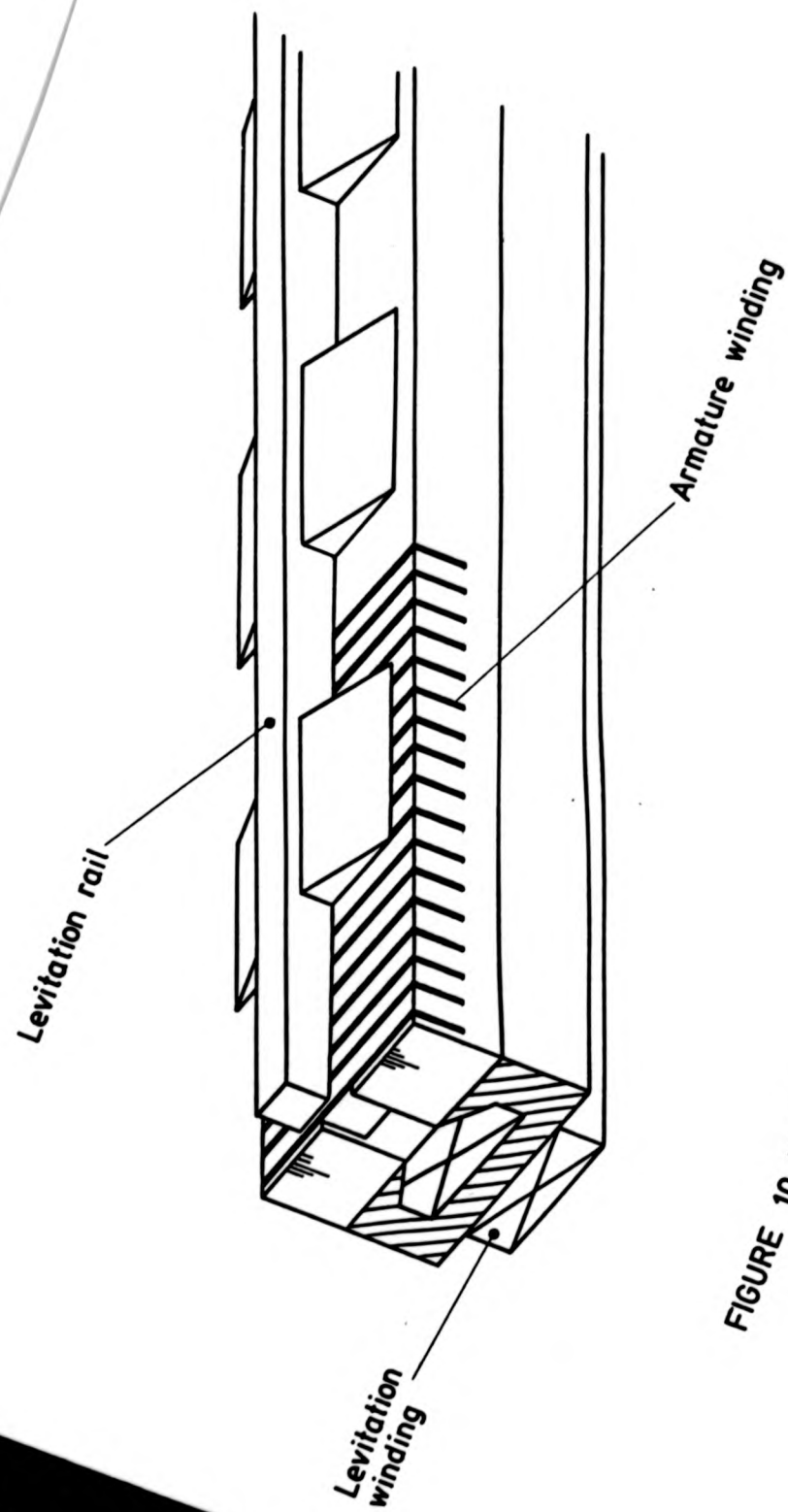


FIGURE 10 KEMPER'S HOMOPOLAR MACHINE WITH LEVITATION

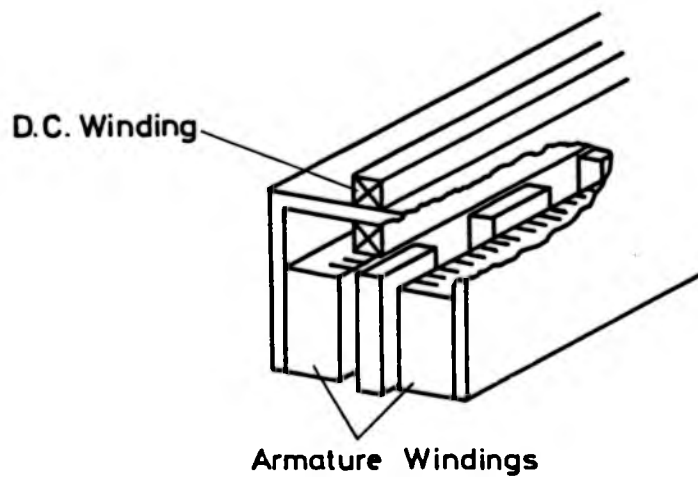


FIGURE 11a. DOUBLE SIDED HL SM WITH YOKE

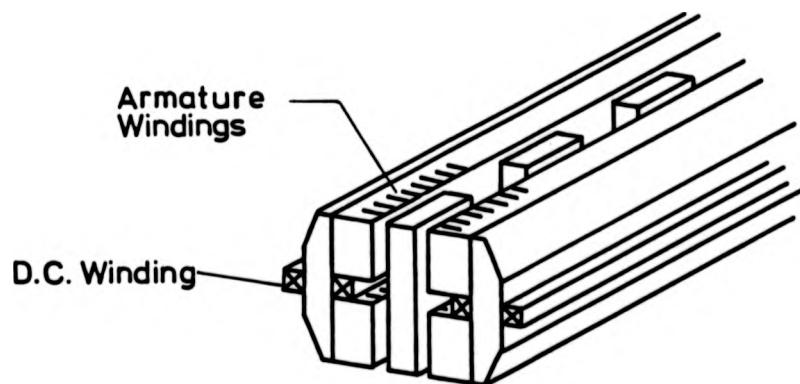


FIGURE 11b DOUBLE SIDED HL SM

An analysis of Leitgeb's yoked double sided HLSM was performed by Rummich⁽¹⁸⁷⁾, and this formed the basis of calculation by Levi in his performance comparisons of LSM with SLIM for the US DOT⁽¹⁷⁵⁻¹⁷⁸⁾. The study showed that both HELSM and HLSM design were flux density limited rather than thermally limited as was the case with SLIM. Higher possible airgaps and improved power to weight ratios despite the increased track complexity prompted continued study by Levi and also General Electric. Eastham had described a variation in winding topology for transverse flux cores in 1973⁽¹⁸⁸⁾ where the laterally adjacent but pole pitch offset similar windings were interconnected twisted coils. This winding could be used to produce a transverse flux homopolar machine⁽¹⁸⁰⁾ where the track structure resembled Leitgeb's single sided design without the thin backing iron (Figure 12). This new interconnection (as opposed to the straight through winding) was analysed by Ooi⁽¹⁸⁹⁾ as part of the General Electric programme, and employed dynamic circuit theory representation of the electromagnetic coupling and force generation. Levi analysed the staggered pole HLSM (Figure 13), using a 2 step Schwartz-Christoffel transformation to determine the effects of salient pole shaping⁽¹⁹⁰⁾. At the same time, General Electric worked through full-scale designs (400 km/h, 3.75MW) for HELSM and HLSM. Because of the predicted high power to weight and thrust to weight ratios for the HLSM (approximately three times the values for SLIM, and six times HELSM) of 2.9 kW/kg and 25.8 N/kg, a self controlled current fed inverter excited HLSM was built rated at 112kW (^(179,191)). The 5 pole machine covered 70° of arc on a 1.4 metre diameter wheel (Table VII), which could run at speeds up to 402 km/h. The first tests used staggered poles and the progressive figure of eight transverse flux armature winding proposed by Eastham. Saturation was apparent in the rotor saliencies, and also in the armature teeth adjacent to the saliencies. Levi adequately explained the effects on the open circuit measured voltage, and the leakage flux fringing modeling

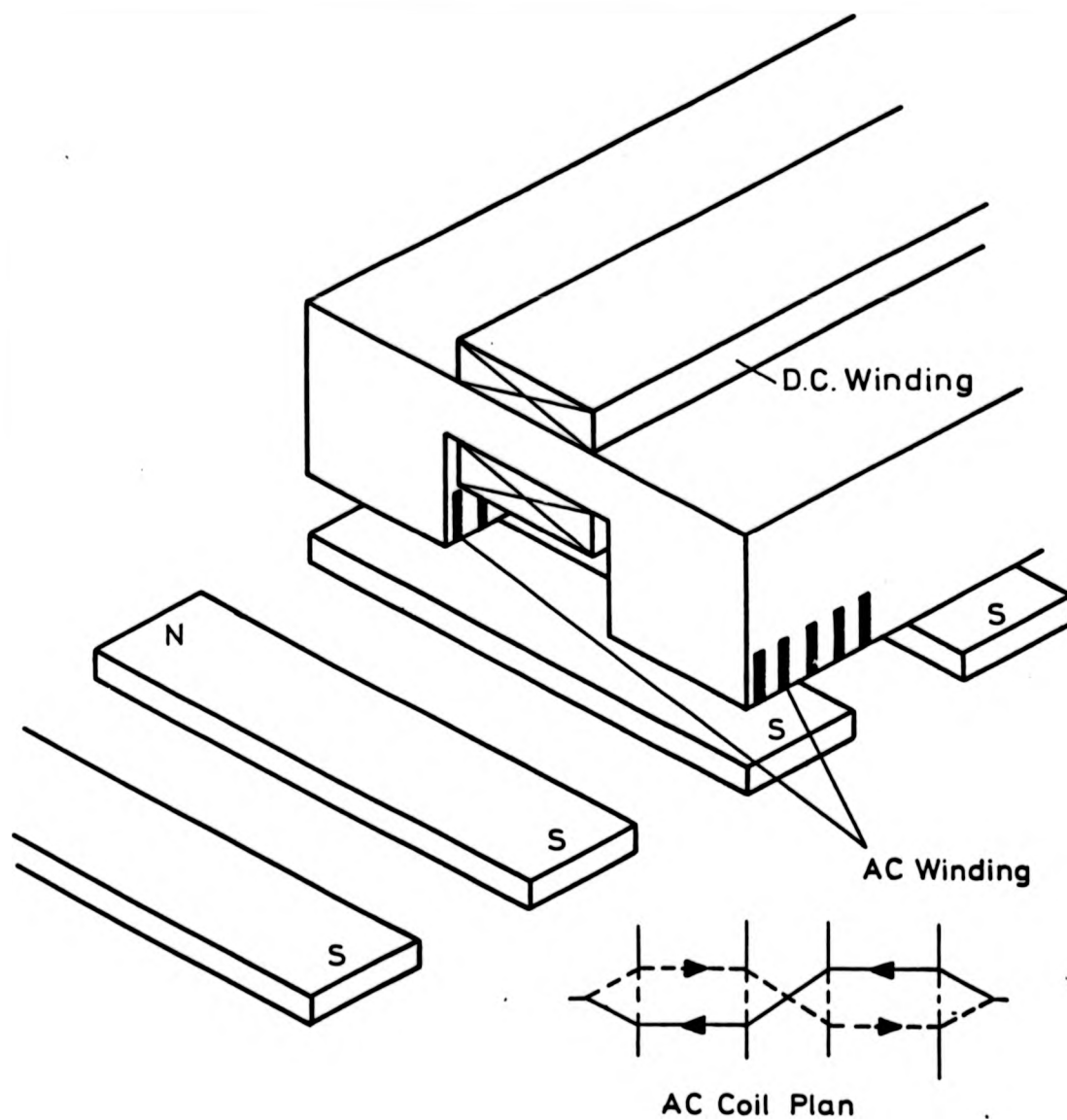


FIGURE 12. ABERDEEN TRANSVERSE FLUX HOMOPOLAR MACHINE

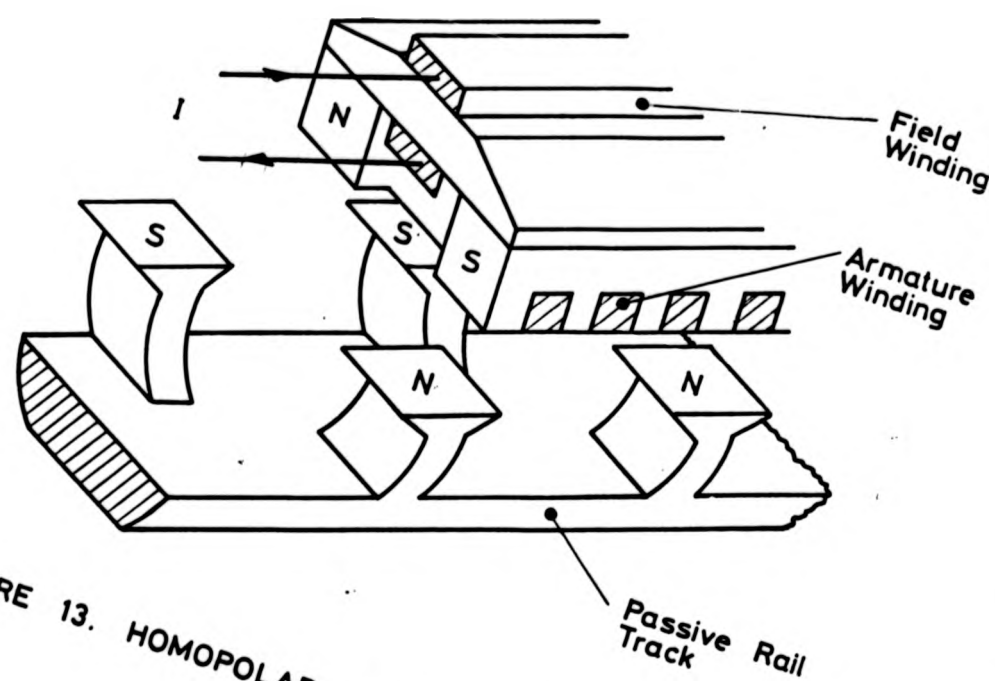


FIGURE 13. HOMOPOLAR INDUCTOR MOTOR

correlated experimental and calculated air gap lines⁽¹⁹⁰⁾.

Levi further examined the control of HLSM fed by current source inverters, and showed that power output maximum could be achieved by running at a unity power factor operating angle⁽¹⁹²⁾. The consequence was that a minimum size machine was possible. Slemon tested a small HLSM on a 2 metre diameter wheel at Toronto, to establish its suitability for urban vehicles⁽¹⁹³⁾. Table VII lists machine details. A current source inverter using the techniques developed for EDS LSM control, drove the armature, and open and short circuit tests together with force measurement suggested that the very simple current and voltage fed equivalent circuits could be used to predict machine performance.

2.5.2.3 Linear Reluctance Motors

The ROMAG system⁽¹⁵⁸⁾ in its simplest form constituted a LRM, in that a polyphase vehicle armature winding reacted against a notched or castellated track magnetic rail. Boldea and Nasar analysed this configuration^(194,195), and identified a further machine variant in which the track was constructed from blocks of ferromagnetic material embedded in a non-magnetic material (e.g. concrete). The segmented secondary LRM could therefore show a much improved track cost compared to the conventional notched rail motor. By the addition of thrust angle feedback, it was possible to achieve controlled thrust and normal forces sufficient for urban vehicles, with motor primaries mounted at each corner. Pole face damper windings were considered necessary to provide induction starting, but a superior method would be to use a variable voltage and frequency inverter which could track the vehicle position.

The group at the University of Sussex examined the segmented track LRM as the subsequent stage in their urban vehicle research, having successfully operated an EMS vehicle with LIM propulsion. Edwards and El-Antably proposed a uniform airgap model with which the field components could be obtained in a closed form, and the normal and traction forces could be

evaluated through a conventional equivalent circuit⁽¹⁹⁶⁾. Airgap reactance coefficients for the direct and quadrature axes were calculated from fundamental flux per pole values and were found to be close to experimental values, once segment end flux leakage is included. Chahal at Brush developed an alternative LRM configuration which used a transverse flux armature core and a ladder secondary. A disadvantage of this system is that the pole flux has to traverse two air gaps for a given mmf, and so has a reduced power to weight ratio compared to a straight axial flux LRM. A further development was the hybrid flux linear reluctance motor (HFLRM) which again used a ladder track, but a conventional axial flux primary. The direct axis flux now follows a hybrid path of longitudinal direction in the primary and the secondary end rings, and transverse in the secondary pole. The quadrature flux is longitudinal in both the primary and secondary^(197,198).

One main problem with LRM is that they exhibit load angle instabilities at speeds or frequencies below the rated values. It is not sufficient to run the machines in closed loop with just a speed following phase locked loop. The Sussex Group examined this problem on their test rig (Table VII) and provided negative damping into the feedback loop to remove the instabilities. Test rig results also confirmed the adequacy of the large uniform airgap model used to derive calculated performance⁽¹⁹⁹⁻²⁰⁰⁾.

Several versions of LRM have been built acting as linear stepping motors, and Finch at Newcastle University has investigated vernier LRM. Although the linear stepper has been applied to a conveyor drive, producing 400N thrust on a 250 kg load travelling at 4 km/h⁽¹⁹⁵⁾, a full size transport version has not been constructed.

2.5.3 Linear DC Motors

An urban vehicle drive which used a double sided track slot lined with permanent magnets, was proposed by the Aerospace Corporation. A vehicle mounted coil array ran in the slot and the coil switching was digitally

synchronized with the relative position of the array to the magnets. A one sixth scale model was built, but the idea was not continued because of the track complexity and cost⁽²⁰²⁾.

Japanese National Railways have persued the development of a DC linear motor (DCLM), in parallel with their EDS LSM research, since 1971. The basic system is outlined in a UK Patent⁽²⁰³⁾, and in more detail by Amemiya⁽²⁰⁴⁾ and Matsui^(205,206). Essentially the track coils are air cored and potted into a vertical fin to give sufficient rigidity and mechanical protection. The vehicle coils are formed onto an iron cored field structure, and are normally conducting (i.e. not cryogenically cooled). The track coil switching is accomplished by "super-forced" commutation, whereby the coil feeding thyristor is force commutated by a reverse voltage some order of magnitude greater than the back emf of the vehicle. A short commutation time is important because of the interrelationship of coil transit time to coil size and the rate of current rise and fall within the coil.

As might be expected, the machine cannot be adequately operated on open loop control. The vehicle motion can be expressed as a second order oscillatory system, with a very small damping coefficient, and the commutation angle oscillates until it breaks past the synchronous point; the machine has only a small margin to prevent stepping out. By applying velocity feedback, the damping coefficient is effectively stabilized at a higher value, providing an efficient operating regime.

To check the operational characteristics of DCLM, a 500 km/h rotating disk and a 500 metre linear test track were built, as well as a 100 metre diameter track used to establish control strategies^(207,208). Tables VI and VII give the main details of the facilities. The rotating disk was constructed out of fibre reinforced plastic and the preformed coils were moulded in. A short time rating of ten minutes was necessary to avoid excessive temperature rise in the disk. The 100 metre diameter track was

used as a control system model to establish that a correct control strategy had been chosen, and a branch with turn out was also included to investigate switch transitions. The 500 metre linear track carried a 3.3 tonne vehicle which could produce a thrust of 2.2 tonnes, or roughly that of two cars of the Shinkansen. The design top speed of 200 km/h is reached in a 240 metre acceleration section, a 70 metre test section being followed by electric and then mechanical braking. Eight field magnets with airgaps of 85mm run at 0.9 Tesla peak, and are energised through a power collecting roller^(209,210). Later tests on pantograph behaviour at high speed provided alternative power pick up, before the track was reconfigured to give both levitation and propulsion with the same coil arrangements, but at the lower speed of 80 km/h⁽²¹¹⁾.

The track coils are driven by a constant current source through a flip flop type inverter. Position indication is usually by means of a cross wire inductive system. An onboard oscillator and antenna links track mounted wires which fed a signal back to the local control of commutation within the flip flop inverter. There are two options for power feeding, the first being 'multiphase feeding' where multiphase square wave currents feed from a substation to the flip flop inverters at each feeding section. The second method is direct current feed, where dc is fed from the substation to each flip flop inverter at the feeding sections. Commercial systems will use dc feed since it is most economical, in terms of lower phase inductance, inverter capacity, and number of feed lines.

Proposed commercial systems are designed for two operating speeds of 300 and 500 km/h, around the conventional JNR train set arrangement of 16 cars, with 100 seats per car. The 300 km/h system would use tyres to provide guidance and some lift, although the majority of lift and the propulsion would come from the DCLM. The 500 km/h system would be fully non contacting (except for current pick up) with the DCLM providing all the lift and propulsion, and an electromagnetic guidance system using null flux

guidance from a controlled current saddle magnet running over a coil array. Expected power levels are 35.1 and 15.6 MW for the two train sets. In order to reduce the weight and power loss in the vehicle magnets, redesign of the magnetic circuit and an enhancement of the current density were accomplished. The choice of cooling was between air, water through hollow conductors, or boiling fluid. Boiling fluid cooling was selected as having the most promise and experimentation determined the optimum dimensions of the coil, tank and condenser circuit⁽²¹²⁾. A fluorinated oil was chosen as the refrigerant, as it had similar physical properties to Freon 113, but its vapour pressure is approximately a quarter of Freon's, resulting in reduced tank wall thickness and a 20-30% weight saving. A trial magnet showed a current density of 4.5 A/mm² in aluminium wire, and a mmf of 100 kA. Using this as a base, the weight of magnets that could lift and propel a 22 tonne vehicle could be reduced from 9.6 tonne/vehicle to 4 tonne/vehicle, with an excitation power of 285kW/vehicle.

2.6 Future Near Term Development

Although the final outcome of the tests at very high speeds at Emsland and in Japan by JAL and JNR will not be known for some time, it is likely that progression to a totally levitated system will be slow, because of world recession and Government reluctance to enter into large capital projects. It is therefore reasonable to expect that the emergence of hybrid systems, namely fairly conventional duorail vehicles with linear motor propulsion, will offer near term advantages over existing methods of propulsion, but not require totally new infrastructure development with all the associated land acquisition cost and environmental impact problems. For urban vehicles, the Toronto ICTS is an example, and Slemon has suggested a permanent magnet LSM propulsion unit for a similar capacity 8 tonne vehicle, where the field is an array of samarium cobalt magnets with iron backing and the track is an air cored three phase winding excited in 200 metre block lengths⁽²¹³⁾.

SLIM's have been used in Japan as booster/retarders in a classification yard since 1974 on a regular basis⁽²¹⁴⁾, and can produce significant savings in reduction of damage resulting from uncontrolled end impacts, and considerably reduce noise levels in the yards. In the USA, it is estimated that remote switch motors and controlled decelerations could save \$6.5 billion (1975 dollars) in the period 1980-2000⁽¹⁶²⁾.

For propulsion units suited to conventional high speed trains, the choice is dependent on whether cryogenic systems can be engineered to meet railway operational conditions. Abel has suggested that a magnet pack containing an isochoric cryostat and a multimagnet array could be simply supported under the power car of an APT type vehicle⁽¹³⁷⁻⁹⁾. At terminif the magnet pack could be replaced with a freshly charged pack to provide a quick turn around. The unsprung mass of the driven axles would no longer be a design constraint, and sufficient propulsive power and braking obtained with a meander air cored track winding could extend the speed range to 300 km/h, and beyond, depending on wheel wear rates.

Similar studies by Nondahl at General Electric were based on SLIM or HLSM drives, the main feature being passive track structures⁽²¹⁵⁾. Five operating modes were chosen, with ratings of 200, 450, 1200, 2400 and 3735 kW, the designs representing vehicles ranging from a New York City subway car (112 km/h) to a High Speed Locomotive (400 km/h). The designs were optimized to produce minimum track weight with similar magnetic and electrical loadings. The main conclusions were that the HLSM worked at a higher power factor, produced greater restoring forces for track misalignments, and gave lower track heating than the SLIM. The SLIM advantages were that there was no need to synchronise train speed and frequency, the machine was easier to construct, lower copper weight, a more easily anchored track structure. Generally, when the output power and available frequency are low the HLSM track is lighter, and similarly, the SLIM track is lighter at higher powers and frequencies. Both schemes

suffer the same disadvantage in that a power collection system is required, whereas an air cored LSM needs no pickup. The ACLSM can further be implemented with cryogenically cooled coils and small airgaps, since there is no requirement for levitation. The air gap field harmonics can be picked up by the vehicle and used to produce on board power when the vehicle is in motion.

Another option is cryogenically cooled coils driven by a dc busbar power collection as part of an ACLSM propelled urban vehicle. These hybrid applications are discussed in a later section.

Kolm and O'Neill have suggested using a basic ACLSM as an electromagnetic launcher. Primarily research has been aimed at lunar transport of materials, and shuttle payload launching. One novel application has been the suggestion of nuclear waste disposal into deep space, and the inevitable use as an electromagnetic gun has also been investigated⁽²¹⁶⁻²¹⁸⁾. However, these systems require energy compression ratios of about 60:1, and suitable energy delivery equipment. The most promising arrangement is a homopolar generator feeding pulsed power into the armature system. For space payload launching, an evacuated 7.8km tube can house a 1 tonne vehicle, which would emerge through a vacuum lock at 12.3 km/s, having been accelerated at 1000 gee, Launch time would be 1.5 seconds, and would require 76 GJ. More reasonable applications include short take off assistance for conventional aircraft: 20 kg vehicles launched at 400 km/h would reach a 600 metre altitude and then act as gliders. Typical launch ramps would be 5m long, and 100 gee would require 0.12 MJ delivered in 0.1 second.

Since 1977, AGT system development has been generally on the decline, with the exception of the German and Japanese effort. The emphasis has changed from that of high speed at low cost (which marked the aspirations of work in the late 60's) to adequately high speed transport at reasonable energy

efficiency, compared to the alternative modes. This has acted against the development of EDS since the aerodynamic drag power doubles on a vehicle going from 400 to 500 km/h, and EDS is more effective at the high speed than EMS. The LIM has been given a reasonable top speed of 300-400km/h when used as an EMS propulsion or as part of an ISPS. LSM have proved to be the preferred propulsion unit, long stator iron cored for EMS vehicles, or air cored for EDS and perhaps high speed duorail trains. HLSM and HELSM show slight improvement over LIM and LRM, but both require current pickup which is likely to preclude their use at high speed. The Japanese DCLM is a serious alternative for a maglev system, but again, requires a current collection system to supply the on board electromagnets.

The three main contenders for AGT propulsion all have track windings which are block supplied, in short lengths approaching the vehicle length in the case of the DCLM, several times the vehicle length for the iron cored LSM, and many times the vehicle length for the cryogenic LSM. The latter two cases do not rely on current collection through brushgear and either use an on board power supply or effectively pick up the air gap harmonics to top up on board battery supplies. Because of the advantages that these machines show over conventional rotary machines driving power wheel sets with the attendant problems of unsprung mass, wheel and rail wear through the adhesion interface and limited acceleration and deceleration rates, it is to be expected that they will be the focus of continued research and development. The final outcome will be a design for a prototype with substantially improved performance compared to a conventional duorail vehicle, and extended speed capability with low initial infrastructure cost and minimal maintenance requirements.

CHAPTER THREE

PERFORMANCE CHARACTERISTICS OF LSM

3. Performance Characteristics of LSM

3.1 Equivalent Circuit Representation

3.1.1 Basic Requirements

If machine performance over a wide range of conditions is to be accurately predicted, it is necessary to formulate a suitable model. Invariably, for electromagnetic devices, an equivalent circuit is used as the basis for investigating performance in terms of either imposed operational constraints, or parameter variation and system sensitivity. The component parts of the circuit should be readily identifiable as relating to particular aspects of the real machine (for example phase resistance, leakage inductance etc) and must, if possible, include all mutually induced effects from other similar linked circuits.

The LSM can be represented by lumped parameters in a representative phase. The representative phase is that identifiable single winding representation of a polyphase armature winding whose magnetomotive force (mmf) coincides with that of the whole polyphase armature sheet mmf. Although it is tempting to split the phase into sections which either link the main field flux or are distant from the vehicle⁽²¹⁹⁾, there is no particular advantage in doing so. In the simple equivalent circuit shown in Figure 14, phase current passes through the phase impedance and is driven by the difference in terminal voltage E_T and the induced back emf E_B . The phase impedance is made up of a resistive term and a reactance based on the overall phase inductance, excluding field linkages. The phase inductance is therefore essentially a leakage inductance, and itself can be decomposed into two terms, a winding self inductance, and a mutual term, formed by the representative phase net mutual linkage with the rest of the armature windings.

The back emf E_B represents the mutual linkage between the armature representative phase and the field winding array. E_B although reflected into the terminals is only induced in the few turns per pole per phase

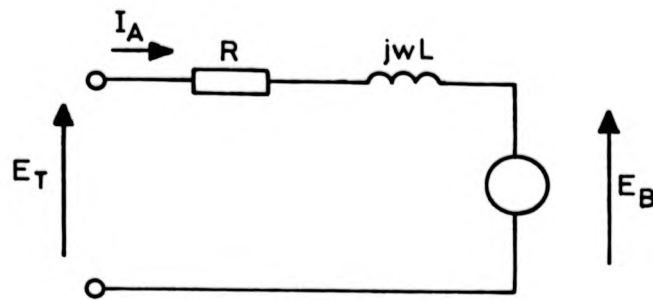


FIGURE 14. VOLTAGE FED EQUIVALENT CIRCUIT

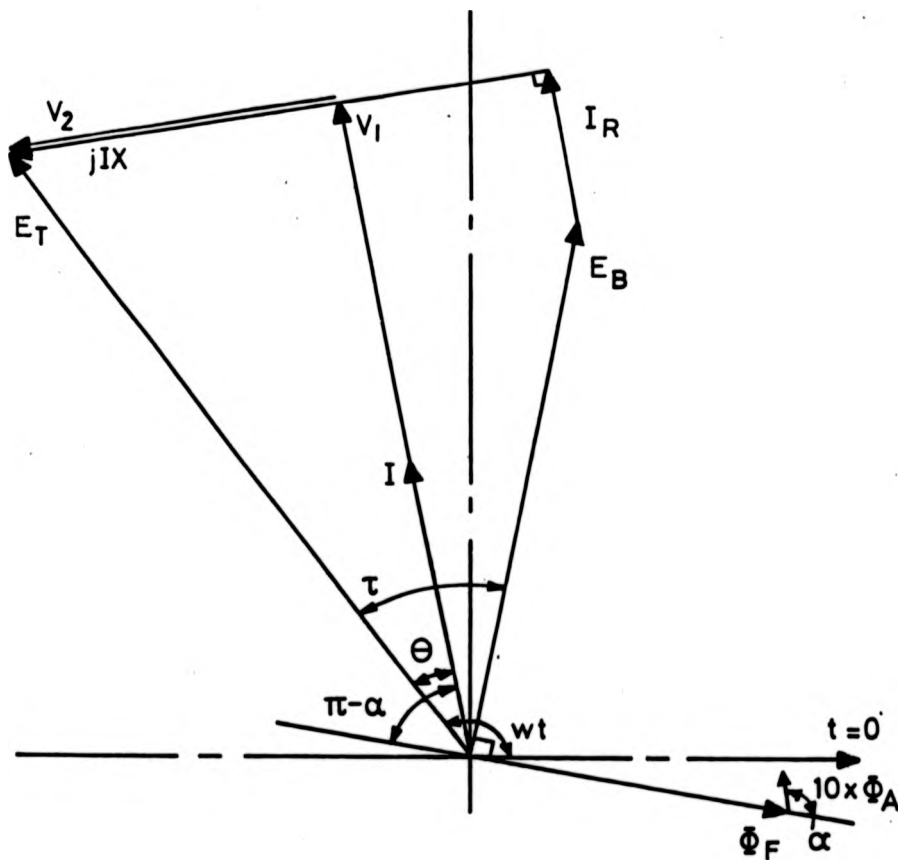


FIGURE 15. PHASOR DIAGRAM FOR REPRESENTATIVE PHASE.

over the short section of the energised armature linking the vehicle field coils. Because the superconducting magnets have such high ampere turns (three orders of magnitude greater than the armature) the field strength at the track level is such that the armature reaction is relatively small, and E_B can approach the terminal voltage even when considerable amounts of power are being transferred.

The field and armature windings are air cored and generally can be broken down into the simple configuration shown previously as Figure 1. Non linearities which are usually associated with conventional iron cored machinery are therefore absent for ACLSM. The track level flux density is generated by a regular disposition of finite coils, and if the coil height to pole pitch ratio is low, multiple harmonics in the induced emf will occur. Each harmonic can be treated separately in the equivalent circuit, and the net effect evaluated, with no loss of generality, or the need to introduce additional components.

Figure 15 shows the representative phasor diagram deduced from the equivalent circuit. The armature flux Φ_A is driven through the machine airgap by the phase mmf. In the machine air gap directly below the magnet coil array the field winding flux Φ_F lags behind the armature flux by a force angle α (also known as the current angle). Φ_F induces in the phase windings the back emf E_B , and this leads the Φ_F phasor by $\frac{\pi}{2}$. As will be seen later, the optimum operation of the machine occurs with $\alpha > \frac{\pi}{2}$, in a region that is normally unstable for synchronous machines without either fast acting AVR's or other auxiliary closed feedback loops in the excitation or terminal control. The back emf lags on the terminal voltage by the load angle τ ; on no-load operation there would be no net current flow, τ would be zero, and the back emf would be exactly balanced by the terminal voltage, E_T . This situation is unreal for LSM; the nearest equivalent would be an evacuated tube vehicle with low drag, or alternatively when the machine is braking and passes through the $\tau = 0$ locus before regenerating.

The phase current I lags on the terminal voltage by the power factor angle θ , and is of course in phase with Φ_A .

3.1.2 Load Angle Derived Equations

A load angle derived equation set is particularly easy to formulate, and so will be introduced first to establish basic relationships. Using phasor representation of the phasor diagram, with the terminal voltage as the time reference,

$$\bar{E}_T = E_T + j0$$

$$\text{then } \bar{E}_B = E_B \cos \tau - jE_B \sin \tau$$

$$\text{and } \bar{I} = I \cos \theta - jI \sin \theta$$

the equivalent circuit gives a solution for the current phasor,

$$\bar{I} = \frac{\bar{E}_T - \bar{E}_B}{R + jX}$$

$$\text{since } I = |\bar{I}| = (\bar{I} \bar{I}^*)^{1/2}$$

$$I = \left[\frac{E_T^2 + E_B^2 - 2E_T E_B \cos \tau}{R^2 + X^2} \right]^{1/2} \quad (1)$$

At the terminals, the instantaneous input power S_T for a machine with m phases is given by

$$S_T = m \bar{E}_T \bar{I}^* = P_T + jQ_T \quad (2)$$

P_T and Q_T are the average power and reactive volt amperes (reactive power)

The magnitude of S_T is given by

$$S_T = \frac{m E_T [E_T^2 + E_B^2 - 2E_T E_B \cos \tau]^{1/2}}{(R^2 + X^2)^{1/2}} \quad (3)$$

Similarly the machine output S_B is given by

$$\bar{S}_B = m \bar{E}_B \bar{I}^* = P_B + jQ_B$$

Taking the real part of \bar{S}_B gives P_B , the mechanical output power,

$$P_B = \frac{mE_B}{R^2 + X^2} [R(E_T \cos \tau - E_B) + X E_T \sin \tau] \quad (4)$$

The expressions for the remaining input and output magnitudes can also be written, which allows the linking terms of power factor $\cos \theta$, efficiency, η and power factor-efficiency product $\eta \cos \theta$ to be evaluated

$$\text{Power factor, } \cos \theta = \frac{P_T}{S_T} = \frac{\frac{R}{X} \left(\frac{E_T}{E_B} - \cos \tau \right) + \sin \tau}{\left(1 + \frac{R^2}{X^2} \right)^{1/2} \left(1 + \frac{E_T}{E_B} \left(\frac{E_T}{E_B} - 2 \cos \tau \right) \right)^{1/2}} \quad (5)$$

$$\text{Efficiency, } \eta = \frac{P_B}{P_T} = \frac{\frac{R}{X} \left(\cos \tau - \frac{E_B}{E_T} \right) + \sin \tau}{\frac{R}{X} \left(\frac{E_T}{E_B} - \cos \tau \right) + \sin \tau} \quad (6)$$

$$\text{Product, } \eta \cos \theta = \frac{P_B}{S_T} = \frac{\frac{R}{X} \left(\cos \tau - \frac{E_B}{E_T} \right) + \sin \tau}{\left(1 + \frac{R^2}{X^2} \right)^{1/2} \left(1 + \frac{E_T}{E_B} \left(\frac{E_T}{E_B} - 2 \cos \tau \right) \right)^{1/2}} \quad (7)$$

Equation (7) is important since it provides the link between the mechanical output power P_B and the required total instantaneous power at the terminals, S_T . If the machine is running at a steady synchronous speed v , then the traction force or thrust F_B is simply given by

$$F_B = \frac{P_B}{v} \quad (8)$$

The current angle α is directly linked to the power factor angle and load angle by

$$\alpha = \frac{\pi}{2} - \theta + \tau \quad (9)$$

as can be seen from the phasor diagram. Equations 5 to 9 are plotted in Figures 16 and 17 for a typical value of $\frac{E_B}{E_T}$ of 0.75 and two representative

values for $\frac{R}{X}$ of 0.3 and 0.6. It is seen that although the

efficiency peaks rapidly with load angle, the power factor is much less sensitive to changes. The efficiency-power factor product, $\eta \cos \theta$ has a broad maximum in the range $15^\circ < \tau < 35^\circ$. The value of load angle at which this maximum occurs is

$$\tau \Big|_{\max. \eta \cos \theta} = \frac{\sqrt{1 + \frac{R^2}{X^2} - \frac{E_B^2}{E_T^2}} - \frac{R}{X}}{1 + \frac{E_B}{E_T}} \quad (10)$$

As mentioned the usefulness of the load angle as a fundamental quantity for analysis is limited, since in an operating system the conditions for no load running will only occur when the machine is about to pass into regeneration while decelerating. On-load conditions make load angle difficult to measure, and the method used, for example, in the CIGGT control strategy is to provide a model to artificially create the track armature, and compare the signal generated for E_B with a real time E_T - derived signal. The vector difference is a measure of τ in the real machine. Sen's analysis of the load angle derived equations^(107,220) is faulty because of an inconsistency in the sign notation used to derive the equations, and results in curious performance characteristics of a revenue vehicle design.

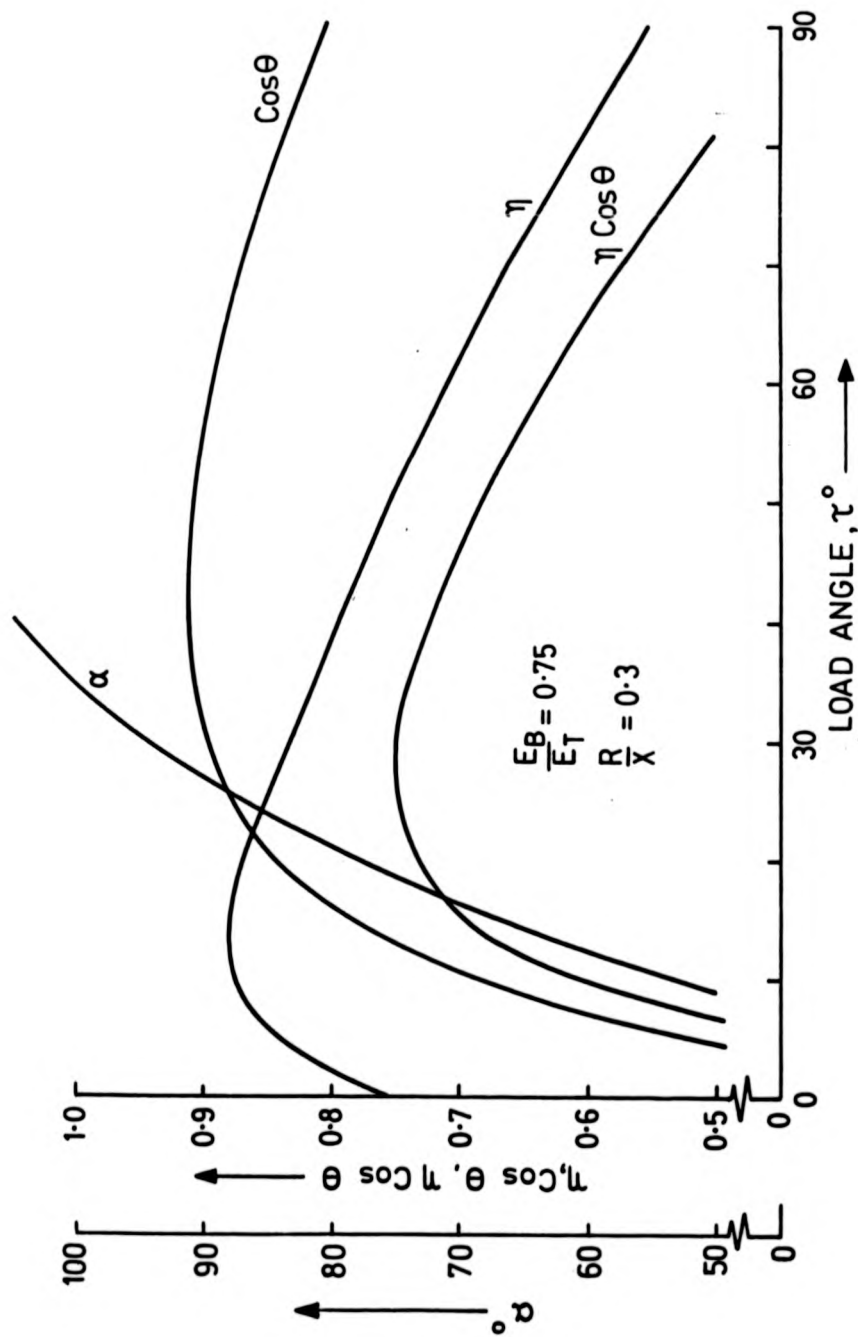


FIGURE 16. EFFICIENCY, η , POWERFACTOR, $\cos \theta$, AND $\eta \cos \theta$ WITH CURRENT ANGLE, α WRT LOAD ANGLE τ

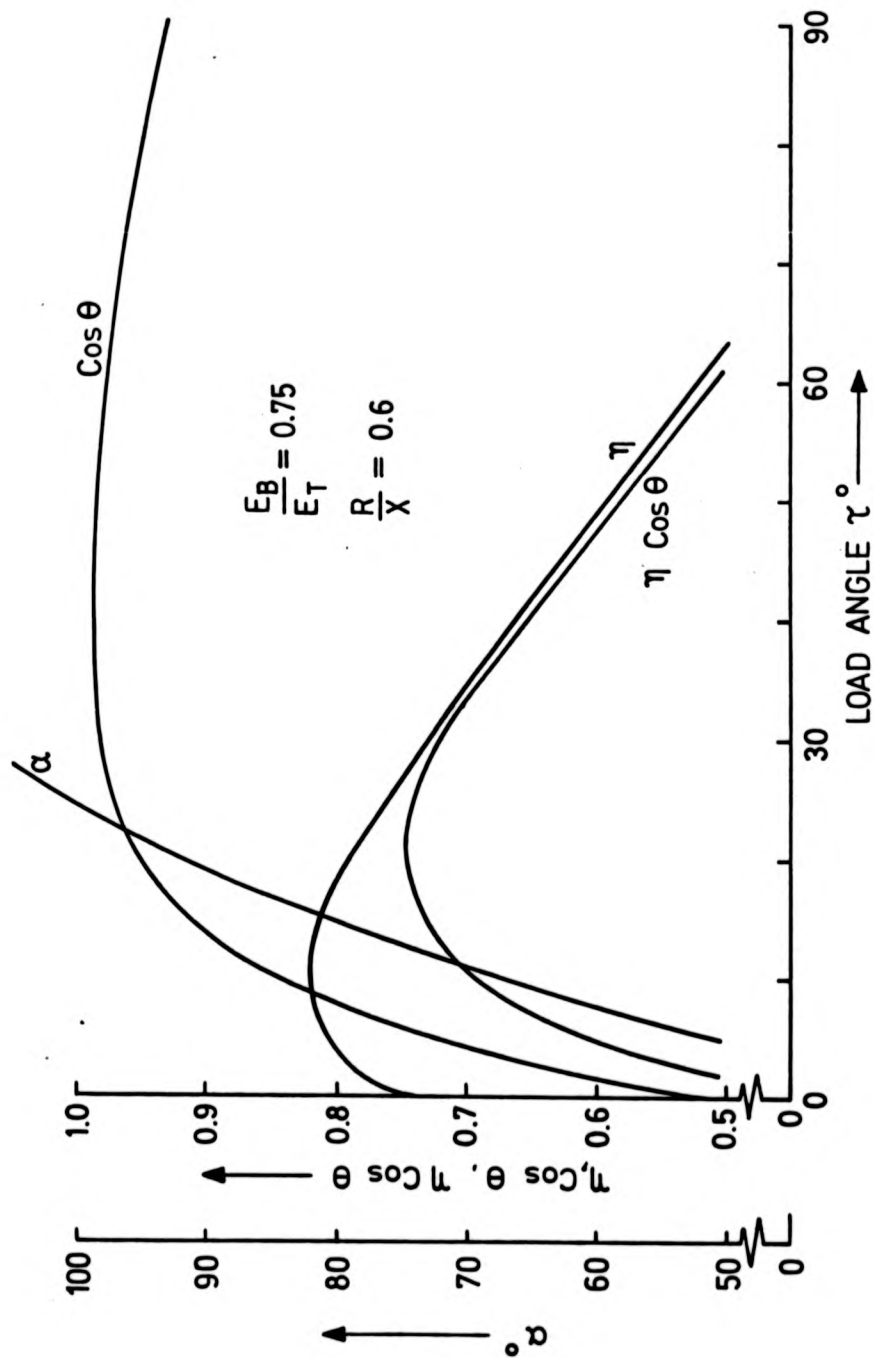


FIGURE 17. EFFICIENCY, η , POWERFACTOR, $\cos \theta$, AND $\eta \cos \theta$ WITH CURRENT ANGLE, α WRT LOAD ANGLE τ .

3.1.3 Current Angle Derived Equations

The current angle is the linear equivalent angle between the peaks of the armature and field mmf distributions. In the phasor diagram, Figure 15, the terminal emf can be split into active (in phase with stator current) and reactive (quadrature phasing to current) components. The appropriate voltages are given by

$$V_1 = E_B \cos(\tau - \theta) + IR = E_B \sin\alpha + IR \quad (11)$$

$$V_2 = -E_B \sin(\tau - \theta) + IX = E_B \cos\alpha + IX \quad (12)$$

The power factor is directly obtained as

$$\cos\theta = \cos\left[\tan^{-1}\left\{\frac{V_2}{V_1}\right\}\right] = \frac{V_1}{(V_1^2 + V_2^2)^{1/2}} \quad (13)$$

and the terminal emf, E_T , is

$$E_T = (V_1^2 + V_2^2)^{1/2} \quad (14)$$

The machine is primarily designed to provide a particular thrust-speed characteristic determined by the required acceleration and load profile. The thrust, F_B , is linked to the back emf, phase current and current angle by

$$F_B = \frac{P_B}{v} = \frac{m E_B I \sin\alpha}{v} \quad (15)$$

Since the induced emf is proportional to speed, the developed thrust is speed independent, and can be controlled by individual manipulation of either phase current I or current angle α , at the inverter.

The machine active input power P_T is given by

$$P_T = P_B + m I^2 R \quad (16)$$

So efficiency is

$$\eta = \frac{P_B}{P_T} = \frac{1}{1 + \frac{m^2 R}{R_B}} = \frac{1}{1 + \frac{P_B R}{m E_B^2 \sin^2 \alpha}} \quad (17)$$

Using (14), (15), the total input power S_T is

$$S_T = m E_T I = \frac{P_B}{\sin \alpha} \left[1 + \frac{P_B^2 (R^2 + X^2)}{m^2 E_B^2 \sin^2 \alpha} + \frac{2 P_B (R + X \cot \alpha)}{m E_B^2} \right]^{1/2} \quad (18)$$

Also

$$P_T = P_B \left[1 + \frac{P_B R}{m E_B^2 \sin^2 \alpha} \right] \quad (19)$$

and

$$Q_T = P_B \left[\cot \alpha + \frac{P_B X}{m E_B^2 \sin^2 \alpha} \right] \quad (20)$$

Finally, the linking expression

$$\eta \cos \theta = \frac{P_B}{S_T} = \frac{E_B}{E_T} \sin \alpha \quad (21)$$

indicates that for a high power factor-efficiency product at a particular thrust loading, the back emf-terminal emf ratio and current angle product must be as large as possible. A typical value range of 70-85% might be achieved for a large machine, when the track installation and energy consumption optimizations are worked through into the design.

By manipulating the current angle at which the motor operates, power conditioning benefits can be achieved. Minimum phase current (equivalent to maximum efficiency), minimum terminal voltage, minimum terminal rating as well as power factor can be chosen depending on the particular requirement⁽²²¹⁾. In most cases the minimum terminal rating option will be chosen since installed conditioning and cabling cost will be proportional to this factor. In revenue service with supply from a Utility, it may show some advantage in maximum peak demand costings to operate some of the scheduled LSMs at leading power factor to compensate the remaining LSM's operating at the more usual lagging power factor. This would ease the

stored energy MVAR obtained from the Utility Grid and any cost benefit may offset the increased superconductor and track conductor cost. Inevitably any trade off of parameters to obtain a particular result will have a detrimental effect on other parameters. In the design process the trade off effects must be understood so that specific parameters are not compromised. As LSM development has progressed, it has become apparent that more system flexibility is possible if sections are supplied by individual inverters, rather than operating the steady state cruise sections on a synchronous near-Utility tie, so that the minimum terminal rating option is likely to be made the preferred choice.

If machine parameters are fixed, a decision has to be made as to which variables should be optimised, and with what constraints. The basic fixed parameters for a certain steady state are simply track armature resistance and reactance, number of phases, and back emf. Machine thrust at the synchronous speed is a parameter which depends on the thrust-speed requirement of the vehicle, and is linked to the output power by equation (15), which effectively fixes $I \sin \alpha$ at a constant value.

For a constant thrust requirement, the value of current angle which minimises efficiency and phase current is

$$\alpha = \frac{c}{\pi} \frac{\pi}{2}$$

$$\text{If } s = \frac{P_B X}{m E_B^2} \quad (22)$$

$$\text{then } E_T = E_B \left[1 + \frac{s^2}{\sin^2 \alpha} \left[\frac{R^2}{X^2} + 1 \right] + 2s \left[\frac{R}{X} + \cos \alpha \right] \right]^{\frac{1}{2}} \quad (23)$$

and the minimum terminal voltage is given for a value of current angle where

$$\alpha = \pi^c - \tan^{-1} \left[s \left[\frac{R^2}{X^2} + 1 \right] \right] \quad (24)$$

Power factor may be maximised by appropriate choice of current angle, or if the back emf component in quadrature to the phase current is larger, equal to or smaller than the reactive voltage drop, then lagging, unity or leading power factor will ensue.

Unity power factor occurs when θ is zero, i.e. terminal voltage and current phasors are in line, which is interpreted as V_2 is also zero. The required value of current angle for unity power factor is

$$\alpha = \frac{\pi}{2} + \frac{1}{2} \sin^{-1} 2s \quad (25)$$

Maximum power factor is similarly obtained as occurring at the value of current angle where

$$\alpha = \pi^c - \cot^{-1} \left\{ \frac{X}{R} \left[\left(1 + \frac{R^2}{X^2} \left(\frac{X}{sR} + 1 \right) \right)^{\frac{1}{2}} - 1 \right] \right\} \quad (26)$$

Maximum power factor efficiency product lies between the individual values of current angle producing the separate maxima, i.e. $\frac{\pi}{2}$ and the value obtained from (26). The value of current angle for which this occurs requires the solution of the cubic equation.

$$\tan^3 \alpha + \left(r + \frac{2R}{X} + \frac{1}{s} \right) \tan^2 \alpha + 3 \tan \alpha + r = 0 \quad (27)$$

$$\text{where} \quad r = 2s \left(1 + \frac{R^2}{X^2} \right) \quad (28)$$

Solving (27) is tedious, since it requires solution of a reduced equation, and the evaluation of its discriminant⁽²²¹⁾. A range of the non dimensional parameters $\frac{R}{X}$ and $s \left(= \frac{P_B X}{m E_B^2} \right)$

for which the value of current angle giving minimum S_T have been evaluated and are shown in Figure 18. As might be expected, an increase in loading, s , requires a reduction in current angle once a break point is reached around $s = 0.6$.

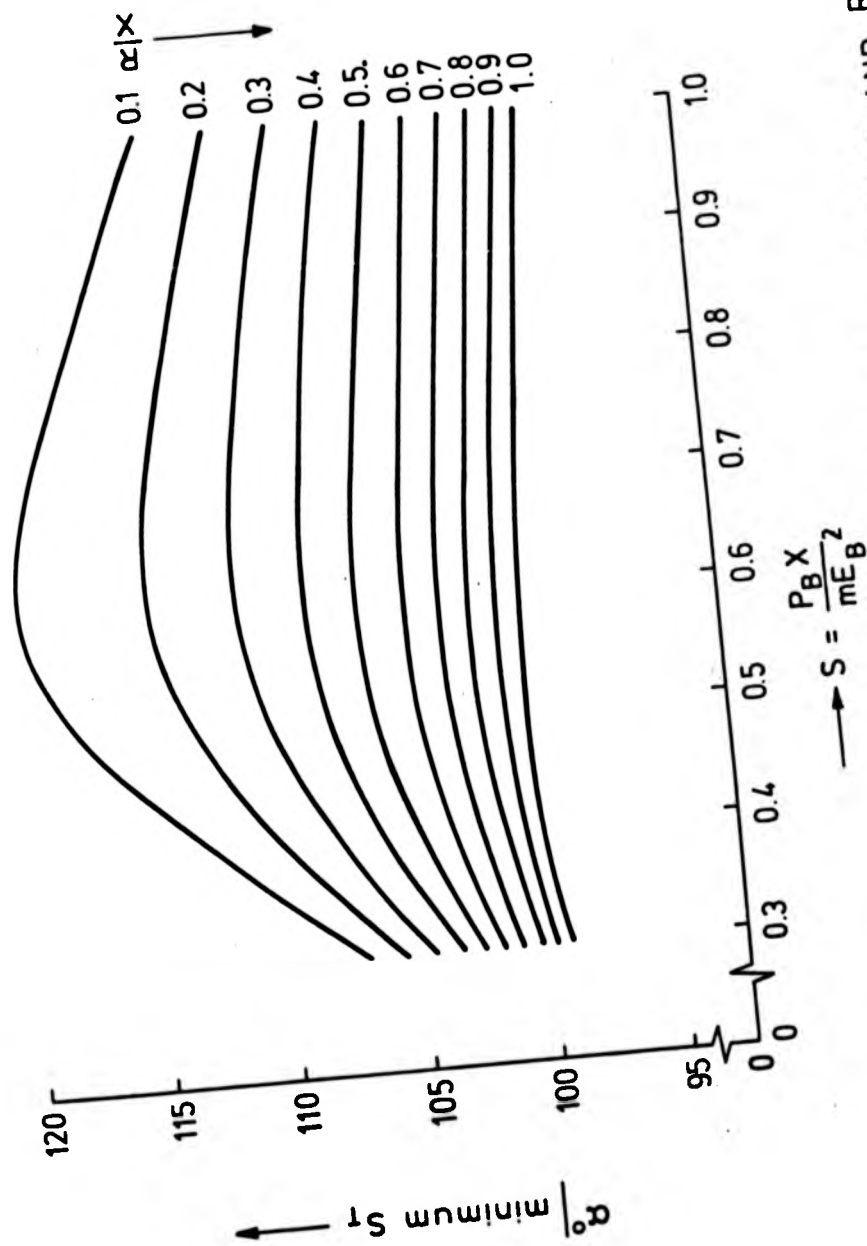


FIGURE 18. CURRENT ANGLE α° FOR MINIMUM S_T WRT S AND $\frac{R}{X}$

3.1.4 Operation at Minimum S_T

Assuming that the inverter operation is set to automatically minimise its terminal rating, to minimise total power flow, then the parameter variation for various loads should be evaluated. The results of a blanket range of calculations for efficiency, powerfactor and their product, terminal voltage, phase current and total input power with various normalizing factors are shown in Figures 19 to 23. The parameters are evaluated for the minimum S_T values of current angle resulting from combinations of the two main non dimensional factors s and $\frac{R}{X}$, over a typical design spread.

The figures are self explanatory. However it is interesting to note the fact that since for a particular track arrangement, inductance does not significantly change with increased conductor section, a low resistance track will always show overall advantage even though it degrades the power factor. Also worth noting is the high power factor efficiency products that are possible at light loadings and low track resistances.

Finally, parameter sensitivity to changes in current angle must be determined to establish any economic advantage gained from optimum running. For the CIGGT revenue vehicle, $P_B = 5.4$ MW, cruise speed is 480 km/h, phase resistance and reactance are 2.8 and 8.89 ohms respectively, for a 5 kilometre block length. The back emf is nominally 4kV. The minimum terminal rating value of current angle is 108° , and Figure 24 shows the terminal total power and voltage and phase current normalized about this value. Efficiency, power factor and their product are also shown for different current angles. In general the form of the curves holds for most large scale LSM designs. In going from maximum efficiency to maximum apparent efficiency operating points, the phase current increases and the terminal voltage drops. The terminal voltage reduces more rapidly than phase current increases, and in this example E_T reduces by 10% while I increases by only 5%. The implication is that the phase current affects

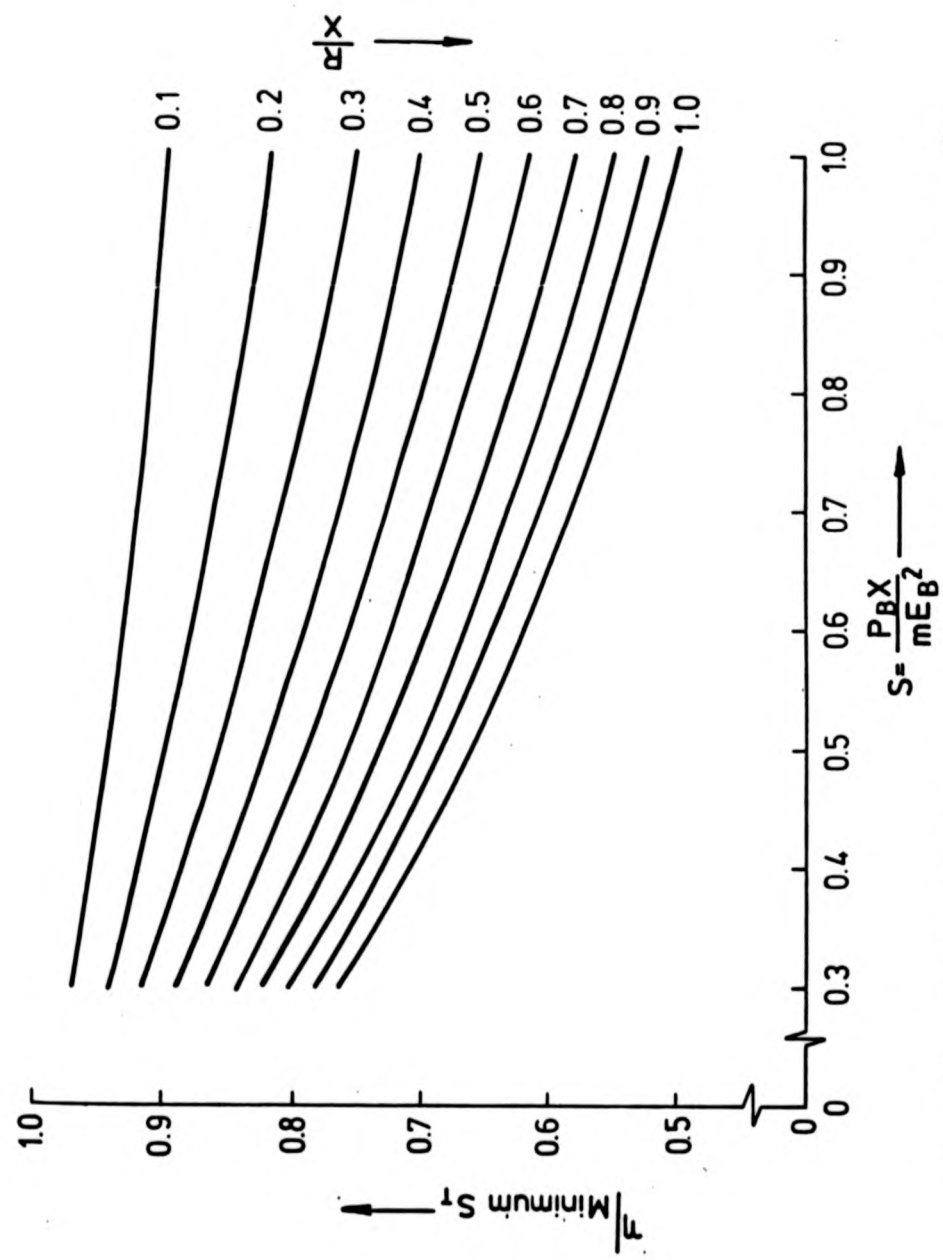


FIGURE 19. EFFICIENCY, η , FOR MINIMUM S_T WRT S AND $\frac{R}{X}$

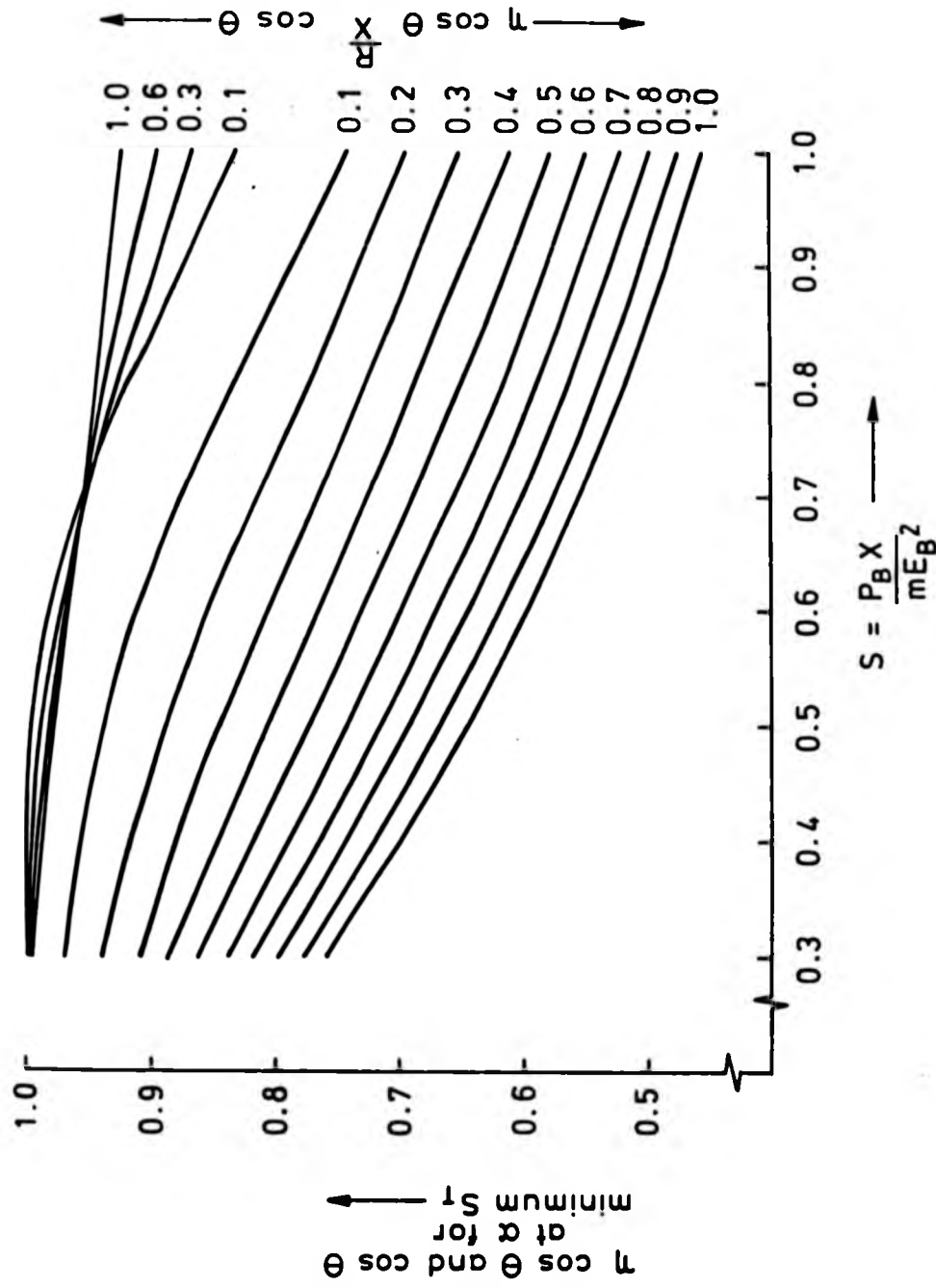


FIGURE 20 POWER FACTOR ($\cos \theta$) POWER FACTOR-EFFICIENCY PRODUCT ($\eta \cos \theta$)
 WRT S AND $\frac{R}{X}$ FOR MINIMUM - $S_T \propto$

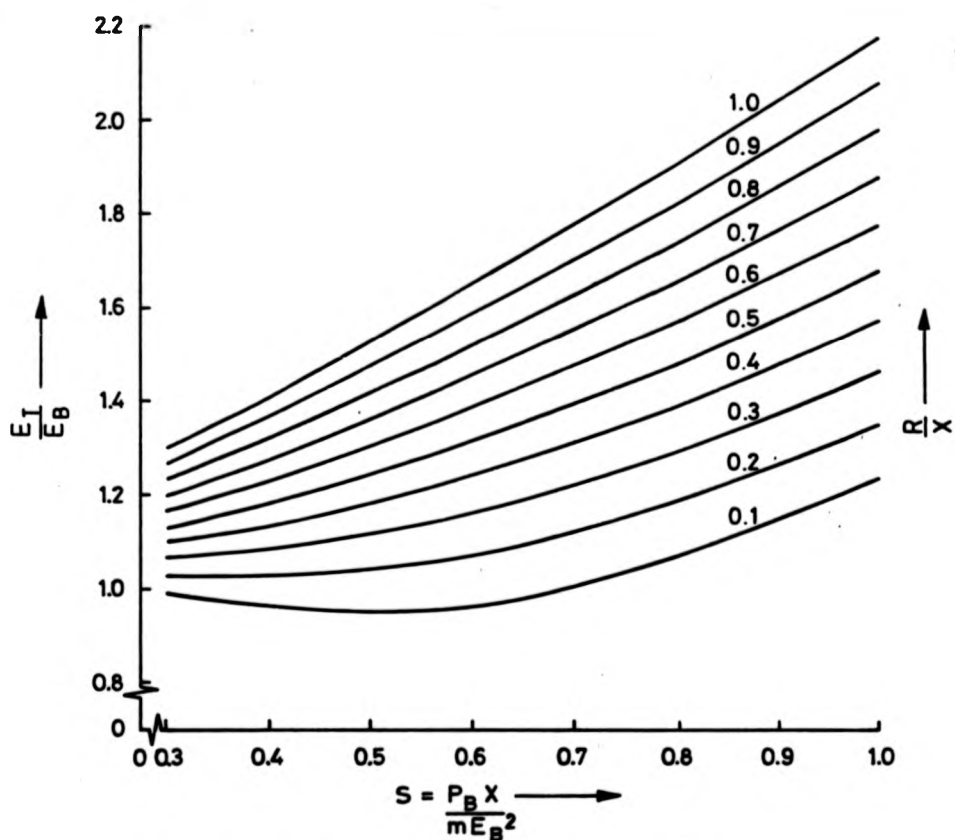


FIGURE 21. NORMALIZED TERMINAL VOLTAGE W.R.T. S
AND $\frac{R}{X}$ FOR MINIMUM $-S_T$ α

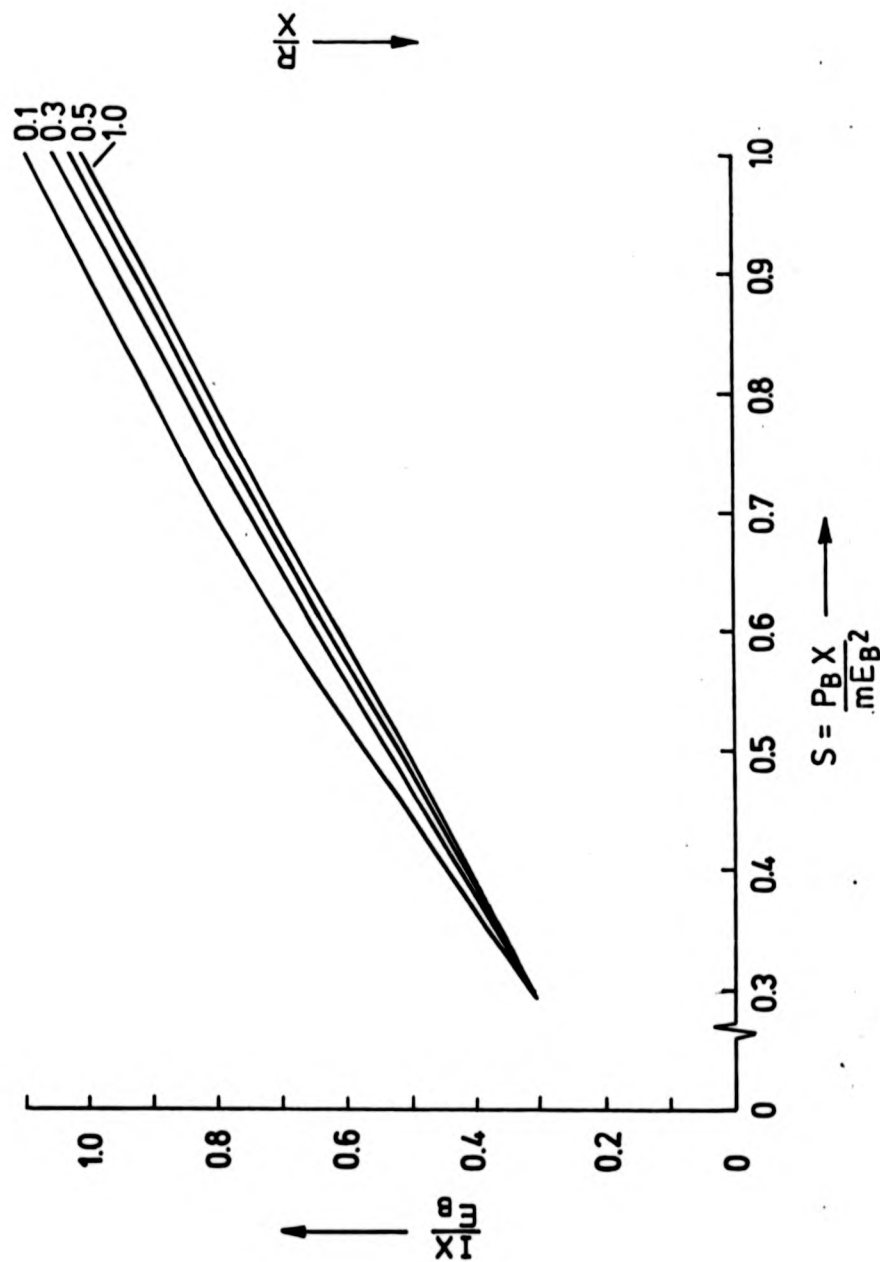


FIGURE 22 NORMALIZED PHASE CURRENT WRT S AND $\frac{R}{X}$ FOR MINIMUM $S_T - \alpha$

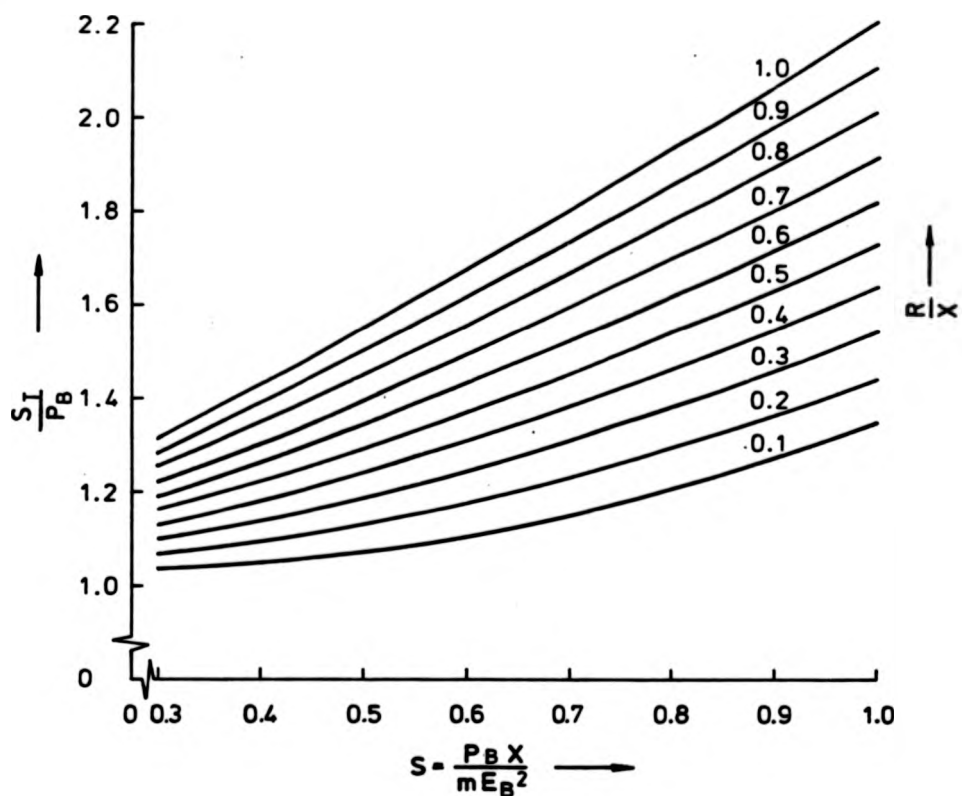


FIGURE 23. NORMALIZED POWER INPUT WRT S AND $\frac{R}{X}$ FOR MINIMUM - $S_T \alpha$

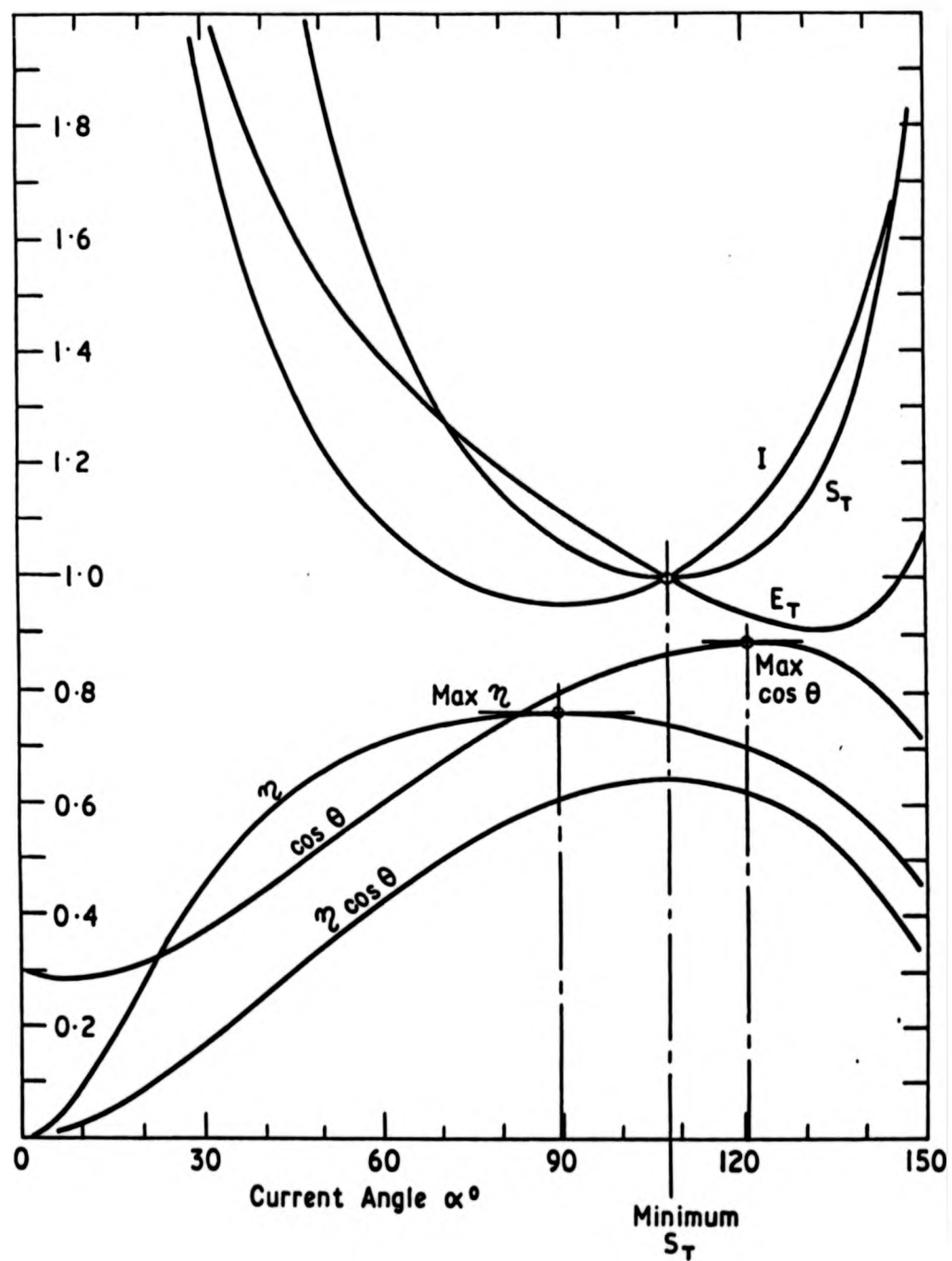


Figure 24. Performance Characteristics of LSM at Cruise.

the track heating and conductor temperature rise and so determines the type of insulation and its ageing, whereas the terminal voltage affects the risk of insulation breakdown, and the inverter semiconductor required blocking voltage and the subsequent cyclical stress.

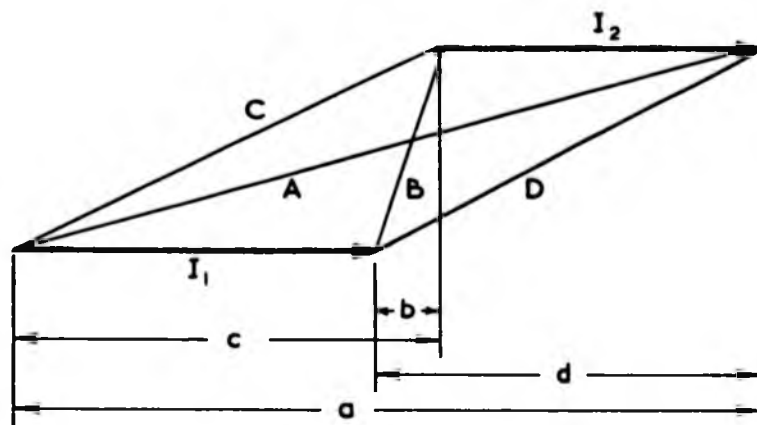
3.2 Inductance and Induced Emf Modelling

3.2.1 Mutual Inductance

In establishing the equivalent circuit model, it has been assumed that the phase inductance and back emf are known singular quantities. There are in fact force and other parameter harmonic pulsations in the model to be considered. Force pulsation occurs because of nonsinusoidal currents flowing in the armature winding, and the nonsinusoidal nature of the main airgap field. If the track windings and the field coil array are decomposed into elemental filaments, the mutual inductance between interacting filaments can be calculated (Figure 25). For LSM design, a common method of calculation is to evaluate the mutual inductance linkage for a vehicle coil and a track array, and derive the force components as gradients of force about a working point (195,219). This involves evaluating mutual inductance six times about a common reference point. Figure 26 shows a suitable coordinate set, and identifies the convention adopted at Warwick for vehicle and track coil dimensions. The alternative solution to evaluate the forces is to lump the effects of vehicle to track linkage effectively into the back emf, E_B . Because the system is iron free, super position can be applied, so harmonics can be treated at each level separately, if required. For a particular mutual field-stator mutual inductance M_{FA} , and superconducting equivalent current i_F , the back emf is given by (107)

$$E_B = \frac{1}{2} \omega \frac{I_F}{F} M_{FA} \quad (29)$$

An alternative to a strict application of mutual inductance formulae for offset rectangular coils, is to evaluate the line integral of a track wavelength vector potential around a vehicle loop. In this way mutual inductance is similarly defined for a unit of current flowing in the track loop. Raytheon had used this method to look at shape effects in different track and vehicle coil geometries.



$$M = \frac{\mu_0}{4\pi} \left\{ \log_e \left[\frac{(A+a)^a (B+b)^b}{(C+c)^c (D+d)^d} \right] + C + D - A - B \right\}$$

Figure 25. Mutual inductance between parallel current elements.

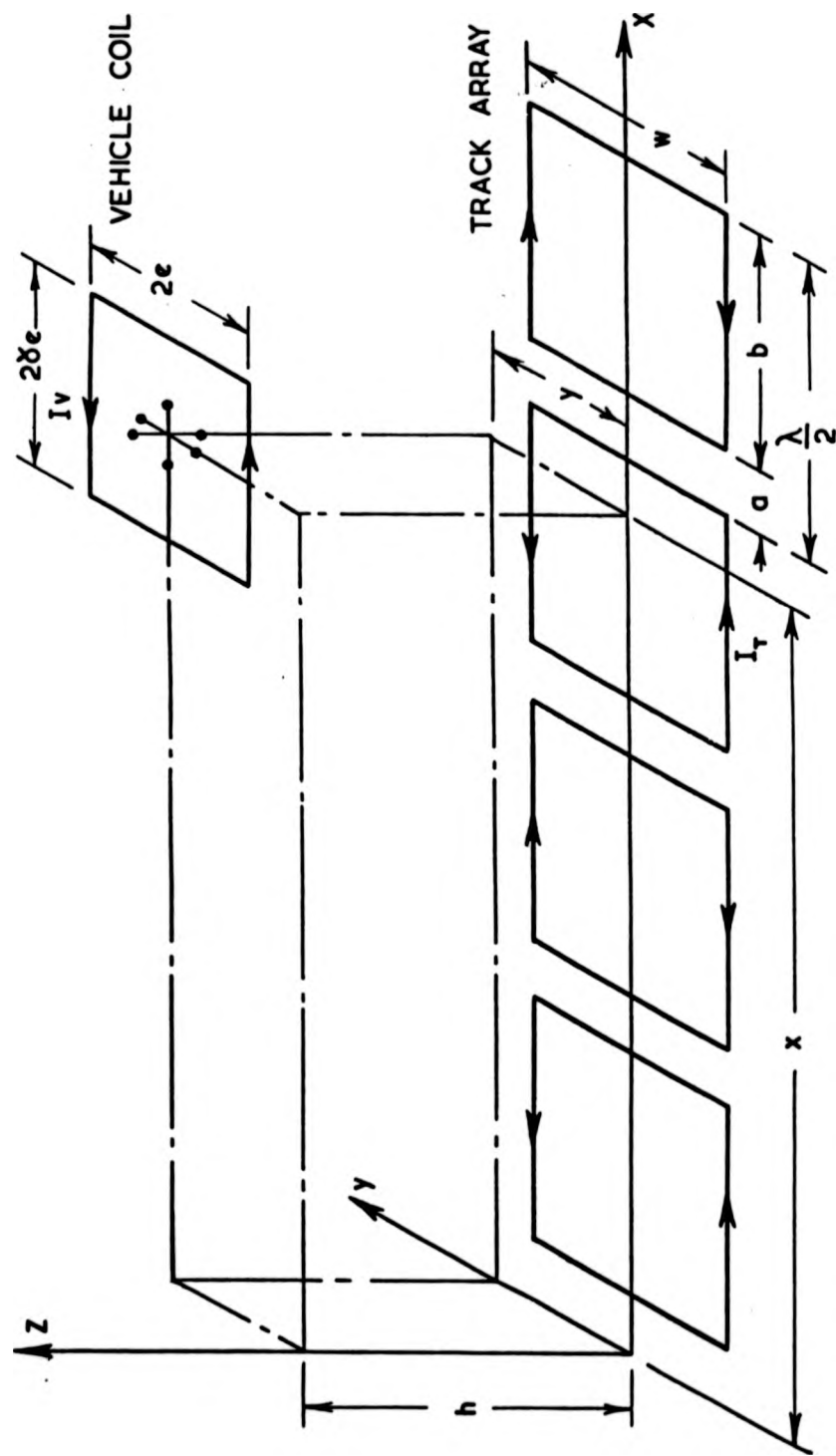


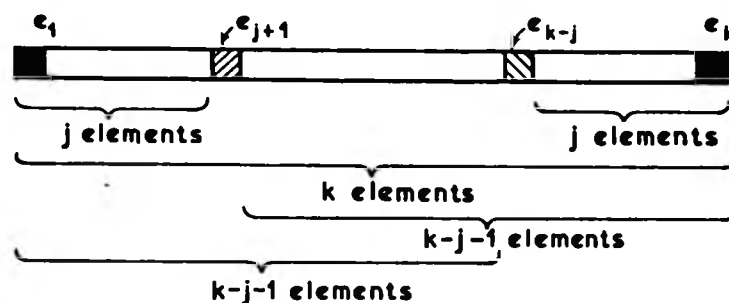
Figure 26. Coordinates for mutual inductance, vehicle coil to track coil array.

3.2.2 Track Inductance

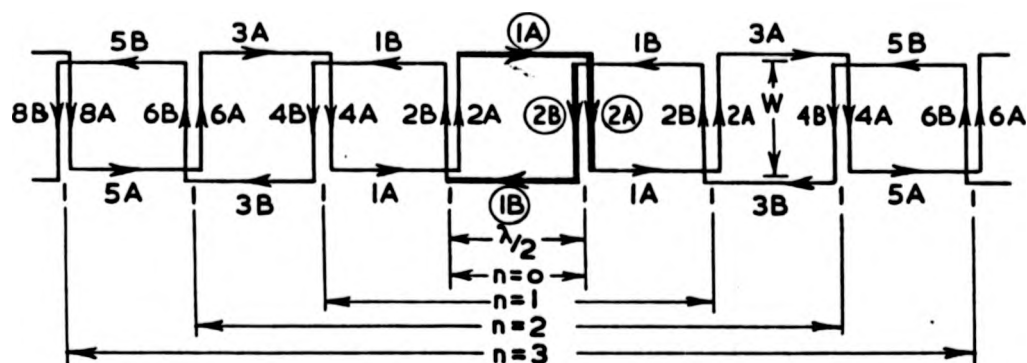
The inductance of the meander coil type winding for the LSM is basically found to consist of two major parts. For one phase a self inductance can be established which relates to the mutual linkage of the phase winding with itself, and for a double layer winding this in fact becomes a quantity which scales linearly with increasing winding energised length. As well as the self linkage, linkages exist with the remaining phases of the machine, and the currents in these phases set up mutual voltages in the original reference phase. These too scale linearly, for the double layer winding. Appendix III gives details of the derivation of both terms. To analyse the self inductance, the concept of an elemental inductance is introduced, being a unit of one phase which is one pole pitch long. If the whole energised phase is made up of, say, k elements, then for a particular element e_{j+1} , its elemental complement e_{k-j} must also exist, so that both have j elements outboard to themselves (Figure 27a). If the elemental inductance interacting to n , or $L_e(n)$ is defined as the self inductance of an element e , and the mutual inductance due to e and the n elements on both sides of e , by writing the contribution of e_{j+1} and e_{k-j} to the phase total self inductance, and rearranging, the total strip self inductance $L_T(k)$ is given by

$$L_T(k) = \sum_{n=0}^{k-1} L_e(n) \quad (30)$$

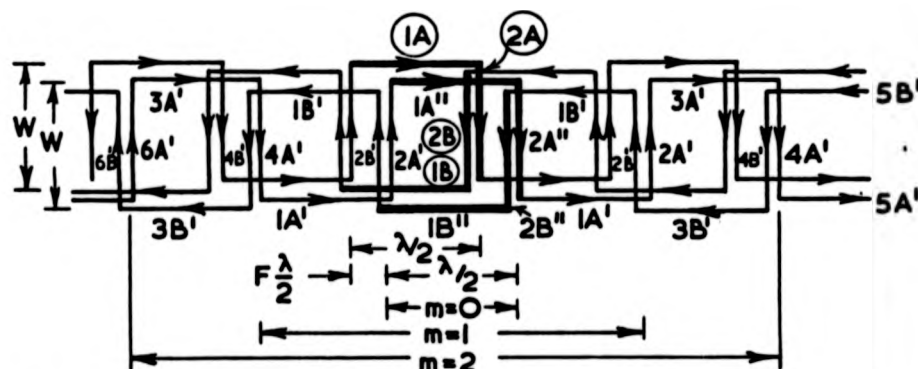
For a double layer winding, an elemental pole pitch is identified, and evaluation of the elementary inductance proceeds as sequential pole pitches are added to either side of the initial element, to n increments. Figure 27b shows the way in which the terms are defined. In fact equation 30 holds for this case too. The two main terms in the total self inductance of the meander winding are termed the initial inductance, L_i , which effectively defines the physical shape of the winding conductor, and one which is a function of the geometric disposition of the conductor, and varies with the pole pitch machine width ratio, the asymptotic inductance L_a . The track phase self inductance, L for a section length G metres long is given by



(a) Subdivision of meander winding into pole pitch elements.



(b) Definition of limbs for self inductance calculation.



(c) Definition of limbs for mutual inductance calculation.

Figure 27. Armature winding representation.

$$L_G = \frac{2G}{\lambda} (L_i + \frac{\lambda}{2} L_d) = G (\frac{2}{\lambda} L_i + L_d) \quad (31)$$

The mutual linkage to the remaining phases from the reference phase is calculated in a similar manner. The form of the mutual inductance must vary cyclically as the displacement between the reference phase and a second phase varies. If F is the fraction of a pole pitch that the second phase is displaced from the first phase, then

$$M(F) = M(F + 2) = -M(1+F) = M(-F)$$

$$\text{and } M(\frac{1}{2}-F) = -M(\frac{1}{2}+F)$$

Figure 27c indicates the disposition of two phases. For a normal three phase arrangement, a second phase is displaced by 120 electrical degrees, or $\frac{2F}{3}$ of a pole pitch.

$$\text{So } M(\frac{2}{3}) = M(\frac{1}{2} + \frac{1}{6})$$

$$\text{and since } M(\frac{1}{2} + F) = -M(\frac{1}{2} - F)$$

$$M(\frac{2}{3}) = -M(\frac{1}{2} - \frac{1}{6}) = -M(\frac{1}{3})$$

similarly

$$M(\frac{4}{3}) = -M(\frac{1}{3})$$

If balanced operation is assumed, phase currents are equal in magnitude and the mutually induced voltages in the reference phase from the other two phases are individually the product of phase current, mutual inductance and $\cos 60^\circ$, so together they can be summated as a full phase current producing a voltage drop in $M(\frac{1}{3})$, for the reference winding, and three phases.

As with the self inductance, the elementary inductance $M_e(m)$ is defined as the interaction of the reference phase with the second reference elements and the m elements either side. The mutual inductance between phases G metres long is

$$M_G = G (\frac{2}{\lambda} M_i + M_d) \quad (32)$$

where again M_i is an initial shape term, and M_a is an asymptotic value, assuming F remains constant. Figure 28 shows the variation of L_a and M_a with the width/pole pitch ratio.

For the three phase case, M_G and L_G combine to give the total phase leakage inductance, L , as

$$L = (L_G - M_G) \quad (33)$$

and this value can be successfully used in further computation or equivalent circuits.

It is found from this type of analysis that a double layer meander winding shows significant improvement over a single layer meander winding. Essentially a single layer would have to be connected remotely, whereas a double layer allows a common terminal point for machine half phases. The effective self inductance of the phase winding is virtually halved.

3.2.3 Back Emf

The back emf, E_b has been chosen as the main linking parameter for field to armature linkage. If this value is known for a full pitched coil moving at synchronous speed, then conventional rotating machinery analysis can be used to establish the open circuit terminal phase voltage, including the effects of short pitching, transposition, and parallel and series interconnection of individual armature conductors into a phase winding. Initial analysis has assumed that the machine is fed with balanced voltages and currents, and operates under steady state conditions. Phase imbalance can in fact be accommodated by using positive and negative sequence analysis.

Taking the case of the generalized vehicle and track coil shown in Figure 29, the vehicle coil energised with I_v AT generates a track level vertical component of flux B_z . The flux linked by an elemental strip dx wide is given by

$$\begin{aligned} d\phi &= \left\{ \int_{-b}^b B_z dy \right\} \cdot dx \\ \text{i.e. } \frac{d\phi}{dx} &= \int_{-b}^b B_z dy \end{aligned} \quad (34)$$

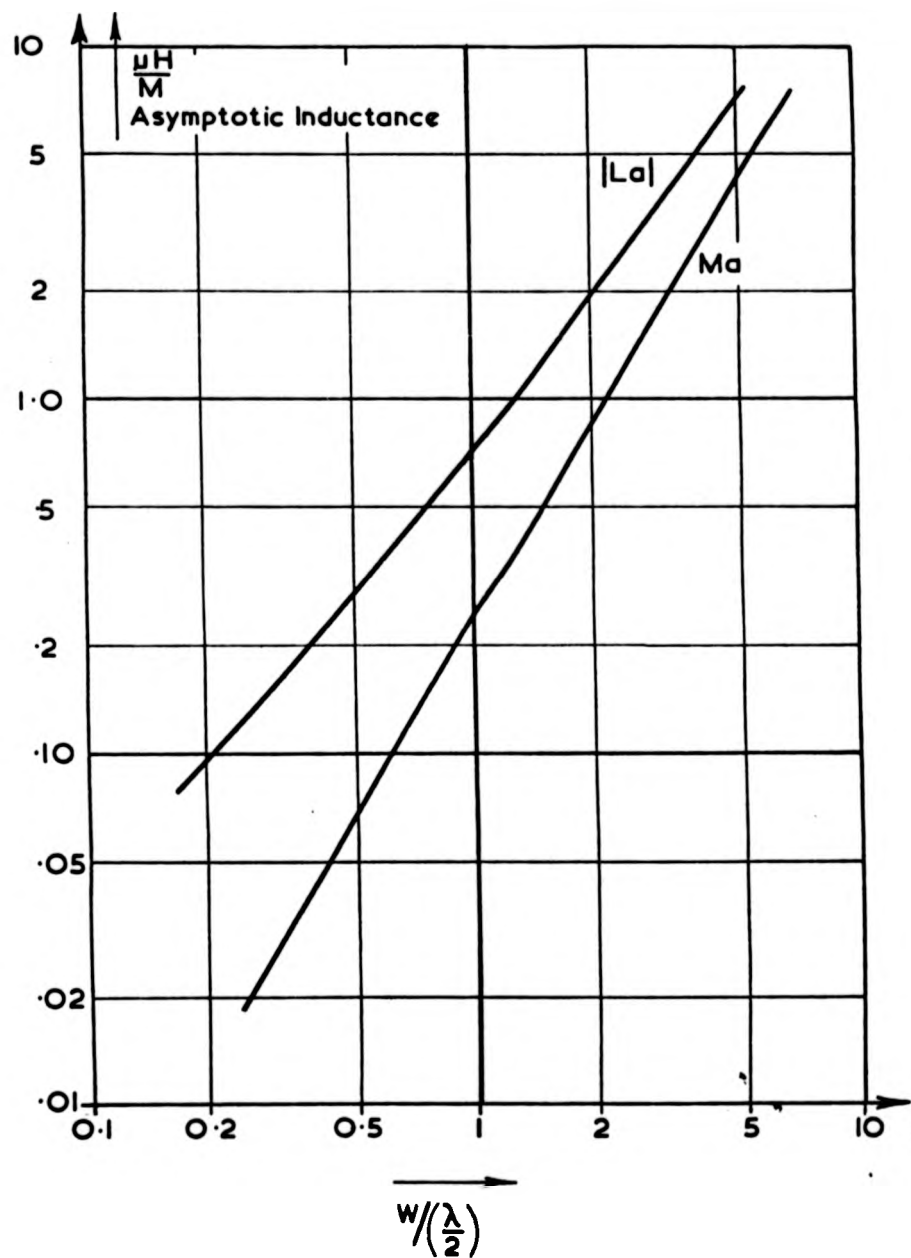


Figure 28. Asymptotic Self and Mutual Inductance as a function of width/pole pitch.

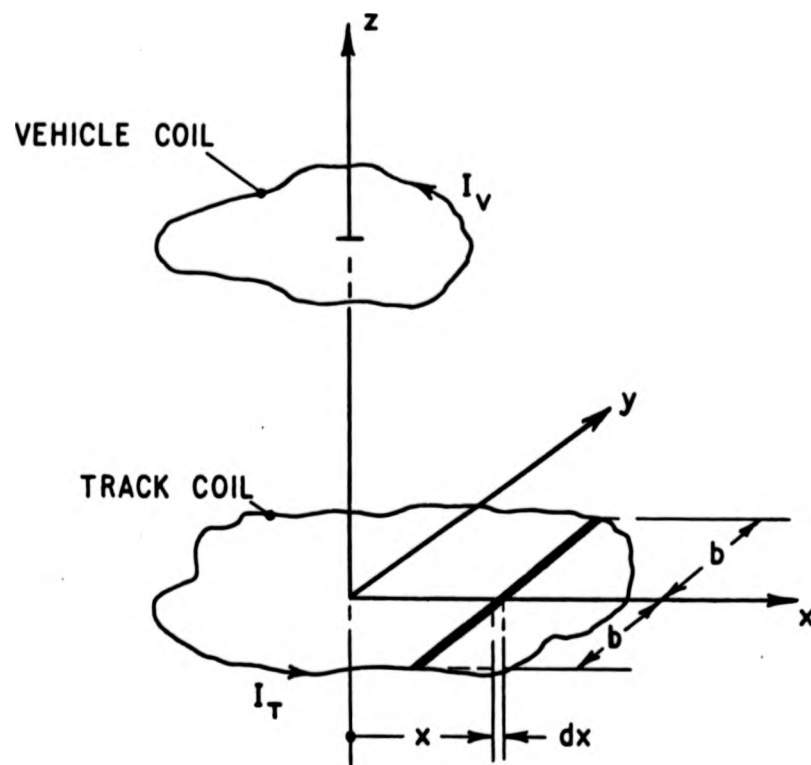


Figure 29. Generalized Vehicle and Track Coils.

The effect of having offset coils is merely to change the limits of integration. For the most common cases of tandem arranged vehicle coils, the zero offset position links the most flux. Equation 34 is valid for whatever topology of coils is finally chosen, independent of end winding geometry. The back emf induced in the track coil by the passage of a vehicle coil is simply equation 34 times the velocity.

Before attempting to evaluate 34, it is worth examining the total effect of an array of coils on the track level flux density distribution. Since the LSM is air cored, superposition can be used to sum the effects of both distant and near coils. It is necessary to establish the order of magnitude of numbers of coils to be included, to give an idea of the likely sensitivity to force calculations. By using a dipole approximation, the effect of neighbouring coils can be determined.

The external field of a current loop can be decomposed into an infinite series of multipoles. In the coil plane,

$$B(r) = \sum_{n=2}^{\infty} \frac{\mu_n}{r^{n+1}} \quad (35)$$

μ_n is the n th pole magnetic moment, and r is the distance from the coil centre line to the field point considered. Since only far off effects are concerned, the higher orders can be neglected. The coil now appears as a dipole, and its field diminishes as the cube of the distance. For the case of the incremental contributions of $2N$ neighbouring coils, with for example, alternating polarities, to the total field of the reference coil, it is found that

$$B_z = \frac{2\mu_2}{(\frac{\Delta}{2})^3} \sum_{n=1}^{N-1} \left(\frac{1}{n^3} - \frac{1}{(n+1)^3} \right) \quad (36)$$

$$n = 1, 3, 5, \dots$$

For an accuracy of better than 0.1%, only 16 neighbouring coils need be considered. Generally, roughly ten coils give an accuracy that is sufficient for most engineering design purposes.

To establish the magnitude of the back emf, an analysis of the flux density under a coil must be made. Powell and Danby attempted to analyse a LSM with a very high harmonic content, and used a simplified expression for rate of change of flux linkage⁽⁷⁹⁾. Atherton attempted to provide a complete solution for a generalised array, but similarly failed to include all the sides of a rectangular magnet in the contribution to the flux⁽¹⁰⁵⁾. Nasar continued the application of a incomplete flux linkage solution in establishing his version of LSM theory⁽¹⁹⁵⁾. While a solution for back emf is of course possible taking into account only the transverse field coil limbs, it can have serious effect on the evaluation of performance, especially for more compact coils where width approaches pole pitch.

A generalized expression has been obtained for the rectangular coil vertical field at an off axis position given by coordinates x, y in Figure 30⁽²²²⁾.

Appendix IV is a copy of this Warwick Maglev Technical Memorandum. The expression includes the contribution of all four sides, and is integrated to give the flux linkage of the coil with a track elemental strip. Essentially the rate of change of flux linkage is a function of five parameters, namely

$$\frac{d\phi}{dx} = \text{fn} (\gamma e, e, b, z, x) \quad (37)$$

γe and e are the vehicle coil half length and width, b is the track half width, z the levitation height, and x the off-coil centre line longitudinal displacement.

It is now possible to fully demonstrate the effect of neighbouring coils on the contribution to rate of change of flux linkage, and hence the effect on back emf. Figure 31 shows three coils from a typical (CIGGT) magnet array, with the rate of change of flux linkage of the reference coil A, and the magnitudes of the contributions of neighbouring left and right hand coils, within the half wavelength centred around A. Also shown is the total rate of change of flux

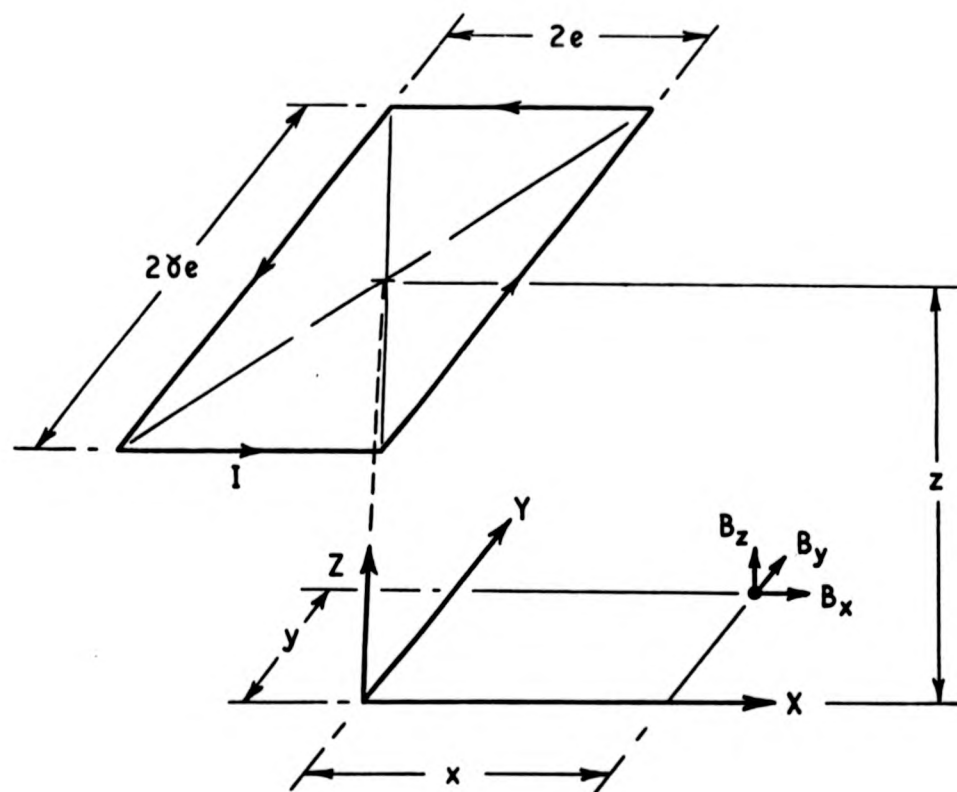


Figure 30. . Field Conventions Adopted for Rectangular Coils.

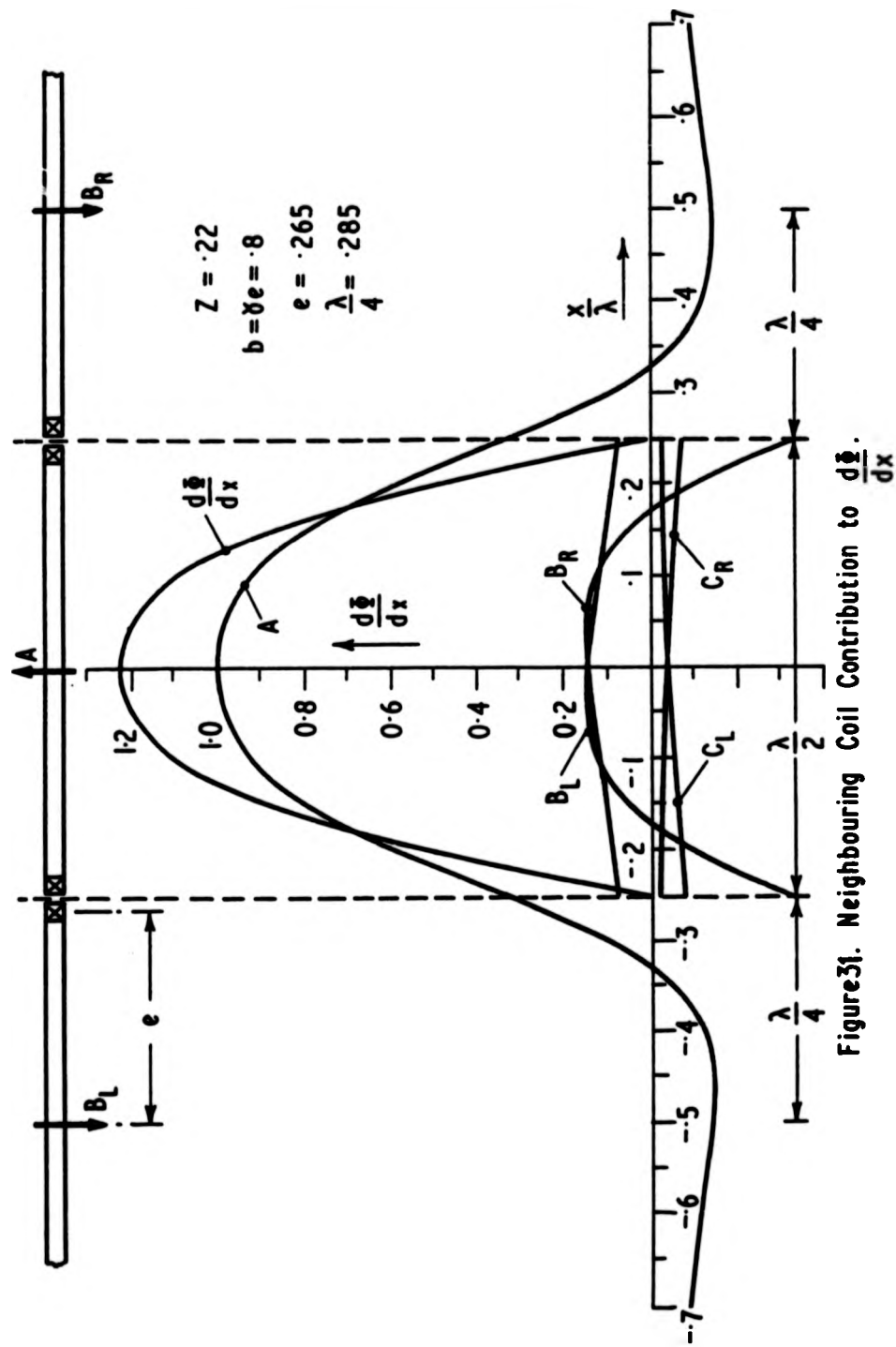


Figure 31. Neighbouring Coil Contribution to $\frac{d\Phi}{dx}$.

linkage, which is forced to zero every half wavelength by conditions of symmetry. In this particular case the effects of two coils ($B_{L,R}$ and $C_{L,R}$) either side of A are included. The effects of additional neighbouring coils on rate of change of flux is shown by Figure 32. Because the case considered is for an alternating array, the successive points alternate about the final value. Also shown is a more rapid convergence, using the incremental difference of successive coil pairs. For this particular case only ten neighbouring coils (i.e. five either side of the first coil) need to be considered to give a reasonable result. The way in which the quarter wavelength value of x is rapidly forced to zero confirms the accuracy of the calculation.

Once the total rate of change of air gap flux linkage with the full pitch track coils is known, its harmonic make up can be evaluated. With the conventions shown for the x axis starting on the vehicle coil centre line, then only odd harmonics will be present in a cosinusoidal summation. Since the air gap flux is dominated by the field contribution, armature reaction will hardly affect the air gap flux distribution. This is much more marked in a linear superconducting machine as opposed to a rotary superconducting machine, where the high field winding mmf is used to increase the machine specific output and the armature reaction is similar to conventional machinery. When the flux waveform is analysed, the choice can be made to short pitch the armature winding to subvert particular harmonics, and phase spread the winding, or to simply operate with only a few turns per phase per pole, establish a star connection and allow harmonic currents to flow through the neutral to the inverter station.

In general the LSM design for Maglev vehicles will operate at an airgap to coil half width ratio near unity, which implies a near sinusoidal flux waveform at the armature. Other applications of the LSM, especially when used to propel contact guided vehicles, will imply a lower ratio, and harmonic fluxes will dominate the design procedure. For the CIGCT machine, the first harmonic has a

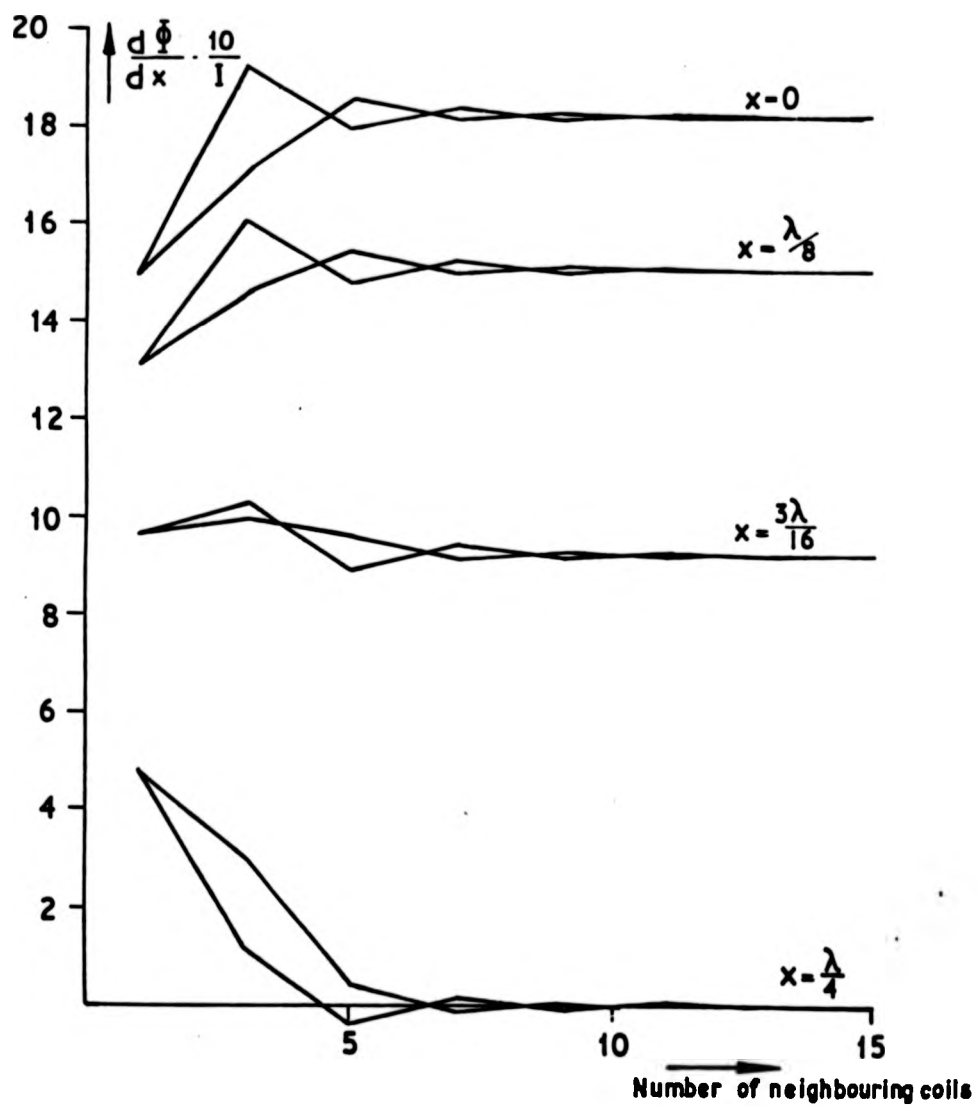


Figure 32. Effect of neighbouring coils on rate of change of flux.

amplitude of 108% of the rms value, with a 9% contribution from the third harmonic, which could be eliminated by a delta connection. There is virtually no harmonic contribution past the ninth harmonic⁽²²³⁾.

Having only dealt with rectangular coils, the field variation at off axis positions for circular and racetrack coils must be defined. Circular coils require the solution of complete elliptical integrals of the first and second kind. Racetrack off axis positions require combinations of straight line element type formulae, with extra terms involving the solution of incomplete elliptical integrals of the first and second kind. The overall technique for solution of rate of change of air gap flux linkage is similar to that used for rectangular coils, but is computationally more awkward. When working at large air gaps an equivalent area rectangular coil can be used for first order approximation, with only a slight loss of accuracy.

Once the harmonics of the back emf are known, the force pulsations on the vehicle, and indeed the force profile can be determined by taking harmonics in turn and applying their values to equation 15. If the current has significant harmonic content, this too can be incorporated to produce the total pulsation of the parasitic harmonic forces.

3.3 Wavelength Optimization

For machine parameter optimization a more general model is required. Operational optimization in choice of a minimum power factor efficiency product working point used an equivalent circuit model. Ideally a wide track giving a long active length per pole, and a short pole pitch, to enable a large number of poles to be used might appear to be the best choice. However, track width is usually determined by the likely infrastructure and compatibility requirements with other systems, as well as vehicle width; pole pitch might be fixed by inverter or cycloconverter upper frequency limits, and cryostat and coil fabrication constraints. A simple model can be formed in which levitation height and track width are the main variable parameters, which are functions of groups of track and vehicle constants.

Thornton analysed a simple model of a finite width track interacting with a two dimensional field distribution from an effectively infinite width magnet array⁽⁹¹⁾. For this case the time averaged thrust force F_B is related to a maximum fundamental thrust force F_M by the current angle. Similarly the normal force F_N is the quadrature variation. F_B and F_N are expressed by

$$F_B = F_M \sin \alpha \quad (38)$$

$$F_N = -F_M \cos \alpha$$

By comparison with equation 15, F_M can be related to the back emf and phase current by

$$F_M = \frac{m}{v} E_B \quad (39)$$

Taking a $\vec{J} \times \vec{B}$ product with the assumption of balanced phase currents and a sinusoidal current sheet representing the magnet array, with a strength of I_v AT per pole, from N poles, then,

$$F_M = 2\mu_0 N m I_v I_T D \frac{w}{\lambda} e^{-2\pi h/\lambda} \quad (40)$$

m and I_T are the number of stator phases and the track per phase current, w , λ and h are track width, wavelength and coil height, and D is a dimensionless constant which expresses the meander winding end turn shape.

Two more useful parameters are P_A , the power loss in the armature per unit track length, and M_A , the meander mass per unit track length. P_A is proportional to the efficiency of the machine, and hence power consumption, and is measured in watts per metre. M_A is proportional to the amount of capital cost in installing the guideway meander conductor, and is in kilogrammes per metre.

$$\text{So } P_A = m I_T^2 \cdot \rho \cdot \frac{(\lambda + 2w)}{2A\lambda} \quad (41)$$

$$\text{and } M_A = m \frac{(\lambda + 2w) A \sigma}{\lambda} \quad (42)$$

where σ and ρ are the density and resistivity of the track conductor.

Combining 41 and 42,

$$M_A P_A = m^2 (\lambda + 2w)^2 \frac{I_T^2 \rho \sigma}{2\lambda^2} \quad (43)$$

and eliminating the track current in (40) with (43)

$$F_M = 2 \mu_0 N I_V \frac{(2M_A P_A)^{\frac{1}{2}} H}{\rho \sigma} \quad (44)$$

$$\text{where } H = \frac{D w}{\lambda + 2w} e^{-2\pi h/\lambda} \quad (45)$$

H embodies width, height and wavelength in a form that can be optimised.

Equation 44 contains (apart from H) items that are very often fixed by economic constraints or material conditions. For example, working the track at a particular P_A implies a choice of efficiency maximum, and for M_A , a track capital repayment cost can be inferred. $N I_V$ is reflected directly into the vehicle cost. It is reasonable, therefore, to assume that these parameters take fixed values, and that design manipulation must be through H.

Thornton chose to maximise the thrust per pole, which implies that a vehicle thrust requirement can be met by simply adding poles. The maglev vehicle however has finite length, which is fixed at an upper limit by a tradeoff between lightness and structural stiffness in torsion and bending moment. Abel, however chose to maximise the thrust per stator conductor length under the vehicle - stator current product, or effectively H divided by wavelength⁽¹³⁰⁾. The power transferred to the finite length vehicle is maximised, which is more reasonable since usually the full vehicle length will be required for propulsion magnets, and may in fact limit the thrust capability in very high powered vehicles.

If the thrust per unit stator length-current product is found for various values of wavelength, the resulting magnitude tends to have a broad maximum, depending on the track width and magnet height. Figure 33 shows the normalized thrust,

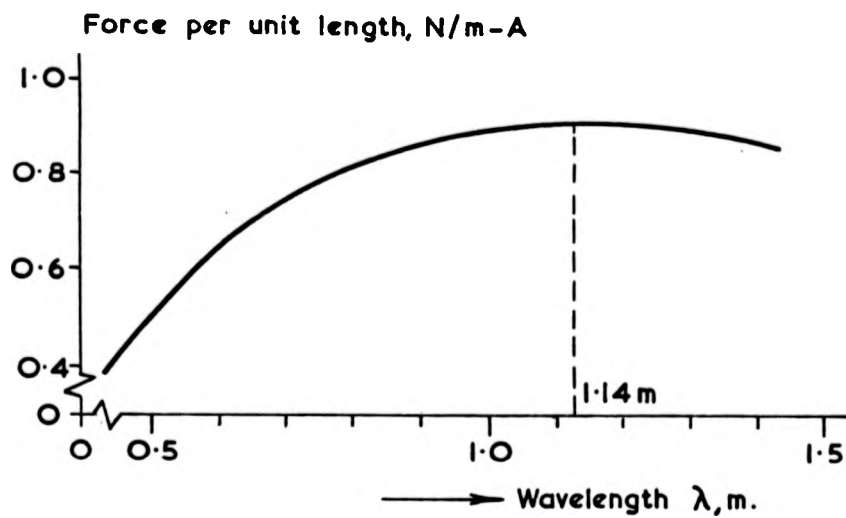


Figure 33. Thrust per unit stator length x current.

and Figure 34 shows the optimum wavelength for a range of magnet heights and track widths. Values for infinitely wide tracks are also shown. The optimum value of wavelength is

$$\lambda = \frac{w - \pi h}{2} \left[\left(\frac{1 + 8 \pi h w}{(w - \pi h)^2} \right)^{\frac{1}{2}} - 1 \right] \quad (46)$$

resulting directly from maximising H divided by wavelength with respect to wavelength.

For the Wolfson LSM design studies, the armature fits between two levitation conductors and is fully spanned by a vehicle coil array. The assumption of a current sheet approximation for the field array is reasonably valid. For a revenue vehicle this validity breaks down, but in fact a mutual inductance derivation of various wavelengths for different track widths and magnet heights leads to similar optimum wavelength. The normal force maximum is generally greater than the thrust force maximum, since the side limbs of the magnets develop significant lift force but do not aid thrust.

3.4 Shape Effects on Coil Stress⁽¹³¹⁾

The use of superconducting magnets as the source of magnetic flux for LSM propulsion has generally been approached from the assumption that it is possible to construct tight corner radius rectangular coils. For the Wolfson design, lateral stiffness and lift to drag ratio considerations suggest that degradation of performance in levitation and guidance would occur if the proposed rectangular tandem array was made up of circular coils. In practice, it is extremely difficult to construct working magnets with tight corner radii without experiencing problems of winding migration and stress concentration at the corners. The usual method of accommodating excessive stresses is to wind circular or racetrack coils. To achieve an optimum design, it is necessary to be able to predict whether it is possible to construct coils which have tight radii at the corners and can still accept the stress levels when energised without all the attendant problems. Usually for a particular vehicle, width is at a premium. For the CIGGT design the width must accommodate the LSM propulsion cryostats as well as levitation cryostats. Propulsion magnet size is

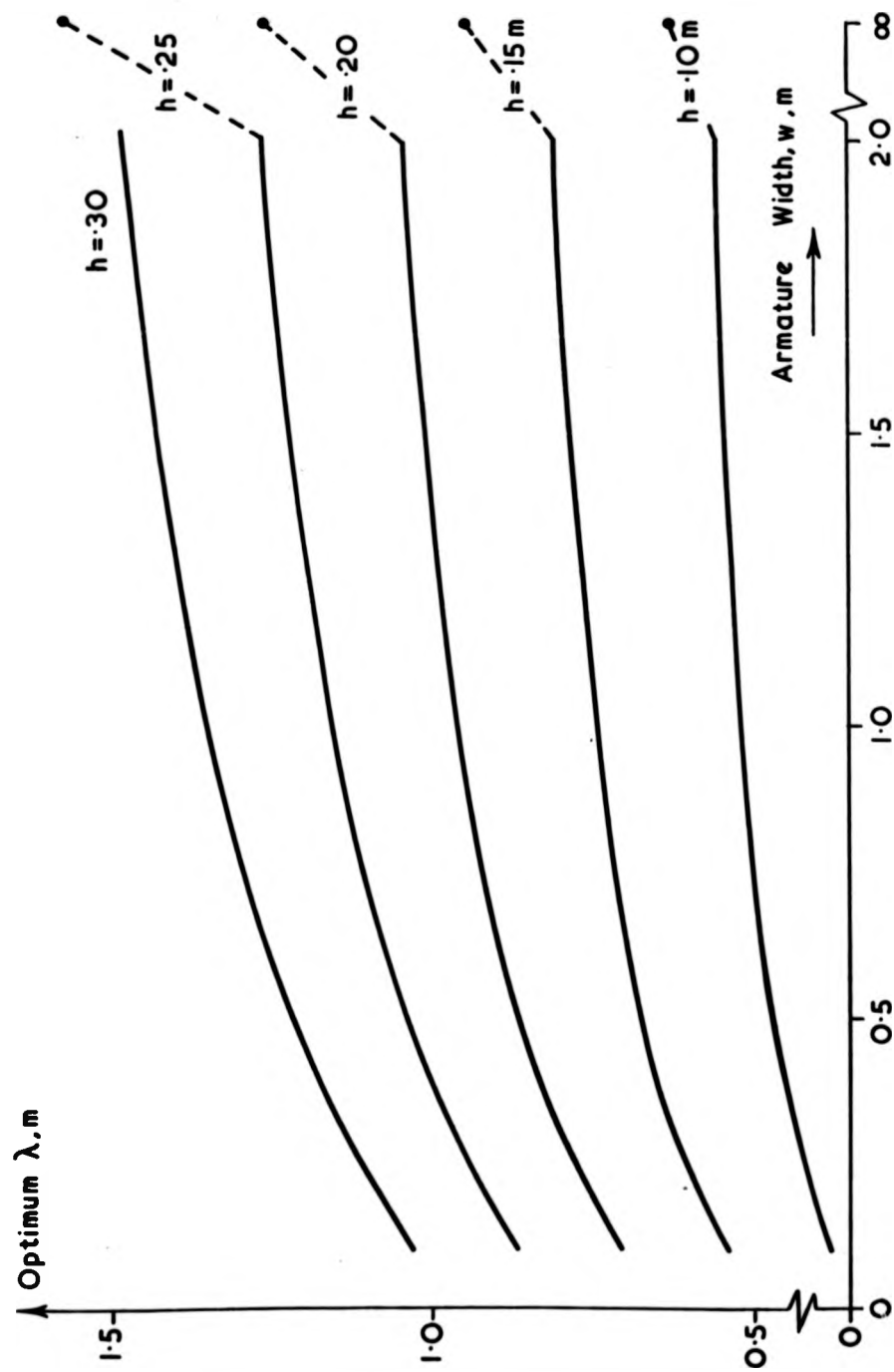


Figure 34. Optimum wavelength for machine width w , and airgap h .

determined by the thrust requirement, passenger density, and hardware costs and generally the wavelength will be in the range of 1-3 metres. For a full race track end wound propulsion coil, the linear motor active length is reduced by about half a wavelength, compared to a rectangular coil. If a dual or transverse-flux motor is adopted, then four sets of end windings will have to be accommodated in the vehicle width, with allowance for levitation magnets included.

The forces on coil systems are generally due to several sources.

Mechanical stresses are induced as the coil is built. Many large superconducting coils are prestressed as they are wound, and additional clamping forces and support increase the inherent stresses. As the coils are cooled down to their working temperature, uneven material contraction can cause thermo-mechanical forces to be generated. Thirdly, as the coils are energised, magnetomechanical forces generate further stress levels. Coil stressing can be attacked at several levels of complexity. Figure 35 shows several simple elements and the way in which the Lorentz forces are generated by the interaction of an elemental current flowing in a coil part in a background field, generated either by the element itself, or an outside source. Usually coils have significant build up in three directions and a finite element solution is suitable, but requires significant computing.

For circular coils, the field level variation throughout the coil section can be evaluated using either tables or direct calculation. Appendix II gives details of the methods used in rectangular and circular solenoid design. The easiest stress analysis is to approximate the coil to a thick/thin cylinder, and model the internal stress boundary condition by a magnetic pressure. A homogeneous thick cylinder theory produces a more accurate solution. Coils are usually anisotropic structures and so account must be taken of the orthotropy, as the stress tensor is evaluated. Mulhall and Prothero analysed a homogeneous anisotropic solenoid⁽²²⁴⁾

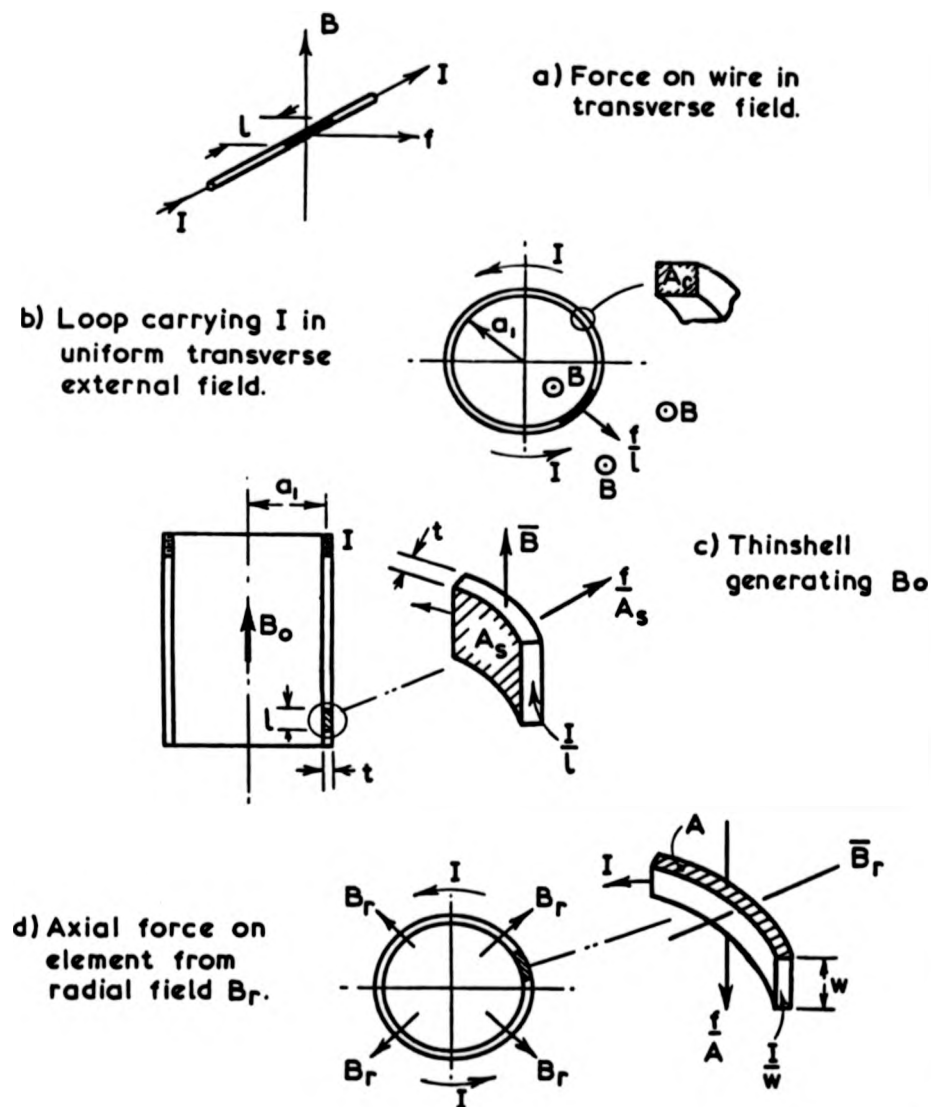


Figure 35. Lorentz forces on simple elements.

by numerically integrating the field generated body force across the coil in the radial direction, to obtain hoop stress values. Abel produced a closed expression for the stress levels for the same case, using the element shown in Figure 36⁽²²⁵⁾. The body force was directly calculated since closed expressions for the radial and circumferential field are known. Montgomery has shown that for circular coils a magnetic pressure approximation approaches an exact solution if the coil build up is small compared to its diameter⁽²²⁶⁾. This condition is usually met by Maglev coils where the strength is of the order of 500 kAT for the motor magnets, and their size is of the order of 0.5-3 x 1-3 metres. If a finite element programme is available, a stress tensor relating strain to stress from equations of continuity and equilibrium would be formed. A typical element is shown in Figure 37 where the element boundary conventions are defined.

When square or rectangular coils are analysed, the exact solution without resort to finite element techniques is difficult. The most critical stress levels will always occur at the corners. A technique developed uses approximate solutions for the stress levels, by effectively matching a magnetic pressure comparison of rectangular and square tubes' stresses with equivalent circular thick walled tubes'. This methodology is acceptable because the free body diagram of sections of a corner radius and a circular coil will be identical.

For the case of a circular coil of mean radius a , winding width (radial build up) s , a magnetic pressure P_M will give hoop stresses σ_θ , radial stress σ_r and shear stress σ_s given by

$$\sigma_\theta = \left(\frac{a}{s} + \frac{s}{4a} \right) P_M \quad (47)$$

$$\sigma_r = - P_M \quad (48)$$

$$\sigma_s = \frac{\sigma_\theta - \sigma_r}{2} = \left(1 + \frac{a}{s} + \frac{s}{4a} \right) \frac{P_M}{2} \quad (49)$$

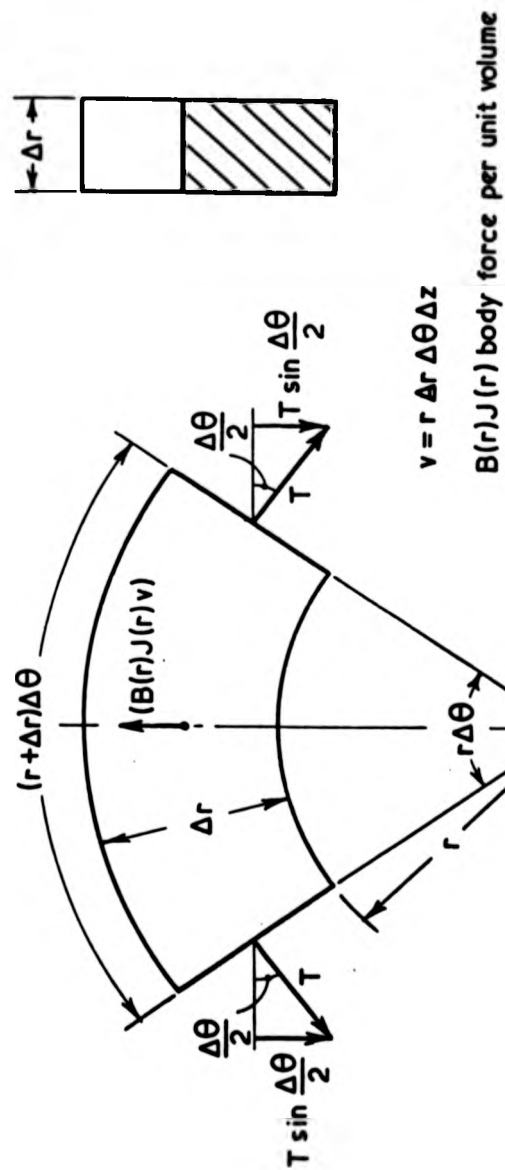


Figure 36. Balance of body forces and restraining forces.

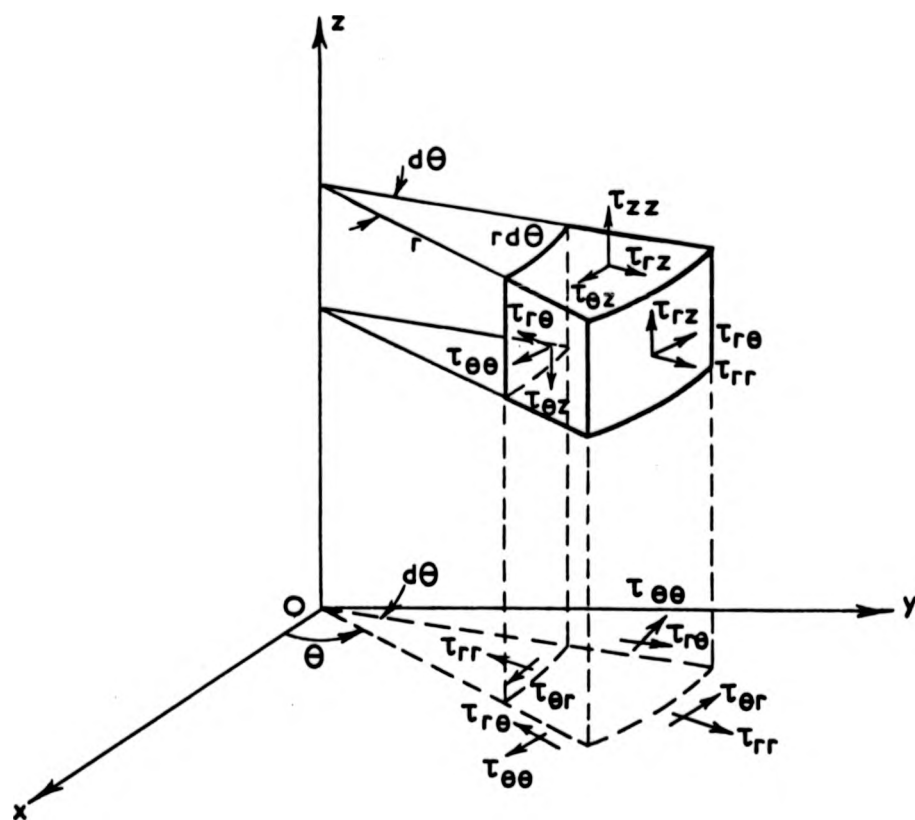


Figure 37. Element for cylindrical coil stressing.

These values are for the inside face of the wound section, where the shear stress is at a maximum.

If the magnetic pressure P_M is taken to be identical to the coil energy density, then to a first approximation

$$P_M = \frac{B^2}{2\mu_0} \quad \text{J/m}^3 \quad (50)$$

where B is the coil flux density. Naturally the coil flux density is modified for the same ampere turns as the corner radius is changed. Figure 38 shows the central field normalized by the factor $\frac{\mu_0 I}{\pi a}$ for the transition from a square coil to a circular coil. The values range from $\frac{\pi}{2}$ (circular) to $2\frac{1}{2}$ (square), and are the combination of field calculations for quadrant and straight line filaments. Although the value of flux density used in equation 50 should be that of the inner face of the coil, the central field value gives a reasonable guide to the exact value.

Roark gives expressions for the corner moment for the simple portal frame and rectangular tube under internal pressure⁽²²⁷⁾. Knowing the bending moment, the hoop stress can be easily obtained at the inner edge. Figure 39 shows the tube and portal frame, with and without radiused corners. For the radiused corner tube, the maximum bending moment is given by

$$M = Cw (2Ye)^2 \quad (51)$$

where C varies from 0 for a circular coil to $1/12$ for a square coil⁽¹³¹⁾ and w is the loading. The hoop fibre stress needs to be modified since the neutral and centroidal axes no longer coincide, and is finally given by

$$\sigma_\theta = 24 \left(\frac{E}{3}\right) C \left[1 + \left(\frac{3}{6n}\right) \left(\frac{1}{(1-\frac{3}{2r})} + 1 \right) \right] P_M \quad (52)$$

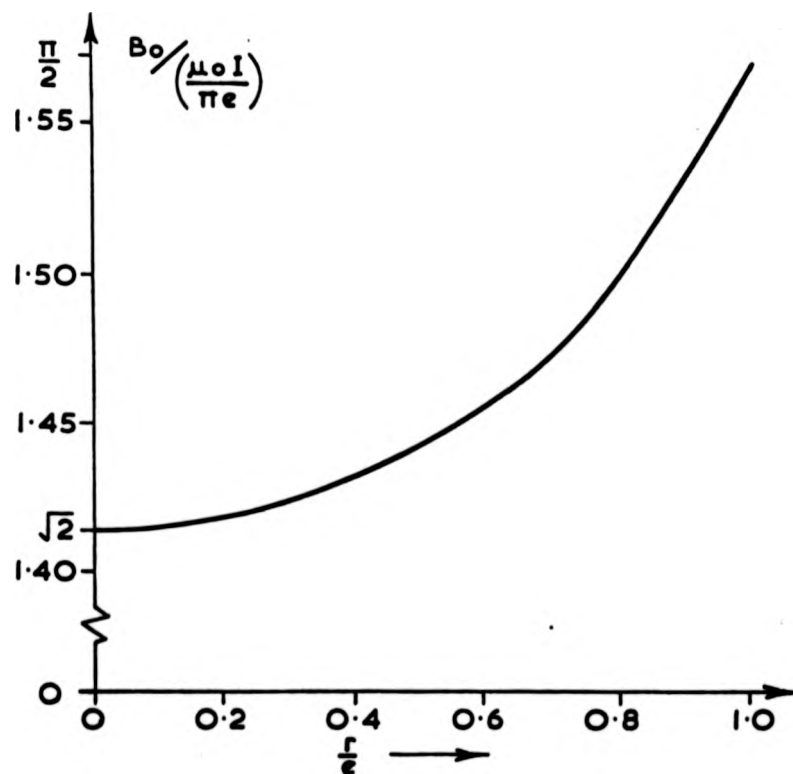
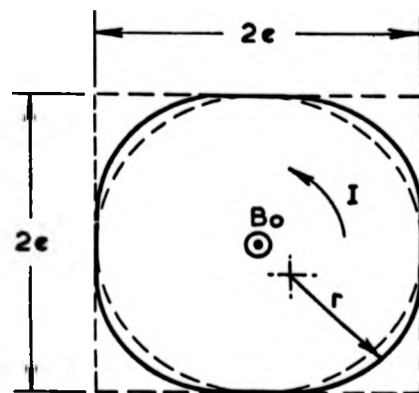
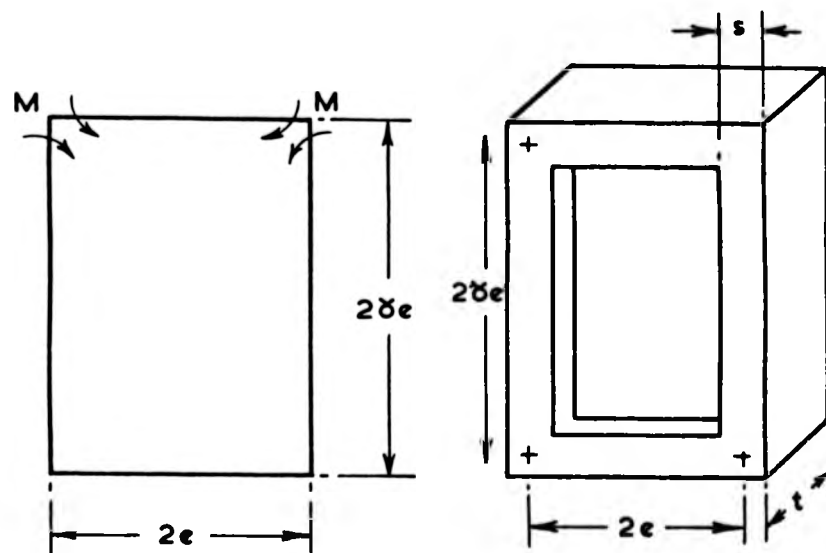
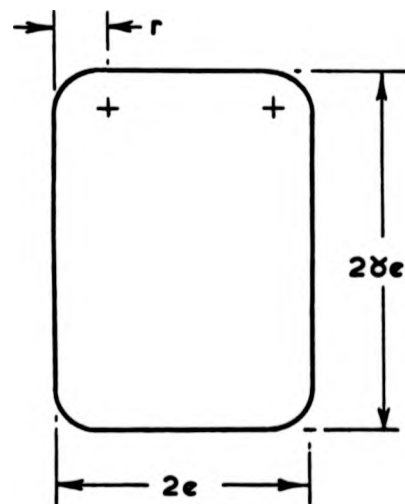


Figure 38. Central field change for transition from square to circular coil.

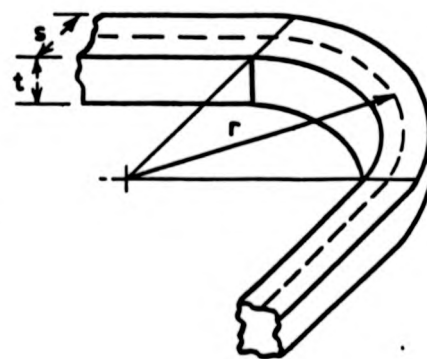


a) Simple portal frame.

b) Rectangular edged tube.



c) Radiused portal frame.



d) Corner section of tube.

Figure 39. Tube equivalents to radiused coils.

Equations 48 and the first half of 49 still hold for the radial and shear stresses.

For a particular wound section (implying buildup and thickness) the radius can be found where the stress levels equal an equivalent circular coil of the same section. The circular equivalent coil can then be analysed using exact solutions including anisotropy. Alternatively, for a particular corner radius determined by factors other than stress levels, accurate computation of stress is provided by the circular equivalent. If this value is excessive a design iteration must be performed.

CHAPTER FOUR
LINEAR COMMUTATOR MOTOR

4. Linear Commutator Motor

4.1 Original Design Philosophy

The idea of using a dc machine with a superconducting field winding seems to have been first considered by Richards and Tinkham in 1972⁽⁸¹⁾. Their concept was to use current reversing switches controlled by the vehicle position to drive dc current into track loops as the vehicle passes. They also expressed concern that the dc linear motor practicability depended on the cost of the large number of switches required. About the same time Atherton proposed a similar scheme, of track coils that were supplied by either ac or dc through bidirectional switches controlled essentially by vehicle position⁽²²⁸⁾. It was felt at the time that this machine variant could avoid any of the expected problems of low speed starting of linear synchronous motors with limited frequency range inverters.

At Warwick University, the reasons for investigating linear commutator motors (LCM) were slightly different. For the 550 metre linear test track, initial designs for LSM had been based on an acceleration length of 250 metres in which a 250 kilogramme vehicle was accelerated at 1.3 gee to 80 metres per second. At this speed the drag power was 32 kW and the inertial power was 108kW, a ratio of 3.4 to 1. On the assumption that a suitable inverter could be acquired for the research programme, the track was first designed for a three block length operation with two blocks permanently connected at any one time, and the acceleration and deceleration blocks switched over as the vehicle entered the central measurement steady state speed section. On evaluating the additional power required to make up losses in the track winding, in addition to the power transferred to the vehicle, it was considered necessary to examine the effect of either providing larger conductor cross section in the main track feeder cable or to supply the track from the feeder at more frequent intervals. Since the track winding is at least two active lengths per wavelength longer than the feeder; a considerable saving could be made in power loss by only energising short lengths of track from the inverter through a feeder line

Figure 40 shows the fraction of power loss for a subdivided track winding with respect to a full length section of track; for the Wolfson design width to half wave-length ratio of 0.375, a 50 metre length has only 66% of the losses of a 250 metre length. Further subdivision only gains at the most another 8%. The track winding would then have 12 bidirectional three phase switches, which would provide a synchronous following of the vehicle, with traversed sections' power being disconnected to leapfrog to the next section. The inverter terminal rating would be reduced, and the individual sections of track would not experience such a long energised time, allowing more time for cooling between runs. If the vehicle magnets were connected to give the same polarity, the track would be wound for a 400mm pole pitch and the ratio of width to pole pitch would be 0.75. The 50 metre block length implied 71% of the 250 metre losses, with a limit of 64%, so the longer pole pitch would be the best choice.

As the concept of short block length continued, it became apparent that the limit was set essentially by the vehicle length, or even single track coils. The power could be ac or dc, provided commutation was possible, and the trackside semiconductors could replace the inverter or cycloconverter units. By phasing the track current relative to the vehicle field, levitation as well as propulsion could be achieved, which coincided with the rest of the Wolfson design of an integrated lift guide and propelled vehicle, using a tandem magnet array. Although the very short energised length LSM, with one coil per bidirectional switch would have to be controlled differently from the multiple wavelength interconnection to an inverter fed tie line, the generic term of LCM was used to describe both types of machine^(124,126). A further subdivision was possible, depending on whether the armature winding was a distributed progressive or concentrated discrete coil winding (Figures 41 and 42).

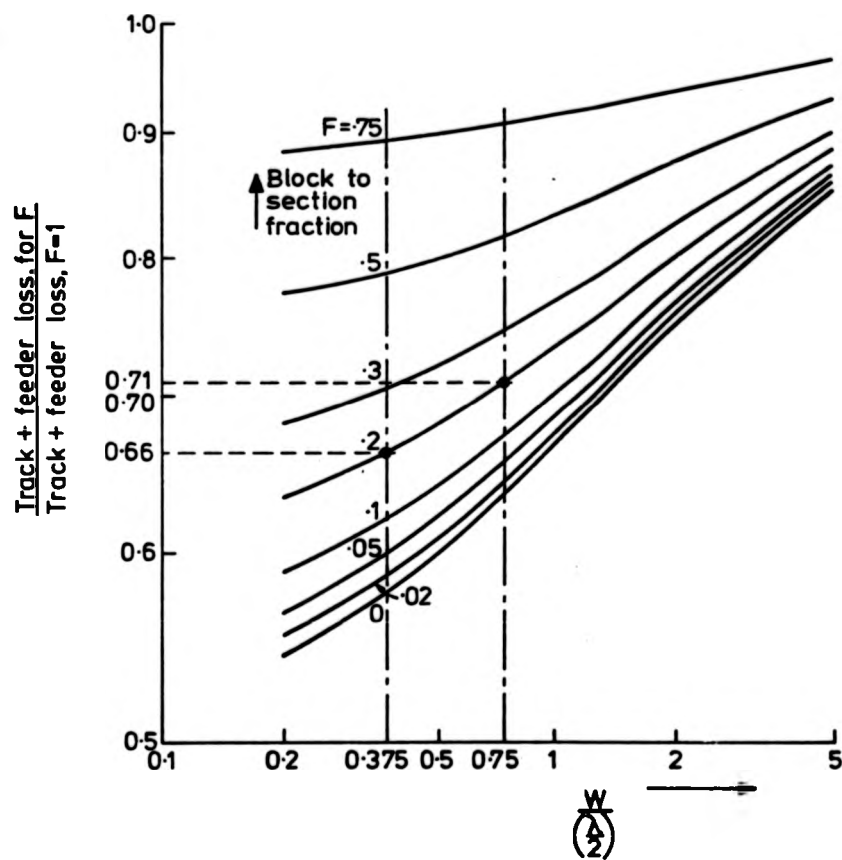


FIGURE 40. FRACTIONAL POWER LOSS IN BLOCK SECTIONED ARMATURE.

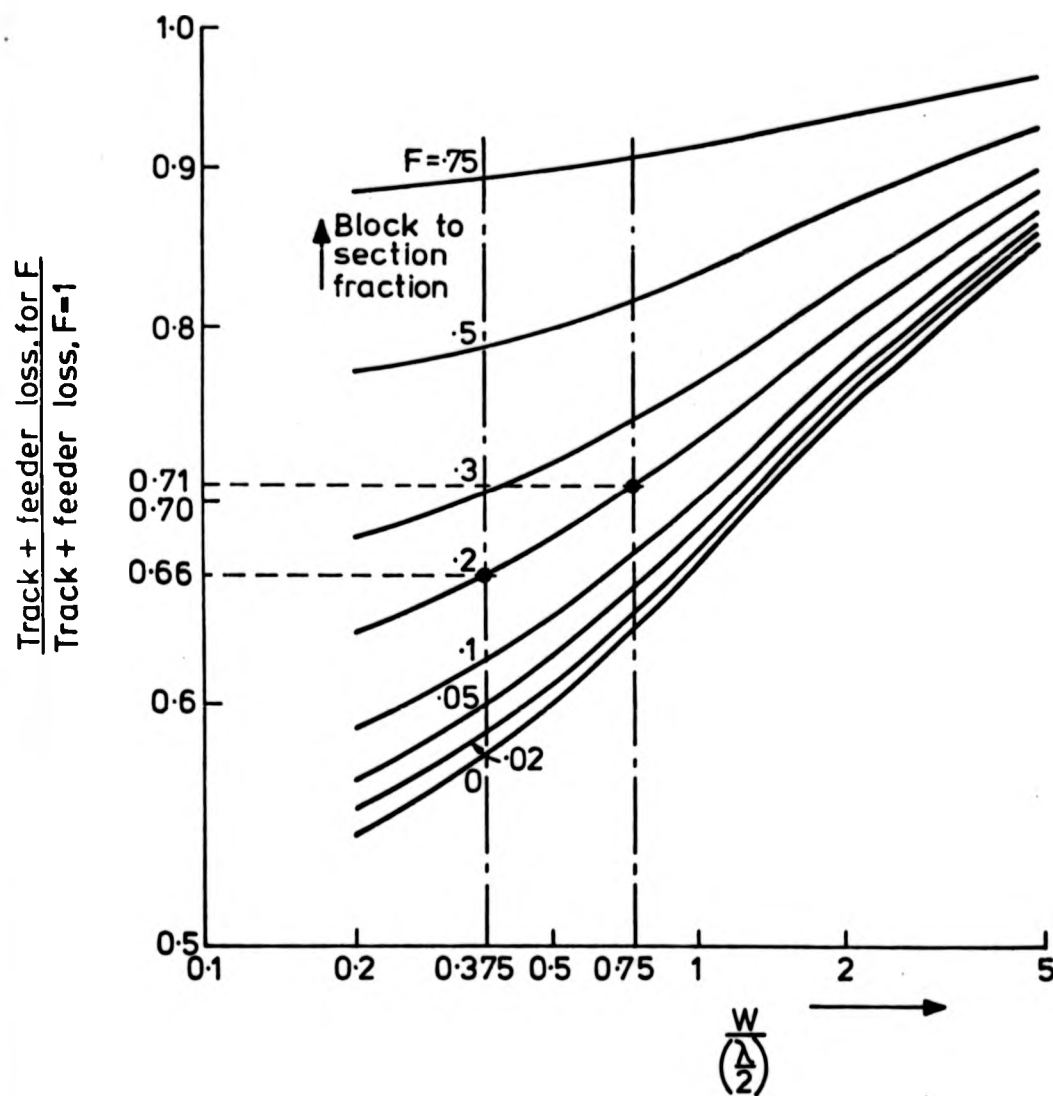


FIGURE 40. FRACTIONAL POWER LOSS IN BLOCK SECTIONED ARMATURE.

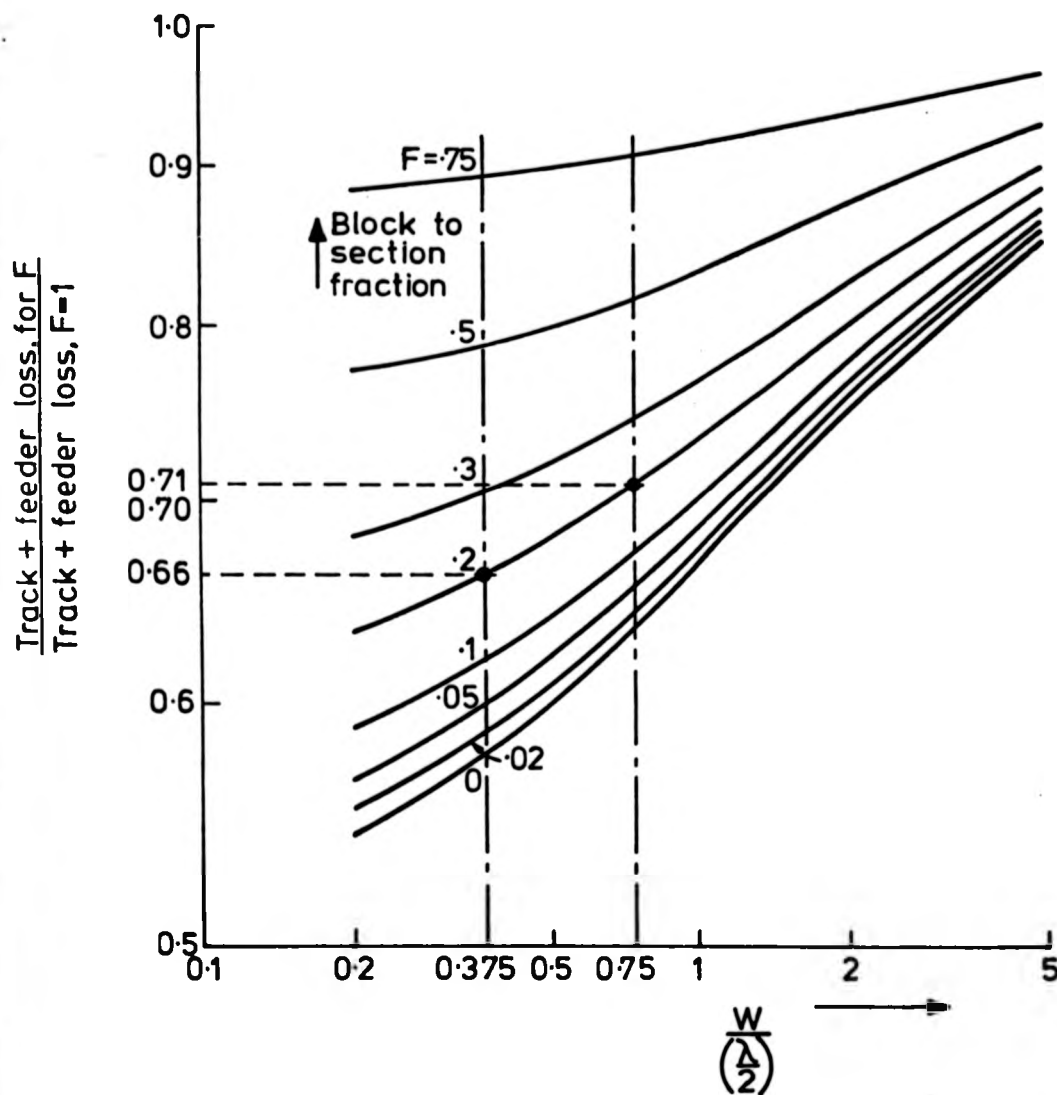


FIGURE 40. FRACTIONAL POWER LOSS IN BLOCK SECTIONED ARMATURE.

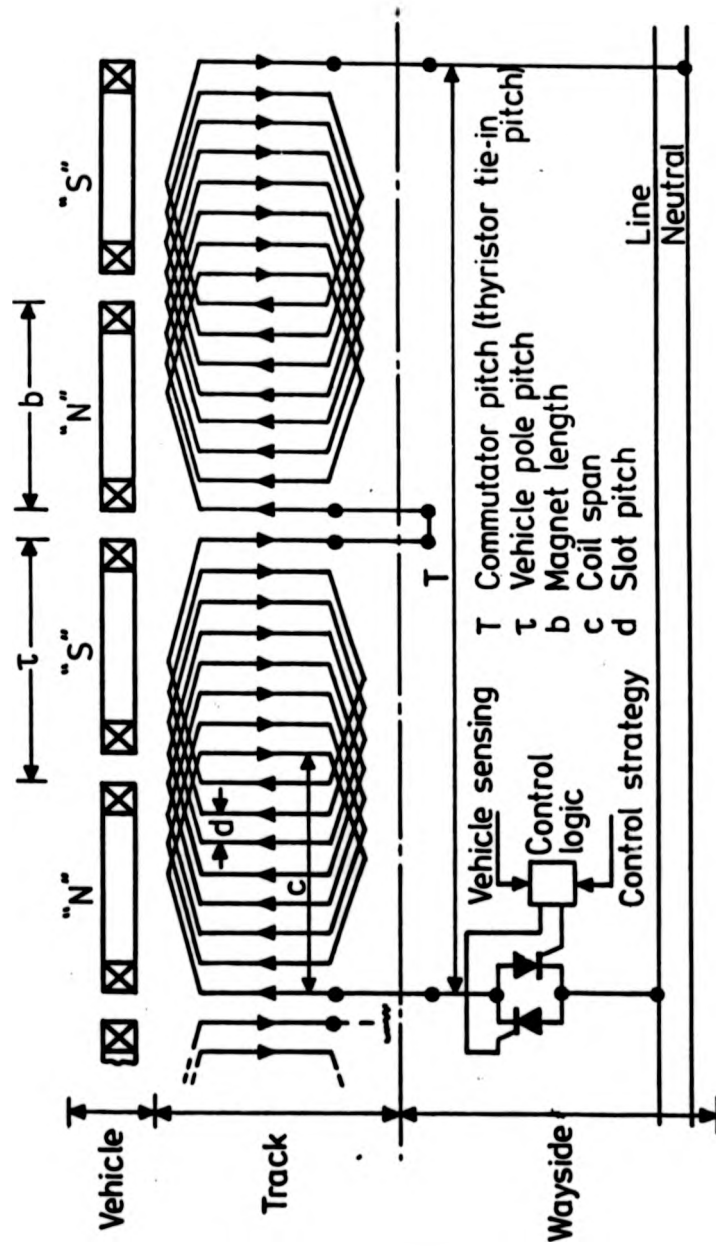


FIGURE 41. L.C.M. DISTRIBUTED PROGRESSIVE WINDING, SERIES CONNECTION OVER TWO POLE PAIRS.

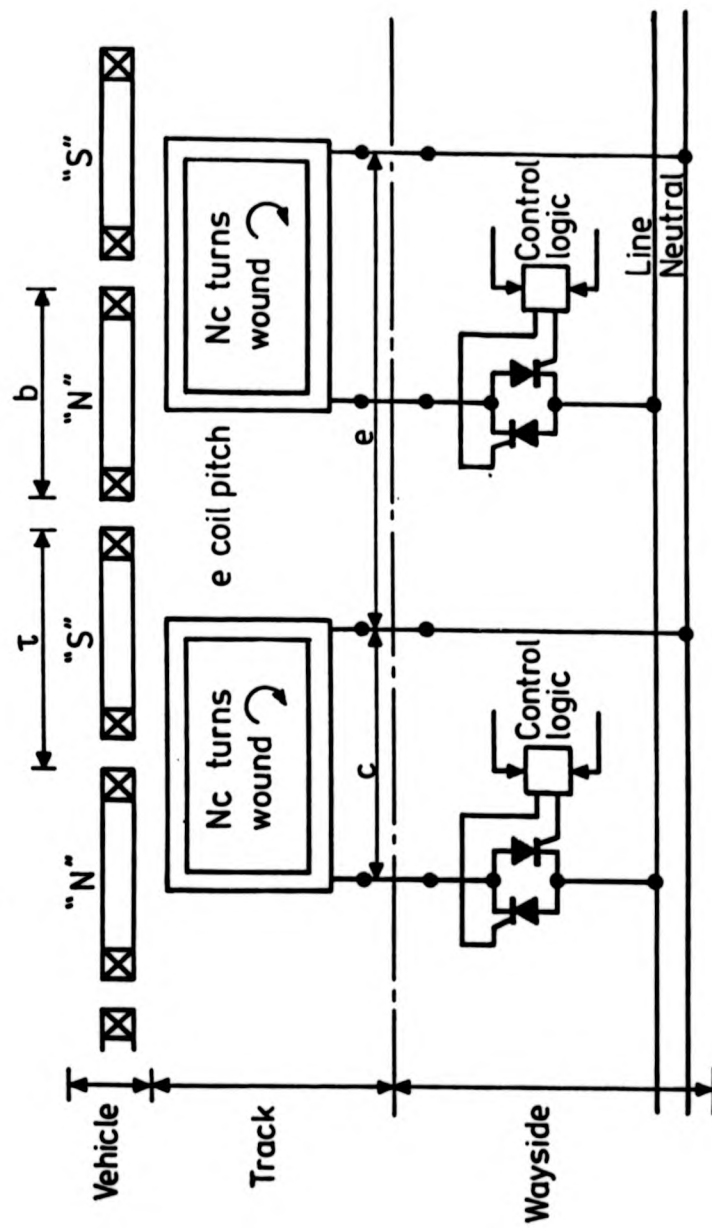


FIGURE 42. L.C.M. DISCRETE WINDING, PARALLEL CONNECTED OVER ONE POLE PAIR.

At the same time as the preliminary track designs were being established, the JNR DCLM was also publicized⁽²⁰⁵⁾. The DCLM used essentially the same philosophy as the switch-per-coil version of the LCM, but the field windings were iron cored normal copper conductors. The JNR work used a dc controlled rectifier feed with a "flip flop" inverter synchronised to propulsion requirements.

Dukowicz, Hoppie and Wang at General Motors had also considered an elementary form of dc propulsion motor, and had filed a US Patent⁽²²⁹⁾. The main claim was for a vehicle with a long length superconducting coil inclined to the horizontal, interacting with a horizontal array of switched coils. The vehicle coil inclination was meant to provide a change in mutual inductance along the direction of motion. The patent loosely describes alternatives with permanent or iron cored magnets, with more than one magnet per vehicle, and overlapping track coils. The practicality of such a system, which relies on the inclination of vehicle coils to provide thrust must be suspect, and would certainly not be easily incorporated into an economic system, because of the waste of vehicle space.

Warwick research continued with the conversion of a 0.5 metre drum used for LSM work, into a LCM model, using mains commutated thyristors to switch individual discrete windings as they passed under three blocks of ferrite magnets. The machine was also used with a specially designed superconducting magnet to examine coil impressed voltage and the possibility of excessive ac loss due to the harmonic content of the machine. With the detailed comparison of the economics of the short energised length LSM form of LCM completed⁽¹³⁰⁾, further study was curtailed because of lack of effort and the change in emphasis of the programme.

The original design philosophy of the LCM, as adopted at Warwick, has been taken up by both JNR and Transrapid. For the Miyazaki test track, the LSM armature winding is energised in block lengths of 29.4 metres, which is only slightly longer than the vehicle length. Transrapid will energise Weh's

design of iron cored LSM at very short lengths; for Emsland the stator will consist of two parallel kilometer blocks connected in series, and the inverter MVA rating is 1.39 times the vehicle required power. With a 6 kilometer feeder cable this rises to a 1.49 increase⁽²³⁰⁾. The need to provide block switching of the iron cored LSM stator arises because of the large track self inductance which results in a very low power factor. Weh has also suggested energising the track in subfractional vehicle lengths of one to two metres, and with four branches of power transistors (in parallel) and diodes (antiparallel) supplying each phase of the stator winding. Two or three of these four quadrant choppers supply a two or three phase winding, and the main feed carries only dc and the substation contains only a transformer and rectifier set.

4.2 Model LCM

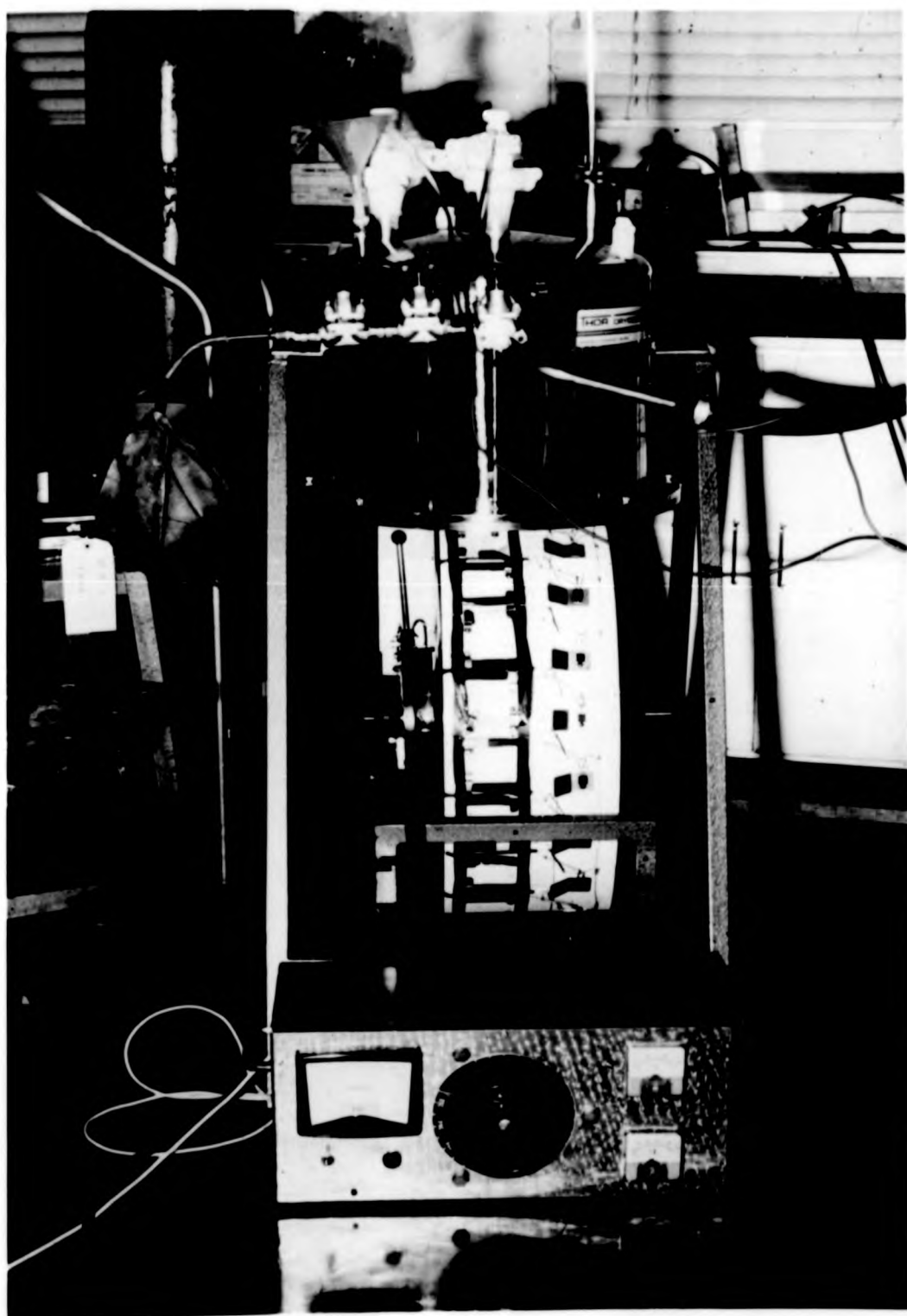
Early in 1974 it was decided at Warwick to produce a working model which demonstrated the LCM concept with a concentrated winding arrangement, and one switch per coil, as shown in Figure 42. The model was based on the 0.5 metre diameter drum that had been used to successfully demonstrate LSM operation. The coils were connected to the 50 Hz mains through slip rings and thyristors rated at 400V and 12A. The thyristor gating signals were provided by a mechanical commutator which gave a pulse as the appropriate coil side passed under one of three blocks of ferrite magnets. The magnets were a full wavelength pitched, and were therefore polarised in the same direction. Thyristor turn off was forced by the mains reversal. Although the drum machine was meant to be for demonstration purposes only, it successfully ran at up to 250 rpm with multiple coil and thyristor failures, indicating the redundancy in this type of machine. A variac controlled the input voltage to the thyristors, and the position at which they were turned on relative to the field magnets was fixed by the position of the brushgear on the commutator. The firing position could be varied by shifting the brushes, so that thrust in either direction could be obtained.

In connection with the Wolfson programme, a superconducting coil was constructed to test the concept of winding square coils with tight corner radii, but was sized to provide an alternative field arrangement for the drum machine. The machine, as shown in Figure 43 produced about twice the thrust with one superconducting magnet compared to three ferrite poles. The main characteristics of the magnet are given in Table VIII. The coil load line cut the critical current line at 90A, which was also the short sample current. A magnet quench through reaching critical field was therefore not anticipated. Cooldown lasted typically six hours from ambient, and the coil appeared to behave good naturedly. Only slight training was observed from the first quench at 42A to repetitive quenches during the first and subsequent cooldowns of 47A.

When the coil was energised over the running machine, the mains voltage waveform effectively commutated by the track windings was observed as a small value impressed voltage on the coil terminals. The radiation shield, cryostat base and coil support attenuated the reaction field to such a level that there appeared to be no significant change in the helium boil off rate with the armature energised, even though the impressed voltage could be observed. This confirmed calculations for the worst case of a machine on the Wolfson test track which had full inverter frequency and a stalled vehicle at low gap. The calculations⁽²³¹⁾ based on Freeman's multilayer region analysis⁽²³²⁾ had indicated that the reaction field would be sufficiently attenuated by the intervening conducting layers, so that the superconductor would be effectively shielded.

The full superconducting machine was demonstrated publicly at the 1975 Intermag Conference in London, and represented the first realization of a practical superconducting commutator machine.

Figure 43 Superconducting Model LCM



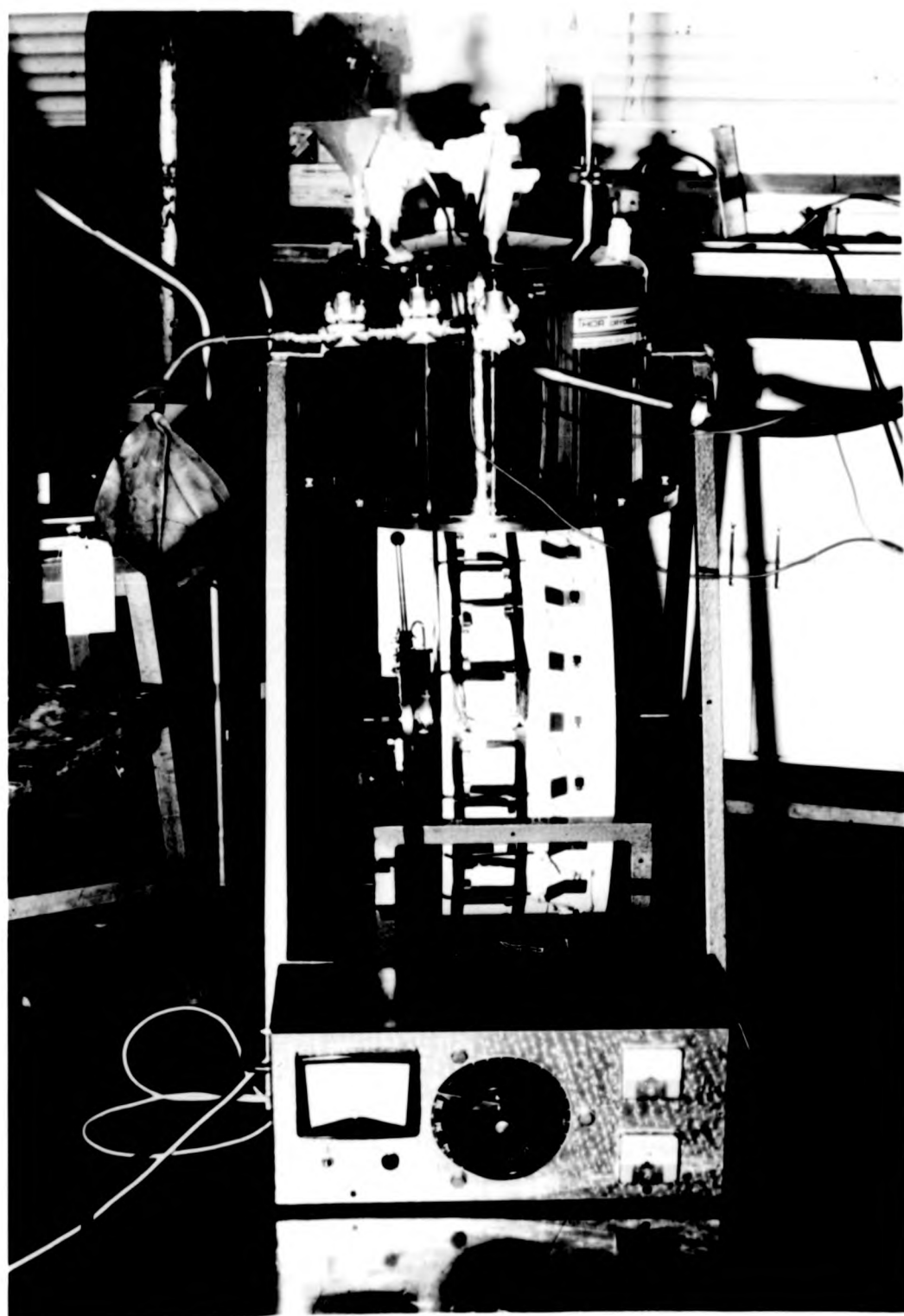


TABLE VIII Characteristics of LCM Superconducting Coil

Conductor

Type	Multifilamentary core wire
Material	Nb-Ti IMI Niomax FM A61/33
Filament diameter	0.028 mm
Wire diameter	0.33mm
Copper/superconductor ratio	1.35:1

Coil

Shape	Square
Meanturn side	115mm
Cross section	15 x 15mm
No turns	1050
No layers	28
Corner radius	10mm
Excitation mode	Persistent current
Short sample current	90A
Quench current	50A
Operating current	35A
Excitation	37 kAT
Overall current density	160 A/mm ²
Winding resistance at 20°C	157 Ω
Inductance	132mH
Stored energy	80 J

Field

Central	10.43 mT/A
Peak	30.4 mT/A
80mm below centre	3.4 mT/A

4.3 Comparison with LSM⁽¹³⁰⁾

Where the very short length LSM is considered, a separate economic assessment needs to be made. If the armature system is accessed too frequently, the track installed cost of the semiconductor or vacuum switches may well exceed the cost of additional track losses associated with greater block lengths. It is by no means immediately apparent where the trade off lies, especially if other factors such as armature power loss and conductor mass can vary, as can interest changes on capital, power cost etc. Also machine design may dictate radical changes in wavelength, and no feel can be given to the effect that this might have on interrelated parameters. Some kind of economic optimisation is required after preliminary machine optimisations have been performed, which can indicate the sensitivity of change in particular parameters on the overall transport system cost. In this way a system optimisation will be achieved, on an iterative basis, by modifying parameters to effect a minimum overall cost, including infrastructure capital repayment, power and running costs.

In searching for a baseline design to compare a short energised LSM with, the CIGGT economic study⁽¹⁰⁷⁾ was finally chosen⁽¹³⁰⁾. The route was based on the Canadian corridor between Toronto and Montreal via Ottawa, approximately 594km. Trip times of about 75 minutes would be possible for vehicles cruising at 504km/h, averaging with stops 475 km/h. The Canadian vehicle has passenger capacity of 100, so with a 60% load factor and 144 trips per day per direction the specified load capacity of the line would be 6.3×10^6 passengers per year. The average number of vehicles per hour was six.

So that an alternative comparison could be made, the MIT Magneplane was reoptimised for 504km/h and minimum terminal rating duty. Thornton had outlined the design of the Magneplane LSM for 360km/h synchronous speed, governed by the top frequency limit on the cycloconverter control. The thrust at this speed was 45 kN developing 4.5 MW of power, of which 3MW was

aerodynamic drag⁽⁹¹⁾. Since the magnetic lift force had saturated, drag power would remain constant at higher speeds, and aerodynamic drag would scale up with velocity ratio cubed. The projected drag was 60kN implying 8.4MW would be required for thrust power. Further optimisation of the current angle required gave an operating point of 113° and terminal rating of 10.1 MVA. Figure 44 shows the operating characteristics for the reworked design with base E_T and I of 3.63kV and 558A. The design works at a high power factor because of the large number of ampere turns per coil (1.25 MAT) and low MIT calculated track inductance. At the original speed of 360km/h Thornton had chosen the design operational point for total power factor correction, which although an improvement over the low current angle initially chosen, could still be bettered by minimum terminal rating operation. High efficiency results from ample allowance in conductor cross section. Table IX gives details of the reworked MIT designs at 360 and 504km/h.

The system costs can be broken down into three parts. Fixed costs are associated with the track conductor and inverter initial installed costs, which are subject to loan repayment amortization. Running costs are dominated by the power required for vehicle propulsion. It is assumed for the purpose of this analysis that maintenance costs will remain relatively unaltered whatever choice is made for the track parameters. A cost equation can be established which lumps together these costs and is expressed as a cost per unit track length, per year. In its most basic form the equation is

$$C = \frac{amk}{100} \frac{A}{\lambda} (1 + \frac{2w}{\lambda}) \sigma C_c + (\frac{P_B}{G} + \frac{am\sigma}{A}) \cdot (1 + \frac{2w}{\lambda}) I_c^2 \left(\frac{C_I k}{200} + 8.76 C_p \frac{\bar{n} G}{\bar{v}} \right) \quad (53)$$

where

C Annual cost \$ per year-metre
G Excited length, metres
a No of parallel paths per phase
m No of phases
 \bar{n} Average vehicle frequency per hour
 \bar{v} Average speed, km/h
 I_c Conductor current (Phase current + a)
w Armature width, metres
 λ Wavelength, metres

C_I Inverter cost, \$ per kVA
 C_p Power cost, \$ per kWh
 C_c cable cost, \$ per kg
A cross section of conductor, m²
 σ Resistivity, ohm-metre
 ρ Density, kg/m³
k Repayment factor, %
 P_B Real power developed, W

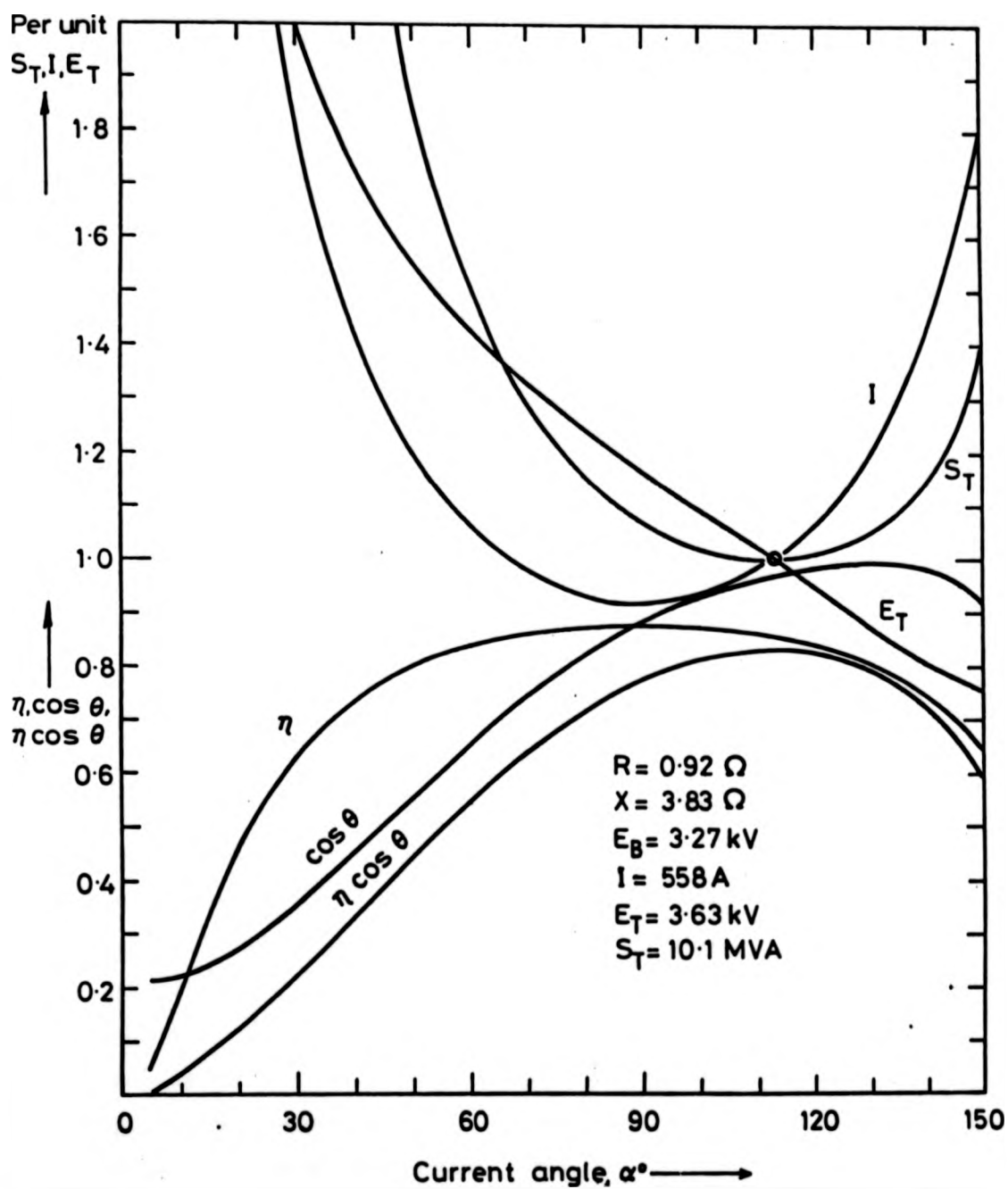


FIGURE 44 PERFORMANCE CHARACTERISTICS OF MIT-LSM

Table IX Magneplane Parameters

Common Factors

Vehicle weight, tonnes	44.8
Length x width x height, m	50 x 3.8 x 4.35
No Passengers	140
Levitation height, m	0.25
No phases	5
Wavelength, m	2.75
Conductor spacing, m	0.275
Stator width, m	2
No Magnets	16
Magnet strength, MAT	1.25
Magnet size major, minor id x od	3.3 x 1.5, 2.4 x 0.6
Magnet pitch m	2.75

Speed Influenced Factors*

Cruise speed, km/h	360	504
Frequency, Hz	36	50.4
Nominal thrust, kN	45	60
Phase current, A	359	558
Back emf, kV	2.31	3.27
Terminal emf, kV	2.55	3.63
Terminal Apparent Power MVA	4.58	10.12
Current Angle °	107.3	112.9
Efficiency	0.87	0.86
Power Factor	0.99	0.97
Apparent Efficiency	0.865	0.83

*Recalculated for minimum terminal MVA

An easier form of equation 53 is found by substitution of the expressions for the power loss and mender mass per unit track length, P_A and M_A , given by equations 41 and 42. The annual unit length track cost becomes

$$C = \frac{k}{100} C_c M_A + \left(\frac{P_B}{G} + P_A \right) \left(\frac{C_I k}{200} + 8.76 C_p \frac{\bar{n}}{\bar{v}} G \right) \quad (54)$$

The cost per passenger kilometer is proportional to $\frac{C}{\bar{n}}$ x vehicle capacity.

M_A and P_B and ultimately the phase current can be replaced by the parameters of thrust and back emf, which are essentially fixed for the design speed. Differentiating 53 with respect to A and G produces values of minimum annual unit cost for a particular choice of wavelength, inverter, cable and power cost. For the range of parameters, families of cost curves can be generated. Figure 45 shows cost C for a fixed cable cost of 8.52 \$/kg, an inverter cost of 25 \$/kVA and a wavelength of 1.14 metres (i.e. the CIGGT optimum wavelength). The power cost C_p is shown varying from 1 to 4 ¢ per kWh, and the minimum points for each cost layer are projected down to the optimum G and A axes. Figure 46 represents four such projections for fixed wavelength and cable cost, but various inverter cost as well as power cost within the carpet plot. If the optimisation is performed for a range of differing wavelengths, an even greater variation in optimum G and A results. Figure 47 displays the loci of G and A optima for different wavelengths. Surprisingly, when the minimum costs associated with the optimum G and A values are calculated, the cost is a slowly rising near linear relationship with wavelength (Figure 48). As inverter cost increases, the gradient of the minimum cost steepens, but not dramatically. For low inverter cost, the gradient is such that a four fold increase in wavelength only increases the cost by approximately 10%. It can be said, therefore, that since cost increases slowly in a monotonic relationship with wavelength, absolute choice of a non-optimum wavelength may not necessarily produce a significant impact on the overall economics of the system. This conclusion is especially important for the integrated system of levitation and propulsion, since other factors strongly influence the choice of pole pitch. Lateral stiffness and lift to drag ratio -

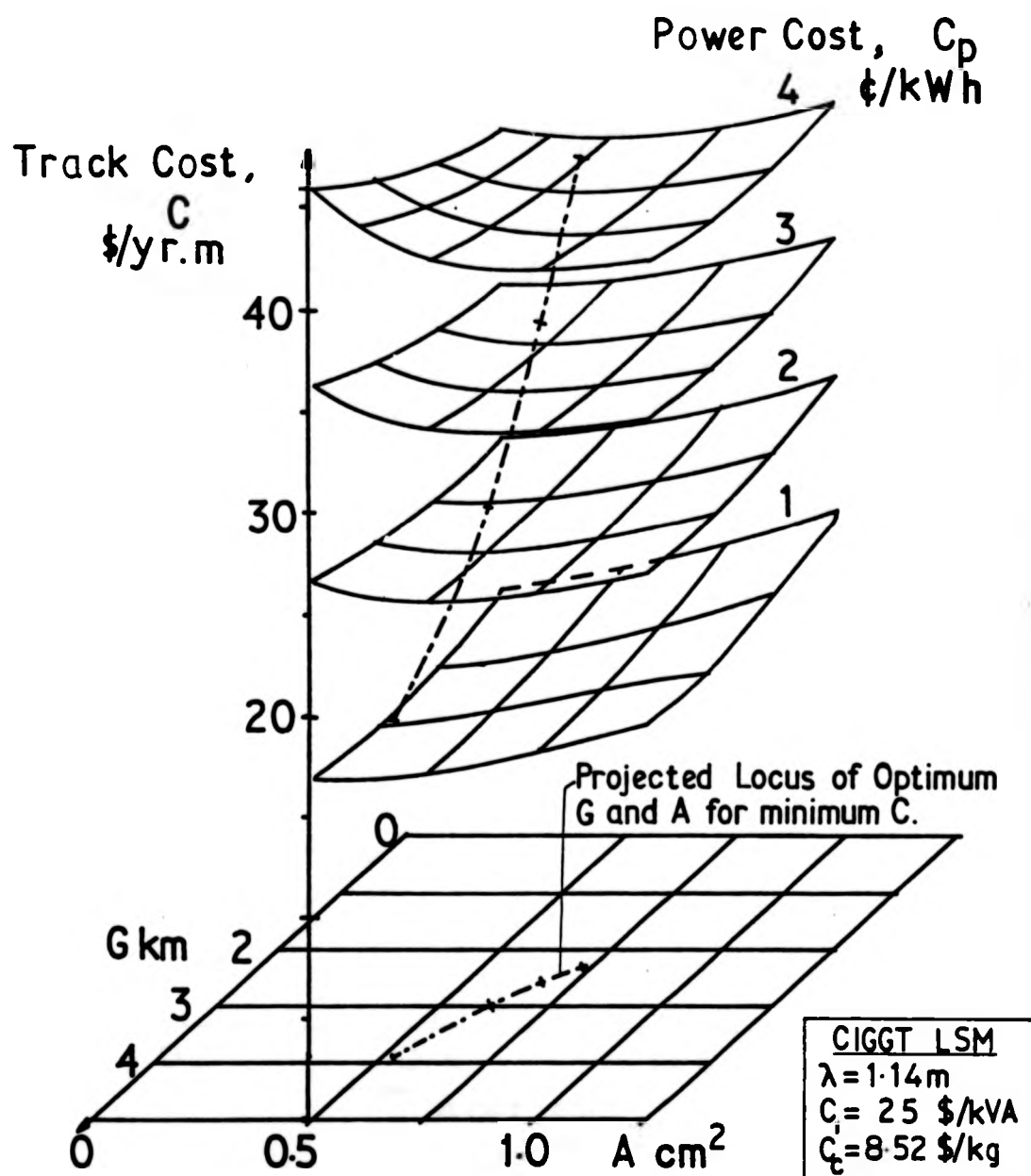


Figure 45. Annual unit track armature cost, C .

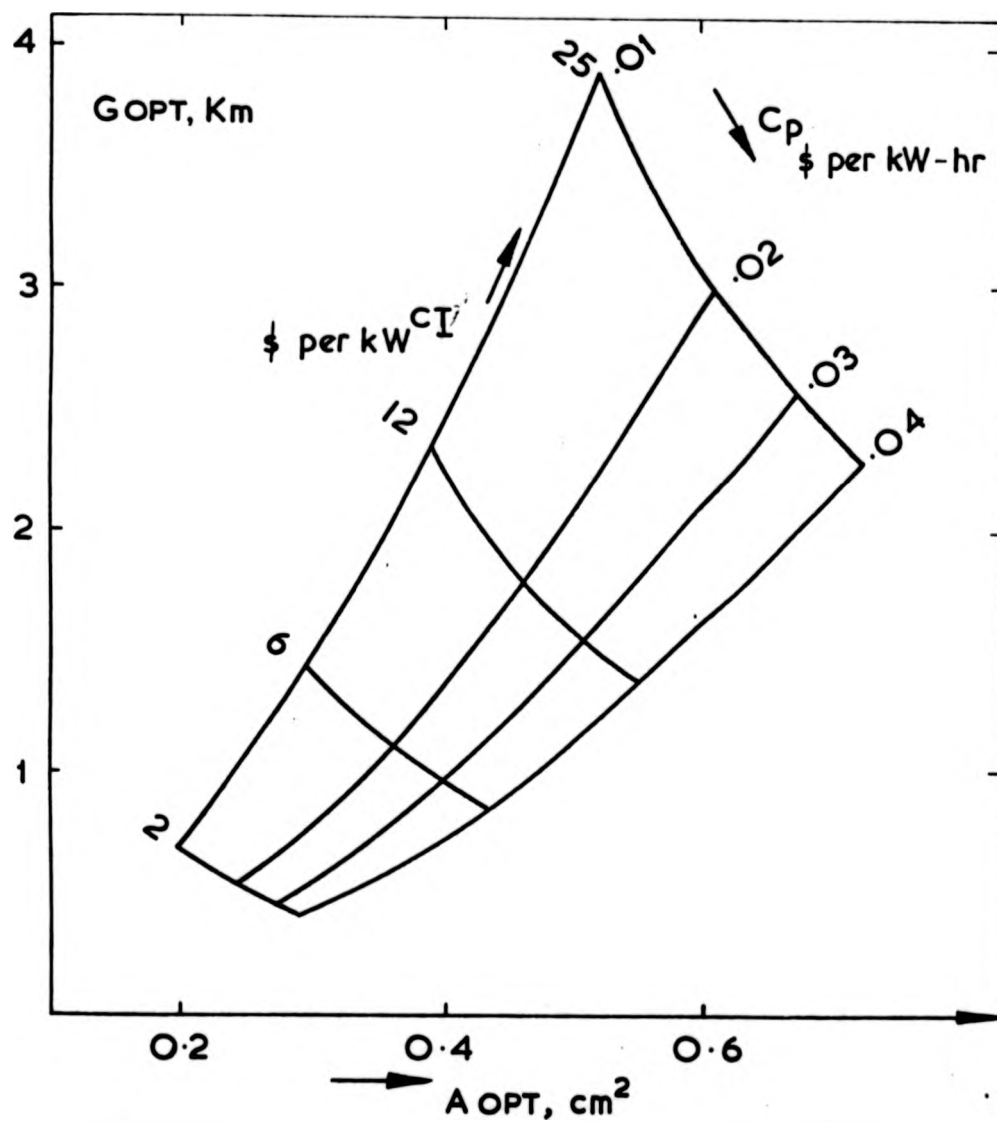


FIG.46. OPTIMISATION FOR G,A.

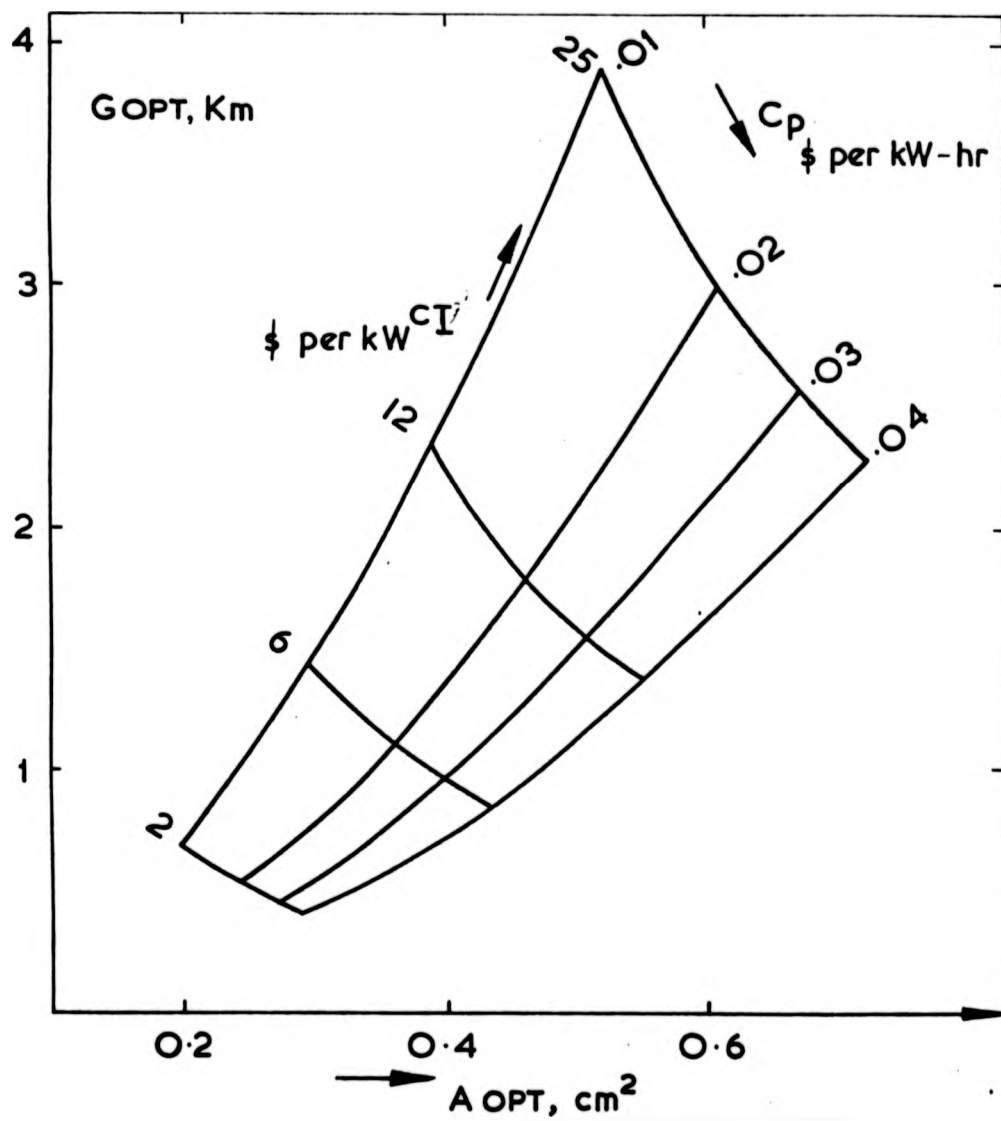


FIG.46. OPTIMISATION FOR G,A.

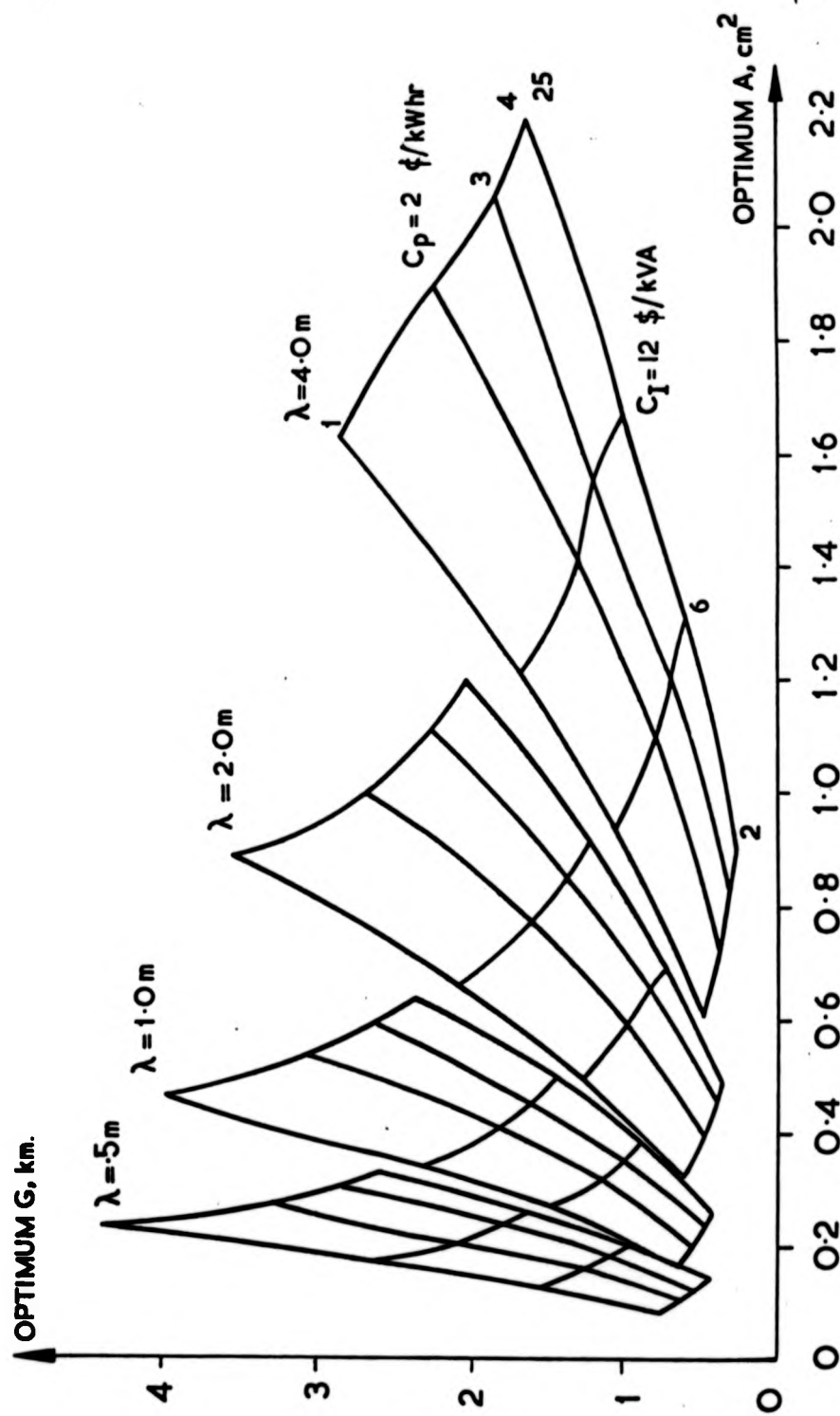


Figure 47. Loci of optimum G, A, for different λ .

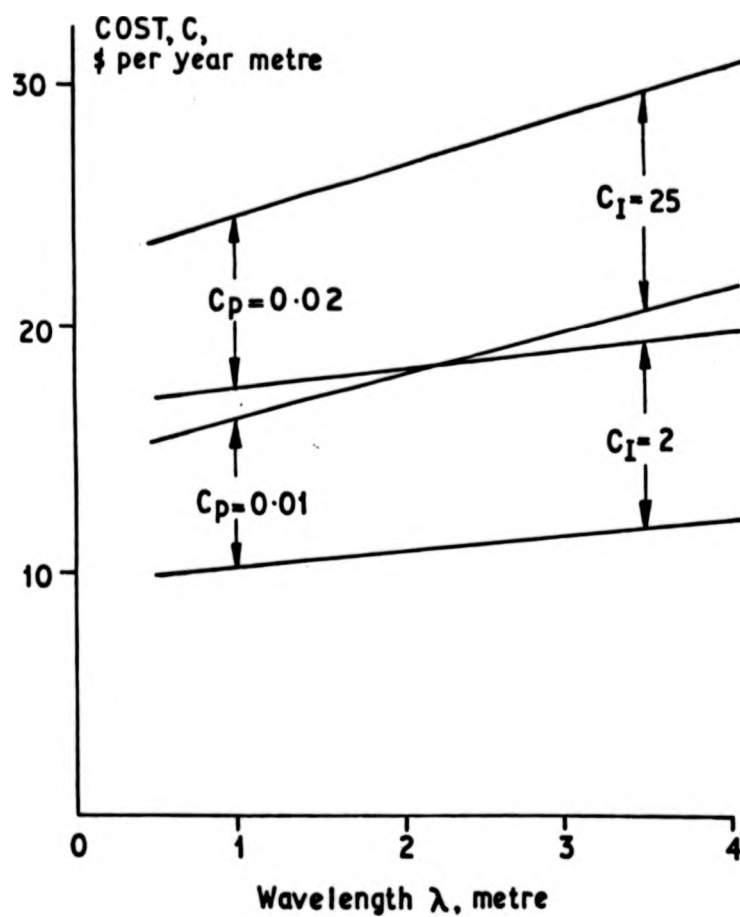


Figure 48. Costs as a function of wavelength.

are all enhanced by relatively long pole pitches, and for the Wolfson revenue vehicle design a 3 metre wavelength was chosen. Optimum G and A were found to be 300 metres and $50\text{mm}^2(130)$, and represents a tradeoff in inverter cost reduction achieved by reduction of track losses and block switching an inverter into many sections.

The LCM Wolfson revenue vehicle was loosely based on a CIGGT type structure, and had similar passenger capacity, and drag characteristics. Table X gives the final choice of parameter values used in the comparison, the machine variants and their resultant optimum cross section, energised length and ultimate journey cost. Although the LCM requires essentially the same propulsive power as the CIGGT vehicle, the reduced block length allows a more efficient power transfer, resulting in lower inverter power handling requirement⁽¹²⁹⁾. Of significance is the result that a LCM propulsion is not necessarily a lot more expensive than an inverter or cycloconverter fed linear synchronous machine. The JNR Miyazaki and the Emsland test facilities both confirm this principle of economic advantage derived from block switching into a frequency converter feed line at frequent intervals.

Table X Optimisation Parameters

Cost Equation Parameters

Amortization, k	15%/annum
Track Conductor cost, C_c	8.25 \$/Kg
Unit Power Cost, C_p	2 ¢ /kWH
Vehicle Frequency, \bar{n}	6 per hour
Load Factor	60%
Average speed \bar{v}	475 km/h
Cruise speed, v	504 km/h
Passenger Throughput	360 passengers/hour

Machine Parameters

	<u>MIT</u>	<u>CIGGT</u>	<u>Warwick</u>
Machine Type	LSM	LSM	LCM
Levitation Height, mm	250	220	240
Wavelength	2.75	1.14	3.0
Conductors/pole	5	6	6
Cruise Power, P_B , MW	8.4	5.6	5.6
No passengers/vehicle	84	60	60
Track cross section, mm^2	100	60	50
Excited length, G , m	5000	3000	300
Conductor Mass, kg/m	3.3	3.5	1.9
Journey Cost, ¢ /pass.km	1	0.8	0.6

Table X Optimisation Parameters

Cost Equation Parameters

Amortization, k	15%/annum
Track Conductor cost, C_c	8.25 \$/Kg
Unit Power Cost, C_p	2 ¢ /kWh
Vehicle Frequency, \bar{n}	6 per hour
Load Factor	60%
Average speed \bar{v}	475 km/h
Cruise speed, v	504 km/h
Passenger Throughput	360 passengers/hour

Machine Parameters

	<u>MIT</u>	<u>CIGGT</u>	<u>Warwick</u>
Machine Type	LSM	LSM	LCM
Levitation Height, mm	250	220	240
Wavelength	2.75	1.14	3.0
Conductors/pole	5	6	6
Cruise Power, P_B , MW	8.4	5.6	5.6
No passengers/vehicle	84	60	60
Track cross section, mm ²	100	60	50
Excited length, G, m	5000	3000	300
Conductor Mass, kg/m	3.3	3.5	1.9
Journey Cost, ¢ /pass.km	1	0.8	0.6

CHAPTER FIVE

MACHINE ECONOMICS AND SYSTEM COMPARISONS

5. Machine Economics and System Comparisons

5.1 The Need for System Comparisons

Future new transport systems will require massive capital expenditure to establish the infrastructure needed for high speed operation. On top of this, the vehicle cost must be added, as well as the running and operating costs. Previous sections have examined system performance and optimization techniques which give the designer and planner a basic structure for overall system economic analysis, for ACLSM. Usually however, the problem is not just to provide an optimum answer for one particular configuration, but to establish the criteria that can be used for comparisons of systems completely different operating or technical bases. Since the decision on whether to proceed or abandon the advanced research and development programmes will often be made at government level, the choice of specific parameters to represent essentially competing systems must be taken with particular care, to avoid confusion and inaccurate judgement.

The major magnetic levitation research and development projects employ linear motor or air fan propulsion for cruise speeds up to 500 km/h. Chapter 2 has given the background details of the status of the various systems, all of which have either reached, or are rapidly approaching, full sized revenue vehicle conceptual design, with a firm understanding of the engineering principles involved, confirmed by high speed rotary or linear testing. Usually one of the main parameters used in comparing levitation and guidance systems is the power to weight ratio, measured in kW/tonne. For the overall system, lift to drag ratio represents another speed dependent variation of power to weight, and specific energy intensity (MJ per passenger-km) indicates the total power consumption. A typical specific energy intensity diagram for various transport modes is shown as Figure 49, using alternative units of Wh per passenger-km. Maglev appears to be competitive with car and rail travel, even though the speeds are much higher, and is considerably cheaper than commercial aircraft^(233,234).

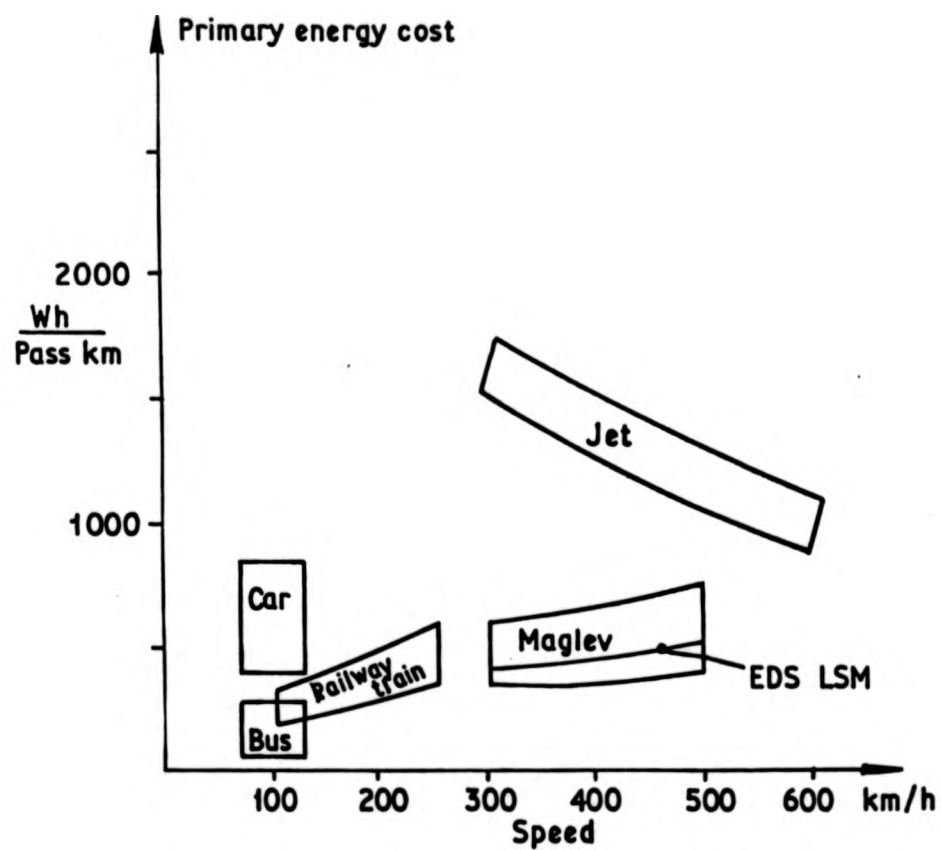


Figure 49. Specific primary energy cost of transport modes.

Of more importance than a rigorous application of specific parameters in system comparisons, is the need to completely identify the energy make up, preferably by evaluating complex power levels reflected through the system to the load presented to the utility. Parameter variation and sensitivity to change must also be included in a reasoned comparison. Finally, wherever possible the systems must be compared at similar benchmarks of speed, passenger density, scheduling and routing.

5.2 German Maglev Revenue Passenger Vehicles

The analysis and design details of proposed German Maglev revenue vehicles are given in the 1977 Statusseminar⁽³⁶⁾, and the basic characteristics are repeated in Table XI. There are two EMS design options, and one EDS German system, with Philco Ford and CIGGT EDS vehicles included in the table. The vehicles are made up from two mirror image sections to allow bidirectional running, with the EDS design speed being 500 km/h, EMS 400km/h. Two propulsion schemes are considered for the EMS vehicle, one being a double sided LIM, and the other, an iron cored LSM in a long stator configuration, supplying lift as well as thrust to ease the on board power requirement. Both the systems designs of EMS and EDS were prepared for a BMFT "System Comparison" to allow a decision to be made on the preferred option to be taken up and pursued to a near full size operational vehicle. Leonhard produced a superficial preliminary system comparison of the three alternatives of Table XI and concluded that none of the systems was sufficiently well developed to allow a clear choice to be made⁽¹³²⁾. This comparison showed the power requirements at the substation, but only included the real power for the main magnetic and aerodynamic drag. Although this represents all the losses for the EDS for a given motor efficiency, no mention was made of, for example, the EMS cooling momentum drag, the short stator dc feed line loss, and the long stator track iron and distribution loss, all of which appear downline from the substation. Furthermore, since the speeds of operation were also different the

TABLE XI Characteristics of Conceptual Maglev Revenue Vehicles

System	PM-EDS	EMS	EMS	PHILCO FORD EDS	CIGCT EDS
Propulsion	LSM	shortstator LIM	long stator ICLSM	Ducted Fan	LSM
Variation		high η low η			
Speed, km/h	500	400	400	483	483
Mass, tonnes	135	170	165	37.3 50.7	28.8
Length, m	56	64	64	33.67 42.9	36.5
No Sections	2	2	2	1	1
No Passengers	200	240	240	80 140	100
Payload, tonnes	20	24	24	7.2 13.2	9.3
Height, m	4.2	4.2	4.0	3.454	3.20
Width, m	3.5	4.2	4.2	2.94 3.454	3.20
Aerodynamic Coefficient, m^2	3.94	4.75	4.75	1.80 2.20	2.42
Substation Spacing, km	15	12	12	-	5
Specific Energy Intensity MJ/pass-km	4.45	6.51*	11.2*	3.63 2.75	3.72

*At 500 km/h

aerodynamic drag power would introduce a further discrepancy; an increase in speed from 400 to 500 km/h results in a doubling of the aerodynamic drag power. Leonhard acknowledged the difficulty in performing a meaningful comparison, and suggested that because of the long term nature of the R&D required, premature decisions in abandoning one system in favour of another were, in fact, unjustified.

The exact power requirements of the different systems can be calculated; including the power factor and motor efficiency allows the substation complex power to be completely specified. When the speed is extrapolated to 500 km/h for the EMS vehicles an additional double sided motor is required for the short stator vehicle, and the weight is increased by 20% to 205 tonnes. The long stator design at 500 km/h requires an increase in gross weight of 10%, to 180 tonnes. Operation of the EDS vehicle at 400 km/h needs no modification to the vehicle, and the LSM can still perform at a near optimum point.

In trying to establish the terminal conditions at the substation for the EMS vehicles, the choice of power factor and efficiency is made difficult because of lack of experimental or even design figures for multimegawatt high speed motors. Winkle suggests calculated efficiencies of 0.6 and 0.78, with associated power factors of 0.5 and 0.65 respectively as the first and second stage of development⁽²³⁵⁾, and the following calculations are based on using these sets of values. Results from the LIMRV tests seem to imply that these figures are representative, although it must be stressed that the EMS LIM requirement is several times the LIMRV power.

The distribution systems for the three options of EDS, and EMS with short or long stator, are shown in Figures 50-52. The EDS system allows leapfrog connections to be made between the track sections and the wayside inverters, with tie reclosures into both directions (not shown). Short stator EMS power is picked up at 4kV and fed via an inverter to the LIM, and through controlled rectifiers to provide on board supply for services and lift and guidance systems. The long stator motor uses a linear

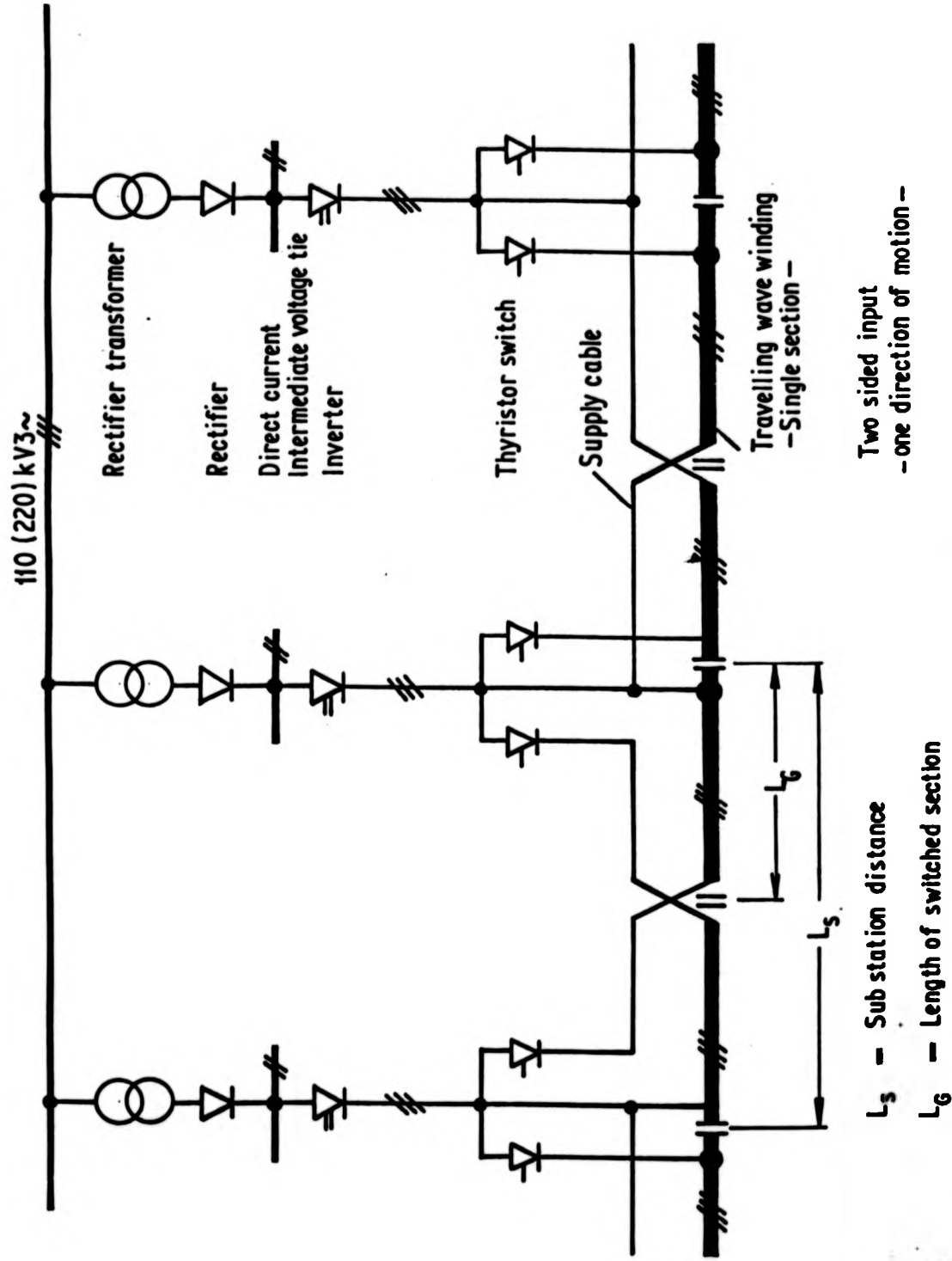


Fig.50. Distribution diagram for the EDS long stator motor propulsion.

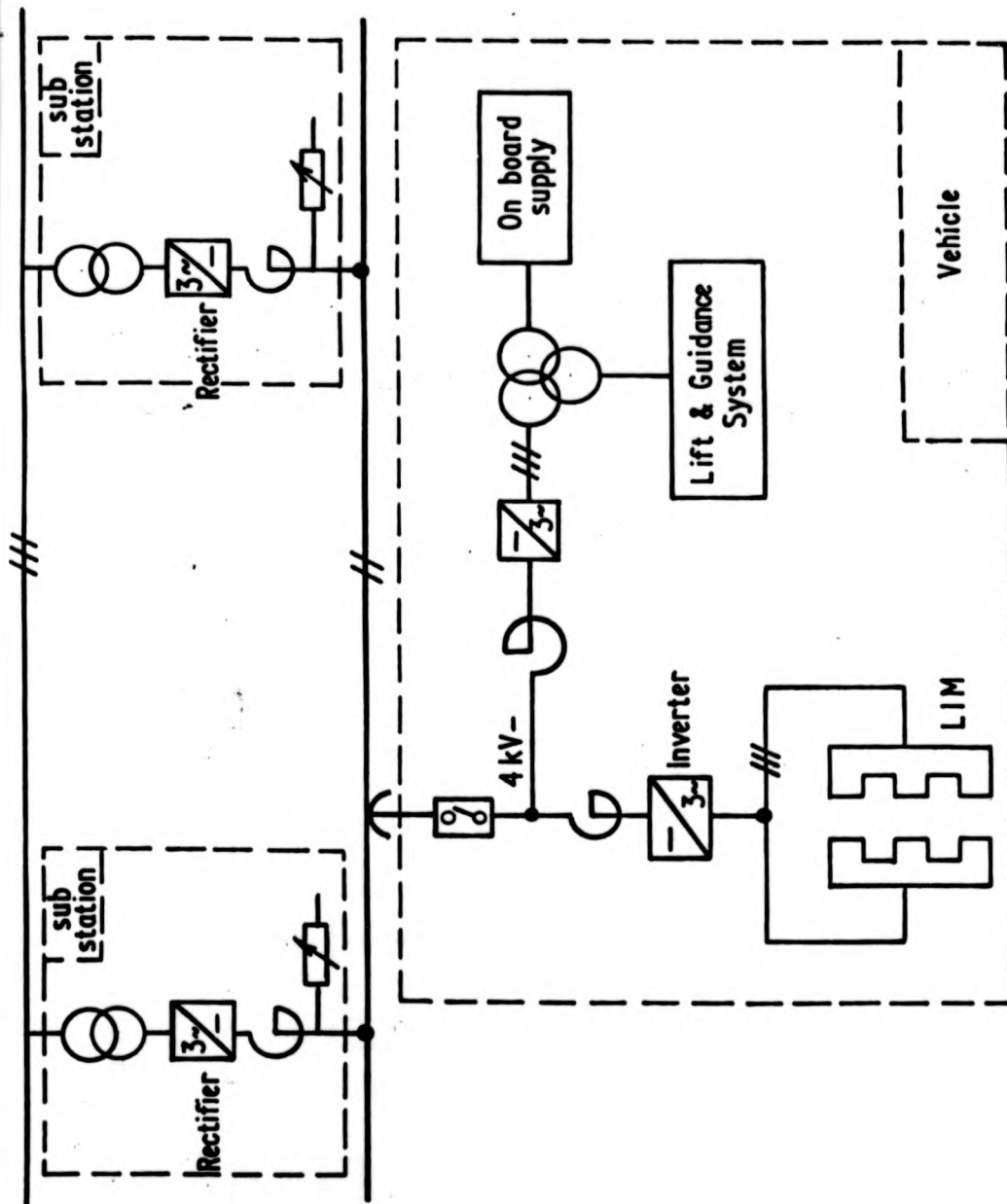


Fig.51. Distribution diagram for the EMS short stator motor propulsion.

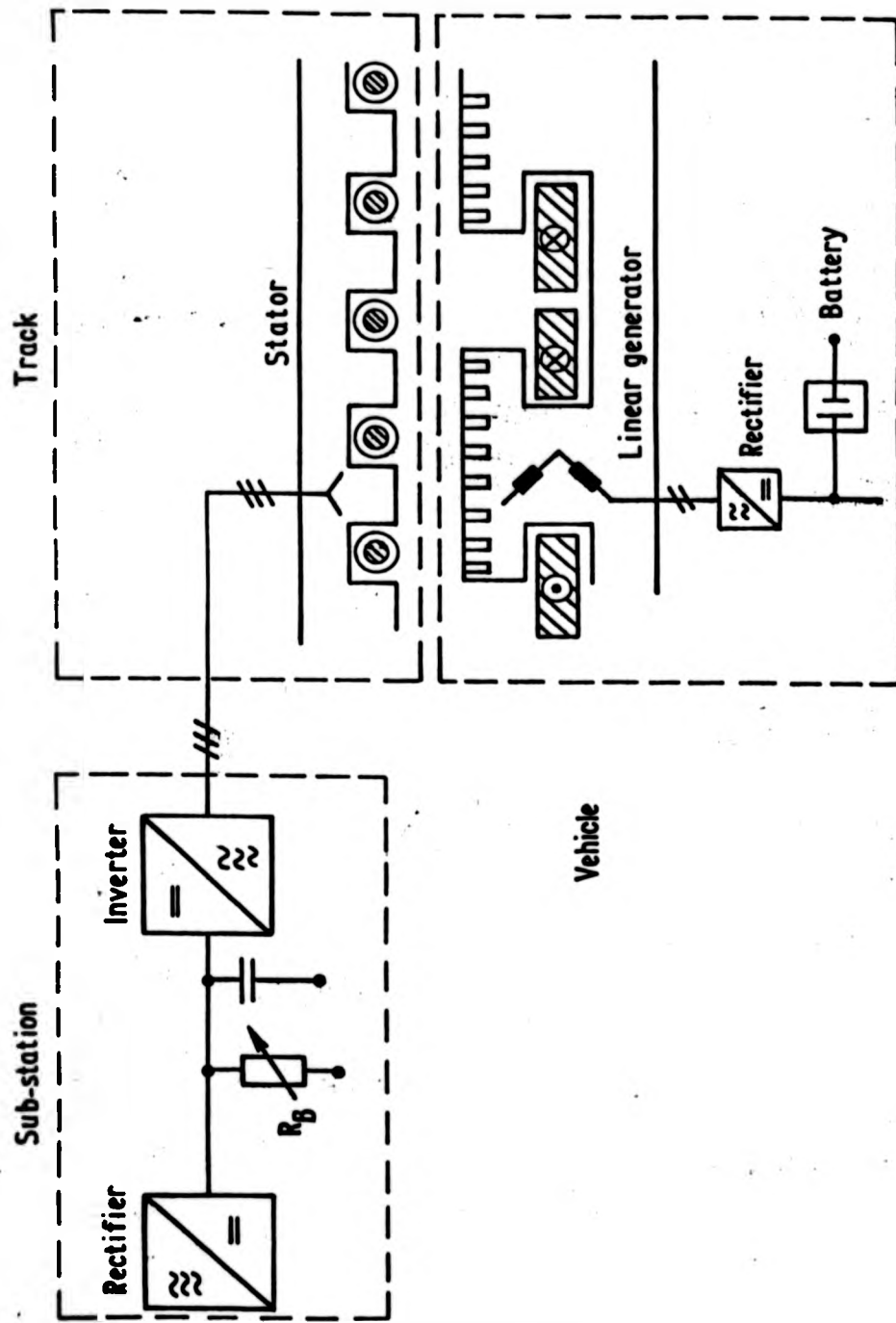


Fig.52. Distribution diagram for the EMS long stator motor propulsion.

generator formed by switching in pole face windings to produce sufficient power for the on board systems above a certain speed. Batteries provide the low speed power.

There are seven main components to the active power requirement for maglev vehicles. Aerodynamic drag is usually a predominant factor in any high speed system, and is proportional to the aerodynamic coefficient, which represents the frontal and surface skin drag, and the velocity squared⁽²³⁶⁾. The magnetic drag for the systems are also speed dependent. For EDS, once the lift and guidance forces have reached a saturation speed, then drag force is inversely proportional to speed, so that drag power is essentially speed independent. For EMS, an approximate relationship is that lift and guidance power scales as (velocity)^(3/2). The EMS Maglev vehicles require entrained air for cooling of the levitation and guidance magnets, as well as the linear machine conductors and the on board power conditioning. The on board systems drag power will scale with the vehicle weight, and represents picked up power to drive the vehicle services such as air conditioning, battery backup charging etcetera. Track winding (EDS) and distribution losses represent the remaining steady state drag values.

Extra power capability is needed to accelerate the vehicle against headwinds, gradients and other inertial forces. Both systems are claimed to be capable of providing propulsion capacity for 3.5% gradients at cruise speed, but the more lenient figure of 0.013 gee was chosen for the comparison. Figure 53 shows the total breakdown of active power requirements for the EDS and EMS systems, at two alternative cruise speeds of 400 and 500 km/h^(133,134). The two options of LIM propelled EMS vehicles are included for comparison purposes to Weh's long stator LSM design. The steady state or cruise power for EDS is the sum of blocks 1, 2 and 5, which are the only system losses. The EMS losses are given in blocks 1 to 5. It should be

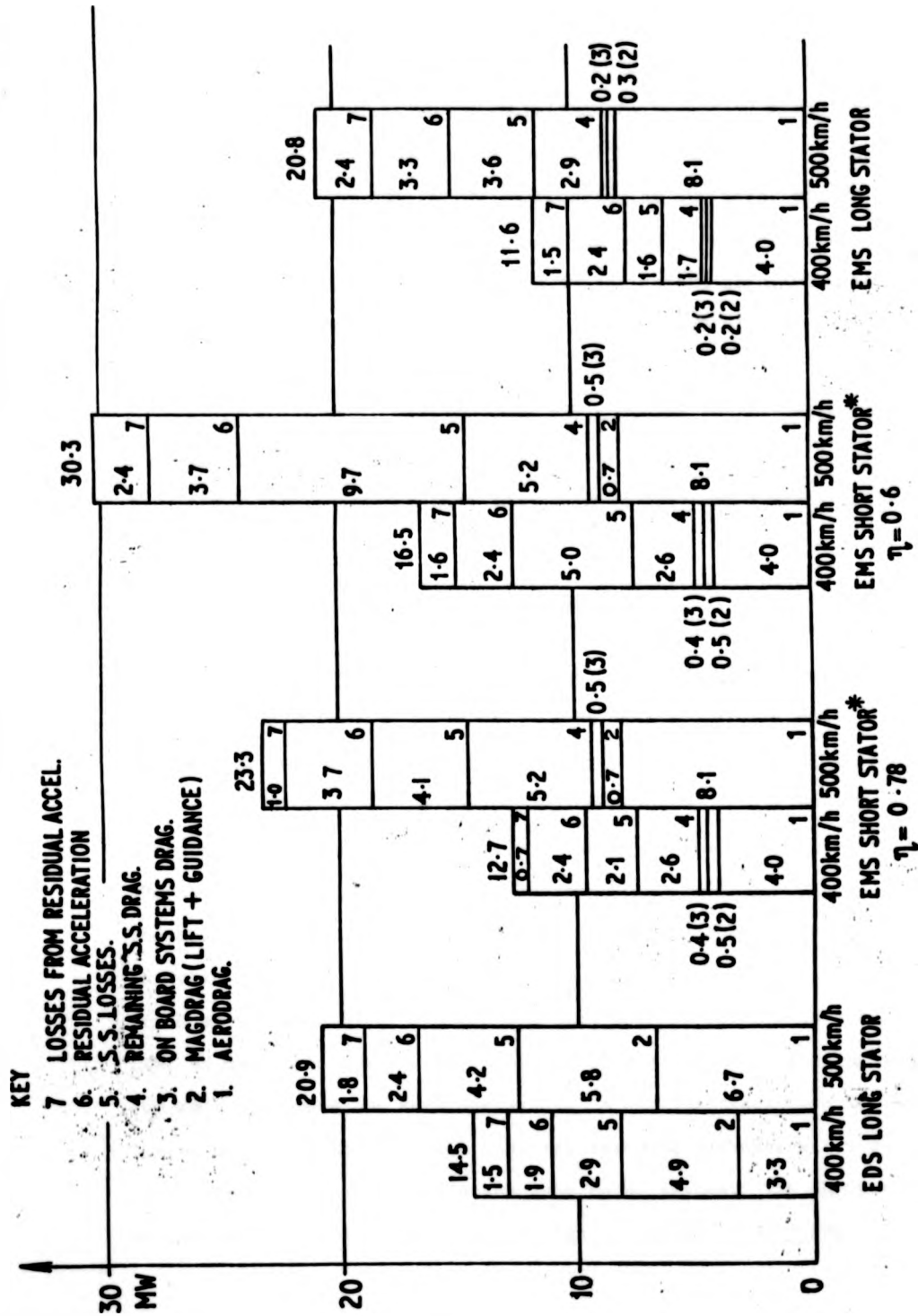


Fig. 53 Total active power of systems (MW) *NOTE. DC DISTRIBUTION & PICKUP LOSS NOT INCLUDED.

noted that the figures used for the EMS long stator should be treated with some scepticism, if only for the reason that detailed overall figures on machine design for the IVA and Emsland vehicles are not readily available. Figure 54 is an alternative presentation of the active power requirements for the four operating regimes of 400 and 500 km/h, steady state or acceleration. The 100% base is the EDS 16.7MW consumption at 500 km/h, steady state. It is apparent that, in terms of real power consumed, the long stator EMS and the EDS are both roughly equivalent when loaded at 500 km/h. The low efficiency LIM short stator EMS uses roughly 45% and the high efficiency LIM EMS 11% more active power. If an estimate is made for the DC line loss for the LIM, before current pickup, of 15%, then the modified EMS/LIM figures are 70 and 31% respectively.

The values here could not have been deduced from the suspension lift-to-drag ratios, or specific powers. For example, the EDS 500 km/h magnetic lift to drag of 32 (equivalent to 36 kW/tonne) is modified by aerodynamic drag so that cruise lift to drag becomes only 15 (92 kW/tonne). Similarly, the EMS short stator magnetic specific power of 3 kW/tonne at 400 km/h (equivalent to a magnetic lift to drag ratio of 370) is modified by the addition of aerodynamic and cooling drag to a steady state value of 44 kW/tonne (a lift to drag ratio of 25). The choice of a suspension subsystem with high magnetic lift to drag ratio does not ensure an overall high ratio because of the aerodynamic and other system losses.

The change in efficiency and power factor of the three systems is indicated in Table XII. The apparent efficiency (power factor - efficiency product) is fixed at either 0.51 or 0.3 for the high and low efficiency versions of the LIM, as mentioned previously. The EDS system loses 7% in going from unloaded 400 km/h to loaded 500 km/h operation. A similar transition for the EMS long stator motor results in a 21% loss representing a conservative estimate, as it ignores non linearities in the iron cored system. The short stator motor values were held constant as the design called for a doubling

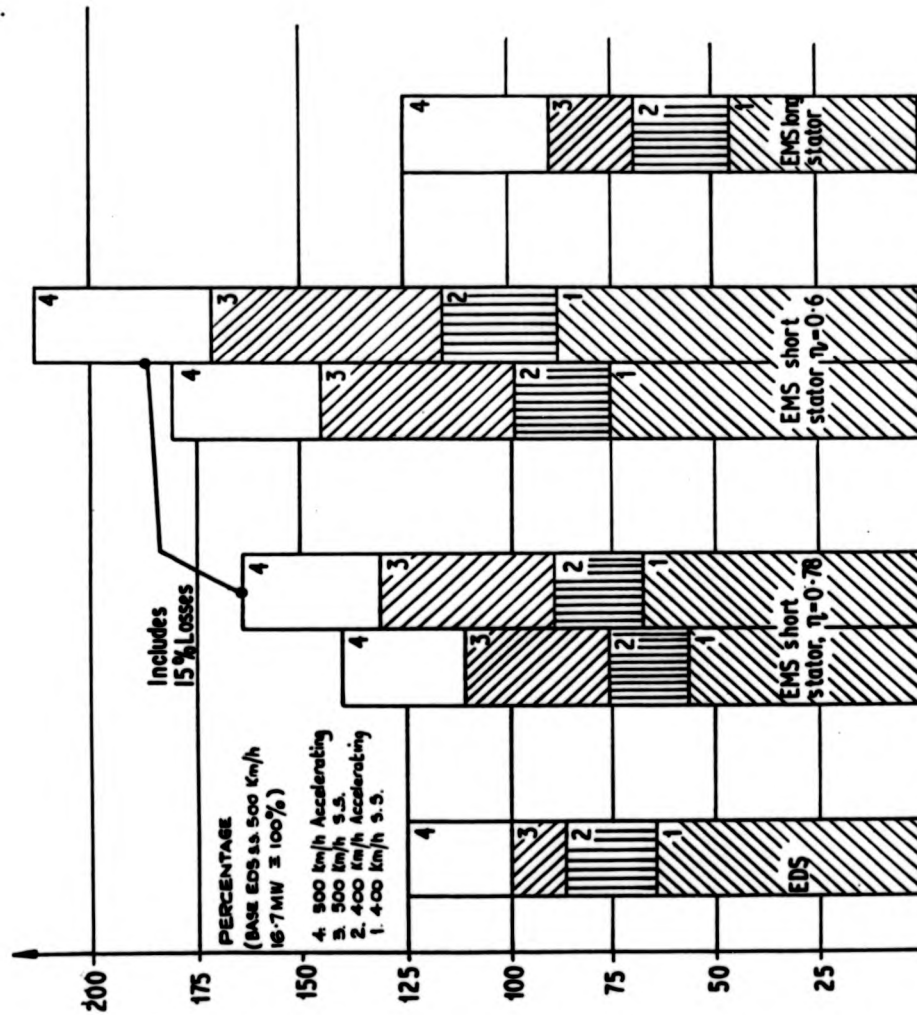


FIG. 54. Relative system active power requirements at 500 and 400 km/h.

TABLE XII Apparent Efficiency of the German Vehicles

	steady state	loaded	steady state	loaded
EDS	0.67	0.62	0.66	0.60
EMS, long stator	0.57	0.46	0.44	0.36
EMS, short stator, high efficiency			0.51	
EMS, short stator, low efficiency			0.30	

up of the motors to give sufficient thrust at the higher speed; each motor remained at much the same output, but would be operating at a different slip.

Using the values in Table XII it is possible to directly obtain the complex or apparent power required at the substation. The reactive power flow in the machine-power network is stored in the leakage and airgap fields, and as such does no useful work. However, the reactive power represents an energy demand that has to be catered for both in plant rating and running cost. An iron cored structure such as a LIM or the EMS long stator motor must have a much lower power factor than a LSM of the same mechanical power output, since air gap magnetization is provided by superconductors requiring no input reactive power, and the armature leakage inductance is small since the track winding is air cored. These points are born out by Figure 55, where complex substation power demand is an ordinate value against the active power for each of the four operating regimes. The success of the electrodynamic system in requiring only small amounts of reactive power to provide propulsion throughout the speed and loading variation is immediately apparent. The size of the ordinate, i.e. the complex power, therefore demonstrates the relative merits of the overall systems, at the substation. Despite the rough equivalence of active power used, the EMS long stator requires 38% more than the EDS base at 500 km/h, and the high efficiency short stator 51% more. Including a line loss the LIM value rises to about 78%. If the lower efficiency short stator EMS is considered, then the figures become increases of 156% and 202% on the EDS base. Figure 56 shows the complex power for the systems, on a percentage base. From this data, a realistic power requirement comparison can be made between the three German Maglev vehicles operating under similar conditions. The comparisons cannot be strictly rigorous, since the EMS and EDS vehicles are primarily designed for different baseline operation. However, the spread of the system total complex power in relation to the actual transferred

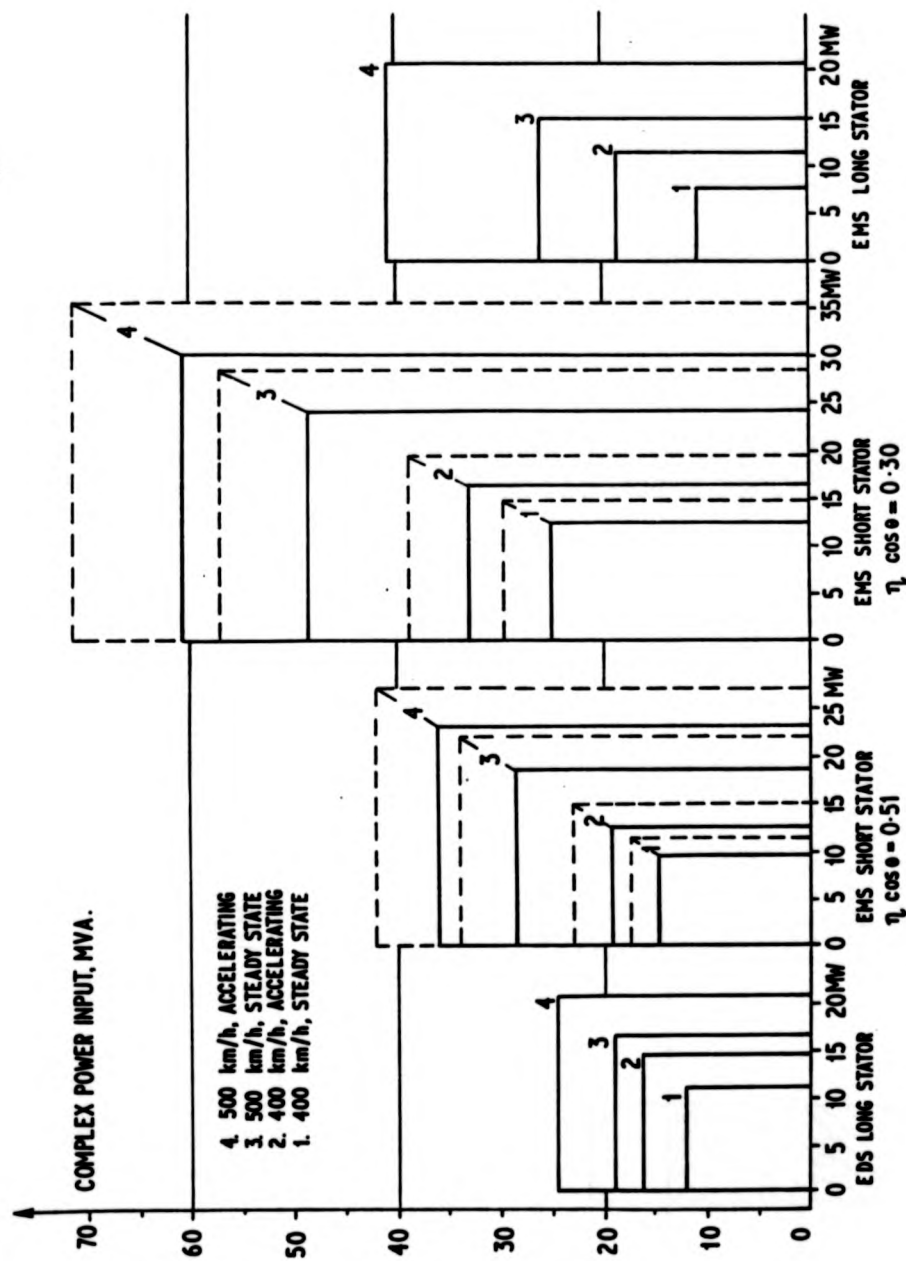


Fig. 55. Total complex and active power of systems. Note: Short stator: Broken lines indicate an included 15 % distribution loss.

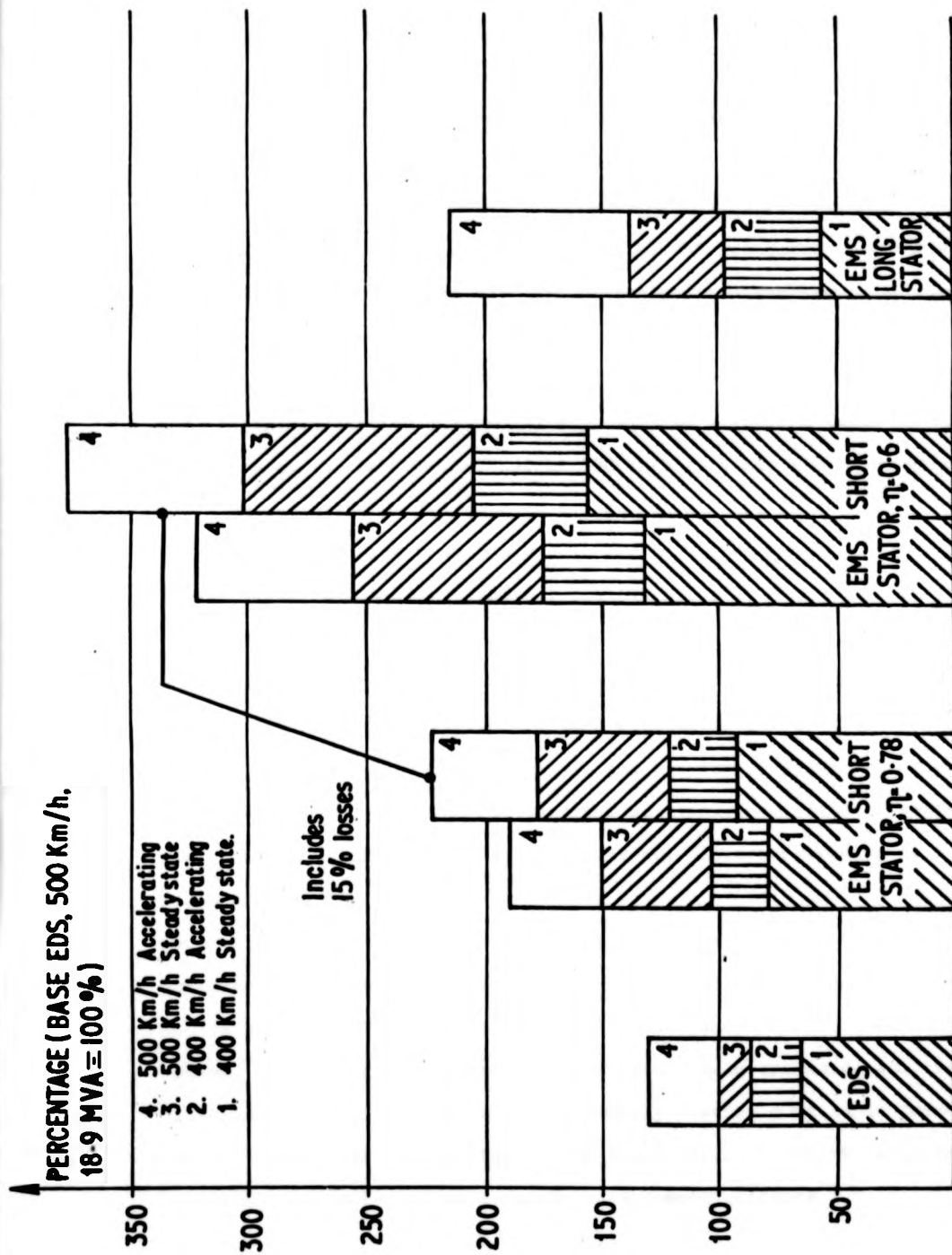


Fig. 5.6. Relative system total complex power requirements at 500 and 400 Km/h.

mechanical power requirement (Figure 55) is indicative of the type of system performance that might be expected for identical service conditions. Several factors emerge from the analysis.

The EDS has good system performance at both 500 and 400 km/h in terms of energy conversion and power consumption, and has scope for increases in power factor and efficiency, depending on the economic costs of power and capital equipment.

The short stator induction machines for the EMS are quite unsuitable for high speed (500 km/h) operation, and are probably also unsuited to 400 km/h operation, primarily because of their high reactive power consumption and hence excessive overall power requirement. For example at 500 km/h the high and low efficiency LIM's respectively required 1.8 and 3 times as much complex power as an EDS-LSM, and at 400 km/h, 1.4 and 2.4 times as much.

The long stator motor EMS appears to need marginally less power than the EDS at 400 km/h (90%) but when loaded, or at the higher speed of 500 km/h, this slight advantage is lost. Another consideration is that this machine concept has only been tested at relatively modest speeds, and so high speed operating characteristics must be regarded as tentative. Results from the Emsland vehicle trials will establish 400 km/h running of the iron cored LSM, and confirm theoretical calculations. To get the supply power factor to a reasonable level, the 1 kilometre track sections, connected in series are tied through a supply cable to the inverter. Inverter spacing is 6 kilometres(230).

Generally, it can be said that using specific power, lift to drag ratio, or specific energy intensity to assess system performance only indicates the active power supplied to make up thrust and losses (if included) in the system. Low power factors in the LIM systems mean trackside and transmission components as well as utility energy supply costing must be in terms of total complex power used by a system. The MVA as well as the MW requirements of a system must be obtained in relation to a common guideway

route together with similar baseline specifications before reasonable comparisons can be made.

5.3 Maglev Vehicle Weight Breakdown

Another area for comparison of vehicle data is that of weight breakdown, and for this study the two additional single section EDS systems are included with the German vehicle data presented in Figure 57⁽¹³⁵⁾. The two EDS vehicles characteristics have been listed in Table XI previously, and are the Philco-Ford⁽⁸⁶⁾ and Canadian^(109,110) conceptual vehicle designs.

Two options are included for Philco-Ford, the baseline 80 passenger vehicle, and their 140 passenger variant. In relative terms, the Philco-Ford and CIGGT designs make available a fifth to a third of their all up weight for payload, whereas all the German vehicles have roughly a 14% allowance. Figure 58 shows the six vehicles' weight breakdown in absolute terms. The overall weight per seat of the German EDS vehicle compared to the CIGGT and Philco-Ford 140 seat vehicles is approximately double. This is largely because of the weight penalty of the heavy duo-rail compatible wheelsets and their emergency integrated guidance system employed, opposed to the lightweight aircraft-type wheels of the other EDS designs. The EMS figures for weight-per-seat demonstrate the large amounts of power conditioning and mechanical hardware in the subsystems penalizing payload capacity.

5.4 Specific Energy Intensity

The specific energy intensity (ψ) of a transport system evaluates the amount of prime energy required per passenger, per kilometre of travel. Within the calculation, the substation converter efficiency, generation and transmission efficiency and load factor for the vehicles are included. In obtaining a value for ψ for non-electrical systems the heating value of the fuel and the journey stage length need to be known. The values of specific energy intensity (including the effects of power factor) for the six vehicle variants considered are shown in Table XI.

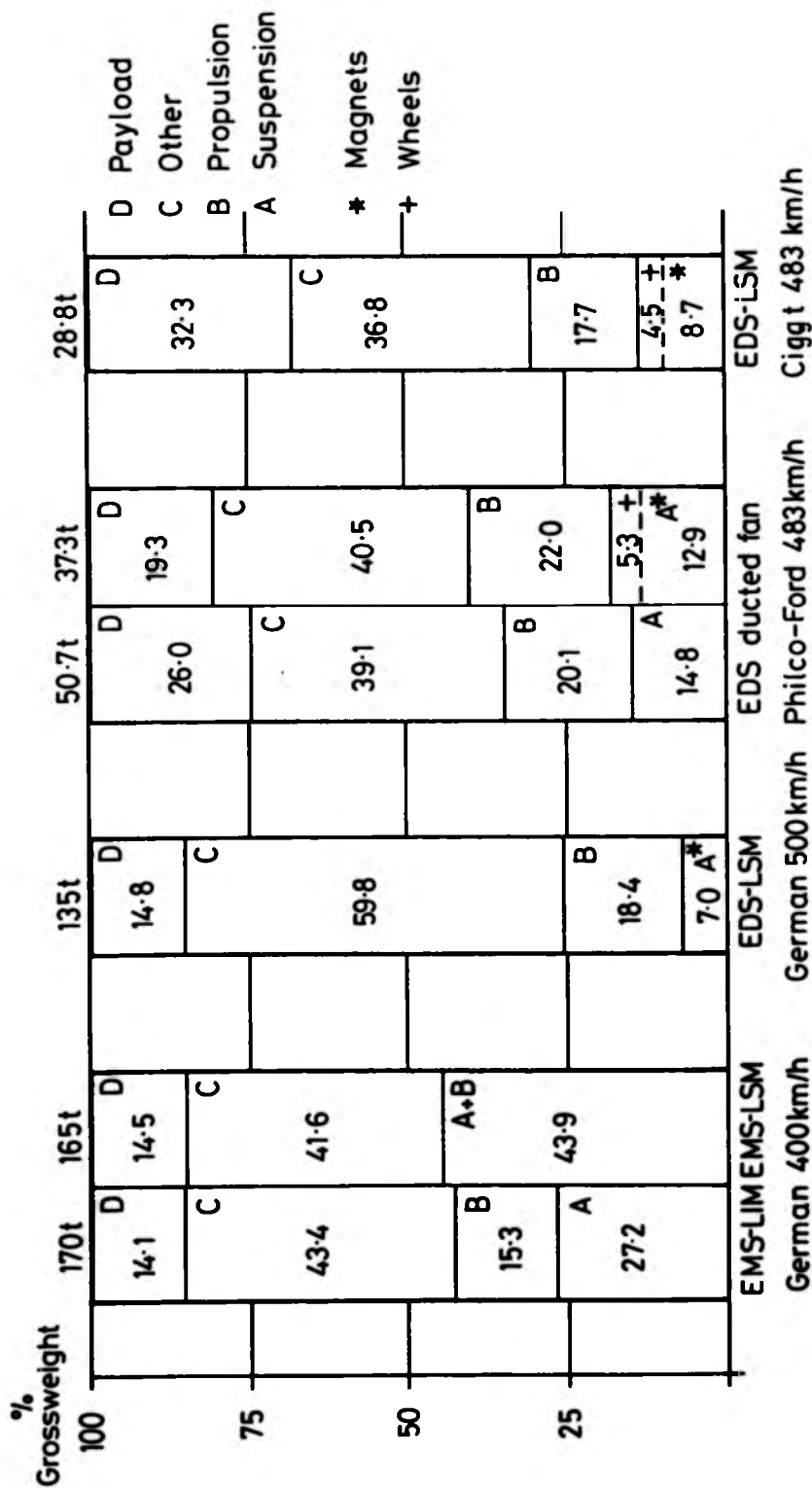


FIGURE 57. SUBSYSTEM WEIGHT BREAKDOWN (% GROSS)

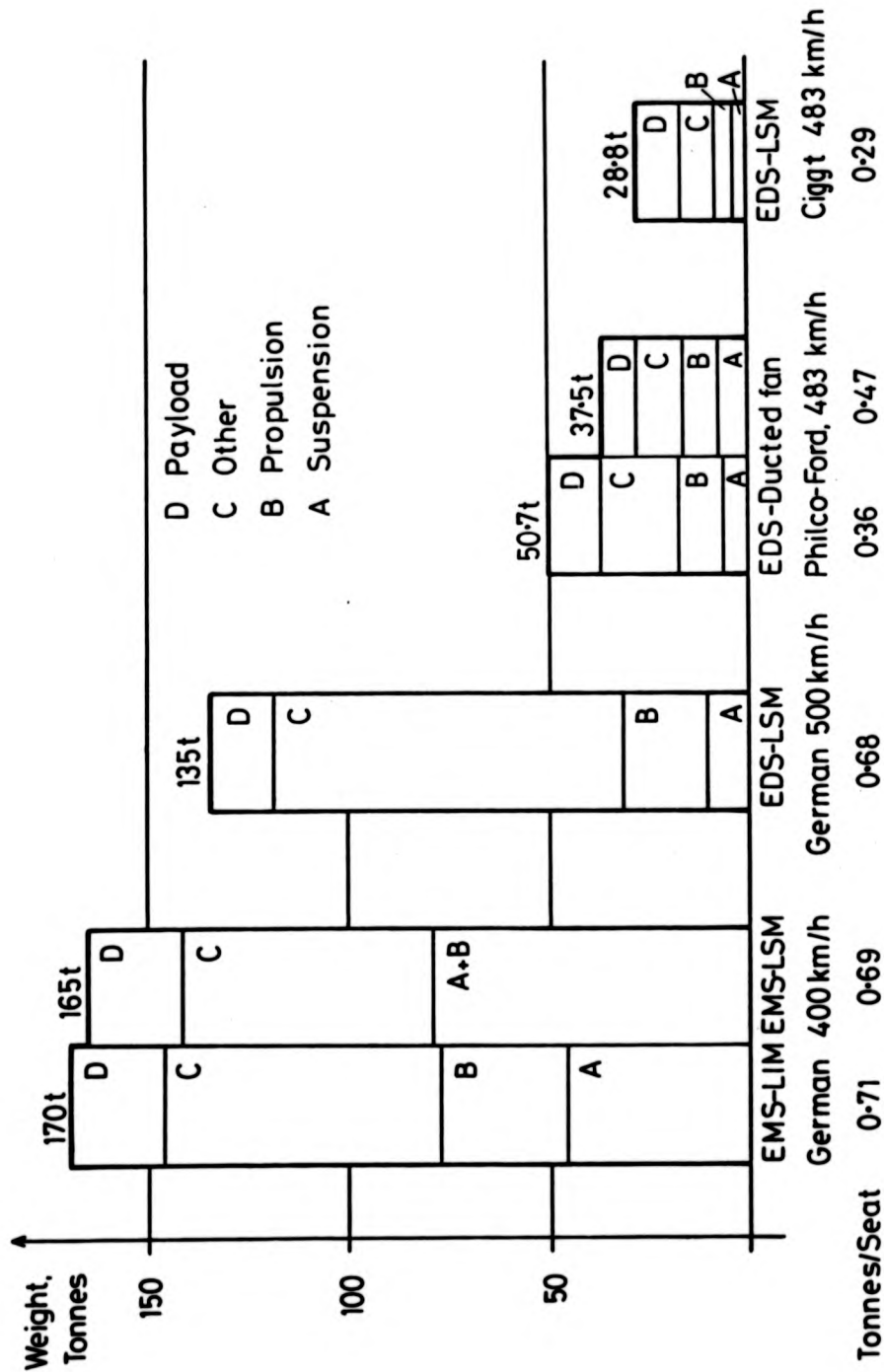


FIGURE 58 SUBSYSTEM WEIGHT BREAKDOWN

The Philco-Ford values are low because of the low aerodynamic coefficients chosen, together with the high magnetic lift to drag ratio obtained with a 25.4mm thick aluminium levitation and guidance conductor. In comparing the CIGGT value of 3.72 MJ per passenger-kilometre with the German EDS value of 4.45, the large vehicle weight of the latter has completely offset the advantage obtained by increasing the vehicle length, as shown by the Philco-Ford difference between short and long vehicles (3.63 and 2.75). Aerodynamic drag per seat decreases with increases in vehicle length, and this effectively means that ϕ will drop with longer vehicles.

Although specific energy intensity is an important factor to consider in making transport comparisons, as has been shown in the sections of the chapter, it is insufficient in completely defining all system parameters adequately, and represents just one part of a total system description.

CHAPTER SIX

FLUX PUMPING AND CRYOGENICALLY COOLED MACHINES

6. Flux Pumping and Cryogenically Cooled Machines

6.1 Pulsed and AC Operation of Coils

Large field value coils tend to use superconductors in the conductor material because of the advantages to be had in the lightweight construction, absence of iron, low power requirement, and the high current density in the conductor section. The majority of applications have been concerned with dc fields produced with very little superimposed ac component. Coil charge and discharge rates are such that only low additional losses occur, and can be easily handled by the refrigeration system at the beginning and end of the coil duty cycle. For maglev systems the ac loss problem stems from air gap harmonics generated by the LSM - the worst case being when the machine stalls and the vehicle sees a full frequency fundamental track mmf before an inverter trip. The other major source is from vehicle transitory motion and track discontinuities influencing the constant flux condition of the coil, and producing a ripple current on the main dc current. The ac loss has been evaluated by several researchers⁽²³⁷⁻²⁴⁰⁾, for this common condition, and loss calculations have been confirmed by experiment.

Work on ac cables running at 50 Hz have used superconductors which are exposed to self-fields generated by the transport current. The field levels are only a few tenths of a Tesla⁽¹¹⁹⁾. The need to develop superconducting coils which can successfully operate at substantial field rates of change has been due to programmes on Superconducting Magnetic Energy Storage (SMES)⁽²⁴¹⁾, and also on Fusion Reactors, especially the large Coil Programme (LCP) and other Tokamak research sponsored by the US DOE^(242,243). It is to be expected that the large scale application of Nb₃Sn or V₃Ga rather than NbTi superconductor material, with their higher T_c(H) values, will promise a higher stability against thermal disturbances caused by excessive eddy current or other ac loss. Since diffusion fabrication of Nb₃Sn in filaments of diameter markedly less than one micron is feasible, as compared to the NbTi size of between one and five microns,

large field amplitudes at industrial frequencies may well be possible, and work to this end is underway⁽²⁴⁴⁾.

If the pulsed operation of superconductors is not feasible for high rates of change of field, then a realistic state of the art alternative solution is to use normal conducting metals such as copper or aluminium and benefit from their reduction of resistivity at low temperatures. A conductivity gain of roughly an order of magnitude is possible from room temperature down to LN₂ temperatures, and this may increase to four orders of magnitude at LHe temperatures. Nitrogen cooled pulsed copper coils have already been used as substitutes for superconducting coils at Warwick in Maglev test applications^(136,245). Their low weight in free open bath cooling allowed more sensitive measurements of force and torque, compared to a cryostat housed superconducting coil. Schauer has discussed the tradeoffs involved in comparing the competitive advantages of cryomagnets (cryogenically cooled magnets) with superconducting coils. The indication is that for only moderate fields in the range 3-4 Tesla, at pulse durations of 5 seconds or shorter, and at temperatures of about 10K, the cryomagnet is a cost effective and technically reliable solution⁽²⁴⁶⁾.

6.2 Application to HSGGT

In a paper by Melville⁽²⁴⁷⁾, the principle of providing thrust for a - Maglev vehicle by reaction of the levitation and guidance magnets to sidepieces set at an angle within the main guideway reaction rails was described. Unfortunately, Melville failed to realise that there was no nett thrust force generated, since for a forward motion, thrust was balanced by an equal and opposite drag force in the second half of the cycle. The concept of a variable reluctance track was considered further at Warwick, where it was seen to fall naturally into a class of machines requiring variable frequency operation of the vehicle magnet currents to achieve superconducting LRM effect with a passive track structure⁽²⁴⁸⁾.

Wipf elaborated on the variable reluctance track concept and also used variable frequency operation of vehicle coils⁽²⁴⁹⁾. The track structure chosen however would be difficult to construct: the choice is a sinusoidal elevation with amplitude of 300mm and period of 6 metres. The coil frequency would be 16.7 Hz for the design speed of 360 km/h. Coil current forcing was derived from a three phase superconducting generator on board which was driven either by a gas turbine or perhaps a LH₂ based turbine. The problem of ac losses was hardly mentioned.

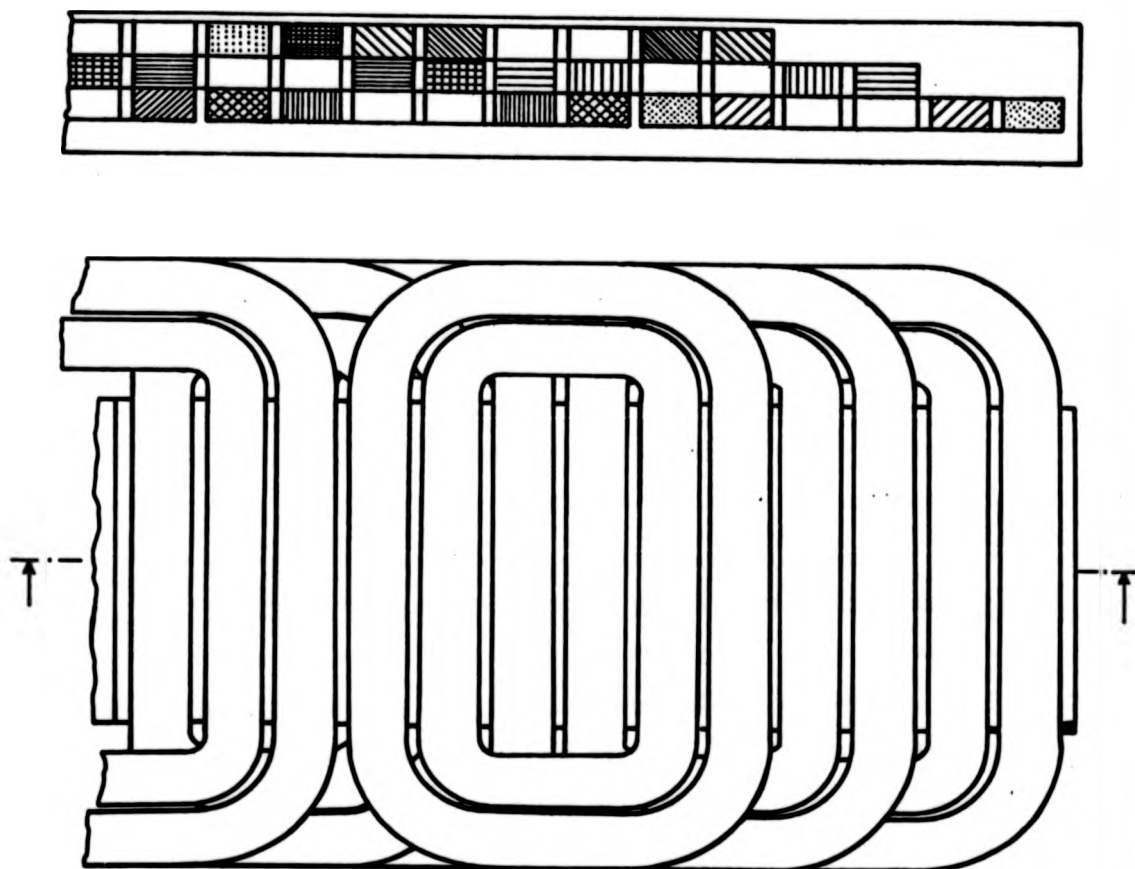
6.3 Flux Pumping Motors (FPM)

6.3.1 Components

The foregoing sections suggest that it may be possible to design a realistic propulsion unit using variable frequency operation of superconductors or cryomagnets, although previous attempts have not produced feasible systems. It is likely that the operating regimes open to such units would be passive track propulsion of duorail or equivalent vehicles, rather than full magnetically levitated vehicles, because of the additional complexity of on board systems compared to an EDS-LSM vehicle.

The coil array construction is based on a three phase, three layer concentric winding arrangement (Figure 59). The three layers provide better volume utilization than a two layer winding and the coils can all be preformed into pancake windings, potted and then assembled into a fabricated array. Coil cross bracing would be eased because the mechanical structure will be very rigid.

The cryostat outer case will probably be a fibre reinforced plastic, perhaps with a eddy current shield on the top face to attenuate field projections into the passenger compartment. The use of plastic cryostats for pulsed coils is already proved⁽²⁴³⁾, and total eddy current loss has a marked reduction. Coil energisation would follow one of four options, depending on the power rates required, and the heat losses that were acceptable. Track structure would be flat and embody ferromagnetic blocks at regular intervals



Three phase, three layer winding.

Figure 59. FLUX PUMPING MOTOR COIL ARRAY.

to provide saliency, although it would be possible to reconfigure the scheme to allow some of the normal attractive force to produce significant lift. As with the Rohr application of ROMAG⁽¹⁵⁸⁾, the track structure could incorporate a cage winding or sheet to produce even more thrust with the machine acting essentially as a superconducting linear induction motor. Using superconductors for airgap magnetization means that the overall power factor will be high, even at large clearances, so the normal problem of low apparent efficiency suffered by conventional LIM and LRM would be avoided. Rotating superconducting induction machines have been proposed⁽²⁵⁰⁾, with a LN₂ primary stator winding and a superconducting rotating secondary. However, the superconductor matrix takes the secondary slip frequencies during start up, until the hysteretic and eddy current losses are sufficiently small to allow the whole cage to be cooled down to the superconductor transition temperature, at relatively low slips. At this point the machine locks into synchronism as the superconductor current oscillates with the cage's transient acceleration and deceleration resulting from load changes.

Some of the advantages of this type of motor result from it being energised from one side. The track could be simple to construct, and if a cage winding or sheet reaction rail was used, there would be no need to synchronise the existing frequency to the vehicle speed. The choice of prime energy for coil power would depend on the application. For low to medium speed operation a dc pickup would be most suitable, with an on board chopper and pulse inverter to supply the coils with a variable amplitude and frequency current source. At higher speeds where current pickup becomes physically awkward and economically unattractive, a gas or hydrogen turbine would almost certainly be chosen, to drive a rotating, perhaps superconducting alternator or dc generator with an inverter following.

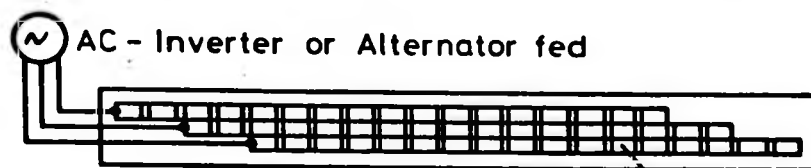
6.3.2 Methods of Coil Energisation

Figure 60 shows four methods for controlling the energy flow into the superconducting (or cryogenically cooled) coil array. The first two methods supply the coils with sinusoidal controlled current from either a current source inverter or an alternator set driven by a prime mover or motor fed from picked up power. The second two methods energise the coils sequentially by either thermal or semiconductor switching.

The first method is probably the most simple, and involves feeding the separate coil phases with alternating currents. The coils within the array are internally connected to form the phase spreads, and a remote star connection within the cryostat obviates the need for another current lead.

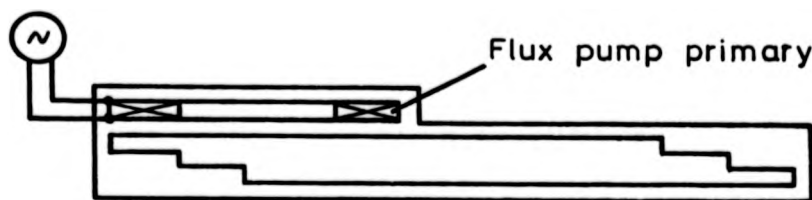
The second method involves the use of a representative phase pitched additional flux pumping coil. The coil is fed with ac as before, but is closely coupled to the first pole pitch of the coil array. By correct choice of coil span and relative cross sectional ampere turns, the whole array will essentially be linked to the single flux pumping coil, since the phase overlap will "pass on" the flux variations. Although this option requires an additional coil to the first, only two current leads are required, for the flux pumping coil, and there are no interconnections to be made between coils in the cryostat. Flux pumps are a proven technology, and can be highly efficient in energy transfer⁽²⁵¹⁾.

The third and fourth schemes are similar in that individual coils are sequentially energised through switches to produce a moving mmf from the vehicle. The function of the inverter is shifted to within the cryostat, and the power feed into the cryostat is dc. The thermally switched flux pump (TSFP) method provides each coil with its own integral thermal switch which is powered up from a source outside the cryostat. The return to a superconducting state after the switch heater is de-energized is accomplished rapidly because of the low thermal inertia of the switch. Homer et al have used this method to produce recovery times as fast as two milliseconds, and have run their switches at about 20Hz to obtain high power densities⁽²⁵²⁾.

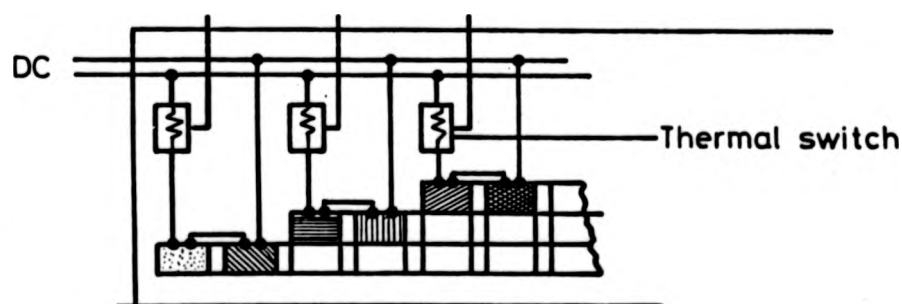


(a) Series Connected Coils

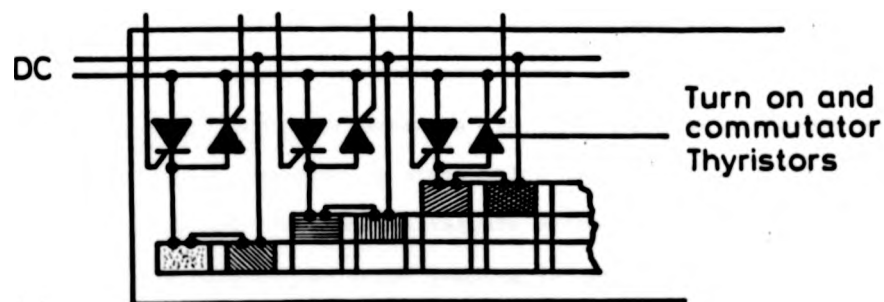
3 layer winding



(b) Representative Phase Flux Pump



(c) Thermally Switched Flux Pump



(d) Semiconductor Switched Flux Pump

FIGURE 60. METHODS OF COIL ENERGISATION.

The semiconductor switched flux pump (SSFP) produces the same effect as the TSFP, but uses either thyristors or transistors to produce the switching action. If thyristors are used, a commutation thyristor will have to be added to produce turn off of the first thyristor. A free wheel diode will not be required because the coil energy will be inductively dumped into the other coils on turn off. The advantage of the thyristor SSFP is that both the switching and commutation thyristors are only given a pulse of energy to turn on and the heat input to the cryogen down the gate leads will be a lot less than the equivalent TSFP heater leads, which are continuously energised when the switch is open. If a transistor switch is used, a continuous base drive is required, but no additional commutation component is necessary. The tradeoffs between thyristor and transistor SSFP and TSFP are difficult to qualify further at this stage. A compromise situation might be to allow the transistor switch to dissipate its base power at a LN₂ shield temperature, and run coil array current leads between LHe and LN₂ levels. The use of active semiconductors at any cryogenic temperature is not widespread, although Alsthom have used freon forced-cooled thyristors in a lightweight chopper circuit for a railway traction application.

The final choice for the best method of energising the coil array will no doubt be dependent on the exact application. If superconducting LIM are proved to be feasible with the expected advances in materials and wire fabrication, then other non-transport applications will develop, in much the same way as have applications of iron cored LIM. The high fields available will allow significant increases in the throughput of processes which use conventional LIM, and open up areas which were previously impractical. Typical examples of LIM application are scrap metal sorting, molten metal stirring, and even liquid metal pumping in foundaries or fast reactors. Liquid metal pumping shows particular advantages because the main pump component is external to the liquid metal, avoids contamination, and can be easily maintained.

6.4 Superconducting Homopolar Linear Synchronous Motors

Various forms of linear homopolar motors were considered during early Maglev development, the most common arrangement being a superconducting coil on the vehicle interacting with a track conductor system that was energised through vehicle brushgear to produce a fixed force angle⁽¹²⁶⁾. There is however, no reason why the Aberdeen Transverse Flux Homopolar Machine (Figure 12), for example, cannot be constructed with the dc flux being sourced from a superconducting racetrack winding. Airgap magnetization could be provided with relatively small amounts of input power making up refrigeration losses. The transverse flux armature coils could still be fixed in laminations carrying the ac flux, so the overall machine would mix superconducting and normally conducting coils. Such combinations using a superconductor to effectively provide a dc bias on the magnetic circuit are presently being tested on a prototype super-transductor or fault limiting device, constructed by Parsons Peebles Power Transformers Ltd and IRD⁽²⁵³⁾.

For large thrusts, the HLSM would effectively span the vehicle width. To provide the iron core at reasonable cross section would produce a very heavy structure. Figure 61 shows an alternative arrangement where the two armature lamination packets are each energised by separate racetrack~ superconducting windings, and the top flux transfer is assisted by the addition of a superconducting screen. The screen effectively compresses the flux and aids the lateral flux linkage. The added advantage is that the passenger compartment is totally screened from extraneous background fields. Whether figure of eight armature windings link both armatures or separate windings are used will depend on the available lateral space for a particular thrust requirement.

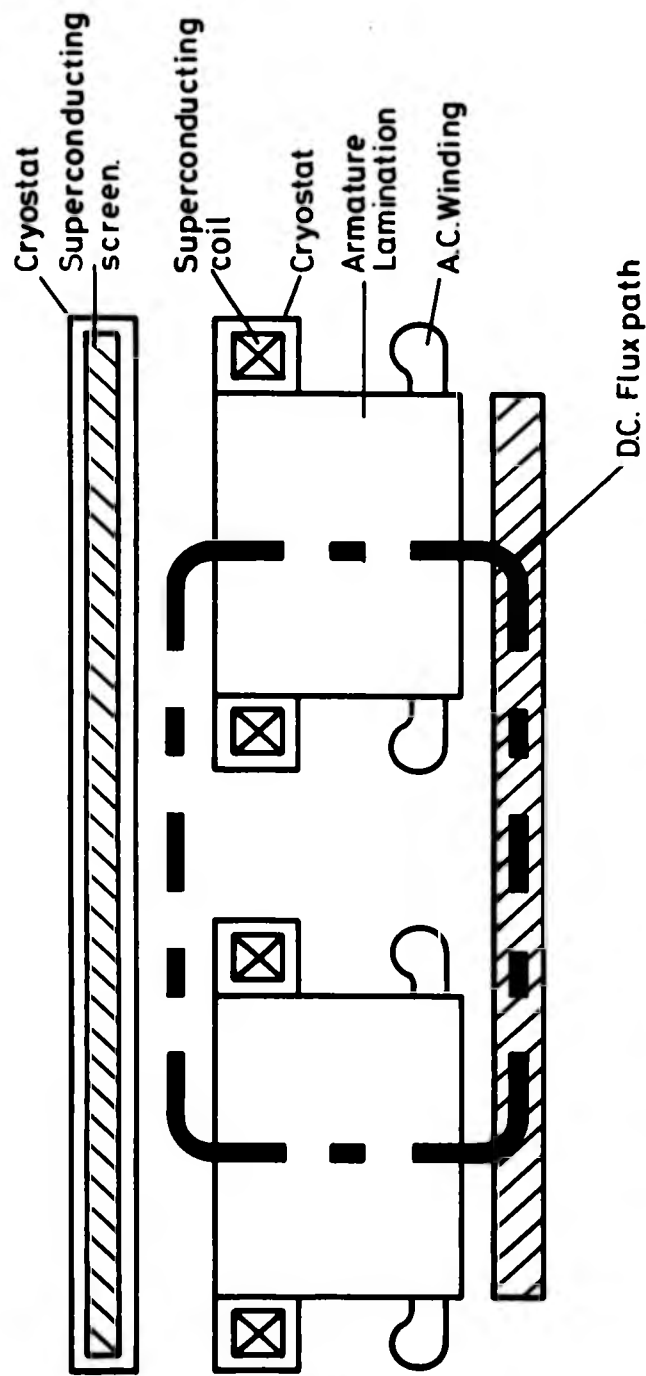


FIGURE 61. SUPERCONDUCTING HOMOPOLAR LINEAR
SYNCHRONOUS MOTOR

CHAPTER SEVEN

HYBRID APPLICATIONS OF ACLSM

7. Hybrid Applications of ACLSM

7.1 Introduction

Railways throughout the world are beginning to rely more heavily on advances in technology to increase their effectiveness as a transport mode compared to the airplane and motorcar. In doing so the emphasis is usually placed on achieving higher average speeds to generate a commercial gain of reduced trip time, with the conflicting constraint of increase of cost usually providing the limiting factor. Technological change in railway practice is usually gradual, but it is possible to improve on existing systems. Aerodynamic drag and energy usage can be reduced by body shape and under body flow styling, and improved suspension design allows increased average speed and hence increases in load factor. Further automation will reduce manpower, but this has a natural bottom limit.

Although some of these effects can be achieved by slight extensions to common practice, others represent distinct changes in philosophy for railway administrations. In particular, the trend has developed to produce fixed formatation articulated-rake trains with integral power for operation in the 200-300 km/h range. Included in this trend has been the development of tilting axis trains such as APT, and the ASEA and FIAT versions. The growing interest in the development of novel techniques of propulsion, guidance and suspension for the very high speeds of 300-500 km/h has not in general been pursued with great vigour by any country's indigenous railway authority (except in Japan). In fact some of the new suspension philosophies have been regarded as rival systems to steel wheel on rail, rather than being accepted as part of an overall transportation solution.

In all the proposed configurations, the method of traction chosen will heavily influence the other sub-systems' design. For example, to meet the tractive power requirement at 400 or 500 km/h either a wheeled trainset with the best of conventional traction motors, or an attractive, magnetically levitated vehicle with linear induction motor drive, would face severe

problems in finding adequate remaining space for payload.

Previous sections have demonstrated maglev characteristics; a development under way in Germany is attempting to qualify the practical limits to conventional railroad. Following on from roller rig tests at up to 500 km/h German Federal Railways(GFR) and Fried.Krupp GmbH are to test a three car 220 tonne 60 metre long vehicle with 12 driven axles⁽²⁵⁴⁾. The power rating will be approximately 12 MW and a top speed of 400 km/h is planned on a converted freight line 23 kilometres long between Rheine and Freren, in North Rhine Westphalia. If the tests are satisfactory, GFR's research department at Minden will determine and develop a suitable configuration for an overall system and its components that could enter revenue service. One aim is to develop the system to 300 km/h, at which point air has no advantage over rail in journey time, for a 500-600 kilometre trip.

Although these tests will not be completed until 1984, it is unlikely that a very high speed system incorporating driven axles will be acceptable in terms of noise generation and track maintenance costs. A possible solution is to provide traction by using a linear machine, and the most suitable system in terms of power transfer is a LSM. The following sections examine the possibility of using an ACLSM as a propulsion device for conventionally railed vehicles.

7.2 Advanced Passenger Train with ACLSM

7.2.1 APT Origin

In the early 1960's British Rail set up a research team to attempt to establish the cause of instability in running freight waggons at high speeds. Above a typical running speed of 80 km/h four wheel waggons tended to derail. At the usual running speed of 70 km/h traffic routing problems would arise when trying to integrate freight and passenger traffic on the same line. Any improvement in freight speed would therefore affect the whole system throughput potential. As a result of the subsequent research a new series of freight bogies allowed freight waggons to run at 50% higher speeds.

The results of the freight analysis and general suspension and vehicle dynamics expertise acquired by British Rail was applied to a proposal to build the Advanced Passenger Train, to similarly extend the useful speed range of trains with no drop in ride quality. This experience was also responsible for BR to be chosen as consultants on vehicle dynamics to the LIMRV programme. The LIMRV ran at up to 400 km/h without flange contact, using the double taper wheel profile chosen by BR for APT.

The concept of providing a tilting suspension on the passenger compartments to allow faster running through curves was chosen as being more cost effective than realignments at greater curve radii and increased cant angles, because British passenger density is generally low. Active control of the tilt using hydraulic jacks was necessary because the simpler passive-damped pendular system could not give sufficient response through tortuous routes, and required an excessively narrow body profile.

Articulation of the train was favoured, since to reduce the track damage rate a lower unsprung mass is required in the wheel sets, which are also subject to a minimum axle loading to sustain ride quality. Articulation of a lightweight train with a low wheel count meets these criteria, and adjacent carriages share common bogies. In general rake length is determined purely by availability of maintenance facilities, and for the London-Glasgow route the rake length can be up to six trailer cars.

Power for traction in the early APT-E (experimental units) was based on British Leyland prototype gas turbines. SNCF also adopted gas turbines for the TGV prototypes. Leyland Truck stopped development of the power units and BR were forced to adopt an electrical power supply, using pantograph equipment. The power car is rated at 3MW. Original plans for 2+12 configuration (two power cars + 12 trailer cars) with the power cars in the middle of the train were dropped in favour of a 1 + 10 make up, with the power car leading. As well as the operational advantage of not having a bisected train, the aerodynamic loading in side gust gives the greatest

The results of the freight analysis and general suspension and vehicle dynamics expertise acquired by British Rail was applied to a proposal to build the Advanced Passenger Train, to similarly extend the useful speed range of trains with no drop in ride quality. This experience was also responsible for BR to be chosen as consultants on vehicle dynamics to the LIMRV programme. The LIMRV ran at up to 400 km/h without flange contact, using the double taper wheel profile chosen by BR for APT.

The concept of providing a tilting suspension on the passenger compartments to allow faster running through curves was chosen as being more cost effective than realignments at greater curve radii and increased cant angles, because British passenger density is generally low. Active control of the tilt using hydraulic jacks was necessary because the simpler passive-damped pendular system could not give sufficient response through tortuous routes, and required an excessively narrow body profile.

Articulation of the train was favoured, since to reduce the track damage rate a lower unsprung mass is required in the wheel sets, which are also subject to a minimum axle loading to sustain ride quality. Articulation of a lightweight train with a low wheel count meets these criteria, and adjacent carriages share common bogies. In general rake length is determined purely by availability of maintenance facilities, and for the London-Glasgow route the rake length can be up to six trailer cars.

Power for traction in the early APT-E (experimental units) was based on British Leyland prototype gas turbines. SNCF also adopted gas turbines for the TGV prototypes. Leyland Truck stopped development of the power units and BR were forced to adopt an electrical power supply, using pantograph equipment. The power car is rated at 3MW. Original plans for 2+12 configuration (two power cars + 12 trailer cars) with the power cars in the middle of the train were dropped in favour of a 1 + 10 make up, with the power car leading. As well as the operational advantage of not having a bisected train, the aerodynamic loading in side gust gives the greatest

The results of the freight analysis and general suspension and vehicle dynamics expertise acquired by British Rail was applied to a proposal to build the Advanced Passenger Train, to similarly extend the useful speed range of trains with no drop in ride quality. This experience was also responsible for BR to be chosen as consultants on vehicle dynamics to the LIMRV programme. The LIMRV ran at up to 400 km/h without flange contact, using the double taper wheel profile chosen by BR for APT.

The concept of providing a tilting suspension on the passenger compartments to allow faster running through curves was chosen as being more cost effective than realignments at greater curve radii and increased cant angles, because British passenger density is generally low. Active control of the tilt using hydraulic jacks was necessary because the simpler passive-damped pendular system could not give sufficient response through tortuous routes, and required an excessively narrow body profile.

Articulation of the train was favoured, since to reduce the track damage rate a lower unsprung mass is required in the wheel sets, which are also subject to a minimum axle loading to sustain ride quality. Articulation of a lightweight train with a low wheel count meets these criteria, and adjacent carriages share common bogies. In general rake length is determined purely by availability of maintenance facilities, and for the London-Glasgow route the rake length can be up to six trailer cars.

Power for traction in the early APT-E (experimental units) was based on British Leyland prototype gas turbines. SNCF also adopted gas turbines for the TGV prototypes. Leyland Truck stopped development of the power units and BR were forced to adopt an electrical power supply, using pantograph equipment. The power car is rated at 3MW. Original plans for 2+12 configuration (two power cars + 12 trailer cars) with the power cars in the middle of the train were dropped in favour of a 1 + 10 make up, with the power car leading. As well as the operational advantage of not having a bisected train, the aerodynamic loading in side gust gives the greatest

moment on the leading car, so a weight increase is of benefit.

The three APT-E units are planned to enter service in late 1981 on the west coast London-Glasgow route. Provided government approval is forthcoming, a 60 train fleet of electric APT-S (S= Service) could fully serve the west coast route in 1985. Although they represent the state of the art in conventional railway practice, their top speed is unlikely to exceed 250 km/h, simply because the maintenance costs will become excessive. Track damage will result from increased power car weight and increased unsprung mass on the axles. Although diesel powered versions of reduced length (say six or seven cars) are planned, they would represent a retrograde step in BR's modernisation and electrification proposals.

7.2.2 Problem Areas in High Speed Running

Whenever a problem area arises in the engineering of a complex system, it is directly reflected in a cost penalty. For a railway system the cost areas are well defined as initial first cost (infrastructure), running cost and maintenance cost. The engineering problems are generally caused by the breakdown of the wheel-rail interface, track damage, ride quality deterioration, and power collection discontinuity.

The wheel rail interface is naturally the most critical area in railway design. Surface contact is limited to the highly stressed area through which the traction power must be transmitted. Adhesion on the driving wheels must be carefully controlled to ensure that wheel slip does not occur during acceleration and that wheel lock does not occur during deceleration. The APT has to brake from 250 km/h to keep within existing signalling distances, at 0.14 gee peak. The hydrokinetic brakes saturate at low speeds, when friction braking takes over. Friction braking needs the provision of wheel slip detection equipment to prevent wheel flats developing under slippery conditions. When the wheels slide rather than purely roll, spalling occurs on the rolling surface from overheating; slip detection has the auxiliary function of monitoring this type of failure.

The acceleration rates on the train are also limited by environmental conditions, the state of the wheel sets' surface, and track profile. By having to generate tractive effort through an essentially slippery surface, power train losses are considerable. Consistent acceleration and deceleration rates cannot be achieved by design factors only.

In general the driven wheel sets are located near or under the power car, whose high axle load allows a higher degree of transmitted tractive effort for a particular track surface condition. There is therefore a requirement for a high axle load for good traction which is in conflict with the desire to produce a lightweight trainset to minimise power demand. The axle load itself results in track damage which has only recently been understood. Track damage is caused by the dynamic loading of the unsprung mass becoming large compared to the static load, and the effect is especially accentuated at joints and crossings. The forces additional to the static loading are known as the P1 and P2 forces, so called because they occur first and second in a force-time history of a rail joint. P1 occurs a $\frac{1}{4}$ - $\frac{1}{2}$ millisecond after meeting a discontinuity and may have an impulse peak up to six times the static load. P2 is a broader response several milliseconds later, at roughly four times the static load. The P1 force is due to a high frequency (500 - 2 kHz) bounce on the Hertzian contact stiffness between wheel and rail, and the P2 force is due to a lower frequency (20 - 100 Hz) bounce of the wheel set on the track foundation stiffness. It is the P2 force which causes the major damage to ballast and leads to track top deterioration as the ballast migrates, but this also sets up a spiral of increasing P1 too.

Vehicle design philosophy is to limit the forces generated to be no greater than a Deltic travelling at 166 km/h. Since the P2 force is largely a function of the axle unsprung mass, it has been found that for any increase in vehicle speeds, the unsprung mass has to be reduced in roughly a velocity squared ratio. APT uses a cardan shaft from the motor driven braked gearbox to a second gearbox on the bogie. The shaft is necessary to take up all the

body movements, especially the tilting motion. The second gearbox on the bogie drives the wheel set through a Quill drive which keeps the unsprung wheel set mass and the primary sprung bogie masses to a minimum. The total unsprung mass is 1.5 tonnes, which is acceptable for 250km/h duty, compared to HST's 2.2 tonnes for 200 km/h and the Deltic's 3.25 tonnes at 160 km/h. A proposed resilient wheel was found to be unsatisfactory because it lacked torsional stiffness. Any required increase in speed is limited therefore by having to reduce the driven wheelset's unsprung mass.

Power collection is likely to remain by pantograph. It is generally accepted that pantograph systems have an upper speed limit although its value is not clearly defined. SNCF have run successfully at up to 280 km/h, and the design speed for the TGV-Electric train sets is 6.3MW power pick up at 270 km/h. The Japanese have run at 256km/h on a timetable service but have considered three phase rigid conductor rail for very high speed current collection. The main problem is that the catenary requires maintenance and repair, as does the brush material on the pantograph head. The original APT 2 + 12 design called for two power cars collecting a total of 6MW for a 270 km/h balance speed.

Figure 62 shows the power and thrust requirements of the 2 + 12 APT with 600 passengers running at constant speed on level track. The 6MW requirement at 270km/h increases to 7.8MW at 300 km/h and 17MW at 400 km/h. The promise of transmitting this level of power, even through a servo controlled pantograph, is daunting and really requires a completely different approach.

7.2.3 ACLSM Extension of APT Capability

The ACLSM for APT propulsion would use the high field superconducting magnet systems similar to EDS Maglev. In the hybrid vehicle the suspension and guidance would for the most part, be provided by the steel wheel on steel rail, but the propulsion and major braking functions would be taken over by the ACLSM. The immediate advantage in choosing an ACLSM over say a LIM or HLMSM with iron cored passive secondaries is that power can be transmitted

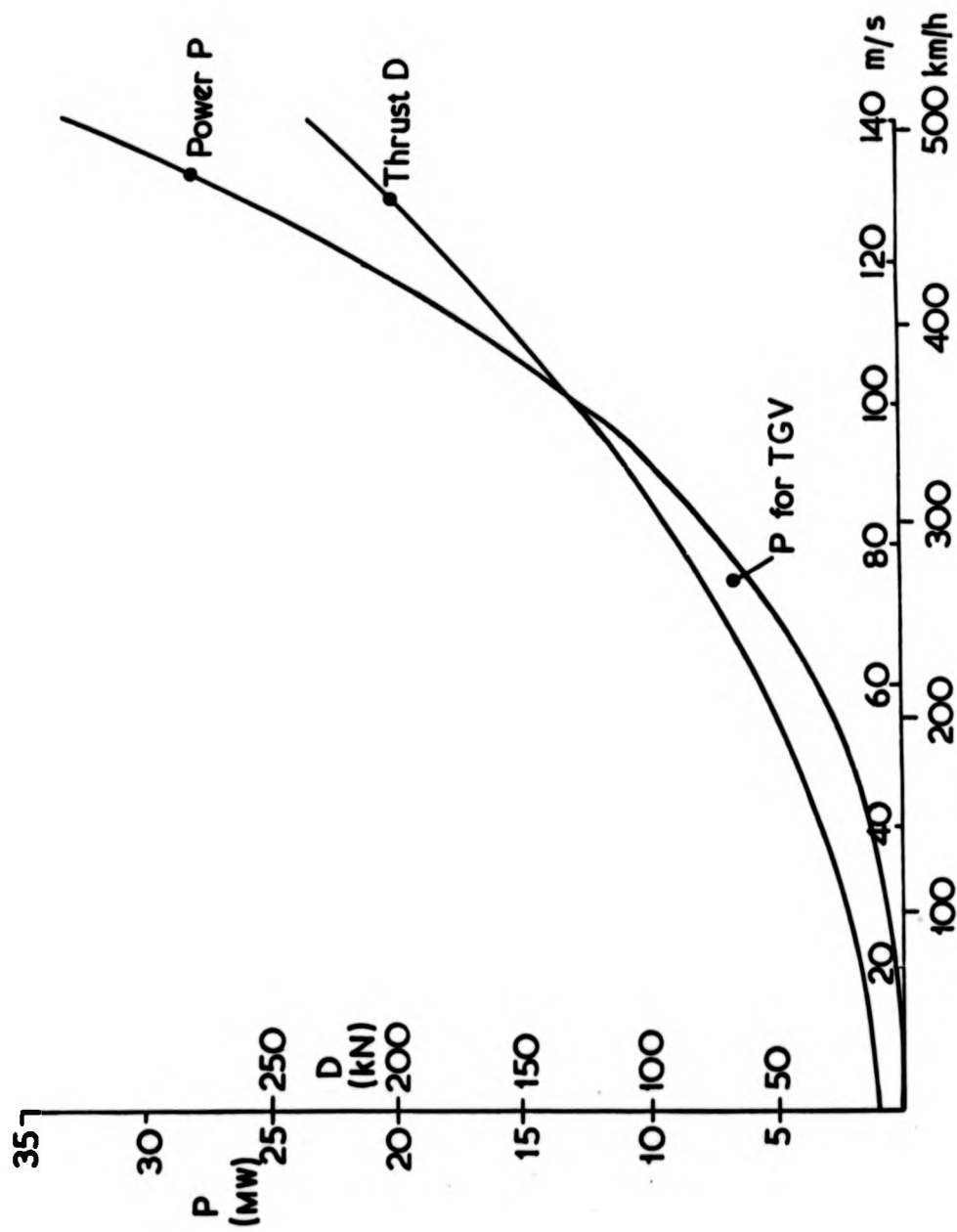


Figure 62. Power requirements for APT.

through the machine airgap to the vehicle for traction, without requiring massive on board generation, or very high power current collection. The pantograph and catenary equipment is immediately superfluous. Braking and acceleration is accomplished through the airgap field without the need to power the wheel sets, avoiding the problems of wheel slip and speed matching. In addition the axle weight in the bogie unsprung mass is allowed more freedom for a lighter structure design that could run at much higher speeds. The magnet system would consist of a multiple array fixed to the train subframe, and would be housed in isochoric cryostats. Persistent current mode operation (with no current leads or external power supply) would be used, and a working day's duty could be achieved before servicing of the cryostat to depressurize and refill was necessary. A totally closed helium cycle is obligatory to conserve a natural resource, and the servicing facility at the termini must have LHe liquefaction and power supplies to re-energise the magnets.

The track winding would be an air cored winding made up of conventional stranded insulated cable laid in a meander configuration either at track surface level or mounted on a slight plinth in the slab track. Figure 63 shows a suggested end view arrangement of plinth armature and cryostat, with an electromagnetic "airgap" clearance of 255mm, and mechanical clearance of 100mm. The plinth might be required to minimise the eddy current drag in the rails from the magnet's motion and the armature winding mmf. An exact analysis of this effect has not been performed since it was found that non magnetic rails were only marginally more expensive than the high quality steel used in conventional rails⁽¹²⁰⁾. The armature conductor would be grouted into the track surface to allow not only good force transmission with minimal strain, but also to provide protection from damage and the environment. The cryostat assembly would form a magnet pad housed in a mounting arrangement that could be easily and automatically decoupled from the train's subframe. This modular approach means that at termini the magnet pads can be rapidly

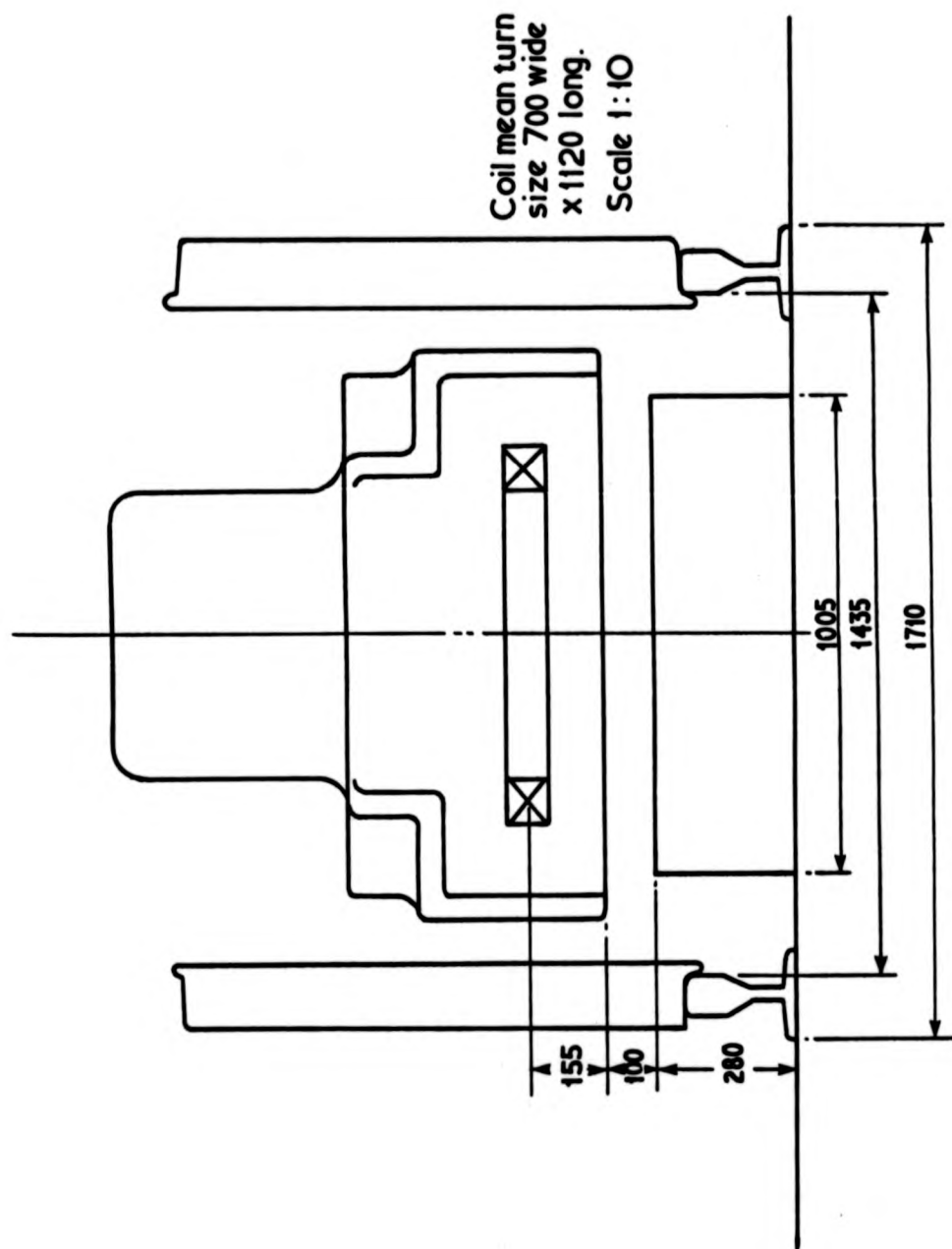
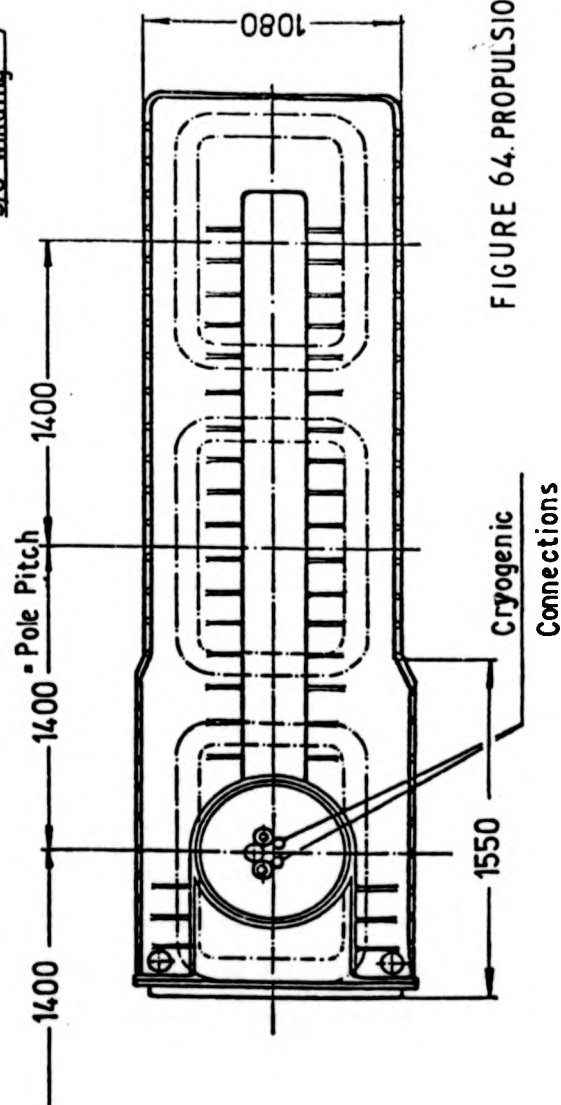
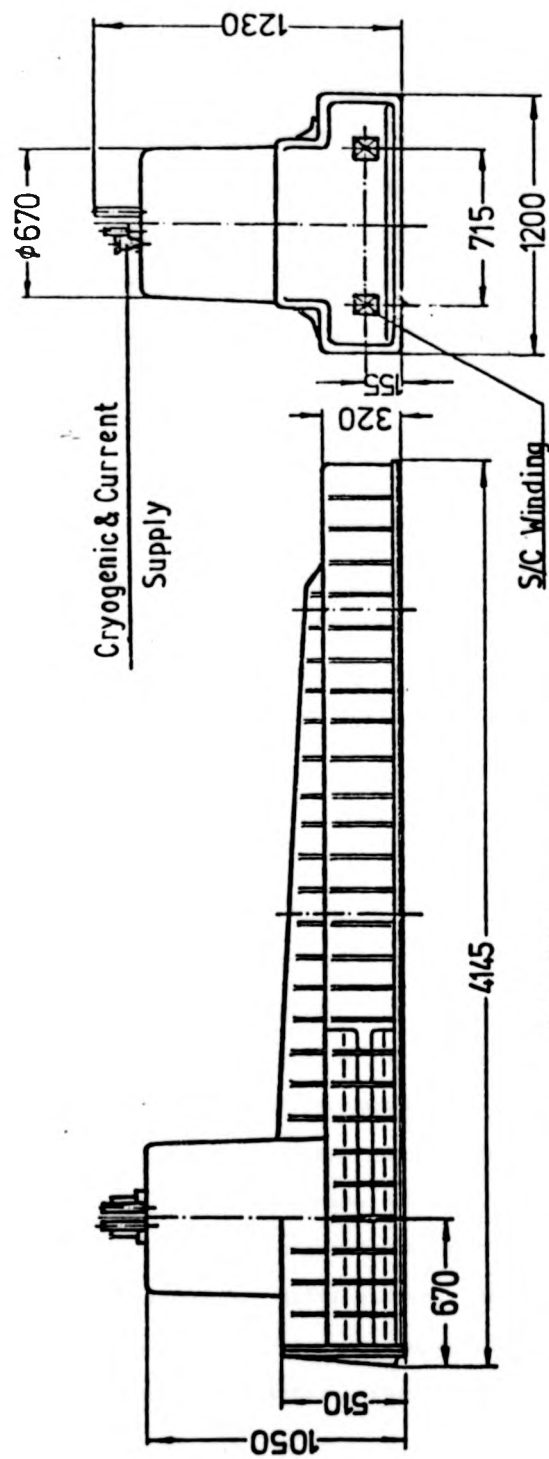


Figure 63. Cryostat End View.

demounted and then taken to a servicing facility where helium transfer through flexible tubing to a liquefier can occur, and connection to a flux pump module will allow magnet recharging and discharging if required. It is quite conceivable that a one to two hour turnaround could be achieved, that would also fit into a daytime operating schedule. If a buffer supply of ready charged cryostats was available, turnaround could be even shorter. An alternative scenario is to provide track incorporated mirror cryostats at the servicing facility, over which the train is positioned. The mirror cryostats would contain flux pumps which would reenergise the coils automatically. On train umbilicals would connect to service ports for LHe transfer. The latter scheme might be preferred by the operator who can afford to effectively spread his servicing operation along many train lengths, rather than concentrating the specialized operations at a service centre and requiring only relatively simple mechanical operations (such as remounting the serviced cryostats to the vehicle body) to be performed at the train.

Conceptually, ACLSM propulsion would not require major technological development, although higher temperature superconductors would ease the temperature rise limitation in isochoric operation. It is possible to design in a system which could make cryogenics operationally easy to handle. A cryostat design such as Figure 64 (Siemens' AVF) would be suitable for conversion to an isochoric duty and ten such units with 30 coils would provide the 90kN required to drive an APT at 300 km/h, with a current sheet track density of about 8kA/m. Using the Emsland design coils and cryostats⁽¹¹⁹⁾ only 3 double sized cryostats (each with six coils) would be required since the active length is greater at 800mm compared to 700mm and the pole pitch at 1 metre is shorter. Two of the double sized cryostats would fit under the existing power car, whose wheelset pitch is 13 metres.

ACLSM adoption would impact all three of the cost criteria. Lower first cost would result since the track bound armature serves as the distribution, pickup and one side of the propulsion motor. Its design is governed more by



Vacuum box: Cast Al without
radiation shield

Weight: 2200 kg.

FIGURE 64. PROPULSION MAGNET AVF/P06, G06.

tradeoff of repayment factor of conductor cost against power cost through the track resistance. Because there is no iron in the track the inductance is very low, and voltage drop in the magnetically unlinked feeding section of the winding must also be similarly low. Because there is no catenary, there are no overhead tensioning devices, and no trackside masts. Load equalisation between sections is unnecessary since the multiphase system is inherently balanced. This would be particularly important for high speeds since loosely tied areas will experience phase imbalance on existing 25kV ac supplies at 132kV feeders.

The armature winding has the option of either being fabricated off site into a "conductor mat" which only requires a minimum of fixing at the installation, or can be automatically track wound into precast blocks which have preformed slots in their surface. The former scheme has the advantage that the conductors are factory formed and installation damage risk is minimised since relatively simple fixing rather than fitting is required. A combined scheme of laying formed and braced conductor into a slip casting machine might provide an alternative method of installation.

Because of the preforming processes involved, track armature lay time will be comparable to catenary stringing time. Lightning protection should be unnecessary, since substantial insulation will be provided by a conventional jacket insulation, and will be aided by epoxy cement grout. The amount of armature material will depend on power density required from the machine. Typically it is in the range of 5-30 kilogramme/metre. The steel rail is roughly 60 kilogramme/metre. Train turbulent windage will allow slightly higher than normal current densities to be used.

The overall machine efficiency and power factor will be high, even though the design limits are set by the economics involved rather than any particular engineering difficulties. Since the main airgap flux is sourced from the vehicle magnets, the magnetization is not reflected into the power supply as a low power factor. For multiple vehicle operation, it may be possible to

operate some of the machines at leading power factors to reduce the overall reactive power consumption and compensate for the line inductance. It is more likely that this effect would not feed through the system since each vehicle will be controlled by one inverter, or a split inverter. Regeneration through the inverters before the main utility connection is made would trade off some of the acceleration and braking loads in the system.

Vehicle cost may be reduced through lightweight construction. APT has attempted to do this by using aluminium extrusions in the body shell design of the passenger sections. The Siemens cryostat weighs approximately 2 tonnes, and would be less for an isochoric design. This can be compared to the main APT incoming transformer weighing 5.3 tonne (53 kW losses), in a 69 tonne power car. The existing power car has very few longitudinal features and is inherently less stiff than a lightly loaded trailer car, so aluminium loses its advantage. Steel was chosen as the main structural material, with the heavy items in the central portion of the car, depressing the natural frequency of the body. With the absence of the majority of the power car equipment, a similar constructional technique could be used to decrease the axle load, and there should be sufficient room to accommodate passengers in the main power car. Naturally, with the absence of driven wheels, the unsprung mass of the power car is reduced too, the wheels being designed for pure rolling.

Maintenance cost will be reduced at the trackside because there is a simple slab track with enclosed conductors. The need for reballasting and catenary adjustment with restringing will have disappeared. Rail damage will be minimal because axle loads of the power car and unsprung mass of wheel sets are all reduced. Provided that armature hot spots do not occur to break down the insulation the track should be essentially maintenance free.

Vehicle maintenance is dominated by the need to reprofile wheel treads. The major causes of the wheel damage are, apart from the unsprung mass

bounce, flats and localised heating producing creep caused by wheel slip. With tractive effort and braking being derived from the motor air gap power transfer, wheel damage and deterioration should be reduced dramatically. Running cost means basically power consumption of the trainset. With the total vehicle construction being lightweight, the inertial power required to accelerate is reduced. Although the steady state power consumption follows a cubic relationship with speed (Figure 62), constant headway limits imposed by signalling means that power requirements will increase as velocity squared. With the omission of the pantograph, the APT has an immediate reduction in the drag force experienced of 8%. Similarly a continued study of underbody flow could possibly reduce aerodynamic drag by as much as 10%.

By being able to provide a magnet pad for any of the trailer cars, it would be possible to match train length to passenger demand more closely. Since synchronous operation is assured, the operation of the system can be either platoon following or exclusive block, depending on the strategy chosen.

Inverter control is already required and this could be incorporated into an overall computer control of all vehicle scheduling, with exact knowledge of vehicle position. Further control of the inverters could provide motion control, for example heave and surge motion control. If vehicle overturning is considered to be a problem, then an attractive normal force can be achieved by altering the machine current angle operation.

Since the armature can be built to match local conditions, additional cross section or armature conductor density may be included where extra acceleration is required, for example near stations and at slow grades.

This will affect infrastructure first cost as well as running cost. For example the Paris-Lyon route is built for maximum gradients of 3.5%, which means only 1.3% of the 427km is made up of bridges. This compares with 30% on the FS Direttissima, and 33% on JNR's Tokaido Section. A reasonable ACLSM design could easily accommodate up to 15% grade climbability at rated

operate some of the machines at leading power factors to reduce the overall reactive power consumption and compensate for the line inductance. It is more likely that this effect would not feed through the system since each vehicle will be controlled by one inverter, or a split inverter. Regeneration through the inverters before the main utility connection is made would trade off some of the acceleration and braking loads in the system.

Vehicle cost may be reduced through lightweight construction. APT has attempted to do this by using aluminium extrusions in the body shell design of the passenger sections. The Siemens cryostat weighs approximately 2 tonnes, and would be less for an isochoric design. This can be compared to the main APT incoming transformer weighing 5.3 tonne (53 kW losses), in a 69 tonne power car. The existing power car has very few longitudinal features and is inherently less stiff than a lightly loaded trailer car, so aluminium loses its advantage. Steel was chosen as the main structural material, with the heavy items in the central portion of the car, depressing the natural frequency of the body. With the absence of the majority of the power car equipment, a similar constructional technique could be used to decrease the axle load, and there should be sufficient room to accommodate passengers in the main power car. Naturally, with the absence of driven wheels, the unsprung mass of the power car is reduced too, the wheels being designed for pure rolling.

Maintenance cost will be reduced at the trackside because there is a simple slab track with enclosed conductors. The need for reballasting and catenary adjustment with restringing will have disappeared. Rail damage will be minimal because axle loads of the power car and unsprung mass of wheel sets are all reduced. Provided that armature hot spots do not occur to break down the insulation the track should be essentially maintenance free.

Vehicle maintenance is dominated by the need to reprofile wheel treads. The major causes of the wheel damage are, apart from the unsprung mass

bounce, flats and localised heating producing creep caused by wheel slip. With tractive effort and braking being derived from the motor air gap power transfer, wheel damage and deterioration should be reduced dramatically. Running cost means basically power consumption of the trainset. With the total vehicle construction being lightweight, the inertial power required to accelerate is reduced. Although the steady state power consumption follows a cubic relationship with speed (Figure 62), constant headway limits imposed by signalling means that power requirements will increase as velocity squared. With the omission of the pantograph, the APT has an immediate reduction in the drag force experienced of 8%. Similarly a continued study of underbody flow could possibly reduce aerodynamic drag by as much as 10%.

By being able to provide a magnet pad for any of the trailer cars, it would be possible to match train length to passenger demand more closely. Since synchronous operation is assured, the operation of the system can be either platoon following or exclusive block, depending on the strategy chosen. Inverter control is already required and this could be incorporated into an overall computer control of all vehicle scheduling, with exact knowledge of vehicle position. Further control of the inverters could provide motion control, for example heave and surge motion control. If vehicle overturning is considered to be a problem, then an attractive normal force can be achieved by altering the machine current angle operation. Since the armature can be built to match local conditions, additional cross section or armature conductor density may be included where extra acceleration is required, for example near stations and at slow grades. This will affect infrastructure first cost as well as running cost. For example the Paris-Lyon route is built for maximum gradients of 3.5%, which means only 1.3% of the 427km is made up of bridges. This compares with 30% on the FS Direttissima, and 33% on JNR's Tokaido Section. A reasonable ACLSM design could easily accommodate up to 15% grade climbability at rated

cruise speed by additional track conductor, without penalizing payload. The ACLSM has scope for improving the overall vehicle performance and has the opportunity for lowering both first cost as well as maintenance and running costs compared to conventional traction drives. Dual running of conventional and ACLSM vehicles is possible since neither scheme requires removal of the alternative facilities. No new infrastructure is required. Freight services would remain unaffected, and might even benefit from LSM drive.

The appearance of an ACLSM propelled APT would not be radically different from the existing vehicle. Because of the higher speed operation, shorter higher loaded vehicles at reduced headways might be expected. Figure 65 gives an impression of a high performance four car vehicle, with removeable cryostat assemblies mounted under the body in between the wheel sets. The vehicle is bidirectional, and passengers are accommodated throughout the front and tail cars, except for small areas containing on board services such as heating and ventilation plant.

7.3 Urban Vehicles with ACLSM

The concept of the ACLSM propelling wheeled vehicles can be extended down in the speed range. Whereas EDS with ACLSM were not considered for urban and low speed operation, the ACLSM on its own can be reconfigured to suit lower speeds. Linear motors have not generally been considered suitable for urban vehicles since the more advanced UMTA projects never really materialised. However with UTDC's, ICTS, the situation may rapidly turnaround, despite their choice of LIM for propulsion. Nondahl at General Electric has studied the alternatives of SLIM and HLSM as propulsive units for design vehicles running at 112 to 400 km/h, requiring 200-3735kW⁽²¹⁵⁾. The track structures are essentially passive, but not necessarily inexpensive. For example the 200 kW SLIM design uses 32 kg/m back iron, and 63kg/m in the 3735 kW design. On top of this the SLIM naturally has aluminium secondary material and there is a current pick up

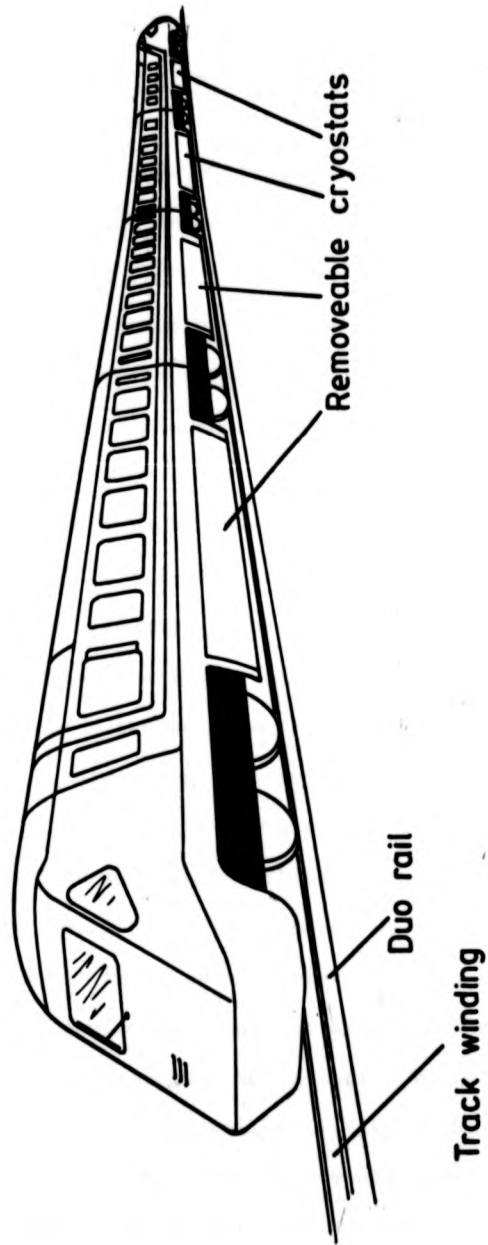


FIGURE 65. APT WITH TRACK WINDING AND REMOVEABLE CRYOSTATS.

system required.

The pressure to reduce the cost of urban rail vehicles has been demonstrated by the Railbus, which consists of two Leyland single-deck bus bodies joined back to back and mounted on a rail underframe supported by high speed freight wagon bogies⁽²⁵⁵⁾. The vehicles are powered by a 150kW diesel for a maximum speed of 120 km/h, with 64 passengers. Vehicle cost for production versions will be about £130k, roughly a third of the price of an equivalent conventional rail vehicle.

Slemon has designed out a LSM vehicle rated at 240kW for urban service at 72 km/h, with an air cored winding, inverters at 200 metres, and a rare earth magnet field assembly weighing about 1 tonne⁽²¹³⁾. Although the machine has good overall performance, the economics are unlikely to be acceptable. Operationally, because the magnets cannot be deenergised, maintenance problems will arise in dealing with magnetic debris picked up from the track.

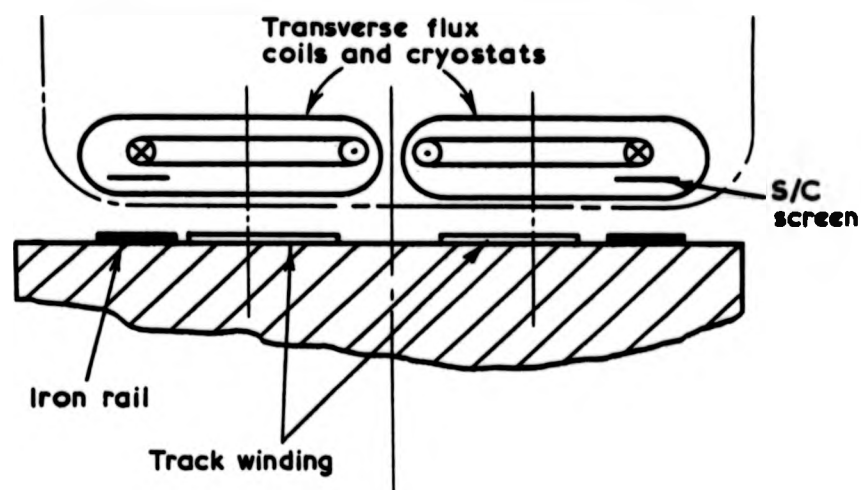
With the continued pressure on cryogenic development from MHD, Fusion, rotating machinery, as well as Maglev the development of reliable and cost effective superconductors will allow an urban vehicle to be equipped with lightweight cryostats. The advantages of the previous section will still apply for simple, low maintenance track, and easily controlled vehicles.

For a typical urban vehicle a thrust of about 12kN is required. This value could be derived from a 3 metre long cryostat assembly with three coils. There would be no particular problems in operation or maintenance if the isochoric magnet pad concept was again applied, since the only part of the vehicle supplying thrust would be easily removeable.

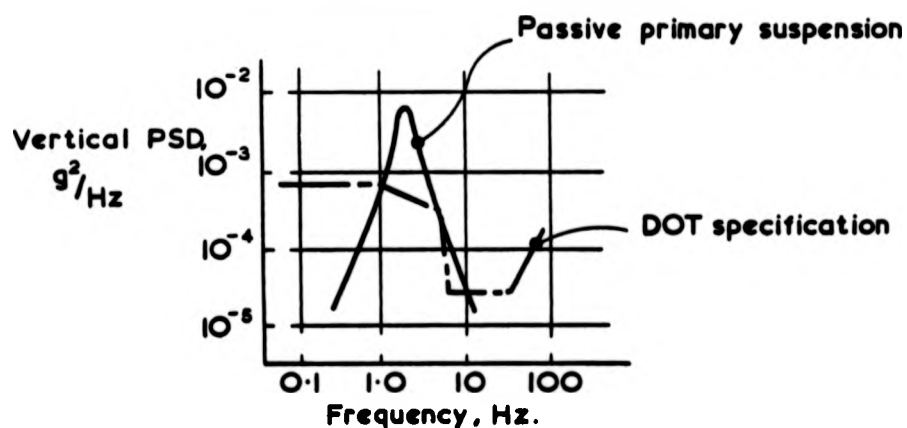
Other field arrangements may prove as suitable. For example, air or iron cored magnets with normal conductors could be used. Power would be generated either on board or picked up through a third rail. To get sufficient ampere turns on the vehicle a cryoresistive coil is likely to be the best option, but at lower ampere turns track and coil windings would need to be iron cored with small mechanical clearances to allow an efficient magnetic circuit to be made.

A form of EDS which might take the place of EMS suspensions at low speed for urban applications, is the mixed u system⁽²⁵⁶⁾. The system involves the use of superconducting screening material between a solenoid and a ferromagnetic rail. Russell suggests a saddle shaped coil formed around an iron rail with a pinch wheel drive on a vertical plate. A more reasonable approach is shown in Figure 66 where a flat track transverse flux motor interacts with a flat iron rail. The superconducting screen is in the same cryostat as the coil and allows lateral stability by edge effect. The transverse motor arrangement is adopted to provide heave roll and surge damping as well as thrust and normal force trim. The PSD expected is shown. To move the ride quality spectra to within the DOT standard, active ride control is necessary, achieved by the LSM. If lateral damping is required then active secondary suspension could be used. A lateral screen working in 'mixed u' but incorporating a persistent current type heater to locally quench it might be an alternative form of lateral active damper, although the heat leak rate is likely to preclude its prolonged action.

The urban vehicle with a passive on board magnet array that was energised at the beginning of the working day, and reacts with a simple controllable air cored track winding running at low power dissipation (and hence high efficiency) is indeed feasible. Its infrastructure is cheap and the track material content is small considering the power that is transferred. Vehicle cost will be low since a lightweight structure with no power conversion equipment on board is all that is required.



a) Mixed - μ suspension and transverse flux (dual motor) linear synchronous propulsion.



b) Typical ride quality results expected for mixed μ suspension and passive primary damping.

Figure 66. Mixed μ suspension and transverse flux linear synchronous motor propulsion.

CHAPTER EIGHT

CONCLUSIONS

8. Conclusions

The most important areas of interest concerning air cored linear machines, their design, development and application to guided ground transportation have been presented. ACLM began as the favoured propulsion unit option for the electrodynamic system of magnetic levitation. The machine characteristics can be represented by an equivalent circuit model with which design performance can be calculated, and the way in which the circuit components are evaluated and optimised is discussed. An analysis of the field to stator flux linkage allows harmonics to be minimised by phase spreading or short pitching the stator winding. Rectangular vehicle coil stresses were modelled by matching the corner body forces to those of a circular coil with a similar field profile and cross section.

For high acceleration loading, the track power dissipated for long section lengths can become excessive. The linear commutator motor was conceived in two main variants to combat this problem. In its most elementary form each track wavelength is energised through a bidirectional chopper from a dc bus. The substation requires only a transformer rectifier set, and the utility is effectively buffered from low power factors. A less sophisticated form uses the LSM geometry with the inverter either at much more frequent intervals or more frequent tie reclosures per inverter, to produce short block lengths of energised track. An economic analysis of the LCM in relation to several LSM designs shows that for low inverter unit cost and short block lengths, a LCM is still an attractive option to LSM for revenue duty, despite the added track complexity. A superconducting model LCM was successfully built and tested. Both the Miyazaki and Emsland high speed linear test facilities have adopted short block length switching to remote converters as the most economic solution with the minimum of overall losses.

A systems comparison of EMS and several EDS full sized designs highlighted the need to perform comparisons on similar baselines of speed, passenger density scheduling and routing, rather than just specifying lift to drag

ratio, specific energy intensity or machine efficiency. In particular the SLIM was shown to be inadequate for 500 km/h operation of German EMS vehicles, and not very efficient in energy conversion at 400 km/h. The Siemens EDS vehicle was also shown to be heavily penalized by its duo-rail compatible low speed suspension system, compared to other EDS designs which used aerospace type vehicle construction, and light weight suspensions.

Several different variations are proposed for a new type of ACLM which uses on board flux pumping either by direct drive from an on board alternator or inverter, or by thermal or semiconductor switching of currents into superconducting or cryogenically cooled coils. The flux pumping motor (FPM) requires a passive track structure with either saliency for reluctance operation, or a sheet secondary for induction motoring. A superconducting HLSC design is also considered.

Finally, the application of ACLM to propulsion of advanced duo rail vehicles is proposed. The gains in speed envelope, reduced track damage and lower installed and maintenance cost are examined. As a short term development, conversion of an APT type vehicle with removable cryostats and coils which operate isochorically would show immediate advantages in reduced operational expense to conventional versions. Extension of the technique to low speed urban vehicle design is also possible, with a simple low maintenance track structure.

In general, development of ACLM has proceeded against a background of increasing world recession, which has limited the need for growth in high speed guided ground transportation expected in the late 1960's. However, the last few years have shown that the basic concepts and design criteria are justified, and can be made to work at the very high speeds of 500km/h.

Although EDS no longer has the impetus of major development in the main industrialised countries, with the exception of Japan, ACLM can be used for other forms of contact guided vehicles, with a less complicated infrastructure required. It is apparent that it is this need that ACLM must satisfy,

otherwise the associated research and development will suffer the same fate as Bachelet's electromagnetic experiments at the turn of the century.

CHAPTER NINE

REFERENCES

References

1. S S Wheeler, C S Bradley, "Improvements in Electric Transportation Systems" UK Patent 4,751:1891, 18 April 1891.
2. "Tangential Traction", Electrician, vol.52, 29 January 1904, p.561-2.
3. H H Wilson, "Electrification of Railways", Trans. Liverpool Engineering Society, vol.26, 1905, p.181-234.
4. A Zehden, "Improvements in Electromagnetic Traction or Driving Apparatus for Railways, Lifts, Machine Tools and Other Apparatus", UK Patent 12,581:1902, 2 June 1902.
5. id., "New Improvements in Electric Traction Apparatus", US Patent 88,145, 4 June 1902.
6. The Electric Carrier Co., "Electric Induction Transport System for Mails", Engineering, vol.96, 10 October 1913, p.501.
7. "Electric Carrier Railways for Rapid Transfer of Mail and Express", Engineering News, vol.70, No.14, 2 October 1913, p.637-9.
8. E Bachlet, "Electromagnetic Levitating and Transmitting Apparatus", UK Patent 9,573:1911, 19 April 1911, also "Levitating Transmitting Apparatus" US Patent 1,020,943, 19 March 1912.
9. "Foucault and Eddy Currents Put to Service", "The Engineer" vol.114, 18 October, 1912, p.414, 420-1.
10. H Kemper, "Schwebende Aufhangung durch elektromagnetische Krafte: eine Moglichkeit fur eine grundsatzlich neue Fortbewegungsart", ETZ-A, Vol.59, No.15, 14 April 1938, p.391-5.
11. id "Elektrisch angetriebene Eisenbahnfahrzeuge mit elektromagnetischer Schwebefuhrung", ibid, vol.74, No.1, January 1953, p.11-14.
12. "A Wound-Rotor Motor 1400 Feet Long", Westinghouse Engineer, vol.6, September 1946, p.160-1.
13. M F Jones, "Launching Aircraft Electrically", Aviation, vol.45, No.10, October 1946, p.62-5.
14. "An Electrical Runway", The Engineer, vol.182, 25 October 1946, p.379-80.
15. J M Shaw, H J H Sketch, J M Logie, "The Theory, Design Construction and Testing of an Electric Launcher", RAE Report No.AERO 2523, EL1484, July 1954.
16. I G Black, R F Gillie, C J Longley, T H Thomas, "Advanced Urban Transport", Warwick University/Lanchester Polytechnic Urban Transport Research Group Working Paper No.21, December 1973.
17. D L Hearn, N H Van Dorn, "Modern Transportation Systems", Automotive Engineering Congress, Detroit, 25 February - 1 March 1974, SAE Preprint No.740225.

18. G P Kalman, "Linear Motors to Power DOT's High Speed Research Vehicles", Railway Gazette International, vol.130, No.10, October 1974, p.378-83.
19. J H Dannan, R N Day, G P Kalman, "A Linear Induction Motor Propulsion System for High Speed Ground Vehicles", Proc.IEEE, vol.61, No.5, May 1973, p.621-30.
20. M Guarino, "Development of the Linear Induction Motor in the United States, Past, Present, and Future," BMFT Statusseminar, 1978.
21. R W Crosby, R J Ravera, "The Transportation Advanced Research Projects Program - An Overview", Proc.Joint Automatic Control Conference, San Francisco, 22-24 June 1977, IEEE Publ.No. 77 CH 1220-3 CS, p.472-80.
22. T G Fellows, "High Speed Surface Transport", Railway Engineering Journal, vol.3, No.2, March 1974, p.1-20.
23. A Garnault, "Technical and Economical Results of the Use of Air Cushion in Guided Ground Transportation", International Automotive Engineering Congress, Detroit, 8-12 January 1973, SAE Paper No.730161.
24. Societe de l'Aerotrain, Publicity Material on Aerotrain Suburbain, "Cergy-Defense" and Aerotrain Tridim.
25. J Bertin, J Berthelot, "Aerotrain Tridim for Urban Transportation, a System Designed to Spare Initial Costs and Energy", Proc.International Hovering Craft, Hydrofoil and Advanced Transit Systems Conference, Brighton, 13-16 May 1974, p.307-15.
26. R G Hoch, M Berthelot, "Use of the Bertin Aerotrain for the Investigation of Flight Effects on Aircraft Engine Exhaust Noise", Third AIAA Conference, Palo Alto, July 1976, Paper No.76-534, also J. of Sound and Vibration, vol.52, No.2, 22 September, 1977, p.153-72.
27. H Yamashita, "Progress of Research and Development on Repulsive Levitation Railway in JNR", Quarterly Reports of the Railway Technical Research Institute, vol.19, No.3, September 1978, p.99-105.
28. R A Nelson, P W Shuldiner, M Miller, R L Winestone, P J Barbato, "Northeast Corridor Transportation Project Report", Office of High Speed Ground Transportation, April 1970, NTIS PB 190929.
29. W D Osmer, "Air Versus High Speed Rail Operating Costs for Intercity Passenger Travel", Boeing Transportation and Logistics Service Report, August 1979.
30. W Herbst, "Weight and Performance Characteristics of Magnetically Suspended High Speed Trains as Compared to Aircraft", 34th Annual Conference of the Society of Allied Weight Engineers, Seattle, 5-8 May 1975, Paper No.SAWE 1059.
31. OECD, "The Future of European Passenger Transport", Brussels, 1973.
32. Birlinghovener Kreis, "Komponenten fur Neue Technologien in Verkehr und Transport" BMFT Project NT91, Final Report, 1971.

33. BMFT, "Spurgebundener Schnellverkehr mit berührungsfreier Fahrtechnik, "Third Statusseminar, Berlin, 18-24 March 1974, BMFT-FBT 74-38 to 40 December 1974, (Also NTIS, N75-33941/65T)
34. G Winkle, "Forschungs-und Entwicklungsstand der elektromagnetischen Schwebetechnik in der Bundesrepublik Deutschland", ETZ-A, vol.96, No.9, September 1975, p.367-73.
35. A Lichtenberg, "Elektrodynamisches Schweben im Fernverkehr der Zukunft", ibid, p.378-83.
36. BMFT, "Spurgeführter Fernverkehr, Magnetbahnwicklung", Sixth Statusseminar, Konstanz, 1977.
37. D Rogg, H Schulz, "Systemtscheidung bei der Magnetschwebetechnik," Eisenbahntechnische Rundschau (ETR), vol.27, No.11, November 1978, p.721-8.
38. "Ministry Takes Over Maglev Projects" Railway Gazette Interntional, vol.134, No.10, October 1978, p.726.
39. HSB Studiengesellschaft mbH, "HSB-Studie uber ein Schnellverkehrssystem", Munich, 1971.
40. C Albrecht, G Bohn, "Neue spurgeführte Transportmittel", (Part I) Physikalische Blatter, vol.32, No.7, July 1976, p.309-26.
41. E Gottzein, K-H Brock, E Schneider, J Pfefferl, "Control Aspects of a Tracked Magnetic Levitation High Speed Test Vehicle", Automatica, Vol.13, No.3, 1977, p.205-23.
42. E Gottzein, W Cramer, "Critical Evaluation of Multivariable Control Techniques Based on Maglev Vehicle Design" Pro.Fourth IFAC International Symposium on Multivariable Technological Systems, Fredericton, July 1977.
43. E Gottzein, R Meisinger, L Miller, "The Magnetic Wheel in the Suspension of High Speed Ground Transportation Vehicles", IEEE Trans. on Vehicular Technology, vol. VT-29, No.1, February 1980, p.17-22.
44. HSB Studiengesellschaft mbH, "Trassierung einer Strecke Hannover-Kassel für ein neuartiges Schnellbahnsystem (EMS-Technik) und Vergleich mit einer Rad-Schiene-Trassierung" Sixth BMFT Statusseminar, Konstanz, 1977, Section W.
45. P A A Koerv, "Control Systems for Operating the Long Stator Maglev Vehicle TRO5", IEEE Trans. on Vehicular Technology, vol. VT-29, No.1, February 1980, p.23-34.
46. P Hartman, H Schulz, "Versuchs-und Demonstrationsanlage Magnetbahn zur Internationalen Verkehrsansstellung 1979 (IVA'79) in Hamburg, "Elektrische Bahnen, vol.77, No.5, May 1979, p.117-22.
47. D J Frenzel, H P Neubar, "Versuchsanlage Magnetbahn im Emsland", ibid, p.122-6.
48. Konsortium Magnetbahn Transrapid, "Im Jahr 1835 war es Nurnberg-Furth. Heute ist es Lathen-Dorpen. Das Emsland macht Bahngeschichte," September 1978, MBB UR

49. Krauss-Maffei, "Transurban TAKT-System", Publicity Material, May 1973, BK5733.
50. H Weh, "Linear Synchronous Motor Development for Urban and Rapid Transit Systems", IEEE Trans. on Magnetics, vol. MAG-15, No.6, November 1979, p.1422-7.
51. H Weh, M Shalaby, "Magnetic Levitation with Controlled Permanent Excitation", IEEE Trans. on Magnetics, Vol. MAG-13, No.5, September 1977, p.1409-11.
52. H Weh, H Mosebach, H May, "Design and Technology of the Iron Core Linear Synchronous Motor for Advanced Ground Transportation", International Conference on Electrical Machines, Brussels, 1978, p. L4/5-1-10.
53. H Weh, H May, "Permanent Magnetic Excitation of Rotating and Linear Synchronous Machines", Journal of Magnetism and Magnetic Materials, vol.9, No.3, October-November 1978, p.173-8.
54. H May, M Shalaby, "Berechnung von geregelten Permanent-Magneten für Tragen, Führen und Antriebsaufgaben", ETZ-A, vol.100, No.2, February 1979, p.63-7.
55. Transrapid-EMS, "Gesellschaft für elektromagnetische Schnellverkehrssysteme", Publicity Material, December 1975.
56. BMFT, "Technology of an Iron Cored Long Stator Motor", Sixth Statusseminar, Konstanz, 1977, Section H.
57. H Weh, "Investigation into EMS Long Stator Technology", ibid Section G.
58. id., "Synchroner Langstatorantrieb mit geregelten, anziehend wirkenden Normalkraften", ETZ-A, vol.96, No.9, September 1975, p.409-13.
59. H Weh, H Mosebach, W Deleroi, "Mechanical Suspended Vehicle with an Active Guideway", Proc. Second International Conference on Hovering Craft, Hydrofoil and Advanced Transit Systems, Amsterdam, May 1976, p.101-9.
60. A Lang, "Propulsion Systems for Magnetically Suspended Vehicles", International Conference on Electrical Machines, Brussels, 1978, p.L3/3-1-10.
61. Y Kyotani, "The Current State of Development of Noncontacting Suspension and Propulsion Systems in Japan", Japanese National Railways, 1977.
62. A Hayashi, "HSST: A Viable Alternative for Rapid Airport-City Centre Transportation", ICAO Bulletin, January 1978, p.21-4.
63. S Nakamura, A Hayashi, "Development of HSST System", Japan Airlines, May 1979.
64. S Nakamura, "Development of High Speed Surface Transport System (HSST)", IEEE Trans. on Magnetics, vol. MAG-15, No.6, November 1979, p.1428-33.

65. J Ideguchi, Private Communication, 7 May 1980
66. S Nakamura, Y Takeuchi, M Takahasi, "Experimental Results of the Single Sided Linear Induction Motor", IEEE Trans. on Magnetics, vol. MAG-15, No.6, November 1979, p.1434-6.
67. Y Hika, Y Takeuchi, "Detail and Experimental Results of Ferromagnetic Levitation System of Japan Air Lines HSST-01/-02 Vehicles", IEEE Trans. on Vehicular Technology, vol. VT-29, No.1, February 1980, p.35-41.
68. S Yamamura, "Magnetic Levitation Technology of Tracked Vehicles - Present Status and Prospects", IEEE Trans. on Magnetics, Vol. MAG-12, No.6, November 1976, p.874-8.
69. B V Jayawant, P K Sinha, A R Wheeler, R J Whorlow, J Willsher "Development of a 1 Ton Magnetically Suspended Vehicle Using Controlled DC Electromagnets", Proc. IEE, Vol. 123, No.9, September 1976, p.941-8.
70. D Linder, "Design and Testing of Low Speed Magnetically Suspended Vehicles", Second Conferences on Advances in Magnetic Materials and their Applications, London 1 - 3 September 1976, IEE Conference Publication No.142, p.96-9.
71. D J Dobbs, D Linder, D S Armstrong, R M Goodal, R J A Bevan, M G Pollard, R W Barwick, R A Williams, "Magnetically Levitated and Wheeled Mintram Comparison Study" BR Technical Report TR EDYN 5, January 1976.
72. "New Maglev Link Opens Door to World Sales", Electrical Review, vol.208, No.10, 13 March 1981, p.21,23.
73. R D Freuchte, R H Nelson, T A Radomski "Power Conditioning Systems for a Magnetically Levitated Test Vehicle" IEEE Power Electronics Specialists Conference, Palo Alto, June 1977, p.275-85; see also IEEE Trans. on Vehicular Technology, vol. VT-29, No.1, February 1980, p.50-60.
74. D A Young "Soviets Drawn to Magnetic Train", Industrial Research/Development, vol.20, No.12, December 1978, p.52.
75. IZV. VUZ Elektromekahnka, No.8, August 1977.
76. J R Powell, "The Magnetic Road: A New Form of Transport", IEEE-ASME Railroad Conference, Atlanta, 25-26 April 1963, Paper No 63-RR-4.
77. J R Powell, G R Danby "High Speed Transport by Magnetically Suspended Trains", Winter Annual Meeting, New York, 27 November - 1 December 1966, Paper No ASME 66-WA/RR-5.
78. Id, "Magnetically Suspended Trains for Very High Speed Transport" Trans. 4th IECEC, Washington, 22-26 September, 1969, p.953-63.
79. Id, "The Linear Synchronous Motor and High Speed Ground Transport", Proc. 6th IECEC, Boston, 3-6 August 1971, p.118-31.
80. C A Guderjahn, S L Wipf, H J Fink, R W Boom, K E MacKenzie, D Williams, T Downey "Magnetic Suspension and Guidance for High Speed Rockets by Superconducting Magnets", J Applied Physics, vol.40, No.5, April 1969, p.2133-40.

81. C A Guderjahn, S L Wipf, "Magnetic Suspension and Guidance for High Speed Trains by Means of Superconducting Magnets and Eddy Currents", Proc.1969 Cryogenic Engineering Conference, California, Advances in Cryogenic Engineering, vol.15, p.117-23.
82. P L Richards, M Tinkham "Magnetic Suspension and Propulsion Systems for High Speed Transportation" J Applied Physics, vol.43, No.6, June 1972, p.2680-91.
83. H T Coffey, F Chilton, L O Hoppie, "Magnetic Levitation of High Speed Ground Vehicles", Proc.Applied Superconductivity Conference, Annapolis. May 1972, IEEE Publication No 72 CHO 632-5 TABSC, p.62-75.
84. H T Coffey "SRI Magnetic Suspension Studies for High Speed Vehicles," Proc.1973 Cryogenic Engineering Conference, Atlanta, Advances in Cryogenic Engineering, Vol.19, p.137-53.
85. J R Reitz, R H Borcherts, L C Davis, T K Hunt, D F Wilkie, "Preliminary Design Studies of Magnetic Suspensions for High Speed Ground Transportation" Final Report to DOT, Report No FRA-RT-73-27, PB 223-237. March 1973.
86. J R Reitz, R H Borcherts, "US Department of Transportation Program in Magnetic Suspension (Repulsion Concept)", IEEE Trans. on Magnetics, Vol. MAG-11, No.2, March 1975, p.615-8.
87. Ford Motor Co. "Conceptual Design and Analysis of the Tracked Magnetically Levitated Vehicle Technology Program (TMLV)- Repulsion Scheme; Vol. I & II, "Final Report to DOT, February 1975, Report No FRA-OR&D-75-21 & 21A.
88. R D Thornton, H H Kolm, "Transportation System Employing an Electromagnetically Suspended, Guided and Propelled Vehicle", US Patent 3,768,417, 30 October 1973.
89. H H Kolm, R D Thornton, "The Magneplane: Guided Electromagnetic Flight", Proc.Applied Superconductivity Conference, Annapolis, May 1972, IEEE Publication No 72 CHO 632-5 TABSC, p.76-85.
90. R D Thornton, "Design Principles for Magnetic Levitation", Proc.IEEE, Vol.61, No.5, May 1973, p.586-97.
91. Id, "The Magneplane Linear Synchronous Motor Propulsion System", Conference on Linear Electric Machines, London, October 1974, IEE Conference Publication No. 120, p.230-5.
92. Y Iwasa, M O Hoenig, H H Kolm, "Design of a Full Scale Magneplane Vehicle" IEEE Trans. on Magnetics, Vol. Mag-10, No.3, September 1974, p.402-5.
93. Y Iwasa, W S Brown, C B Wallace "An Operational 1/25 Scale Magneplane System with Superconducting Coils" IEEE Trans on Magnetics, Vol. MAG-11, No.5, September 1975, p.1490-2.
94. C H Tang, W J Harrold, R S Chu "A Review of the Magneplane Project" IEEE Trans on Magnetics, Vol. MAG-11, No.2, March 1975, p.623-6.

95. C H Tang "Evaluation of Guideway Edge Effects" Presented by H H Kolm at Intermag Conference, London, 14-17 April 1975.
96. K Oshima, Y Kyotani "High Speed Transportation Levitated by Superconducting Magnet" Proc. 1973 Cryogenic Engineering Conference, Atlanta, Advances in Cryogenic Engineering, Vol.19, p.127-136.
97. Y Usami, J Fujie, S Fujiwara, "Studies on Linear Motor in the Institute of JNR" Conference on Linear Electric Machines, London, October 1974, IEE Conference Publication No.120, p.131-6.
98. Y Kyotani, Development of Superconducting Levitated Trains in Japan", Cryogenics, Vol.15, No.7, July 1975, p.372-6.
99. N Maki, H Okuda, T Tatsumi, J Fujie, T Iwahana, "A Combined System of Propulsion and Guidance by Linear Synchronous Motors", Tenth Annual Meeting of IEEE IAS, IEEE Conference Record 1975, IEEE Publication No 75 CHO 999-31A, p.956-961.
100. H Ogiwara, N Takano, "Development of Superconducting Magnets for a Magnetically Suspended High Speed Train in Toshiba", Proc.Fifth International Cryogenic Engineering Conference, Kyoto, May 1974, p.94-6.
101. H Yamashita, "Progress of Research and Development on Repulsive Levitation Railway in JNR, "Quarterly Reports of Railway Technical Research Institute, Vol.19, No.3, September 1978, p.99-105.
102. "Special Issue on Levitation Railway", Railway Technical Research Institute Quarterly Reports, Vol.17, No.4, December 1976, p.145-181, and Vol.21, No.1, March 1980, p.1-56.
103. T Ohtsuka, Y Kyotani "Superconducting Maglev Tests" IEEE Trans. on Magnetics, Vol. MAG-15, No.6, November 1979, p.1416-21.
104. Id, "Recent Progress in Superconducting Magnetic Levitation Tests in Japan" Proc.IAS Annual Meeting, Cincinnati, 28 September-30 October 1980, p.238-43.
105. Canadian Maglev Group "Study of Magnetic Levitation and Linear Synchronous Motor Propulsion" Annual Report for 1972, Phase I Contract Report to TDA, December 1972.
106. Id, "Analysis of Superconducting Magnetic Levitation and Linear Synchronous Motor Propulsion for High Speed Guided Ground Transportation" Annual Report for 1973, Phase II, Contract Interim Report to TDA, March 1974.
107. Id "Superconducting Magnetic Levitation and Linear Synchronous Motor Propulsion for High Speed Guided Ground Transportation" Phase II Contract Report to TDA, CIGGT Report No 75-5, March 1975.
108. Id, "Superconducting Linear Synchronous Motor Propulsion and Magnetic Levitation for High Speed Guided Ground Transportation", Phase III Contract Interim Report to TDA (Transport Canada), CIGGT Report No 76-7, March 1976.
109. Id, "Electrodynamic Suspension and Linear Synchronous Motor Propulsion for High Speed Guided Ground Transportation", Phase III Contract Report to Transport Canada Research and Development Centre, CIGGT Report No 77-13, September 1977. (Summary published separately as "The Canadian High Speed Magnetically Levitated Vehicle System, CIGGT Report No 77-12 September 1977, Verbatim Canadian Electrical Engineering Journal, vol.3, No.2, April 1978, p.3-26.

110. W F Hayes, "High Speed Electrodynamic Maglev Guided Ground Transportation System Conceptual Design Study", Final Report to Transport Canada Research and Development Centre, NRC Report No LTR-CS-176, September 1977.
111. Id, Private communication, 23 March 1979.
112. S A Haines "Going with Gauss, Maglev on Track", Science Dimension, Vol.12, No.6, June 1980, p.10-14.
113. C Albrecht, W Elsel, H Franksen, C P Parsch, K Wilhelm "Superconducting Levitated Systems :First Results with the Experimental Facility at Erlangen", Proc.Fifth International Cryogenic Engineering Conference, Kyoto, May 1974, IPC Science & Technology Press, p.28-34.
114. J Miericke, L Urankar, "Theory of Electrodynamic Levitation with a Continuous Sheet" Applied Physcs, Vol.2, 1973 p.202-211, ibid, vol.3, 1974, p.67-76.
115. P Klocker, C P Parsch, "ROSY, a Rotating Test Rig for Air Cored Linear Synchronous Motors", Siemens Review, Vol.65, No.10, October 1978, p.435-9.
116. J P Gibson, S Lingaya, "Control System for Air Cored Linear Synchronous Motors", ibid, p.439-43.
117. B Boning, W Leonhard "Propulsion Control of a Track Powered Linear Synchronous Motor for a Magnetically Levitated Vehicle on the Basis of Power Measurement in the Invertor Station", Proc.International Conference on Electrical Machines, Brussels, September 1978, p.L5/1-1-9.
118. J P Gibson, C P Parsch, "The Air Cored Linear Synchronous Motor as a Drive for Magnetically Levitated Vehicles", IAS Annual Meeting, Toronto, 1-5 October 1978.
119. G Bogner, "Applied Superconductivity Activities at Siemens", IEEE Trans on Magnetics, Vol. MAG.15, No.1, January 1979, p.824-7.
120. C P Parsch, Private Communication, 20 February 1980.
121. I A Alston, J M Clark, J T Hayden "Magnetic Suspension and Guidance of High Speed Vehicles" Final Report to Science Research Council, Cranfield CTS, Report 2, December 1972.
122. R G Rhodes, A R Eastham, M P Allen, B Mellen, "Magnetic Suspension of High Speed Trains" Report to Science Research Council, October 1972.
123. I A Alston "Superconducting Magnet Suspensions in High Speed Ground Transport" Cranfield CTS Report 5, August 1973, also TRRL Supplementary Report SR 28UC.
124. E Abel, A E Corbett, B E Mulhall, R G Rhodes, "Levitation and Propulsion of Guided Vehicles Using Superconducting Magnets" Conference on Linear Electric Machines, London, 21-23 October 1974, IEE Conference Publication No.120, p.223-9.

125. P E Burke, S Kuntz, G R Slemon "A Dual Linear Synchronous Motor for Maglev Vehicles" IEEE Trans. on Magnetics Vol. MAG 13, No.5, September 1977, p.1415-7.
126. R E Rhodes, B E Mulhall, E Abel, "Flying Land Vehicles using Superconducting Magnets", International Conference on Hovering Craft, Hydrofoil and Advanced Transit Systems, Brighton, 13-16 May 1974, p.157-66.
127. J P Howell, J Y Wong, R G Rhodes, B E Mulhall, "Stability of Magnetically Levitated Vehicles over a Split Guideway". IEEE Trans. on Magnetics, Vol. MAG-11, No.5, September 1975, p.1487-9.
128. R G Rhodes, B E Mulhall, E Abel, J P Howell, J L Mahtani, J Y Wong, Wolfson Progress Report to July 1975.
129. R G Rhodes, B E Mulhall, E Abel, J P Howell, M E Hunt, J L Mahtani, Wolfson Progress Report to September 1976.
130. E Abel, J L Mahtani, B E Mulhall, R G Rhodes, "An Assessment of Linear Superconducting Motors for Maglev" Second Conference on Advances in Magnetic Materials and their Applications, London, 1-3 September 1976, IEE Conference Publication No.142, p.125-7.
131. E Abel, J P Howell, J L Mahtani, R G Rhodes "Design Criteria for Rectangular Superconducting Coils for Transport Applications", Proc. Sixth International Conference on Magnet Technology (MT-6) Bratislava, 29 August - 2 September 1977, p.165-71.
132. W Leonhard "Technische Alternativen bei der Magnetschwebbahn" VDI Nach, 15 April 1977, p.42-3.
133. E Abel, "A Study of the Power Consumption of German Maglev Passenger Vehicles (EDS and EMS), Internal Memo, January 1978.
134. E Abel, R G Rhodes "Power Consumption for Alternative Maglev Systems" Electronics and Power, Vol.24, No.9, September 1978, p.673-4.
135. E Abel, J L Mahtani, R G Rhodes "Linear Machine Power Requirements and System Comparisons", IEEE Trans. on Magnetics, Vol. MAG-14, No.5, September 1978, p.918-20.
136. R G Rhodes, E Abel, J L Mahtani, "Magnetic Levitation and Linear Motor Propulsion for High Speed Vehicles" Report to the Science Research Council, January 1979.
137. E Abel, "A Cooperative Research Programme to Investigate the Application of Air Cored Linear Synchronous Machines to Advanced Ground Transport" Internal Memo, Warwick Maglev Group, December, 1978.
138. Id, "Linear Synchronous Machines as Traction Drives for Trains" Internal Memo, Warwick Maglev Group, January 1979.
139. R G Rhodes, E Abel, J L Mahtani, J H Rakels, "The Superconducting LSM for Vehicle Propulsion" Conference on Superconducting Electrical Machines, Oxford, 19-20 April, 1979, Paper No.18.

140. D S Armstrong, J W Teape, "Air Cored Linear Synchronous Motor : Model Tests", Colloquium on Advanced Ground Transportation Schemes, London 18 April 1979, IEE Digest No 1979/27, p.7.1 - 7.4.
141. H Autruffe, D Lancien, R Moulin "Les Etudes de Sustenation Magnetique a la SNCF" Rev.Gen.Chemins de Fer, Vol.94, No.9, September 1975, p.497-522.
142. D Lancien, R Moulin, "Moteur Lineaire Synchrone a Inducteur Supraconducteur" RGE, Vol.84, No. 7/8, July-August 1975, p.553-65.
143. E R Laithwaite, "Induction Machines for Special Purposes" London, Newnes, 1966.
144. S Yamamura, "Theory of Linear Induction Motors" New York, Wiley, 1972.
145. J A Wagner, "Bibliography on the Linear Induction Motor in High Speed Ground Transportation, Preprint to IEEE PES Summer Meeting, San Francisco, 9-14 July 1972, Paper C72-448-9, p.1-8.
146. E R Laithwaite, S A Nasar, "Linear Motion Electrical Machines", Proc. EEE, Vol.58, No.4, April 1970, p.531-42.
147. E R Laithwaite, "Linear Electric Machines - A Personal View", vol.63, No.2 February 1975, p.250-285.
148. M Pouloujadoff "Linear Induction Machines : I. History and Theory of Operation" IEEE Spectrum, vol.8 No.2, February 1971, p.72-80.
149. id; "Linear Induction Machines : II. Applications", ibid, vol 8, No.3, March 1971, p.79-86.
150. G P Kalman, D Irani, A Simpson "Electrical Propulsion System for Linear Induction Motor Test Vehicle", Proc.Fourth Intersociety Energy Conversion Engineering Conference, Washington, 22-26 September 1969, p.807-17.
151. K M Chirgwin "Test Results from the US Linear Induction Motor Research Vehicle Program" Conference on Linear Electric Machines, London, 21-23 October 1974, IEE Conference Publication No.120, p.236-43, plus addendum.
152. J J Stickler, "Comparison of Theories for High Speed Linear Induction Motors" IEEE Trans. on Vehicular Technology, vol. VT-29, No.1, February 1980, p.65-71.
153. R J A Bevan, G Kalman "Non Uniform Power Distribution in Linear Induction Motors due to End Effects", IEEE Trans. on Power Apparatus & Systems, vol. PAS-98, No.5, September-October 1979, p.1516-21.
154. E R Laithwaite, J F Eastham, H R Bolton, T G Fellows, "Linear Motors with Transverse Flux" Proc.IEE, Vol.118, No.12, December 1971, p.1761-7, Discussion ibid, vol.119, No.12, December 1972, p.1727-9.
155. J F Eastham, E R Laithwaite, "Linear Induction Motors as Electromagnetic Rivers" Proc. IEE, vol.121, No.10, October 1974, p.1099-1108.

156. J F Eastham, Discussion Meeting organised by the Science Research Council, London 18 January 1978.
157. W Farrer, IEE Discussion Meeting "Linear Induction Motors" London, 25 May 1978.
158. J A Ross, "ROMAG Transportation System" Proc.IEEE, vol.61, No.5, May 1973, p.617-20.
159. W J Holt, J A Ross, "New Developments in Magnetic Suspension and Propulsion for Transportation", IAS Annual, 1976, p.133-7.
160. R G Rule, R G Guillard, "Combined Magnetic Levitation and Propulsion : the Mag-Transit Concept", IEEE Trans on Vehicular Technology, vol. VT-29, No.1, February 1980, p.41-9.
161. L del Cid, V Nene, "The Three Axial Forces of an Offset LIM" presented at Intermagnetics Conference, Florence, 9-12 May, 1978.
162. V D Nene, Private Communication, 2 August 1978.
163. R M Katz, A R Eastham, G E Dawson, D A Atherton, C L Schwalm, "Integrated Magnetic Suspension and Propulsion of Guided Ground Transportation Vehicles with a SLIM", IEEE Trans on Magnetics, vol. MAG-15, No.6, November 1979, p.1437-9, also IEEE Trans. on Vehicular Technology, vol. VT-29, No.1, February 1980, p.61-4.
164. G E Dawson, C L Schwalm, "Microcomputer Data System for Maglev Test Facility", Proc. International Symposium on Mini and Microcomputers, Montreal, 11-18 November 1977, IEEE Publ. No. 77CH134-4C, p.189-93.
165. A R Eastham, R M Katz "The Operation of a Single Sided Linear Induction Motor with Squirrel Cage and Solid Steel Reaction Rails" IEEE Trans on Magnetics, vol. MAG-16, No.5, September 1980, p.722-4.
166. G Sobolewski, D Gilmore "An Interim Report on the Development of a Light Steerable Axle Truck for Rail Passenger Vehicles", Proc. Biennial CIGGT Seminar on Railway Research, The Eighties : A New Rail Era, Kingston, 29-30 January 1978,, CIGGT Report No 78-5, April 1978, p.61-72.
167. G E Brown "Linear Induction Motors for Intermediate Capacity Transit Systems" ibid, p.173-8.
168. C D English, G E Brown, "The Linear Induction Motor Propulsion System in Urban Transportation", IEEE Industry Applications Society Conference, Chicago, 11-14 October 1976, IEEE Publ.No. 76 CH 112-1-IA, p.138-44.
169. "UTDC's Test Track Completed" Railway Gazette International, vol.134, No.6, June 1978, p.382.
170. "Automated Transit Planned in Ontario" ibid, vol.134, No.11, November 1978, p.831.
171. A K Wallace, J H Parker, G E Dawson, "Slip Control for LIM Propelled Transit Vehicles" IEEE Trans. on Magnetics, vol. MAG-16, No.5, September, 1980, p.710-12.

172. "AC Motors for Traction" Brush Electrical Machines Ltd, Publicity Material, 1977.
173. J Chahal, IEE Discussion Meeting, "Linear Induction Motors" London, 25 May 1978.
174. J J Pierro, "Linear Electric Motor", US Patent 3,456, 136, 15 July 1969.
175. M Guarino, "Integrated Linear Electric Motor Propulsion Systems for High Speed Transportation", Conference on Linear Electric Motors and High Speed Electric Propulsion, Lyon 15 May 1974, Grenoble 16-17 May, 1974.
176. E Levi, "Linear Synchronous Motors for High Speed Ground Transportation" IEEE Trans. on Magnetics, vol. MAG-9, No.3, September 1973, p.242-7.
177. Id. "High Speed, Iron Cored, Synchronously Operating Linear Motors", Conference on Linear Electric Machines, London, 21-23 October 1974, IEE Conference Publication No.120, p.236-43.
178. Id. "Development of the Design for Iron Cored Synchronously Operating Linear Motors", Private communication, 7 July 1978.
179. T R Haller, W R Mischler "A Comparison of Linear Induction and Linear Synchronous Motors for High Speed Ground Transportation" IEEE Trans. on Magnetics, vol. MAG-14, No.5, September 1978, p.924-6.
180. J F Eastham "Iron Cored Linear Synchronous Machines" Electronics and Power, vol.23, No.3, March 1977, p.239-42.
181. M J Balchin "Operating Characteristics of a Heteropolar Linear Synchronous Motor" Colloquium on Advanced Ground Transportation Schemes, London, 18 April, 1979, IEE Digest No 1979/27, p. 4.1-4.4
182. A J Davis, J S Chahal, W Farrer, "A Study of Linear Synchronous Motors at Brush Electrical Machines Limited", ibid, p.5.1-5.4.
183. R M Davis, S.A.E. El-Drieny, D J Rhodes, "Linear Synchronous Motor Design and Performance" ibid, p.6.1-6.5
184. W Leitgeb, "Linearmotoren fur Fahrzeugantriebe", Siemens Zeitschrift, vol.45, 1971, p.177-80.
185. H Buchberger, W Leitgeb "Fahrzeugantriebe mit synchronen Linearmotoren", Elektrische Bahnen, vol.46, No.4, April 1975, p.82-5.
186. W Leitgeb "Bauarten von Wanderfeldmaschinen fur den spurgebundenen Schnellverkehr" VDI-Z, vol.117, No.2, January 1975, p.57-63.
187. E Rummich "Machines Lineaires Synchrones" Bull. ASE, vol.63, No.23, 11 November 1972, p.1338-44.
188. J F Eastham, E R Laithwaite, "Linear Motor Topology", Proc. IEE, Vol.120, No.3, March 1973, p.337-43.
189. B-T Ooi, "Homopolar Linear Synchronous Motor Dynamic Equivalents" IEEE Trans. on Magnetics, Vol. MAG-13, No.5, September 1977, p.1424-6.

190. E Levi, J P Lee, F Lalezari, M Gemelos, "Computer Aided Conformal Mapping of Magnetic Fluxes in Saturated Inductor Motors" *ibid*, Vol. MAG-14, No.5, September 1978, p.927-9.
191. B K Bose, T A Lipo, "Control and Simulation of a Current Fed Linear Inductor Machine" *IEEE Trans. on Industry Applications*, Vol. IA-15, No.6, November/December 1979, p.591-600.
192. E Levi, L Birenbaum, Z Zabar, "Concerning the Design of Inductor Synchronous Motors fed by Current Source Inverters", *IEEE Trans. on Magnetics*, Vol. MAG-13, No.5, September 1977, p.1421-3.
193. G R Slemon, "A Homopolar Linear Synchronous Motor" *International Conference on Electrical Machines*, Brussels, 11-13 September 1978, p. L4/4-1 - 10.
194. I Boldea, S A Nasar, "Thrust and Normal Forces in a Segmented Linear Reluctance Motor", *Proc IEE*, Vol.122, No.9, September 1975, p.922-4.
195. S A Nasar, I Boldea, "Linear Motion Electric Machines" Wiley Interscience, 1976.
196. J D Edwards, A M El Antably "Segmental Rotor Linear Reluctance Motors with Large Airgaps" *Proc.IEE*, Vol.125, No.3, March 1978, p.209-14.
197. J S Chahal, "Linear Reluctance Machines for Urban Transport", *International Conference on Electrical Machines*, Brussels, 11-13 September 1978, p. L4/1-1 - 10.
198. J S Chahal, A J Davis "A Study of Linear Reluctance Machines at Brush Electrical Machines Limited" *Colloquium on Advanced Ground Transportation Schemes*, London, 18 April 1979, *IEE Digest No 1979/27*, p.5.5-5.8.
199. G Williams, J D Edwards, P Lindon, A M El-Antably, P D Luke, "Linear Reluctance Machines for Traction and Suspension of Guided Vehicles" *ibid*, p.8.1-8.2.
200. P Lindon, G Williams, P D Luke, A M El-Antably, J D Edwards "Closed Loop Control of Linear Reluctance Motors for Traction Applications", *Second International Conference on Electrical Variable Speed Drives*, London 25-27 September, 1979, *IEE Conference Publication No.179*, p.191-5.
201. A M El-Antably, J D Edwards, G Williams, P Lindon, P D Luke, "Steady State Performance Characteristics of Linear Reluctance Motors" *IEEE Trans. on Magnetics*, Vol.MAG-15, No.6 November 1979, p.1440-2.
202. D Kaye "Linear Motor for Mass Transport Improved by Pulsed Techniques" *Electronic Design*, Vol.19, No.10, 13 May 1971, p.30.
203. Japanese National Railways "Improvements in Propulsion Systems", *UK Patent 1,360,834*, 24 July 1974.
204. Y Amemiya, S Aiba, "Tractive Characteristics of DC Linear Motor with a Constant Current Applied to Ground Coil", *Electrical Engineering in Japan*, Vol.94, No.10, October 1974, p.97-103.

205. K Matsui, T Umemori, Y Taketsuna, Y Hosoda "DC Linear Motor Controlled by Thyristors and the Testing Equipment for its High Speed Characteristics" Conference on Linear Electric Machines, London 21-23 October 1974, IEE Conference Publication No.120, p.149-54.
206. K Matsui, T Umemori, M Toyoshima, K Katakami, S Osawa, "Ground Coil Assembly of a Linear Induction Motor with DC Levitating Armature for High Speed Vehicle", US Patent 3,855,485, 17 December 1974.
207. T Umemori, "Construction and Characteristics of Linear Thyristor Motors" Electrical Engineering in Japan, Vol.98, No.1, January-February 1978, p.28-36.
208. Id, "Power Supply and Control of Linear Thyristor Motors" *ibid*, p.96-105
209. T Umemori, M Kawashima, M Oda, S Otisawa, "Development of DC Linear Motor, I Fundamental Construction and Feasibility" IEEE PES Summer Meeting, Los Angeles, 16-21 July 1978, Paper F78 757-7.
210. T Umemori, Y Hosoda, M Iwasaki, M Toyoshima, "Development of a DC Linear Motor, II, Research for a Ground Coil and a Field Magnet", *ibid*, Paper F 78 756-9.
211. T Umemori "Construction and Characteristics of DC Linear Motor" Quarterly Reports of the Railway Technical Institute Vol.21, No.1 March 1980, p.22-8.
212. T Umemori, S Kumazawa, Y Furuto, T Kamoshida, "Study on Miniaturization of Electromagnet for DC Linear Motor" IEEE Trans. on Magnetics, Vol. MAG-16, No.5, September 1980, p.713-5.
213. G R Slemon, P E Burke, N Terzis, "A Linear Synchronous Motor for Urban Transit using Rare Earth Magnets" IEEE Trans. on Magnetics, Vol. MAG-14, No.5, September 1978, p.921-3.
214. K Murato, K Takei, Y Akihama, H Takahashi, H Akabane "Type L4 Linear Motor System Wagon Booster/Retarder for Shiohama Shunting Yard of the JNR", Hitachi Review, Vol.24, No.6, June 1975, p.269-76.
215. T Nondahl "Design Studies for Single Sided Linear Electric Motors : Homopolar Synchronous and Induction", Electric Machines and Electromechanics, Vol.5, No.1, January-February 1980, p.1-14.
216. G K O'Neill, H H Kolm, "Mass Driver for Lunar Transport and as a Reaction Engine" Journal of the Astronomical Sciences, Vol.25, No.4, October-December, 1977, p.349-63.
217. "The Electromagnetic Gun" International Defense Review, Vol.13, No.5, May 1980.
218. H H Kolm, P Mongeau, F Williams "Electromagnetic Launchers" IEEE Trans on Magnetics, Vol. MAG-16, No.5, September 1980, p.719-21.
219. A H Greene, W J Harrold, R S Kasevich, C H Tang, E Weiss, "Magneplane Linear Synchronous Motor Study" Final Report to MIT, Raytheon Company, Equipment Division, June 1973.
220. P C Sen "On Linear Synchronous Motor (LSM) for High Speed Propulsion" IAS Annual, 1975, p.261-7, and slightly modified as IEEE Trans. on Magnetics, Vol. MAG-11, No.5, September 1975, p.1484-6.

221. E Abel, "Linear Synchronous Machine Design for Minimum Terminal Rating" Technical Memo No.4, Warwick Maglev Group, March 1975, revised August 1978.
222. Id, "Flux Linkage and Induced Emf in Air Cored Machines" Technical Memo No.10, Warwick Maglev Group, February 1976, revised November 1978.
223. Id, "Fourier Analysis of Linear Machine Airgap Fluxes" Technical Memo No.13, Warwick Maglev Group, May 1975, revised November 1978.
224. B E Mulhall, D H Prothero, "Mechanical Stresses in Solenoid Coils", J Physics D, Vol.6, 1973, p.1973-7.
225. E Abel, unpublished work at University of Warwick, 1976.
226. D B Montgomery, "Solenoid Magnet Design" Wiley, New York, 1969.
227. R J Roark, "Formulas for Stress and Strain", McGraw Hill, New York, 1965.
228. D L Atherton, "Proposed Propulsion System for Magnetically Levitated Guided Ground Transportation" Proc. 1972 Applied Superconductivity Conference, Annapolis, May 1972, IEEE Conference Publication No. 72 CHOC.
229. J K Dukowicz, L O Hoppie, T C Wang "DC Magnetic Propulsion and Levitation System for High Speed Vehicles", US Patent No. 3,815,511, 11 June 1974.
230. H Weh, "Future Developments in Electromagnetic Lift, Guidance and Propulsion Systems" International Conference on Transportation Technology, Hamburg, June 1979, p.218-38.
231. E Abel, "Multilayer Region Analysis" unpublished work, University of Warwick, February 1974.
232. E M Freeman, Travelling Waves in Induction Machines : Input Impedance and Equivalent Circuits, PEE, Vol.115, No.12, December 1968, p.1772-5.
233. R Zurek, "Methods of Levitation for Tracked High Speed Traffic", Endeavour, Vol.2, No.3, 1978, p.108-14.
234. K Glatzel, G Khurdok, D Rogg "The Development of the Magnetically Suspended Transportation System in the Federal Republic of Germany" IEEE Trans. on Vehicular Technology, Vol. VT.29, No.1, February 1980, p.3-16.
235. G Winkle, "Forschungs-und Entwicklungsstand der Elektromagnetischen Schwebetechnik in der Bundesrepublik Deutschland" ETZ-A, Vol.96, No.9, September 1975, p.367-73.
236. E Abel, "Aerodynamic Drag on German Revenue Vehicles, Internal Memo, University of Warwick, October 1977.
237. T Satow, M Tanaka, T Ogama, "AC Losses in Multifilamentary Superconducting Composites for Levitated Trains Under AC and DC Magnetic Fields" Proc. 1973 Cryogenic Engineering Conference, Atlanta, Advances in Cryogenic Engineering, Vol.19, p.154-61.

238. T K Hunt "AC Losses in Superconducting Magnets at Low Excitation Levels" J.Appl.Physics, Vol.45, No.2 February 1974, p.907-13.
239. G Ries, "AC Losses in Multifilamentary Superconductors at Technical Frequencies" IEEE Trans. on Magnetics, Vol. MAG-13, No.1, January 1977, p.524-9.
240. M E Hunt, J H Rakels, R G Rhodes, "The Effects of Magnetic Field Oscillations on Losses in Superconducting Composites", Cryogenics, Vol.22, No.7, July 1980, p.390-4.
241. J D Rogers, H J Boenig, W V Hassenzahl, R I Schermer, "Superconducting Magnetic Energy Storage For Electric Utilities and Fusion Systems", Proc.Joint Automatic Control Conference (JACC/78) Philadelphia, 18-20 October 1978, p.71-84.
242. J W H Chi "Conceptual Design of a Hollow Cable Conductor for the Large Coil Program" IEEE Trans. on Magnetics, Vol. MAG-15, No.1, January 1979, p.337-9.
243. S H Kim, S T Wang, W F Praeg, C I Krieger, M Lieberg, "Performance Tests of a 1.5 MJ Pulsed Superconducting Coil and its Cryostat" ibid, p.840-2.
244. K Kwasnitza, D Salathe, D G Howe, D U Gubser, "Pulsed Magnetic Field Losses and Critical Current Densities of V_3Ga and Nb_3Sn Multifilament Superconductors", Cryogenics, Vol.22, No.2, February 1980, p.101-6.
245. E Abel, "Cryogenic Precooling of Coils for Pulse Operation" Technical Memo No.7, Warwick Maglev Group, August 1978.
246. W Schauer, "Conductor Materials for Cryomagnets" Proc. Fifth International Conference on Magnet Technology (MT-5), Rome, April 1975, p.629-43.
247. P H Melville, "Magnetic Propulsion for Magnetically Levitated Trains", Cryogenics, Vol.13, No.12, December 1973, p.716-7.
248. P H Melville, M N Wilson, B E Mulhall, "Propulsion of Magnetically Levitated Vehicles" ibid, Vol.15, No.5, May 1975, p.295.
249. S L Wipf "Propulsion of Magnetically Levitated Trains", ibid, Vol.16, No.5, May 1976, p.281-8.
250. H Brechna, H Kronig, "Three Phase Induction Motor with a Superconductive Cage Winding" IEEE Trans. on Magnetics, Vol.13, No.1, January 1979, p.715-8.
251. S P Bernard, D L Atherton "High Efficiency Flux Pump Power Supply Using Inductive Current Transfer" Rev.Sci.Instrum. Vol.48, No.10, October 1977, p.1250-2.
252. G J Homer, P J Houzago, C A Scott, M N Wilson, "A Thermally Switched Flux Pump" Rutherford Laboratory, Report RL-74-134, October 1974, (Also as IEEE Trans. on Magnetics Vol. MAG-11, No.2, 1975, p.576-9).
253. T C Bartram, "A Superconducting Fault Limiter : Its Construction and Testing" Conference on Superconducting Electrical Machines, Oxford 19-20 April 1979, Paper No.20.

238. T K Hunt "AC Losses in Superconducting Magnets at Low Excitation Levels" J.Appl.Physics, Vol.45, No.2 February 1974, p.907-13.
239. G Ries, "AC Losses in Multifilamentary Superconductors at Technical Frequencies" IEEE Trans. on Magnetics, Vol. MAG-13, No.1, January 1977, p.524-9.
240. M E Hunt, J H Rakels, R G Rhodes, "The Effects of Magnetic Field Oscillations on Losses in Superconducting Composites", Cryogenics, Vol.22, No.7, July 1980, p.390-4.
241. J D Rogers, H J Boenig, W V Hassenzahl, R I Schermer, "Superconducting Magnetic Energy Storage For Electric Utilities and Fusion Systems", Proc.Joint Automatic Control Conference (JACC/78) Philadelphia, 18-20 October 1978, p.71-84.
242. J W H Chi "Conceptual Design of a Hollow Cable Conductor for the Large Coil Program" IEEE Trans. on Magnetics, Vol. MAG-15, No.1, January 1979, p.337-9.
243. S H Kim, S T Wang, W F Praeg, C I Krieger, M Lieberg, "Performance Tests of a 1.5 MJ Pulsed Superconducting Coil and its Cryostat" ibid, p.840-2.
244. K Kwasnitza, D Salathe, D G Howe, D U Gubser, "Pulsed Magnetic Field Losses and Critical Current Densities of V_3Ga and Nb_3Sn Multifilament Superconductors", Cryogenics, Vol.22, No.2, February 1980, p.101-6.
245. E Abel, "Cryogenic Precooling of Coils for Pulse Operation" Technical Memo No.7, Warwick Maglev Group, August 1978.
246. W Schauer, "Conductor Materials for Cryomagnets" Proc. Fifth International Conference on Magnet Technology (MT-5), Rome, April 1975, p.629-43.
247. P H Melville, "Magnetic Propulsion for Magnetically Levitated Trains", Cryogenics, Vol.13, No.12, December 1973, p.716-7.
248. P H Melville, M N Wilson, B E Mulhall, "Propulsion of Magnetically Levitated Vehicles" ibid, Vol.15, No.5, May 1975, p.295.
249. S L Wipf "Propulsion of Magnetically Levitated Trains", ibid, Vol.16, No.5, May 1976, p.281-8.
250. H Brechna, H Kronig, "Three Phase Induction Motor with a Superconductive Cage Winding" IEEE Trans. on Magnetics, Vol.13, No.1, January 1979, p.715-8.
251. S P Bernard, D L Atherton "High Efficiency Flux Pump Power Supply Using Inductive Current Transfer" Rev.Sci.Instrum. Vol.48, No.10, October 1977, p.1250-2.
252. G J Homer, P J Houzgo, C A Scott, M N Wilson, "A Thermally Switched Flux Pump" Rutherford Laboratory, Report RL-74-134, October 1974, (Also as IEEE Trans. on Magnetics Vol. MAG-11, No.2, 1975, p.576-9).
253. T C Bartram, "A Superconducting Fault Limiter : Its Construction and Testing" Conference on Superconducting Electrical Machines, Oxford 19-20 April 1979, Paper No.20.

254. "Upgrading Wheel/Rail Systems" Machine Design, Vol.51, No.9, 26 April 1979, p.52,
255. "The Bus That Will Ride Warwickshires Rails" Engineering Today Vol.5, No.17, p.17.
256. F M Russell "Mixed- μ Magnetic Levitation for Advanced Ground Transport System" Rutherford Laboratory RL-77-076/B, December 1977.
257. J D Cockroft "The Design of Coils for the Production of Strong Magnetic Fields" Phil.Trans. Royal Society, Vol.227, 31 May 1928, p.317-43.
258. D E Morris, R A Kilgore, "The Magnetic Field on the Axis of Circular Cylindrical Coils" NASA TN D-1013, April 1962.
259. G V Brown, L Flax, "Superposition Calculation of Thick Solenoid Fields from Semi-Infinite Solenoid Tables" NASA TN D-2494, September 1964.
260. F W Grover, "Inductance Calculations" Dover, New York, 1946.
261. T H Fawzi, P E Burke "The Accurate Computation of Self and Mutual Inductances of Circular Coils" IEEE Trans. on Power Apparatus and Systems, Vol. PAS-97, No.2, March/April 1978, p.464-8.
262. D B Montgomery, "Solenoid Magnet Design" Wiley Interscience, New York, 1969.
263. W Y Cheu "Interactive Computer Program for Coil Geometry Data Base Generation and Manipulation" IEEE Trans. on Magnetics, Vol. Mag-14, No.6, November 1978, p.1180-5.
264. D B Montgomery "The Generation of High Magnetic Fields" Reports on Progress in Physics, Vol.26, Institute of Physics and the Physical Society, 1963.

D52158

VOL 1

END

145

D52158/84

Vol. 2

ABEL. E.

Total pages = 426

WARWICK.

AIR CORED LINEAR MACHINES
FOR GROUND TRANSPORTATION

E Abel, B.Sc, CEng, MIEE

submitted for the degree of

Department of Engineering Science

University of Warwick

September 1981

Volume Two of two volumes

AIR CORED LINEAR MACHINES
FOR GROUND TRANSPORTATION

E Abel, B.Sc, CEng, MIEE

submitted for the degree of PhD

Department of Engineering Science

University of Warwick

September 1981

Volume Two of two volumes

	<u>VOLUME TWO</u>	Page No
APPENDIX I	BIBLIOGRAPHY	177
	1. Scope of the Bibliography	177
	2. Books	178
	3. Special Issues	178
	4. Conference Proceedings	179
	5. Indexed Papers List	180
	5.1 Papers	180
	5.2 Author Index	228
	5.3 Corporate Index	236
APPENDIX II	SOLENOID MAGNET DESIGN	241
	1. Introduction	241
	2. Circular Coils	242
	2.1 Basic Field and Power Relationships	242
	2.2 Off Axis Field of a Finite Solenoid	246
	3. Rectangular Coils	247
	3.1 Line Filament Solutions	247
	3.2 Finite Sections	249
	4. Racetrack Coils	251
APPENDIX III	DERIVATION OF TRACK INDUCTANCE	
	1. Introduction	253
	2. Track Inductance	254
	2.1 Phase Leakage Inductance	254
	2.2 Elemental Inductance	254
	3. Self Inductance Structure	255
	4. Mutual Inductance Structure	258
APPENDIX IV	FLUX LINKAGE AND INDUCED EMF IN AIR CORED MACHINES (Reference 222)	
	1. Introduction	262
	2. Derivation of Back Emf Relationships	262
	3. Rectangular Coils	268
	4. Circular and Racetrack Coils	272
	5. Conclusions	273
	Appendix. Rate of Change of Flux Linkage for a Rectangular Coil	274
APPENDIX V	COMPARISONS OF ALTERNATIVE MAGLEV REVENUE VEHICLE SYSTEMS	
	1. Reference 134, Electronics and Power	291
	2. Reference 135, IEEE Transactions on Magnetics	294

APPENDIX I - BIBLIOGRAPHY

1. Scope of the Bibliography

This bibliography contains over 400 references to published literature relevant to linear synchronous machines. Since the development of this type of machine is so closely coupled to that of magnetic levitation, some of the more important EDS maglev references are included, particularly the Ford and Stanford reports for the US Department of Transportation. The earliest references are to essentially ac induction devices, which were suggested as forms of guided transport to assist or complement the existing rail systems. Linear induction motors are covered by Wagner's bibliography, the more general papers of Poloujadoff and Laithwaite, and the books by Laithwaite, Nasar and Yamamura. Also included are references to iron cored linear synchronous machines, and the homopolar and heteropolar variants. The linear dc machine or linear thyristor machine with iron cored field is similarly listed, as are the more relevant EMS papers. Generally the majority of references are freely available. The exceptions are a few Warwick University internal publications, and the German Statusseminar proceedings. Special issues and IEEE Transactions on Magnetics (for INTERMAG and Applied Superconductivity Conferences) will find about 94 of the references, and the remaining listed conferences include a further 86 papers.

2. Books

- 1) F W Grover (NBS)
Inductance Calculations
Dover, New York, 1962
- 2) G R Polgreen
New Applications of Modern Magnets
MacDonald, London, 1966
- 3) E R Laithwaite (Imperial College)
Induction Machines for Special Purposes
Newnes, London, 1966
- 4) Id
Propulsion Without Wheels
English Universities Press, London 1966
- 5) Id
Linear Electric Motors
Mills & Boon, London, 1971
- 6) S Yamamura (Univ. of Tokyo)
Theory of Linear Induction Motors
Wiley, Chichester, Sussex 1972
- 7) A G Hammitt
Aerodynamics of High Speed Ground Transportation
Western Periodicals, North Hollywood, California, 1973
- 8) S A Nasar, I Boldea (Univ. of Kentucky)
Linear Motion Electric Machines
Wiley - Interscience, New York, 1976

3. Special Issues

- 1) Ground Transportation in the Eighties, P.I.E.E. Vol.61, No.5, May 1973
- 2) New Systems Challenge the Steel Wheel, Railway Gazette International, Vol.130, No.10, October 1974.
- 3) Ground Transportation, Trans. ASME, Vol.96, Series G, No.2, June 1974.
- 4) High Speed Electric Propulsion, Revue Generale de l'Electricite, Vol.84 No.2 February 1975.
- 5) Maglev Issue, Cryogenics, Vol.15, No.7, July 1975.
- 6) Levitation and Propulsion Technology, ETZ-A, Vol.96, No.9, September, 1975.
- 7) Levitation Railway, Quarterly Reports of the Railway Technical Research Institute, Vol.17, No.4, December 1976.
- 8) IEEE Trans. on Vehicular Technology, Vol.VT-29, No.1, February 1980.

2. Books

- 1) F W Grover (NBS)
Inductance Calculations
Dover, New York, 1962
- 2) G R Polgreen
New Applications of Modern Magnets
MacDonald, London, 1966
- 3) E R Laithwaite (Imperial College)
Induction Machines for Special Purposes
Newnes, London, 1966
- 4) Id
Propulsion Without Wheels
English Universities Press, London 1966
- 5) Id
Linear Electric Motors
Mills & Boon, London, 1971
- 6) S Yamamura (Univ. of Tokyo)
Theory of Linear Induction Motors
Wiley, Chichester, Sussex 1972
- 7) A G Hammitt
Aerodynamics of High Speed Ground Transportation
Western Periodicals, North Hollywood, California, 1973
- 8) S A Nasar, I Boldea (Univ. of Kentucky)
Linear Motion Electric Machines
Wiley - Interscience, New York, 1976

3. Special Issues

- 1) Ground Transportation in the Eighties, P.I.E.E. Vol.61, No.5, May 1973
- 2) New Systems Challenge the Steel Wheel, Railway Gazette International, Vol.130, No.10, October 1974.
- 3) Ground Transportation, Trans. ASME, Vol.96, Series G, No.2, June 1974.
- 4) High Speed Electric Propulsion, Revue Generale de l'Electricite, Vol.84 No.2 February 1975.
- 5) Maglev Issue, Cryogenics, Vol.15, No.7, July 1975.
- 6) Levitation and Propulsion Technology, ETZ-A, Vol.96, No.9, September, 1975.
- 7) Levitation Railway, Quarterly Reports of the Railway Technical Research Institute, Vol.17, No.4, December 1976.
- 8) IEEE Trans. on Vehicular Technology, Vol.VT-29, No.1, February 1980.

- 9) Levitation Railway, Quarterly Reports of the Railway Technical Research Institute, Vol.21, No.1, March 1980.

4. Conference Proceedings

- 1) Seventeenth Annual Conference on Magnetism and Magnetic Materials, Chicago, 16-19 November 1971, AIP Conference Proceedings, Vol.5
- 2) Second BMFT Statusseminar, Friedrichsruhe, February 1972.
- 3) Applied Superconductivity Conference, Annapolis, 1-3 May, 1972, IEEE Publication No. 72 CHO682-5-TABSC.
- 4) Fourth International Cryogenic Engineering Conference (ICEC4), Eindhoven, 24-26 May 1972, IPC Science & Technology Press.
- 5) Fourth International Conference on Magnet Technology (MT-4), Brookhaven, September 1972.
- 6) 1973 Cryogenic Engineering Conference, Atlanta, 8-10 August 1973, Advances in Cryogenic Engineering, Vol.19.
- 7) Intermag-73, Washington, 24-27 April 1973, IEEE Transactions on Magnetics, Vol. MAG-9, No.3, September 1973.
- 8) Third BMFT Statusseminar, Berlin, 18-21 March 1974.
- 9) Fifth International Cryogenic Engineering Conference (ICEC5), Kyoto, 7-10 May 1974, IPC Science & Technology Press.
- 10) International Conference on Hovering Craft, Hydrofoil, and Advanced Transit Systems, Brighton, 13-16 May 1974.
- 11) Control Aspects of New Forms of Guided Land Transport, London, 28-30 August, 1974, IEE Conference Publication No.117.
- 12) Intermag-74 Toronto, 14-17 May 1974, IEEE Transactions on Magnetics, Vol. MAG-10, No.3, September 1974.
- 13) IFAC Symposium of Control in Power Electronics and Electrical Drives, Dusseldorf, 7-9 October 1974.
- 14) Linear Electric Machines, London, 21-23 October, 1974, IEE Conference Publication No.120.
- 15) International Conference on High Speed Ground Transportation, Tempe, 7-10 January 1975.
- 16) Fourth BMFT Statusseminar, Schliersee, 10-12 March 1975.
- 17) Applied Superconductivity Conference, Argonne, 30 September-2 October 1974, IEEE Transactions on Magnetics, Vol.MAG-11, No.2, March 1975.
- 18) Fifth International Conference on Magnet Technology (MT-5), Rome, 21-25 April 1975.

- 19) Intermag-75, London, 14-17 April 1975, IEEE Transactions on Magnetism, Vol. MAG-11, No.5, September 1975.
- 20) Fifth BMFT Statusseminar, Bad Kissingen, March 1976.
- 21) 1976 Industrial Electronics and Control Instrumentation Meeting, (IECI'76), Philadelphia, 8-10 March 1976, IEEE No.76CH1117-1 IECI.
- 22) Sixth International Cryogenic Engineering Conference (ICEC6), Grenoble, 11-14 May 1976, IPC Science & Technology Press.
- 23) Second International Conference on Hovering Craft, Hydrofoil, and Advanced Transit Systems, Amsterdam, 17-20 May 1976.
- 24) Second Conference on Advances in Magnetic Materials and their Applications, (AMMA), London 1-3 September 1976, IEE Conference Publication No.142.
- 25) Intermag-76, Pittsburgh, 15-18 June 1976, IEEE Transactions on Magnetism, Vol. MAG-12, No.6, November 1976.
- 26) Sixth BMFT Statusseminar, Konstanz, March 1977.
- 27) Sixth International Conference on Magnet Technology (MT-6) Bratislava, 29 August-2 September 1977.
- 28) Intermag-77, Los Angeles, 6-9 June 1977, IEEE Transactions on Magnetism, Vol. MAG-13, No.5, September 1977.
- 29) Seventh BMFT Statusseminar, Willingen, 1978.
- 30) Biennial CIEET Seminar on Railway Research "The Eighties : A New Rail Era", Kingston, 29-30 January 1978, CIGGT Report No.78-5.
- 31) Intermag-78, Florence, 9-12 May 1978, IEEE Transactions on Magnetism, Vol. MAG-14, No.5, September, 1978.
- 32) International Conference on Electrical Machines, Brussels, 11-13 September, 1978.
- 33) IEE Colloquium on Advanced Ground Transportation Schemes, London, 18 April 1979, IEE Digest No 1979/27.
- 34) Intermag-79, New York, 17-20 July 1979, IEEE Transactions on Magnetism, Vol. MAG-15, No.6, November 1979.
- 35) Intermag-80, Boston, 21-24 April 1980, IEEE Transaction on Magnetism, Vol. MAG-16, No.5, September 1980.

5. Indexed Papers List

The papers are listed as closely as possible in published date order. The first number set refers to the year of publication, the second set to the month (zero indicates unknown month), and the final number set is an arbitrary rank within the month.

An author and a corporate index are included as sections 5.2 and 5.3

- 19) Intermag-75, London, 14-17 April 1975, IEEE Transactions on Magnetics, Vol. MAG-11, No.5, September 1975.
- 20) Fifth BMFT Statusseminar, Bad Kissingen, March 1976.
- 21) 1976 Industrial Electronics and Control Instrumentation Meeting, (IECI'76), Philadelphia, 8-10 March 1976, IEEE No.76CH1117-1 IECI.
- 22) Sixth International Cryogenic Engineering Conference (ICEC6), Grenoble, 11-14 May 1976, IPC Science & Technology Press.
- 23) Second International Conference on Hovering Craft, Hydrofoil, and Advanced Transit Systems, Amsterdam, 17-20 May 1976.
- 24) Second Conference on Advances in Magnetic Materials and their Applications, (AMMA), London 1-3 September 1976, IEE Conference Publication No.142.
- 25) Intermag-76, Pittsburgh, 15-18 June 1976, IEEE Transactions on Magnetics, Vol. MAG-12, No.6, November 1976.
- 26) Sixth BMFT Statusseminar, Konstanz, March 1977.
- 27) Sixth International Conference on Magnet Technology (MT-6) Bratislava, 29 August-2 September 1977.
- 28) Intermag-77, Los Angeles, 6-9 June 1977, IEEE Transactions on Magnetics, Vol. MAG-13, No.5, September 1977.
- 29) Seventh BMFT Statusseminar, Willingen, 1978.
- 30) Biennial CIEET Seminar on Railway Research "The Eighties : A New Rail Era", Kingston, 29-30 January 1978, CIGGT Report No.78-5.
- 31) Intermag-78, Florence, 9-12 May 1978, IEEE Transactions on Magnetics, Vol. MAG-14, No.5, September, 1978.
- 32) International Conference on Electrical Machines, Brussels, 11-13 September, 1978.
- 33) IEE Colloquium on Advanced Ground Transportation Schemes, London, 18 April 1979, IEE Digest No 1979/27.
- 34) Intermag-79, New York, 17-20 July 1979, IEEE Transactions on Magnetics, Vol. MAG-15, No.6, November 1979.
- 35) Intermag-80, Boston, 21-24 April 1980, IEEE Transaction on Magnetics, Vol. MAG-16, No.5, September 1980.

5. Indexed Papers List

The papers are listed as closely as possible in published date order. The first number set refers to the year of publication, the second set to the month (zero indicates unknown month), and the final number set is an arbitrary rank within the month.

An author and a corporate index are included as sections 5.2 and 5.3

5.1 Papers

5.0.1

A Zehden
New improvements in electric traction apparatus.
US Patent 732, 312, 1905.

5.0.2

H W Wilson
Electrification of Railways
Trans. Liverpool Engineering Society, Vol.26, 1905, p.181-234

12.3.1

E Bachelet
Levitating Transmitting Apparatus
US Patent, 1,020,943, 19 March 1912

12.10.1

Anon
Foucault and eddy currents put to service.
The Engineer, Vol.114, 18 October 1912, p.414, 420-1

13.10.1

Anon
An electric induction transport system for mails.
Eng.News, Vol.70, 2 October, 1913, p.637-9: 9 October 1913, p702-4
Engineering, Vol.96, 10 October 1913, p.501.

38.4.1

H Kemper
Schwebende Aufhangung durch elektromagnetischen Krafte,
eine moglichkeit fur eine grundsatzlich neue Fahrtbenegungsart
ETZ-A, Vol.59, No.15, 14 April 1938, p.391-5

46.9.1

A wound rotor motor 1400 feet long.
Westinghouse Engineer, Vol.6, September, 1946, p.160-1

46.10.1

M F Jones (Westinghouse Electric Corp)
Launching Aircraft Electrically
Aviation, Vol.45, No.10, October 1946, p.62-5.

53.1.1

H Kemper
Elektrische angetriebene Eisenbahnfahrzeuge mit elektromagnetischer
Schwebefuhrung
ETZ-A Vol.74, No.1, January 1953, p.11-14.

62.0.1

F W Grover (NBS)
Inductance Calculations
Dover, New York, 1962

63.4.1

J R Powell (Brookhaven Natl.Lab)
The Magnetic road : a new form of transport
IEEE - ASME Railroad Conf. Atlanta, 25-26 April 1963, ASME paper No
63-RR-4, p1-8.

66.0.1

E R Laithwaite (Imperial College)
Induction Machines for special purposes
Newnes, London, 1966

66.0.2

G R Polgreen
New applications of modern magnets
MacDonald, London, 1966.

66.11.1

J R Powell, G R Danby (Brookhaven Natl.Lab)
High speed transport by magnetically suspended trains.
ASME Winter Annual Meeting 27 November - 1 December 1966, New York,
ASME Paper No 66-WA/RR-5, p.1-11.

68.8.1

R D Thornton (MIT)
High frequency motors for electric propulsion
Proc. IECEC '68, Boulder, 13-17 August 1968, IEEE Publ. No. 68C
21-ENERGY, p.797-804.

69.4.1

C A Guderjahn, S L Wipf, H J Fink (Atomic Int.Dir. of North American
Rockwell Corp). R W Boom (Univ. of Wisconsin), K E Mackenzie (Univ.
of California, D Williams, T Downey (Saudi Labs).
Magnetic suspension and guidance for high speed rockets by
superconducting magnets.
J.Appl.Physics, Vol.40, No.5, April 1969, p.2133-40.

69.5.1

E R Laithwaite (Imperial College), F T Barwell (University College,
Swansea).
Application of linear induction motors to high speed transport
systems.
PIEE, Vol.116, No.5, May 1969, p.713-24.

62.0.1

F W Grover (NBS)
Inductance Calculations
Dover, New York, 1962

63.4.1

J R Powell (Brookhaven Natl.Lab)
The Magnetic road : a new form of transport
IEEE - ASME Railroad Conf. Atlanta, 25-26 April 1963, ASME paper No
63-RR-4, pl-8.

66.0.1

E R Laithwaite (Imperial College)
Induction Machines for special purposes
Newnes, London, 1966

66.0.2

G R Polgreen
New applications of modern magnets
MacDonald, London, 1966.

66.11.1

J R Powell, G R Danby (Brookhaven Natl.Lab)
High speed transport by magnetically suspended trains.
ASME Winter Annual Meeting 27 November - 1 December 1966, New York,
ASME Paper No 66-WA/RR-5, p.1-11.

68.8.1

R D Thornton (MIT)
High frequency motors for electric propulsion
Proc. IECEC '68, Boulder, 13-17 August 1968, IEEE Publ. No. 68C
21-ENERGY, p.797-804.

69.4.1

C A Guderjahn, S L Wipf, H J Fink (Atomic Int.Dir. of North American
Rockwell Corp). R W Boom (Univ. of Wisconsin), K E Mackenzie (Univ.
of California, D Williams, T Downey (Saudi Labs).
Magnetic suspension and guidance for high speed rockets by
superconducting magnets.
J.Appl.Physics, Vol.40, No.5, April 1969, p.2133-40.

69.5.1

E R Laithwaite (Imperial College), F T Barwell (University College,
Swansea).
Application of linear induction motors to high speed transport
systems.
PIEE, Vol.116, No.5, May 1969, p.713-24.

69.6.1

C A Guderjahn, S L Wipf (Atomics Int.Div. North American Rockwell Corporation)
Magnetic suspension and guidance for high speed trains by means of superconducting magnets and eddy currents.
Proc. 1969 Cryogenic Engineering Conference, California 16-18 June 1969, Advances in Cryogenic Engineering, Vol.15, p.117-123.

69.9.1

J R Powell, G T Danby (Brookhaven Natl.Lab)
Magnetically suspended trains for very high speed transport.
Proc. 4th IECEC Conf. Washington, 22-26 September 1969, p.953-63.

70.4.1

E R Laithwaite (Imperial College), S A Nasar (University of Kentucky)
Linear motion electrical machines
Proc. IEEE, Vol.58, No.4, April 1970, p.531-42

70.5.1

G Bogner (Siemens AG)
Applications of superconductivity
Proc. Third International Cryogenic Engineering Conference, (ICEC3) Berlin, 25-7 March 1970, Iliffe Science and Technology Publications Ltd, p.35-49.

71.1.1

E R Polgreen
The ideal magnet - fully controllable permanent magnets for power and transport.
Electronics and Power, Vol.17, No.1 January 1971, p.31-4

71.2.1

M Poloujadoff (Univ. of Grenoble)
Linear induction machines
IEEE Spectrum, Vol.8, No.2 February 1971, p.72-80.

71.3.1

M Poloujadoff (University of Grenoble)
Linear induction machines
IEEE Spectrum, Vol.8, NO.3, March 1971, p.79-86.

71.6.1

C Guderjahn, S L Wipf (Atomic Int.Div. North American Rockwell Corp)
Magnetically levitated transportation
Cryogenics, Vol.11, No.6, June 1971, p.171-8

71.6.2

J R Powell, G T Danby (Brookhaven Natl.Lab)
Magnetic suspension for levitated vehicles
Ibid, p.192-204.

71.8.1

J R Powell, G T Danby (Brookhaven Natl.Lab)
The linear synchronous motor and high speed ground transport.
Pro. 6th IECEC Conf, Boston, 3-6 August 1971, p.118-31

71.9.1

Y Asagoe, Y Sinryo, E Ohno (Mitsubishi)
Fundamental study of high speed ground transportation.
Mitsubishi Denki Engineer, Sept 1971, p10-19.

71.11.1

P L Richards (Univ, of California)
Magnetic suspension and propulsion systems for high speed
transportation
Seventeenth Annual Conference on Magnetism and Magnetic Materials,
Chicago 16-19 November 1971, AIP Conf. Proc. Vol.5 Pt.2, p.935-7.

71.11.2

J T Harding (US Dept of Transportation)
Progress in magnetic suspension applied to high speed ground
transportation.
Ibid, p938-48).

71.11.3

H Stablein (Krupp Forschungsinstitut)
Permanent magnets - materials and applications, review of permanent
magnet materials
Ibid, p.950-69.

71.11.4

D J Iden (Univ. of Dayton), C E Ehrenfried, H J Garrett
(Wright-Patterson AFB)
Present and future applications of high coercive force magnets
Ibid, p1026-46.

71.11.5

H Tanaka
The linear motor
Japan Electronic Engineering, No.60, November 1971, p.34-40

71.12.1

E R Laithwaite, J F Eastham, H R Bolton, T G Fellows (Imperial
College)
Linear motors with transverse flux
Proc. IEE, Vol.118, No.12, December 1971, p.1761-7.
Discussion, ibid, Vol.119, No.12, December 1972, p.1727-9.

71.12.2

R G Rhodes, A R Eastham (Univ. of Warwick)
Magnetic suspension for high speed trains
Hovering Craft and Hydrofoil, Vol.11, No.3, December 1971 p.12-26

72.0.1

C Guderjahn (Rockwell Int)
Hybrid magnetically levitated bus
Proc. Greater Los Angeles Area Transportation Symposia 1972-73,
p.209-14

72.0.2

Y Kyotani (JNR)
Magnetic levitation research vehicle
Japanese Railway Engineering No4, 1972, p6-9

72.0.3

Bundesministerium für Forschungs und Technologie
Spurgebundener Schnellverkehr mit beruhungsfreier Fahrtechnik. (High
speed ground transportation with magnetic levitation techniques)
Proc. Second Statusseminar, Friedrichsruhr, February 1972

72.1.1

H J Gutt (Siemens AG)
Applications of travelling field motors of the sector and liner
type.
Siemens Review vol. 39, No.1, January 1972, p.32-6.

72.2.1

D L Atherton (Queen's Univ.)
Magnetic levitation and linear motor for guided ground
transportation.
Seminar on Transportation Research and Education, CIGGT, Queen's
University, Kingston, CIGGT Report No 72-10, 7-8 February 1972.

72.2.2

Ford Motor Co
Technical feasibility of magnetic levitation as a suspension system
for high speed ground vehicles.
Final report, February 1971 - February 1972 on Task I, US DOT report
No FRA-RT-72-40, PB 210-506, February 1972

72.2.3

Stanford Research Inst.
The feasibility of magnetically levitating high speed ground
vehicles.
Final report, February 1972 on Task I, US DOT Report No
FRA-RT-72-39, PB 210-505, February 1972.

72.3.1

W J Harrold (Raytheon Co)
Calculation of equipotentials and flux lines in axially symmetrical
permanent magnet assemblies by computer.
IEEE Trans on Magnetics, Vol. MAG.8 No.1, March 1972, p.23-9.

72.4.1

R E Rhodes, A R Eastham, M P Allen, B Mellen (Univ. of Warwick)
Magnetic suspension of high speed trains
Interim report to SRC for October 1971 - April 1972.

72.5.1

J R Reitz (Ford Motor Co)
The role of superconducting magnets in tracked magnetic cushion
vehicles for high speed transportation.
Proc. 1972 Applied Superconductivity Conf. Annapolis, 1-3 May 1972,
IEEE Publ. No 72CHO682-5-TABSC, p.57-61.

72.5.2

H T Coffey, F Chilton, L O Hoppie (SRI)
Magnetic levitation of high speed ground vehicles
Ibid, p.62-75

72.5.3

H H Kolm, R D Thornton (MIT)
The Magneplane: guided electromagnetic flight
Ibid, p.76-85

72.5.4

G Danby, J Powell (Brookhaven National Laboratory)
Integrated systems for magnetic suspension and propulsion of
vehicles.
Ibid, p.120-6.

72.5.5

D L Atherton (Queen's University)
Proposed propulsion system for magnetically levitated guided
ground transportation.
Ibid, p.129-151

72.5.6

K Oshima (Univ. of Tokyo), Y Kyotani (JNR)
The Japanese magnetically suspended train project
Proc. Fourth International Cryogenic Engineering Conference (ICEC4),
Eindhoven, 24-26 May 1972, IPC Science & Technology Press, p.26-34.

72.5.7

I A Alston, J T Hayden (Cranfield Inst. of Technology)
A preliminary technical assessment of magnetically suspended trains
Ibid, p.198-201

72.6.1

P L Richards (Univ. of California) M Tinkham (Harvard Univ)
Magnetic suspension and propulsion systems for high speed
transportation.
J Appl. Phys. Vol.43, No.6, June 1972, p.2680-91.

72.7.1

J A Wagner (San Jose State College)
Bibliography on the linear induction motor in high speed ground
transportation.
IEEE Power Engineering Society Summer Meeting, San Francisco,
9-14 July 1972, paper C72 448-9, p.1-8

72.9.1

S Yamamura (Univ of Tokyo)
Theory of Linear Induction Motors
John Wiley, September 1972

72.9.2

H H Kolm (MIT)
The prolonged adolescence of superconductivity
Proc. Fourth International Conference on Magnet Technology (MT-4),
Brookhaven, 1972, p3-7

72.9.3

K Hirai, S Akiyama, H Fujino, K Onodera (Fuji Electric Co)
A lightweight superconducting magnet for a test facility of
magnetic suspension for vehicles.
Ibid, p41-8.

72.9.4

H Ogiwara, N Takano, M Yonemitsu (Toshiba)
Experimental studies on magnetically suspended high speed trains
using large superconducting magnets.
Ibid, p70-9

72.10.1

JNR
Test run success of experimental car using linear synchronous motor
and superconducting magnetic levitation.
JNR Quarterly Bulletin, No.13 & 14, October 1972, p1-4

72.10.2

E J Ward (F R A Dept of Transportation)
Linear electric motors for high speed ground transport.
Electronics and Aerospace Systems Convention (EASCON 72) 16-18
October 1972, IEEE, p169-73.

72.11.1

E Rummich (T U Vienne)
Machines lineaires synchrones. Theori et realisation pratiques
Bull ASE, Vol.63, No.23, 11 November 1972, p1338-44.

72.11.2

C H Tang, W J Harrold (Raytheon Co)
Lift and drag force calculations and magnet design for the Magneplane model.
Proc. 18th Annual Conference on Magnetism and Magnetic Materials .
Denver, 28 November - 1 December 1972, AIP Conference. Proc. No.10
Pt.1, p.598-602.

72.12.1

Canadian Maglev Group
Study of magnetic levitation and linear synchronous motor propulsion
Phase I Contract Report, CIGGT Report No 73-1, December 1972

72.12.2

I A Alston, J M Clark, J T Hayden (Cranfield Inst of Technology)
Magnetic suspension and guidance of high speed vehicles
Final report to SRC, Cranfield CTS Report 2, December 1972

72.12.3

D L Atherton, L E E Love, P O Prentiss (Queen's Univ)
Magnetic Levitation: linear synchronous motor efficiency
Can J of Physics, Vol.50, No.24, 15 December, 1972, p3143-6

73.0.1

Toshiba's research and development of large type superconductivity magnets for magnetically levitated high speed trains.
Toshiba descriptive leaflet.

73.1.1

A Garnault (Societe de l'Aerotrain)
Technical and economic results of the use of air cushion in guided ground transportation.
International Automotive Engineering Congress, Detroit 8-12 Jan.1973
SEA paper No 730161,p.1-16

73.2.1

Stanford Research Inst.
Study of a magnetically levitated vehicle
Final report, February 1973 on Task II, US DOT Report No
DOT-FR-73-24, PB 221-696, February 1973

73.3.1

Ford Motor Co
Preliminary design studies of magnetic suspensions for high speed ground transportation
Final report, February 1972 - March 1973 on Tasks II and III, US DOT Report No FRA-RT-73-27, PB 223-237, March 1973
See also 73.6.2

73.3.2

G R Slemon (Univ of Toronto) J B Forsythe (Garrett Manufacturing Ltd) S B Dewan (Univ of Toronto)
Controlled-power-angle synchronous motor inverter drive system.
IEEE Trans on Industry Applications, Vol. 1A-9, No.2, March/April 1973 p.216-9.

73.4.1

J F Leonard, D W Jackson, P A Wheeler (United Engineers)
Report on a study of the magneplane power system and guideway
United Engineers and Constructors Inc. Boston, April 1973

73.4.2

R D Thornton (MIT)
Flying low with maglev
IEEE Spectrum, Vol.10, No.4, April 1973, p.47-54

73.4.3

R D Thornton (MIT)
Design principles for induced-current magnetic levitation systems
Digests of the 1973 INTERMAG Conference Washington 24-27 April 1973,
IEEE Publ. No 73 CHO 723-7-MAG, p.9.1

73.5.1

R H Borcherts, L C Davis, J R Reitz, D F Wilkie (Ford Motor Co)
Baseline specifications for a magnetically suspended high speed vehicle.
Proc. IEEE, Vol.61, No.5, May 1973, p.569-78

73.5.2

E Ohno, M Iwamoto, T Yamada (Mitsubishi)
Characteristics of superconductive suspension and propulsion for high speed trains.
Ibid, p.579-86

73.5.3

R D Thornton (MIT)
Design principles for magnetic levitation
Ibid p.586-98

73.5.4

Y Iwasa (MIT)
Magnetic shielding for maglev vehicle
Ibid, p.598-603

73.5.5

R L Forgacs (Ford Motor Co)
Evacuated tubes versus jet aircraft for high speed transport
Ibid, p.604-16

73.5.6

J A Ross (Rohr Industries, Ltd)
ROMAG transportation system
Ibid,p.617-20

73.5.7

J H Dannan, R N Day, G P Kalman (AiResearch Manufacturing Co)
A linear induction motor propulsion system for high speed ground
vehicles.
Ibid,p.621-30

73.6.1

A H Greene, W J Harrold, R S Kasevich, C H Tang, E Weiss, (Raytheon
Co)
Magneplane linear synchronous motor study, final report for MIT,
June 1973.

73.6.2

Ford Motor Co
Preliminary design studies of magnetic suspensions for high speed
ground transportation: Volume II: Experimental ride simulation
studies.
Final report, June 1972-June 1973, US DOT Report No FRA-RT-73-27A,
PB 224 893/8, PB 230 489/7, June 1973 see also 73.3.1.

73.7.1

L C Davies, R H Borcherts (Ford Motor Co)
Superconducting paddle wheels, screws and other propulsion units for
high speed ground transportation.
J. Appl.Phys. Vol.44, No.7, July 1973, p.3294-99

73.7.2

R G Rhodes
Report on the Wolfson Maglev Project
Univ. of Warwick report, July 1973

73.7.3

Univ. of Toronto
Reference Design Linear Synchronous Motor
Univ. of Toronto note, 26 July 1973

73.8.1

I A Alston (Cranfield Inst. of Technology)
Superconducting magnet suspensions in high speed ground transport
Cranfield CTS Report 5. (Also TRRL Supplementary Report SR 72 UC)
August 1975.

73.8.2

K Oshima (Univ of Tokyo), Y Kyotani (JNR)
High speed transportation levitated by superconducting magnet,
Proc. 1973 Cryogenic Engineering Conf. Atlanta, 8-10 August
Advances in Cryogenic Engineering, Vol.19, p.127-36.

73.8.3

H T Coffey (SRI)
SRI Magnetic suspension studies for high speed vehicles
Ibid, p.137-53

73.8.4

T Satow, M Tanaka, T Ogama (Mitsubishi Electric Corp)
AC losses in multifilamentary superconducting composites for
levitated trains under ac and dc magnetic fields.
Ibid, p.154-61

73.9.1

Anon
Levitated vehicles : how magnetic forces can outperform the air
cushion.
Design Engineering September 1973, p.51-4

73.9.2

Anon
Hardware for high speed in 1973
Railway Gazette International Vol. 129, No.9, September 1973,
p.336-43

73.9.3

E Levi (Poly.Inst. of Brooklyn)
Linear synchronous motors for high speed ground transportation.
IEEE Trans on Magnetics, Vol. MAG.9 Nq.3, September 1973, p242-8

73.9.4

W J Harrold, C H Tang (Raytheon Co)
Optimization of magnet configuration for the Magneplane Model
Ibid, p.248-52

73.9.5

E Ohno, M Iwamoto, O Ogino, T Kawamura, M Shinob (Mitsubishi)
Studies on magnetic levitation for high speed trains
Mitsubishi Electrical Engineer No 37, September 1973, p 23-9.

73.10.1

H H Kolm, R D Thornton (MIT)
Electromagnetic flight
Scientific American, Vol.229, No.4, October 1973, p.17-23

73.10.2

Univ of Warwick
Wolfson Magnetic Levitation Project - Memo 1
8 October 1973

73.10.3

R D Thornton, H H Kolm (MIT)
Transportation system employing an electromagnetically suspended,
guided and propelled vehicle.
US Patent 3,768,417, 30 October 1973

73.11.2

W J Harrold, R S Kasevich, C H Tang, N P Viens (Raytheon Co)
Electromagnetic propulsion for magnetically levitated vehicles
19th Annual Conference on Magnetism and Magnetic Materials, Boston
13-16 November 1973, AIP Conf. Proc. No. 18 Pt.2 p.1340-44.

73.11.3

C Albrecht (Siemens AG, Erlangen)
Zukünftige Hochgeschwindigkeitsbahnen : Berührungsloses Tragen und
Führen mit supraleitenden Magneten.
De Ingenieur, Vol.85, No.48 29 November 1973, p.943-51.

73.12.1.

Univ of Warwick
Wolfson Magnetic Levitation Project - Memo 2
Progress, September - December 1973

73.12.2

P H. Melville (CERL)
Magnetic propulsion for magnetically levitated trains
Cryogenics, Vol.13, No 12, December 1973, p.716-7.

74.0.1

J Allen (Culham Lab)
The electromagnetically levitated vehicle of Emile Bachelet, a
contemporary technical comment, 1912-1914.
Culham Laboratory, report No CR 74-74, 1974

74.0.2

R Yasumochi, H Kobayashi, K Fuke, Y Takeyama (Fuji Electric Co Ltd)
Characteristics of the linear synchronous motor for magnetically
suspended vehicle.
Fuji Electrical Review, Vol.20, No.1, 1974, p.26-32.

74.2.1

R L Byer, R F Begley, G R Stewart, (Stanford Univ)
Superconducting, magnetically levitated merry-go-round
American Journal of Physics, Vol.42, No.2 February 1974, p111-25

74.2.2

D L Hearn, N H Van Dorn (Rohr Industries Inc)
Modern transportation systems
Automotive Engineering Congress, Detroit, 25 February - 1 March 1974
SAE preprint 740225, p.1-16.

74.2.3

T K Hunt (Ford Motor Co)
A C Losses in superconducting magnets at low excitation levels
J.Appl.Phys. Vol.45, No.2, February 1974, p.907-13

74.3.1

D L Atherton, A R Eastham (Queen's Univ)
Flat guidance schemes for magnetically levitated high speed guided
ground transport.
J.Appl.Phys.Vol.45, No.3, March 1974, p.1398-1405.

74.3.2

Canadian Maglev Group
Analysis of superconducting magnetic levitation and linear
synchronous motor propulsion for high speed guided ground
transportation.
Annual Report for 1973, CIGGT Report No 74-8, March 1974.

74.3.3

T G Fellows (THL)
High speed surface transport
Railway Engineering Journal, Vol.3, No.2, March 1974, p.4-20.

74.4.1

Univ of Warwick
Wolfson Magnetic Levitation Project - Memo 3
Progress to April 1974, 4 April 1974.

74.4.2

Ford Motor Co
Parameter optimization studies of magnetic suspensions or high speed
ground transportation
Final report, June 1973 - April 1974 on Tasks IV and V. US DOT
Report No FRA-ORD/D-74-42, Pb 238773/6, April 1974.

74.5.1

G R Slemon, S B Dewan (Univ of Toronto) J W A Wilson, (Reliance
Electric Co)
Synchronous motor drive with current source inverter
IEEE Trans on Industry Applications, Vol. IA-10, No.3. May/June 1974
p.412-6.

74.5.2

Y Kyotani (JNR)
High speed railways in Japan
Proc. Fifth International Cryogenic Engineering Conference (ICECS),
Kyoto, 7-10 May 1974, IPC Science and Technology Press, p.17-20

74.5.3

R H Borcherts, (Ford Motor Co)
The use of superconductivity in the USA transportation programme.
Ibid p.26-7

74.5.4

C Albrecht, W Elsel, H Franksen, C P Parsch, K Wilhelm (Siemens AG)
Superconducting levitated systems: first results with the
experimental facility at Erlangen.
Ibid, p.28-34

74.5.5

G Prast (Phillips Research Labs)
On board refrigeration for high speed trains
Ibid, p35-6

74.5.6

St Asztalos, W Baldus, R Kneuer, A Stephan (Linde AG)
On board cryogenic systems for magnetic levitation of trains:
cryogenic system of EET.
Ibid, p.37-41

74.5.7

R D.Thornton, Y Iwasa, H H Kolm (MIT)
The Magneplane system
Ibid, p42-5

74.5.8

D L Atherton, A R Eastham (Queen's Univ)
High-speed maglev studies in Canada
Ibid p.46-50

74.5.9

T Takahashi, N Maki, T Miyashita, (Hitachi Ltd)
Combined system for propulsion and guidance of magnetically suspended
vehicles.
Ibid, p.78-81.

74.5.10

T Kasahara, R Saito, Y Kazawa, N Tada, T Takahashi, H Kimura, S Sato
(Hitachi)
A superconducting magnet for ML-100
Ibid p.82-5

74.5.11

H Ichikawa, H Ogiwara (Toshiba)
Design considerations for superconducting magnets as a maglev pad.
Ibid p86-9

74.5.12

E Ohno, M Iwamoto, O Ogino, T Kawamura (Mitsubishi)
Development of superconducting magnets for magnetically levitated trains
Ibid p90-3

74.5.13

H Ogiwara, N Takano (Toshiba)
Development of superconducting magnets for a magnetically suspended high speed train in Toshiba.
Ibid p94-6

74.5.14

H Nakashima, K Arima (JNR)
Vertical cryostat for guidance and propulsion of superconducting magnetic levitation vehicle.
Ibid p.97-8

74.5.15

K Arima, H Nakashima, T Kuzuu (JNR)
Refrigeration system for magnetically levitated trains
Ibid p99-101

74.5.16

Y Ishizaki, T Kuroda, (Univ of Tokyo), T Ohtsuka (Tohoku Univ)
Sealed cryostat system for magnetically levitated vehicles
Ibid, p102-5

74.5.17

T Satow, K Fukuhara, T Yamada, M Iwamoto, M Shinobu (Mitsubishi)
Removable current leads for superconducting magnets
Ibid, p.403-5

74.5.18

H Kimura, H Ogata, S Sato, H Tomeoku (Hitachi Ltd)
Force cooled superconducting magnet with doughnut shaped cryostat
Ibid, p417-9

74.5.19

C G Swanson (Mitre Corp), A F Lampros (FRA, US Dept of Transportation)
Tracked Air Cushion Vehicle (TACV) research and development by the US Department of Transportation
Proc. International Hovering Craft, Hydrofoil and Advanced Transit Systems Conf. Brighton, 13-16 May 1974, p57-68

74.5.20

R G Rhodes, B E Mulhall, E Abel (Univ of Warwick)
Flying land vehicles using superconducting magnets
Ibid p157-66

74.5.21

G E Dawson, V I John (Queen's Univ)
Performance characteristics of variable speed linear synchronous motor.
Digests of the INTERMAG Conference, Toronto, 14-17 May 1974
IEEE Conf. Publ. No 74 CHO 852-4 MAG, p19-7.

74.5.22

M Guarino Jr (US Dept of Transportation)
Integrated linear electric motor propulsion systems for high speed transportation
International Symposium on Linear Electric Motors, Lyon and Grenoble
15-17 May 1974

74.6.1

F B Metzger (Hamilton Standard)
Quiet air propulsion for high speed ground transportation
High Speed Ground Transportation Journal, Vol.8 No.2 Summer 1974,
p33-9.

74.6.2

D L Atherton, A R Eastham (Queen's Univ)
Electrodynamic magnetic levitation development in Canada
Ibid p101-10

74.6.3

S Watabe, T Yamaguchi, Y Tamura, A Mase, T Yamaya (Toshiba)
Propulsion control system for super high speed transportation
Toshiba Review Vol.29, No.6 June 1974, p551-65.

74.7.1

Japanese National Railways
Improvements in propulsion systems
UK Patent 1,360,834, 24 July 1974

74.8.1

R G Rhodes, B E Mulhall, E Abel (Univ of Warwick)
Maglev vehicle oscillations and damping mechanisms
Conference on Control Aspects of New Forms of Guided Land Transport,
London, 28-30 August 1974, IEE Conference Publ. No.117, p.214-20.

74.09.1

Univ of Warwick
Wolfson Maglev Project
Progress Report to September 1974

74.9.2

H H Kolm (MIT)
Electromagnetic flight
IEEE Trans on Magnetics Vol MAG-10, No.3, September 1974 p.397

74.9.3

R G Rhodes, B E Mulhall, J P Howell, E Abel (Univ of Warwick)
The Wolfson Maglev project
Ibid p398-401

74.9.4

Y Iwasa, M O Hoenig, H H Kolm (MIT)
Design of a full sized Magneplane vehicle
Ibid p402-5

74.9.5

D W Jackson (Unitd Engineers & Constructors Inc)
Magneplane power supply costs
Ibid p406-9

74.9.6

D L Atherton, A R Eastham (Queen's Univ)
Guidance of a high speed vehicle with electrodynamic suspension
ibid p413-6.

74.9.7

A H Greene, W J Harrold, R S Kasevich, F P Morrison, C H Tang
(Raytheon Co)
LSM control of maglev vehicle ride quality
Ibid p431-4

74.9.8

G R Slemon, R A Turton, P E Burke (Univ of Toronto)
A linear synchronous motor for high speed ground transport
Ibid p435-8

74.9.9

P E Burke, R A Turton, G R Slemon (Univ of Toronto)
The calculation of eddy losses in guideway conductors and
structural members of high speed vehicles.
Ibid p.462-5

74.9.10

Y Amemiya, S Aiba (Nagoya Univ)
Tractive characteristics of DC linear motor with a constant voltage
applied to ground coil.
Electrical Engineering in Japan, Vol.94, No.5, September-October 1974
p.97-103

74.10.1

D L Atherton, A R Eastham (Queen's Univ)
Propulsion requirements for high speed vehicles with electrodynamic suspension.
IEEE 9th Annual IAS Meeting, Pittsburgh, 7-10 October, 1974 IEEE Publication No 74 CHO 833 HIA paper LT-WED-AMI, p.695-700 See also 77.5.1.

74.10.2

H Lehman
Latest developments affecting magnetic levitation vehicles
Rail International Vol.10, October 1974, p.629-37.

74.10.3

W Mrha (Brown Boveri, Mannheim)
Führung eines Linearmotors (LIM) durch eine elektrohydraulische Regelung
Proc. IFAC Symposium, Control in Power Electronics and Electrical Drives Dusseldorf, 7-9 October 1974, Vol.II, p.495-507.

74.10.4

Anon
Levitation line up 1974
Railway Gazette International, Vol.130, No.10, October 1974, p.377

74.10.5

G P Kalman (AiResearch Manuf.Co. Garrett Corp.)
Linear motors to power DoT's high speed research vehicles
Ibid, p.378

74.10.6

A W Bond (Harris Audey Lea & Brooks)
Aerospace investors are taken for a ride
ibid p.389-9

74.10.7

Y Usami, J Fujie, S Fujiwara (JNR)
Studies on linear motor in the Institute of JNR
Conference on Linear Electric Machines, London, 21-23 October 1974
IEE Conf. Publ. No.120, p.131-6

74.10.8

G R Slemon, R A Turton, P E Burke, S B Dewan (Univ of Toronto)
Analysis of control of a linear synchronous motor for high speed ground transport.
Ibid p.143-8

74.10.9

K Matsui, T Umemori (JNR) Y Taketsuna, Y Hosoda (Sumito Electric Industries)
DC linear motor controlled by thyristors and the testing equipment for its high speed characteristics.
Ibid p.149-54

74.10.1

D L Atherton, A R Eastham (Queen's Univ)
Propulsion requirements for high speed vehicles with electrodynamic suspension.
IEEE 9th Annual IAS Meeting, Pittsburgh, 7-10 October, 1974 IEEE Publication No 74 CHO 833 HIA paper LT-WED-AMI, p.695-700 See also 77.5.1.

74.10.2

H Lehman
Latest developments affecting magnetic levitation vehicles
Rail International Vol.10, October 1974, p.629-37.

74.10.3

W Mrha (Brown Boveri, Mannheim)
Führung eines Linearmotors (LIM) durch eine elektrohydraulische Regelung
Proc. IFAC Symposium, Control in Power Electronics and Electrical Drives Dusseldorf, 7-9 October 1974, Vol.II, p.495-507.

74.10.4

Anon
Levitation line up 1974
Railway Gazette International, Vol.130, No.10, October 1974, p.377

74.10.5

G P Kalman (AiResearch Manuf.Co. Garrett Corp.)
Linear motors to power DoT's high speed research vehicles
Ibid, p.378

74.10.6

A W Bond (Harris Audey Lea & Brooks)
Aerospace investors are taken for a ride
ibid p.389-9

74.10.7

Y Usami, J Fujie, S Fujiwara (JNR)
Studies on linear motor in the Institute of JNR
Conference on Linear Electric Machines, London, 21-23 October 1974
IEE Conf. Publ. No.120, p.131-6

74.10.8

G R Slemon, R A Turton, P E Burke, S B Dewan (Univ of Toronto)
Analysis of control of a linear synchronous motor for high speed ground transport.
Ibid p.143-8

74.10.9

K Matsui, T Umemori (JNR) Y Takatsuna, Y Hosoda (Sumito Electric Industries)
DC linear motor controlled by thyristors and the testing equipment for its high speed characteristics.
Ibid p.149-54

74.10.10

E Levi (Poly-Inst of New York)
High speed, iron-cored synchronously operating linear motors
Ibid p.155-60

74.10.11

E Abel, A E Corbett, B E Mulhall, R E Rhodes (Univ of Warwick)
Levitation and propulsion of guided vehicles using superconducting magnets.
Ibid p.223-9

74.10.12

R D Thornton (MIT)
The Magneplane linear synchronous motor propulsion system.
Ibid p.230-5

74.10.13

J F Eastham (Univ of Aberdeen), E R Laithwaite (Imperial College)
Linear Induction Motors as Electromagnetic Rivers
PIEE, Vol.121, No.10. October 1974, p.1099-1108.

74.12.1

H Ichikawa, H Ogiwara (Toshiba)
Design considerations of superconducting magnets as a maglev pad
IEEE Trans on Magnetics, Vol. MAG 10. No.4, December 1974,
p.1099-1103.

74.12.2

Bundesministerium fur Forschungs und Technologie
Spurgebundener Schnellverkehr mit beruhrungsfreier Fahrtechnik (High speed ground transportation with magnetic levitation techniques).
Proc. Third Statusseminar, Berlin, 18-21 March 1974, BMFT-FB-T-74-38 & 40, December 1974.

74.12.3

K Matsui, T Umemori (JNR) M Toyoshima, K Katakami, S Osawa (Hitachi Cable Ltd)
Ground coil assembly of a linear induction motor with dc levitating armature for high speed vehicle.
US Patent 3,855,485, 17 December 1974.

75.1.1

W Leitgeb (Siemens AG)
Bauarten von Wanderfeldmaschinen fur den spurgebundenen Schnellverkehr.
VDI-Z, Vol.117, No.2, January 1975, p.57-63.

75.2.1

Philco-Ford Corp
Conceptual design and analysis of the tracked magnetically levitated vehicle technology program (TMLV),. Repulsion Scheme.
Volume I. Technical studies. Vol.II, Appendices A-F Vol.III, Appendix G, 5 DOF computer programme. Executive summary
Final report June 1974-January 1975, US DOT Report No FRA/ORD 75-21/21A/21B/21C, PB 247 931/932/933/934 (Paper copy set as PB247 930-SET) February 1975.

75.2.2

E R Laithwaite (Imperial College)
Linear electric machines - a personal view.
Proc IEEE, Vol.63, No.2, February 1975, p.250-90.

75.2.3.

A Wiart, (Jeumont-Schneider)
Groupe propulseur a moteur lineaire et convertisseur electromonique
R.G.E. Vol.84, No.2, Feb.1975, p.112-9.

75.3.1

Canadian Maglev Group
Superconducting magnetic levitation and linear synchronous motor
propulsion for high speed guided ground transportation.
Phase II Contract Report, CIGGT Report No 75-5, March 1975.

75.3.2

H Weh (T U Braunschweig)
Elektrische Linearantriebe - Stand der Entwicklung
Naturwissenschaften Vol.62, No.3, March 1975, p.113-7.

75.3.3

W Heinz (Universitat Karlsruhe)
Research work on superconducting magnet systems in Germany
IEEE Trans on Magnetics, Vol. MAG.11, No.2 March 1975, p.147-53

75.3.4

T Ohtsuka (Tohoku Univ), Y Kyotani (JNR)
Superconducting levitated high speed ground transportation project
in Japan.
Ibid, p.608-14.

75.3.5

J R Reitz, R H Borcherts (Ford Motor Co)
US Dept of Transportation program in magnetic suspension (repulsion
concept)
Ibid p.615-8.

75.3.6

H Kimura, H Ogata, S Sato, R Saito, N Tada (Hitachi Ltd)
Superconducting magnet with tube type cryostat for magnetically
suspended train.
Ibid, p.619-22.

75.3.7

C H Tang, W J Harrold, R S Chu (Raytheon Co)
A review of the Magneplane project.
Ibid, p.623-6

75.3.8

D L Atherton, A R Eastham (Queen's University)
Superconducting Maglev and LSM development in Canada.
Ibid, p.627-32.

75.3.9

Stanford Research Inst.
An evaluation of the dynamics of a magnetically levitated vehicle
Final report, March 1973-March 1974 on Task III, US DOT report No
FRA-ORD/D-74-41, PB 236 671, March 1975.

75.3.10

Bundesministerium fur Forschungs und Technologie
Spurgefuehrter Fernverkehr. Teil a : Spurgebundener Schnellverkehr
mit beruhungsfreier Fahrtechnik. (Long distance rail transportation
Part A : Rapid rail transportation using non contact techniques)
Proc. Fourth Statusseminar, Schliersee, 10-12 March 1975, BMFT-FB-T-
75-36-PTA.

75.4.1

H Buchberger, W Leitgeb
Fahrzengantriebe mit synchronen linear motoren.
Elektrische Bahnen, Vol.46, No.4, April 1975, p.82-5.

75.4.2

H Autruffe (SNCF)
Problems arising in connection with the use of superconducting coils
in a passenger transport system.
Proc. Fifth International Conference on Magnetic Technology (MT-5),
Rome 21-25 April 1975, p.468-76.

75.4.3

R G Rhodes, B E Mulhall (Univ of Warwick)
Superconducting magnets for levitated high speed vehicles.
Ibid p.493-6.

75.4.4

W Schauer (Karlsruhe University)
Conductor materials for cryomagnets
Ibid p.629-43

75.4.5

C H Tang (Raytheon Co)
Evaluation of guideway edge effects
Digests of the Intermag Conf. London 14-17 April 1975, IEEE
Conf. Publ. No. 75 CHO 932-4 MAG. New York, p.28-12.

75.4.6

H Weh (TU Braunschweig)
Adhesion free transportation with integrated generation of three
controllable force components.
Ibid, p.28.5

75.4.7

Ford Motor Co

Parameter optimization studies of magnetic suspensions for high speed ground transportation.

Final report, June 1973-April 1974 on Tasks IV and V, US DOT report No. FRA-ORD/D-74-42, PB238 773, April 1974.

75.5.1

P H Melville (CERL) B E Mulhall (Univ of Warwick) M N Wilson, (Rutherford Lab)

Propulsion of magnetically levitated vehicles

Cryogenics Vol.15, No.5, May 1975, p.295.

75.5.2

G Wiegner (Siemens)

Der Antrieb des Versuchsfahrzeuges Zur Erprobung der elektrodynamischen Schwebetechnik - Beispiel eines Linearmotorantriebes

Elektrische Bahnen, Vol.46, No.5, May 1975, p.118-124

75.6.1

Canadian Maglev Group

Maglev test facilities at Queen's University

Descriptive information, June 1975

75.7.1

D L Atherton, A R Eastham (Queen's Univ)

Superconducting magnetic levitation and linear synchronous motor development - the Canadian program.

Proc. 1975 Cryogenic Engineering Conference, Kingston, 22-25, July 1975, Advances in Cryogenic Engineering, Vol.21, Plenum, paper A-1 p.1-8.

75.7.2

D Lancien, R Moulin, (SNCF)

Moteur lineaire synchrone a inducteur supraconducteur

RGE, Vol.84, No. 7/8, July-August 1975, p.553-64

75.7.3

R D Thornton (MIT)

Magnetic levitation and propulsion 1975

IEEE Trans. on Magnetics, Vol. MAG.11, No.4, July 1975, p.981-99

75.7.4

Warwick Maglev Group

Wolfson Magnetic Levitation Project

Progress report to July 1975

75.7.5

Y Kyotani (JNR)
Development of superconducting levitated trains in Japan.
Cryogenics, Vol.15, No.7, July 1975, p.372-6

75.7.6

H H Kolm, R D Thornton, Y Iwasa, W S Brown (MIT)
The Magneplane system
Ibid, p.377-84

75.7.7

R H Borcherts (Ford Motor Co)
Repulsion magnetic suspension research - US progress to date
Ibid p.385-93

75.7.8

D L Atherton, A R Eastham (Queen's Univ)
Canadian developments in superconducting Maglev and linear
synchronous motors
Ibid p.395-402

75.7.9

R G Rhodes, B E Mulhall (Warwick Univ)
The Wolfson magnetic levitation project
Ibid, Vol. 403-5

75.9.1

I Boldea (Poly Inst "TR VUIA") S A Nasar (Univ of Kentucky)
Thrust and normal forces in a segmented secondary linear reluctance
motor.
PIEE, Vol.122, No.9, September 1975, p.922-4

75.9.2

G Winkle (Transrapid - EMS)
Forschungs-und Entwicklungsstand der elektromagnetischen
Schwebetechnik in der Bundesrepublik Deutschland
ETZ-A, Vol.96, No.9, September 1975, p.367-73

75.9.3

A Lichtenberg (Siemens AG)
Elektrodynamisches Schweben in Fernverkehr der Zukunft
Ibid, p.378-83

75.9.4

C Albrecht (Siemens AG)
Elektrodynamische Trag-Führungs-systeme
Ibid p.383-90

75.9.5

J Holtz (Siemens AG)
Kraftkomponenten und deren betriebliche steuerung beim eisenlosen
Synchronlinearmotor
Ibid p.396-400

75.9.6

W Deleroi, P Grumbkow, H Weh (T U Braunschweig), U Feldmann,
P K Sattler (Inst fur Elektrische Maschinen der RWTH) G Kratz
(AEG-Telefunken), P Appun, H Buchberger, M Reutmeister (Siemens AG)
Kurzstator-Linearmotoren-stand und Entwicklung
Ibid p.401-9

75.9.7

H Weh (TU Braunschweig)
Synchroner Langstatorantrieb mit geregelten, anziehend wirkenden
Normalkraften
Ibid p.409-13

75.9.8

G R Slemon (Univ of Toronto)
The Canadian Maglev Project on High Speed Interurban transportation
Ibid p.1478-83

75.9.9

P C Sen (Queen's Univ)
On linear synchronous motors (LSM) for high speed propulsion
Ibid p.1484-6
See also 75.9.14

75.9.10

J P Howell, J Y Wong, R E Rhodes, B E Mulhall (Univ of Warwick)
Stability of Magnetically levitated vehicles over a split guideway
Ibid p.1487-9

75.9.11

Y Iwasa, W S Brown, C B Wallace (MIT)
An operational 1/25 scale Magneplane system with superconducting
coils.
Ibid p.1490-2

75.9.12

W S Brown (MIT)
The effect of long magnets on inductive maglev ride quality
Ibid, p.1498-1500

75.9.13

P E Burke (Univ of Toronto)
The use of stranded conductors to reduce eddy losses in guideway
conductors of high speed vehicles.
Ibid, p.1501-3

75.9.14

P C Sen (Queen's Univ)

On linear synchronous motor (LSM) for high speed propulsion
Tenth Annual Meeting of IEEE IAS Atlanta, 28 September-20 October 1975
IEEE Conference Record 1975, IEEE Publication No 75 CHO 999-31A.
Paper 10-E, p.261-7

75.9.15

N Maki, H Okuda, T Tatsumi (Hitachi Ltd) J Fujie, T Iwahana (JNR)
A combined system of propulsion and guidance by linear synchronous
motors.
Ibid, paper 42-D, p.956-63
See also 77.7.1

75.9.16

H Autruffe, D Lancien, R Moulin (SNCF)
Magnetic levitation studies at the SNCF
Rev.Gen.Chemins de Fer. Vol.94, No.9 September 1975, p.497-522

75.11.1

T Iwahana (JNR)
Study of superconducting magnetic suspension and guidance
characteristics on loop tracks.
IEE Trans on Magnetics Vol. MAG.11, No.6, November 1975, p.1704-11

76.0.1

Trans rapid - EMS
Gesellschaft fur elektromagnetische Schnellverkehrssysteme
Publicity folder

76.0.2

S A Nasar, I Boldea (Univ of Kentucky)
Linear Motion Electric Machines
Wiley-Interscience 1976

76.0.3

Allgemeine Elektrizitäts-Gesellschaft (AEG-Telefunken, Brown Boveri &
Cie, Siemens)
Spurgebundener Schnellverkehr mit berührungs freier
Fahrtechnik (Rapid rail transportation using non contact technology)
Proc. Fifth Statusseminar des Bundesministeriums für Forschungs und
Technologie, Bad Kissingen 1976

76.1.1

D J Dobbs, D Linder, D S Armstrong, R M Goodall, R J A Bevan,
M G Pollard, R W Barwick, R A Williams (British Rail)
Magnetically levitated and wheeled minitram comparison study
British Railways Board R & D Division Technical Report TR EDYN5,
January 1976.

76.1.2

J Holtz (Siemens AG)
Parameterabhängigkeit der Kräfte und der Betriebsreaktanz des
eisenlosen Synchronlinearmotors
Siemens Forsch und Entwicklungsber, Vol.5, No.1, January 1976,
p.39-46.

76.3.1

G E Dawson, C L Schwalm, E Unteregelsbacher (Queen's Univ)
A device to measure force angle of a linear synchronous motor.
Proc.1976 Industrial Electronics and Control Instrumentation Meeting
(IECI '76) Philadelphia, 8-10 March 1976, IEEE Publication No.76
CH 1117-1 IECI, New York, p.85-8.
See also 76.11.7.

76.3.2

D J Clarke, P C Sen (Queen's Univ)
A versatile three phase oscillator
Ibid p112-6.

76.3.3

Canadian Maglev Group
Superconducting linear synchronous motor propulsion and magnetic
levitation for high speed guided ground transportation
Interim Phase III Contract Report, CIGGT Report No 76-7, March 1976.

76.3.4

S Aiba, Y Amemiya (Nagoya Univ)
Tractive properties of DC linear motors under constant current
drive.
Electrical Engineering in Japan, Vol.96, No.2, March-April 1976,
p.23-9.

76.5.1

S L Wipf (Los Alamos Scientific Lab)
Propulsion of magnetically levitated trains
Cryogenics, Vol.16, No.5 May 1976, p.281-8

76.5.2

R G Rhodes, B E Mulhall (Univ of Warwick)
A superconducting maglev test facility for high speed transport.
Proc. Sixth International Cryogenic Engineering Conference, (ICEC6)
Grenoble, 11-14 May 1976, IPC Science & Technology Press, p.489-91.

76.5.3

W Mückli, D Rogg (Dornier System GmbH)
Research and Development in the field of high speed levitated
transportation in the Federal Republic of Germany
Second International Conf on Hovering Craft Hydrofoils and Advanced
Transit Systems, Amsterdam, 17-20 May 1976, p.1-9.

76.5.4

H Weh, H Mosebach, W Deleroi (TU Braunschweig)
Mechanical suspended vehicle with an active guideway
Ibid p.101-9

76.7.1

C Albrecht (Siemens AG) G Bohn (Transrapid-EMS)
Neue spurgeführte Transportmittel (Teil I).
Physikalische Blätter, Vol.32, No.7, July 1976, p.309-26
See 77.3.3 for Part II.

76.7.2

Anon
Development of power converter control system for linear motors
Technocrat, Vol.9 No.7 July 1976, p.57.

76.7.3

T Saijo (JNR)
Thrust and levitation force of linear synchronous motors for
propulsion and levitation use.
Electrical Engineering in Japan, Vol.96, No.4, July-August 1976,
p.67-74.

76.8.1

J Gibson, J Holtz, S Lingaya (Siemens AG)
Control of a linear synchronous motor for magnetically levitated
vehicles.
Proc. IFAC Symposium on Control in Transportation Systems, Columbus,
9-13 August 1976, p.143-51.

76.8.2

N Maki, H Okuda, K Nakamura (Hitachi Ltd)
Characteristics of linear synchronous motor for high speed
levitation trains.
Hitachi Review, Vol.25, No.8, August 1976, p.270.

76.9.1

Warwick Maglev Group
Wolfson Magnetic Levitation Project
Progress Report to September 1976.

76.9.2

C Albrecht (Siemens AG)
Development of levitated vehicles with superconducting magnets.
Second Conference on Advances in Magnetic Materials and their
Applications, London, 1-3 September 1976, IEE Conference Publication
No.142, p.113-6

76.9.3

E Abel, J L Mahtani, B E Mulhall, R G Rhodes (Univ of Warwick)
An assessment of linear superconducting motors for maglev.
Ibid, p.125-7

76.10.1

W J Holt, J A Ross (Rohr Industries Inc)
New developments in magnetic suspension and propulsion for
transportation.
IEEE Industry Applications Society Conference, Chicago, 11-14 October
1976, IEEE Catalogue No 76CH1122-1-IA, p.133-7.

76.10.2

C D English, G E Brown, (Spar Aerospace Products Ltd)
The linear induction motor propulsion system in urban transportation
Ibid p.138-54.

76.11.1

B E Mulhall, R G Rhodes (Univ of Warwick)
Sealed liquid helium cryostats for mobile superconducting
magnets
Cryogenics, Vol.16, No.11 November 1976, 682-3.

76.11.2

G R Slemon, S B Dewan, J Cunningham, R A Turton (Univ of Toronto)
D L Atherton, A R Eastham (Queens University)
Experimental results on a linear synchronous motor
IEEE Trans. on Magnetism, Vol. MAG-12, No.6, November 1976, p.873

76.11.3

S Yamamura (Univ of Tokyo)
Magnetic levitation technology of tracked vehicles present status
and prospect
Ibid p.874-8.

76.11.4

T Akinbiyi, P E Burke (Univ of Toronto) B T Ooi (McGill Univ)
A Comparison of ladder and sheet guideways for electrodynamic
levitation of high speed vehicles.
Ibid p.879-81.

76.11.5

P E Burke, T Akinbiyi (Univ of Toronto)
The design of flat ladder and coil guideway systems for high speed
trains
Ibid p.882-4.

76.11.6

G E Dawson, P C Sen, D J Clarke, S Lakhavani, (Queen's Univ)
Linear synchronous motor feedback controls
Ibid, p.885-8.

76.11.7

G E Dawson, C L Schwalm, E Unteregelsbacher (Queen's Univ)
A device to measure force angle of a linear synchronous motor
IEEE Trans on Industrial Electronics and Control Instrumentation,
Vol. IECI-2 No.4, November 1976, p.406-9. See also 76.3.1

76.12.1

T Hobara (JNR)
On research and development of levitation railway
Quarterly Reports of the Railway Technical Research Institute,
Vol.17, No.4, December 1976, 3 pages preceding p.145.

76.12.2

T Morii (JNR)
Development of guideway for levitated ground transportation.
Ibid p.145-50

76.12.3

T Fujimura, N Kataoka (JNR)
Power supply train control
Ibid p.151-56, 165.

76.12.4

H Yamashita (JNR)
Repulsive levitation and propulsion
Ibid p.157-65.

76.12.5

A Matsuura (JNR)
Dynamic property of guideway girder
Ibid p.166-9

76.12.6

T Saijo (JNR)
Power supply and control system for railway by linear synchronous
motor traction.
Ibid, p.170-3

76.12.7

M Miyamoto (JNR)
Motion characteristics of magnetically levitated vehicle
Ibid, p.174-7

76.12.8

T Iwahana (JNR)
Characteristics of superconducting magnetic suspension and guidance
on loop tracks.
Ibid p.178-81.

76.12.9

B E Mulhall (Warwick Univ) D H Prothero (IRD)
Protection of superconducting coil by means of secondary winding
Cryogenics, Vol.16, No.12, December 1976, p.705-8.

77.0.1

G Bogner (Siemens AG)
Large scale applications of superconductivity
NATO Advanced Study Institute Series B, Vol.21 Superconductor
Applications: SQUIDS and Machines, Plenum, New York 1977, Editors
B.B. Schwartz, S Foner, Chapter 20, p.547-737

77.0.2

Brush Electrical Machines Ltd
AC motors for traction
Publicity folder from BEM Traction Division 1977

77.0.3

Bundesministerium fur Forschungs und Technologie
Spurgeführter Fernverkehr, Magnetbahnentwicklung
(Guided track transportation, Maglev development).
Proc. Sixth Statusseminar, Constance, 1977.

77.0.4

Y Kyotani (JNR)
The current state of development of noncontacting suspension and
propulsion systems in Japan
Technical Development Department, JNR, 1977.

77.1.1

D L Atherton, A R Eastham (Queen's Univ), J A Cunningham, S B Dewan
G R Slemon, R A Turton (Univ of Toronto)
Superconducting linear synchronous motor tests
IEEE Trans on Magnetics, Vol. MAG-13, No.1 January 1977, p.776-9.

77.3.1

W Farrer (Brush Electrical Machines) R Davis (Nottingham Univ)
Linear synchronous motors investigated
Electronics & Power, Vol.23, No.3, March 1977, p.199

77.3.2

J F Eastham (Aberdeen Univ)
Iron cored linear synchronous machines
Ibid p.239-42.

77.3.3

C Albrecht (Siemens AG), G Bohn (Transrapid-EMS)
Neue spurgeführte Transportmittel (Teil II)
Physikalische Blätter, Vol.33, No.3, March 1977, p.103-18
See 76.7.1 for Part I.

77.4.1

D L Atherton, J A Cunningham, S B Dewan, A R Eastham, G R Slemon,
R A Turton (Queen's and Toronto Univ)
Design, analysis and test results for a superconducting linear
synchronous motor
Proc. IEE, Vol.124, No.4, April 1977, p.363-72.

77.4.2

W Leonhard (TU Braunschweig)
Technische Alternativen bei der Magnetschwebbahn
VDI Nach No.15, 15 April 1977, p.42-3
See also 78.4.2.

77.4.3

Anon
German trans-Europe maglev train experiment on time
Electrical Review, vol.200, No.16, 22 April 1977, p.9

77.5.1

D L Atherton, A R Eastham (Queen's Univ)
Propulsion requirements for high speed vehicles with electrodynamic
suspension
IEEE Trans on Industry Applications, Vol. IA-13, No.3, May/June 1977
p268-73.
See also 74.10.1

77.6.1

R W Crosby, R J Ravera (US Dept of Transportation)
The transportation advanced research projects program-an overview
1977 Joint Automatic Control Conf. San Francisco, 22-4 June 1977
IEEE E Publ.No. 77CH 1220-3CS, p.472-80

77.6.2

P R Belanger, R Guillemette (McGill Univ)
Passive suspension design for a magnetically levitated vehicle
Ibid p.1476-86.
See also 77.12.1

77.6.3

S Kawase, T Kawamura, S Fujimori (JNR)
Open loop control of linear thyristor motor
Quarterly Reports of the Railway Technical Research Institute,
Vol.18, No.2, June 1977, p.81-2.

77.7.1

N Maki, H Okuda, T Tatsumi (Hitachi Ltd) J Fujie, T Iwahana (JNR)
A combined system of propulsion and guidance by linear synchronous
motors.
IEEE Trans on Power Apparatus Systems, Vol. PAS-96, No.4, July/
August 1977, p.1109-1116
See also 75.9.15

77.4.1

D L Atherton, J A Cunningham, S B Dewan, A R Eastham, G R Slemon,
R A Turton (Queen's and Toronto Univ)
Design, analysis and test results for a superconducting linear
synchronous motor
Proc. IEE, Vol.124, No.4, April 1977, p.363-72.

77.4.2

W Leonhard (TU Braunschweig)
Technische Alternativen bei der Magnetschwebbahn
VDI Nach No.15, 15 April 1977, p.42-3
See also 78.4.2.

77.4.3

Anon
German trans-Europe maglev train experiment on time
Electrical Review, vol.200, No.16, 22 April 1977, p.9

77.5.1

D L Atherton, A R Eastham (Queen's Univ)
Propulsion requirements for high speed vehicles with electrodynamic
suspension
IEEE Trans on Industry Applications, Vol. IA-13, No.3, May/June 1977
p268-73.
See also 74.10.1

77.6.1

R W Crosby, R J Ravera (US Dept of Transportation)
The transportation advanced research projects program-an overview
1977 Joint Automatic Control Conf. San Francisco, 22-4 June 1977
IEEE E Publ.No. 77CH 1220-3CS, p.472-80

77.6.2

P R Belanger, R Guillemette (McGill Univ)
Passive suspension design for a magnetically levitated vehicle
Ibid p.1476-86.
See also 77.12.1

77.6.3

S Kawase, T Kawamura, S Fujimori (JNR)
Open loop control of linear thyristor motor
Quarterly Reports of the Railway Technical Research Institute,
Vol.18, No.2, June 1977, p.81-2.

77.7.1

N Maki, H Okuda, T Tatsumi (Hitachi Ltd) J Fujie, T Iwahana (JNR)
A combined system of propulsion and guidance by linear synchronous
motors.
IEEE Trans on Power Apparatus Systems, Vol. PAS-96, No.4, July/
August 1977, p.1109-1116
See also 75.9.15

77.8.1

E Abel, J P Howell, J L Mahtani, R G Rhodes, (Univ of Warwick)
Design criteria for rectangular superconducting coils for transport applications.
Proc.Sixth International Conference on Magnet Technology (MT-6)
Bratislava, 29 August-2 September 1977, p.163-171.

77.8.2

C Albrecht (Siemens AG)
Experience with superconducting magnets for levitating the 17 tons test carrier EET at 150km/h.
Ibid p.177-82

77.8.3

M E Hunt, R G Rhodes, (Univ of Warwick)
Power losses in superconducting multifilamentary composites
Ibid p.738-42.

77.9.1

W F Hayes (NRC Canada)
High speed electrodynamic maglev guided ground transportation system conceptual design study final report, March 1976-September 1977.
Report No LTR-CS-176 for Transport Canada, September 1977.

77.9.2

H Weh (TU Braunschweig) M Shalaby (Al-Azhar-Univ)
Magnetic levitation with controlled permanent excitation.
IEEE Trans on Magnetics, Vol MAG.13 No.8, Sept 1977, p.1409-11

77.9.3

P E Burke, S Kuntz, G R Slemon, (Univ of Toronto)
A dual linear synchronous motor for maglev vehicles
Ibid p.1415-7

77.9.4

E Levi.L Birenbaum, Z Zabar (Poly Inst of New York)
Concerning the design of inductor synchronous motors fed by current source inverters.
Ibid p.1421-3

77.9.5

B-T Ooi (McGill Univ)
Homopolar linear synchronous motor dynamic equivalents
Ibid p.1424-6

77.9.6

Canadian Maglev Group
The Canadian high speed magnetically levitated vehicle system
Phase III Contract Summary Report, CIGGT Report No 77-12, September 1977.

77.10.1

S P Bernard, D L Atherton (Queens Univ)
High efficiency flux pump power supply using inductive current transfer
Rev.Sci.Instrum.Vol.48, No.10, October 1977, p.1250-2

77.10.2

G K O'Neill (Princeton Univ) H H Kolm (MIT)
Mass driver for lunar transport and as a reaction engine
J Astronautical Sciences, Vol.25, No.4, October-December 1977
p.349-63

77.10.3

B Boning (TU Braunschweig)
Microcomputer based data acquisition and propulsion control for a track powered linear synchronous motor for high speed ground transportation
Proc.Second IFAC Symposium on Control in Power Electronics and Electrical Drives, Dusseldorf, 7-9 October 1977, p.827-33

77.11.1

G E Dawson, C L Schwalm (Queen's Univ)
Microcomputer data system for Maglev test facility.
Proc.International Symp.on Mini and Micro Computers, Montreal
11-18 November 1977, IEEE Publication No 77CH134-4C, p.189-93.

77.12.1

P R Belanger, R Guillemette (McGill Univ)
Passive suspension design for a magnetically levitated vehicle
Trans ASME, J.Dyn.Syst.Meas & Control, Vol.99 No.4, December 1977
See also 77.6.2.

78.0.1

Konsortium Magnetbahn Transrapid
Im Jahr 1835 War es Nurnberg-Furth. Heute ist es Lathen-Dorpen
Das Emsland macht Bahngeschichte.
Publicity Leaflet, 1978.

78.0.02

D V Sveharnik
Scope for linear electric drives on electric rolling stock and problems in application
Electric Technology USSR, No.4, 1978, p.69-82

78.0.3

E Levi (Poly Inst of New York)
Linear Propulsion
Standard handbook for Electrical Engineers, 11th Edition
McGraw Hill, 1978, p.23-104 - 23-120

78.0.4

M Guarino (US Dept of Transportation)
Development of the linear motor in the United States, past, present and future.
Proc. Seventh Annual Statusseminar on Guided Ground Transportation, for BMFT, Willingen, 1978.

78.0.5

E Levi (Poly Institute of New York)
Development of the design for iron-cored synchronously operating linear motors.
Ibid

78.0.6

V D Nene (Mitre Corp)
Mitre propulsion work under FRA sponsorship
Ibid

78.0.7

Bundesministerium fur Forschungs und Technologie
Proc. Seventh Statusseminar on Guided Ground Transportation Willingen, 1978

78.1.1

A Hayashi (Japan Air Lines)
HSST: a viable alternative for rapid airport-city centre transportation
ICAO Bulletin, January 1978, 0.21-4

78.1.2

E Abel
A study of the power consumption of German Maglev passenger vehicles (EDS and EMS)
Warwick Maglev Group, Internal Memo, January 1978.

78.1.3

T Umemori (JNR)
Construction and characteristics of linear thyristor motors
Electrical Engineering in Japan, Vol.98, No.1, January-February 1978 p.28-36

78.1.4

T Umemori (JNR)
Power supply and control of linear thyristor motors
Electrical Engineering in Japan, Vol.98, No.1, January-February 1978 p.96-105

78.1.5

G Sobolewski, D Gilmore (Canadair Services Ltd)
An interim report on the development of a light steerable axle truck for rail passenger vehicles
Proc. Biennial CIGGT Seminar on Railway Research "The Eighties: A New Rail Era" Kingston, 29-30 January 1978, CIGGT Report No.78-5.

78.1.6

G E Brown (Spar Aerospace Products Ltd)
Linear induction motors for intermediate capacity transit systems
Ibid p.173-8

78.1.7

G R Slemon (Univ of Toronto)
Linear synchronous motor propulsion for urban systems
Ibid p.179-87

78.1.8

N E Rudback (Transport Canada) W F Hayes (NRC) A R Eastham (CIGGT)
Status of magnetically levitated high speed guided ground
transportation
Ibid p.399-418

78.2.1

Wolfson Magnetic Levitation Group
The electrodynamic system of levitation and LSM propulsion
Dept of Engineering, Univ of Warwick, 24 February 1978

78.3.1

H J Dull, C P Parsch (Siemens AG) F Vegelaun (AEG Telefunken)
H Wiechens (Siemens AG)
Der eisenlose Synchronlinearmotor als Fahrzeugantrieb in einem
neuartigen Schnellverkehrssystem
ETR Vol.27, No.3, March 1978, p.143-50

78.3.2

J D Edwards, A M El-Antably (Univ of Sussex)
Segmental-rotor linear reluctance motors with large airgaps
Proc. IEE, Vol.125, No.3, March 1975, p.209-14

78.3.3

P Klocker, C P Parsch (Siemens AG)
ROSY, ein Rotationsprufstand zum Erproben des eisenlosen
Synchronlinearmotors
Siemens Zeitschrift, Vol.52, No.3, March 1978, p.108-113 See also
78.10.1

78.3.4

J P Gibson, S Lingaya (Siemens AG Erlangen)
Regaleinrichtung fur den eisenlosen Synchronlinearmotor
Ibid p.113-7. See also 78.10.2.

78.3.5

T Saijo (JNR)
Control system of cycloconverter for linear synchronous motors
Electr. Eng Jpn, Vol.98, No.2, March-April 1978, p.45-52.

78.3.6

S Okuma, Y Amemiya (Nagoya Univ)
Stability and its improvement of combined propulsion and guidance
system for high speed trains.
Electrical Engineering in Japan, Vol.98, No.2. March-April 1978
p.61-9

78.4.1

Anon
JNR tests dc linear motor
Railway Gazette International, Vol.134, No.4, April 1978, p.219

78.4.2

W Leonhard (TU Braunschweig)
Technical alternatives for a maglev system
Electronics & Power, Vol.24, No.4 April 1978.
Transl. of VDI Nach, No.15, 15 April 1977, p.42-3, by R G Rhodes
and J H Rakels (Univ of Warwick)
See also 77.4.2

78.4.3

D L Atherton, G E Dawson, A R Eastham (Queens Univ) P R Belanger,
B T Ooi, P Silvester (McGill Univ), P E Burke, G R Slemon (Univ of
Toronto) W F Hayes (NRC)
The Canadian high speed magnetically levitated vehicle system
Canadian Electrical Engineering Journal, Vol.3, No.2 April 1978,
p.3-26.

78.5.1

W Farrer (Brush Electrical Machines)
Linear Induction Motors, IEE Discussion Meeting, London 25 May 1978

78.5.2

J S Chahal (Brush Electrical Machines)
Ibid

78.7.1

S Kuntz (Garrett-AiResearch) P E Burke, G R Slemon (Univ of Toronto)
Active damping of maglev vehicles using superconducting linear
synchronous motors.
Electrical Machines and Electromechanics, Vol.2, No.3
July-September 1978, p.371-84.

78.7.2

T Umemori (JNR), M Kawashima, (Sumitomo Electric Industries Ltd)
M Oda, (Furukawa Electric Co Ltd) S Ohsawa (Hitachi Cable Ltd)
Development of DC linear motor (I) - fundamental construction and
feasibility
IEEE Power Engineering Society Summer Meeting, Los Angeles 16-21
July 1978, paper F 78 757-7, p.1-9
and also as IEEE Trans Vol. PAS-98, No.4, July-August 1979, p.1456-
65

78.7.3

T Umemori (JNR) Y Hosoda (Sumitomo Electric Industries, Ltd)
M Iwasaki (Furukawa Electric Co Ltd) M Toyoshima (Hitachi Cable Ltd)
Development of a DC linear motor (II) - research for a ground
coil and field magnet
Ibid, paper F78 756-9, p.1-9
Also as IEEE Trans Vol. PAS-98, No.5, September-October 1979,
p.1786-95

78.9.1

E Abel, R G Rhodes (Univ of Warwick)
Power consumption for alternative maglev systems
Electronics & Power, Vol.24, No.9, September 1978, p.673-4

78.9.2

E Abel, J L Mahtani, R G Rhodes (Univ of Warwick)
Linear machine power requirements and system comparisons
IEEE Trans on Magnetics Vol MAG.14, No.5, Sept 1978,
p.918-20

78.9.3

G R Slemon, P E Burke, N Terzis (Univ of Toronto)
A linear synchronous motor for urban transit using rare
earth magnets
Ibid p.921-4

78.9.4

T R Haller, W R Mischler (General Electric Co)
A comparison of linear induction and linear synchronous motors for
high speed ground transportation
Ibid, p.924-6.

78.9.5

E Levi, J P Lee, F Lalezari, M Gamalos (Poly Inst of New York)
Computer-aided conformal mapping of magnetic fluxes in saturated
inductor motors
Ibid p.927-9.

78.9.6

A Lang (Transrapid EMS)
Propulsion systems for magnetically suspended vehicles
Proc. International Conf on Electrical Machines, Brussels,
11-13 Sept 1978, p. L3/3-1-10

78.9.7

M Reutmeister (TU Graz)
Comparison between asynchronous and synchronous linear motor of
short stator construction
Ibid, p.L3/5-1-11

78.9.8

J S Chahal (Brush Electrical Machines Ltd)
Linear reluctance machines for urban transport
Ibid, p L4/1-1-10

78.9.9

S Lingaya, C P Parsch (Siemens AG)
Characteristics of the force components of an air cored linear
synchronous motor with superconducting excitation magnets.
Ibid, p.L4/2-1-11

78. 9.10

C P Parsch (Siemens AG) G Wiegner (BBC)
The air cored linear synchronous motor: the state of the art
in Erlangen
Ibid p.L4/3-1-13

78.9.11

G R Slemon (Univ of Toronto)
A homopolar linear synchronous motor
Ibid p. L4/4-1-10

78.9.12

H Weh, H Mosebach, M May (TU Braunschweig)
Design and technology of the iron core linear synchronous motor for
advanced ground transportation
Ibid p L4/5-1-10

78.9.13

B Boning, W Leonhard (TU Braunschweig)
Propulsion control of a track powered linear synchronous motor
for a magnetically levitated vehicle on the basis of power
measurement in the inverter station.
Ibid, p L5/1-1-9

78.9.14

U Claussen, W Leonhard (TU Braunschweig)
Microprocessor controlled linear synchronous motor as positioning
drive
Ibid p L5/2-1-9

78.9.15

H Yamashita (JNR)
Progress of research and development on repulsive levitation railway
in JNR
Q.Rep Railw Tech Res.Inst.Vol.19, No.3, September 1978, p.99-105.

78.9.16

R Zurek (Transrapid-EMS)
Methods of levitation for tracked high speed traffic,
Endeavour, Vol.2, No.3 1978, p.108-14.

78.10.1

P Klocker, C P Parsch (Siemens AG)
Rosy, a rotating test rig for air-cored linear synchronous motors.
Siemens Rev. Vol.45 No.10, October 1978, p.434-9
See also 78.3.3

78.10.2

J P Gibson, S Lingaya (Siemens AG)
Control system for air-cored linear synchronous motors
Ibid p.439-43
See also 78.3.4

78.10.3

J P Gibson, C P Parsch (Siemens AG)
The air cored linear synchronous motor as a drive for
magnetically levitated vehicles
IEEE-IAS Annual Meeting Toronto 1-5, October 1978, p.337-44

78.10.4

H Weh, H May (TU Braunschweig)
Permanent magnetic excitation of rotating and linear
synchronous machines
J Magn & Magn.Mater. Vol.9, No1-3, October-November 1978 p173-8

78.11.1

C P Parsch, G Wiegner (Siemens AG)
The air cored linear synchronous motor: the state of the art
in Erlangen
International Symposium on Superconductive Magnetic Levitated
Trains Miyazaki, 9-10 November 1978.

78.11.2

R G Rhodes (Univ of Warwick)
The superconductive magnetic train in Japan
Report on a visit to Japan, November 1978

78.12.1

E Abel
A cooperative research programme to investigate the application of
air cored linear synchronous machines to advanced ground transport
Warwick Maglev Group unpublished memo December 1978

78.12.2

D A Young
Soviets drawn to magnetic train
Industrial Research/Development Vol.20, No.12, December 1978, p.52

79.1.1

E Abel
Linear synchronous machines as traction drives for trains
Warwick Maglev Group unpublished memo, January 1979.

79.1.2

R G Rhodes, E Abel, J L Mahtani (Univ of Warwick)
Magnetic levitation and linear motor propulsion for high speed vehicles
Report to the Science Research Council, January 1979

79.1.3

G Bogner (Siemens AG)
Applied superconductivity activities at Siemens
IEEE Trans. on Magnetism, Vol. MAG-15, No.1, January 1979, p.824-7.

79.1.4

N Borg (Farebrother & Partners)
Discussion on a possible co-operative research programme for the
investigation of a linear synchronous motor propulsion system for
advanced ground transport.
Notes on meeting between Univ of Warwick, British Rail, BICC,
Balfour Beatty, Brush Electrical Machines, Farebrother & Partners.
Derby 31 January 1979.

79.2.1

H May, M Shalaby, H Weh (TU Braunschweig)
Design of controlled permanent magnets for levitation, guidance
and drive applications.
ETZ-A No.2, February 1979, p.63-7.

79.3.1

G Kratz (BMFT)
Der Linearmotor in der Antriebstechnik
Techn.Mitt AEG-Telefunken, Vol.69, No.3, March 1979 p.65-73

79.4.1

Japan Air Lines
Development of the Japan Air Lines High Speed Surface Transport.
HSST Information, Japan Air Lines, April 1979.

79.4.2

W Cramer (MBB)
Design criteria of magnetic levitation systems for high speed
vehicles.
Colloquium on Advanced Ground Transportation Schemes, London, 18 April
1979, IEE Digest No 1979/27, p. 1.1-1.6.

79.4.3

S Nakamura (JAL)
Development of the HSST
Ibid p.2.1-2.4

79.4.4

C P Parsch, J P Gibson (Siemens AG)
The air cored linear synchronous motor : basic operation and test
facilities in Erlangen.
Ibid p.3.1-3.4

79.4.5

M J Balchin (Univ of Bath)

Operating Characteristics of a heteropolar linear synchronous motor

Ibid p.4.1-4.4

79.4.6

A J Davis, J S Chahal, W Farrer (Brush Electrical Machines Ltd)

A study of linear synchronous motors at Brush Electrical Machines Ltd

Ibid p 5.1-5.4

79.4.7

J S Chahal, A J Davis, (Brush Electrical Machines Ltd)

A study of linear reluctance machines at Brush Electrical Machines Ltd.

Ibid p.5.5-5.8

79.4.8

R M Davis, S A E El-Drieny, D J Rhodes (Univ of Nottingham)

Linear synchronous motor design and performance

Ibid p 6.1-6.5

79.4.9

R G Rhodes (Univ of Warwick) E Abel (UKAEA), J L Mahtani

J H Rakels (Univ of Warwick)

The superconducting LSM for vehicle propulsion.

Conference on Superconducting Electrical Machines, Oxford
19-20 April 1979, paper No.19.

79.4.10

Anon

Maglev to take off at Hamburg/French may revive Aerotrain

Electrical Review, Vol.204, No.16, 27 April 1979, p.5.

79.5.1

P Hartmann (Dornier-System), H Schulz (BMFT)

Versuchs- und Demonstrationsanlage Magnetbahn zur Internationalen

Verkehrsausstellung 1979 (IVA '79) in Hamburg

Elektrische Bahnen Vol.77, No.5, May 1979, p.117-22

79.5.2

D J Frenzel (BMFT), H P Neubaur (Dornier System)

Versuchsanlage Magnetbahn in Emsland

Ibid p 122-6

79.5.3

S Nakamura, A Hayashi (Japan Air Lines)

Development of HSST system

Japan Air Lines, May 1979

79.5.4

T Saijo (JNR)

Feeder Sectioning of linear synchronous motors for high speed railway
Electrical Engineering in Japan, Vol.98, No.3, May-June 1979 p51-9.

79.6.1

High speed ground transport for 21st century

Electric Review International Vol.204, No.22, 8 June, 1979, p12-13

79.7.1

G R Slemon (Univ of Toronto)

An experimental study of a homopolar linear synchronous motor.

Electr.Mach & Electromech. Vol.4, No.1, July-August 1979, p.59-70.

79.8.1

P Klocker (Siemens AG)

Der eisenlose Synchronlinearmotor-ein Antrieb für
Schnellverkehrsmittel.

Elektrotechnik, Vol.61, No. 15/16, 24 August 1979, p.12-16

79.9.1

D L Atherton (Queen's Univ)

Shunt protection for superconducting maglev magnets

Cryogenics, Vol.19, No.9, September 1979, p 537-41.

79.9.2

S Lingaya, C P Parsch (Siemens AG)

Characteristics of the force components of an air cored linear
synchronous motor with superconducting excitation magnets

Electric Machines and Electromechanics, Vol.4, No2-3,
September-October 1979, p.113-23.

79.9.3

G Wiegner (BBC)

Magnetschwebbahn - Grosversuch mit einem synchronen Langstatormotor

BBC Nachr Vol.61, No.9, September 1979, p.311-9.

79.9.4

Anon

JNR's Linear Motorcar

Technocrat, Vol.12, No.9, September 1979 p.68.

79.9.5

P Lindon, G Williams, P D Luke, A M El-Antably, J D Edwards
(Univ of Sussex)

Closed loop control of linear reluctance motors for traction
applications.

Proc.Second International Conference on Electrical Variable Speed
Drives, London 25-27 September 1979, IEE Conf.Publ.NO.179, p191-5.

79.9.6

D B Charchas (Univ of Toronto)
A dynamics simulation for a high speed magnetically levitated
guided ground vehicle
Trans ASME, J.Dyn.Syst.Meas & Control, Vol.101, No.3, September 1979
p223-9.

79.11.1

B K Bose, (General Electric Co) T A Lipo (Purdue Univ)
Control and simulation of a current fed linear inductor machine
IEEE Trans. on Industry Applications, Vol. IA-15, No.6, November/
December 1979, p.591-600.

79.11.2

T Ohtsuka (Tohoku Univ) Y Kyotani (JNR)
Superconducting maglev tests
IEEE Trans on Magnetics, Vol.MAG-15, No.6, November 1979, p1416-21

79.11.3

H Weh (TU Braunschweig)
Linear synchronous motor development for urban and rapid transit
systems.
Ibid, p.1422-7.

79.11.4

S Nakamura (Japan Air Lines)
Development of high speed surface transport system (HSST)
Ibid p.1428-33.

79.11.5

S Nakamura, Y Takeuchi, M Takahashi (Japan Air Lines)
Experimental results of the single sided linear induction motor
Ibid p.1434-6.

79.11.6

R M Katz (Mitre Corp) A R Eastham, G E Dawson, D A Atherton
C L Schwalm (CIGGT)
Integrated magnetic suspension and propulsion of guided ground
transportation vehicles with a SLIM.
Ibid p.1437-9.

79.11.7

A M El-Antably, J D Edwards, G Williams, P Lindon, P D Luke
(Univ of Sussex)
Steady state performance characteristics of linear reluctance motors
Ibid p.1440-2

79.11.8

J H Parker (Urban Transportation Development Corporation Ltd)
G E Dawson (Queen's University on leave to Canadair Services Ltd)
LIM propulsion system development for transit.
Ibid p.1443

79.11.9

P E Burke (Univ of Toronto)

The design of reinforcing steel systems for maglev guideways
Ibid p.1497-9.

79.12.1

M J Balchin, J F Eastham (Univ of Bath)

Characteristics of a heteropolar linear synchronous machine with
passive secondary.

IEE J.Electr.Power Appl. Vol.2, No.6, December 1979, p.213-8

80.1.1

Anon

504 Km/h was attained

Technocrat, Vol.13, No.1, January 1980, p.69.

80.1.2

D L Atherton (Queens Univ)

Maglev using permanent magnets

IEEE Trans. on Magnetics, Vol. MAG.16, No.1. January 1980,
p.146-8

80.1.3

T A Nondahl (General Electric Co)

Design studies for single sided linear electric motors : homopolar
synchronous and induction.

Electric Machines & Electromechanics, Vol.5, No.1, January-February
1980, p.1-14.

80.2.1

C P Parsch (Siemens AG)

Private communication 20 February 1980.

80.2.2

C J Adriance (Boeing Aerospace Co)

Guest Editorial

IEEE Trans on Vehicular Technology, Vol VT.29, No.1, February 1980,
p1-2.

80.2.3

K Glatzel, G Khurdok, D Rogg (Dornier System GmbH)

The development of the magnetically suspended transportation system
in the Federal Republic of Germany)

Ibid p.3-17.

80.2.4

E Gottzein, R Meisinger, L Miller (MBB)

The "magnetic wheel" in the suspension of high speed ground
transportation vehicles.

Ibid p.17-23.

80.2.5

P A A Koerv (MBB)

Control systems for operating the long stator maglev vehicle TR05
Ibid p.23-34

80.2.6

Y Hikasa, Y Takeuchi (Japan Air Lines)

Detail and experimental results of ferromagnetic levitation
system of Japan Air Lines HSST-01/02 vehicles
Ibid p.35-41

80.2.7

R E Rule, R G Gilliland (Boeing Aerospace Co)

Combined magnetic levitation and propulsion the Mag-Transit concept
Ibid p.41-9.

80.2.8

R D Fruechte, R H Nelson, T A Radomski (General Motors)

Power conditioning systems for a magnetically levitated test
vehicle

Ibid p.50-60.

Also IEEE Power Electronics Specialists Conference Record, June 1977
IEEE Publ.No.77CH1213-8AES

80.2.9

R M Katz (Mitre Corp) A R Eastham (Queen's Univ), G E Dawson,
D L Atherton, C L Schwalm (CIGGT)

Integrated magnetic suspension and propulsion of guided ground
transportation vehicles with a SLIM

Ibid p.61-4.

80.2.10

J J Stickler (US Dept of Transportation)

Comparison of theories for high speed linear induction motors
Ibid p.65-71

80.2.11

T M Barrow (US Dept of Transportation)

Comparison of combined versus separate lift/propulsion systems
Ibid p.71-80.

80.3.1

K Glatzel (Dornier System GmbH) H Schulz (BMFT)

Transportation: the promise of maglev
IEEE Spectrum, Vol.17, No.3, March 1980, p.63-6.

80.3.2

Y Sato, S Kishimoto, S Miura, K Takeshita (JNR)

Tolerance of Guideway Irregularity and its Control on the
Miyazaki Test Track

Quarterly Reports of the Railway Technical Research Institute, Vol.
21, No.1, March 1980 p1-8

80.3.3

J Mizuno (JNR)
Theoretical Performance of Synchronous Motor Generator
Interconnected with Power System to variable load
Ibid p.9-14

80.3.4

T Saijo (JNR)
Power Feeding Characteristics of Ground Primary Type Linear Motor
Railway
Ibid p15-21

80.3.5

T Umemori (JNR)
Construction and Characteristics of DC Linear Motor
Ibid p22-8

80.3.6

T Sasaki (JNR)
Application of Train Detector using Inductive Wires to Feeder
Sectioning Control.
Ibid p29-34.

80.3.7

H Nakashima, T Herai (JNR)
Cooling Characteristics of Super Conducting Magnet Cooled with the
Helium Refrigerator
Ibid p35-9

80.3.8

S Yasukawa, S Yuda (JNR)
A Linear Synchronous Motor Control Method and its Feasibility
Ibid p40-3

80.3.9

M Miyamoto (JNR)
A Dynamic Response of Magnetically Levitated Flexible Vehicle to
Random Track Irregularities
Ibid p44-8

80.3.10

S Fujwara (JNR)
Damping Characteristics of the Repulsive Magnetic Levitation Vehicle
Ibid p49-52

80.3.11

K Kasai
Test Results in the Miyazaki Test Track for Magnetic Levitation
Vehicle
Ibid p53-6

80.4.1

E J Lerner

Superconductivity : will its potential be realized?
High Technology, Vol.1, No.3 April 1980 p64-71

80.5.1

J Ideguchi (Japan Air Lines)

Personal communication, 7 May 1980

80.7.1

P Mnich (TUV Rheinland), K D Hubner (TU Braunschweig)
Tragkraftschwankungen bei Magnetschwebefahrzeugen mit
integrierten synchronem Linearantrieb und ihre sicherheitstechnische Bedeutung.
Archiv fur Elektrotechnik, Vol.62, No.4-5, July 1980, p301-8

80.9.1

A K Wallace (Canadair Services Ltd) J H Parker (UTDC) G E Dawson
(Queen's Univ)
Slip control for LIM propelled transit vehicles
IEEE Trans on Magnetics, Vol. MAG.16 No.5, September 1980, p710-2

80.9.2

T Umemori (JNR) S Kumazawa, Y Furuto, T Kamoshida (Furukawa Electric Co)
Study on miniaturization of electromagnet for DC Linear Motor
Ibid p713-5.

80.9.3

H H Kolm, P Mongeau, F Williams (MIT)
Electromagnetic launchers
Ibid p719-21

80.9.4

A R Eastham (Queens Univ) R M Katz (Mitre Corp)
The operation of a single sided linear induction motor with squirrel cage and solid steel reaction rails
Ibid p722-4

80.10.1

Anon

Metro-Cammell catches the Canadian connection
Engineering Today Vol.4, No.39, 21 October 1980, p.15

81.3.1

Anon

Maglev Drives for a \$100M Export Market
Ibid Vol.5, No.8, 2 March 1981, p.8.

5.2 Author Index

A

Abel E	74.5.20, 74.8.1, 74.9.3, 74.10.11, 76.9.3, 77.8.1, 78.1.2, 78.9.1, 78.9.2, 78.12.1, 79.1.1, 79.1.2, 79.4.9
Adriance J	80.2.2
Aiba, S	74.9.10, 76.3.4.
Akinbiyi T	76.11.4, 76.11.5
Akiyama S	72.9.3
Albrecht C	73.11.3, 74.5.4, 75.9.4, 76.7.1, 76.9.2, 77.3.3 77.8.2
Allen J	74.0.1
Allen M P	72.4.1
Alston I A	72.5.7, 72.12.2, 73.8.1
Amemiya Y	74.9.10, 76.3.4, 78.3.6
Appun P	75.9.6
Arima K	74.5.14, 74.5.15
Armstrong D S	76.1.1
Asagoe Y	71.9.1
Asztalos St	74.5.6
Atherton D L	72.2.1, 72.5.5, 72.12.3, 74.3.1, 74.5.8, 74.6.2, 74.9.6, 74.10.1, 75.3.8, 75.7.1, 75.7.8, 76.11.2, 77.1.1, 77.4.1, 77.5.1, 77.10.1, 78.4.3, 79.9.1, 79.11.6, 80.1.2, 80.2.9
Autruffe H	75.4.2, 76.9.16

B

Bachelet E	12.0.1, 12.10.1
Balchin M J	79.4.5, 79.12.1
Baldus W	74.5.6
Barrows T M	80.2.11
Barwell F T	69.5.1
Barwick R W	76.1.1
Begley R F	74.2.1
Belanger P R	77.6.2, 77.12.1
Bernard S P	77.10.1
Bevan R J A	76.1.1
Birenbaum L	77.9.4
Bogner G	70.5.1, 77.0.1, 79.1.3
Bohn G	76.7.1, 77.3.3
Boldea I	75.9.1, 76.0.2.
Bolton H R	71.12.1
Bond A W	74.10.6
Boning B	77.10.3, 78.9.13
Boom R W	69.4.1
Borcherts R H	73.5.1, 73.7.1, 74.5.3, 75.3.5, 75.7.7
Borg N	79.1.4
Bose B K	79.11.1
Brown G E	76.10.2, 78.1.6
Brown W S	75.7.6, 75.9.11, 75.9.12
Buchberger H	75.4.1, 75.9.6
Burke P E	74.9.8, 74.9.9, 74.10.8, 75.9.13, 76.11.4, 76.11.5, 77.9.3, 78.7.1, 78.9.3, 79.11.9
Byer R L	74.2.1

C

Chahal J S	78.5.2, 78.9.8, 79.4.6, 79.4.7
Cherchas D B	79.9.6
Chilton F	72.5.2
Chu R S	75.3.7
Clark J M	72.12.2
Clarke D J	76.3.2, 76.11.6
Claussen U	78.9.14
Coffey H T	75.5.2, 73.8.3
Corbett A E	74.10.11
Cramer W	79.4.2
Crosby R W	77.6.1
Cunningham J	76.11.2, 77.1.1, 77.4.1

D

Danby G R	66.11.1, 69.9.1, 71.6.2, 71.8.1, 72.5.4
Dannan J H	73.5.7
Davis A J	79.4.6, 79.4.7
Davis L C	73.5.1, 73.7.1
Davis R M	77.3.1, 79.4.8
Dawson G E	74.5.21, 76.3.1, 76.11.6, 76.11.7, 77.11.1 79.11.6, 79.11.8, 80.2.9, 80.9.1
Day R N	73.5.7
Deleroi W	75.9.6, 76.5.4
Dewan S B	74.5.1, 74.10.8, 76.11.2, 77.1.1, 77.4.1
Dobbs D J	76.1.1
Downey T	69.4.1
Dull H J	78.3.1

E

Eastham A R	71.12.2, 72.4.1, 74.3.1, 74.5.8, 74.6.2, 74.9.6., 74.10.1, 75.3.8, 75.7.1, 75.7.8, 76.11.2, 77.1.1, 77.4.1, 77.5.1, 78.1.8, 79.11.6, 80.2.9, 80.9.4
Eastham J F	71.12.1, 74.10.13, 77.3.2, 79.12.1
Edwards J D	78.3.2, 79.9.5, 79.11.7
Ehrenfried C E	71.11.4
El-Antably A M	78.3.2, 79.9.5, 79.11.7
El-Drieny S A E	79.4.8
Elsel W	74.5.4
English C D	76.10.2

F

Farrer W	77.3.1, 78.5.1, 79.4.6
Feldmann U	75.9.6
Fellows T G	71.12.1, 74.3.3
Fink H J	69.4.1
Forgacs R L	73.5.5
Forsythe J B	73.3.2
Franken H	74.5.4
Frenzel D J	79.5.2
Fruechte R D	80.2.8
Fujie J	74.10.7, 75.9.15, 77.7.1
Fujimori S	77.6.3
Fujimura T	76.12.3

C

Chahal J S	78.5.2, 78.9.8, 79.4.6, 79.4.7
Cherchas D B	79.9.6
Chilton F	72.5.2
Chu R S	75.3.7
Clark J M	72.12.2
Clarke D J	76.3.2, 76.11.6
Claussen U	78.9.14
Coffey H T	75.5.2, 73.8.3
Corbett A E	74.10.11
Cramer W	79.4.2
Crosby R W	77.6.1
Cunningham J	76.11.2, 77.1.1, 77.4.1

D

Danby G R	66.11.1, 69.9.1, 71.6.2, 71.8.1, 72.5.4
Dannan J H	73.5.7
Davis A J	79.4.6, 79.4.7
Davis L C	73.5.1, 73.7.1
Davis R M	77.3.1, 79.4.8
Dawson G E	74.5.21, 76.3.1, 76.11.6, 76.11.7, 77.11.1 79.11.6, 79.11.8, 80.2.9, 80.9.1
Day R N	73.5.7
Deleroi W	75.9.6, 76.5.4
Dewan S B	74.5.1, 74.10.8, 76.11.2, 77.1.1, 77.4.1
Dobbs D J	76.1.1
Downey T	69.4.1
Dull H J	78.3.1

E

Eastham A R	71.12.2, 72.4.1, 74.3.1, 74.5.8, 74.6.2, 74.9.6., 74.10.1, 75.3.8, 75.7.1, 75.7.8, 76.11.2, 77.1.1, 77.4.1, 77.5.1, 78.1.8, 79.11.6, 80.2.9, 80.9.4
Eastham J F	71.12.1, 74.10.13, 77.3.2, 79.12.1
Edwards J D	78.3.2, 79.9.5, 79.11.7
Ehrenfried C E	71.11.4
El-Antably A M	78.3.2, 79.9.5, 79.11.7
El-Drieny S A E	79.4.8
Elsel W	74.5.4
English C D	76.10.2

F

Farrer W	77.3.1, 78.5.1, 79.4.6
Feldmann U	75.9.6
Fellows T G	71.12.1, 74.3.3
Fink H J	69.4.1
Forgacs R L	73.5.5
Forsythe J B	73.3.2
Franken H	74.5.4
Frenzel D J	79.5.2
Fruechte R D	80.2.8
Fujie J	74.10.7, 75.9.15, 77.7.1
Fujimori S	77.6.3
Fujimura T	76.12.3

Fujino H	72.9.3
Fujiwara S	74.10.7, 80.3.10
Fuke K	74.0.2
Fukuhara K	74.5.17
Furuto Y	80.9.2

G

Garnault A	73.1.1
Garrett H J	71.11.4
Gemelos M	78.9.5
Gibson J	76.8.1, 78.3.4, 78.10.2, 78.10.3, 79.4.4
Gilmore D	78.1.5
Glatzel K	80.2.3, 80.3.1
Goodall R M	76.1.1
Gottzein E	80.2.4
Green A H	73.6.1, 74.9.7
Grover F W	62.0.1
Grumbkow P	75.9.6
Guarino M	74.5.22, 78.0.4
Guderjahn C A	69.4.1, 69.6.1, 71.6.1, 72.0.1
Guillemette R	77.6.2, 77.12.1
Guilliland R G	80.2.7
Gutt H J	72.1.1

H

Harding J T	71.11.2
Haller T R	78.9.4
Harrold W J	72.3.1, 72.11.2, 73.6.1, 73.9.4, 74.9.7, 75.3.7
Hartmann P	79.5.1
Hayashi A	78.1.1, 79.5.3
Hayden J T	72.5.7, 72.12.2, 73.11.2
Hayes W F	77.9.1, 78.1.8
Hearn D L	74.2.2
Heinz W	75.3.3
Heraï T	80.3.7
Hikasa Y	80.2.6
Hirai K	72.9.3
Hobara T	76.12.1
Hoenig M O	74.9.4
Holt W J	76.10.1
Holtz J	75.9.5, 76.1.2, 76.8.1
Hoppie L O	72.5.2
Hosoda Y	74.10.9, 78.7.3
Howell J P	74.9.3., 75.9.10, 77.8.1
Hubner K-D	80.7.1
Hunt M E	77.8.3
Hunt T K	74.2.3

I

Ichikawa H	74.5.11, 74.12.1
Ideguchi J	80.5.1
Iden D J	71.11.4
Ishizaki Y	74.5.16
Iwahana T	75.9.15, 75.11.1, 76.12.8, 77.7.1
Iwanoto M	73.5.2, 73.9.5, 74.5.12, 74.5.17

Iwasa Y	73.5.4, 74.5.7, 74.9.4, 75.7.6, 75.9.11
Iwasaki M	78.7.3

J

Jackson D W	73.4.1, 74.9.5
John V I	74.5.21
Jones M F	46.10.1

K

Kalman G P	73.5.7, 74.10.5
Kamoshida T	80.9.2
Kasahara T	74.5.10
Kasai K	80.3.11
Kasevich R S	73.6.1, 73.11.2, 74.9.7
Katakami K	74.12.3
Kataoka N	76.12.3
Katz R M	79.11.6, 80.2.9, 80.9.4
Kawamura T	73.9.5, 74.5.12, 77.6.3
Kawase S	77.6.3
Kawashima M	78.7.2
Kazawa Y	74.5.10
Kemper H	38.4.1, 53.1.1
Khurdok G	80.2.3
Kimura H	74.5.10, 74.5.18, 75.3.6
Kishimoto S	80.3.2
Klocker P	78.3.3, 78.10.1, 79.8.1
Kneuer R	74.5.6
Kobayashi H	74.0.2
Koerv P A A	80.2.5
Kolm H H	72.5.3, 72.9.2, 73.10.1 73.10.3, 74.5.7, 74.9.2
	74.9.4, 80.9.3
Kratz G	75.9.6, 79.3.1
Kumazawa S	80.9.2
Kuntz S	77.9.3, 78.7.1
Kuroda T	74.5.16
Kuzuu T	74.5.15
Kyotani Y	72.0.2, 72.5.6, 73.8.2, 74.5.2, 75.3.4, 75.7.5, -
	77.0.4, 79.11.2

L

Laithwaite E R	66.0.1, 69.5.1, 70.4.1, 71.12.1, 74.10.13, 75.2.2
Lakhavani S	76.11.6
Lalezari F	78.9.5
Lampros A F	74.5.19
Lancien D	75.7.2, 76.9.16
Lang A	78.9.6
Lee J P	78.9.5
Lehman H	74.10.2
Leitgeb W	75.1.1, 75.4.1
Leonard J F	73.4.1
Leonhard W	77.4.2, 78.4.2, 78.9.13, 78.9.14
Lerner E J	80.4.1
Levi E	73.9.3, 74.10.10, 77.9.4, 78.0.3, 78.0.5, 78.9.5
Lichtenberg A	75.9.3
Linder D	76.1.1

Lindon P	79.9.5, 79.11.7
Lingaya S	76.8.1, 78.3.4, 78.9.9, 78.10.2, 79.9.2
Lipo T A	79.11.1
Love L E G	72.12.3
Luke P D	79.9.5, 79.11.7

M

Mackenzie K E	69.4.1
Mahtani J L	76.9.3, 77.8.1, 78.9.2, 79.1.2, 79.4.9
Maki N	74.5.9, 75.9.15, 76.8.2, 77.7.1
Mase A	74.6.3
Matsui K	74.10.9, 74.12.3
Matsuura A	76.12.5
May H	78.9.12, 78.10.4, 79.2.1
Meisinger R	80.2.4
Mellen B	72.4.1
Melville P H	73.12.2, 75.5.1
Metger F B	74.6.1
Miller L	80.2.4
Mischler W R	78.9.4
Miura S	80.3.2
Miyamoto M	76.12.7, 80.3.9
Miyashita T	74.5.9
Mizuno J	80.3.3
Mnich P	80.7.1
Mongeau P	80.9.3
Morii T	76.12.2
Morrison F P	74.9.7
Mosebach H	76.5.4, 78.9.12
Moulin R	75.7.2, 76.9.16
Mrha W	74.10.3
Muckli W	76.5.3
Mulhall B E	74.5.20, 74.8.1, 74.9.3, 74.10.11, 75.4.3, 75.5.1, 75.7.9, 75.9.10, 76.5.2, 76.9.3, 76.11.1, 76.12.9

N

Nakamura K	76.8.2
Nakamura S	79.4.3, 79.5.3, 79.11.4, 79.11.5
Nakashima H	74.5.14, 74.5.15, 80.3.7
Nasar S A	70.4.1, 75.9.1, 76.0.2
Nelson R H	80.2.8
Nene V D	78.0.6
Neubaur H P	79.5.2
Nondahl T A	80.1.3

O

Oda M	78.7.2
Ogama T	73.8.4
Ogata G	74.5.18, 75.3.6
Ogino O	73.9.5, 74.5.12
Ogiwara G	72.9.4, 74.5.11, 74.5.13, 74.12.1
Ohno E	71.9.1, 73.5.2, 73.9.5, 74.5.12
Ohsawa S	78.7.2
Ohtsuka T	74.5.16, 75.3.4, 79.11.2
Okuda H	75.9.15, 76.8.2, 77.7.1

Okuma S	78.3.6
O'Neill G K	77.10.2
Onodera K	72.9.3
Ooi B T	76.11.4, 77.9.5
Osawa S	74.12.3
Oshima K	72.5.6, 73.8.2

P

Parker J H	79.11.8, 80.9.1
Parsch C P	74.5.4, 73.8.1, 78.3.3, 78.9.9, 78.9.10, 78.10.1
	78.10.3, 78.11.1, 79.4.4, 79.9.2, 80.2.1
Polgreen G R	66.0.2, 71.1.1
Pollard M G	76.1.1
Poloujadoff M	71.2.1, 71.3.1
Powell J R	63.4.1, 66.11.1, 69.9.1, 71.6.2, 71.8.1, 72.5.4
Prast G	74.5.5
Prentiss P O	72.12.3
Prothero D H	76.12.9

R

Radomski T A	80.2.8
Rakels J H	78.4.2, 79.4.9
Ravera R J	77.6.1
Reitz J R	72.5.1, 73.5.1, 75.3.5
Rentmeister M	75.9.6, 78.9.7
Rhodes D J	79.4.8
Rhodes R G	71.12.2, 72.4.1, 73.7.2, 74.5.20, 74.8.1, 74.9.3
	74.10.10, 75.4.3, 75.7.9, 75.9.10, 76.5.2, 76.9.3,
	76.11.1, 77.8.1, 77.8.3, 78.4.2, 78.9.1, 78.9.2
	78.11.2, 79.1.2, 79.4.9.
Rogg D	76.5.3, 80.2.3
Ross J A	73.5.6, 76.10.1
Rudback N E	78.1.8
Rule R G	80.2.7
Rummich E	72.11.1

S

Saijo T	76.7.3, 76.12.6, 78.3.5, 79.5.4, 80.3.4,
Saito R	74.5.10, 75.3.6
Sasaki T	80.3.6
Sato S	74.5.10, 74.5.18, 75.3.6
Sato Y	80.3.2
Satow T	73.8.4, 74.5.17
Sattler P K	75.9.6
Schauer W	75.4.4
Schulz H	79.5.1, 80.3.1
Schwalm C L	76.3.1, 76.11.7, 77.11.1, 79.11.6, 80.2.9
Sen P C	75.9.9, 75.9.14, 76.3.2, 76.11.6
Shalaby M	77.9.2, 79.2.1
Shinobu M	73.9.5, 74.5.17
Sinryo Y	71.9.1
Slemon G R	73.32, 74.5.1, 74.9.8, 74.9.9, 74.10.8, 75.9.8
	76.11.2, 77.1.1, 77.4.1, 77.9.3, 78.1.7, 78.7.1
	78.9.3, 78.9.11, 79.7.1
Sobolewski G	78.1.5

Stablein H	71.11.3
Stephan A	74.5.6
Stewart G R	74.2.1
Stickler J J	80.2.10
Svecharnik D V	78.0.2
Swanson C G	74.5.19

T

Tada N	74.5.10, 75.3.6.
Takahashi M	79.11.5
Takahashi T	74.5.9, 74.5.10
Takano N	72.9.4, 74.5.13
Takeshita K	80.3.2
Taketsuna Y	74.10.9
Takeuchi Y	79.11.5, 80.2.6
Takeyama Y	74.0.2
Tamura Y	74.6.3
Tanaka H	71.11.5
Tanaka M	73.8.4
Tang C H	72.11.2, 73.6.1, 73.9.5, 73.11.2, 74.9.7, 75.3.7
	75.4.5
Tatsumi T	75.9.15, 77.7.1
Terzis N	78.9.3
Thornton R D	68.8.1, 72.5.3, 73.4.2, 73.4.3, 73.5.3, 73.10.1,
	73.10.3, 74.5.7, 74.10.12, 75.7.3, 75.7.6
Tinkham M	72.6.1
Tomeoku H	74.5.18
Toyoshima M	74.12.3, 78.7.3
Turton R A	74.9.8, 74.9.9, 74.10.8, 76.11.2, 77.1.1, 77.4.1

U

Umemori T	74.10.9, 74.12.3, 78.1.3, 78.1.4, 78.7.2, 78.7.3,
	80.3.5, 80.9.2
Unteregelsbacher E	76.3.1, 76.11.7
Usami Y	74.10.7

V

Van Dorn N H	74.2.2
Vegelahn F	78.3.1
Viens N P	73.11.2

W

Wagner J A	72.7.1
Wallace A K	80.9.1
Wallace C B	75.9.11
Ward E J	72.10.2
Watabe S	74.6.3
Weh H	75.3.2, 75.4.6, 75.9.6, 75.9.7, 76.5.4, 77.9.2,
	78.9.12, 78.10.4, 79.2.1, 79.11.3
Weiss E	73.6.1
Wheeler P A	73.4.1
Wiart A	75.2.3
Wiechens H	78.3.1

Wiegner G	78.9.10, 78.11.1, 79.9.3
Wilhelm K	74.5.4
Wilkie D F	73.5.1
Williams D	69.4.1
Williams F	80.9.3
Williams G	79.9.5, 79.11.7
Williams R A	76.1.1
Wilson H W	5.0.2
Wilson J W A	74.5.1
Wilson M N	75.5.1
Winkle G	75.9.2
Wipf S L	69.4.1, 69.6.1, 71.6.1, 76.5.1
Wong J Y	75.9.10

Y

Yamada T	73.5.2, 74.5.17
Yamaguchi T	74.6.3
Yamamura S	72.9.1, 76.11.3
Yamashita H	76.12.4, 78.9.15
Yamaya T	74.6.3
Yasukawa S	80.3.8
Yasumochi R	74.0.2
Yonemitsu H	72.9.4
Young D A	78.12.2
Yuda S	80.3.8

Z

Zabar Z	77.9.4
Zehden A	5.0.1
Zurek R	78.9.16

5.3 Corporate Index

A

Aberdeen University	74.10.13, 77.3.2
AEG-Telefunken	75.9.6, 78.3.1
AIResearch Manufacturing Co	73.5.7, 74.10.5, 78.7.1
Al-Azhar University	77.9.2
Atomics International	69.4.1, 69.6.1, 71.6.1, 72.0.1

B

Bath, University of	79.4.5, 79.12.1
Boeing Aerospace Co	80.2.2, 80.2.7
Braunschweig TU	75.3.2, 75.4.6, 75.9.6, 75.9.7, 76.5.4, 77.4.2, 77.9.2, 77.10.3, 78.4.2, 78.9.12, 78.9.13, 78.9.14, 78.10.4, 79.2.1, 79.11.3, 80.7.1
British Rail	76.1.1, 81.3.1
Brookhaven National Laboratory	63.4.1, 66.11.1, 69.9.1, 71.6.2, 71.8.1, 72.5.4
Brooklyn, Polytechnic Institute of,	73.9.3
Brown Boveri Cie	74.10.3, 79.9.3
Brush Electrical Machines Ltd	77.0.2, 77.3.1, 78.5.1, 78.5.2, 78.9.8, 79.4.6, 79.4.7, 81.3.1
Bundesministerium fur Forschungs und Technologie (BMFT)	72.0.3, 74.12.2, 75.3.10, 76.0.3 77.0.3, 78.0.7, 79.3.1, 79.5.1 79.5.2, 80.3.1

C

California, University of	69.4.1, 71.11.1, 72.6.1
Canadair Services Ltd	78.1.5, 79.11.8, 80.9.1
Canadian Institute for Guided Ground Transportation (CIGGT)	72.12.1, 74.3.2, 75.3.1, 75.6.1 76.3.3, 77.9.6, 78.1.8, 79.11.6, 80.2.9
Central Electricity Research Lab	73.12.2, 75.5.1
Cranfield Institute of Technology	72.5.7, 72.12.2, 73.8.1
Culham Laboratory	74.0.1

D

Dayton, University of	71.11.4
Domier System GmbH	76.5.3, 79.5.1, 79.5.2, 80.2.3, 80.3.1

E

Electric Carrier Co	13.10.1
---------------------	---------

F

Farebrother, JEC & Partners	79.1.4
Ford Motor Co	72.2.2, 72.5.1, 73.3.1, 73.5.1 73.5.5, 73.6.2, 73.7.1, 74.2.3 74.4.2, 74.5.3, 75.3.5, 75.4.7, 75.7.7

5.3 Corporate Index

A

Aberdeen University	74.10.13, 77.3.2
AEG-Telefunken	75.9.6, 78.3.1
AIResearch Manufacturing Co	73.5.7, 74.10.5, 78.7.1
Al-Azhar University	77.9.2
Atomics International	69.4.1, 69.6.1, 71.6.1, 72.0.1

B

Bath, University of	79.4.5, 79.12.1
Boeing Aerospace Co	80.2.2, 80.2.7
Braunschweig TU	75.3.2, 75.4.6, 75.9.6, 75.9.7, 76.5.4, 77.4.2, 77.9.2, 77.10.3, 78.4.2, 78.9.12, 78.9.13, 78.9.14, 78.10.4, 79.2.1, 79.11.3, 80.7.1
British Rail	76.1.1, 81.3.1
Brookhaven National Laboratory	63.4.1, 66.11.1, 69.9.1, 71.6.2, 71.8.1, 72.5.4
Brooklyn, Polytechnic Institute of,	73.9.3
Brown Boveri Cie	74.10.3, 79.9.3
Brush Electrical Machines Ltd	77.0.2, 77.3.1, 78.5.1, 78.5.2, 78.9.8, 79.4.6, 79.4.7, 81.3.1
Bundesministerium fur Forschungs und Technologie (BMFT)	72.0.3, 74.12.2, 75.3.10, 76.0.3 77.0.3, 78.0.7, 79.3.1, 79.5.1 79.5.2, 80.3.1

C

California, University of	69.4.1, 71.11.1, 72.6.1
Canadair Services Ltd	78.1.5, 79.11.8, 80.9.1
Canadian Institute for Guided Ground Transportation (CIGGT)	72.12.1, 74.3.2, 75.3.1, 75.6.1 76.3.3, 77.9.6, 78.1.8, 79.11.6, 80.2.9
Central Electricity Research Lab	73.12.2, 75.5.1
Cranfield Institute of Technology	72.5.7, 72.12.2, 73.8.1
Culham Laboratory	74.0.1

D

Dayton, University of	71.11.4
Domier System GmbH	76.5.3, 79.5.1, 79.5.2, 80.2.3, 80.3.1

E

Electric Carrier Co	13.10.1
---------------------	---------

F

Farebrother, JEC & Partners	79.1.4
Ford Motor Co	72.2.2, 72.5.1, 73.3.1, 73.5.1 73.5.5, 73.6.2, 73.7.1, 74.2.3 74.4.2, 74.5.3, 75.3.5, 75.4.7, 75.7.7

Fuji Electric Co	72.9.3, 74.0.2
Furukawa Electric Co Ltd	78.7.2, 80.9.2

G

Garrett Manufacturing Ltd	73.3.2, 73.5.7, 74.10.5, 78.7.1
General Electric Co	78.9.4, 79.11.1, 80.1.3
General Motors	80.2.8
Graz T U	78.9.7
Grenoble, University of	71.2.1, 71.3.1

H

Hamilton Standard	74.6.1
Harris Auday Lea & Brooks	74.10.6
Harvard University	72.6.1
Hitachi Ltd	74.5.9, 74.5.10, 74.5.18, 74.12.3, 75.3.6, 75.9.15, 76.8.2, 77.7.1, 78.7.2, 78.7.3

I

Imperial College	66.0.1, 70.4.1, 71.12.1, 74.10.13, 75.2.2
International Research & Development Co	76.12.9

J

Japan Air Lines	78.1.1, 79.4.1, 79.4.3, 79.5.3 79.11.4, 79.11.5, 80.2.6, 80.5.1
Japanese National Railways	72.0.2, 72.5.6, 72.10.1, 73.8.2 74.5.2, 74.5.14, 74.5.15, 74.7.1 74.10.7, 74.10.9, 74.12.3, 75.3.4, 75.7.5, 75.9.15, 75.11.1 76.7.2, 76.7.3, 76.12.1, 76.12.2 76.12.3, 76.12.4, 76.12.5, 76.12.6, 76.12.7, 76.12.8 77.0.4, 77.6.3, 77.7.1, 78.1.3 78.1.4, 78.3.5, 78.4.1, 78.9.15 79.5.4, 79.9.4, 79.11.2, 80.1.1 80.3.2, 80.3.3, 80.3.4, 80.3.5 80.3.6, 80.3.7, 80.3.8, 80.3.9 80.3.10, 80.3.11, 80.9.2 75.2.3
Jeumont-Schneider	

K

Karlsruhe, Universitat der	75.3.3, 75.4.4
Kentucky, University of	70.4.1, 75.9.1, 76.0.2
Konsortium Magnetbahn Transrapid	78.0.1, 79.4.10, 79.6.1
Krupp	71.11.3

L

Linde A G	74.5.6
Los Alamos Scientific Laboratories	76.5.1

M

MBB	79.4.2, 80.2.4, 80.2.5
McGill University	76.11.4, 77.6.2, 77.9.5, 77.12.1
Metro-Cammell	80.10.1
MIT	68.8.1, 72.5.3, 72.9.2, 73.4.2
	73.4.3, 73.5.3, 73.5.4, 73.10.1
	73.10.3, 74.5.7, 74.9.2, 74.9.4
	74.10.12, 75.7.3, 75.7.6,
	75.9.11, 75.9.12, 77.10.2
	80.9.3
Mitre Corporation	74.5.19, 78.0.6, 79.11.6,
	80.2.9, 80.9.4
Mitsubishi	71.9.1, 73.5.2, 73.8.4, 73.9.5
	74.5.12, 74.5.17

N

Nagoya University	74.9.10, 76.3.4, 78.3.6
National Research Council, Canada	77.9.1, 78.1.8
New York, Polytechnic Institute of	74.10.10, 77.9.4, 78.0.3,
	78.0.5, 78.9.5
North American Rockwell Corp	69.4.1, 69.6.1, 71.6.1
	72.0.1
Nottingham University	77.3.1, 79.4.8

P

People Mover Group	81.3.1
Philco-Ford Corporation	75.2.1
Phillips Research Laboratories	74.5.5
Princeton University	77.10.2
Purdue University	79.11.1

Q

Queen's University	72.2.1, 72.5.5, 72.12.3, 74.3.1
	74.5.8, 74.5.21, 74.6.2, 74.9.6
	74.10.1, 75.3.8, 75.7.1, 75.7.8
	75.9.9, 75.9.14, 76.3.1, 76.3.2
	76.11.2, 76.11.6, 76.11.7,
	77.1.1, 77.4.1, 77.5.1, 77.10.1
	77.11.1, 78.4.3, 79.9.1, 79.11.8
	80.1.2, 80.2.9, 80.9.1, 80.9.4

R

Raytheon Company	72.3.1, 72.11.2, 73.6.1, 73.9.4
	73.11.2, 74.9.7, 75.3.7, 75.4.5
Reliance Electric Company	74.5.1
Rheinland TU	80.7.1
Rohr Industries Inc	73.5.6 74.2.2, 76.10.1
Rutherford Laboratory	75.5.1
RWTH, Institut fur Elektrische Maschinen	75.9.6

S

Sandia Laboratories	69.4.1
San Jose State College	72.7.1
Siemens AG	70.5.1, 72.1.1, 73.11.3
	74.5.4, 75.1.1, 75.4.1, 75.9.3
	75.9.5, 75.9.6, 76.1.2, 76.7.1
	76.8.1, 76.9.2, 77.0.1,
	77.3.3, 77.4.3, 77.8.2, 78.3.1,
	78.3.3, 78.3.4, 78.9.9, 78.9.10
	78.10.1, 78.10.2, 78.10.3,
	78.11.1, 79.1.3, 79.4.4, 79.8.1
	79.9.2, 80.2.1
SNCF	75.4.2, 75.7.2, 76.9.16
Societe de l'Aerotrain	73.1.1, 79.4.10
Spar Aerospace Products Ltd	76.10.2, 78.1.6
Stanford Research Institute	72.2.3, 72.5.2, 73.2.1, 73.8.3,
	75.3.9
Stanford University	74.2.1
Sumitomo Electric Industries Ltd	74.10.9, 78.7.2, 78.7.3
Sussex, University of	78.3.2, 79.9.5, 79.11.7

T

Tohoku, University of	74.5.16, 75.3.4, 79.11.2
Tokyo, University of	72.5.6, 72.9.1, 73.8.2, 74.5.16
	76.11.3,
Toronto, University of	73.3.2, 73.7.3, 74.5.1, 74.9.8
	74.9.9, 74.10.8, 75.9.8, 75.9.13
	76.11.2, 76.11.4, 76.11.5,
	77.1.1, 77.4.1, 77.9.3, 78.1.7,
	78.7.1, 78.9.3, 78.9.11, 79.7.1,
	79.9.6, 79.11.9
Toshiba	72.9.4, 73.0.1, 74.5.11,
	74.5.13, 74.6.3, 74.12.1
Tracked Hovercraft Ltd	74.3.3
Transport Canada	78.1.8
Transrapid-EMS	75.9.2, 76.0.1, 76.7.1, 77.3.3,
	78.9.6, 78.9.16, 79.4.10,
	79.6.1, 79.9.5
Traian Vuia, Polytechnic Institute of	75.9.1

U

UKAEA	74.0.1, 79.4.9
United Engineers	73.4.1, 74.9.5
University College, Swansea	69.5.1
US Department of Transportation	71.11.2, 72.10.2, 74.5.19,
	74.5.22, 77.6.1, 78.0.4
	80.2.10, 80.2.11
UTDC Ltd	79.11.8, 80.9.1, 80.10.1

V

Vienne TU	72.11.1
-----------	---------

W

Warwick, University of

71.12.2, 72.4.1, 73.7.2,
73.10.2, 73.12.1, 74.4.1,
74.5.20, 74.8.1, 74.9.1,
74.9.3, 74.10.11, 75.4.3
75.5.1, 75.7.4, 75.7.9,
75.9.10, 76.5.2, 76.9.1, 76.9.3
76.11.1, 76.12.9, 77.8.1,
77.8.3, 78.1.2, 78.2.1,
78.4.2, 78.9.1, 78.9.2,
78.11.2, 78.12.1, 79.1.1
79.1.2, 79.4.9.
46.9.1, 46.10.1
69.4.1
71.11.4

Westinghouse

Wisconsin, University of

Wright-Patterson AFB

W

Warwick, University of

71.12.2, 72.4.1, 73.7.2,
73.10.2, 73.12.1, 74.4.1,
74.5.20, 74.8.1, 74.9.1,
74.9.3, 74.10.11, 75.4.3
75.5.1, 75.7.4, 75.7.9,
75.9.10, 76.5.2, 76.9.1, 76.9.3
76.11.1, 76.12.9, 77.8.1,
77.8.3, 78.1.2, 78.2.1,
78.4.2, 78.9.1, 78.9.2,
78.11.2, 78.12.1, 79.1.1
79.1.2, 79.4.9.
46.9.1, 46.10.1
69.4.1
71.11.4

Westinghouse
Wisconsin, University of
Wright-Patterson AFB

APPENDIX II

1. Introduction

The purpose of this appendix is to provide a detailed description of the design and construction of the solenoid magnet used in the experiment.

The solenoid magnet is a cylindrical device consisting of a coil of wire wound around a central core. The core is made of a material with a high magnetic permeability, such as iron or steel.

The coil is made of a material with a low resistance, such as copper or aluminum. The current flowing through the coil creates a magnetic field that is directed along the axis of the solenoid.

The magnetic field is used to deflect the particles in the experiment. The deflection is proportional to the current flowing through the coil and the length of the solenoid.

APPENDIX II

SOLENOID MAGNET DESIGN

The solenoid magnet is a cylindrical device consisting of a coil of wire wound around a central core. The core is made of a material with a high magnetic permeability, such as iron or steel.

The coil is made of a material with a low resistance, such as copper or aluminum. The current flowing through the coil creates a magnetic field that is directed along the axis of the solenoid.

The magnetic field is used to deflect the particles in the experiment. The deflection is proportional to the current flowing through the coil and the length of the solenoid.

The solenoid magnet is designed to operate at a current of 10 amperes. The length of the solenoid is 10 cm. The diameter of the solenoid is 5 cm.

The solenoid magnet is made of a material with a high magnetic permeability, such as iron or steel. The coil is made of a material with a low resistance, such as copper or aluminum.

The solenoid magnet is used to deflect the particles in the experiment. The deflection is proportional to the current flowing through the coil and the length of the solenoid.

APPENDIX II SOLENOID MAGNET DESIGN

1. Introduction

The design of adequate performance ACLM for propelling advanced ground transport vehicles ultimately relies on the assumption that the inductances and field profiles of the coils in the vehicle array can be correctly predicted. Fortunately the absence of ferromagnetic material means that the calculations involve linear field strength - flux density relationships, and superposition can be readily applied.

Design procedures for circular coils have been available for sometime⁽²⁵⁷⁾, and parameter variation was investigated by Maxwell, who established inductance and maximum efficiency relationships. More recently field analyses of thick solenoids both on and off axis were performed under NASA sponsorship^(258,259). Coil mutual and self inductance calculations were made easier by tabulations and simplified formulae assembled by Grover⁽²⁶⁰⁾, and Fawzi later produced an algorithm that could be used for coaxial current sheets which meant that faster calculation cycle time was possible⁽²⁶¹⁾. Previous computing methods had generally stored Grover's tables, which leads to limited and uncontrolled accuracies at certain geometries.

For Maglev, circular coils do not necessarily represent an optimum geometry. For the Warwick system this is considered in Chapter 3. The common choice is for rectangular or even square coils with tight corner radii. The corners represent problem areas because the self field is concentrated by the rapid change in direction of the current, and the subsequently generated body forces must be accommodated by the coil structure and support. The corner field will also determine the load line of the coil and its intercept with the critical field locus. Field calculations then must be made for straight line filaments and bars, and the corner effects evaluated.

A racetrack winding is often used to provide a rectangular coil equivalent, and inductance matching is based on an equal area criteria. This

APPENDIX II SOLENOID MAGNET DESIGN

1. Introduction

The design of adequate performance ACLM for propelling advanced ground transport vehicles ultimately relies on the assumption that the inductances and field profiles of the coils in the vehicle array can be correctly predicted. Fortunately the absence of ferromagnetic material means that the calculations involve linear field strength - flux density relationships, and superposition can be readily applied.

Design procedures for circular coils have been available for sometime⁽²⁵⁷⁾, and parameter variation was investigated by Maxwell, who established inductance and maximum efficiency relationships. More recently field analyses of thick solenoids both on and off axis were performed under NASA sponsorship^(258,259). Coil mutual and self inductance calculations were made easier by tabulations and simplified formulae assembled by Grover⁽²⁶⁰⁾, and Fawzi later produced an algorithm that could be used for coaxial current sheets which meant that faster calculation cycle time was possible⁽²⁶¹⁾. Previous computing methods had generally stored Grover's tables, which leads to limited and uncontrolled accuracies at certain geometries.

For Maglev, circular coils do not necessarily represent an optimum geometry. For the Warwick system this is considered in Chapter 3. The common choice is for rectangular or even square coils with tight corner radii. The corners represent problem areas because the self field is concentrated by the rapid change in direction of the current, and the subsequently generated body forces must be accommodated by the coil structure and support. The corner field will also determine the load line of the coil and its intercept with the critical field locus. Field calculations then must be made for straight line filaments and bars, and the corner effects evaluated.

A racetrack winding is often used to provide a rectangular coil equivalent, and inductance matching is based on an equal area criteria. This

configuration is more easily wound than a tight corner coil since there is reduced chance of the wire riding up and splaying on the corners, and migrating when energised. Montgomery has briefly looked at rectangular coil field analysis by approximating the coil with four straight bars, overlapping at the corners⁽²⁶²⁾. Unfortunately the published material is inconsistent in its notation, so reworking has proved to be necessary. For a period of time the design procedure involving different coil geometries and their field distributions seemed only soluble by large mainframe computer programmes. The Rutherford Laboratory's GFUN and TOSCA represent quite complex software which can handle a wide range of intricate magnetic systems. A similar installation is General Atomics' interactive computer programme GMAN used in conjunction with the field analysis programme EFFI, developed by the Lawrence Livermore Laboratory⁽²⁶³⁾. These systems are necessary to work through a finished detailed design, but can prove costly in trying to just establish the basic configurations that need further study, and the parameter sensitivity to major changes in design strategy. This appendix sets out the techniques that can be used to produce reasonably accurate solutions to field problems for circular, rectangular and racetrack coils, both on and off the geometric axis. The solution to equations can be found using pocket or desk top programmable scientific calculators. This enables the design process to proceed rapidly, without the initial need to establish a large data and software base to accurately analyse coil structures which will then prove unsatisfactory and need to be discarded.

2. Circular Coils

2.1 Basic Field and Power Relationships

Figure 67 shows the simple elemental current loop for which the on axis field B_z is given by the Biot-Savart relationship. At a position z from the coil plane, and for a loop current of I amperes, the field is

$$B_z = \mu_0 \frac{I}{2} \cdot \frac{a^2}{(a^2 + z^2)^{3/2}} \quad (55)$$

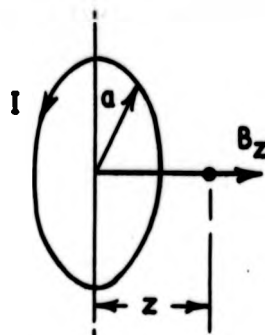


Figure 67. The Elemental Loop.

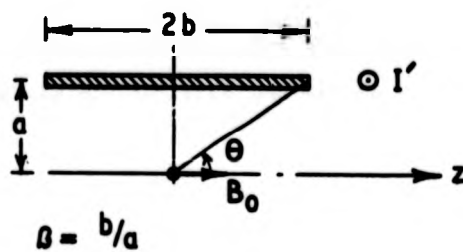


Figure 68. Current Sheet.

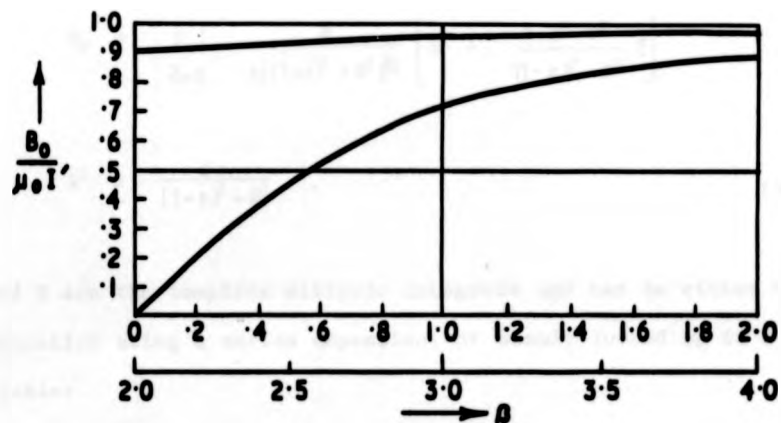


Figure 69. Saturation of Current Sheet Central Field.

where a is the loop radius. The central field is simply

$$B_0 = \frac{\mu_0 I}{2a} \quad (56)$$

so generally,

$$B_z = B_0 \frac{a^3}{(a^2 + z^2)^{3/2}} \quad (57)$$

The off axis field of a circular filament is given by expressions involving complete elliptical integrals of the first and second kind. For a loop radius a , carrying I amperes in an anticlockwise direction in plan, the field components in the vertical and radial direction are B_z and B_r . The field point below the coil plane is defined as being sg vertically and ea horizontally from the coil centre.

The fields and modulus, k , are given by

$$B_z = \frac{\mu_0 I}{2\pi a} \cdot \frac{1}{[(1+e)^2 + s^2]^{1/2}} \left[K + \frac{1-e^2-s^2}{(1-e)^2 + s^2} E \right] \quad (58a)$$

$$B_r = \frac{\mu_0 I}{2\pi a} \cdot \frac{s}{e[(1+e)^2 + s^2]^{1/2}} \left[K - \frac{1+e^2+s^2}{(1-e)^2 + s^2} E \right] \quad (58b)$$

$$k^2 = \frac{4e}{(1+e)^2 + s^2} \quad (58c)$$

K and E are the complete elliptic integrals and can be either evaluated by calculation using a series expansion, or simply looked up in a suitable set of tables.

The elemental loop can be used to generate the field expressions for current sheets by integrating between the beginning and ends of the single layer coil equivalent. The sheet is defined by the strength I' , ampere turns per metre, and axial aspect ratio β , the ratio of sheet length to diameter (Figure 68). It can be shown that the central field B_0 is given by

$$B_0 = \mu_0 I' \cos \theta = \mu_0 I' \frac{\beta}{(1 + \beta^2)^{1/2}} \quad (59)$$

where $I' = \frac{NI}{2b}$, $\beta = \frac{b}{a}$ (60)

I is the turn current and N the number of turns. Figure 69 shows the saturating effect of length on the central field; for $\beta = 2$ the central field is already at $\sim 90\%$ of its infinite length value.

Integrating the effect of the current loop over a finite build coil (Figure 70), with inner and outer radii a_1 and a_2 such that

$$\alpha = \frac{a_2}{a_1} \quad \text{and} \quad \beta = \frac{b}{a_1} \quad (61)$$

produces a central field given by

$$B_0 = \mu_0 j \lambda a_1 \beta \ln \left[\frac{\alpha + (\alpha^2 + \beta^2)^{1/2}}{1 + (1 + \beta^2)^{1/2}} \right] \quad (62)$$

or $B_0 = \mu_0 j \lambda a_1 \beta (\sinh^{-1}(\frac{\alpha}{\beta}) - \sinh^{-1}(\frac{1}{\beta}))$ (63)

$j\lambda$ is the overall current density per unit cross section,

$$\text{i.e. } j\lambda = \frac{NI}{2b(a_2 - a_1)} = \frac{NI}{2a_1\beta(\alpha - 1)} \quad (64)$$

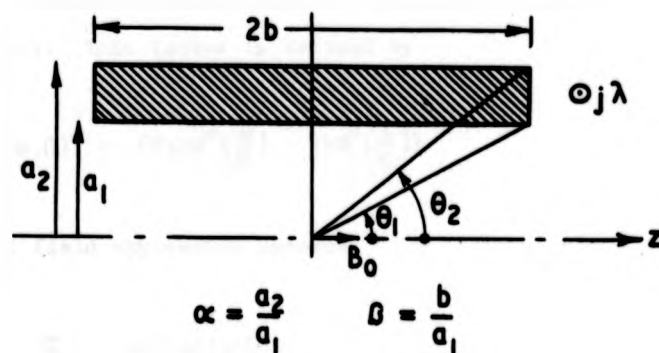


Figure 70. Finite Thickness Uniform Current Density Solenoid.

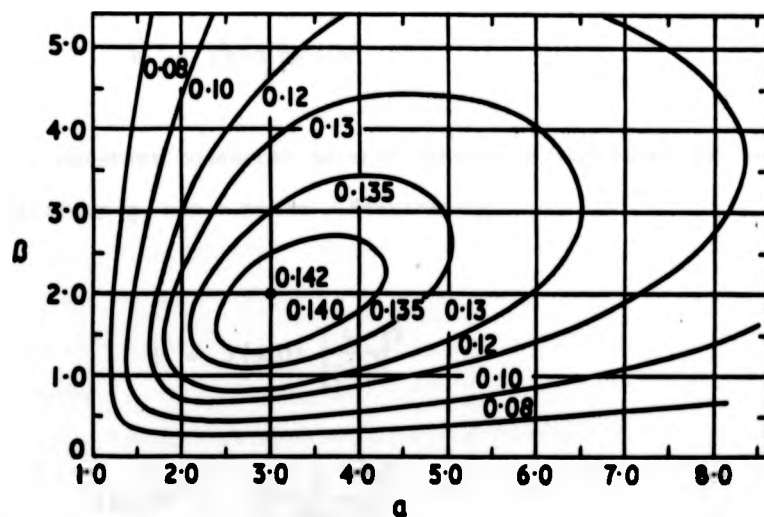


Figure 71. Constant Fabry Factor $G = (\alpha, D)$
Contours for a Uniform Current Density Coil.

j is the current density and λ the space factor.

Examination of 62 and 63 reveals that the central field is in fact given by the product of overall current density, inner coil radius and a geometry dependent factor. This factor is defined by

$$F(\alpha, \beta) = \beta(\sinh^{-1}(\frac{\alpha}{\beta}) - \sinh^{-1}(\frac{1}{\beta})) \quad (65)$$

so the central field expression becomes

$$B_0 = \mu_0 j \lambda a F(\alpha, \beta) \quad (66)$$

For a resistive coil, the power required for a particular magnetic field can be evaluated, knowing the conductor resistivity and coil volume. The total power absorbed is

$$W = j^2 \rho \lambda a^3 2\pi \beta (\alpha^2 - 1) \quad (67)$$

where the constant conductor current density j A/m² flows in the conductor of resistivity ρ ohm - metre. Rearranging,

$$j = J(\alpha, \beta) \left[\frac{W}{\rho \lambda a^3} \right]^{1/2} \quad (68)$$

$$\text{where } J(\alpha, \beta) = \left[\frac{1}{2\pi \beta (\alpha^2 - 1)} \right]^{1/2} \quad (69)$$

$J(\alpha, \beta)$ is the coil current density factor, relating conductor current density to the coil total power. The central field can be derived as a function of W , J and F such that

$$B_0 = \mu_0 F(\alpha, \beta) J(\alpha, \beta) \left[\frac{W\lambda}{\rho a_1} \right]^{1/2} \quad (70)$$

or

$$B_0 = \mu_0 G(\alpha, \beta) \left[\frac{W\lambda}{\rho a_1} \right]^{1/2} \quad (71)$$

$G(\alpha, \beta)$ is the totally geometrically dependent term known as the Fabry Factor, and links the field produced by a coil to the power input required. G has a maximum of 0.142 near $\alpha = 3$ and $\beta = 2$. Figure 71 shows the contours of Fabry Factor for various α and β of a uniform current density coil, and the moderate gradient allows some choice in α and β with minimal degradation of G .

2.2 Off-Axis Field of a Finite Solenoid

Calculating the off axis field of a finite solenoid is possible by integrating the effect of a current carrying element such as is shown in Figure 72, throughout the solenoid. This technique is most successful off-axis and at medium distance from the coil, but can be complicated for regions within the coil itself because of discontinuities in the functions encountered.

A more simple method is to break down the solenoid into a set of four semi infinite solenoids as shown in Figure 73. The advantage of the semi infinite solenoid, which has a zero inner radius and a uniform current density extending from the axis to the outer radius, is that the field at a point can be represented by only two nondimensional variables, the normalized radial and axial coordinates of the field point. Reference 259 shows how

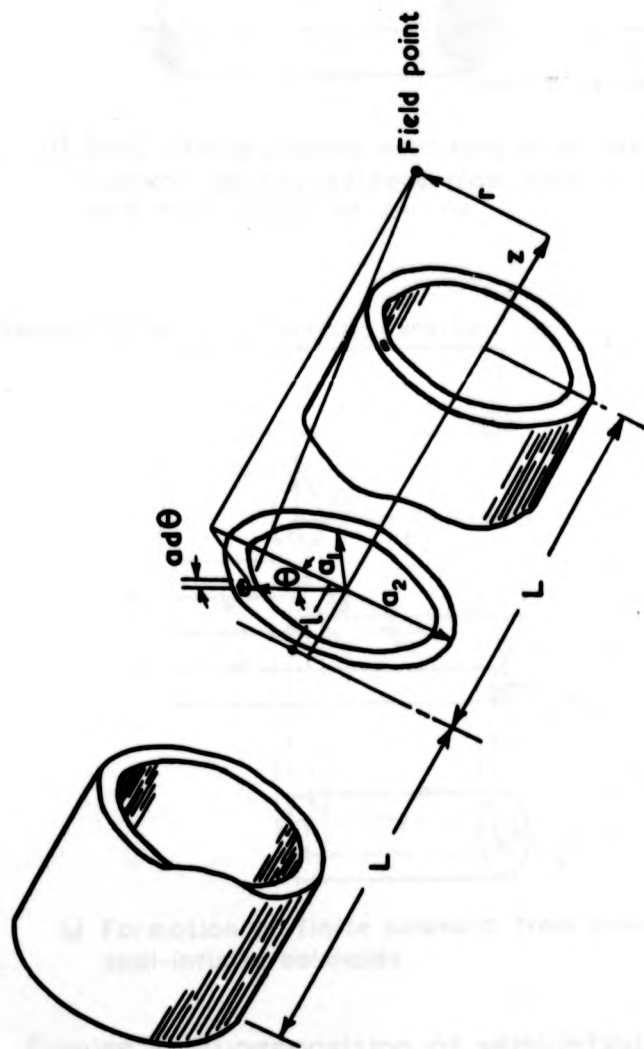
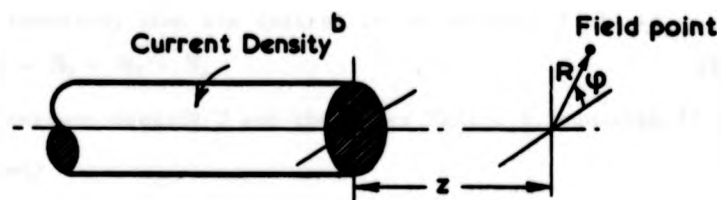
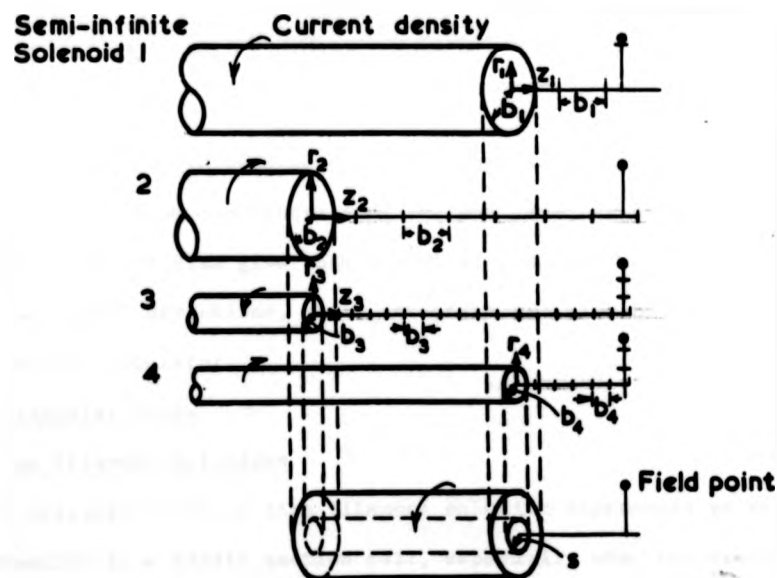


Figure 72. Coil geometry for calculating off axis field for a thick coil.



- a) Semi-infinite solenoid with zero inner radius. Current density extends from axis to $R=b$, and from $z=0$ to $z=-\infty$.



- b) Formation of finite solenoid from four semi-infinite solenoids.

Figure 73. Superposition of semi-infinite solenoids.

superposition four semi infinite solenoids produces the same field function as the finite solenoid (Figure 73b). If the field component (radial or axial) of the solenoids is H_1, H_2, H_3, H_4 , from the same sensed current density rotation, then the desired thick solenoid field is

$$H = H_1 - H_2 + H_3 - H_4 \quad (72)$$

Dividing by the current density J and the inner radius s , equation 72 is nondimensionalized:

$$\frac{H}{Js} = \frac{H_1}{Js} - \frac{H_2}{Js} + \frac{H_3}{Js} - \frac{H_4}{Js}$$

With semiinfinite solenoid radii b_1, b_2, b_3, b_4 , where $b_3 = b_4 = s$, and $b_1 = b_2 = \alpha s$, and if quantities such as $H_1/Jb_1 = h_1$ etc,

$$\frac{H}{Js} = \alpha h_1 - \alpha h_2 + h_3 - h_4 \quad (73)$$

Each solenoid value is nondimensionalized by its outer radius as a unit of length, working from the centre line and end face, as shown in Figure 73b. Although Brown and Flax give both graphical and tabular solutions for h , in radial and axial directions, their integrals can also be evaluated on a programmable calculator.

3. Rectangular Coils

3.1 Line Filament Solutions

As with circular coils, a line filament solution represents an easy first approximation to a finite section coil, especially when the required field point is some distance away. For close field points, a filament solution can still be used if it is based on a geometric mean distance (GMD) approximation of the finite coil build (Figure 74). The field expressions derive from the Biot-Savart relationship applied to the current element $d\mathbf{l}$, which carries a current I and produces an elemental field $d\mathbf{B}$ at the origin of an orthogonal coordinate set. \mathbf{s} is the vector from the current element to the origin

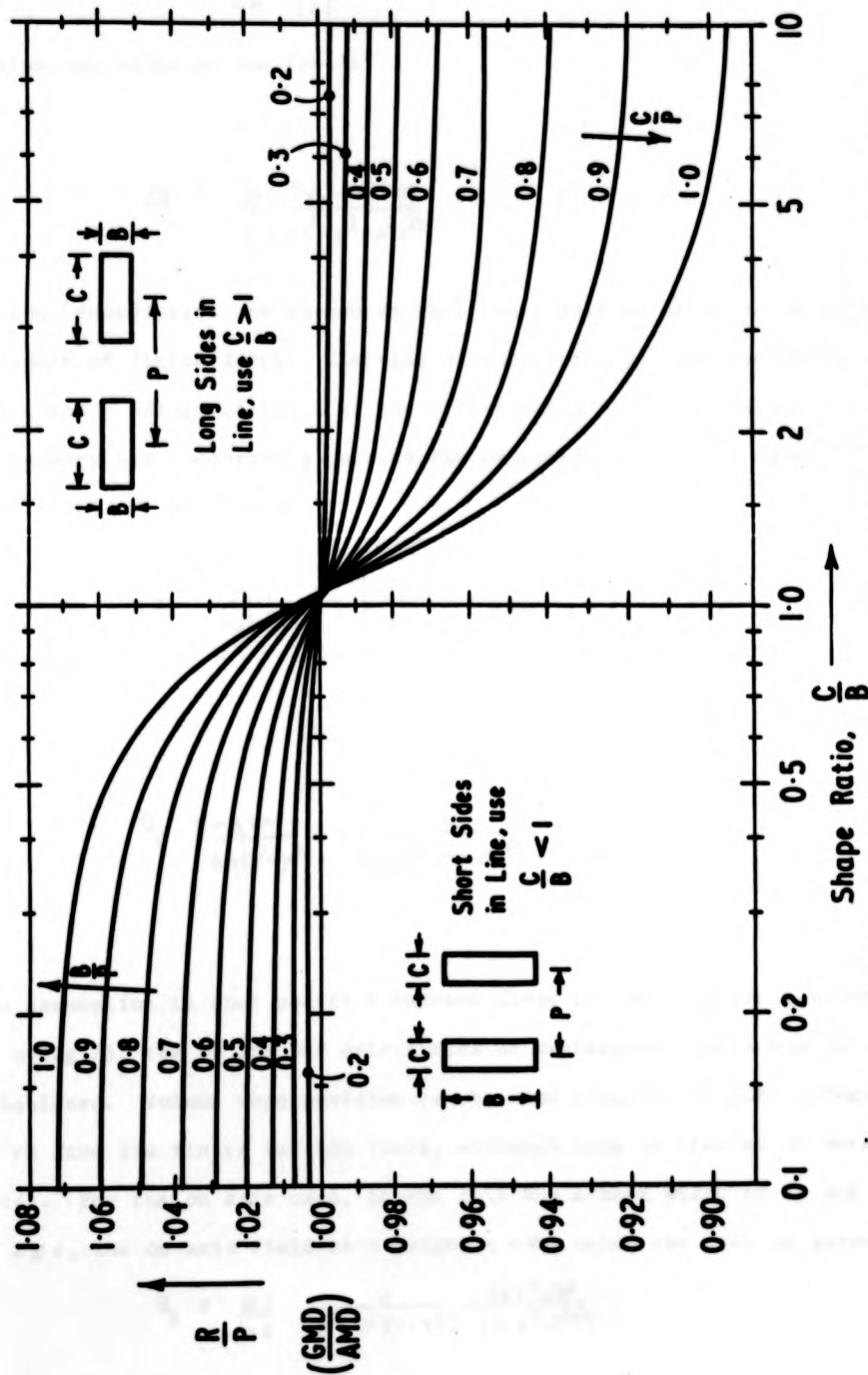


Figure 74. Geometric/Arithmetic Mean Distance for Equal Parallel Rectangles.

(Figure 75). The field is given by

$$\underline{dB} = \frac{\mu_0 I}{4\pi} \frac{d\mathbf{l} \times \mathbf{s}}{|\mathbf{s}|^3}$$

Evaluation produces the result

$$\underline{dB} = \frac{\mu_0 I}{4\pi} \frac{(y\mathbf{i} - x\mathbf{j}) dz}{(x^2 + y^2 + z^2)^{3/2}} \quad (74)$$

If the coordinates are chosen so that the z axis is parallel to a current filament of finite length, starting at coordinate z_1 , and finishing at z_2 , the x and y values of field at the origin can be found by using 74. Montgomery has incorrectly stated the expressions for this case⁽²⁶²⁾, they should be written as

$$B_x = \frac{\mu_0 I y}{4\pi(x^2 + y^2)} \left[\frac{z_2}{(x^2 + y^2 + z_2^2)^{1/2}} - \frac{z_1}{(x^2 + y^2 + z_1^2)^{1/2}} \right] \quad (75)$$

$$B_y = \frac{-\mu_0 I x}{4\pi(x^2 + y^2)} \left[\frac{z_2}{(x^2 + y^2 + z_2^2)^{1/2}} - \frac{z_1}{(x^2 + y^2 + z_1^2)^{1/2}} \right]$$

The assumption is that positive current flows in the positive z direction. By using 75, the on and off axis fields of rectangular coils can be easily calculated. Volume superposition can be used (Figure 76) with integration of 74 to find the finite section field, although this is treated in more detail later. For the on axis case, if the coil has a base width of $2a$ and breadth of $2b$, the on axis field at a height $z = 0$ below the coil is given by

$$B_z = \frac{\mu_0 I}{\pi a} \frac{a}{(a^2 + b^2)(1 + b^2)} \cdot \frac{1 + a^2 + 2b^2}{(1 + a^2 + b^2)^{1/2}} \quad (76)$$

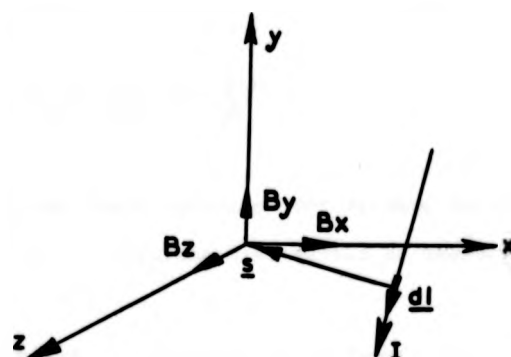


Figure 75. Current element $d\mathbf{l}$

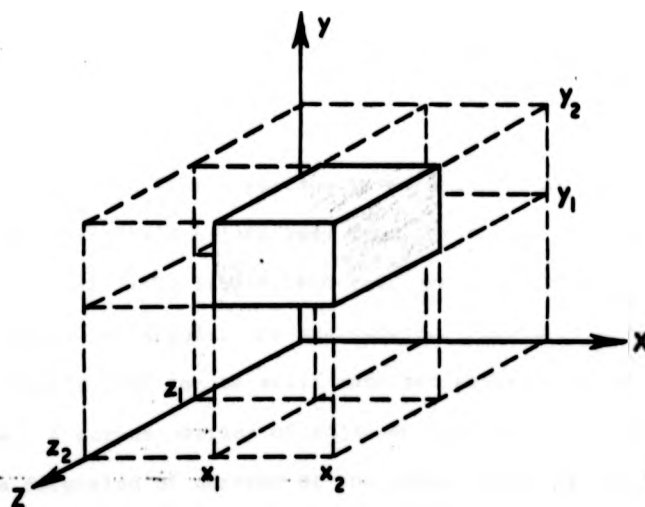


Figure 76. Volume superposition.

The central field ($z = 0$) is simply

$$B_0 = \frac{\mu_0 I}{\pi a} \left(1 + \frac{1}{4}\right)^{1/2} \quad (77)$$

Figure 77 shows the axial field variation for various heights and width to breadth ratios. The circle with the same radius as the coil half width is given for comparison.

The off axis field profile is indicated for a square coil by Figure 78 which is a plot of the vertical field for a point equidistant from two of the coil sides, at various heights. The shape of the profile indicates the high harmonic content of the flux variation when a magnet array is made up of alternating coils at levitation heights much less than the coil half width. The rapid fall off of field as the reference point moves under the transverse coil side is also readily apparent.

3.2 Finite Sections

The rectangular coil with finite section is more difficult to successfully evaluate. For general field points away from the actual wound section, and indeed for the central field itself, the coil limbs can often be approximated by the finite length rectangular bar equivalent. Figure 79 shows, for example, how a square coil can be split into bar equivalents to include the corner sections. A corner overlay of adjacent bars would accommodate the rapid change on direction of current at the corner more successfully. For the case when very long coil sides are present, the infinitely long rectangular bar can be used with superposition as in Figure 79 to evaluate field values. Figure 80 shows an infinitely long rectangular bar, with one edge running along the z axis. The field components B_x and B_y at the origin ($B_z = 0$) are given by the expressions shown. Essentially equation 74 can be double integrated over the x and y limits from 0 to $+x$ and $+y$. Normalizing by the x value (i.e. to give a bar of unit width and height $y = \frac{y}{x}$)

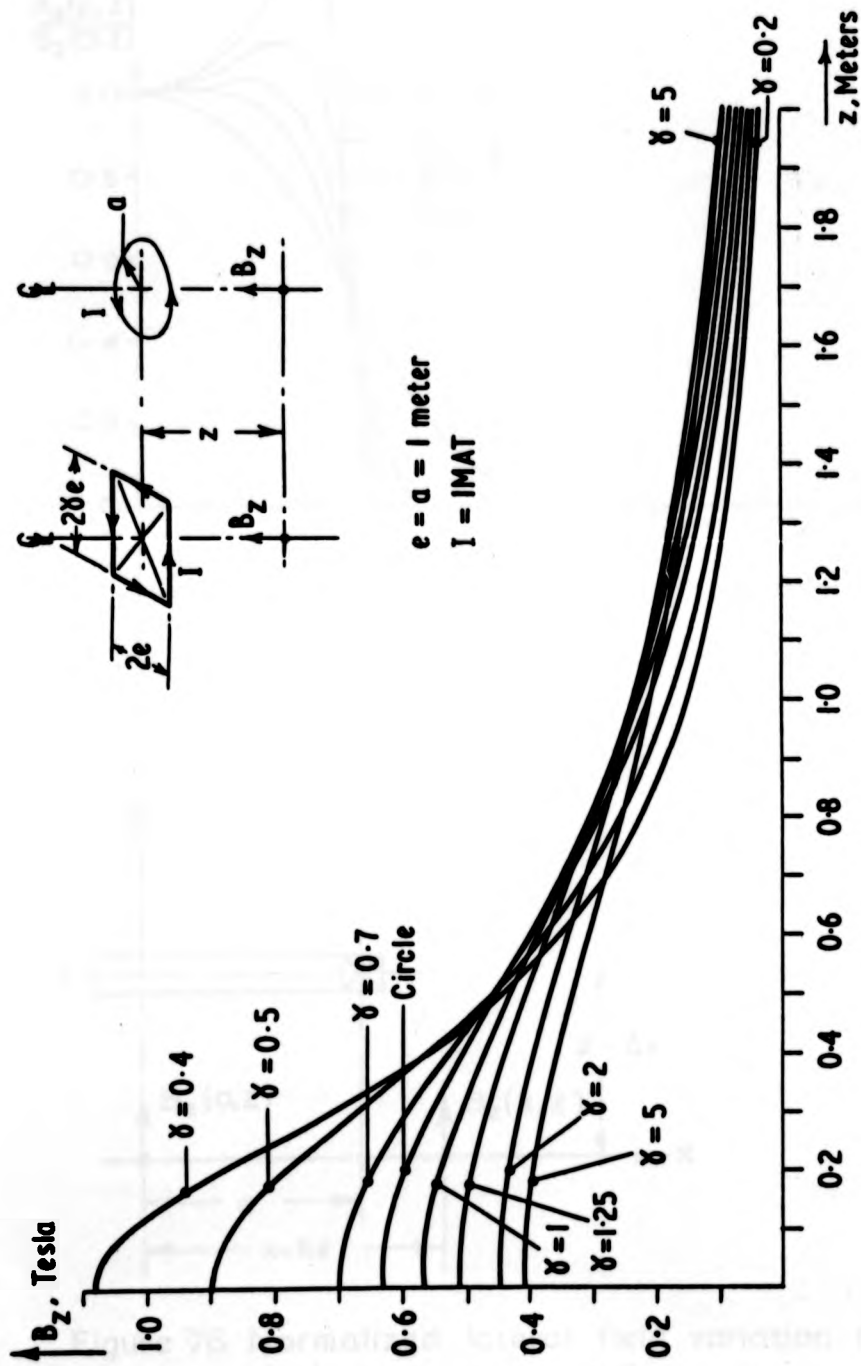


Figure 77. Axial Field Variation at Height z for Rectangular and Circular Coils.

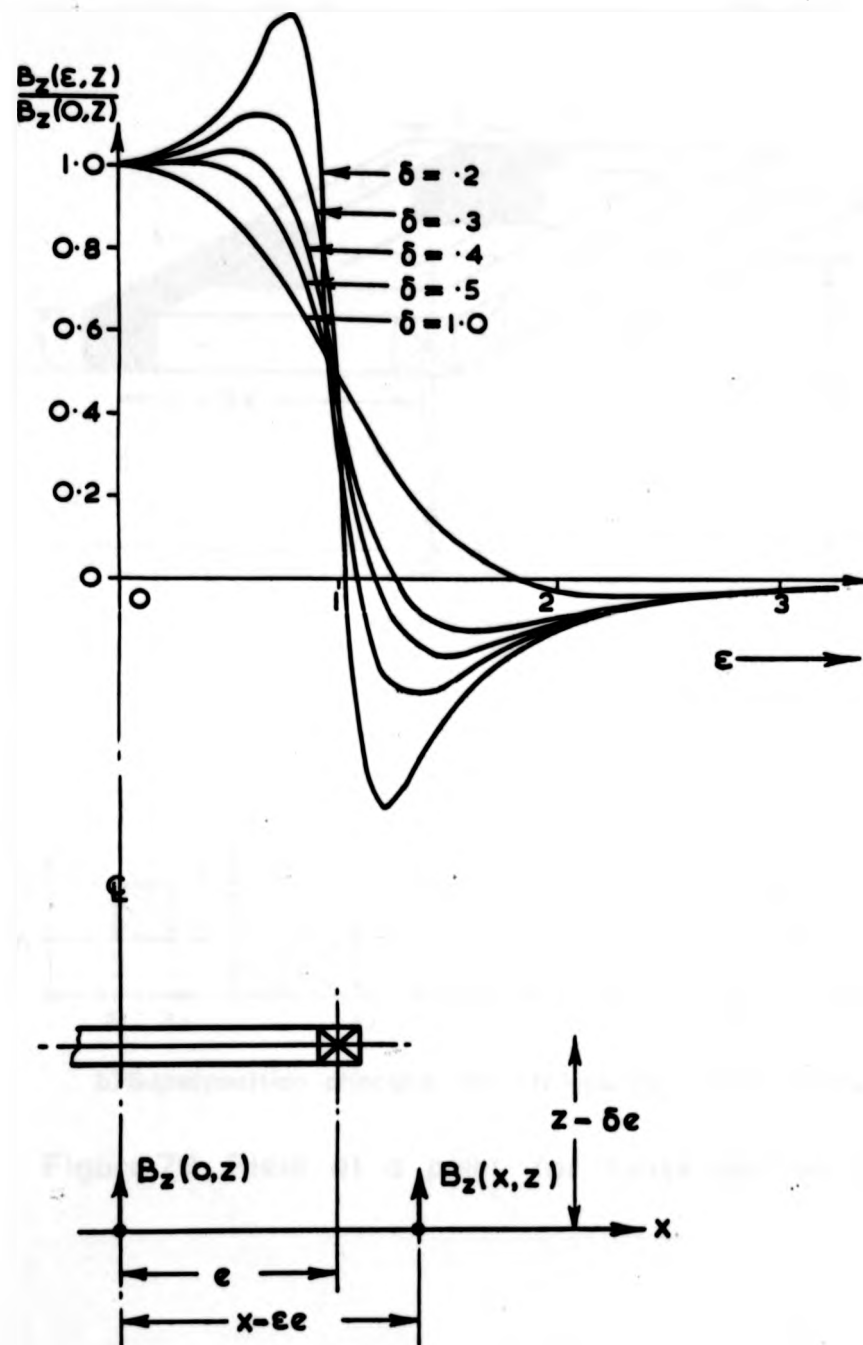


Figure 78. Normalized lateral field variation for a single turn square coil.

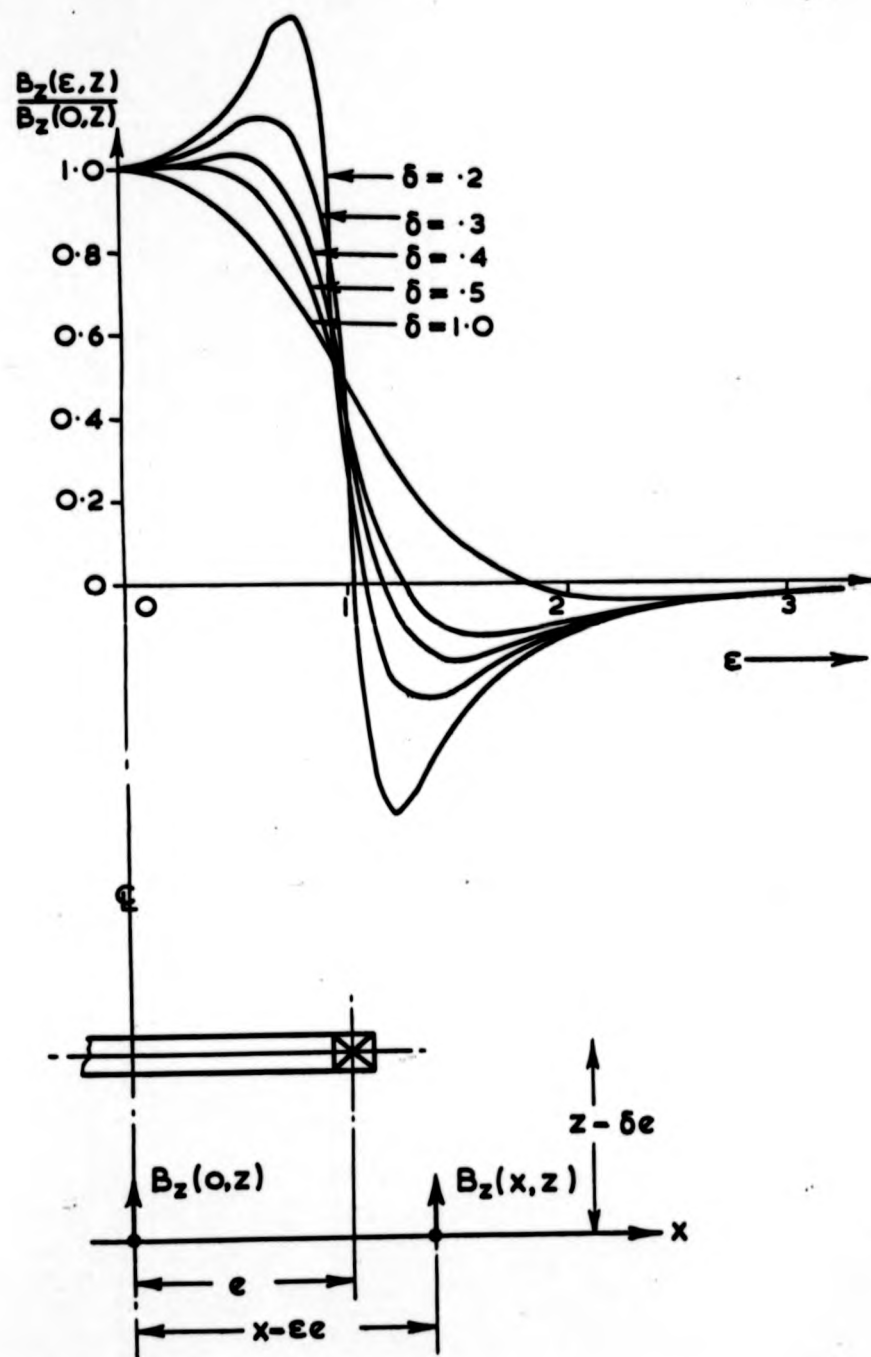


Figure 78. Normalized lateral field variation for a single turn square coil.

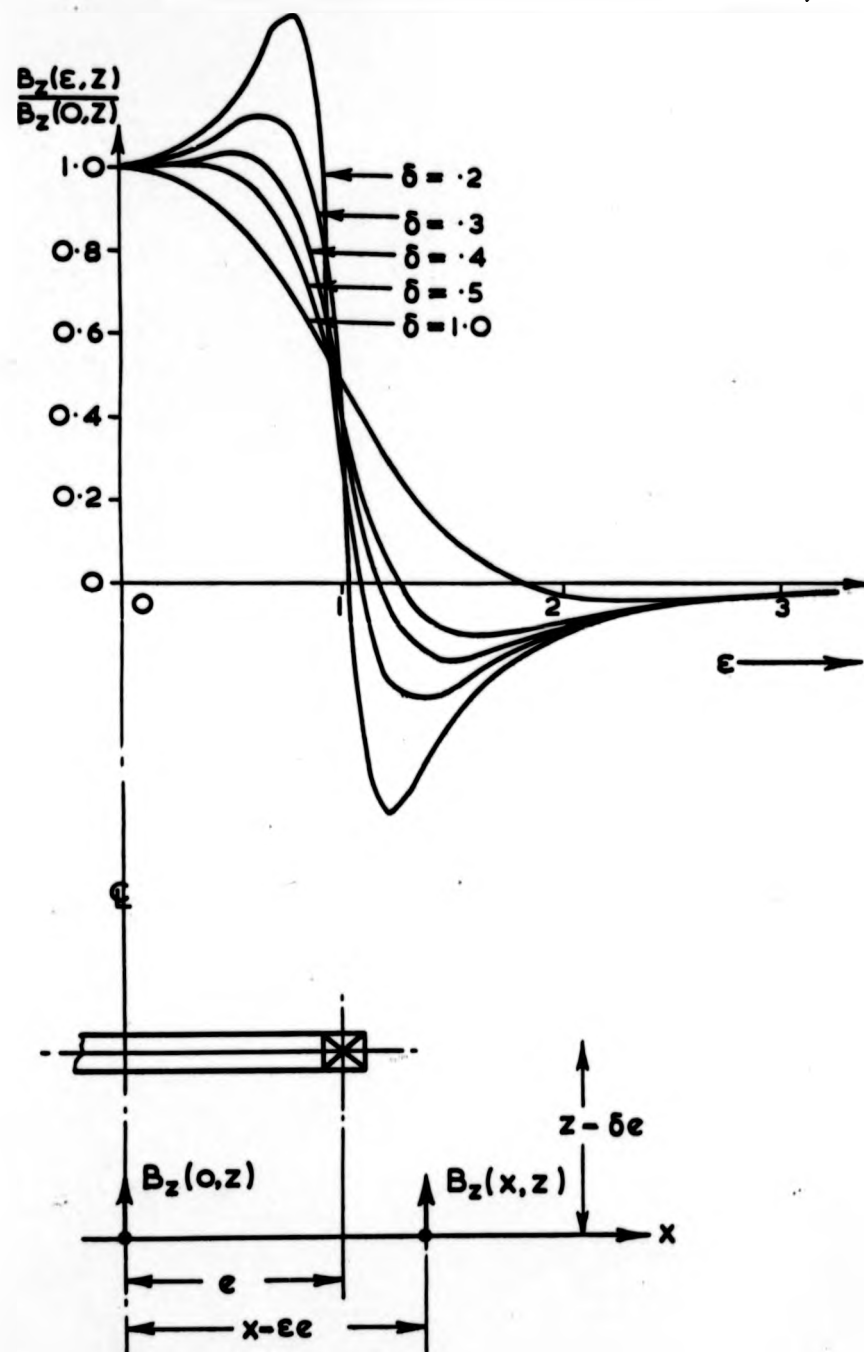
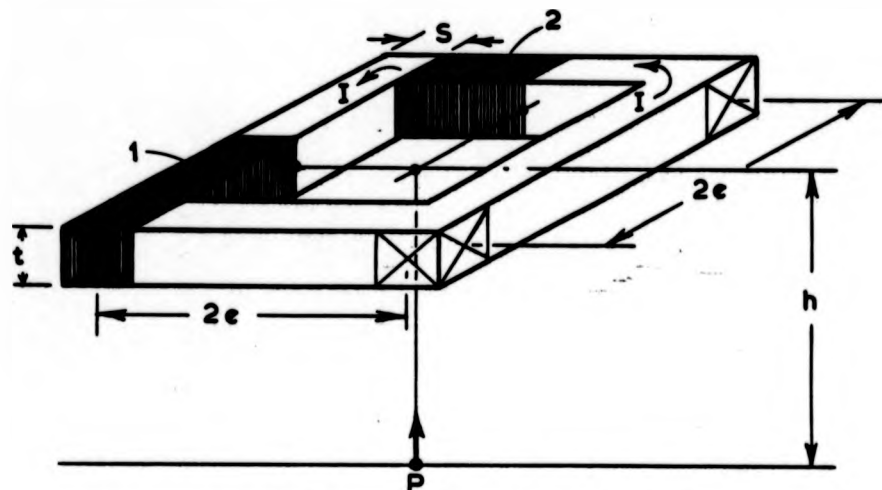
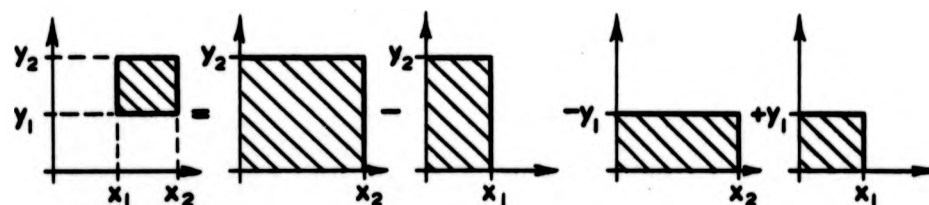


Figure 78. Normalized lateral field variation for a single turn square coil.



a) Subdivision of square coil for on-axis field.



b) Superposition principle for off-corner field points.

Figure 79. Field at a point for finite section coils.

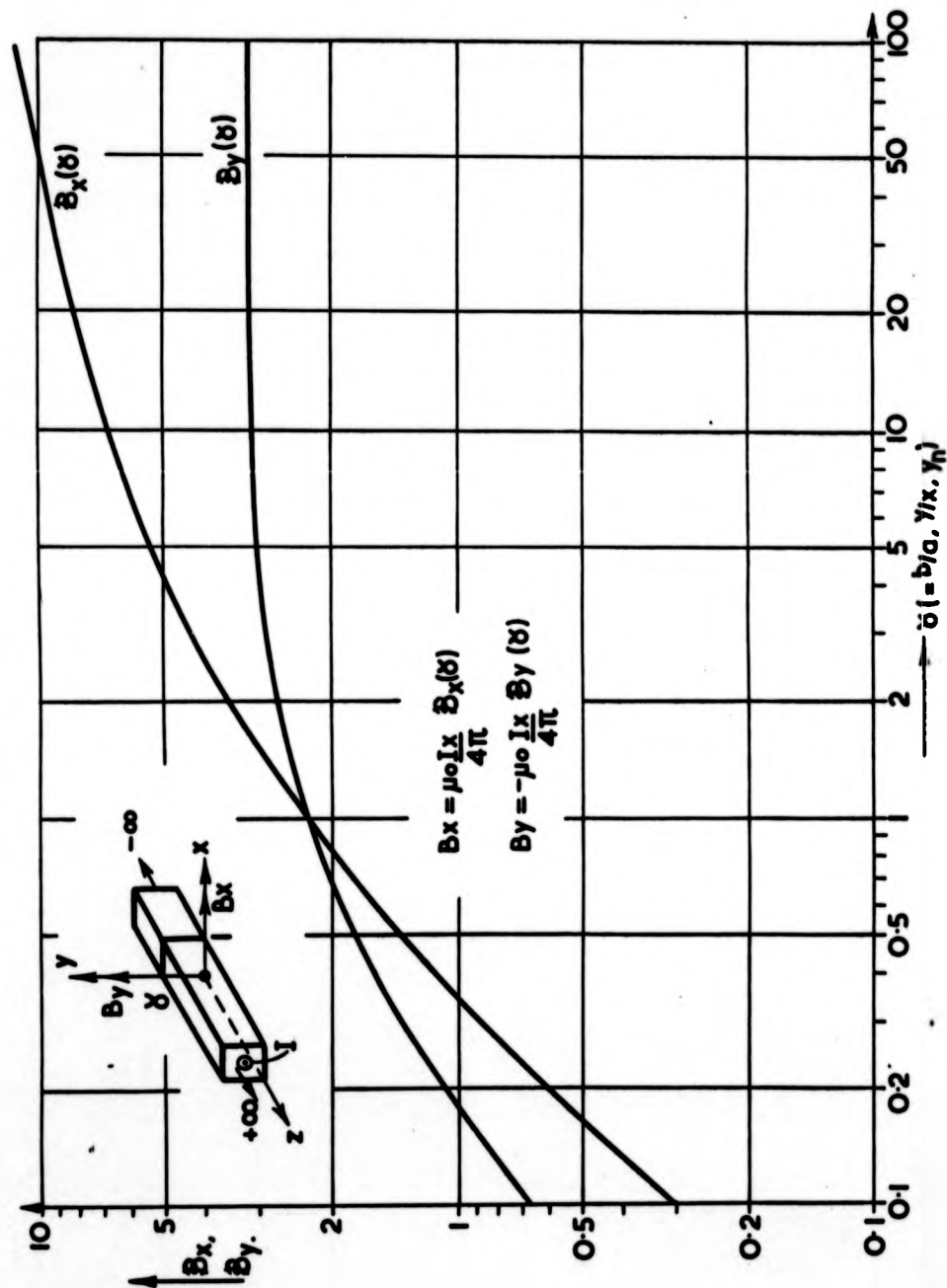


Figure 80. Field functions for unit width infinitely long rectangular bar.

produces field values

$$B_x = \frac{\mu_0 I x}{4\pi} \left[\ln(y^2 + 1) + 2y \tan^{-1}\left(\frac{1}{y}\right) \right]$$

$$B_y = -\frac{\mu_0 I x}{4\pi} \left[y \ln\left(1 + \frac{1}{y^2}\right) + 2 \tan^{-1} y \right]$$
(78)

The field functions are the values within square brackets and are plotted in Figure 80 for various shape ratios y . Superposition as demonstrated by Figure 79 allows the field components distant from an infinitely long rectangular bar to be determined.

Similar field functions can be obtained for finite length rectangular bars. Here the bar stretches from the origin to a finite value of z , and similarly has one edge aligned to the z axis, in the positive quadrant of x and y . Triple integration of 74 and normalizing the coordinates by x to give unit width and bar height $y_n = \frac{y}{x}$ and bar length $z_n = \frac{z}{x}$, with I replaced by

$j\lambda \, dy \, dx$ ($j\lambda$ is the overall current density), produces

$$B_x = \frac{\mu_0 j\lambda x}{4\pi} \mathcal{B}_x^*$$

$$B_y = -\frac{\mu_0 j\lambda x}{4\pi} \mathcal{B}_y^*$$
(79)

where

$$\mathcal{B}_x^* = z_n \ln \left[\frac{[1 + (1 + z_n^2)^{1/2}][1 + \frac{y_n^2}{2}]^{1/2}}{1 + (1 + y_n^2 + z_n^2)^{1/2}} \right] + \ln \left[\frac{[z_n + (1 + z_n^2)^{1/2}][1 + y_n^2]^{1/2}}{z_n + (1 + y_n^2 + z_n^2)^{1/2}} \right] + y_n \tan^{-1} \left[\frac{z_n}{y_n (1 + y_n^2 + z_n^2)^{1/2}} \right]$$

$$\mathcal{B}_y^* = z_n \ln \left[\frac{[y_n + (1 + y_n^2 + z_n^2)^{1/2}][1 + \frac{1}{z_n^2}]^{1/2}}{y_n + (1 + y_n^2 + z_n^2)^{1/2}} \right] + y_n \ln \left[\frac{[z_n + (1 + y_n^2 + z_n^2)^{1/2}][1 + \frac{1}{y_n^2}]^{1/2}}{z_n + (1 + y_n^2 + z_n^2)^{1/2}} \right] + \tan^{-1} \left[\frac{y_n z_n}{(1 + y_n^2 + z_n^2)^{1/2}} \right]$$
(80)

Figure 81 and 82 plot the field functions given by equations 80 for the unit width normalized height and length bars, and have also been transferred to a programmable calculator.

4. Racetrack Coils

Field solutions for finite section racetrack coils usually require a complex program which will present finite element approximation to the coil dimensions using a standard suite of building bricks or generated volumes. A filamentary approximation is however possible, using a combination of formulae for finite length straight wires and a field solution for a filamentary quadrant or half circle. Figure 83 shows how the coil sides are broken into four groups to enable the field components to be evaluated. If the coil has straight elements on all four sides, then a quadrant field expression (rather than semi-circle) must be used for each of the corner radii.

Figure 84 shows a coordinate set for evaluating the field at a point P produced by a quadrant of a circular current filament. P is chosen to lie on the x axis, and the Biot Savart expression is used with the appropriate vectors to give the three field components. If the limits on α are chosen to be $\pm \frac{\pi}{4}$ instead of 0 and $\frac{\pi}{2}$, then B_y is zero, and with the coil elevation z and radius r normalized by the offset of P from the coil centreline, h so that

$$z = hZ$$

$$r = hR$$

then

$$B_x = -\frac{\mu_0 I}{2\pi h} \int_0^{\pi/4} \frac{RZ \cos \alpha \, d\alpha}{(1+R^2+Z^2-2RZ\cos \alpha)^{3/2}}$$

(81)

$$B_z = +\frac{\mu_0 I}{2\pi h} \int_0^{\pi/4} \frac{(R^2 - RZ \cos \alpha) \, d\alpha}{(1+R^2+Z^2-2RZ\cos \alpha)^{3/2}}$$

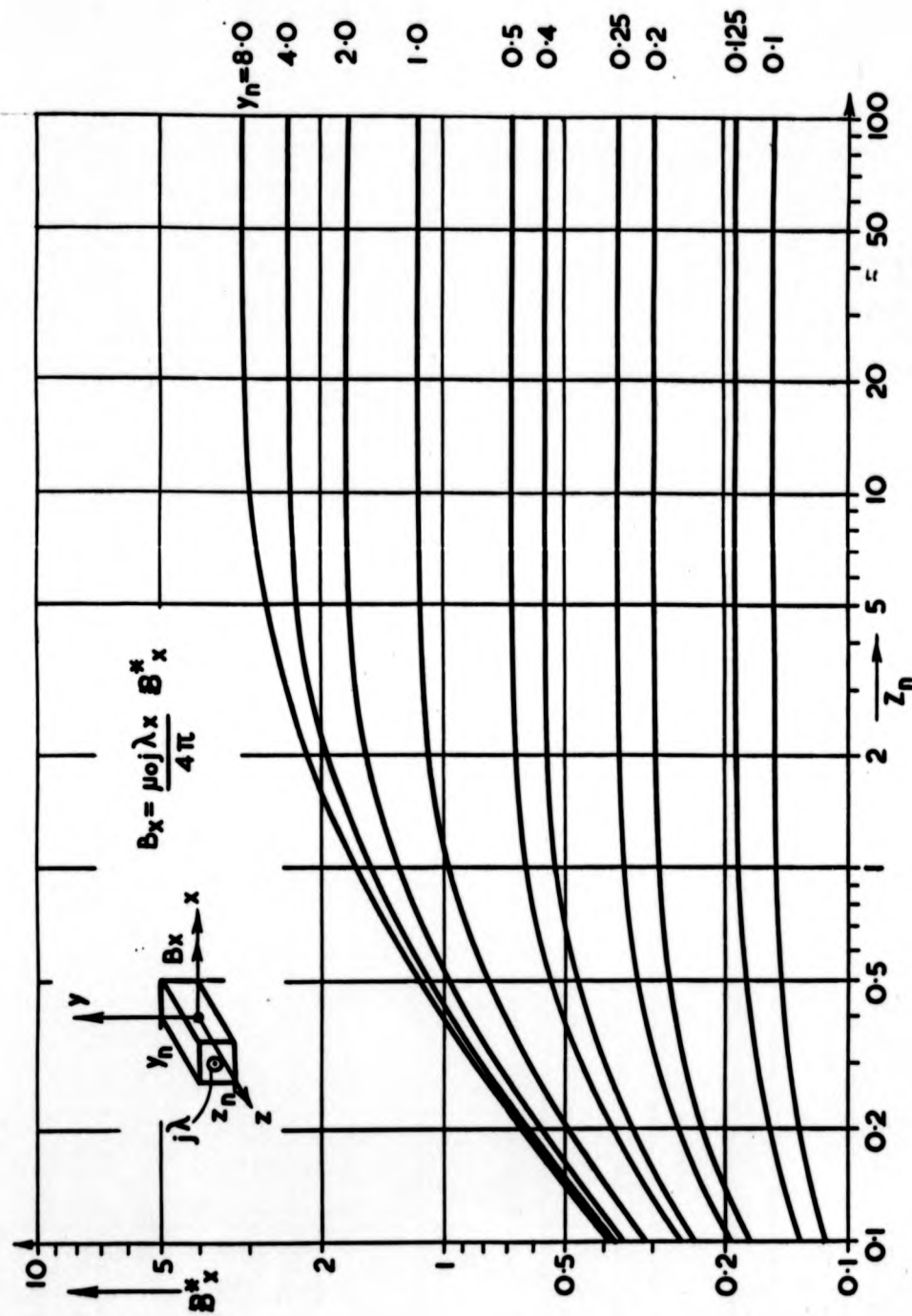


Figure 81. Field functions for unit width finite length rectangular bar.

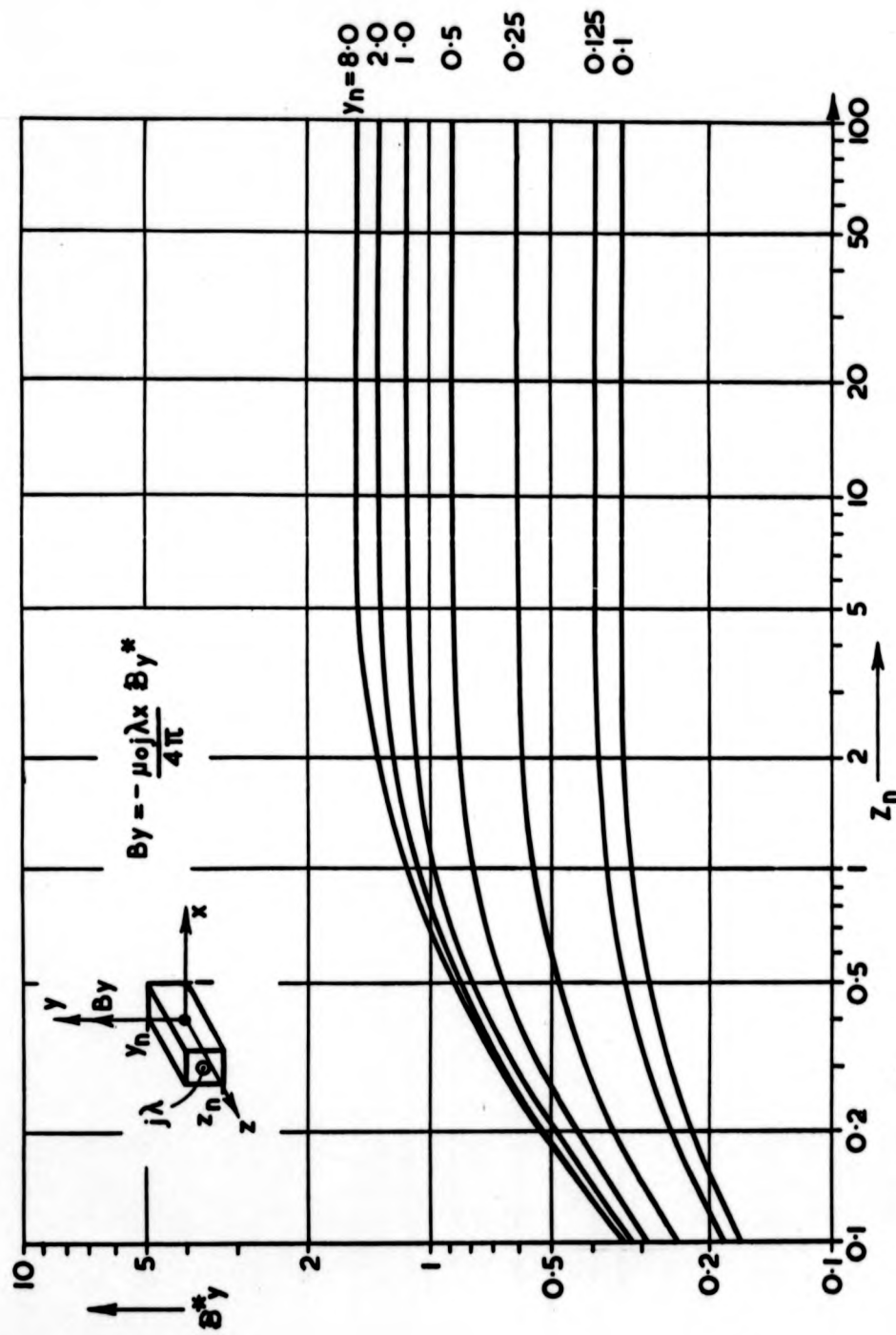


Figure 82. Field functions for unit width finite length rectangular bar.

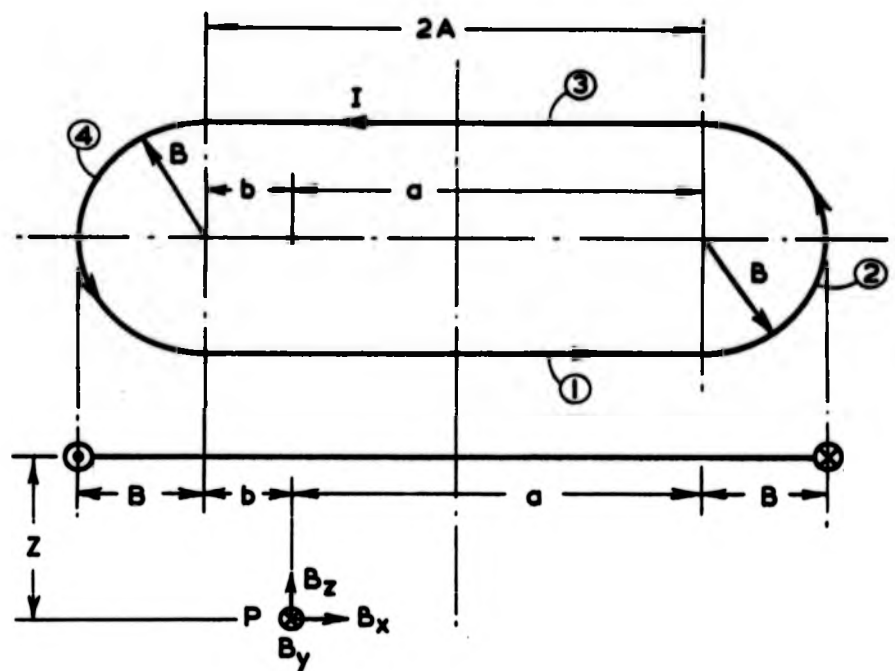


Figure 83. Race-track coil field components, off axis.

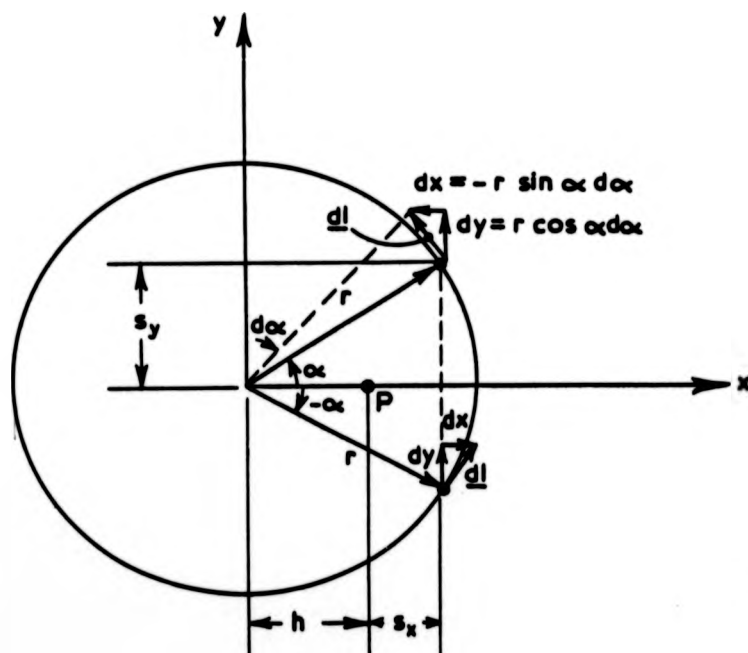
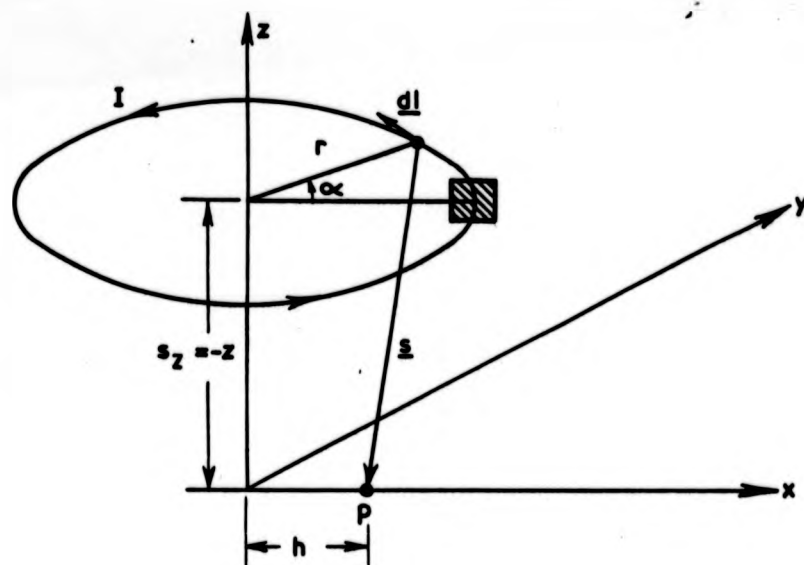


Figure 84. Off-axis field for quadrant of a circular current filament.

Equation 81 can be evaluated after some manipulation as expressions involving incomplete elliptic integrals of the first and second kind, but requiring only values of Z and R to define the modulus and argument. This technique was used to evaluate the central fields of finite corner radius rectangular coils discussed in 3.4.

APPENDIX III

DERIVATION OF TRACK INDUCTANCE

APPENDIX III DERIVATION OF TRACK INDUCTANCE

1. Introduction

This appendix gives details of the derivation of initial and asymptotic self and mutual inductances as discussed in section 3.2.2. Calculation is eased by the use of superposition, which is valid since the winding is air cored and magnetically linear. The essence in calculating both self and mutual inductance of either single or double layer meander windings is the concept of an elemental inductance of a track segment of one phase, which is one pole pitch long. Calculation of the per unit track length self inductance of this half wavelength element, and then the subsequent addition of adjacent elements, yields a series, which for a double layer winding converges to a finite value. The additional terms which are far from the initial segment can be represented as line filaments, and have characteristics determined by the track width to pole pitch ratio. The whole expression splits into two terms which relate to the finite size of the winding (i.e. its cross sectional area or aspect ratio, as well as the relevant limb length) and the track width to pole pitch ratio linked with the number of adjacent segment pairs involved (i.e. linked to the track section length). The first term is defined as the initial inductance, since its evaluation centres on the initial elemental segment with no additional side segment contributions. The second term, the asymptotic inductance, is so called since evaluation of the running total of terms involving width to pole pitch ratio and the number of included adjacent segment pairs tends to an asymptotic limit.

The mechanics of the calculation are the same when applied to finding the mutual inductance between two double layer phases. The expressions involve an additional term which is effectively the fractional physical displacement between phases. However, because of the close coupling of the initial

segments, it is necessary to include up to two adjacent segment pairs to each initial element, per phase, into the initial term.

2. Track Inductance

2.1 Phase Leakage Inductance

It is assumed that the track phase winding self inductance can be represented as a summation of the self inductance of an isolated single phase meander winding, and the mutual inductance of the other two (or remaining) phases, reflected into the reference phase. If L_G represents the phase isolated self inductance, and M_G represents the mutual contribution from another phase, for a section length G , then the total phase leakage inductance is simply

$$L = L_G - M_G \quad (1)$$

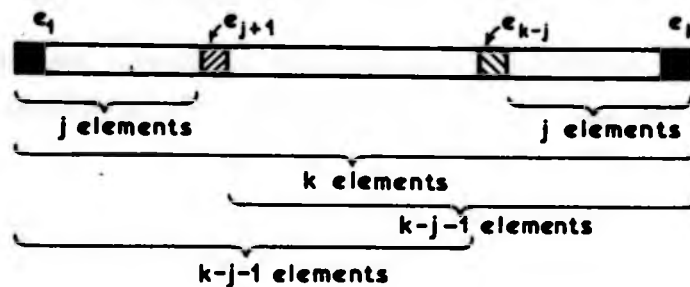
since the current magnitudes in the remaining phases combine to a full phase equivalent mutual.

2.2 Elemental Inductance

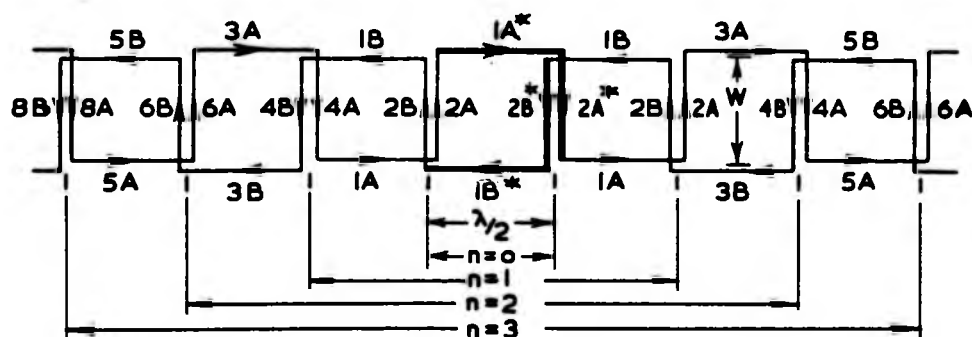
A track meander phase winding (single or double layer) can be modelled as a concatenation of single pole pitch long elements, as shown in Figure 1(a). For a section length made up of k elements, a particular element e_{j+1} can exist with an elemental complement e_{k-j} , so that both have j elements outboard to themselves. If the self inductance of any element e and the mutual inductance contribution to e from the n elements on both sides of e is defined as the elementary inductance interacting to n , or $L_e(n)$, then the contribution of e_{j+1} and e_{k-j} to the phase total self inductance is

$$L(e_{j+1}) = L_s(e_{j+1}) + M(e_{j+1}) \cdot j_L + M(e_{j+1}) \cdot (k-j-1)_R$$

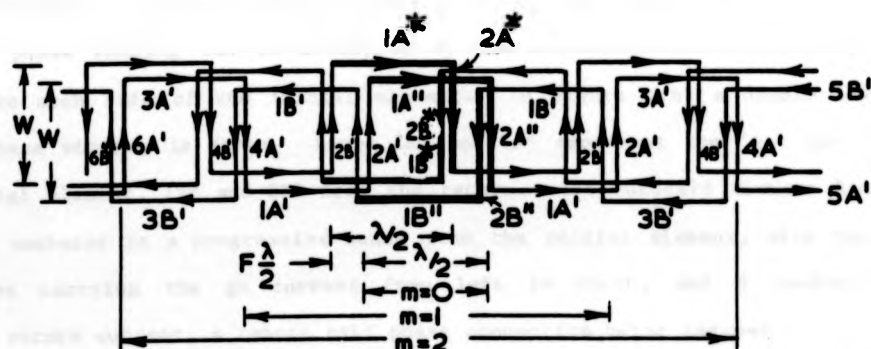
and



(a) Subdivision of meander winding into pole pitch elements.



(b) Definition of limbs for self inductance calculation.



(c) Definition of limbs for mutual inductance calculation.

Figure 1. Armature winding representation.

$$L(a_{k-j}) = L_s(a_{k-j}) + M(a_{k-j}) \cdot j_R + M(a_{k-j}) \cdot (k-j-1)_L$$

where suffices R and L relate to right and left hand outboard contributions. Adding, and remembering that terms which relate to a_{j+1} and a_{k-j} must be similar,

$$\begin{aligned} L(a_{j+1}) + L(a_{k-j}) &= [L_s(a_{j+1}) + M(a_{j+1}) \cdot j_L + M(a_{k-j}) \cdot j_R] \\ &+ [L_s(a_{k-j}) + M(a_{k-j}) \cdot (k-j-1)_L + M(a_{j+1}) \cdot (k-j-1)_R] \end{aligned}$$

so

$$L(a_{j+1}) + L(a_{k-j}) = L_e(j) + L_e(k-j-1)$$

Since the total strip self inductance $L_T(k)$ from k elements is given by

$$L_T(k) = \sum_{i=1}^k L(e_i)$$

then

$$L_T(k) = \sum_{n=0}^{k-1} L_e(n) \quad (2)$$

3. Self Inductance Structure

Equation 2 suggests that the evaluation of the self inductance of an isolated phase winding can be attempted by the successive addition of pole pitches to each side of the initial element. In Figure 1(b) a double layer single phase winding is shown. Limbs 1A* and 2A* represent the 'go' part of the initial element, 1B* and 2B* form the return. The outboard element limbs are then numbered in a progressive sense from the initial element, with the A conductors carrying the go current from left to right, and B conductors carrying return current, a remote half phase connection being assumed.

For the initial element, the reaction with the adjacent segments can be written as

$$L_e = L_L + L_T \quad (L \text{ and } T \text{ for longitudinal and transverse limb interactions}) \quad (3)$$

By symmetry, the longitudinal interactions to 1A* and 1B* are identical, so

$$L_L = 2L_{L1A} \quad (4)$$

L_{L1A} , the longitudinal interactions to 1A*, is composed of the self inductance of 1A*, L_1 , the mutual inductance with 1B*, M_1 , as well as the mutual interaction to opposing and colinear longitudinal filaments, from both sides of the initial element.

$$L_{L1A} = L_1 + 2(M_{1B} + M_{3A} + M_{5B} + M_{7A} + \dots) \text{ colinear terms} \\ + M_1 + 2(M_{1A} + M_{3B} + M_{5A} + M_{7B} + \dots) \text{ opposing terms} \quad (5)$$

For the transverse terms, only 2A* and 2B* are close coupled. It can be shown that the self inductance, L_2 , of two parallel strips 2A* and 2B* with the same current and direction connected in series is equivalent to four times the self inductance of a single strip with double thickness, L_{2A2B}

$$L_2 = 4 L_{2A2B} \quad (6)$$

Therefore,

$$L_T = L_2 + 8(M_{2A} + M_{4A} + M_{6A} + M_{8A} + \dots) \quad (7)$$

However note that for $n=0$, only L_2 is involved, and for $n=1$, L_2 is added to $8M_{2A}$ and $4M_{4A}$. The next step $n=2$ adds $4M_{4A}$ and $4M_{6A}$.

The way in which $L_e(n)$ is generated is established by using equations 3-7

$$L_e(n) = 2(L_1 + M_1) + L_2 + 4(M_{1A} + M_{3B} + M_{5A} + M_{7B} + \dots) \\ + 4(M_{1B} + M_{3A} + M_{5B} + M_{7A} + \dots) + 8(M_{2A} + M_{4A} + M_{6A} + M_{8A} + \dots) \quad (8)$$

generally, for $n \geq 2$

$$L_e(n) = L_e(n-1) + 4(M_{(2n-1)A} + M_{(2n-1)B} + M_{2nA} + M_{(2n+2)A}) \quad (9)$$

From the form of equation 8 it can be seen that when n is large, $L_e(n)$ attains a steady state limiting value. With the same provision it follows that $L_T(k)$ will assume the form of a block of initial terms with subsequent monotonic increases whose rate is determined by pole pitch.

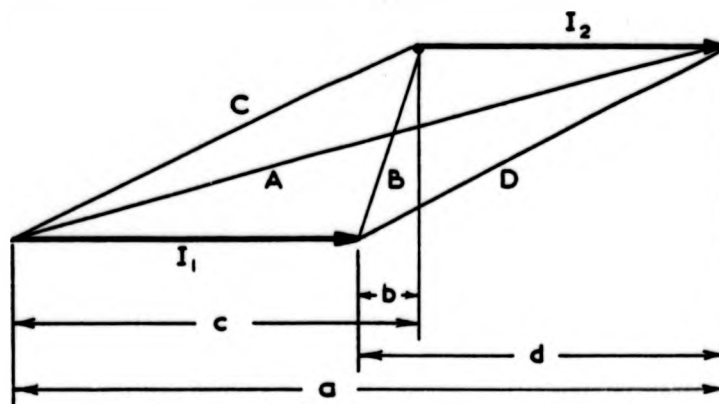
Grover⁽²⁶⁰⁾ gives expressions for evaluating self and mutual inductances. For L_1 and L_2 , the standard expression used includes a term which allows for the finite section of the conductor. For M_1 and the subsequent mutuals, calculation is through either an expression such as given in Figure 2, or Grover's Q factor, which will give identical results.

Evaluation of the incremental term in equation 9, normalised by the pole pitch, reveals that

- . colinear longitudinal filaments' normalised inductance varies as a function of n only,
- . opposing longitudinal filaments' normalised inductance varies as n and width to pole pitch ratio only,
- . transverse filaments' normalised inductance similarly varies only as n and width to pole pitch ratio.

A running summation of the incremental terms normalised by the pole pitch and k , will reach an asymptotic value, defined as L_a , such that

$$L_a = \frac{2}{k\lambda} \cdot 4 \sum_{n=0}^{k-1} (M_{(2n-1)A} + M_{(2n-1)B} + M_{2nA} + M_{(2n+2)A}) \quad (10)$$



$$M = \frac{\mu_0}{4\pi} \left\{ \log_e \left[\frac{(A+a)^a (B+b)^b}{(C+c)^c (D+d)^d} \right] + C + D - A - B \right\}$$

Figure 2. Mutual inductance between parallel current elements.

Equation 2 can be rewritten as

$$L_T(k) = k L_e(0) + (k-1) (4M_{2A}) + \frac{k\lambda}{2} L_a$$

and since

$$\begin{aligned} k &\approx \frac{2G}{\lambda} \text{ and } L_e(0) = 2(L_1 + M_1) + L_2, \\ L_T(k) &= \frac{2G}{\lambda} L_1 + G L_a = G \left(\frac{2}{\lambda} L_1 + L_a \right) \end{aligned} \quad (11)$$

where

$$L_1 = 2(L_1 + M_1) + L_2 + 4M_{2A}$$

The strip self inductance L_G used in equation 1 and the main text is the same quantity as $L_T(k)$.

4. Mutual Inductance Structure

Mutual inductance calculation follows the same strategy as self inductance calculation. The parallel expression to equation 2 is given by

$$M_T(k) = \sum_{m=0}^k M_e(m) \quad (12)$$

where $M_T(k)$ is the total mutual inductance between two phases of LSM, with k elements. The calculation can be performed for various relative phase displacements, and the main text explains how the remaining phase effects can be lumped together to refer to the first phase. Figure 1c shows the limb representation between a reference phase and a second double layer phase winding displaced by a fraction F of a wavelength.

Because of the intimate positioning of the limbs with low values of F , the initial inductance must include limbs up to $m=2$. However, the same structure emerges, with the final result

$$M_T(k) = M_G = G\left(\frac{2}{\lambda} M_1 + M_a\right) \quad (13)$$

where M_1 and M_a are the initial and asymptotic inductances respectively.

Figure 3 shows L_a and M_a for a range of width to pole pitch ratios.
(L_a is invariably negative.)

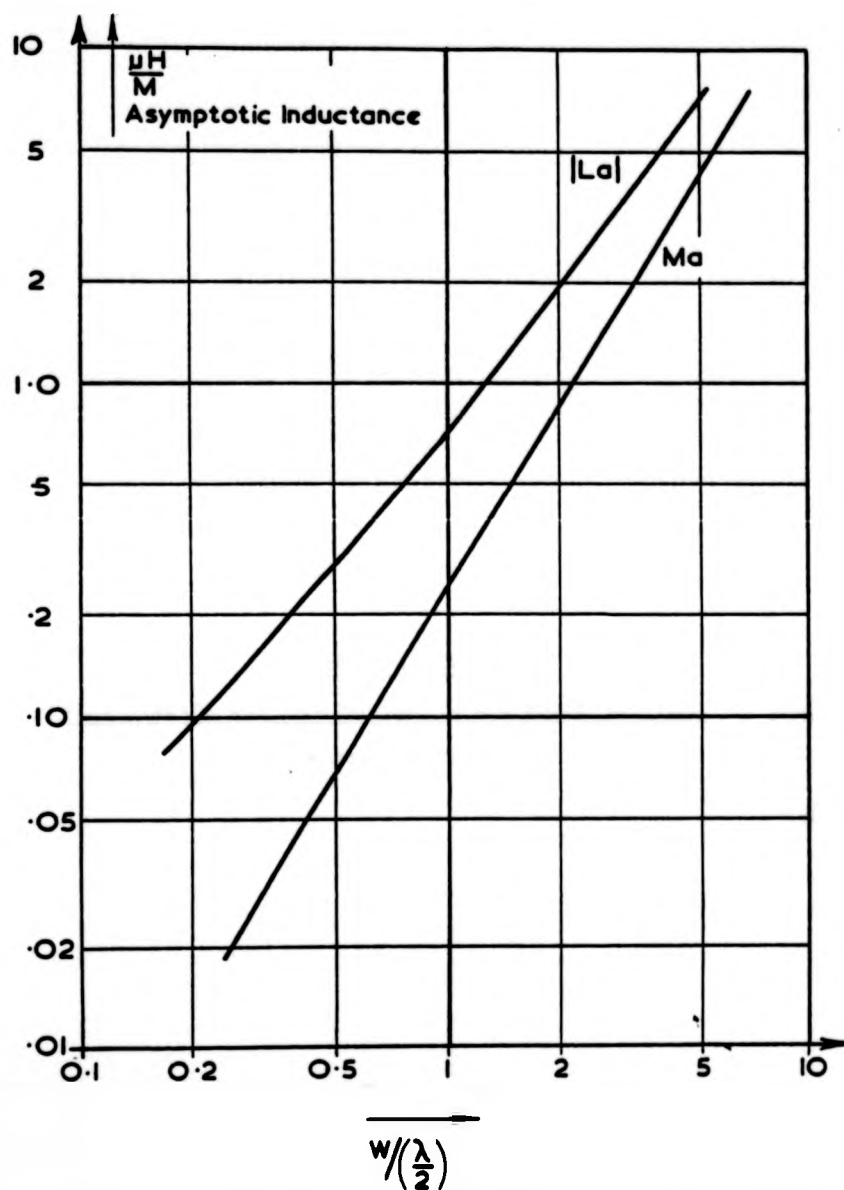


Figure 3. Asymptotic Self and Mutual Inductance as a function of width/pole pitch.

APPENDIX IV

FLUX LINKAGE AND INDUCED EMF IN AIR CORED MACHINES

(Reference 222)

TECHNICAL MEMORANDUM NO. 10

TITLE : FLUX LINKAGE AND INDUCED EMF IN AIR
CORED MACHINES.

AUTHOR : E. ABEL

DATE : FEBRUARY 1976.
REVISED NOVEMBER 1978.

CONTENTS

1	Introduction	1
2	Derivation of Back Emf Relationships	2
	2.1 Relationship with Rate of Change of Flux Linkage	2
	2.2 Rate of Change of Flux Linkage	2
	2.3 The Effect of Neighbouring Coils	4
	2.3.1 Dipole Approximation of Field	4
	2.3.2 Effect on Rate of Change of Flux Linkage	5
3	Rectangular Coils	7
	3.1 Evaluation of $\frac{d\phi}{dx}$	7
	3.2 Evaluation of $\frac{d\phi}{dx}$	8
	3.3 Harmonics in the Air Gap Flux Linkage	11
4	Circular and Racetrack Coils	11
5	Conclusions	12

APPENDIX I - Rate of Change of Flux Linkage for a Rectangular Coil

1	Flux Density Under a Rectangular Coil	A-1
2	Evaluation of $\int_{-b}^b B_z dy$	A-2
3	Rate of change of Flux Linkage	A-4
4	Solution of Equation A-10	A-6

Flux Linkage and Induced EMF in Air Cored Machines

1 INTRODUCTION

For the efficient design of air cored linear superconducting machinery it is necessary to be able to calculate accurately the emf induced in an armature phase winding by the superconducting magnets moving at a particular speed. If this value is known, for example, for a full pitched coil, conventional rotating machinery procedures can be used to establish the open circuit terminal phase voltage (the back emf). In this way the effects of short pitching, transposition and parallel and series interconnection of the individual conductor bars into a phase winding can also be calculated.

In common with machine practice, it is assumed that the machine is fed with balanced voltages or currents, and is operating in steady-state conditions. Phase inbalance can in fact be treated by using the concept of positive, zero and negative sequence currents, but will not be discussed further in this memorandum.

2 DERIVATION OF BACK EMF RELATIONSHIPS

2.1 Relationship with Rate of Change of Flux Linkage

The electromagnetic induction equation relates the emf e induced in a circuit which experiences a rate of change of flux linkage $\frac{d\phi}{dt}$.

$$e = - \frac{d\phi}{dt} \quad (1)$$

If the field winding is moving at a synchronous velocity v m/s, and the spatial variation of the flux linkage ϕ weber-turns is known for the field coil, then the temporal back emf e_B in the armature can be deduced from:

$$\begin{aligned} e_B &= - \frac{d\phi}{dt} \\ &= - \frac{d\phi}{dx} \cdot \frac{dx}{dt} \\ \text{or } e_B &= - v \cdot \frac{d\phi}{dx} \quad (2) \end{aligned}$$

i.e., for balanced conditions, the temporal variation in back emf is proportional to the product of the synchronous velocity and the spatial variation of flux linkage.

2.2 Rate of Change of Flux Linkage

The rate of change of flux linkage may be calculated from knowledge of the vertical flux density at the track level produced by the superconducting coil.

Figure 1 shows a generalised current coil, with positive sensed current flowing. The vertical z axis is positioned so that it lies along the axial line of maximum field, normal to the coil plane. The x axis lies parallel to the direction of motion of the vehicle coil array. The track coils may be modelled as closed turns of full pitch, and for ease of calculation in this particular case are assumed to be symmetrical in the y plane, and parallel to the vehicle coil.

Consider a transverse strip of width dx located a distance x from the coil axis (Figure 1). The vertical flux density seen by the strip varies along its width in a manner determined by coil geometry dimensions, and current. The flux dφ linked by the strip is simply given by

$$d\phi = \left(\int_{-b}^b B_z dy \right) dx \quad \text{weber-turns} \quad (3)$$

$$\text{i.e. } \frac{d\phi}{dx} = \int_{-b}^b B_z dy \quad \text{weber-turns/metre} \quad (4)$$

The effect of having the track coils offset is merely to alter the limits of integration. For the most common cases of tandem arranged vehicle coils the zero offset position links the most flux.

Note that expression (4) is valid whatever topology of coils is chosen, with whatever end winding geometry.

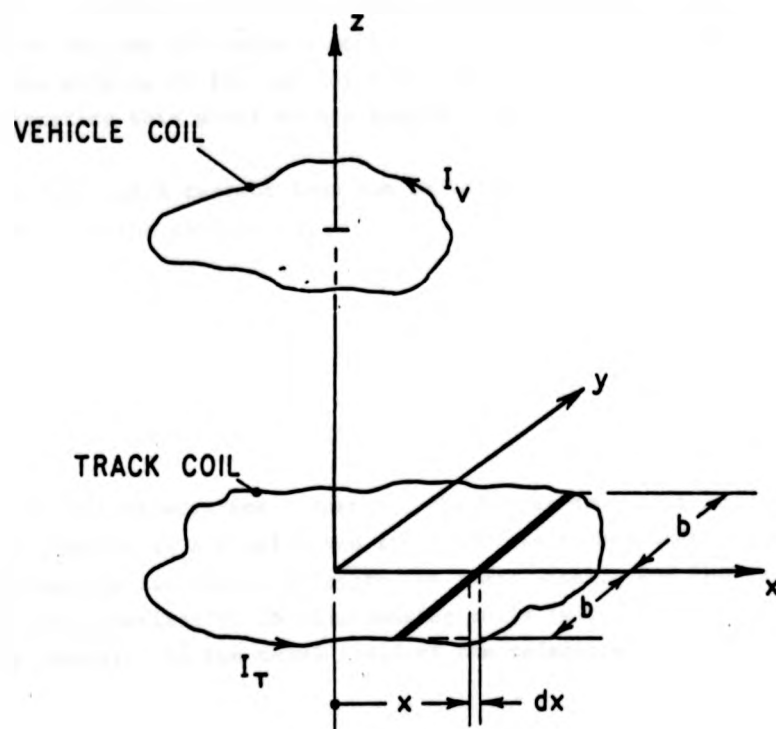


Figure 1. Generalized Vehicle and Track Coils.

2.3 The Effect of Neighbouring Coils

2.3.1 Dipole Approximation of Field

Because the LSM is air cored, the fields produced by vehicle coil arrays can be superposed. In effect it is not normally necessary to perform the calculation to include all vehicle coils, if the array is composed of a large number, as the effects of far-off coils become negligibly small. It is worth demonstrating this point with a simple example.

The external field of a current loop can be decomposed into an infinite series of multipoles. In the coil plane,

$$B(r) = \sum_{n=2}^{\infty} \frac{\mu_n}{r^{n+1}} \quad (5)$$

μ_n is the nth pole magnetic moment, and r is the distance from the coil centre line to the field point considered.

Since only far-off effects are concerned, the higher orders can be neglected. The coil now appears as a dipole, and its field diminishes as the cube of the distance (twice the distance, one eighth the field, etc). For the case of incremental contributions of $2N$ neighbouring coils (with, for this example, alternating polarity) to the total field of the reference coil, on its centre line,

$$B_z = - \frac{2\mu_2}{(\frac{\lambda}{2})^3} + \frac{2\mu_2}{(\frac{2\lambda}{2})^3} - \frac{2\mu_2}{(\frac{3\lambda}{2})^3} + \dots \quad (6)$$

where $\frac{\lambda}{2}$ is the pole pitch of the magnet array and μ_2 the dipole moment of the coils (assumed to be equal). Equation 6 can be generalised to

$$B_z = - \frac{2\mu_2}{(\frac{\lambda}{2})^3} \sum_{n=1}^N \frac{(-1)^{n-1}}{n^3}, \quad n = 1, 2, 3, 4 \dots \quad (7)$$

When N is even, grouping together the terms in pairs reduces (7) to:

$$B_z = - \frac{2\mu_2}{(\frac{\lambda}{2})^3} \sum_{n=1}^{N-1} \left(\frac{1}{n^3} - \frac{1}{(n+1)^3} \right), \quad n = 1, 3, 5 \dots \quad (8)$$

2.3 The Effect of Neighbouring Coils

2.3.1 Dipole Approximation of Field

Because the LSM is air cored, the fields produced by vehicle coil arrays can be superposed. In effect it is not normally necessary to perform the calculation to include all vehicle coils, if the array is composed of a large number, as the effects of far-off coils become negligibly small. It is worth demonstrating this point with a simple example.

The external field of a current loop can be decomposed into an infinite series of multipoles. In the coil plane,

$$B(r) = \sum_{n=2}^{\infty} \frac{\mu_n}{r^{n+1}} \quad (5)$$

μ_n is the nth pole magnetic moment, and r is the distance from the coil centre line to the field point considered.

Since only far-off effects are concerned, the higher orders can be neglected. The coil now appears as a dipole, and its field diminishes as the cube of the distance (twice the distance, one eighth the field, etc). For the case of incremental contributions of $2N$ neighbouring coils (with, for this example, alternating polarity) to the total field of the reference coil, on its centre line,

$$B_z = - \frac{2\mu_2}{(\frac{\lambda}{2})^3} + \frac{2\mu_2}{(\frac{2\lambda}{2})^3} - \frac{2\mu_2}{(\frac{3\lambda}{2})^3} + \dots \quad (6)$$

where $\frac{\lambda}{2}$ is the pole pitch of the magnet array and μ_2 the dipole moment of the coils (assumed to be equal). Equation 6 can be generalised to

$$B_z = - \frac{2\mu_2}{(\frac{\lambda}{2})^3} \sum_{n=1}^N \frac{(-1)^{n-1}}{n^3}, \quad n = 1, 2, 3, 4 \dots \quad (7)$$

When N is even, grouping together the terms in pairs reduces (7) to:

$$B_z = - \frac{2\mu_2}{(\frac{\lambda}{2})^3} \sum_{n=1}^{N-1} \left(\frac{1}{n^3} - \frac{1}{(n+1)^3} \right), \quad n = 1, 3, 5 \dots \quad (8)$$

The first few terms of equation (8), under the summation, are shown in Table 1.

n	$\frac{1}{n^3} - \frac{1}{(n+1)^3}$
1	0.875
3	0.021412
5	0.003370
7	0.000962
9	0.000372
11	0.000173
13	0.000091
15	0.000052

TABLE 1 Initial Terms of Summation from Equation (8)

For an accuracy of better than 0.1% only 16 neighbouring coils ($n=7$, $N=8$) need be considered. Generally, roughly ten coils give an accuracy sufficient for most engineering design purposes.

2.3.2 Effect on Rate of Change of Flux Linkage

Figure 2 shows three coils from a typical alternating magnet array, with the rate of change of flux linkage $\frac{d\phi}{dx}$ of the reference coil A and the magnitudes of $\frac{d\phi}{dx}$ for neighbouring right and left hand coils within the half wavelength centred around A. Also shown is the total rate of change of flux linkage, which is forced to zero every $\frac{\lambda}{2}$ by conditions of symmetry.

The total effect of neighbouring coils on the value of rate of change of flux linkage for the range $0 < x < \frac{\lambda}{4}$ can be obtained as

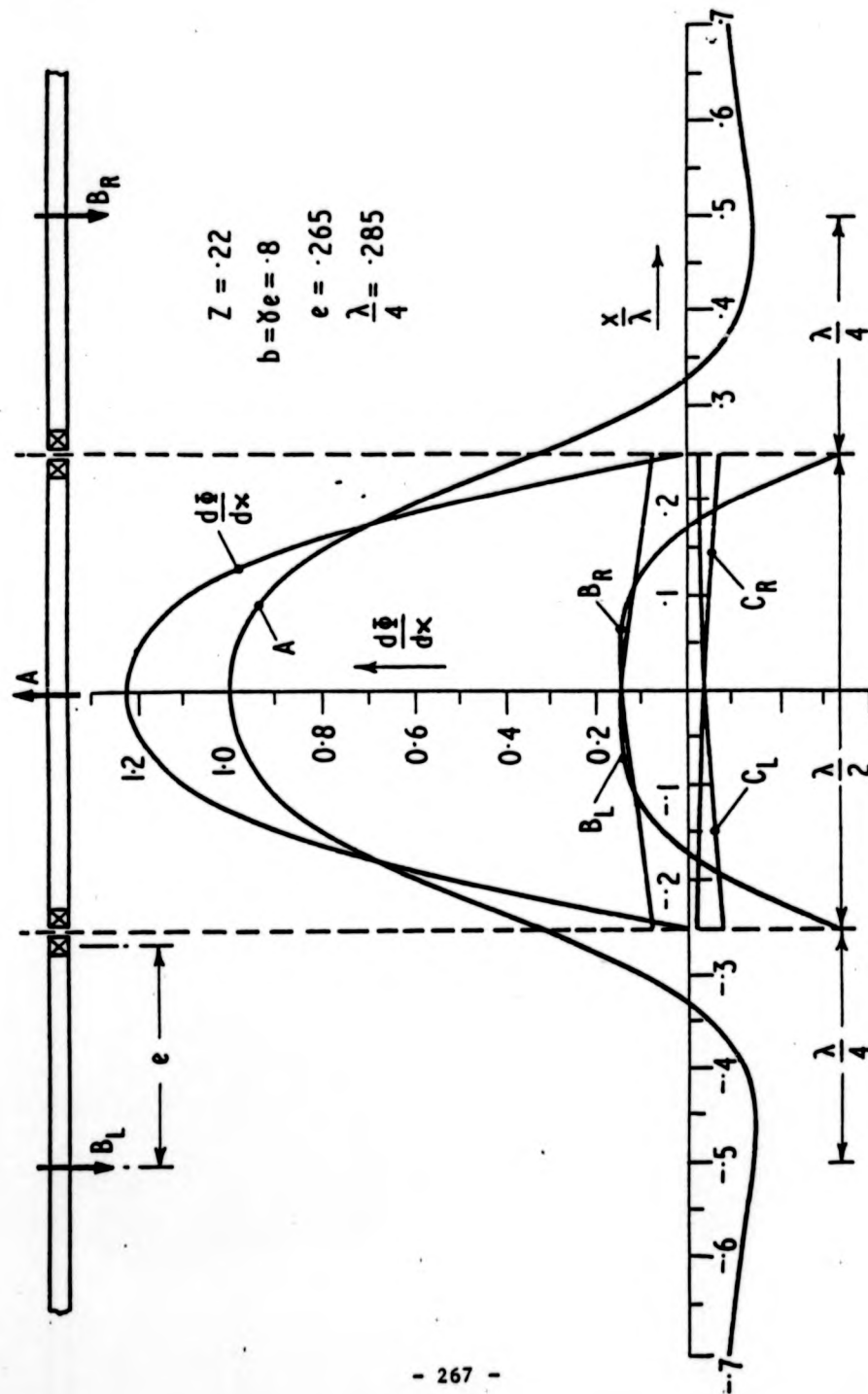


Figure 2. Neighbouring Coil Contribution to $\frac{d\Phi}{dx}$.

$$\begin{aligned} \frac{d\phi}{dx} = & \frac{d\phi}{dx} \Big|_x - \frac{d\phi}{dx} \Big|_{\frac{\lambda}{2} - x} - \frac{d\phi}{dx} \Big|_{\frac{\lambda}{2} + x} + \frac{d\phi}{dx} \Big|_{\lambda - x} + \frac{d\phi}{dx} \Big|_{\lambda + x} \\ & \quad \quad \quad A \quad \quad \quad B_R \quad \quad \quad B_L \quad \quad \quad C_R \quad \quad \quad C_L \\ & - \frac{d\phi}{dx} \Big|_{\frac{3\lambda}{2} - x} - \frac{d\phi}{dx} \Big|_{\frac{3\lambda}{2} + x} + \frac{d\phi}{dx} \Big|_{2\lambda - x} + \frac{d\phi}{dx} \Big|_{2\lambda + x} - \dots \\ & \quad \quad \quad D_R \quad \quad \quad D_L \quad \quad \quad E_R \quad \quad \quad E_L \end{aligned}$$

$$\text{i.e.} \quad \frac{d\phi}{dx} = \frac{d\phi}{dx} \Big|_x + \sum (-1)^n \frac{d\phi}{dx} \Big|_{\frac{n\lambda}{2} \pm x}, \quad n = 1, 2, 3, \dots \quad (9)$$

For the optional designs involving only the same sensed magnets, (Magneplane, Wolfson 0.4 m pole pitch) n takes only even values in equation 9, and may be expressed as

$$\frac{d\phi}{dx} = \frac{d\phi}{dx} \Big|_x + \sum \frac{d\phi}{dx} \Big|_{n\lambda \pm x}, \quad n = 1, 2, 3, \dots \quad (10)$$

3 RECTANGULAR COILS

3.1 Evaluation of $\frac{d\phi}{dx}$

Appendix I evaluates the rate of change of flux linkage with respect to the off axis track element as a function of coil half width and length, track half width, coil height and longitudinal off axis position.

$$\text{i.e.} \quad \frac{d\phi}{dx} = \text{fn}(\gamma_e, e, b, z, x) \quad (11)$$

Equation A-11 can be slightly simplified by considering the common design case $\gamma_e = b$ (i.e. track width = coil width), and equation A-12 results. Both equations can be solved relatively easily using the substitutions (A-13 to A-15) which are:

$$E = \frac{a \pm x}{z} \quad (12)$$

$$R1 = \sqrt{\left(\frac{xe + b}{z}\right)^2 + E^2 + 1} \quad (13)$$

$$R2 = \sqrt{\left(\frac{xe - b}{z}\right)^2 + E^2 + 1} \quad (14)$$

so that, for a particular off axis position, x.

$$\begin{aligned} \frac{d\phi}{dx} \cdot \frac{10}{I} = & \left[\frac{2E}{1+E^2} (R1 - R2) + \ln \left\{ \frac{(R1 - E)(R2 + E)}{(R2 - E)(R1 + E)} \right\} \right] \bigg|_{E = \frac{e+x}{z}} \\ & + \left[\frac{2E}{1+E^2} (R1 - R2) + \ln \left\{ \frac{(R1 - E)(R2 + E)}{(R2 - E)(R1 + E)} \right\} \right] \bigg|_{E = \frac{e-x}{z}} \end{aligned} \quad (15)$$

The Appendix also shows the variation of (15) with x, and describes how to use the program.

3.2 Evaluation of $\frac{d\phi}{dx}$

Equation (9) has shown how the successive neighbouring coils' $\frac{d\phi}{dx}$ contributes to the total $\frac{d\phi}{dx}$. For a particular coil, its effect within the range $0 < x < \frac{\lambda}{4}$ under the first coil can be found by incrementing or decreasing the $\frac{n\lambda}{2} \pm x$ term by the amount $\frac{\lambda}{4q}$, where q is the number of divisions of $\frac{\lambda}{2}$ chosen for harmonic analysis. Having done this for each successive coil, the following array is obtained.

A	B _R	B _L	C _R	C _L
0	$\frac{\lambda}{4}$	$\frac{\lambda}{4}$	λ	
$\frac{\lambda}{4} \cdot q$	$\frac{\lambda}{4} \frac{(2q-1)}{q}$	$\frac{\lambda}{4} \frac{(2q+1)}{q}$	$\frac{\lambda}{4} \frac{(4q-1)}{q}$	$\frac{\lambda}{4} \frac{(4q+1)}{q}$
$\frac{\lambda}{4} \frac{(q-1)}{q}$	$\frac{\lambda}{4} \frac{(q+1)}{q}$	$\frac{\lambda}{4} \frac{(3q-1)}{q}$	$\frac{\lambda}{4} \frac{(3q+1)}{q}$	$\frac{\lambda}{4} \frac{(5q-1)}{q}$
	$\frac{\lambda}{4}$	$3\frac{\lambda}{4}$		$5\frac{\lambda}{4}$

TABLE 2 Values of x to be used in Program to evaluate (9)

The number of rows is simply $q+1$ and the number of columns is the total number of coils included. It is worthwhile evaluating the first row and finding the point where an incremental pair of coils alter $\left. \frac{d\phi}{dx} \right|_x$ by, say, less than 1%, and using this as the value for the numbers of columns for subsequent rows.

When the $\frac{d\phi}{dx}$ values obtained using Table 2 are summated as in (9) (taking into account the coil polarities) then the total flux linked by the elemental strip dx is found, being a one dimensional array of size $q+1$.

Figure 3 shows the effect on $\frac{d\phi}{dx}$ of including neighbouring coils. Because the case considered is for an alternating array, the successive points alternate about the final value. Also shown is a more rapid convergence, using the incremental difference of successive coil pairs. For this particular case, only ten neighbouring coils (i.e. five on either side of the first coil) need to be considered to give a reasonable result. Note also the way in which the $x = \frac{\lambda}{4}$ value is rapidly forced to zero by the symmetry of the coil array.

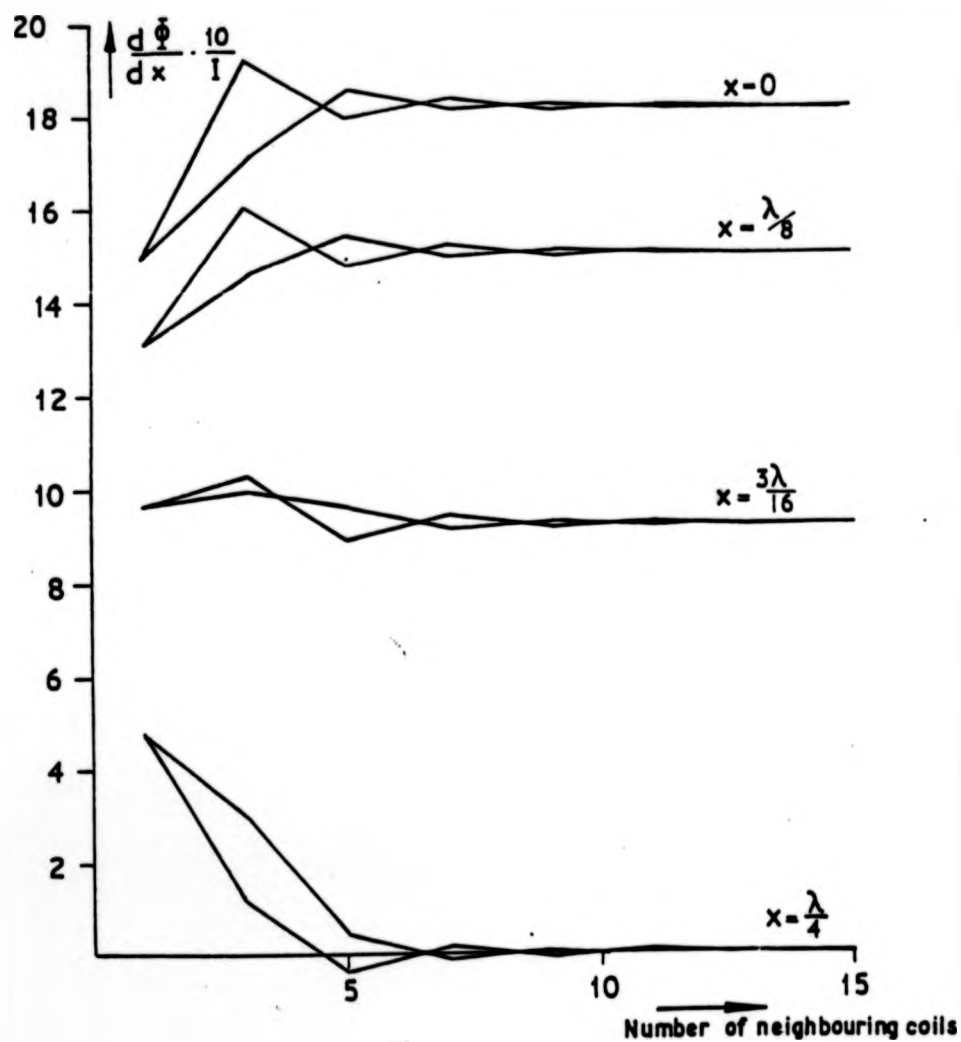


Figure 3. Effect of neighbouring coils on rate of change of flux.

The parameter values used for the figures for rectangular coils are given in Table 3.

Vehicle coil half length	e	0.265
Vehicle coil half width	γe	0.8
Vehicle to track separation	z	0.22
Track half width	b	0.8
Quarter Wavelength	$\lambda/4$	0.285

TABLE 3 Rectangular Coil Parameters

3.3 Harmonics in the Air Gap Flux Linkage

Once the total rate of change of air gap flux linkage with the full pitch track coils is known, its harmonic make-up can be evaluated. If $\frac{d\phi}{dx}$ is evaluated at $x = q\lambda$ positions in the quarter wavelength (note $x = \lambda/4$, $\frac{d\phi}{dx} = 0$) the Fourier coefficients can be found for the first $2q+1$ harmonics. With the conventions used, $x = 0$ for maximum linkage and $x = \frac{\lambda}{4}$ for zero linkage for the elemental strip, so only odd harmonics will be present in a cosinusoidal summation. For a fuller treatment of harmonic analysis, refer to TM 13, Fourier Analysis of Linear Machine Airgap Fluxes.

4 CIRCULAR AND RACETRACK COILS

The field variation at off axis positions for circular coils involves solution of complete elliptical integrals of the first and second kind. Racetrack off axis positions involve combinations of straight line element type formulae, with extra terms involving solution of incomplete elliptical integrals of the first and second kind. The overall technique for solution of rate of change of air gap flux linkage is similar to that used for rectangular coils, but is computationally more awkward. When working at large airgaps, an equivalent area rectangular coil can be used for first order approximation, with only a slight loss of accuracy.

5 CONCLUSIONS

The way in which the rate of change of flux linkage between a track coil and an array of vehicle magnets varies has been demonstrated, with particular reference to rectangular coils. From this, the temporal variation of induced emf in the air cored machine can be directly computed, complete with harmonic content, and so the vehicle force profile with any pulsations present can be established.

1st Draft: February 1976

Revised: November 1978

APPENDIX I - RATE OF CHANGE OF FLUX LINKAGE FOR A RECTANGULAR COIL

1 Flux Density Under a Rectangular Coil

Using the Biot-Savart relationship, the field for a finite length straight conductor can be found. For a rectangular coil with sides $2e$, and $2ye$ (Figure A-1) the vertical field at a point (x, y) can be found by superposition of the field from the four sides to be given by

$$\begin{aligned}
 B_z = & \frac{\mu I}{4\pi} \frac{e+x}{(e+x)^2+z^2} \left(\frac{ye+y}{[(e+x)^2+(ye+y)^2+z^2]^{3/2}} + \frac{ye-y}{[(e+x)^2+(ye-y)^2+z^2]^{3/2}} \right) \\
 & + \frac{e-x}{(e-x)^2+z^2} \left(\frac{ye+y}{[(e-x)^2+(ye+y)^2+z^2]^{3/2}} + \frac{ye-y}{[(e-x)^2+(ye-y)^2+z^2]^{3/2}} \right) \\
 & + \frac{ye+y}{(ye+y)^2+z^2} \left(\frac{e+x}{[(e+x)^2+(ye+y)^2+z^2]^{3/2}} + \frac{e-x}{[(e-x)^2+(ye+y)^2+z^2]^{3/2}} \right) \\
 & + \frac{ye-y}{(ye-y)^2+z^2} \left(\frac{e+x}{[(e+x)^2+(ye-y)^2+z^2]^{3/2}} + \frac{e-x}{[(e-x)^2+(ye-y)^2+z^2]^{3/2}} \right)
 \end{aligned}$$

(A-1)

Integration of expression A-1 is tedious, but is eased by similarities throughout the terms. Re-writing A-1, replacing the terms sequentially,

$$B_z = \frac{\mu I}{4\pi} [(A+B) + (C+D) + (E+F) + (G+H)] \quad (A-2)$$

2 Evaluation of $\int_{-b}^b B_z dy$

Taking the terms in the square brackets of A-2,

$$\int_{-b}^b A dy = \frac{a+x}{[(a+x)^2 + z^2]} \int_{-b}^b \frac{(ye+y) dy}{[(a+x)^2 + (ye+y)^2 + z^2]^{\frac{1}{2}}} \quad (A-2)$$

$$= \frac{a+x}{(a+x)^2 + z^2} \left[\left[(a+x)^2 + (ye+b)^2 + z^2 \right]^{\frac{1}{2}} - \left[(a+x)^2 + (ye-b)^2 + z^2 \right]^{\frac{1}{2}} \right] \quad (A-3)$$

It is found that similarly, $\int_{-b}^b B dy = \int_{-b}^b A dy \quad (A-4)$

Also

$$\int_{-b}^b C dy \text{ and } \int_{-b}^b D dy \text{ are merely the previous expressions with } -x$$

replacing x which does not affect the integration.

So

$$\int_{-b}^b C dy = \int_{-b}^b D dy, \text{ and normalizing by } z^2$$

$$= \frac{a-x}{\left(\frac{a-x}{z}\right)^2 + 1} \left[\left[\left(\frac{ye+b}{z}\right)^2 + \left(\frac{a-x}{z}\right)^2 + 1 \right]^{\frac{1}{2}} - \left[\left(\frac{ye-b}{z}\right)^2 + \left(\frac{a-x}{z}\right)^2 + 1 \right]^{\frac{1}{2}} \right] \quad (A-5)$$

$$\int_{-b}^b E dy = a+x \int_{-b}^b \frac{(ye+y) dy}{((ye+y)^2 + z^2) ((a+x)^2 + (ye+y)^2 + z^2)^{\frac{1}{2}}} \quad (A-6)$$

using the substitution

$$t^2 = (\gamma e + y)^2 + (e + x)^2 + z^2$$

$$\text{then } 2t \, dt = 2(\gamma e + y) \, dy$$

$$\text{and } t_u = \text{upper limit} = \left[(\gamma e + b)^2 + (e + x)^2 + z^2 \right]^{\frac{1}{2}}$$

$$t_l = \text{lower limit} = \left[(\gamma e - b)^2 + (e + x)^2 + z^2 \right]^{\frac{1}{2}}$$

So

$$\int_{-b}^b E \, dy = e + x \int_{t_l}^{t_u} \frac{dt}{t^2 - (e + x)^2}$$

since in the denominator the coefficient of t^2 is unity, i.e. > 0 , and also $-(e + x)^2 < 0$,

$$\int_{-b}^b E \, dy = \frac{1}{2\sqrt{(e + x)^2}} \ln \left[\frac{t \sqrt{1 - \sqrt{(e + x)^2}}}{t \sqrt{1 + \sqrt{(e + x)^2}}} \right]_{t_l}^{t_u} = \frac{1}{2} \ln \frac{t_u - (e + x)}{t_l - (e + x)} \bigg|_{t_l}^{t_u}$$

So

$$\begin{aligned} \int_{-b}^b E \, dy &= \frac{1}{2} \ln \frac{t_u - (e + x)}{t_l - (e + x)} - \frac{1}{2} \ln \frac{t_u + (e + x)}{t_l + (e + x)} \\ &= \frac{1}{2} \ln \left\{ \frac{\left[\left(\frac{\gamma e + b}{2} \right)^2 + \left(\frac{e + x}{2} \right)^2 + 1 \right]^{\frac{1}{2}} - \left(\frac{e + x}{2} \right)}{\left[\left(\frac{\gamma e - b}{2} \right)^2 + \left(\frac{e + x}{2} \right)^2 + 1 \right]^{\frac{1}{2}} - \left(\frac{e + x}{2} \right)} \right\} - \frac{1}{2} \ln \left\{ \frac{\left[\left(\frac{\gamma e + b}{2} \right)^2 + \left(\frac{e + x}{2} \right)^2 + 1 \right]^{\frac{1}{2}} + \left(\frac{e + x}{2} \right)}{\left[\left(\frac{\gamma e - b}{2} \right)^2 + \left(\frac{e + x}{2} \right)^2 + 1 \right]^{\frac{1}{2}} + \left(\frac{e + x}{2} \right)} \right\} \end{aligned}$$

As with $\int B$ and $\int A$, the change of sign for y effects the limits and term signs of $\int G$, which evaluate as equivalent to $\int E$

$$\text{i.e. } \int_{-b}^b G \, dy = \int_{-b}^b E \, dy \quad (\text{A-8})$$

Also as with C and D, F and H are the same as E and G, with x replaced by $-x$, so

$$\int_{-b}^b F \, dy = \int_{-b}^b H \, dy$$

$$= \frac{1}{2} \ln \left\{ \frac{\left[\left(\frac{ye+b}{2} \right)^2 + \left(\frac{e-x}{2} \right)^2 + 1 \right]^{1/2} - \left(\frac{e-x}{2} \right)}{\left[\left(\frac{ye-b}{2} \right)^2 + \left(\frac{e-x}{2} \right)^2 + 1 \right]^{1/2} - \left(\frac{e-x}{2} \right)} \right\} - \frac{1}{2} \ln \left\{ \frac{\left[\left(\frac{ye+b}{2} \right)^2 + \left(\frac{e-x}{2} \right)^2 + 1 \right]^{1/2} + \left(\frac{e-x}{2} \right)}{\left[\left(\frac{ye-b}{2} \right)^2 + \left(\frac{e-x}{2} \right)^2 + 1 \right]^{1/2} + \left(\frac{e-x}{2} \right)} \right\} \quad (\text{A-9})$$

3 Rate of Change of Flux Linkage

The flux linkage $d\phi$ of an element of track dx , x from the centre of the field coil axis, is simply

$$d\phi = \left(\int_{-b}^b B_z \, dy \right) dx \quad (\text{A-10})$$

where the vertical field component B_z at the track surface is considered between the track coil width $2b$.

Using expression A-2 through to A-10, the rate of change of flux linkage, $d\phi/dx$ is given by

$$\frac{d\phi}{dx} = \frac{4\pi \cdot 10^{-7} \cdot I \cdot 10^6}{4\pi} \left[\int_{-b}^b (A + B + C + D + E + F + G + H) \, dy \right] \text{ weber-turns per metre}$$

where I is the field coil current in MAT.

i.e.

$$\begin{aligned}
\frac{d\phi}{dx} &= \frac{I}{10} \left[\frac{2 \frac{e+x}{z}}{\left(\frac{e+x}{z}\right)^2 + 1} \left(\sqrt{\left(\frac{ye+b}{z}\right)^2 + \left(\frac{e+x}{z}\right)^2 + 1} - \sqrt{\left(\frac{ye-b}{z}\right)^2 + \left(\frac{e+x}{z}\right)^2 + 1} \right) \right. \\
&\quad + \ln \left\{ \frac{\sqrt{\left(\frac{ye+b}{z}\right)^2 + \left(\frac{e+x}{z}\right)^2 + 1} - \frac{e+x}{z}}{\sqrt{\left(\frac{ye-b}{z}\right)^2 + \left(\frac{e+x}{z}\right)^2 + 1} - \frac{e+x}{z}} \right\} - \ln \left\{ \frac{\sqrt{\left(\frac{ye+b}{z}\right)^2 + \left(\frac{e+x}{z}\right)^2 + 1} + \frac{e+x}{z}}{\sqrt{\left(\frac{ye-b}{z}\right)^2 + \left(\frac{e+x}{z}\right)^2 + 1} + \frac{e+x}{z}} \right\} \\
&\quad + \frac{2 \frac{e-x}{z}}{\left(\frac{e-x}{z}\right)^2 + 1} \left(\sqrt{\left(\frac{ye+b}{z}\right)^2 + \left(\frac{e-x}{z}\right)^2 + 1} - \sqrt{\left(\frac{ye-b}{z}\right)^2 + \left(\frac{e-x}{z}\right)^2 + 1} \right) \\
&\quad + \ln \left\{ \frac{\sqrt{\left(\frac{ye+b}{z}\right)^2 + \left(\frac{e-x}{z}\right)^2 + 1} - \frac{e-x}{z}}{\sqrt{\left(\frac{ye-b}{z}\right)^2 + \left(\frac{e-x}{z}\right)^2 + 1} - \frac{e-x}{z}} \right\} - \ln \left\{ \frac{\sqrt{\left(\frac{ye+b}{z}\right)^2 + \left(\frac{e-x}{z}\right)^2 + 1} + \frac{e-x}{z}}{\sqrt{\left(\frac{ye-b}{z}\right)^2 + \left(\frac{e-x}{z}\right)^2 + 1} + \frac{e-x}{z}} \right\} \Bigg]
\end{aligned}$$

(A-11)

For the case when the coil width ($2ye$) equals the track armature width ($2b$)
A-11 becomes

$$\begin{aligned}
 \frac{d\phi}{dx} = & \frac{I}{10} \left[\frac{2 \frac{e+x}{z}}{\left(\frac{e+x}{z}\right)^2 + 1} \left(\sqrt{\left(\frac{2b}{z}\right)^2 + \left(\frac{e+x}{z}\right)^2 + 1} - \sqrt{\left(\frac{e+x}{z}\right)^2 + 1} \right) \right. \\
 & + \ln \left\{ \frac{\sqrt{\left(\frac{2b}{z}\right)^2 + \left(\frac{e+x}{z}\right)^2 + 1} - \frac{e+x}{z}}{\sqrt{\left(\frac{e+x}{z}\right)^2 + 1} - \frac{e+x}{z}} \right\} - \ln \left\{ \frac{\sqrt{\left(\frac{2b}{z}\right)^2 + \left(\frac{e+x}{z}\right)^2 + 1} + \frac{e+x}{z}}{\sqrt{\left(\frac{e+x}{z}\right)^2 + 1} + \frac{e+x}{z}} \right\} \\
 & + \frac{2 \frac{e-x}{z}}{\left(\frac{e-x}{z}\right)^2 + 1} \left(\sqrt{\left(\frac{2b}{z}\right)^2 + \left(\frac{e-x}{z}\right)^2 + 1} - \sqrt{\left(\frac{e-x}{z}\right)^2 + 1} \right) \\
 & + \ln \left\{ \frac{\sqrt{\left(\frac{2b}{z}\right)^2 + \left(\frac{e-x}{z}\right)^2 + 1} - \frac{e-x}{z}}{\sqrt{\left(\frac{e-x}{z}\right)^2 + 1} - \frac{e-x}{z}} \right\} - \ln \left\{ \frac{\sqrt{\left(\frac{2b}{z}\right)^2 + \left(\frac{e-x}{z}\right)^2 + 1} + \frac{e-x}{z}}{\sqrt{\left(\frac{e-x}{z}\right)^2 + 1} + \frac{e-x}{z}} \right\} \Bigg]
 \end{aligned}$$

(A-12)

both A-11 and A-12 can be solved fairly easily using the HP 9100 A calculator.

4 Solution of Equation A-10

Observing the form of equation A-11 it is apparent that the last three terms are simply the first three terms with $\frac{e+x}{z}$ replacing $\frac{e-x}{z}$. Further more the first three terms are composed of combinations of two square roots, and $\frac{e+x}{z}$.

Substituting

$$E = \frac{a \pm x}{z} \quad \begin{array}{l} (+ve \text{ for 1st 3 terms} \\ -ve \text{ for 2nd 3 terms}) \end{array} \quad (A-13)$$

$$R1 = \sqrt{\left(\frac{ye + b}{z}\right)^2 + E^2 + 1} \quad (A-14)$$

$$R2 = \sqrt{\left(\frac{ye - b}{z}\right)^2 + E^2 + 1} \quad (A-15)$$

A-11 becomes, therefore

$$\begin{aligned} \frac{d\phi}{dx} \cdot \frac{10}{I} = & \left[\frac{2E}{1 + E^2} (R1 - R2) + \ln \left(\frac{(R1 - E)(R2 + E)}{(R2 - E)(R1 + E)} \right) \right] \bigg|_{E = \frac{a+x}{z}} \\ & + \left[\frac{2E}{1 + E^2} (R1 - R2) + \ln \left(\frac{(R1 - E)(R2 + E)}{(R2 - E)(R1 + E)} \right) \right] \bigg|_{E = \frac{a-x}{z}} \end{aligned} \quad (A-16)$$

The programme steps to evaluate A-16 are shown in Figures A-2 - 3, with annotated listings in Figures A-4 - 5, and are available for use on magnetic card. To use the card, load side one, start the programme, load z , ye and b , and run the programme. The values of

$$1 + \left(\frac{ye \pm b}{z}\right)^2$$

are given in the y and z registers at step 19. The second side of the card is loaded, and the two previous values are loaded in registers d and c respectively. Values of a and z are written in steps 02 - 05 and 07 - 0b respectively. The value of x for which A-16 is required is loaded into the y register, and the programme is started.

The next few steps (68 - 7c) are for use in evaluating the effect of neighbouring coils on a strip confined to $0 < x < \frac{\lambda}{4}$ under the first coil,

and is discussed in section 3.2 of the main text.

The plotter options are used to provide graphical displays of $\frac{d\phi}{dx}$, and have to be written over the steps used for printing. The step size in x is entered in 77 - 79 or 78 - 7a, and whether this is added or subtracted from initial x , in step 01 or 00. Horizontal scaling sets x times 5000, i.e. 2.5 x per mm. Vertical scaling is 200 times the $\frac{d\phi}{dx} \cdot \frac{10}{I}$ value, i.e. $0.1 \frac{d\phi}{dx} \cdot \frac{10}{I}$ per mm. Both can be changed by over-writing steps 69 - 71 or 6a - 72, if required.

The second option allows the $\frac{d\phi}{dx} \cdot \frac{10}{I}$ term (F) to be negated, but this requires a manual continue to be used after step 7d. This option was used to plot Figure 2 of the main text.

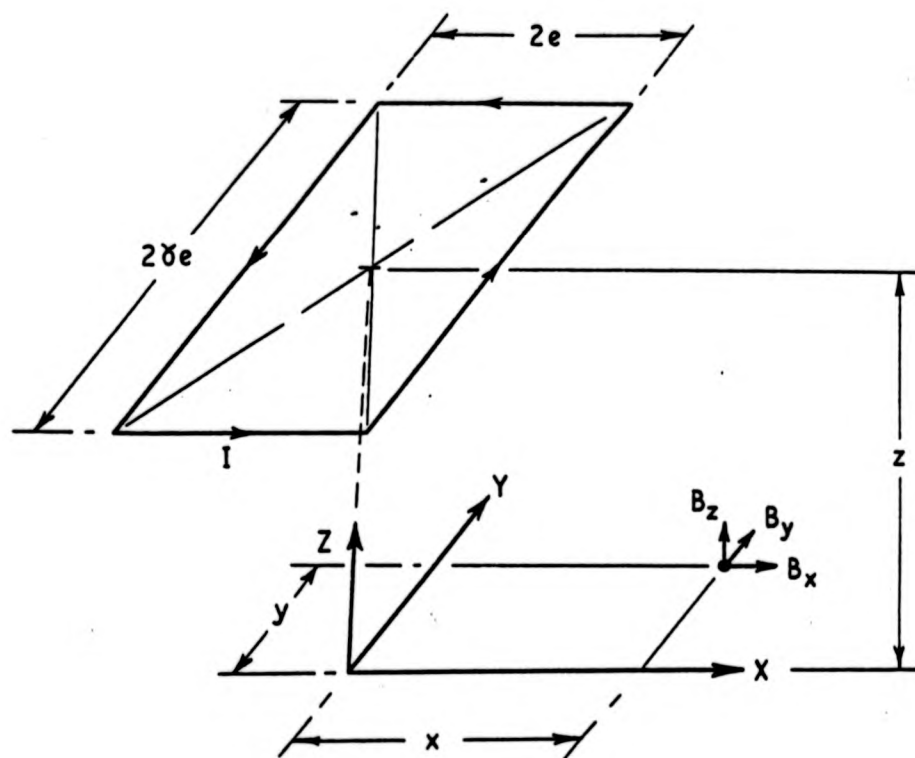


Figure A-1. Field Conventions Adopted for Rectangular Coils.

0.0	-20	3.0	-15	6.0	-02
0.1	-41	3.1	-35	6.1	-00
0.2	-60	3.2	-55	6.2	-27
0.3	-33	3.3	-21	6.3	-12
0.4	-24	3.4	-00	6.4	-27
0.5	-12	3.5	-01	6.5	-47
0.6	-34	3.6	-53	6.6	-47
0.7	-12	3.7	-06	6.7	-15
0.8	-22	3.8	-01	6.8	-41
0.9	-35	3.9	-25	6.9	-20
0.3	-30	3.3	-40	6.3	-41
0.6	-31	3.6	-15	6.6	-23
0.2	-35	3.2	-12	6.2	-17
0.4	-25	3.4	-27	6.4	-40
1.0	-31	4.0	-02	7.0	-14
1.1	-36	4.1	-33	7.1	-35
1.2	-25	4.2	-40	7.2	-11
1.3	-31	4.3	-12	7.3	-00
1.4	-36	4.4	-00	7.4	-36
1.5	-01	4.5	-27	7.5	-40
1.6	-33	4.6	-41	7.6	-16
1.7	-22	4.7	-33	7.7	-25
1.8	-33	4.8	-15	7.8	-25
1.9	-41	4.9	-30	7.9	-41
2.0	-20	4.3	-33	7.3	-27
1.6	-01	4.6	-27	7.6	-02
1.2	-27	4.2	-15	7.2	-35
1.4	-00	4.4	-35	7.4	-25
2.0	-41	5.0	-55	8.0	-60
2.1	-60	5.1	-21	8.1	-01
2.2	-02	5.2	-00	8.2	-33
2.3	-33	5.3	-01	8.3	-17
2.4	-40	5.4	-53	8.4	-50
2.5	-12	5.5	-06	8.5	-11
2.6	-00	5.6	-01	8.6	-13
2.7	-27	5.7	-25	8.7	-00
2.8	-41	5.8	-40	8.8	-41
2.9	-33	5.9	-15	8.9	-27
2.3	-15	5.3	-12	8.3	-16
2.6	-30	5.6	-27	8.6	-22
2.5	-34	5.5	-44	8.5	-36
2.4	-27	5.4	-02	8.4	-31

FIGURE A-2 (1) Input values for side two (2) $\frac{d\bar{f}}{dx}$ (3) Fourier coefficients

9.0	-----73
9.1	-----36
9.2	-----01
9.3	-----30
9.4	-----60
9.5	-----12
9.6	-----27
9.7	-----44
9.8	-----10
9.9	-----01
9.3	-----02
9.6	-----30
9.2	-----35
9.4	-----15
2.0	-----36
2.1	-----14
2.2	-----27
2.3	-----17
2.4	-----31
2.5	-----30
2.6	-----45
2.7	-----41
2.8	-----46

Figure A-2 continued

0.0-----40	3.0-----40	6.0-----10
0.1-----11	3.1-----15	6.1-----33
0.2-----47	3.2-----14	6.2-----25
0.3-----47	3.3-----27	6.3-----24
0.4-----47	3.4-----12	6.4-----11
0.5-----47	3.5-----34	6.5-----30
0.6-----33	3.6-----27	6.6-----32
0.7-----47	3.7-----13	6.7-----45
0.8-----47	3.8-----30	6.8-----27
0.9-----47	3.9-----34	6.9-----47
0.2-----47	3.2-----31	6.2-----47
0.6-----35	3.6-----35	6.6-----47
0.2-----40	3.2-----13	6.2-----47
0.4-----12	3.4-----22	6.4-----47
1.0-----12	4.0-----33	7.0-----47
1.1-----36	4.1-----31	7.1-----47
1.2-----27	4.2-----36	7.2-----33
1.3-----36	4.3-----14	7.3-----47
1.4-----16	4.4-----22	7.4-----47
1.5-----33	4.5-----33	7.5-----47
1.6-----25	4.6-----25	7.6-----47
1.7-----76	4.7-----35	7.7-----47
1.8-----23	4.8-----15	7.8-----47
1.9-----13	4.9-----30	7.9-----53
1.3-----17	4.3-----65	7.3-----00
1.6-----33	4.6-----33	7.6-----00
1.2-----25	4.2-----43	7.2-----46
1.4-----76	4.4-----05	
2.0-----23	5.0-----16	
2.1-----14	5.1-----54	
2.2-----27	5.2-----40	
2.3-----13	5.3-----10	
2.4-----34	5.4-----24	
2.5-----12	5.5-----11	
2.6-----36	5.6-----32	
2.7-----02	5.7-----01	
2.8-----36	5.8-----36	
2.9-----01	5.9-----44	
2.3-----22	5.3-----00	
2.6-----33	5.6-----00	
2.2-----25	5.2-----25	
2.4-----35	5.4-----24	

FIGURE A-3 Evaluation of $\frac{d\phi}{dx} \cdot \frac{10}{I}$ for Rectangular Coils

6.7-----27	6.7-----27
6.8-----31	6.8-----31
6.9-----02	6.9-----32
6.3-----00	6.3-----02
6.6-----00	6.6-----00
6.2-----36	6.2-----00
6.4-----05	6.4-----36
7.0-----26	7.0-----05
7.1-----03	7.1-----26
7.2-----22	7.2-----03
7.3-----36	7.3-----22
7.4-----31	7.4-----36
7.5-----42	7.5-----31
7.6-----25	7.6-----42
7.7-----21	7.7-----25
7.8-----47	7.8-----21
7.9-----47	7.9-----47
7.3-----22	7.3-----47
7.6-----44	7.6-----22
7.2-----00	7.2-----30
7.4-----00	7.4-----46
0.0-----30	0.0-----33
0.1-----33	0.1-----40
0.2-----40	0.2-----11
0.3-----11	0.3-----47
0.4-----47	0.4-----47
0.5-----47	0.5-----47
0.6-----47	0.6-----33
0.7-----33	
0.8-----47	5.6-----01
0.9-----47	
0.3-----47	
0.6-----35	
5.6-----02	

FIGURE A-3 Continued

A - 14 SIDE ONE OF MAGNETIC CARD

1) Evaluates input for side 2. 2) Evaluates coil array $\frac{d^2}{dx^2}$ 3) Evaluates Fourier coefficient

Key	N	1	2	3	4	5	6	7	8	9	0	1	2	3	4	5	6	7	8	9	0
0 CLEAR 20	0	0	0	3	f	15	$\frac{1}{2}$	R+L	$\frac{1}{2}$	6	2	02									
STOP 41	b	8e	z		$\frac{1}{2}$	35		$\frac{1}{2}$	$\frac{1}{2}$		0	00	0								
Acc+ 60					y	55		y			f	27	0	0							
+ 33		8e+b				21					e	12	n								
y \rightarrow (1) 24						00	0				f	27	n	n	0						
e 12		8e				01	01				CONTINUE 47										
- 34		8e-b									CONTINUE 47										
e 12	8e+b					1P x > y 53															
ROLL 22	z	8e+b 8e-b				6	06				f	15	$\frac{1}{2}$	n	0						
\div 35						1	01				STOP 41										
x \rightarrow y 30	8e+b	z					25	$\frac{1}{2}$	$\frac{1}{2}$	$\frac{1}{2}$											
ROLL 31	z	8e-b					40				3 CLEAR 20	0	0	0							
\div 35		8e-b					f	15			STOP 41	q	n	0							
f 25	8e+b	8e-b					e	12	n			x \rightarrow (1) 23									
ROLL 31	8e+b	8e-b					f	27	n	n		d	17								
1 X 36												y \rightarrow (1) 40									
2 f 25	8e+b	8e-b					2	02	2			b	14								
3 ROLL 31	8e+b	8e-b					+	33	n+2			\div 35		n/q							
4 x 36							y \rightarrow (1) 40					9	11	9							
5 1 01							e	12				0	00	90							
6 + 33		1 \rightarrow (1) $\frac{1}{2}$					0	00	0			x	36	90n/q							
7 ROLL 22	8e+b	1 \rightarrow (1) $\frac{1}{2}$					f	27	0	0	n	y \rightarrow (1) 40									
8 + 33		1 \rightarrow (1) $\frac{1}{2}$					STOP 41	R _n	L _n	n		c	16								
9 STOP 41							+	33	R+L			f	25	90n/q	0	0					
0 CLEAR 20	0	0	0	0			f	15	$\frac{1}{2}$			f	25	0	0	0					
1 01	1						x \rightarrow y 30	R _n	$\frac{1}{2}$			STOP 41	y ₀	0	0	0					
2 f 27	1	1	0				+	33	$\frac{1}{2}$			f	27	y ₀	y ₀	0					
3 0 00	0	1	0				f	15	$\frac{1}{2}$			z	02	2							
4 STOP 41	A	1	0				\div 35		$\frac{1}{2}$			\div 35	$\frac{1}{2}$	$\frac{1}{2}$	0(12)	0					
1 Acc+ 60							y	55	$\frac{1}{2}$												
2 2 02	2							21													
3 + 33							0	00	0												
4 y \rightarrow (1) 40							1	01	01												
e 12							1P x > y 53														
0 00	0						6	06													
f 27	0	0	n				1	01													
STOP 41	R _n	L _n	n				f	25	$\frac{1}{2}$	$\frac{1}{2}$	$\frac{1}{2}$										
+	33	R+L					y \rightarrow (1) 40														
f	15	$\frac{1}{2}$					f	15													
x \rightarrow y 30	R+L	$\frac{1}{2}$					e	12	n												
- 34	R+L	$\frac{1}{2}$					f	27	n	n											
f 27	R+L	$\frac{1}{2}$					STOP 41	2	02												

FIGURE A-4 Program Steps for Side One

③ cont.

8	Acc+	60	$y_0/2$	$d(i)$	0				
1		01							
+		33		$1+i$					
d		17	q						
IFx=y		50							
9		11							
a		13							
0		00	0	i	0				
STOP		41	y_i	i	0				
↑		27	y_i	y_i	i				
c		16	90%						
Roll+		22	i	90%	y_i				
x		36	90%						
Roll+		31	90%	y_i	i				
90	cos x	73	$\cos 2x$						
1	x	36	$y_i \cos 2x$						
2	1	01	1						
3	$x \rightarrow y$	30	$y \cos 2x$	1					
4	Acc+	60							
5	e	12	z_i						
6	↑	27	z_i	z_i	1				
7	STOP	44							
8	8	10							
9	1	04							
2	2	02	2	q	(0)				
b	$x \rightarrow y$	30	q	2					
c	$\frac{e}{f}$	35	$\frac{2}{q}$						
d	f	15	$\frac{q}{2}$						
a	x	36	a_n						
1	b	14	n						
2	↑	27	n	n	a_n				
3	d	17	q						
4	Roll+	3	n	a_n	q				
5	$x \rightarrow y$	30	a_n	1	q				
6	PRINT	45	a_n	n	q				
7	STOP	41							
8	END	46							

FIGURE A-4 Continued

Evaluation of $\frac{dI}{dx} \cdot \frac{10}{I} \Big|_x$ for rectangular coils .NB y, etc registers filled before start.

FIGURE A-5 Program Steps for Side Two

A - 16 SIDE TWO OF MAGNETIC CARD

Evaluation of $\frac{dy}{dx} \cdot \frac{10}{I}$ for rectangular coils. NB y, etc registers filled before start.

0	y → 40	x	3	y → 40	1+E ²	A	2E(R1-R2)	6	8	10	B + 1000 A H (C1)	C1
1	5	11		f	15				+	33	$\frac{dy}{dx} \cdot \frac{10}{I}$	
2		47		b	14	R1			+	25	$\frac{dy}{dx} \cdot \frac{10}{I}$	
3		47		p	27	R1	R1	A	y → 24			
4	e	47		c	12	E			9	11	-x	
5		47		-	34		R-E		x → 30	-x	$\frac{dy}{dx} \cdot \frac{10}{I}$	
6		47	e	p	27	E	E	R1-E	GIVEN	32	x	
7	+	33	x+E	a	13	R2			PRINT	45	x	$\frac{dy}{dx} \cdot \frac{10}{I}$
8		47		x → 30	E	R2			p	27	x	$\frac{dy}{dx} \cdot \frac{10}{I}$
9		47		-	34		R2-E			47		
10		47		Roll	31	R2-E	R1-E	E		47		
11		47		÷	35		R1-E	R2-E		47		
12	y → 40			a	13	R2				47		
13	e	12		Roll	22	E	R2	R1-E		47		
14	e	12	E	+	33		R2+E			47		
15	x	36	E ²	Roll	31	R2+E	R1-E	E		47		
16	p	27	E	x	36					47		
17	x	36	E ²	b	14	R1			+/	33	x + $\frac{dy}{dx} \cdot \frac{10}{I}$	
18	c	16	$1 + (\frac{dy}{dx})^2$	Roll	22	E	R1	C1	END	47		
19	+	33	R2	+	33		R1-E	C1	STOP	47		
20	p	25	R2 ²	p	25	R1-E	C1	C1	LIMIT	47		
21	√x	76	R2	÷	35		C1	C1	x →	47		
22	x → 23			f	15	A				47	x = x + $\frac{dy}{dx} \cdot \frac{10}{I}$	
23	a	13		x → 30	100	A			IF x > 512	512		
24	d	17	$1 + (\frac{dy}{dx})^2$	lnx	65	100			0	00		
25	+	33	R1	+	33		A + 1000		0	00		
26	p	25	R1 ²	IF F.A.	43				END	46		
27	√x	76	R1	5	05							
28	x → 23			c	16							
29	b	14		SET FILE	54							
30	p	27	R1	y → 40								
31	a	13	R2	8	10							
32	-	34	R1-R2	y → 24								
33	e	12	E	9	11	x						
34	x	36	E(R1-R2)	GIVEN	32							
35	2	02	2	1	01	-1						
36	x	36	2E(R1-R2)	x	36	-x						
37	1	01	1	GO TO	44							
38	Roll	22	E ²	0	00							
39	+	33	1+E ²	0	00							
40	+	25	1+E ² 2E(R1-R2) 4(R1-R2)	25	100	C1	C1					
41	35	A		y → 24								

FIGURE A-5 Program Steps for Side Two

SIDE TWO, $d\phi/dx$ for rectangular coils, cont.

PLOTTER OPTIONS											
6	↑	27	x	x	F	67	↑	27	x	x	F
	Roll ↑	31	x	F	x		Roll ↑	31	x	F	x
	2	02	2				9	CHESLEN	32	-	
	0	00	20				3	2	02	-2	
	0	00	200				6	0	00	-20	
	x	36		200F			5	0	00	-200	
	5	05					10	x	36		200F
7	ENTER	26				7	5	05	5		
1	3	03	5000			1	ENTER	26			
2	Roll ↑	22	x	5000	200F	2	3	03	5000		
3	x	36		5000x		3	Roll ↑	22	x	5000	-200F
4	Roll ↑	31	5000x	200F	x	4	x	36		5000x	
5	FMT	42				5	Roll ↑	31	5000x	-200F	x
6	↑	25				6	FMT	42			
7	.	21				7	↑	25			
8		47				8	.	21			
9	} x _s	47	x _s			9		47			
10	Roll ↑	22	x	x _s	200F	10	} x _s	47	x _s		
11	Go To	44				11	Roll ↑	22	x	x _s	-200F
12	0	00				12	x	30	x _s	x	
13	0	00				13	END	46	PRESS	CONTINUE	
14	x	30	x _s	x		14	0	+/-	33/34	x _s x _s	
15	+/-	33/34		x _s x _s		15	1	y-x()	40		
16	y-x()	40				16	2	9	11		
17	9	11				17	3		47		
18		47				18	4	} e	47		
19	e	47				19	5		47	e	
20	e	47	e			20	6	+	33	e+x	
21	+	33		e+x		21	7			As before, until	
22		47				22	8			step	
23		47				23	9				
24		47				24	10				
25	÷	35		E		25	11	01		As before, until	
26	2	02				26	12			step 67	

FIGURE A-5 Continued

APPENDIX V

COMPARISONS OF ALTERNATIVE MAGLEV REVENUE VEHICLE SYSTEMS

(References 134 and 135)

1. Reference 134, E. Abel, R.G. Rhodes, "Power Consumption for Alternative Maglev Systems", Electronics and Power, Vol.24, No.9, September 1978, pp.673-4.

Power consumption for alternative maglev systems

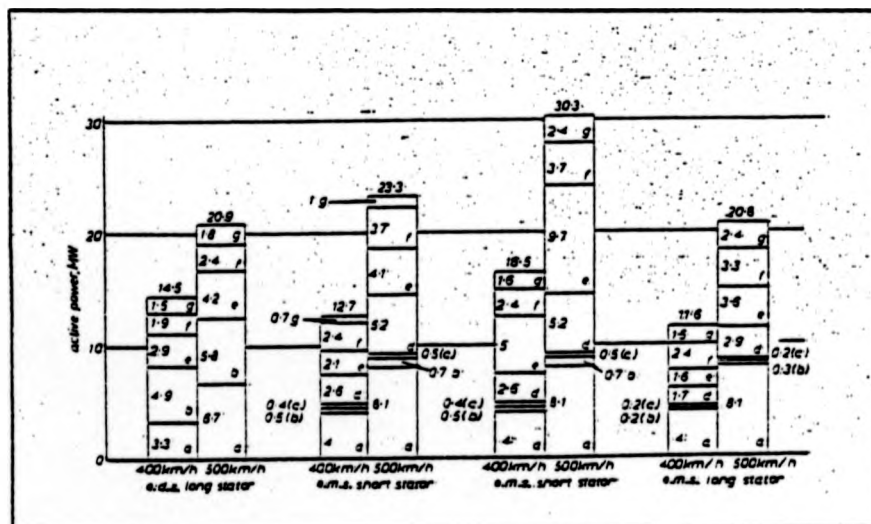
by E. Abel, B.Sc., C.Eng., M.I.E.E., and Prof. R. G. Rhodes

Two alternative systems for a high speed train are being developed in W. Germany, namely, the electrodynamic system of levitation utilising superconducting magnets and the long-stator synchronous motor for propulsion (e.d.s.), and the electromagnetic attraction system of suspension using controlled electromagnets combined with either the short-stator linear induction motor or the long-stator synchronous motor for propulsion (e.m.s.).

Edward Abel and Prof. Rhodes are with the Department of Engineering, University of Warwick, Coventry, War. CV4 7AL, England

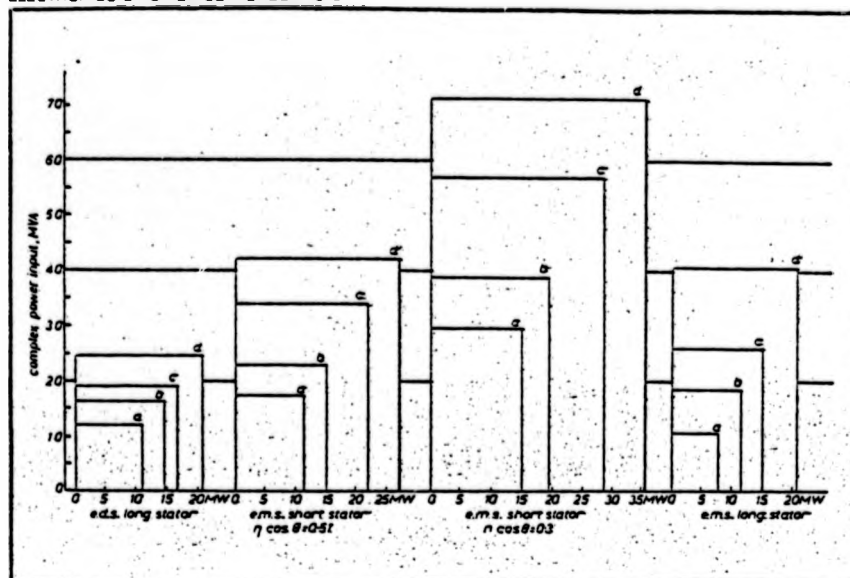
0013-5127/78/0578 - 0873 \$1.50/0
© IEE: 1978

In a recent publication¹ the design details, performance characteristics and power requirements of these systems have been contrasted and compared, and the general conclusion was that the development of either system had not proceeded sufficiently far for a clear decision to be taken between them. However, it was felt that the figures quoted in the above references for the power consumption of the respective systems are somewhat misleading, in that only the active power supplied to the vehicle is considered. The complex power requirements at the wayside substations, on the other hand, have been ignored. However, when these are taken into account, particularly for the case of the linear induction machine (l.i.m.), it has a marked effect when the total powers are compared.



1 Total active power of systems, D.C. distribution and pickup loss not included for both e.m.s. short stator ($\eta = 0.78$ and $\eta = 0.6$, respectively)

- a Aerodrag
- b Magdrag (H & guidance)
- c On-board systems drag
- d Remaining subsystem drag
- e Subsystem losses
- f Residual acceleration
- g Losses from residual acceleration



2 Total Complex and active power of systems

- a 400 km/h, steady state
b 400 km/h, accelerating
c 500 km/h, steady state
d 500 km/h, accelerating

The purpose of this study was to obtain a more realistic assessment of the respective overall power requirements from published figures¹⁻⁴ for the competitive systems, and the aggregated powers are presented in the form of the block diagrams shown in Figs. 1 and 2. In assembling this data, it was discovered that very little factual information on power factor and efficiency could be found for the e.m.s. propulsion systems. However, for the purpose of calculating the complex power requirements for the short-stator l.i.m., two designs were considered with efficiencies of 0.78 and 0.60, respectively, and efficiency/power factor products of 0.51 and 0.30.

In the determination of the overall power consumption of the respective systems, the following energy requirements were considered:

- aerodynamic drag
- magnetic drag resulting from both lift and guidance
- on-board systems drag, i.e. the power supplied to the vehicle for on-board systems
- remaining steady-state drag, i.e. cooling air inlet drag
- steady-state losses (due to motor inefficiency)
- residual acceleration, i.e. extra power to accelerate against headwinds, gradients etc.
- losses from residual acceleration.

In Fig. 1 the total composite active-power requirements of the different systems have been plotted for the two speeds 400 and 500 km/h, respectively, and, in Fig. 2, both the total complex and active power requirements are presented.

It is clear from these results that the e.d.s. system

with the long-stator motor (l.s.m.) propulsion requires considerably less energy than the other variants of the e.m.s. system under these assessed operating conditions. It seems equally obvious that the short-stator l.i.m. would be quite unsuitable for operational speeds of 500 km/h and even very doubtful for 400 km/h. Although the e.m.s. long-stator system would appear to have reasonable characteristics at 400 km/h, it becomes seriously degraded at 500 km/h. But it is felt that, because of the relatively meagre published information on this system, not very much reliance can be placed on these results. It can be concluded, therefore, that from the available published evidence on the relative power requirements of these proposed systems, the e.d.s. (cryogenic) design with l.s.m. propulsion (long stator) would appear to have the most promise for the required operating speeds of 400 to 500 km/h.

References

- 1 LEONHARD, W. 'Technische Alternativen bei der Magnetbahnentwicklung'. VDI Nachr., 15th April 1977, pp. 42-43. Translated by RHODES, R.G. and RAKELIS, J.H. 'Technical alternatives for a maglev system'. *Electron. & Power*, 1978, 24, pp. 293-296.
- 2 'Spurgleitender Fernverkehr: Magnetbahnentwicklung'. Proc. 6th Status Seminar des Bundesministeriums für Forschung und Technologie, Konstanz, 1977.
- 3 ALBRECHT, C. 'Development of levitated vehicles with superconducting magnets'. *IEEE Conf. Publ.* 142, 1976 pp. 113-116.
- 4 HEBBAST W. 'Weight and performance characteristics of magnetically suspended high speed trains as compared to aircraft'. Presented at the 14th Conference of Society of Allied Weight Engineers, Seattle, 5th-8th May 1975.
- 5 WINKLE, G. 'Forschungs- und Entwicklungsstand der Elektromagnetischen Schwebetechnik in der Bundesrepublik Deutschland'. *ETZ-A* 1975, 96, pp. 367-373.

2. Reference 135, E. Abel, J.L. Mahtani, R.G. Rhodes, "Linear Machine Power Requirements and System Comparisons", IEEE Transactions on Magnetics, Vol.MAG-14, No.5, September 1978, pp.918-20.

LINEAR MACHINE POWER REQUIREMENTS AND SYSTEM COMPARISONS

E. Abel*, J.L. Mahceni*, R.G. Rhodes*

ABSTRACT

The revenue vehicle designs of the two German Maglev groups are analysed and the complex power requirements at the trackside substation calculated. The two systems are the Electromagnetic System (EMS) with either linear induction motor (LIM) or long stator motor propulsion, and the Electrodynamic System (EDS) with linear synchronous motor (LSM) propulsion. The operational conditions considered were 400 and 500 km/h velocities either at steady state cruise or with a grade or headwind additional loading. It is found that the LSM of the EDS system is the most suitable form of propulsion for these operating conditions, the long stator motor for the EMS having apparently reasonable characteristics at 400 km/h, but becoming degraded at 500 km/h, and the LIM's studied being unsuited to the high speed range. These results highlight the necessity to compare not only the active power supplied to a vehicle, but also the complex power at wayside substations to be able to indicate the overall efficiencies and power factors of the competing systems.

The German, the Canadian and the Philco-Ford EDS designs are also compared by weight make-up and specific energy intensity. These results show that the advantage gained from a lightweight aircraft-type construction, coupled with the relatively longer body, is lost in the German design because of the extra dead weight of the wheel sets required for running on conventional dual-rail with the resultant heavier body structure. The respective machine power factors are included in the intensity calculations to link in reactive power storage.

INTRODUCTION

Several countries are engaged in research and development projects which employ magnetic levitation (Maglev) and linear motor or air-fan propulsion as component parts of high speed (up to 500 km/h) guided ground transport vehicles. The various systems can be divided into two major categories, the electrodynamic system (EDS) and the electromagnetic system (EMS). The main difference is that the former employ "repulsive" levitation and cryogenic magnets, and the latter "attractive" levitation and conventional iron-cored magnets. The state-of-the-art for both types of Maglev is such that system comparisons are being made between full-sized revenue-carrying vehicle designs on specific routes. Because of the complexity and profusion of parameters involved it is customary to choose a few specific parameters for detailed comparison which will hopefully embody the major characteristics and performance of a system. Two parameters frequently chosen are the power-to-weight ratio of the levitation and guidance system (kW/tonne) and the specific energy intensity, (kWh/passenger-km). However, to make meaningful comparisons, the way in which other factors may dominate the choice of these and other primary parameters must be clarified.

THE GERMAN SYSTEM

The analysis and design details of the German Maglev revenue vehicles are given in the 1977 Status-seminar¹ and the basic characteristics are repeated in Table I. The vehicles are made up from two sections, the EDS design speed being 500 km/h and the EMS 400 km/h. Two propulsion schemes are considered for the EMS vehicle, i.e. the double-sided linear induction motor (LIM), and the long stator motor which also incorporates a lift

function in the suspension system.

TABLE I. Characteristics of German Vehicles.

System	EDS	EMS
Stator configuration	long	short
Speed, km/h	500	400
Mass, tonnes	135	170
Length, m	56	64
No. sections	2	2
No. passengers	200	240
Payload, tonnes	20	24
Height, m	4.2	4.2
Width, m	3.3	4.2
Aerodynamic coefficient, m^2	3.94	4.75
Substation spacing, km	15	12

A preliminary system comparison has been made of the three alternatives², concluding that none of the systems was sufficiently developed to allow a clear choice to be made. Although this comparison showed the power requirement at the substation, it only included the real power for the main magnetic and aerodynamic drag. Although this represents all the losses for the EDS for a given motor efficiency, no mention was made of the EMS cooling momentum drag, the short stator d.c. line loss and the long stator track iron and distribution loss, all of which appear downline from the substation. Furthermore, since the speeds of operation were also different the aerodynamic drag power would introduce a further discrepancy, e.g. an increase of speed from 400 to 500 km/h would result in a doubling of the aerodynamic dragpower. A study was performed to establish the exact power requirements of the different systems, including power factor and motor efficiency values enabling estimates of substation complex power to be made³. When the speed is extrapolated to 500 km/h for the EMS vehicles an additional double-sided motor is required for the short stator vehicle, and the weight is increased by 20% to 205 tonnes. The long stator design at 500 km/h requires an increase in gross weight of 10%, to 180 tonnes⁴. Operation of the EDS at the lower speed of 400 km/h should not be too far from an optimized design.

In considering the values of power factor and efficiency to use in establishing terminal conditions at the substation for the EMS vehicles, it was obvious that there were few published test results or even design figures for multi-megawatt high speed motors. Reference 5 suggests calculated efficiencies of 0.8 and 0.78 and associated power factors of 0.5 and 0.65 respectively at the first and second stage of development, and calculations have been made using both these sets of values. The breakdown of active power (Fig. 1) was:-

- (1) Aerodynamic drag
- (2) Magnetic drag from lift and guidance
- (3) On-board system power (excluding any on-board batteries or generators).
- (4) Remaining steady-state drag, viz. cooling air inlet drag.
- (5) Steady-state losses due to motor inefficiency.
- (6) Residual acceleration, viz. extra power to accelerate against headwinds, gradients, etc.
- (7) Losses from residual acceleration.

The value of 0.013g residual acceleration was taken for the EDS in common with other values used in (1) for the EMS analysis. The system sets claim propulsion capacity for 3.32 gradients at cruise speeds. The steady-state or cruise power for the EDS is the sum of blocks 1, 2 and 5 in Fig. 1 which are the only system losses. The EMS cruise power is given by the sum of blocks 1 to 5. It must be noted that the figures used for the EMS long stator should be treated with some scepticism, if only for the reason that no large-scale experimental performance characteristics have yet been reported. It is

Manuscript received March 20, 1978.

* Department of Engineering, University of Warwick, Coventry, CV4 7AL.

0018-9464/78/0000-0918\$00.75 © 1978 IEEE

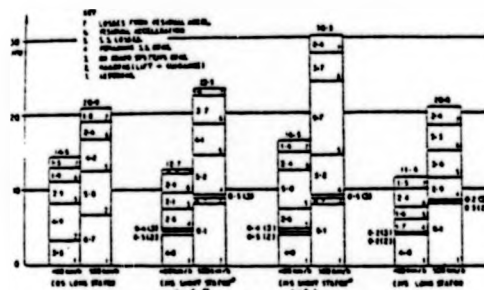


Fig. 1. Total active power of systems (MW). Note: D.C. distribution and pickup loss not included.

apparent that, in terms of real power consumed, the long stator LIM and the EDS are both roughly equivalent when loaded at 500 km/h. The low efficiency LIM (short stator) EDS was roughly 45% and the high efficiency LIM/EDS 11% more active power. If an estimate is also made of the D.C. line loss for the LIM, before current pickup, of 15%, the modified EDS/LIM figures are 70% and 31% respectively.

The values shown here could not have been deduced from the suspension lift-to-drag ratios or specific powers. For example the EDS 500 km/h magnetic lift-to-drag ratio of 32 (equivalent to 36 kW/tonne) is modified by aerodynamic drag so that cruise lift-to-drag becomes 15 (92 kW/tonne). Similarly, the EDS short stator magnetic specific power of 3 kW/tonne at 400 km/h (equivalent to magnetic lift-to-drag ratio of 370) is modified by the addition of aerodynamic and cooling drag to a steady-state value of 46 kW/tonne (lift-to-drag ratio of 15). The choice of a suspension subsystem with high magnetic lift-to-drag ratio does not ensure an overall high ratio because of the aerodynamic and other system losses.

TABLE II. Apparent efficiency (powerfactor - efficiency product) of the German Vehicles

	400 km/h		500 km/h	
	steady state loaded		steady state loaded	
EDS	0.87	0.82	0.86	0.80
EDS, long stator	0.37	0.44	0.44	0.38
EDS, short stator, high efficiency	0.31	0.31	0.31	0.31
EDS, short stator, low efficiency	0.30	0.30	0.30	0.30

The change in efficiency and power factor of the three systems as loading and speed vary is indicated in Table II. The EDS system loses 7% in going from unloaded 400 km/h to loaded 500 km/h operation. A similar transition for the EDS long stator motor results in a 21% loss representing a conservative estimate as it ignores non-linearities in the iron-cored system. The short stator values were held constant as the design called for a doubling up of the motors to give sufficient thrust at the higher speed; each motor remained at much the same output, but would be operating at different slip.

The power factor of a system enables the complex power to be evaluated from a substation active power. Reactive power flow in a machine-power network is stated in the leakage inductances of the system and air gap of the machine, and as such does no useful work. However reactive power represents a power demand that has to be catered for both in plant rating and energy cost. An iron-cored structure such as a LIM or the EDS long stator motor must have a much lower power factor than a linear synchronous motor (LSM) of the same mechanical power output, since airgap magnetization is provided by superconductors requiring an input reactive power, and the structure leakage inductance is small since the track winding is air-cored. These points are born out by

Figure 2, which shows the complex substation power as an ordinate against the active power for each of the four operating conditions of the system. The success of the electrodynamic system in requiring small amounts of reactive power to provide propulsion throughout the speed and loading variation considered is apparent. The size of the ordinates, i.e. the complex power, therefore demonstrates the relative merits of the overall systems, at the substation. Despite the rough equivalence of active power used, the EDS long stator requires 30% more than the EDS base, and the high efficiency short stator 51% more. Including a line loss the LIM value rises to a 78% increase. If the lower efficiency short stator EDS is considered, then the figures become increases of 154% and 202% on the EDS 100% base.

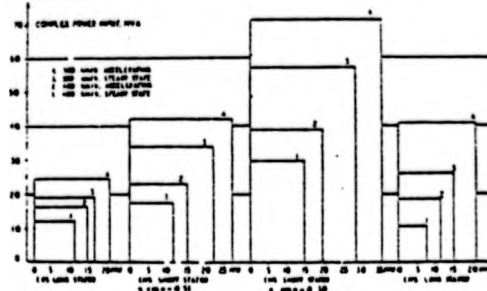


Fig. 2. Total complex and active power of systems.

From this data a power requirement comparison can be made between the three German Maglev vehicles operating under similar conditions. The comparisons cannot be strictly rigorous, since the EDS and EDS vehicles are primarily designed for different baseline operation. However, the spread of system total complex power, at the trackside substations, (Figure 2) is indicative of the type of system performance to be expected for identical service conditions. Several factors have emerged from the analysis:-

(i) The EDS has good system performance at both 500 and 400 km/h in terms of energy conversion and power consumption, and has scope for increases in power factor and efficiency, depending on economic costs of power and capital equipment.

(ii) The short stator induction machines for the EDS are quite unsuitable for high speed (500 km/h) operation, and are probably also unsuited to 400 km/h operation, primarily because of their high reactive power consumption and hence excessive overall power requirements. For example at 500 km/h the high and low-efficiency LIM's respectively required 1.8 and 3 times as much complex power as an EDS/LIM, and at 400 km/h, 1.4 and 2.4 times as much.

(iii) The long stator motor EDS appears to need marginally less power than the EDS at 400 km/h (90%), but when loaded, or at the higher speed of 500 km/h, this slight advantage is lost. Another consideration is that this machine concept has only been tested at low speed, so high-speed operating characteristics must only be regarded as tentative.

(iv) Using specific power, lift-to-drag ratio or specific energy intensity to assess system performance only indicates the active power supplied to mass up thrust and losses (if included) in the system. Low power factors in the LIM system means trackside and transmission components as well as utility energy supply costing must be in terms of total complex power used by a system. The MVA as well as the MW requirements of a system must be obtained in relation to a common guideway

route together with similar baseline specifications before reasonable comparisons can be made.

MAGLEV VEHICLE WEIGHT BREAKDOWN

Another area for comparison of vehicle data is that of weight breakdown and for this study two additional single section EDS systems are included with the German vehicle data presented in Figure 3, i.e., the Philco-Ford¹ and the Canadian^{2,7} conceptual vehicle designs (see Table III). Two options are included for Philco-Ford, the baseline 80-passenger vehicle, and the 140-passenger vehicle.

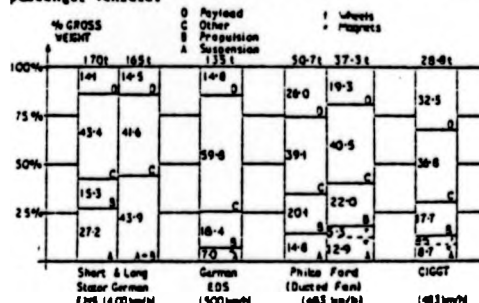


Fig. 3. Subsystem weight breakdown (X Gross).

TABLE III. Characteristics of conceptual EDS Vehicles.

System	Philco-Ford	CIGGT
Propulsion	Ducted Fan	LSM
Speed, km/h	483	483(6)
Mass, tonnes	37.3	50.7
Length, m	33.67	42.9
No. passengers	80	140
Payload, tonnes	7.2	13.2
Height, m	1.454	1.20
Width, m	2.94	3.454
Aerodynamic coefficient, m ²	1.80	2.20
		2.42(6)
		2.38(7)

Figure 4 shows the weight information scaled in tonnes for the six vehicles. The overall weight per seat of the German EDS vehicle compared to CIGGT and the 140 seat Philco-Ford designs is approximately double. This is largely because of the weight penalty of the heavy dual-rail compatible wheelless opposed to lightweight aircraft-type wheels of the other EDS designs. The EDS figures for weight-per-seat demonstrate the large amount of power-conditioning and mechanical hardware in the subsystem, which is also borne out by the payload variations from 14.1% (EDS) to 32.3% (CIGGT).

SPECIFIC ENERGY INTENSITY

The specific energy intensity (ϵ) of a transport system evaluates the amount of prime energy required per passenger, per kilometer of travel. Within the calculation, the substation converter efficiency, generation and transmission efficiency, and load factor for the vehicles are included. In obtaining values for (ϵ) for non-electrical systems the heating value of the fuel and the journey range length need to be known. The values of specific energy intensity (including power factor) for the six vehicle designs considered is shown in Table IV.

The Philco-Ford values are low because of the low aerodynamic coefficients chosen together with the high magnetic lift-to-drag ratio obtained with a 2.34m thick aluminum reaction rail. In comparing the CIGGT value with the German EDS, the large vehicle weight of the

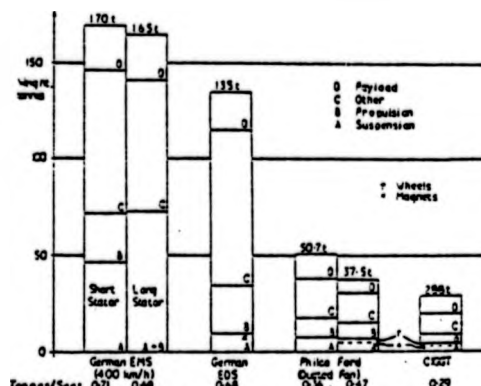


Fig. 4. Subsystem weight breakdown.

TABLE IV. Specific Energy Intensity.

System	Short	Long	EDS	Philco-Ford	CIGGT
Speed	500	500	500	483	483
high η low η	8.31	11.2	3.1	4.43	2.75
ϵ	8.31	11.2	3.1	4.43	2.75

latter has completely offset the advantage obtained by increasing the vehicle length as shown by the Philco-Ford difference between short and long vehicles. This decrease in ϵ occurs since passenger number increases more rapidly than drag on the extended vehicle.

CONCLUSIONS

The study evaluates and compares total substation power required by the German revenue vehicle designs. The evidence suggests that the linear induction motor does not appear to be a good choice for a propulsion subsystem at 500 km/h or indeed at 400 km/h. The long stator motor (EDS) is likewise degraded when loaded at 400 km/h or run at 500 km/h. The EDS/LSM on the other hand appears to have the most promise for the required operating speed range of 400-500 km/h.

When compared with other EDS designs the German system is shown to be limited by its excessive dead weight as a consequence of the requirement for conventional dual-rail compatibility.

In evaluating any system it has been shown that it is necessary to completely identify the energy make-up rather than specify particular parameters such as lift-to-drag ratio or specific power intensity in isolation.

REFERENCES

1. "Spurgeführter Fernverkehr Magnetantriebsentwicklung", Proc. 6th Statussammlung des Bundesministeriums für Forschung und Technologie, Konstanz, 1977.
2. V. Leunhard, "Technische Alternativen bei der Magnetbahn", VDI Nachr., No. 13, 13 April 1977, pp. 42-3.
3. E. Abel, "A Study of the Power Consumption of German Maglev Passenger Vehicles, (EDS and EDS)", Internal Mem. University of Warwick, January 1978.
4. G. Winkler, "Forschungs- und Entwicklungsstand der Elektromagnetischen Schwebebahntechnik in der Bundesrepublik Deutschland", ITZ-a, Vol. 16, No. 9, 1973, pp. 367-73.
5. T. B. Clark, R. L. Foss, "Conceptual Design and Analysis of the Tracked Magnetically Levitated Vehicle Technology Program - Repulsion Section", Vol. 1 & 2, PB 247931/2, Report No. PRA-OR 1 5-75-11-11a, US Dept. of Transportation, February 1975.
6. W. F. Hayes, "High-Speed Electrodynamics Maglev Guided Ground Transportation System Conceptual Design Study", NRC Canada, Report No. LTR-CR-178, September 1977.
7. Canadian Maglev Group, "The Canadian High Speed Magnetically Levitated Vehicle System", Summary Report, CIGGT Report No. 77-12, September 1977.

D52158

VOL

END